

Alma Mater Studiorum – Università di Bologna

DOTTORATO DI RICERCA IN

Scienze Chimiche

Ciclo XXXI

**Settore Concorsuale: 03/C1**

**Settore Scientifico Disciplinare: CHIM/06**

**Synthesis and biological potential of new active  $\beta$ -lactam based  
compounds**

**Presentata da: Giulia Martelli**

**Coordinatore Dottorato**

**Prof. Aldo Roda**

**Supervisore**

**Prof. Daria Giacomini**

**Esame finale anno 2019**



## Table of contents

ABSTRACT .....	4
1. INTRODUCTION.....	9
2. NOVEL $\beta$ -LACTAM COMPOUNDS ACTIVE AS ANTIBACTERIAL AGENTS .....	10
2.1 MOLECULES WITH ANTIBACTERIAL ACTIVITY .....	10
2.2 $\beta$ -LACTAM ANTIBIOTICS .....	12
2.3 ANTIMICROBIAL RESISTANCE.....	14
2.3.1 <i>Resistance mechanisms</i> .....	16
2.4 MULTI-TARGET DRUGS AND CYSTIC FIBROSIS .....	18
2.5 DEVELOPMENT OF MONOCYCLIC $\beta$ -LACTAM ANTIBACTERIALS.....	19
2.6 DUAL ACTIVE ANTIBACTERIAL-ANTIOXIDANT $\beta$ -LACTAMS.....	24
2.6.1. <i>Synthesis of azetidinones</i> .....	25
2.6.2 <i>Antibacterial activity</i> .....	26
2.6.3 <i>Antioxidant activity</i> .....	28
2.7 VECTORIZATION AND <i>IN VIVO</i> BIODISTRIBUTION OF A SELECTED 4-ALKYLIDENE- $\beta$ -LACTAM.....	30
2.7.1 <i>Synthesis of azetidinones</i> .....	30
2.7.2 <i>Formulation of SLNs for the loading of the lead compound</i> .....	31
2.7.3 <i>Cytotoxicity and antibacterial activity</i> .....	31
2.7.4 <i>Preliminar in vivo activity</i> .....	33
2.8 OTHER ANTIBACTERIAL ALKYLIDENE $\beta$ -LACTAMS .....	34
2.8.1 <i>Synthesis of azetidinones</i> .....	35
2.8.2 <i>Antibacterial activity</i> .....	37
2.9 CARBAMATE $\beta$ -LACTAMS .....	38
2.9.1 <i>Synthesis of azetidinones</i> .....	39
2.9.2 <i>Antibacterial activity</i> .....	42
2.10 $\beta$ -LACTAM BASED ANTIBACTERIAL BIOMATERIALS .....	45
2.10.1 <i>Biomaterials and hydroxyapatite (HA)</i> .....	45
2.10.2 <i>Synthesis of azetidinones</i> .....	46
2.10.3 <i>Loading of azetidinones on HA</i> .....	47
2.10.4 <i>Characterization of azetidinone-HA samples</i> .....	50
2.10.5 <i>Azetidinone release studies</i> .....	51
2.10.6 <i>Antibacterial activity</i> .....	52
2.10.7 <i>Cytotoxicity tests</i> .....	54
2.11 OTHER <i>N</i> -THIO-SUBSTITUTED $\beta$ -LACTAMS.....	55
2.11.1 <i>Synthesis of azetidinones</i> .....	56
2.12 CONCLUDING REMARKS .....	58
2.13 EXPERIMENTAL SECTION .....	60
2.13.1 <i>General information</i> .....	60
2.13.2 <i>Synthetic general procedures</i> .....	60
2.13.3 <i>Synthesis of dual active antibacterial-antioxidant <math>\beta</math>-lactams</i> .....	62
2.13.4 <i>Synthesis of alkylidene-<math>\beta</math>-lactams for vectorization and in vivo biodistribution</i> .....	68
2.13.5 <i>Synthesis of other antibacterial alkylidene-<math>\beta</math>-lactams</i> .....	69
2.13.6 <i>Synthesis of <math>\beta</math>-lactam carbamates</i> .....	71
2.13.7 <i>Development of <math>\beta</math>-lactam-based antibacterial biomaterials</i> .....	75
2.13.7.1 <i>Loading of azetidinones</i> .....	75
2.13.7.2 <i>In vitro release</i> .....	76
2.13.7.3 <i>Synthesis of <i>N</i>-thio-substituted-azetidinones</i> .....	76
2.13.8 <i>Synthesis of other <i>N</i>-thio-substituted <math>\beta</math>-lactams</i> .....	77

<b>3. NOVEL <math>\beta</math>-LACTAM COMPOUNDS ACTIVE AS INTEGRIN LIGANDS .....</b>	<b>80</b>
3.1 MULTIFACETED ACTIVITIES OF $\beta$ -LACTAM COMPOUNDS .....	80
3.1.1 <i><math>\beta</math>-lactams as enzyme inhibitors</i> .....	80
3.1.2 <i><math>\beta</math>-lactams as integrin ligands</i> .....	82
3.1.2.1 Integrins .....	82
3.1.2.2 Integrin ligands .....	84
3.1.2.3 Integrin activation: internalization, trafficking and endocytosis .....	86
3.2 DEVELOPMENT OF A NEW INTEGRIN-LIGAND LIBRARY .....	88
3.2.1 <i>Synthesis of azetidinones</i> .....	88
3.2.2 <i>Biological evaluations</i> .....	94
3.2.2.1 Cell adhesion and solid-phase binding assays .....	94
3.2.2.2 Effects of selected $\beta$ -lactams on integrin-mediated ERK phosphorylation .....	98
3.2.2.3 Effects on selected $\beta$ -lactams to HUTS-21 epitope exposure .....	100
3.2.3 <i>Molecular Modeling</i> .....	100
3.3 OTHER $\beta$ -LACTAM BASED INTEGRIN LIGANDS .....	102
3.3.1 <i>Synthesis of azetidinones</i> .....	103
3.3.2 <i>Biological evaluations</i> .....	107
3.4 STUDIES ON INTEGRIN INTERNALIZATION MEDIATED BY $\beta$ -LACTAM COMPOUNDS .....	110
3.5 FLUORESCENT $\beta$ -LACTAM COMPOUNDS .....	111
3.5.1 <i>Imaging and bioimaging</i> .....	112
3.5.2 <i>Fluorophores</i> .....	112
3.5.3 <i>Development of <math>\beta</math>-lactam-fluorophore conjugates</i> .....	113
3.5.3.1 <i>Synthesis of azetidinones</i> .....	113
3.5.3.2 <i>Spectrophotometric evaluations</i> .....	119
3.5.3.3 <i>Biological evaluations</i> .....	120
3.6 CYTOTOXIC $\beta$ -LACTAM COMPOUNDS .....	122
3.6.1 <i>Cytotoxic agents and Targeted drug delivery systems</i> .....	122
3.6.2 <i>Development of cytotoxic conjugates</i> .....	124
3.6.3 <i>Biological evaluations</i> .....	128
3.7 LOADING OF $\beta$ -LACTAM INTEGRIN LIGANDS ON SR-HYDROXYAPATITE .....	130
3.7.1 <i>Loading of azetidinones on Sr-HA</i> .....	131
3.7.2 <i>Characterization of azetidinone-Sr-HA samples</i> .....	133
3.7.3 <i>Azetidinone release study</i> .....	135
3.8 LOADING OF AGONIST $\beta$ -LACTAM INTEGRIN LIGANDS ON PLLA NANOFIBERS .....	136
3.8.1 <i>Loading of azetidinones on PLLA</i> .....	138
3.8.2 <i>Characterization of azetidinones-PLLA-samples</i> .....	138
3.8.3 <i>Azetidinone release study</i> .....	141
3.8.4 <i>Biological evaluations</i> .....	145
3.9 CONCLUDING REMARKS .....	147
3.10 EXPERIMENTAL SECTION .....	150
3.10.1 <i>General information</i> .....	150
3.10.2 <i>Synthetic general procedures</i> .....	150
3.10.3 <i>Synthesis of the new integrin ligand library</i> .....	151
3.10.4 <i>Synthesis of other <math>\beta</math>-lactam based integrin ligands</i> .....	160
3.10.5 <i>Synthesis of fluorescent <math>\beta</math>-lactam compounds</i> .....	164
3.10.6 <i>Synthesis of cytotoxic <math>\beta</math>-lactam compounds</i> .....	169
3.10.7 <i>Loading of <math>\beta</math>-lactam compounds on Sr-HA</i> .....	171
3.10.7.1 <i>Loading of azetidinones</i> .....	171
3.10.7.2 <i>In vitro release</i> .....	172

3.10.7.3 HPLC analysis parameters .....	172
3.10.8 Loading of $\beta$ -lactam compounds on PLLA.....	172
3.10.8.1 Quantification of azetidinones loaded on PLLA .....	173
3.10.8.2 <i>In vitro</i> release.....	173
<b>4. BIOCATALYSIS AS A PROMISING SYNTHETIC STRATEGY.....</b>	<b>174</b>
4.1 BIOCATALYSIS AND ENZYMES.....	174
4.1.1 <i>Hydrolases and Lipases</i> .....	176
4.2 KINETIC RESOLUTIONS WITH LIPASES .....	177
4.2.1 <i>Development of enantiomerically pure <math>\beta</math>-lactam integrin ligands</i> .....	179
4.2.2 <i>Biological evaluations</i> .....	189
4.3 OXIDATION REACTIONS .....	190
4.3.1 <i>Amine oxidation</i> .....	190
4.3.2 <i>Amine oxidation with Sodium periodate/TEMPO system</i> .....	192
4.3.3 <i>Oxidative couplings</i> .....	199
4.3.4 <i>Biocatalytic oxidation reaction: laccases</i> .....	200
4.3.5 <i>Development of the oxidative amidation</i> .....	203
4.4 ENZYMATIC CARBOXYLATION OF BIPHENYL COMPOUNDS .....	209
4.4.1 <i>(De)carboxylases</i> .....	209
4.4.2 <i>Stereorecognition in biphenyl compounds</i> .....	212
4.5 CONCLUDING REMARKS .....	220
4.6 EXPERIMENTAL SECTION .....	222
4.6.1 <i>General information</i> .....	222
4.6.2 <i>Synthesis of enantiomerically pure <math>\beta</math>-lactams</i> .....	222
4.6.2.1 <i>Chiral HPLC parameters</i> .....	224
4.6.3 <i>Synthesis for amine oxidation with Sodium periodate/TEMPO system</i> .....	224
4.6.4 <i>Synthesis for oxidative amidation</i> .....	227
4.6.5 <i>Enzymatic ortho-carboxylations</i> .....	228
4.6.5.1 <i>General information</i> .....	228
4.6.5.2 <i>Site-directed mutagenesis</i> .....	228
4.6.5.3 <i>Heterologous expression of (De)carboxylases in <i>E. coli</i></i> .....	228
4.6.5.4 <i>Synthesis of biphenyl compounds</i> .....	229
<b>REFERENCES.....</b>	<b>234</b>

## Abstract

Since the discovery of Penicillin (Fleming, 1928),  $\beta$ -lactam compounds (azetidin-2-ones) represent an important class of four-membered cyclic amides. Starting from the antimicrobial potency exerted by naturally occurring bicyclic compounds (penicillins and cephalosporins), nowadays new variants with monocyclic structure are showing new and specific biological activities.<sup>1</sup>  $\beta$ -lactam compounds are still the main agents used to treat bacterial infections, nevertheless the widespread emergence of resistance to antibiotics in pathogenic bacteria now represents a serious threat to global health, prompting to the development of new antibacterial agents. During the last two decades researches demonstrated that structural modifications of monocyclic  $\beta$ -lactams are an effective tool for the discovery of innovative antibacterial compounds.

Recently, new monocyclic  $\beta$ -lactam compounds with an alkyldiene moiety conjugated to a benzyl ester in the C4 position of the ring were reported. In these derivatives the carbon-carbon double bond directly linked to the azetidinone conferred an increased aptitude toward ring-opening reactions leading to an enhancement of antibacterial potency against Gram-positive pathogens.<sup>2-4</sup>

Starting from this 4-alkyldiene-azetidinone scaffold, we developed new  $\beta$ -lactams that combined in one molecule the antibacterial and the antioxidant activities, thus realizing dual active compounds with a synergistic action for the potential treatment of chronic infections such as those in cystic fibrosis (CF) pathology, where a persistent colonization by drug-resistant pathogens is often associated with epithelial damage by pulmonary oxidative stress.<sup>5</sup> The novel derivatives were functionalized on the C3 side chain of the  $\beta$ -lactam ring with some natural polyphenols (caffeic, ferulic, or sinapic acid) for activating the antioxidant potency (Figure A1). The new derivatives were tested *in vitro* for antibacterial and antioxidant activities including multidrug-resistant strains from CF patients. The best candidates showed good activities against multidrug resistant clinical isolates of MRSA (MICs 2-8 mg/L) and TEAC (Trolox Equivalent Antioxidant Capacity) values 2.5 times higher than those known for compounds currently used as antioxidants.

Exploiting the 4-alkyldiene-azetidinone scaffold, the effect of a carbamate group was also explored,<sup>6</sup> since organic carbamates have frequently been employed as pharmaceuticals (e.g. Linezolid). The new molecules were designed to have an aryl, benzyl, or phenethyl-carbamate group on the C3 hydroxyethyl side chain (Figure A2) and tested for their antibacterial efficacy against Gram-positive and Gram-negative bacterial strains. Overall phenethyl-carbamates resulted selective antibacterials against multi drugs resistant Gram-positive species with MIC potencies of 2-4 mg/L.

The efficacy against *S. aureus*, including methicillin resistant strains (MRSA), of some monocyclic  $\beta$ -lactams with an alkylthio-group on the nitrogen atom has recently been reported, with the *N*-methylthio substituent proving to be essential for antimicrobial activity.<sup>4</sup> Therefore we developed a library of different *N*-thio-substituted azetidinones (Figure A3) and studied the loading of some of these derivatives on hydroxyapatite (HA) nanocrystals in order to get functionalized materials able to couple the bioactivity of HA with the antibacterial properties of the  $\beta$ -lactams.<sup>7</sup> The new *N*-thio-azetidinone-functionalized hydroxyapatites were then evaluated against Gram-positive and Gram-negative reference bacteria as well as antibiotic-resistant strains from clinical isolates obtained from surgical bone biopsies. All tested

azetidinone-HA samples displayed a significant antibacterial activity against *S. aureus* and *E. coli*, resulting promising as new functional biomaterials with enhanced antibacterial activity.

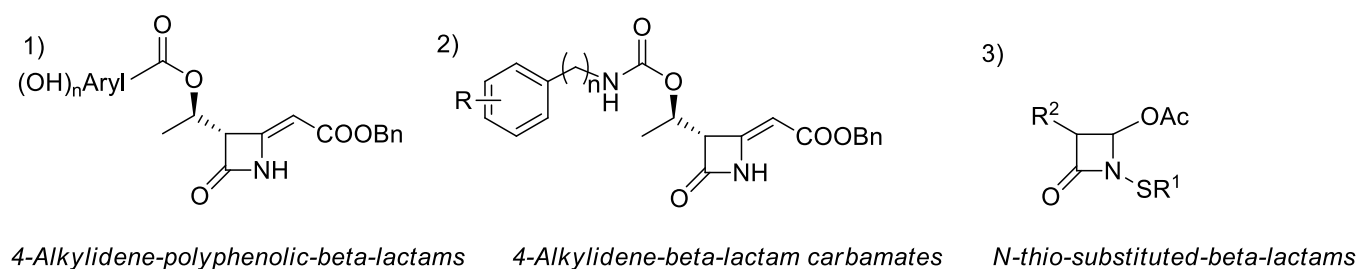


**Figure A.** General selected structures of  $\beta$ -lactam compounds active as antibacterials

Even if azetidinones first attracted attention for their antibacterial properties, over the past few decades the  $\beta$ -lactam core structure offered a unique approach to the design and synthesis of new derivatives with diverse biological properties. As a matter of fact, new  $\beta$ -lactam compounds demonstrated biological activity as inhibitors of a wide range of enzymes.<sup>1</sup> Among receptor ligands that are structurally based on the  $\beta$ -lactam scaffold, only few azetidinones have been shown to exhibit activity against integrins. Integrins are heterodimeric  $\alpha/\beta$  transmembrane receptors that mediate dynamic adhesive cell-cell and cell-matrix interactions regulating crucial aspects of cellular functions, such as migration, adhesion, differentiation, growth and survival. Because of the important roles of integrins and their ligands in immune responses, leukocyte traffic, haemostasis, and cancer, their potential as a therapeutic target is now widely recognized.<sup>8</sup>

To date, most efforts have focused on the development of small ligands that can modulate integrins. Peptidic and non-peptidic ligands that have been developed are all related to the minimal recognition RGD (Arg-Gly-Asp) or MPUPA (4([(N-2-methylphenyl)ureido]-phenylacetyl) motifs present on endogenous extra-cellular matrix (ECM) ligands of some integrin classes.

Recent research efforts have also focused on improving the pharmacological parameters of the synthetic ligands mainly by altering the polarity and the rigidity of the scaffolds. According to this, we designed and developed a library of  $\beta$ -lactam derivatives that were specifically designed by a structure-based strategy to target RGD-binding and leukocyte integrins.<sup>9</sup> The approach used for the design of the new molecules was based on rationalization from known integrin ligands. The incorporation of a conformational constrain was obtained by the insertion of the  $\beta$ -lactam scaffold, a rigid core that, by reducing the conformational degrees of freedom, could favor directional non-covalent bonding for ligand-receptor recognition. The ring was indeed functionalized with different side chains bearing an acid and a basic terminus to mimic the RGD peptide or the MPUPA moiety, for enhancing selectivity and modulating the affinity toward the receptor.

The biological activities of these new compounds were evaluated by investigating their effects on integrin-mediated cell adhesion in suitable cell lines expressing the RGD integrins  $\alpha_v\beta_3$ ,  $\alpha_v\beta_5$ ,  $\alpha_v\beta_6$ ,  $\alpha_5\beta_1$ , and  $\alpha_{11b}\beta_3$ , and leukocyte integrins  $\alpha_4\beta_1$  and  $\alpha_L\beta_2$ . A structure-activity analysis of this new series of azetidinones allowed to identify structural elements associated with integrin selectivity and we obtained selective and potent agonists at a nanomolar level that could promote cell adhesion mediated by  $\alpha_v\beta_3$ ,  $\alpha_v\beta_5$ ,  $\alpha_5\beta_1$ , or  $\alpha_4\beta_1$  integrin, as well as antagonists that were selective for RGD-binding integrins or leukocyte integrins (Figure B).

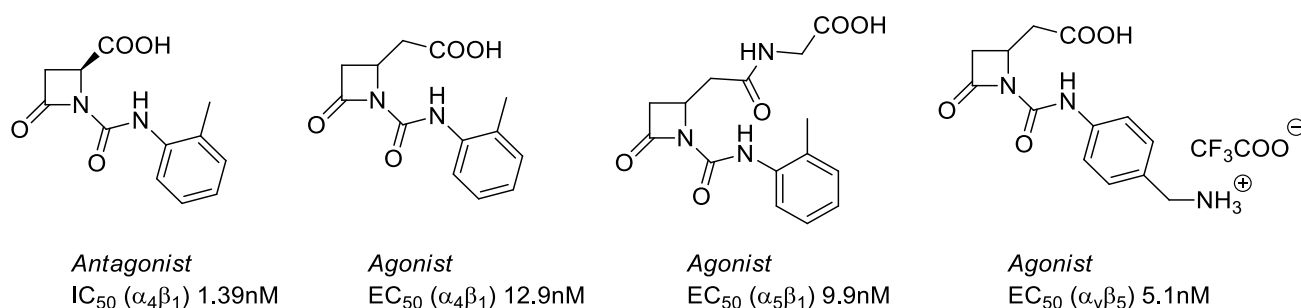


**Figure B.** Selected structures of  $\beta$ -lactam compounds active and selective as integrin ligands

Nowadays extensive efforts have been made to develop ligands active as integrin antagonists, whereas less attention has been paid to the discovery of agonists; nevertheless integrin agonists could open up novel opportunities for therapeutics, which gain benefits to increase integrin-dependent cell adhesion and proliferation.<sup>10</sup> In fact, integrin agonists could enhance the effects of stem cell-based therapies and induce human stem cells to differentiate. According to this, we decided to exploit the agonist behavior of some of our ligands to develop novel  $\beta$ -lactam based biomaterials as biocompatible scaffolds displaying an enhanced adhesion ability toward stem cells. Both adsorption on hydroxyapatite (HA) nanocrystals and loading on PLLA (poly-L-lactic acid) nanofibers were successfully performed and the resulting materials were assayed toward integrin- and human mesenchymal stem cells (hMSCs)-mediated adhesion.

These new insights into integrin functions required a better investigation of agonist and antagonist effects on several integrin-mediated processes such as cell adhesion, internalization and trafficking. Trafficking is a complex process through which the cell internalizes ECM molecules or receptors into the cytoplasm through endocytosis mechanisms, allowing a constant integrin recycling.<sup>11</sup>

According to this, we evaluated integrin internalization with confocal microscopy analysis by means of an integrin transfected with a green fluorescence protein (GFP). From these studies it emerged that our agonist synthetic compounds could induce integrin internalization as well as fibronectin (FN), the endogenous ligand, while antagonists prevented integrin internalization. After these promising results, we moved to the conjugation of the most active agonist candidates with fluorescent tags for evaluating a possible internalization of the compound itself inside the cell.

In particular, conjugation with two fluorophore molecules (Rhodamine B and fluorescein isothiocyanate, FITC) was performed on the C3 position of azetidiones (Figure C1) and the new obtained fluorescent ligands maintained an integrin affinity as agonists at a micromolar level. Preliminary fluorescence bio-imaging investigations revealed a possible internalization of the Rhodamine-conjugated-ligand into the cellular cytoplasm.

Therefore, in order to design a drug-delivery system that could enter selectively into cancer cells *via* endocytosis upon integrin binding, two cytotoxic molecules were incorporated on the  $\beta$ -lactam scaffold, thus replacing the fluorophore moieties. Accordingly, 5-fluorouracil (5-FU) and Doxorubicin were conjugated on the C3 hydroxyethyl chain after an appropriate cytotoxic derivatization and linker insertion (Figure C2).



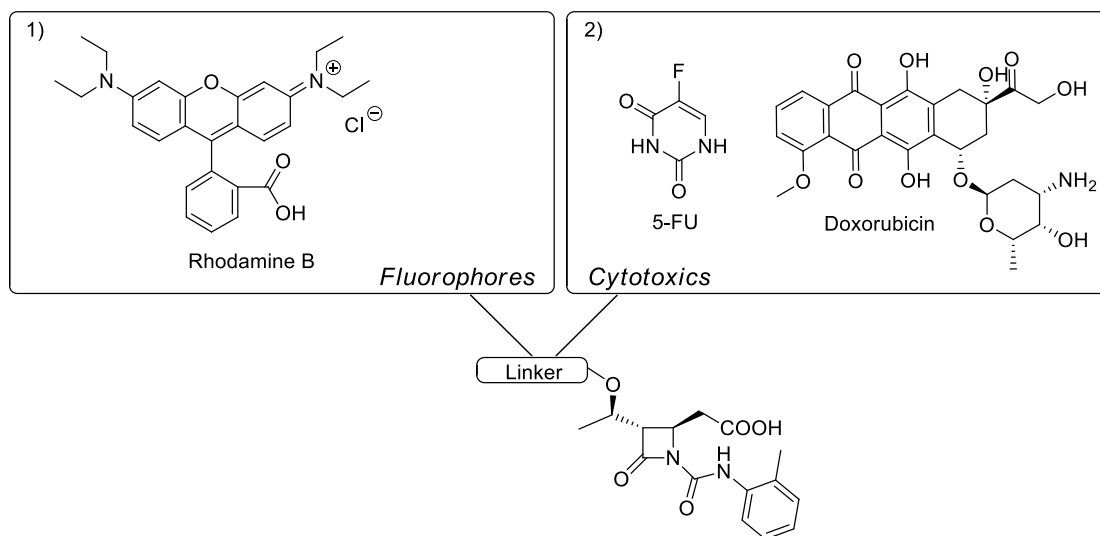


**Figure C.** Selected structure of a  $\beta$ -lactam compound conjugated with fluorophores or cytotoxic drugs

From docking studies on some selected derivatives among integrin ligands, it emerged how the receptor active site could discriminate between two enantiomers in their binding mode, hence indicating that the ligands could have different biological activities according to their specific absolute configuration. We then decided to develop a biocatalytic protocol for obtaining, through an enzymatic kinetic resolution (KR) mediated by lipases, an enantiomerically pure  $\beta$ -lactam intermediate, necessary for the development of the racemic integrin ligands library. In this way it was possible to obtain some selected couples of  $\beta$ -lactam enantiomers with excellent enantiomeric excesses to be tested in cell adhesion assays (Figure D).

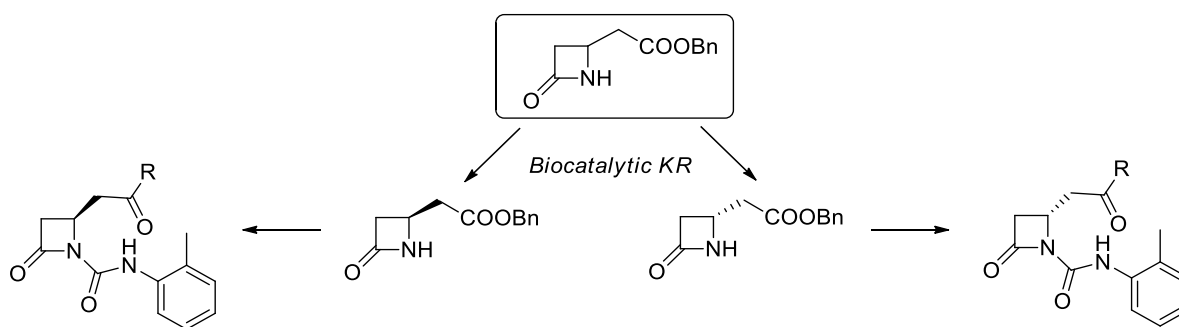


**Figure D.** Schematic strategy for the synthesis of enantiomerically pure  $\beta$ -lactam integrin ligands through biocatalysis

As just demonstrated, biocatalysis has become nowadays a standard tool for the production of fine chemicals and its application in the pharmaceutical field dominates heavily. In fact, the use of enzymes or redox biocatalysts in synthetic organic chemistry processes is becoming an alternative way to obtain enantiomerically pure products or for the resolution of racemates,<sup>12</sup> leading to many advantages such as mild work conditions, reduction of extrasteps and no toxic waste production.

To cite some developed applications, a kinetic resolution on *ortho*-substituted biphenyl compounds mediated by decarboxylases was studied for obtaining an enantioselective synthesis of atropoisomers, and an amidation oxidative coupling mediated by laccase/TEMPO system in aqueous medium was performed.

In the field of oxidation processes, selectivity and sustainable reaction conditions are key issues for the development of new eco-friendly methodologies for amine oxidation. Indeed, selectivity is often a critical point because of the large number of possible products, and many systems still need metal-containing reagents and produce toxic or hazardous wastes. According to this, we investigated some inorganic metal-free oxidants for oxidation of amines, and NaIO<sub>4</sub>/TEMPO turned out to be the most efficient and selective system for benzylamines oxidation to benzaldehydes in aqueous-organic medium. Furthermore, oxidation of secondary amines gave selective oxidation on the benzylic portion thus realizing an oxidative deprotection of the *N*-benzyl group with an easy amine recovery.

- 1 P. Galletti and D. Giacomini, *Current Medicinal Chemistry*, 2011, **18**, 4265.
- 2 F. Broccolo, G. Cainelli, G. Caltabiano, C. E. A. Cocuzza, C. G. Fortuna, P. Galletti, D. Giacomini, G. Musumarra, R. Musumeci and A. Quintavalla, *J. Med. Chem.*, 2006, **49**, 2804.
- 3 P. Galletti, C. E. A. Cocuzza, M. Pori, A. Quintavalla, R. Musumeci and D. Giacomini, *ChemMedChem*, 2011, **6**, 1919.
- 4 R. Cervellati, P. Galletti, E. Greco, C. E. A. Cocuzza, R. Musumeci, L. Bardini, F. Paolucci, M. Pori, R. Soldati and D. Giacomini, *Eur. J. Med. Chem.*, 2013, **60**, 340.
- 5 D. Giacomini, R. Musumeci, P. Galletti, G. Martelli, L. Assennato, G. Sacchetti, A. Guerrini, E. Calaresu, M. Martinelli and C. E. A. Cocuzza, *Eur. J. Med. Chem.*, 2017, **140**, 604.
- 6 D. Giacomini, G. Martelli, M. Piccichè, E. Calaresu, C. E. A. Cocuzza and R. Musumeci, *ChemMedChem*, 2017, **12**, 1525.
- 7 D. Giacomini, P. Torricelli, G. A. Gentilomi, E. Boanini, M. Gazzano, F. Bonvicini, E. Benetti, R. Soldati, G. Martelli, K. Rubini and A. Bigi, *Scientific Reports*, 2017, **7**:2712.
- 8 P. Galletti, R. Soldati, M. Pori, M. Durso, A. Tolomelli, L. Gentilucci, S. D. Dattoli, M. Baiula, S. Spampinato and D. Giacomini, *Eur. J. Med. Chem.*, 2014, **83**, 284.
- 9 M. Baiula, P. Galletti, G. Martelli, R. Soldati, L. Belvisi, M. Civera, S. D. Dattoli, S. Spampinato, D. Giacomini, *J. Med. Chem.*, 2016, **59**, 9721.
- 10 A. Tolomelli, P. Galletti, M. Baiula and D. Giacomini, *Cancers*, 2017, **9**, 78.
- 11 C. Le Roy and J. L. Wrana, *Nat. Rev. Mol. Cell Biol.*, 2005, **6**, 112.
- 12 A.J.J. Straathof, S. Panke, A. Schmid, *Curr. Opin. Biotechnol.*, 2002, **13**, 548.

# 1. Introduction

This thesis is divided in three main chapters and reports the research work performed during my three year-PhD programme under the supervision of Prof. Daria Giacomini at the Department of Chemistry, University of Bologna.

The main subject of this dissertation concerns the design and synthesis of new classes of monocyclic  $\beta$ -lactam compounds and their biological potential.

$\beta$ -lactams in fact are really evergreen bioactive molecules, primarily known for their efficiency as antibiotics, but more recently considered also for a great number of diverse activities.

The search for novel active azetidinone compounds has been deeply studied and pioneered within my research group since more than 10 years, and with this thesis work we aim at demonstrating how a wide structural variability on a fixed monocyclic azetidinone scaffold could give rise to novel candidates displaying different biological activities and innovative promising applications (Figure 1.1).

Specifically, Chapter 2 comprises the synthesis of new  $\beta$ -lactam-based antimicrobial agents against multidrug-resistant pathogens. Chapter 3 concerns the design of novel  $\beta$ -lactam derivatives active as integrin ligands. Finally, Chapter 4 covers other more variegated projects including biocatalytic approaches for the synthesis of enantiomerically pure azetidinones, and studies toward oxidative processes mediated by enzymes or metal-free oxidants.

The work performed during a three months-exchange period (funded by a Marco Polo grant) at Karl Franzens University of Graz under the supervision of Prof. Kurt Faber is also included in this section.

In general, my work dealt with the design, synthesis and complete characterization of the new compounds and functional materials including the release studies. Biological assays on the developed molecules or biomaterials were conducted in collaboration with other research groups, as specified in the main body text.

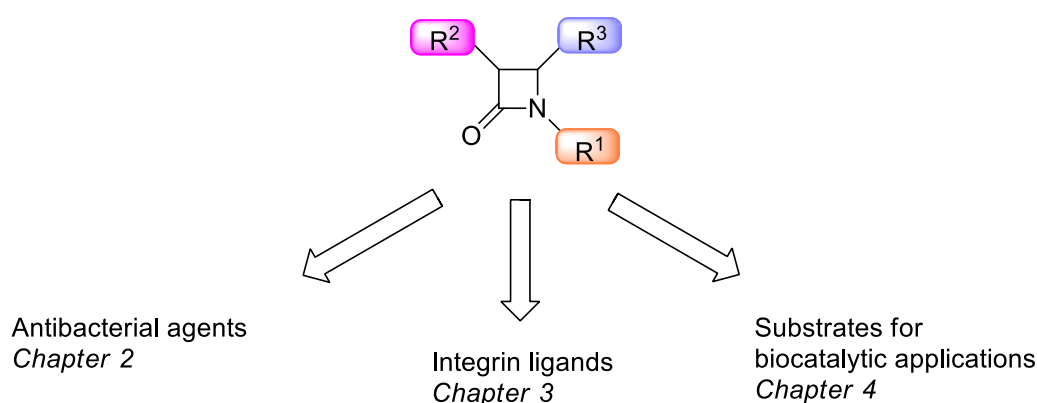


**Figure 1.1.** Sketch of the possible applications of monocyclic  $\beta$ -lactam compounds described in this PhD thesis

## 2. Novel $\beta$ -lactam compounds active as antibacterial agents

### 2.1 Molecules with antibacterial activity

The term 'antibiotic' comes from the Greek 'anti' (against) and 'bios' (life) and was introduced by Selman Waksman in 1942 to indicate those substances produced by some microorganisms and characterized by an antagonistic effect against the growth of other bacterial species, thus excluding non-microbial origin compounds.<sup>1</sup> Nowadays the term also refers to synthetic or semi-synthetic compounds, obtained from naturally occurring molecules appropriately modified by synthetic strategies. Antibiotics are distinguished in bacteriostatic (if block the bacterial growth preventing its reproduction) and bactericides (if directly kill the pathogens). The antibiotic molecules are classified according to different mechanisms of action that are closely related to their chemical structure and spectrum of activity:

- Molecules acting as competitive inhibitors of enzymes involved in the synthesis and replication of nucleic acids, i.e. sulfonamides (Sulfamerazine), quinolones (Nalidixic acid) and fluoroquinolones (Levofloxacin) (Figure 2.1).

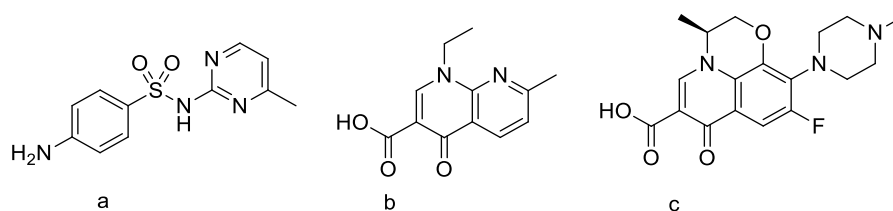


Figure 2.1. Sulfamerazine (a), Nalidixic acid (b), Levofloxacin (c)

- Bacteriostatic molecules interfering with protein synthesis, such as aminoglycosides (Streptomycin), macrolides (Erythromycin) and tetracyclines (Chlortetracycline) (Figure 2.2).

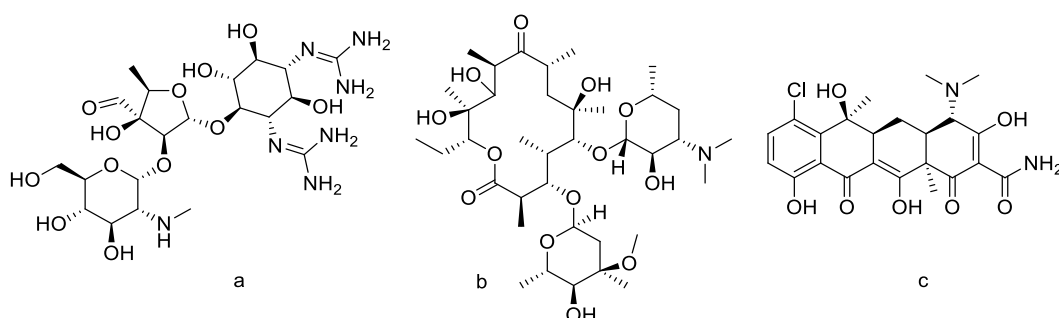
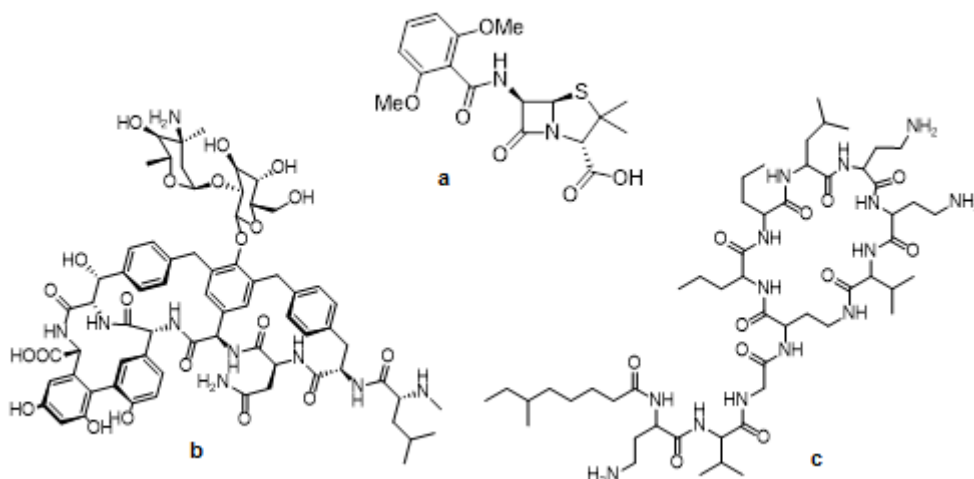


Figure 2.2. Streptomycin (a), Erythromycin (b), Chlortetracycline (c)

- Bactericidal molecules interfering with bacterial cell wall construction, such as penicillins (Methicillin), cephalosporins and carbapenems or with cell membrane construction, such as glycopeptides (Vancomycin) or polymyxins (Colistin) (Figure 2.3).



**Figure 2.3.** Methicillin (a), Vancomycin (b), Colistin (c)

- Molecules constituted by a lipidic portion connected to a peptide i.e. lipopeptides (Daptomycin) (Figure 2.4), which display a unique mechanism of action, interacting directly with the bacterial cell membrane and leading to the inhibition of proteins and nucleic acids synthesis and thus to the death of the cell.<sup>2</sup>

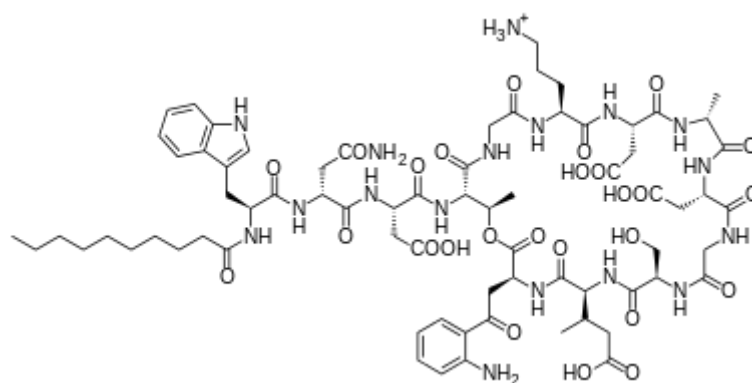


**Figure 2.4.** Daptomycin

- Oxazolidinones, total-synthesis compounds that are considered bacteriostatic with slow bactericidal action. This class is currently represented by a single commercial molecule, linezolid (LZD) (Figure 2.5).<sup>3</sup> Linezolid acts as a protein synthesis inhibitor by binding to peptidyl transferase, an enzyme present on bacterial ribosomes responsible for the process of mRNA translation. Unlike most of other protein synthesis inhibitors acting on the elongation phase, linezolid exhibits a unique mechanism of action acting on the initiation step of protein synthesis.<sup>4</sup> Nevertheless, after a few years of its introduction and marketing, bacterial strains of *Staphylococcus aureus* and *Enterococcus* resistant to linezolid have been evolved and spread.

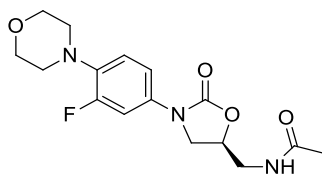


Figure 2.5. Linezolid

## 2.2 $\beta$ -lactam antibiotics

$\beta$ -lactams are a large class of compounds characterized by the presence of the azetidin-2-one ring. Since their discovery and introduction in therapy by Alexander Fleming,<sup>5</sup>  $\beta$ -lactam antibiotics proved to be chemotherapeutics of incomparable effectiveness, with a broad spectrum of activity and low toxicity, still representing the main agents for treating bacterial infections.<sup>6</sup>

Bicyclic  $\beta$ -lactam antibiotics were originally divided into penicillins, where the azetidinone is condensed with a 5-term thiazolidine ring ('penam' core) and cephalosporins, whose  $\beta$ -lactam nucleus is condensed with a six-membered dihydrothiazinic ring. Nowadays all the semi-synthetic variants of the aforementioned classes derive from 6-aminopenicillanic acid (6-APA) and 7-aminocephalosporanic acid (7-ACA) as precursors. Other  $\beta$ -lactam-based families are represented by clavams (or oxapenams), clavams and the most modern carbapenems ('penem' core), containing a 2,3-dihydropyrrole ring fused with the azetidinone (Figure 2.6).

With the discovery of monobactams, i.e. monocyclic  $\beta$ -lactams, in the late 1970s, it was demonstrated for the first time that the antibacterial activity of azetidinone compounds was not strictly related to the typical bicyclic structure of penicillins, cephalosporins or carbapenems,<sup>7</sup> thus making the search for new monocyclic  $\beta$ -lactam antibiotics extremely active. By far, the only commercially available compound is Aztreonam (Figure 2.6), a monobactam showing remarkable specificity against Gram-negative aerobic bacteria and excellent resistance against  $\beta$ -lactamases.<sup>8</sup>

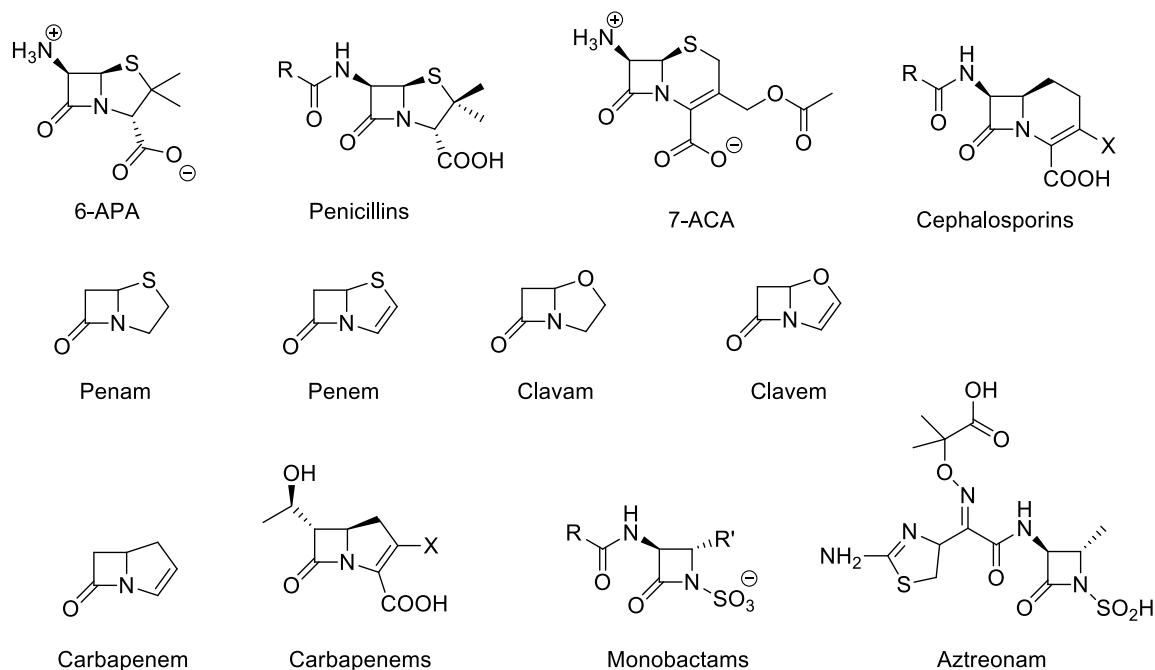
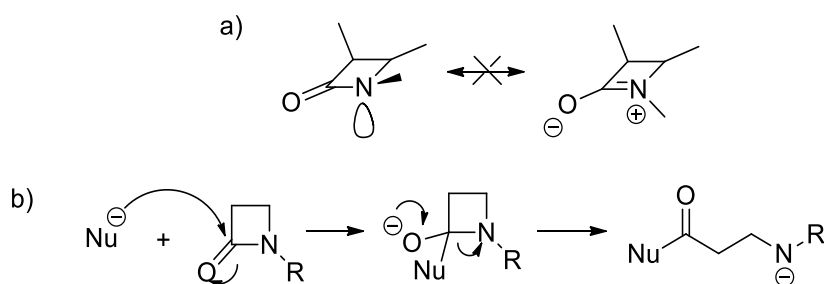


**Figure 2.6.** Structure variability of  $\beta$ -lactam compounds

The biological activity of  $\beta$ -lactam antibiotics is closely linked to the intrinsic strain of the azetidinone ring, due to the deformation of its  $sp^3$ -carbon bond angles (lower than  $109.5^\circ$ ) and its eclipsed bonds. These structural features lead to a remarkable reactivity of the amide group; in fact, the delocalization of the nitrogen lone pair is prevented since the charge separation resonance structure would otherwise present two  $sp^2$  hybridized atoms on a four membered ring leading to an extremely hindered planar complex (Scheme 2.1a). The enhanced electrophilic character of the amide carbon atom renders it more susceptible to nucleophilic attacks giving a consequent opening of the  $\beta$ -lactam ring through a classic nucleophilic acyl substitution (Scheme 2.1b).



**Scheme 2.1.** a) Prevented amide resonance in  $\beta$ -lactam ring; b) nucleophilic acyl substitution on  $\beta$ -lactam compounds

This mechanism is extremely important since it is involved in the antibacterial action exerted by  $\beta$ -lactams. As above-mentioned, these molecules affect the action of the enzymes responsible for the cross-linkers synthesis in peptidoglycan, the main component of bacterial cell wall.<sup>9</sup> Peptidoglycan is a heteropolymer able to confer a high mechanical resistance to the bacterial cell wall because of its branched structure. It is constituted by an amino-sugar polymer (alternating *N*-acetyl glucosamine (NAG) and *N*-

acetyl muramic acid (NAM) monomers) that is in turn bound to a tetrapeptide sequence (*L*)Ala-(*D*)Glu-(*L*)Lys-(*D*)Ala derivatized on the lysine residue with pentaglycine bridges (Figure 2.7).

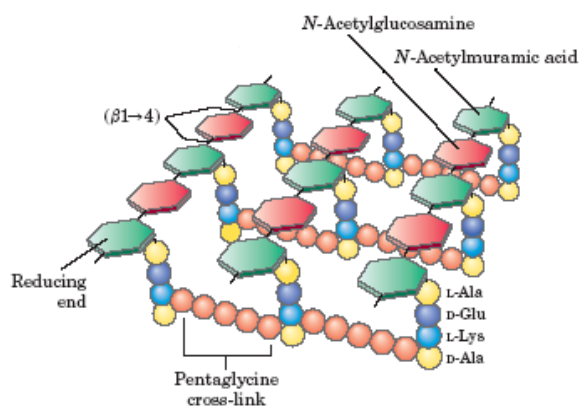
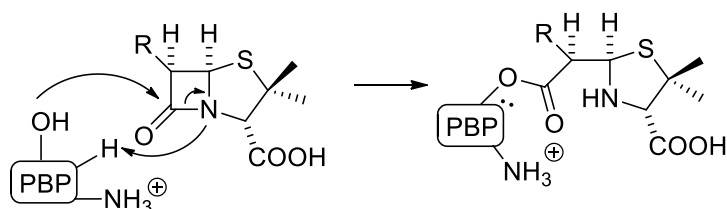


**Figure 2.7.** Structure of peptidoglycan. Figure adapted from ref.<sup>10</sup>

One of the final steps in the peptidoglycan biosynthesis is the formation of these pentaglycinic units catalysed by *D,D*-transpeptidase, a serine dependent enzyme belonging to the penicillin binding-proteins (PBPs). PBPs constitute the bacterial target of penicillin antibiotics that are responsible for the covalent binding of a transpeptidase serine residue on the  $\beta$ -lactam carbonyl through an enzymatic nucleophilic attack. A stable  $\beta$ -lactam-transpeptidase complex is thus obtained leading to an irreversible inhibition of the enzyme (Scheme 2.2); when peptidoglycan synthesis is prevented, the exceeding internal pressure causes the lysis of the cell and the consequent death of the bacterium.



**Scheme 2.2.** Mechanism of antibacterial action exhibited by penicillins on inhibiting the Penicillin Binding Proteins (PBPs)

## 2.3 Antimicrobial resistance

Over the last 20 years, the phenomenon of antimicrobial resistance (AMR) has been raising dangerous levels in all parts of the world,<sup>11</sup> since the past decades have seen a dramatic increase in human-pathogenic bacteria that are resistant to one or multiple antibiotics (Figure 2.8).



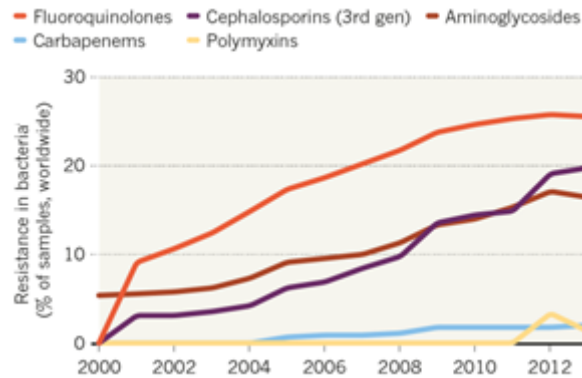


**Figure 2.8.** Spread of antibacterial resistance against common antibiotics. Figure adapted from ref.<sup>12</sup>

Whereas antibiotic resistance was once largely confined to hospitals and long-term care facilities, it has now emerged in community settings. The main source of antibiotic resistance is paradoxically linked to their use: resistance is indeed an inevitable phenomenon directly related to bacterial easy mutagenesis that is greatly amplified by the mis- and over-use of antibiotics. In fact, broad-spectrum antibiotics are often inappropriately prescribed instead of those responsible for a specific disease or even unnecessarily employed to treat viral infections. In addition, antibiotics are also used in agriculture, aquaculture and farm breeding, favoring the onset of resistant bacterial strains. Therefore, a considerable quantity of marketed foodstuffs could be contaminated with antibiotic-resistant bacteria that have been selected during animal treatment and can be transmitted to humans through food ingestion.<sup>13</sup>

Examples of resistant bacteria of notable incidence are: methicillin-resistant *Staphylococcus aureus* (MRSA),<sup>14</sup> vancomycin-resistant *Staphylococcus aureus* (VRSA) and vancomycin-resistant *Enterococci* (VRE)<sup>15</sup> among Gram-positive pathogens, or Gram-negative bacilli such as *Pseudomonas aeruginosa* or *Escherichia coli* that produce specific enzymes such as extended-spectrum  $\beta$ -lactamases (ESBL).<sup>16</sup> Most of the cited microorganisms are generally resistant to diverse classes of antimicrobial agents and are therefore called multi-resistant microorganisms. The first penicillin-resistant *Staphylococcus aureus* strains dated back to 1942; in order to contrast them, penicillin was replaced with methicillin, but resistance phenomena occurred soon also against this antibiotic. From then on for about four decades (from the early 1940s to the late 1970s), the pharmaceutical industry provided a steady flow of new antibiotics, including several agents with new mechanisms of action.<sup>17</sup> Nevertheless, since then only two new classes of antibiotics, oxazolidinones and lipopeptides, which include the already described linezolid and daptomycin, have been marketed in Europe to treat infections caused by multidrug-resistant Gram-positive bacteria<sup>18</sup> and meanwhile, resistance among Gram-negative bacteria has been increasing relentlessly, with only few new active antibacterial agents reaching the market in the last decade (Figure 2.9).

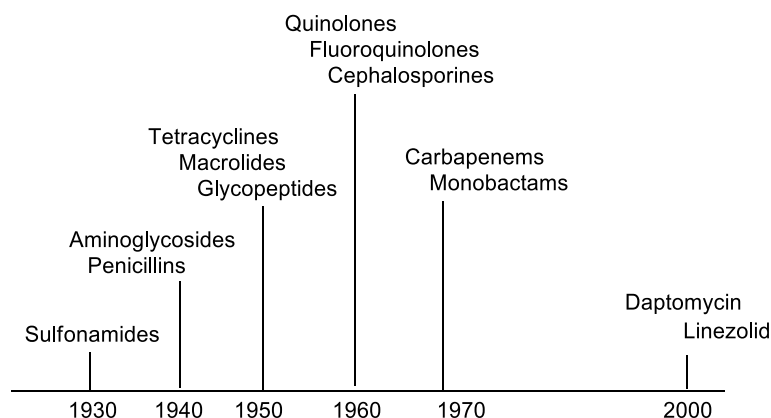


**Figure 2.9.** Antibacterial agents discovery from 1930s to 2000s

In extreme cases, multidrug-resistant bacteria are no longer susceptible to any of the licensed antibacterial agents prompting to move toward a “post-antibiotic” era in which common infections and minor injuries cannot be healed.<sup>10</sup> The World Health Organization (WHO) has identified antimicrobial resistance as one of the greatest threats to human health and has adopted a global action plan which outlines five objectives:<sup>19</sup> to increase awareness of the problem with effective communication and education; to strengthen knowledge on the mechanisms and on the spread of resistance; to reduce the incidence of infections and to optimize the use of antimicrobial agents, with particular attention being addressed to increasing investments for the development of new antimicrobial agents. In 2010, the Infectious Diseases Society of America (IDSA) launched the initiative “10 x 20” aimed at developing new antibacterial drugs.<sup>20</sup> More recently, the European commission adopted in 2017 a dedicated action plan against antimicrobial resistance.<sup>21</sup> This action boosted research, development and innovation that should provide novel solutions and tools to prevent and treat infectious diseases, improve diagnosis, and control the spread of AMR. The proposed research strategy covers the full “One Health” spectrum, addressing human and animal health as well as the role of the environment and taking into account the priorities set out in the above-mentioned WHO global action plan on AMR.

### 2.3.1 Resistance mechanisms

New resistance mechanisms are emerging and spreading globally, threatening our ability to treat common infectious diseases.<sup>10</sup> Various types of resistance can be distinguished: the natural or intrinsic resistance is linked to the genetic, structural or physiological characteristics of a microorganism and is specific for each species;<sup>22</sup> the acquired resistance instead arises from genetic modifications through mutations or by exchange of genetic material between microorganisms.<sup>23</sup> It can be also described the endogenous resistance, which is vertically inherited only by the progeny through the duplication of chromosomal genes, and is rare since the mutational events occur at rather low frequency, generally between  $10^{-7}$  and  $10^{-10}$ . Finally, the horizontal exogenous resistance is linked to accessory genetic elements, which transfer the genetic determinants of resistance among bacteria also belonging to different species.<sup>24</sup>

As already described in Paragraph 2.1, the antibacterial action results from the interaction of an antibiotic agent on a specific vital biological mechanism of the bacterial species, such as inhibition of cell wall synthesis, protein synthesis or nucleic acid replication. The mechanisms of resistance developed are

essentially four and not infrequently the same pathogen may adopt more than one, thus increasing the difficulty of pharmacological treatments (Figure 2.10).

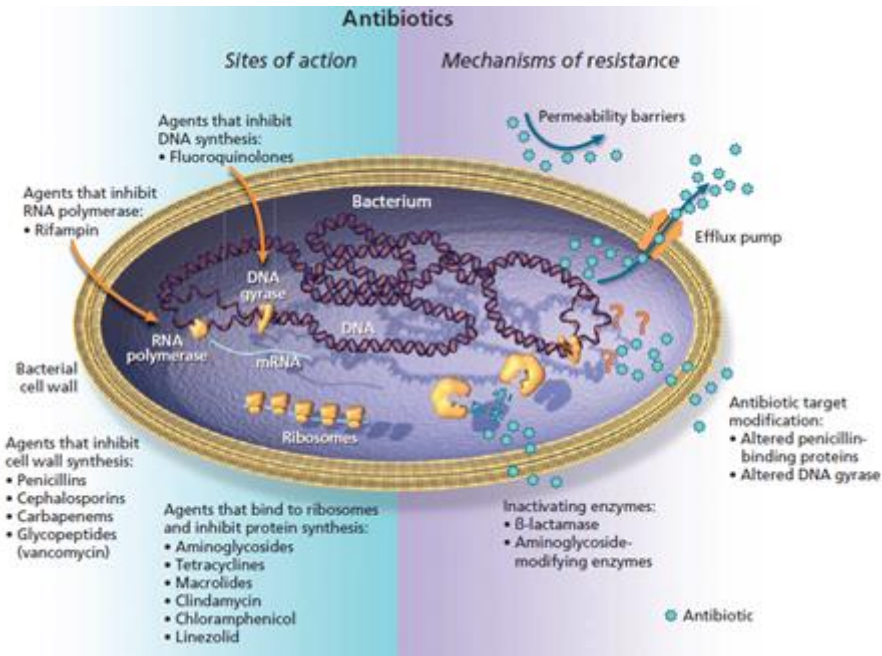


**Figure 2.10.** Antibacterial resistance mechanisms and sites of action of common antibiotics. Figure adapted from ref.<sup>25</sup>

1. Specific modification of the binding site, leading to the loss or decrease of affinity of the drug for its target. An example is constituted by MRSA strains, which evolved after a few years from the introduction of penicillins through a horizontal genetic mutation: the mutation encodes the synthesis of PBP2a (penicillin binding-protein 2a) that, replacing the natural D,D-transpeptidase (PBP), impedes the target-antibiotic site interaction and prevents penicillins to exploit their function.<sup>26</sup>
2. Modification of the outer membrane, leading to a decrease of the bacterial wall permeability (typical for Gram-negative bacteria). In order to allow the flow of essential components through the outer membrane, the bacterial cell produces the so-called porins that allow the diffusion of molecules, including antibiotics, into the cytoplasm. Genetic mutations modify the structure of the outer membrane proteins leading to a permeability barrier that prevents the access of the antibiotic to its binding site.<sup>27</sup>
3. Upregulation of the mechanisms controlling the outflow of antibiotics. Instead of preventing the penetration of antibiotics into the active site, some microorganisms have developed an active efflux mechanism, through efflux pumps, which expels the antibiotics from the cytoplasm.<sup>28</sup>
4. Enzymatic inactivation of the antibacterial agent by modification of its active portion. This is undoubtedly the most effective mechanism of bacterial resistance; a typical example involves MSSA (Methicillin-susceptible *Staphylococcus aureus*) bacterial strains and their production of  $\beta$ -lactamases, enzymes able of hydrolysing the  $\beta$ -lactam ring of penicillins, cephalosporins and carbapenems. To combat these resistant bacterial strains, specific  $\beta$ -lactamase inhibitors, such as Clavulanic acid, Tazobactam and Sulbactam, are administered in addition to the actual antibiotic molecules (Figure 2.11).

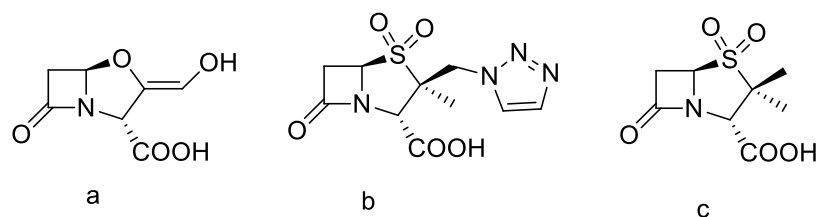


**Figure 2.11.** Clavulanic acid (a), Tazobactam (b), Sulbactam (c)

## 2.4 Multi-target drugs and cystic fibrosis

The above-described phenomena point to the need of new antibacterial agents able to fight chronic infections caused by multidrug resistant bacterial strains.

Our understanding of the pathogenesis of diseases has advanced enormously in recent decades. As a consequence, drug research aims mainly at achieving selectivity for a given target.<sup>29</sup> However, many diseases are multifactorial and cannot be treated acting on a single biological target, since they depend on multiple genetic factors, and sometimes also on environmental aspects. Drugs hitting a single target may be thus inadequate for the treatment of diseases like neurodegenerative syndromes, diabetes, cardiovascular diseases, and cancer, which involve multiple pathogenic factors.<sup>30</sup> The most famous examples of multifactorial diseases are Alzheimer and Cystic Fibrosis (CF).

Facing these new challenges, the principle of ‘one molecule, one target’ that has thoroughly been followed in pharmaceutical and medicinal science since nowadays is now giving space to a new approach based on Multi Target Drug Ligands (MTDL), firstly defined by Melchiorre *et al* in 2008,<sup>29</sup> in which a single chemical compound is able to modulate multiple targets simultaneously, with superior efficacy and safety profiles.<sup>31</sup> Not surprisingly, the MTDL strategy has now been incorporated in routine therapeutic drug design,<sup>32</sup> and the considerable number of multi-target derivatives described in the last ten years points out the growing confidence that this new approach could lead to better therapeutic solutions for the aforementioned multigenic diseases.

Clearly, the use of MTDLs presents both advantages and disadvantages. The benefits of using multiple targeting lead drugs can be resumed as follows:

- a single way of administration simplifies the assumption of the drug in comparison to the use of different pharmaceuticals, preventing errors derived from a wrong posology;
- a single pathway of metabolism and elimination drastically reduces the number of metabolites and their side effects;
- the risk of interferences among different drugs is avoided;
- the production costs are substantially decreased.

Nevertheless, the following complications may be encountered:

- a greater difficulty in the design and synthesis of the molecule, due to its enhanced complexity;
- a diminished range of applications linked to the higher selectivity and specificity of the drug.

In order to gain multi-targeting in a single therapy solution, two approaches are possible: the selection of molecules with an in-built capacity to act on two or more targets, and/or the combination of two or more pharmacophores in a single molecule.<sup>31</sup>

A valuable contribution in design and synthesis of new multi-target compounds could arise in the development of dual-active molecules effective as antioxidant and antibacterial agents in the treatment of chronic infections such as cystic fibrosis, a severe genetic pulmonary disease. In CF patients high levels of systemic oxidative stress have been documented over the years.<sup>33</sup> Oxidative stress is generated by an imbalance increase of ROS/RNS (reactive oxygen species/reactive nitrogen species) that can damage all classes of cellular macromolecules as proteins, lipids and nucleic acids with strong effects on human metabolic pathways, causing the onset of several disorders such as airways inflammation and progressive epithelial tissue damage.<sup>34</sup> In infectious conditions, the production of ROS by activated neutrophils represents an important mechanism to kill bacteria but, whereas in healthy individuals it is properly counteracted by endogenous antioxidants agents,<sup>33</sup> in CF patients the defence systems are ineffective and an increased production of ROS may be associated with cell dysfunctions and disease progression.<sup>35</sup> In addition, a persistent colonization by pathogenic bacteria occurs in CF patients and it was reported that both oxidative stress and the repeated use of antibacterial agents could contribute to the selection of resistant bacterial strains, such as *Pseudomonas aeruginosa* (incidence 43%) and *Staphylococcus aureus* (incidence 73.1%).<sup>36</sup> A rise in *S. aureus* infections has been reported in CF patients, with an increase in the prevalence of highly virulent, methicillin-resistant *S. aureus* strains.<sup>37</sup> Lungs in CF patients are hence exposed to a vicious cycle of infection, inflammation, and obstruction. Interrupting this cycle with innovative agents might slow the disease progression, improve the quality of life, and delay respiratory failure.<sup>11</sup>

## 2.5 Development of monocyclic $\beta$ -lactam antibacterials

In this context a series of monocyclic  $\beta$ -lactams active as antibacterial agents against resistant strains were successfully realized during the last ten years by my research group. In particular, the new class of 4-(2-oxoethylidene)azetidin-2-ones (or 4-alkylidene azetidiones) has been developed<sup>38</sup> (Figure 2.12).

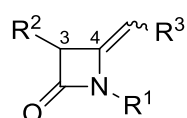
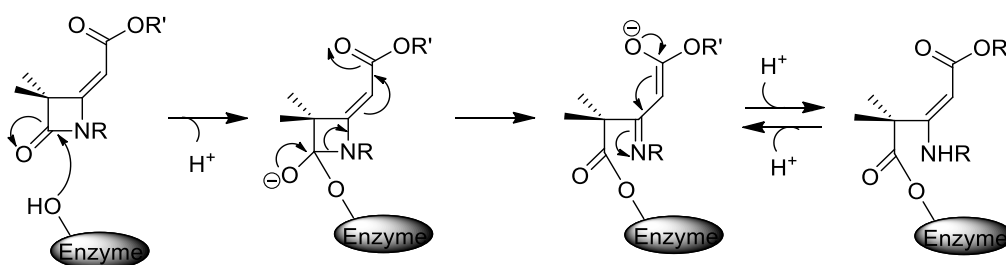


**Figure 2.12.** General structure of 4-alkylideneazetidiones

The synthesis of these compounds was achieved by a novel Lewis acid mediated reaction of acyldiazocompounds with 4-acetoxyazetidin-2-ones. Using this approach, C3- and C4-substituted 4-alkylideneazetidin-2-ones were obtained depending on the starting azetidione and  $\alpha$ -diazocarbonyl compound. The products revealed a general excellent (*Z*) diastereoselection of the C4 double bond even if variable amounts of (*E*) isomers could be obtained depending on the nature of the C3 side chain, the Lewis acid, and the  $\beta$ -lactam nitrogen protection. VT (variable temperature) NMR spectroscopic experiments and X-ray structural analysis of crystalline derivatives demonstrated the presence of an intramolecular hydrogen bond in (*Z*) isomers driving the stereochemical outcome of the reaction.<sup>38</sup>

In these derivatives the carbon-carbon double bond directly linked to the azetidione ring confers an increased aptitude toward ring-opening reactions by suitable enzymes. In this perspective, the C=C acts

as an electron-withdrawing group delocalizing the negative charge originated in the enzyme- $\beta$ -lactam complex (Scheme 2.3).



**Scheme 2.3.** Ring-opening mechanism in 4-alkylidene-azetidinones by serine-dependent enzymes

Over the years several reactions of functionalizations have been studied on this type of substrates varying the substituents on different positions of the ring and evaluating how the structure variability could influence the antibacterial activity exhibited by the relative compounds.<sup>39</sup>

Many of the newly obtained 4-alkylidene-azetidinones resulted effective in bacterial inhibition showing a significant potency against resistant Gram-positive pathogens.<sup>39c</sup> Some examples are reported in Figure 2.13 together with the corresponding antibacterial activity expressed as minimum inhibitory concentration (MIC) in mg/L.

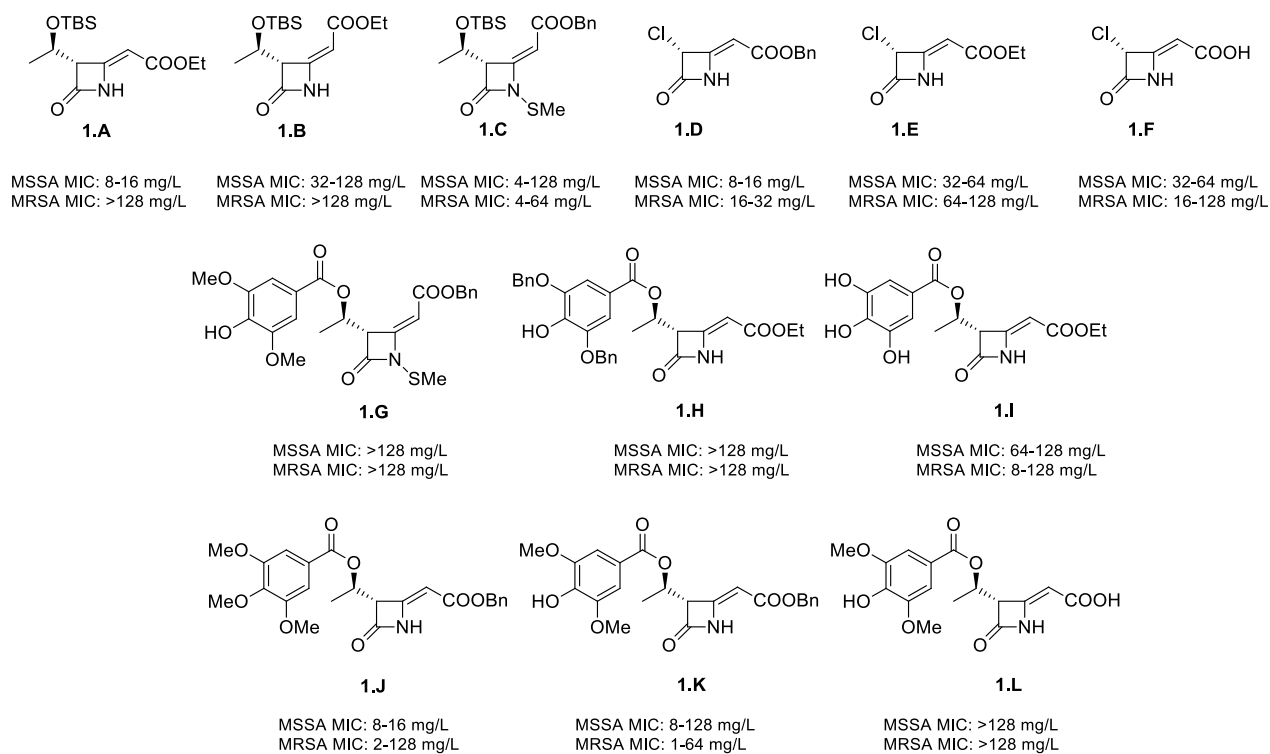


**Figure 2.13.** 4-alkylidene-azetidinone derivatives previously reported. Relative antibacterial activities expressed as MIC in mg/L are reported<sup>17, 39c-e</sup>

Concerning the antibacterial activity, some structural features resulted particularly important for a valuable potency: it was observed that the 4-alkylidene function with a (*Z*) stereochemistry favours the biological activity compared to (*E*) stereoisomers if the nitrogen atom of the  $\beta$ -lactam is not substituted (compound **1.A** vs **1.B**);<sup>39b</sup> only alkylidenes with (*E*) stereochemistry could be derivatized with a *N*-thiomethyl group making the corresponding derivative more active as antibacterial (compound **1.C**).<sup>40</sup> Several esters conjugated to the double bond have been then studied; among these different substitutions, the presence of a benzyl ester strongly improved the potency compared to the ethyl ester or the carboxylic acid<sup>17</sup> (see compounds **1.D** vs **1.E** and **1.F** or **1.K** vs **1.L**). Furthermore, it was observed that coupling a phenolic ester with *N*-methylthio-4-alkylidene- $\beta$ -lactams resulted in inactivation,<sup>17</sup> hence showing the need to include an unsubstituted-NH atom in these compounds (see inactive compound **1.G**). A study conducted by Marchand-Brynaert,<sup>41</sup> aimed at determining the structural elements necessary for a  $\beta$ -lactam to present inhibitory activity, showed the importance of the substituents on the C3 position of the ring for modulating the interaction with the specific binding site present on D,D-transpeptidases. In this regard, various functionalizations have been evaluated, i.e. the introduction of halogens or a protected  $\alpha$ -hydroxyethyl chain<sup>39c</sup> (compounds **1.A-1.F**), as displayed for carbapenem derivatives. Thienamycin (Figure 2.14), a carbapenem antibiotic, shows indeed a broad spectrum of action against important Gram-negative bacterial strains, exhibiting also good stability against  $\beta$ -lactamases. These biological properties seem to be closely related to the presence of the hydroxyethyl chain that is probably able to prevent the recognition of carbapenems by  $\beta$ -lactamases.<sup>42</sup>

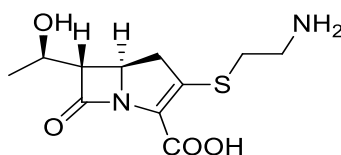


Figure 2.14. Thienamycin

Since in recent years there has been a growing attention on plant-derived antimicrobials as an alternative to antibiotics, for their efficacy and low tendency in developing bacterial resistance,<sup>11</sup> the C3 hydroxyethyl side chain was further derivatized with some plant-derived and differently substituted benzoic acids<sup>17,39c</sup> (compounds **1.G-1.L**), revealing in some cases promising antibacterial activities<sup>39c</sup> (compounds **1.J-1.K**).

It is also worth to mention that the similar activities against both MRSA and MSSA provide evidence that PBP2a does not represent the biological target of these new azetidinones.<sup>17</sup> In fact, as it was previously mentioned, bacterial resistance is adopted by MRSA through a modification of the  $\beta$ -lactam antibiotics binding site *via* the synthesis of PBP2a that has low affinity for  $\beta$ -lactams, thus not allowing the bactericidal action. For MSSA instead, the resistance is obtained by the production of  $\beta$ -lactamases that deactivate the  $\beta$ -lactam compound through a ring opening reaction.

In general, the actual marketed  $\beta$ -lactam antibiotics generally display a different activity on MRSA and MSSA strains, with the latter being extremely lower than the former. Therefore, the derivatives in Figure 2.13, which show a comparable antibacterial potency between the two bacterial strains, probably act with an alternative mechanism that does not involve the interaction with the PBP2a protein.

Also the presence of other electron withdrawing groups on the C4 position of the ring was evaluated,<sup>17,39e</sup> with the acetoxy moiety being a suitable candidate already present in some commercially available azetidiones commonly employed for the synthesis of  $\beta$ -lactam derivatives (compounds **1.M** and **1.O**, Figure 2.15).

A thiomethyl derivatization on  $\beta$ -lactam nitrogen was performed (Figure 2.15) and the combination of *N*-SMe and acetoxy group on C4 position clearly increased potency against Gram-positive bacteria over the corresponding -NH derivatives that were completely inactive<sup>17</sup> (compounds **1.N** and **1.P** vs **1.M** and **1.O**, respectively).

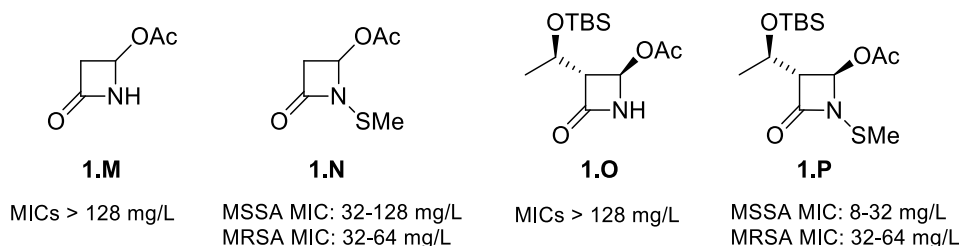
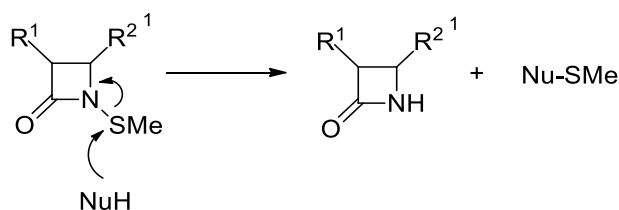


**Figure 2.15.** *N*-thiomethylated  $\beta$ -lactam compounds previously reported. Relative antibacterial activities expressed as MIC in mg/L are reported<sup>17</sup>

In particular, compound **1.P** showed activity against MSSA, MRSA, and *S. epidermidis*, whereas the C3-unsubstituted analogue **1.M** showed activity against MSSA, MRSA, *E. faecalis*, and Gram-negative *E. coli*.<sup>17</sup>

The synthesis and the biological evaluation as antibacterial agents of some monocyclic azetidiones with an alkylthio group on the  $\beta$ -lactam nitrogen was reported for the first time by Turos and co-workers.<sup>43</sup> They also investigated a mechanism of action for these derivatives, which are thought to block type II fatty acid biosynthesis in *S. aureus* through an initial transfer of the *N*-alkylthio moiety from the nitrogen atom onto a cellular target. In particular,  $\beta$ -lactam compounds should react rapidly with coenzyme A (CoA) to produce an alkyl-CoA mixed disulfide species, which then interferes with fatty acid biosynthesis.<sup>44</sup> In this perspective the  $\beta$ -lactams developed by Turos *et al.* appeared to act as prodrugs without any special structural features needed for the activity, other than being relatively lipophilic and able to serve as a leaving group during nucleophilic attack on sulphur (Scheme 2.4).



**Scheme 2.4.** *N*-alkylthioazetidiones as thiomethyl-transfer agents

Another suggested mechanism arises from a possible delayed bacteriostatic effect exerted by *N*-thiolated azetidiones *via* inhibition of protein biosynthesis in bacteria. Therefore, the bacteriostatic activity found



for *N*-thiomethylazetidiones **1.N** and **1.P** could suggest a mechanism of action as thiomethylating agents such as that reported by Tuross and colleagues.

Finally, a small library of *N*-thiomethylated  $\beta$ -lactams with an acetoxy group in C4 was armed with polyphenolic side chains in order to combine in one structure antioxidant and antibacterial activities as two synergistic pharmacological properties that could provide new promising leads useful in adverse clinical conditions such as those displayed in cystic fibrosis patients.

In Figure 2.16 some examples of these compounds are reported, with the phenolic residue on the hydroxyethyl side chain activating the antioxidant activity, evaluated by TEAC (Trolox Equivalent Antioxidant Capacity) tests.<sup>39e</sup>

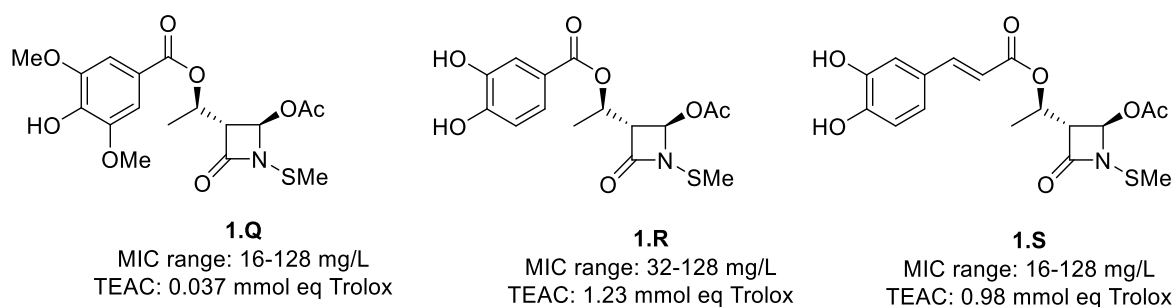


**Figure 2.16.**  $\beta$ -lactam compounds with antibacterial and antioxidant activities previously reported. Relative MIC ranges in mg/L toward MRSA strains and TEAC-DPPH values expressed as mmol eq. Trolox are reported<sup>39e</sup>

Among  $\beta$ -lactams with polyphenolic esters on 3-hydroxyethyl side-chain, compound **1.Q** with a syringic moiety got scarce antioxidant potency, but compounds **1.R** and **1.S** are good antioxidants (TEAC 1.23 and 0.98 mmol equiv. Trolox respectively). Nevertheless, all derivatives displayed a discrete, but not excellent, antibacterial activity against MRSA strains (MICs range 16-128 mg/L or 32-128 mg/L).<sup>39e</sup>

As a general trend, to activate the antioxidant potency of the tested compounds to a significant extent, the presence of two or three phenolic OH groups is necessary, and the OH group on the C(3) of the phenyl ring considerably improved the activity.<sup>39d</sup>

It is then important to highlight that in this class of monocyclic  $\beta$ -lactam derivatives the antibacterial potency is mainly activated by the presence of a good electron-withdrawing group on the C4 position of the ring such as 4-alkylidene- or 4-acetoxy moieties. Whenever such substituents were absent, as in compounds **1.T** and **1.U** (Figure 2.17), the antibacterial potency was completely lost.<sup>45</sup>

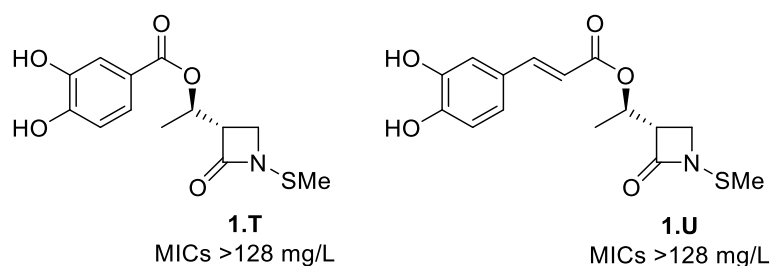


**Figure 2.17.**  $\beta$ -lactam compounds with unfunctionalized C4 position

## 2.6 Dual active antibacterial-antioxidant $\beta$ -lactams

As part of an ongoing project on the synthesis of dual-target monocyclic  $\beta$ -lactams, specifically designed to address resistant bacterial strains and to have antioxidant activities, we broadened the scope of the previously reported studies<sup>39</sup> by functionalizing the antibacterial core of 4-alkylidene-azetidinones with different polyphenolic moieties for efficiently combining in one structure both antioxidant and antibacterial activities (Chart 2.1).<sup>46</sup>

In designing the novel derivatives, some structural features that resulted particularly important for a valuable antibacterial potency were inserted on the azetidinone, i.e. the alkylidene function with a (*Z*) stereochemistry, a benzyl ester on C4 position and the presence of an unsubstituted-NH group. Starting from this scaffold, different polyphenolic moieties from some plant-derived benzoic acids were inserted on C3 position. Moreover, since polyphenol-substituted  $\beta$ -lactams presented a decreased antioxidant activity if compared with their corresponding polyhydroxybenzoates,<sup>39d</sup> we considered that an extension of the side chain linking the phenolic aromatic ring to the rest of the structure might provide a greater exposure of the phenolic OH residues, modulating the antioxidant activity without disturbing the antibacterial potency. Relying on the commonly occurring structures in natural polyphenols, we identified the C6-C3 leitmotiv of hydroxycinnamic acids (such as coumaric, caffeic, ferulic, or sinapic) as promising group.<sup>47</sup> Hydroxycinnamic acids have in fact been described as chain-breaking antioxidants acting through radical scavenging activity that is related to their hydrogen or electron donating capacity and to the ability to delocalize/stabilize the resulting phenoxyl radical within their structure. In the study of the phenol-protection strategy, we also considered the methylenedioxy moiety, present in many natural products, as an interesting substructure to be held in the target compounds for evaluating its antibacterial activity (Chart 2.1).

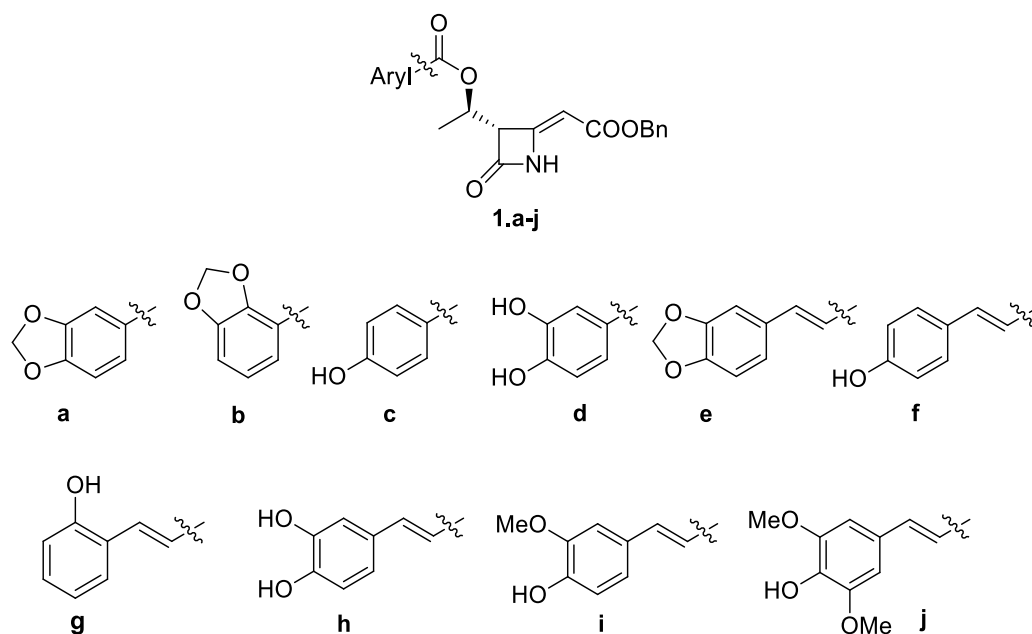
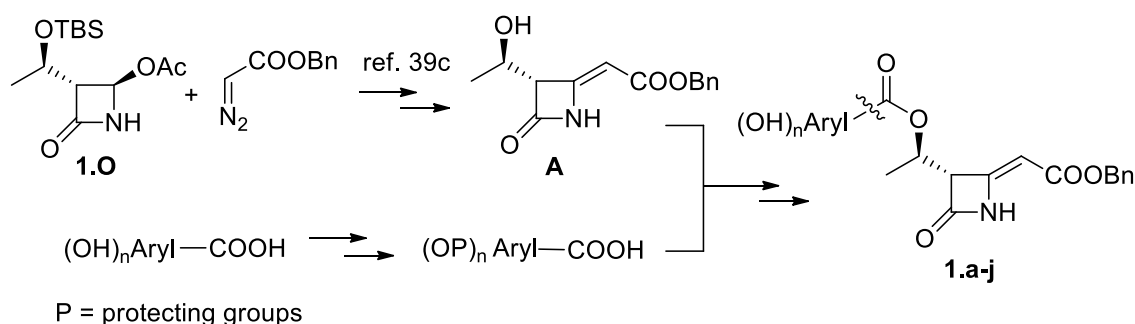


**Chart 2.1.** Novel  $\beta$ -lactam derivatives **1.a-j** designed to have a dual antibacterial-antioxidant activity

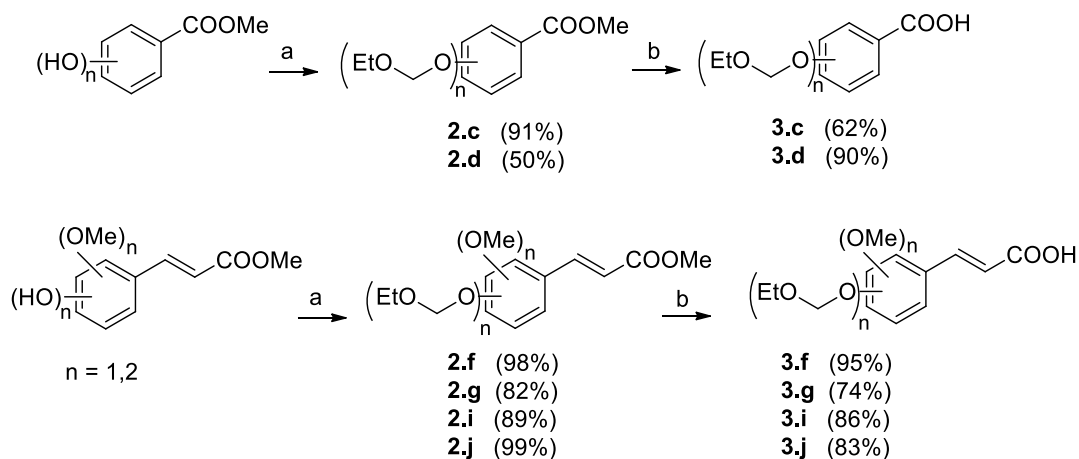
### 2.6.1. Synthesis of azetidinones

All target compounds were prepared according to a convergent synthetic strategy that comprised the preparation of the 3-hydroxyethyl-4-alkylidene  $\beta$ -lactam **A**, obtained with a two-step protocol starting from the commercially available (3*R*,4*R*)-4-acetoxy-3-[(1*R*)-1-(tert-butyl)dimethylsilyloxy]ethyl]azetidin-2-one **1.O** and benzyl diazoacetate,<sup>38</sup> and a following -OTBS group deprotection in acidic conditions. The esterification of alcohol **A** with polyphenolic acids duly protected on the -OH groups yielded the target compounds after phenols deprotection, when required (Scheme 2.5).



**Scheme 2.5.** Convergent synthesis of new 4-alkylidene- $\beta$ -lactams with polyphenolic residues

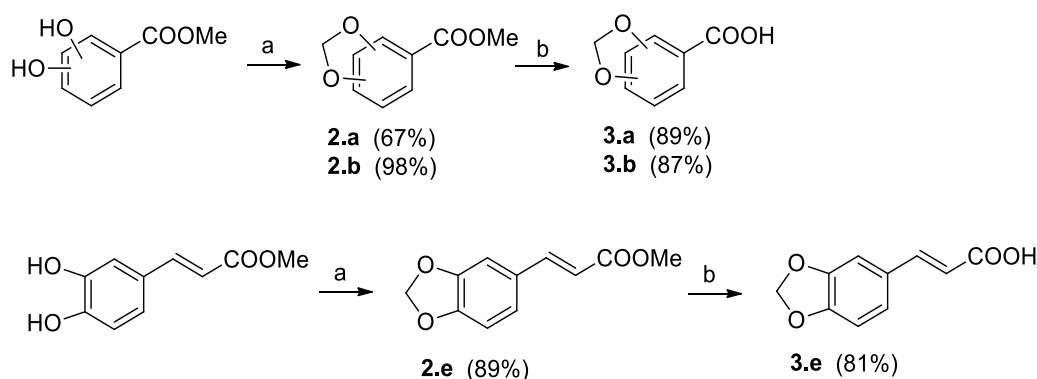
The *O*-protected aryl acids were in turn prepared from their corresponding methyl esters exploiting a phenolic oxygen protection with chloromethylethylether (EOMCl) followed by alkaline hydrolysis (Scheme 2.6), according to what previously optimized for the *O*-protected caffeic acid **3.h**.<sup>39e</sup>



**Scheme 2.6.** Synthesis of *O*-protected phenolic acids **3.c-d**, **3.f-g**, and **3.i-j**. Reagents and conditions: a) NaH, EOMCl, THF, 0 °C to rt, 2 h; b) NaOH 5 M, THF/CH<sub>3</sub>OH 1:1, 40 °C, 4 h. Yields of isolated products are reported in brackets

The EOM ether turned out to be an effective protecting group that can be easily inserted, and selectively removed at late stage of the synthesis with a mild procedure without damaging the  $\beta$ -lactam ring in final compounds. The dioxymethylene group was inserted on suitable methyl esters (i.e. 2,3-dihydroxy-

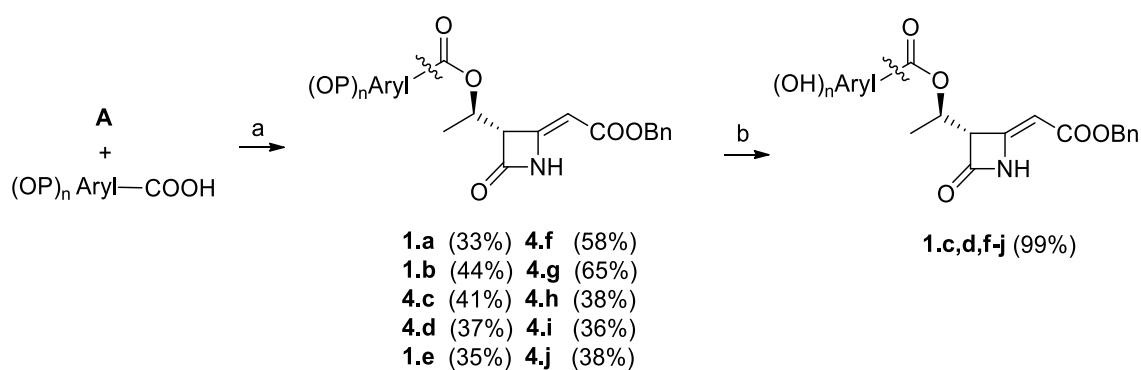
methyl-benzoate, 3,4-dihydroxy-methyl-benzoate and (*E*)-methyl 3-(3,4-dihydroxyphenyl)acrylate) with diiodomethane and potassium carbonate according to a procedure reported by Alam *et al.* (Scheme 2.7).<sup>48</sup>



**Scheme 2.7.** Synthesis of methylenedioxy-protected acids **3.a,b,e**. Reagents and conditions: a)  $\text{CH}_2\text{I}_2$ ,  $\text{K}_2\text{CO}_3$ , DMF, 110 °C, 5 h; b) NaOH 5 M, THF/ $\text{CH}_3\text{OH}$  1:1, 40 °C, 4 h. Yields of isolated products are reported in brackets

The 3-hydroxyethyl side chain of  $\beta$ -lactam **A** was then derivatized as phenolic or polyphenolic aromatic ester with the appropriate *O*-protected acid **3.a-j** by treatment with *N,N'*-dicyclohexylcarbodiimide (DCC) and a catalytic amount of 4-dimethylaminopyridine (DMAP) in dichloromethane (Scheme 2.8) according to the well-known Steglich esterification.<sup>49</sup> Yields were slightly affected by this step probably for the steric hindrance of the secondary alcohol group of intermediate **A** that could obstruct the nucleophilic attack on the acid-DCC adduct.

Esters **4.c**, **4.d**, and **4.f-j** were finally treated with trifluoroacetic acid (TFA) to eliminate the EOM protection<sup>39e</sup> and afford the target  $\beta$ -lactams **1.c**, **1.d**, and **1.f-j** in quantitative yields (Scheme 2.8).



**Scheme 2.8.** Synthesis of target compounds **1.a-j**. Reagents and conditions: a) DCC, DMAP,  $\text{CH}_2\text{Cl}_2$ , 0 °C then rt, 16 h; b)  $\text{CF}_3\text{COOH}$ ,  $\text{CH}_2\text{Cl}_2$ , 0 °C then rt. Yields of isolated compounds are reported in brackets

### 2.6.2 Antibacterial activity

(in collaboration with Prof. C. E. A. Cocuzza and Dr. R. Musumeci, University of Milano)

Antibacterial activity screening of compounds **1.a-j** was carried out against recent, well-characterized clinical isolates. Most of the bacterial strains were specifically selected to exhibit a multidrug-resistant phenotype against penicillins/cephalosporins, linezolid, or vancomycin. Antimicrobial activities of the

compounds are listed in Table 2.1, with potency being shown as minimum inhibitory concentration values (MICs) expressed in mg/L. Only MIC values equal to or less than 128 mg/L against corresponding bacterial species were reported as remarkable activities. Values ranging from 1-8 mg/L are to be considered very good and were highlighted in bold. Commercially available vancomycin (VA) and cefuroxime (FUR) were used as reference compounds (see Table 2.1).

The *in vitro* antimicrobial susceptibility analysis indicated antibacterial activity only against Gram-positive bacteria, while none of the tested compounds exhibited an appreciable antibacterial effect against studied Gram-negative bacteria (results not included in Table 2.1). However, the lack of activity of the tested compounds against Gram-negative bacteria confirmed a general trend of this class of monocyclic azetidinones as previously observed.<sup>17,39c,e</sup> This inefficiency could be due to a reduced uptake through the outer membrane of Gram-negative bacteria, and unfortunately, the presence of a catechol moiety was not sufficient to allow bacterial cell penetration *via* the siderophore receptors of Gram-negative bacteria.<sup>50</sup> Another reason could find place in a possible deactivation mediated by  $\beta$ -lactamases in the periplasmic space between outer and cytoplasmic membranes.

**Table 2.1** Antibacterial activity of new  $\beta$ -lactam derivatives **1.a-j**. Results are expressed as MIC values (mg/L) for compounds **1.a-j**, vancomycin (VA) and cefuroxime (FUR) as reference compounds

Organism ID	1.a	1.b	1.c	1.d	1.e	1.f	1.g	1.h	1.i	1.j	VA	FUR
<i>S. aureus</i> ATCC 29213	<b>2</b>	16	<b>2</b>	16	>128	<b>8</b>	<b>2</b>	>128	<b>4</b>	>128	0.5	2
<i>S. aureus</i> SAU-1	<b>2</b>	<b>2</b>	<b>2</b>	16	>128	<b>4</b>	<b>1</b>	>128	<b>4</b>	<b>8</b>	1	>128
<i>S. aureus</i> 44674	<b>4</b>	>128	>128	<b>8</b>	>128	<b>4</b>	>128	>128	<b>4</b>	<b>8</b>	4	8
<i>S. aureus</i> 69856	<b>8</b>	>128	>128	<b>4</b>	>128	<b>8</b>	>128	>128	<b>8</b>	>128	0.5	1
<i>S. aureus</i> 39249	<b>4</b>	>128	>128	<b>4</b>	>128	<b>4</b>	>128	>128	<b>8</b>	<b>8</b>	2	2
<i>S. hominis</i> $\alpha$ 26	<b>4</b>	<b>8</b>	16	>128	128	<b>4</b>	<b>2</b>	>128	<b>4</b>	<b>4</b>	1	8
<i>S. epidermidis</i> G1027	<b>4</b>	>128	>128	16	>128	<b>8</b>	>128	>128	<b>4</b>	>128	2	32
<i>S. epidermidis</i> 3226	<b>8</b>	>128	>128	16	>128	<b>8</b>	>128	>128	<b>8</b>	>128	1	0.5
<i>E. faecalis</i> ATCC 29212	>128	>128	>128	128	>128	>128	>128	>128	>128	>128	2	>128
<i>E. faecalis</i> 4150	>128	>128	>128	128	>128	64	>128	>128	<b>8</b>	>128	0.25	>128
<i>E. faecium</i> VRE 2	>128	>128	>128	128	>128	>128	>128	>128	>128	>128	>128	>128

Notably, compounds **1.a**, **1.f**, and **1.i** produced significant antibacterial activities against the tested Gram-positive bacteria grouped in *staphylococci* with excellent MIC values between 2 and 8 mg/L. Other compounds, such as **1.b**, **1.c**, **1.g**, and **1.j** showed a selective activity towards some *S. aureus* and *S. hominis* resistant strains with MICs ranging from 1 to 16 mg/L. Compound **1.g** showed the most promising activity against strains of *S. aureus* ATCC 29213, *S. aureus* SAU-1, and *S. hominis*  $\alpha$ 26, the latter two characterized by an extensive condition of multidrug resistance and high resistance to linezolid (MIC values 2, 1, and 2 mg/L, respectively). It is noteworthy that against *S. aureus* SAU-1 **1.g** was as active as vancomycin, whereas cefuroxime, a second-generation cephalosporin, was completely inactive.

Among the three methylenedioxy-derivatives, whilst **1.e** was found completely inactive, **1.a** showed a good and broad activity and **1.b** with an oxygen atom at *ortho* position of the aromatic ring resulted in a selective activity against *S. aureus* ATCC 29213 and *S. aureus* SAU-1. The association of *ortho* substitution and selectivity was observed also comparing *para*-substituted **1.f** (broad activity) and *ortho* substituted **1.g** (more selective). The catechol- and caffeoyl-derivatives **1.d** and **1.h** possessing two vicinal OH groups were less or no active, whereas monomethylether **1.i** recovered an appreciable potency, as well as the coumaroyl derivative **1.f** (against *staphylococci* MICs = 4-8 mg/L). Relying on the cinnamyl series, the most and the less lipophilic compounds **1.e** and **1.h** were both inactive, whereas compounds with an intermediate lipophilicity **1.f**, **1.g**, **1.i**, and **1.j** showed good activities. Notably, only compounds **1.f** and **1.i** showed some potency against *E. faecalis* strain (MIC values = 64 and 8 mg/L, respectively), while all other compounds exhibited an exclusively anti-staphylococcal activity.

### 2.6.3 Antioxidant activity

(in collaboration with Prof. G. Sacchetti, University of Ferrara)

Antioxidant activity determination based on different approaches was carried out with the objective to ensure a better comparison of the results and cover a wider range of possible applications for the novel molecules. Therefore, the  $\beta$ -lactam derivatives were subjected to TEAC (Trolox® equivalent antioxidant capacity) assay, based on the ability of the compounds to scavenge the DPPH (2,2-diphenyl-1-picrylhydrazyl) and ABTS (2,2'-azino-bis(3-ethylbenzothiazoline-6-sulphonic acid)) radical cations, compared to the same scavenging ability of Trolox®, a water-soluble derivative of vitamin E with potent antioxidant properties.<sup>51</sup>

Compounds **1.b** and **1.e** were not tested because the absence of OH groups precluded from antioxidant activity, as obtained for **1.a** (Table 2.2). The presence of a single phenolic group in derivatives **1.c**, **1.f**, and **1.g** was not enough to give radical-scavenging ability and values obtained for these compounds are not significant for antioxidant applications, even though ferulic and sinapic esters exhibited a slightly better activity than the others, in line with previously reported results.<sup>39d,e</sup> The best performances were instead recorded with compounds **1.d** and **1.h** with a catechol group; in DPPH assay they displayed antioxidant capacity 2.6 and 1.7 times higher than that expressed by 1 mmol of Trolox®, respectively. Analogously, **1.d** and **1.h** evidenced the same outcomes with ABTS test, even if with lower values, being however comparable with those expressed by active antioxidant natural compounds such as ascorbic acid and  $\alpha$ -tocopherol.<sup>52</sup>

**Table 2.2** Antioxidant activity of selected new  $\beta$ -lactam derivatives based on DPPH and ABTS assays. Results are expressed as mmol of Trolox Equivalent Antioxidant Capacity (TEAC)  $\pm$  Standard Deviation (SD)

Comp.	TEAC-DPPH	TEAC-ABTS
<b>1.a</b>	0.012 $\pm$ 0.001	nd
<b>1.c</b>	0.007 $\pm$ 0.001	0.010 $\pm$ 0.001
<b>1.d</b>	2.590 $\pm$ 0.220	1.300 $\pm$ 0.138
<b>1.f</b>	0.003 $\pm$ 0.001	0.053 $\pm$ 0.006
<b>1.g</b>	0.002 $\pm$ 0.001	0.143 $\pm$ 0.015
<b>1.h</b>	1.670 $\pm$ 0.178	1.030 $\pm$ 0.110
<b>1.i</b>	0.142 $\pm$ 0.015	0.284 $\pm$ 0.030
<b>1.j</b>	0.191 $\pm$ 0.020	0.232 $\pm$ 0.025

nd = not detectable

As an overall result, a number of novel compounds with good antibacterial activity against *staphylococci*, particularly multidrug-resistant clinical isolates of MRSA, have been discovered, with the best candidates showing impressive MIC activities of 2-8 mg/L and thus selectable for further *in vivo* evaluations. In addition, among the new compounds, two derivatives with a catechol moiety on the side chain revealed a strong antioxidant capacity in TEAC-DPPH and TEAC-ABTS assays being significantly more active than Trolox®. In particular molecule **1.d** displayed a considerable dual antibacterial-antioxidant activity (Figure 2.18), reinforcing the idea that phytochemicals moieties can be used for the development of new alkylidene- $\beta$ -lactams with a synergistic action for the potential treatment of those infections where the oxidative stress could increase specific resistant variants.<sup>53</sup>

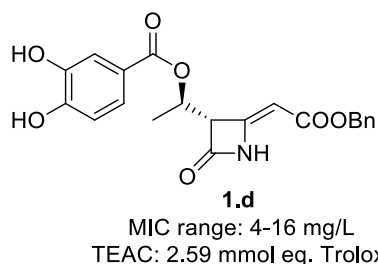


**Figure 2.18.** Best candidate compound **1.d** with potent antibacterial and antioxidant activities. MIC ranges in mg/L toward MRSA strains and TEAC-DPPH value expressed as mmol eq. Trolox are reported

## 2.7 Vectorization and *in vivo* biodistribution of a selected 4-alkylidene- $\beta$ -lactam

Firstly described in 1961,<sup>54</sup> Methicillin-resistant *Staphylococcus aureus* represents one of the recently re-prioritized “superbugs” by WHO for investments in new drugs.<sup>55</sup> Known at the beginning to be responsible of hospital outbreaks (healthcare associated MRSA, HA-MRSA),<sup>56</sup> it mutated in 2000s its epidemiology into the community-associated MRSA (CA-MRSA) and more recently it differentiated another epidemiological phenotype associated with livestock exposure (LA-MRSA). The treatment is based on vancomycin and daptomycin as first-line agents,<sup>57</sup> but their use is not without side effects, such as duration-dependent nephrotoxicity, slow bacterial killing, variable tissue penetration, and selection of MRSA strains with intermediate or high resistance.<sup>58</sup>

Another threat with alarming increasing rates is *S. aureus* colonizing the airways and causing recurrent respiratory infections in cystic fibrosis patients. A grave peculiarity of *S. aureus* isolated from CF patients is indeed the growth modality through the selection of small colony variants (SCVs), whose phenotype may carry to an intrinsic antibiotic resistance profile without evoking the host immune response.<sup>59</sup> Treating such conditions necessitates frequent intravenous administrations of high-dose antibiotics, but, even with this aggressive treatment, complete eradication of infection is hard to achieve because of bacteria ability to form biofilms.

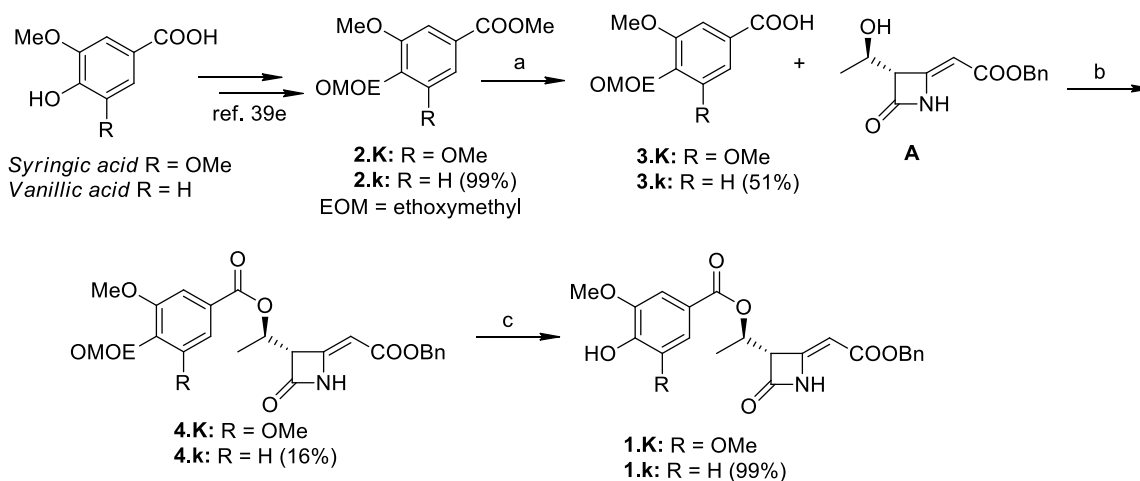
Lungs are the primary gate for respiratory infections and hence for their treatment; they are characterized by a large surface area and a thin epithelium layer that could improve drug absorption and efficacy.<sup>60</sup> Moreover, lungs are highly perfused by blood allowing faster absorption of inhaled drugs and onset of action. Pulmonary drug delivery systems represent an applicable alternative to both oral and parenteral routes of administration, since bypassing hepatic metabolism and consequently lowering the administrated doses could reflect in side effect reduction and drug bioavailability enhancement.<sup>61</sup>

In light of all these considerations, we decided to consider MRSA infections in difficult environments such as those related to chronic CF patients and selected the already reported compound **1.K** among the alkylidene-azetidinone series as potentially suitable for the eradication of such complex pathogens. It was then further investigated its antibacterial activity against multi drug-resistant *S. aureus* from CF clinical isolates and its cytotoxicity. In addition, a formulation of this derivative in solid-lipid-nanoparticles (SLNs) was evaluated together with a preliminar *in vivo* biodistribution study of the molecule itself and vectorized in nanoparticles (**1.K-SLN**).

### 2.7.1 Synthesis of azetidinones

The synthesis of the identified lead compound **1.K** was previously reported<sup>39c</sup> (see Paragraph 2.5) and accomplished through the procedure reported in Scheme 2.9 optimized for a gram-scale preparation starting from the  $\beta$ -lactam intermediate **A** coupled with *O*-EOM-syringic acid.<sup>39e</sup> The new  $\beta$ -lactam **1.k** was identified to be a suitable internal standard for HPLC-MS-MS analysis of *ex-vivo* samples. Compound **1.k** was obtained with a synthetic procedure similar to that developed for **1.K** but starting from *O*-EOM-vanillic acid (Scheme 2.9). Briefly, *O*-protected syringic and vanillic acids **3.K** and **3.k** were prepared from their corresponding methyl esters exploiting a phenolic oxygen protection with chloromethylethylether (EOM) followed by alkaline hydrolysis. The 3-hydroxyethyl side chain of  $\beta$ -lactam **A** was then coupled with the protected aryl acids through an esterification reaction mediated by DCC and DMAP, followed by EOM group deprotection in acid conditions.





**Scheme 2.9.** Synthesis of target  $\beta$ -lactams **1.K** and **1.k**. Reagents and conditions: a) NaOH 5 M, THF/CH<sub>3</sub>OH 1:1, 40 °C, 4 h; b) DCC, DMAP, CH<sub>2</sub>Cl<sub>2</sub>, 0 °C then rt, 16 h; c) CF<sub>3</sub>COOH, CH<sub>2</sub>Cl<sub>2</sub>, 0 °C then rt, 6 h. Yields of isolated compounds are reported in brackets

### 2.7.2 Formulation of SLNs for the loading of the lead compound (in collaboration with P. Gasco, Nanovector S.r.l.)

SLNs were prepared by warm micro-emulsion technique.<sup>62</sup> Several different excipients to load compound **1.K** in solid lipid nanoparticles were tested. After a preliminary screening, formulation based on a tripalmitin matrix was chosen for its stability in physiological buffers and for its high drug loading efficiency. The final formulation of **1.K-SLN** resulted in an efficient drug incorporation into the lipid carriers, with a final drug loading value of 7.5% (weight to weight, drug to total lipids).

The content of compound **1.K** in **1.K-SLN** was determined by HPLC-UV analysis and its morphology was performed by Field Emission Scanning Electron Microscopy (FESEM) in collaboration with DISAT, Polytechnic of Turin, Italy (data not shown).

### 2.7.3 Cytotoxicity and antibacterial activity

(in collaboration with Prof. C. E. A. Cocuzza and Dr. R. Musumeci, University of Milano)

The potential non selective toxicity of compound **1.K** and the encapsulated **1.K-SLN** was evaluated by cell viability assay performed in adenocarcinoma alveolar basal epithelial cells (A549). A549 cell line was chosen as suitable model of respiratory system for drug toxicity and targeting studies because of its high degree of morphological and functional differentiation *in vitro*.

Results obtained with MTT cell viability assay showed about 25% cell death of A549 treated with the minor dose of compound **1.K** (40 mg/L), reaching 50% of cytotoxicity with a doubled dose (80 mg/L). These results are similar to those obtained with the standard compound **1.k** (30% cell death of A549 treated with 80 mg/L). However, 60% cell death was reached after treatment with compound **1.k** at 120 mg/L (Figure 2.19).

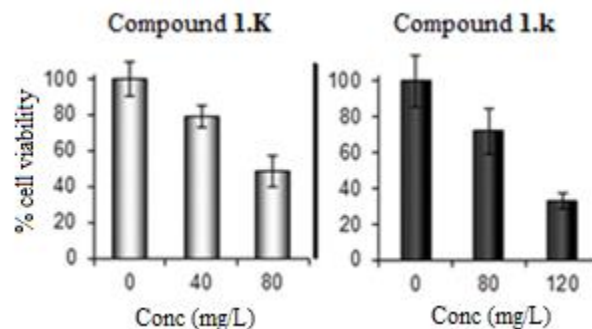


**Figure 2.19.** Cytotoxicity of compounds **1.K** and **1.k** against A549 cells

In order to evaluate the cytotoxicity of the lead compound **1.K** vehiculated in SLN, A549 were treated with increasing concentrations (20-80 mg/L) of **1.K-SLN** (Figure 2.20). In parallel, the cytotoxicity of SLN lipid formulation alone was analyzed, treating the cells with unloaded SLNs. **1.K-SLN** showed an increasing cytotoxic effect reaching the LC<sub>50</sub> at 80 mg/L, as well as compound **1.K** alone. About 20-25% mortality was also observed in cells treated with SLNs alone independently to lipid concentrations administrated, probably due to the formulation of the nanoparticles. Hence, in *in vitro* studies, lipid and surfactant composition employed to constitute SLNs might interfere with cellular viability or MTT assay.

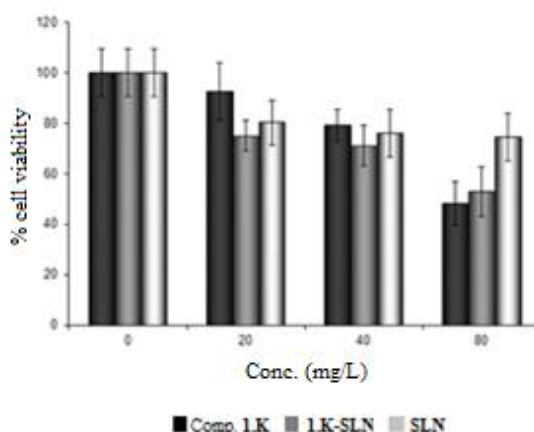


**Figure 2.20.** Cytotoxicity of compound **1.K** alone (black), vehiculated **1.K-SLN** (dark grey), and SLN alone (light grey)

Antibacterial activity of compound **1.K** alone compared to **1.K-SLN** was evaluated with 96 *S. aureus* strains isolated from 58 chronically colonized CF pediatric patients followed up by the CF Regional Reference Centre, Fondazione IRCCS Cà Granda, Milano during 2011 to 2014. Out of the 96 strains, 80 (83%) were identified as methicillin-resistant (MRSA) and 16 (17%) as methicillin-susceptible (MSSA). None were found to be vancomycin or linezolid resistant.

From the antibacterial tests against representative MRSA and MSSA strains, compound **1.K** exhibited a MIC range of 2-32 mg/L, whereas vehiculated **1.K-SLN** displayed a MIC range of 2->128 mg/L, including really promising values of 2-32 mg/L toward most of the tested bacteria. SLN alone were found to not possess antibacterial activity with MIC values >128 mg/L in any case.

2.7.4 Preliminary *in vivo* activity  
(in collaboration with G. Sancini, University of Milano)

Biodistribution in mice of the lead compound **1.K** in the free form and in the vehicular form **1.K-SLN** was preliminary evaluated through intratracheal (IT) instillation on two groups of mice, as previously described.<sup>63</sup> The extracts from harvested samples of lungs, brain, liver, kidney, and spleen were analyzed by HPLC-MS-MS in the presence of the internal standard compound **1.k** having a chemical structure similar to that of the lead compound **1.K** but a different molecular weight. The mass spectrum can be used to derive quantitative information on **1.K** by comparing the peak areas of the analyte (lead compound **1.K**) and of the internal standard **1.k**. The first group of 5 mice (ID 1-5) was treated with the lead in vehicular form (**1.K-SLN**), the second group of mice (ID 6-10) was treated with the lead in the free form (**1.K**). Biodistribution was evaluated in five major organs and accumulation amounts by aerosol administration were obtained. The results are reported in Table 2.3 expressed in nmoles/gram of the organ or sampled tissue.

**Table 2.3.** Detected concentrations of compound **1.K** in homogenate samples of mice lungs, brain, liver, kidney, and spleen by HPLC-MS-MS analyses; ID1-5 were treated with **1.K-SLN**, ID6-10 were treated with **1.K** in its free form

ID (mouse)	Weight (g)	Kidney (nmol/g)	Liver (nmol/g)	Lungs (nmol/g)	Brain (nmol/g)	Spleen (nmol/g)
1	43.2	0.021	0.0066	0.0007	n.d.	n.d.
2	40.5	0.031	0.0173	0.0006	n.d.	n.d.
3	33.8	0.068	0.0119	0.0074	n.d.	n.d.
4	34.9	0.005	0.0038	n.d.	n.d.	n.d.
5	37.3	0.067	0.0119	n.d.	n.d.	n.d.
<b>media</b>	38	0.04	0.010	0.003	n.c	n.c.
<b>std dev.</b>	3	0.03	0.005	0.004	n.c.	n.c.
6	44.1	0.005	n.d.	0.0098	n.d.	n.d.
7	33.2	n.d.	0.0015	0.0010	n.d.	n.d.
8	25.9	0.002	n.d.	0.0097	n.d.	n.d.
9	30.7	0.003	n.d.	0.0185	n.d.	n.d.
10	30.4	n.d.	n.d.	0.0149	n.d.	n.d.
<b>media</b>	33	0.003	n.c.	0.011	n.c.	n.c.
<b>std dev.</b>	7	0.002	n.c.	0.007	n.c.	n.c.

n.d. =non detectable; n.c.=non calculable

After a single administration, the lead compound was mainly detected in kidney, liver, and lungs. In brain and spleen tissue **1.K** was not detected or cannot be quantitatively determined. The concentrations of the

vehiculated and free drug detected in tissues of different animals are graphically outlined in Figure 2.21. The lead compound **1.K** in the free form had the high concentration in lungs, whereas in the vehiculated form **1.K-SLN** was more concentrated in kidneys, followed by liver.

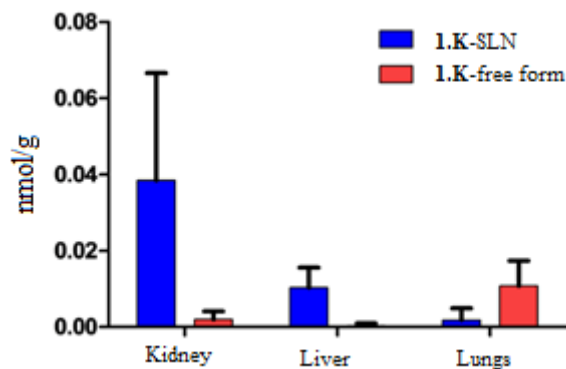


**Figure 2.21.** Biodistribution data of the lead compound in its free (**1.K**) and vehicular form (**1.K-SLN**)

The resulting diversified data opened the possibility for the lead compound to target different organs, according to its diverse formulation. In its free form, **1.K** was able to reach the main biological target of pulmonary diseases such as CF, i. e. the lungs. In the vehiculated form instead, it was possible to mainly reach diverse (and usually more complicated to target) organs such as kidney and liver, both constituting a site of dangerous and hard-to-threat infections.

## 2.8 Other antibacterial alkylidene $\beta$ -lactams

In the last two decades, significant research on natural antimicrobial peptides (AMPs) demonstrated their potential as therapeutic candidates,<sup>64</sup> being essential components of the innate immune system of all multicellular organisms.<sup>65</sup> A hypothesized mechanism of action involves the permeabilization of the bacterial cell membrane that leads to cell death.<sup>66</sup> The selectivity of AMPs toward bacterial cells compared to mammalian cells is mainly due to differences in the lipid components of the respective cell membranes.

This particular interaction of AMPs renders bacterial resistance difficult to strengthen, giving them a strong advantage over conventional antibiotics.<sup>67</sup> However, their clinical development has been hampered due to their toxicity, poor bioavailability and low proteolytic stability.<sup>68</sup> This led to the development of synthetic mimetics of antimicrobial peptides (SMAMPs), with the aim of overcoming the problems associated with AMPs while maintaining the essential characteristics for antimicrobial activity.<sup>69</sup> One of the major design parameters for the development of SMAMPs is facial amphiphilicity (FA), since most AMPs fold into amphiphilic structures when they interact with the bacterial cell membrane. Natural AMPs in fact commonly bear both positive and hydrophobic groups into an amphiphilic structure, with the positive charge constituting the driving force for the electrostatic interaction between AMPs and the negatively charged bacterial membrane, and the lipophilic residues facilitating the insertion into the hydrophobic core.<sup>65</sup>

The systematic structure-activity relationship (SAR) studied on SMAMPs led to the evolution of numerous compounds with a direct antimicrobial activity and a reduced toxicity, some of which have already been included in clinical development.<sup>70</sup> As an example, Thaker *et al.*<sup>71</sup> recently reported novel mimetic AMP derivatives with aromatic residues of benzene or naphthalene as hydrophobic core, whereas the ionic character was conferred through the introduction of ethanol- or propanol-amine chains directly linked to aromatic residues through an ether bond (Figure 2.22). The series of aryl-based SMAMPs that were designed *via* systematic tuning of hydrophobicity and cationic charge, exhibited a strong antibacterial potency while being non-toxic to host cells, with increasing activities on enhancing the number of the cationic amine chains.<sup>72</sup>

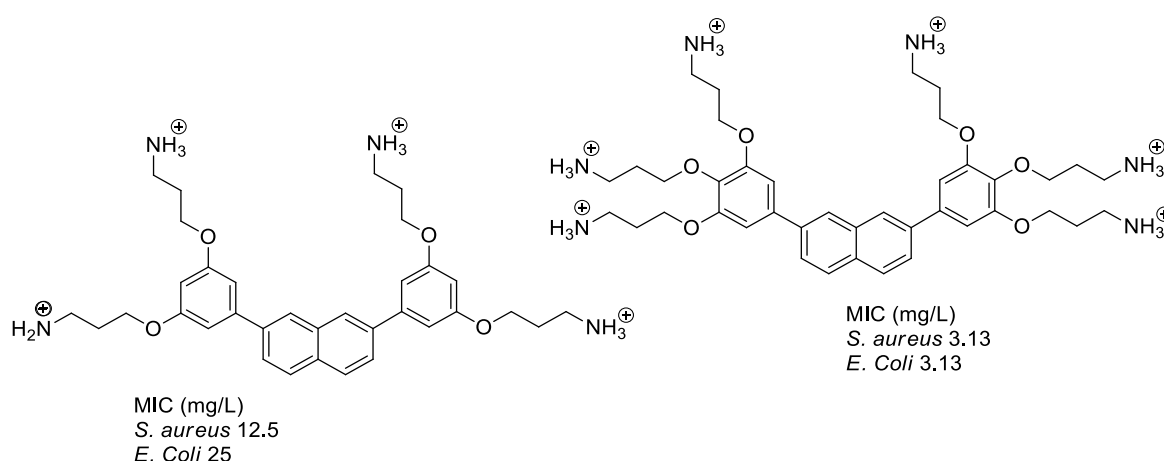
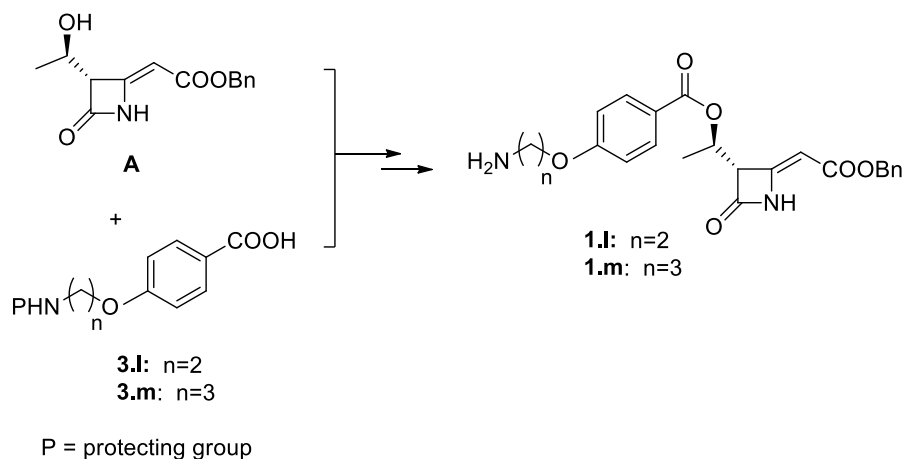


**Figure 2.22.** SMAMPs derivatives with potent antibacterial activities. MIC values in mg/L toward *S. aureus* and *E. Coli* strains are reported<sup>72</sup>

According to these results and aiming at the development of new compounds that could overcome bacterial resistance phenomena and switch the selectivity also towards Gram-negative pathogens, we designed two novel alkylidene-azetidinone compounds functionalizing the C3 position with phenolic residues linked to ethyl- and propyl-amines. The rational hypothesis took in account that the new derivatives could mimic, as far as possible, the specific activity of AMPs on bacterial membranes. In our case, the amphiphilic effect could arise from the positive charges on protonated primary amine terminals and from the presence of two aryl portions in the molecular scaffold (on C3 and C4 position of the ring), which could guarantee a hydrophobic character.

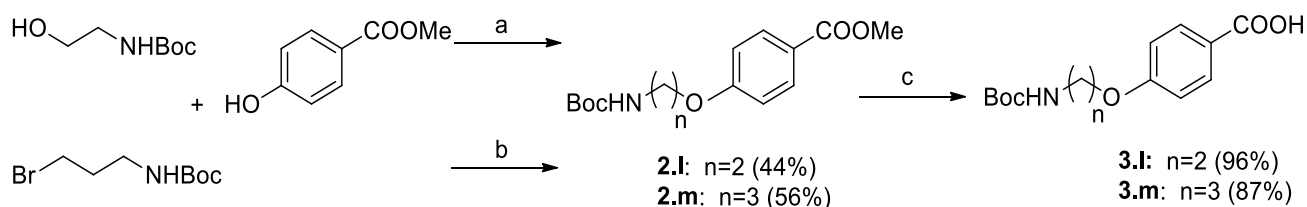
### 2.8.1 Synthesis of azetidinones

The synthetic strategy followed for the synthesis of the new alkylidene- $\beta$ -lactams **1.l** and **1.m** consisted in a convergent procedure comprising a final coupling reaction between  $\beta$ -lactam intermediate **A** with an alcoholic functionality and two different benzoic carboxylic acids **3.l** and **3.m**, both characterized by a protected amine chain of different lengths linked to a *para*-phenolic group (Scheme 2.10).



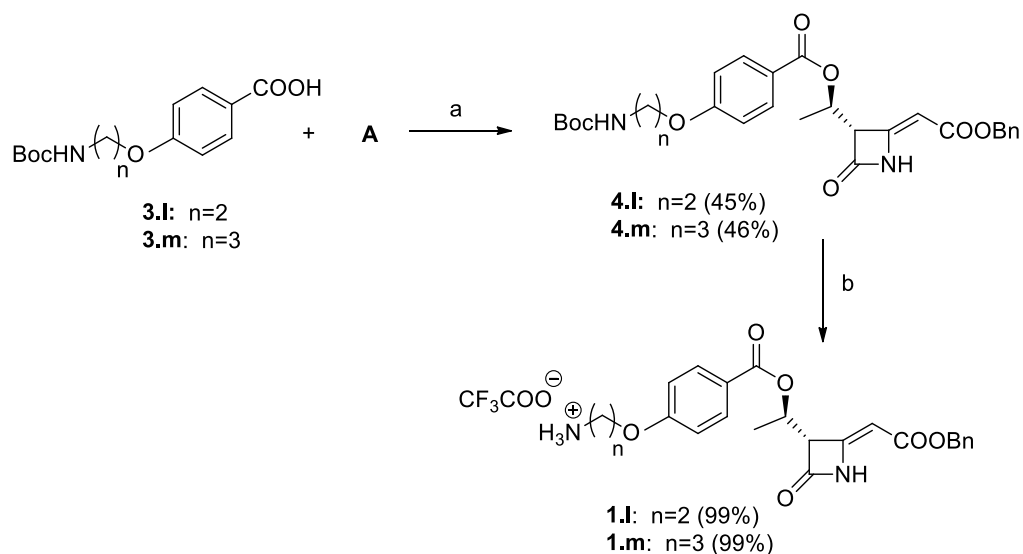
**Scheme 2.10.** Convergent synthesis of new 4-alkylidene- $\beta$ -lactams **1.l** and **1.m**

Preparation of  $\beta$ -lactam **A** was already described; aryl acids **3.l** and **3.m** with an amine terminal functionality were synthesized from *p*-hydroxybenzoic methyl ester whose phenolic group was derivatized with ethanolamine and 3-bromopropylamine duly protected on the –NH function with a Boc group. In particular, coupling with *N*-Boc-ethanolamine was performed *via* Mitsunobu reaction conditions<sup>73</sup> mediated by triphenylphospine and diisopropylazodicarboxylate (DIAD) to give **2.l**. Derivative **2.m** instead was gained through a Williamson reaction<sup>74</sup> with  $K_2CO_3$  in DMF between *N*-Boc-3-bromopropylamine and *p*-hydroxybenzoic methyl ester. The final stage comprised for both compounds **2.l** and **2.m** an alkaline hydrolysis to obtain the free carboxylic acids **3.l** and **3.m** (Scheme 2.11).



**Scheme 2.11.** Synthesis of carboxylic acids **3.l** and **3.m**. Reagents and conditions: a)  $PPh_3$ , DIAD, THF, 0 °C then rt, 3h; b)  $K_2CO_3$ , DMF/ $H_2O$  10:1, 45 °C then rt, 30 h; c) NaOH 5 M, THF/ $CH_3OH$  1:1, 40 °C, 4 h. Yields of isolated products are reported in brackets

The synthesized NH-protected benzoic acids **3.l** and **3.m** were then coupled with  $\beta$ -lactam **A** through the already described Steglich esterification. Also in this case the resulting esters **4.l** and **4.m** were subjected to a deprotection reaction mediated by trifluoroacetic acid to eliminate the Boc group on the amine terminus and to afford the target  $\beta$ -lactams **1.l** and **1.m** in quantitative yields (Scheme 2.12).



**Scheme 2.12.** Synthesis of target compounds **1.l** and **1.m**. Reagents and conditions: a) DCC, DMAP, CH<sub>2</sub>Cl<sub>2</sub>, 0 °C then rt, 16 h; b) CF<sub>3</sub>COOH, CH<sub>2</sub>Cl<sub>2</sub>, 0 °C then rt, 6 h. Yields of isolated compounds are reported in brackets

### 2.8.2 Antibacterial activity

(in collaboration with Prof. C. E. A. Cocuzza and Dr. R. Musumeci, University of Milano)

Antibacterial activity tests of the new alkylidene-azetidinones **1.l** and **1.m** were performed against recent clinical isolates. Also in this case the bacterial strains are well-known for exhibiting a multidrug-resistant phenotype against penicillins/cephalosporins, linezolid, or vancomycin. Antimicrobial activities of the compounds are listed in Table 2.4 expressed as MICs in mg/L. Unfortunately, the insertion of a protonated amine terminus on the new derivatives was not able to furnish any appreciable antimicrobial activity against Gram-negative bacterial strains (data not shown). Nevertheless, a strong antibacterial potency was detected against various *S. aureus* and *S. epidermidis* resistant strains with MIC values ranging from 4 to 32 mg/L and from 8 to 16 mg/L, respectively. In general, the presence of a longer amine side chain in compound **1.m** was found to slightly improve the potency against the tested bacteria compared to **1.l**.

**Table 2.4.** Antibacterial activity of new  $\beta$ -lactam derivatives **1.l** and **1.m**. Results are expressed as MIC values (mg/L) for compounds **1.l** and **1.m**, vancomycin (VA) and cefuroxime (FUR) as reference compounds

Organism ID	1.l	1.m	VA	FUR
<i>S. aureus</i> ATCC 29213	128	16	0.5	2
<i>S. aureus</i> FM80	32	32	1	>128
<i>S. aureus</i> 44674	<b>8</b>	<b>4</b>	4	8
<i>S. aureus</i> 69856	<b>4</b>	<b>4</b>	0.5	1
<i>S. hominis</i> $\alpha$ 26	128	>128	1	8
<i>S. epidermidis</i> G1027	16	16	2	32
<i>S. epidermidis</i> 3226	16	<b>8</b>	1	0.5
<i>E. faecalis</i> ATCC 29212	>128	>128	2	>128
<i>E. faecium</i> VRE 2	128	>128	>128	>128

## 2.9 Carbamate $\beta$ -lactams

Searching for novel derivatives with antibacterial potency, we decided to insert a carbamate moiety on 4-alkylidene- $\beta$ -lactam structure for exploring the effect of this new functional group on biological activity.<sup>75</sup> This choice reflects the properties of organic carbamates, which have frequently been employed as pharmaceuticals, such as, for instance, linezolid in the class of oxazolidinone antibiotics (Figure 2.23).<sup>76</sup> In recent years, several reports indicated that the carbamate linkage present in between the active pharmacophores of various synthetic or semisynthetic molecules increased their biological activities.<sup>77</sup> For instance, Stephen *et al.* recently described some analogues of ethyl-*N*-(2-phenethyl) carbamate as biofilm inhibitors of methicillin-resistant *S. aureus* strains.<sup>78</sup> Moreover, considering bicyclic  $\beta$ -lactams, Yoshizawa *et al.* reported for some cephalosporins with a carbamate derivatization on a pyridine group (Figure 2.23a) an enhanced antibacterial activity against resistant strains of MRSA and *Pseudomonas aeruginosa* compared to the underivatized analogue (Figure 2.23b).<sup>79</sup> A further example of cephalosporin functionalization with a linezolid-like moiety was given by Yan *et al.* that obtained some cephalosporin-oxazolidinone conjugates linked by a carbamate function (Figure 2.23c). The new derivatives showed an antimicrobial activity that was comparable to that exhibited for cephalosporin and oxazolidinone alone, but meanwhile displayed an enhanced resistance against  $\beta$ -lactamases.<sup>80</sup>



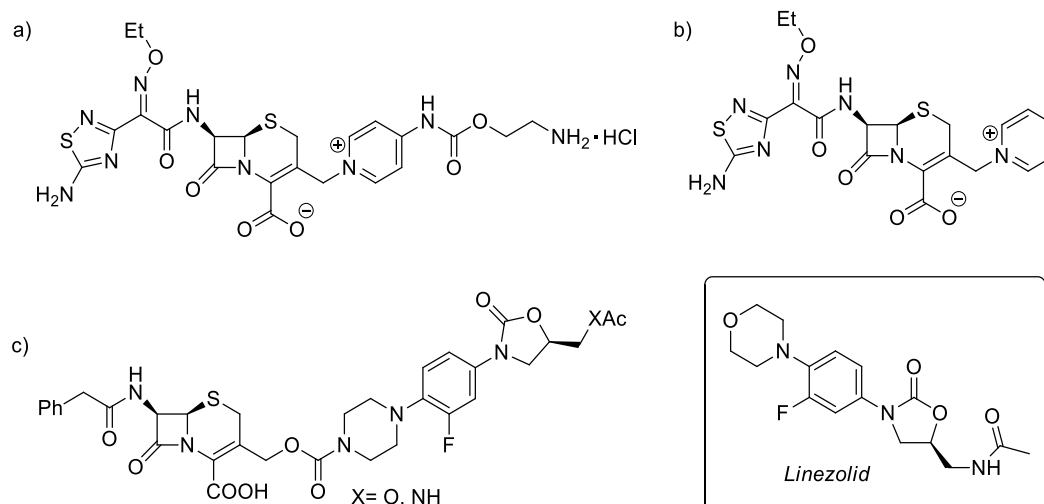


**Figure 2.23.** Cephalosporin-analogues with antibacterial activities. Structure of antibiotic Linezolid is also reported<sup>79,80</sup>

For the development of this project we designed and synthesized 21 novel molecules bearing an aryl, benzyl, or phenethyl-carbamate moiety on C3 position of the  $\beta$ -lactam ring, and also included in the new library two carbamates armed with a linezolid-like molecular fragment (Chart 2.2).

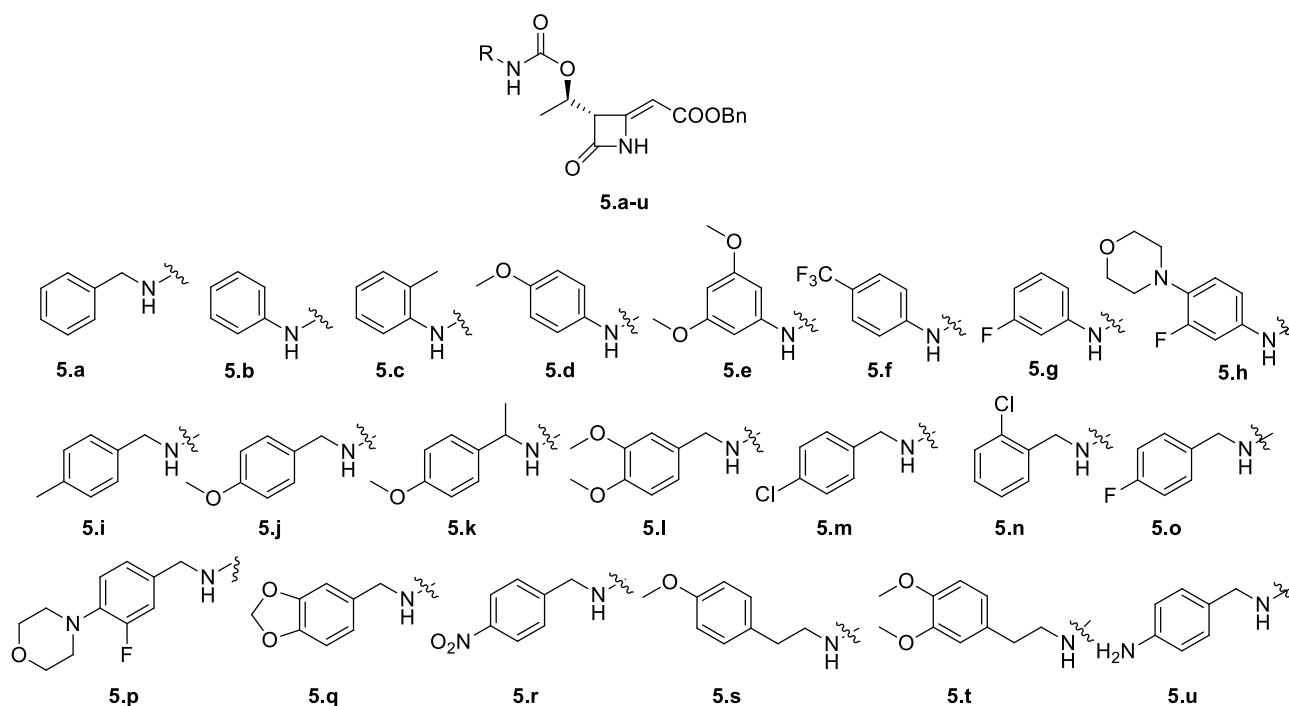


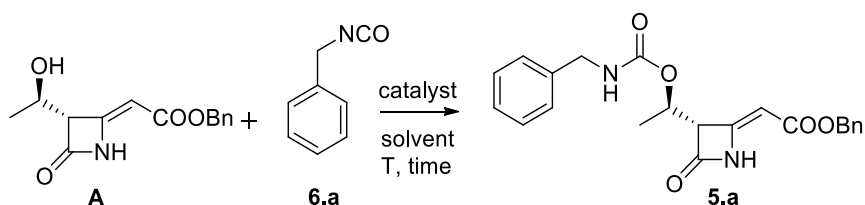
**Chart 2.2.** New  $\beta$ -lactam carbamate derivatives **5.a-u**

### 2.9.1 Synthesis of azetidinones

The synthesis of the new carbamate library was carried out exploiting the reaction between alcohols and isocyanates<sup>81</sup> and developed starting from  $\beta$ -lactam **A** as common precursor, whose synthesis has already been described. For the development of a suitable method tailored for 4-alkylidene- $\beta$ -lactams,

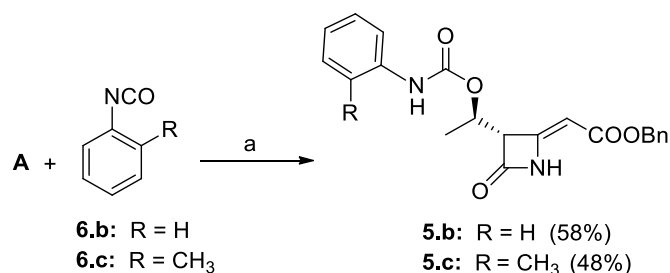
we chose the condensation between the commercially available *N*-benzylisocyanate **6.a** and alkylidene azetidinone **A** as model reaction (Table 2.5). Initially, a base-mediated reaction in CH<sub>2</sub>Cl<sub>2</sub> or acetonitrile (entries 1-4) was investigated,<sup>79</sup> but potassium carbonate, triethylamine, or 4-dimethylaminopyridine gave a mixture of several products in the crude.<sup>39b</sup> After liquid chromatography, carbamate **5.a** was obtained only with DMAP as catalyst in very low yields (entry 4). On the other hand, the uncatalyzed reaction did not proceed at all (entry 5). Then we attempted neat reaction conditions simply by mixing azetidinone **A** with the liquid isocyanate **6.a** in the absence of any catalyst or solvent. In this case the reaction was very slow but selective and no by-products were detected. However, conversions were not complete and consequently, yields of **5.a** were poor even on increasing the isocyanate equivalents (entries 6-8). However, encouraging results were obtained on enhancing the reaction temperature or under microwave (MW) irradiation<sup>82</sup> (entries 8-10). With MW a better result was obtained under a solvent-free condition rather than with chlorobenzene as a solvent (entries 9-10).

**Table 2.5.** Study of the reaction conditions for the synthesis of **5.a**



Entry	Solvent	6.a (equiv)	Catalyst (equiv)	T (°C)	Time (h)	Yield (%)
1	CH <sub>3</sub> CN	1.2	K <sub>2</sub> CO <sub>3</sub> (1.5)	rt	3	-
2	CH <sub>2</sub> Cl <sub>2</sub>	1.2	TEA (1.5)	rt	3	traces
3	CH <sub>2</sub> Cl <sub>2</sub>	1.2	TEA (1.5)	rt	16	traces
4	CH <sub>2</sub> Cl <sub>2</sub>	1.5	DMAP(0.1)	rt	3	8
5	CH <sub>2</sub> Cl <sub>2</sub>	1.5	-	rt	6	traces
6	-	1.5	-	rt	19	23
7	-	2.5	-	rt	20	25
8	-	1.5	-	40	7	50
9	-	1.5	-	MW 400W	40 min	56
10	PhCl	1.5	-	MW 400W	40 min	38
11	CH <sub>2</sub> Cl <sub>2</sub>	1.1	Ti(OBu) <sub>4</sub> (0.1)	rt	20	20
12	CH <sub>2</sub> Cl <sub>2</sub>	1.5	Ti(OBu) <sub>4</sub> (0.1)	rt	20	28
13	CH <sub>2</sub> Cl <sub>2</sub>	1.1	TiCl <sub>4</sub> (0.1)	rt	19	16
14	CH <sub>2</sub> Cl <sub>2</sub>	1.1	TiCl <sub>4</sub> (0.1)	rt	72	50
15	CH <sub>2</sub> Cl <sub>2</sub>	1.5	TiCl <sub>4</sub> (0.1)	rt	20	35
16	CH <sub>2</sub> Cl <sub>2</sub>	2	TiCl <sub>4</sub> (0.1)	rt	20	56
17	CH <sub>2</sub> Cl <sub>2</sub>	1.5	TiCl <sub>4</sub> (0.1)	40	6	91
18	CH <sub>2</sub> Cl <sub>2</sub>	1.5	HCl (0.1)	rt	20	27

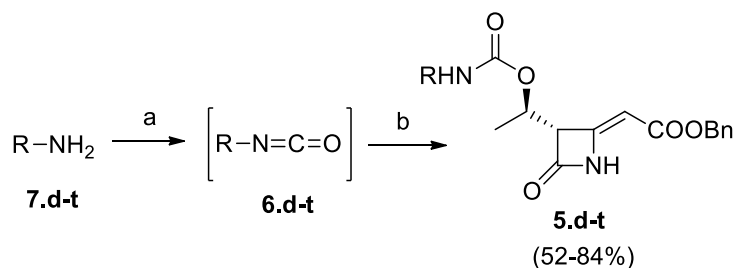
The MW methodology was exploited with other two commercially available isocyanates, phenyl isocyanate **6.b** and *o*-tolyl isocyanate **6.c**, for giving the corresponding carbamates **5.b** and **5.c** that were successfully isolated in acceptable yields after flash-chromatography (Scheme 2.13).



**Scheme 2.13.** Synthesis of  $\beta$ -lactam carbamates **5.b** and **5.c**. Reagents and conditions: a) MW 400 W, neat, 40 min. Yields of isolated compounds are reported in brackets

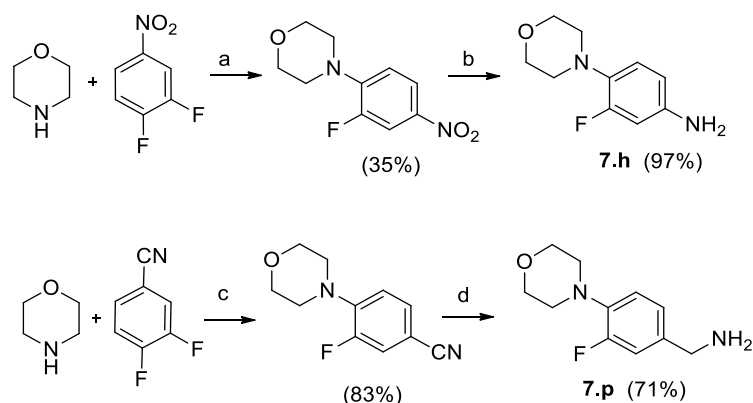
Since Feledziak *et al.* used  $\text{Ti}(\text{O}i\text{Bu})_4$  and isocyanates for inserting a carbamate group on the C3-hydroxyethyl chain of *N*-acylated  $\beta$ -lactams,<sup>83</sup> the synthesis of **5.a** was evaluated under acid catalysis conditions (entries 11-18). Nevertheless,  $\text{Ti}(\text{O}i\text{Bu})_4$  was not satisfying on 4-alkylidene- $\beta$ -lactams (entries 11-12), because of the formation of considerable amounts of the corresponding benzyl butoxycarbamate as by-product. The use of  $\text{TiCl}_4$  gave better results instead (entries 13-17), and with 1.5 equivalents of isocyanate in  $\text{CH}_2\text{Cl}_2$  at reflux temperature (entry 17) target compound **5.a** was obtained in excellent yields (91%) together with a relative decrease of the reaction time for a complete consumption of the starting material (6h instead of 20h when the reaction was carried out at reflux instead of room temperature). A reaction mediated by HCl 12M as catalyst was attempted (entry 18), but it resulted much less efficient than  $\text{TiCl}_4$ .

With the optimized conditions in hand, the scope of the reaction was then investigated. Since many aryl- or benzyl-isocyanates are not commercially available, we developed a method which allowed to synthesize isocyanates *in situ* starting from the corresponding amines, triphosgene, and TEA in dichloromethane (Scheme 2.14). In all cases the formation of isocyanates was confirmed through FT-IR analysis by monitoring the intensity of the characteristic N=C=O stretching absorption at around  $2270\text{ cm}^{-1}$ . The freshly prepared isocyanates were immediately reacted with alcohol **A** and  $\text{TiCl}_4$  in dichloromethane to yield the desired  $\beta$ -lactam carbamates with generally good yields.



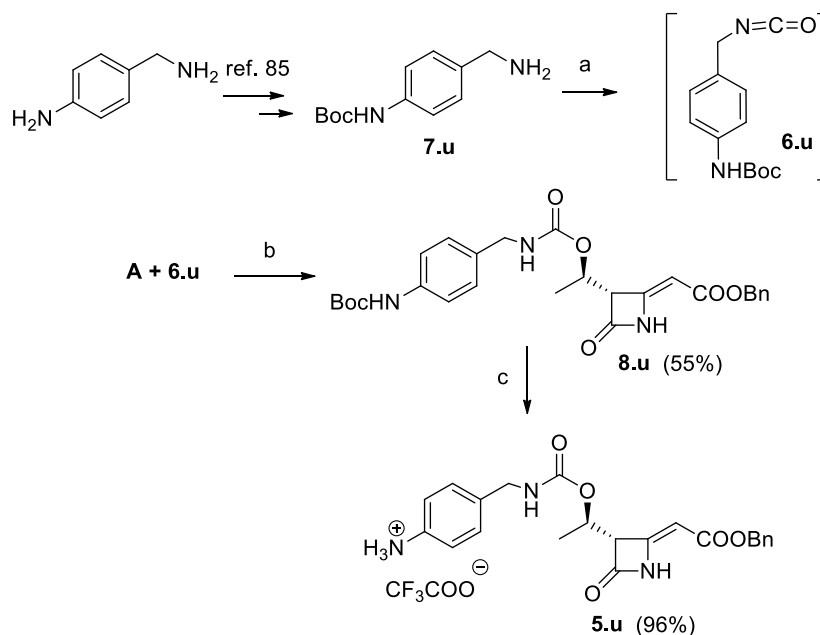
**Scheme 2.14.** Synthesis of  $\beta$ -lactam carbamates **5.d-t**. Reagents and conditions: a) triphosgene, TEA,  $\text{CH}_2\text{Cl}_2$ ,  $0\text{ }^\circ\text{C}$  then reflux, 3h; b) **A**,  $\text{TiCl}_4$  (10 mol%),  $\text{CH}_2\text{Cl}_2$ , rt, 18 h. Range of yields of isolated compounds are reported in brackets

This method was applied to a series of commercially available anilines, benzylamines, and phenethylamines, except for linezolid-like amines **7.h** and **7.p** that were synthesized according to procedures reported in literature<sup>84</sup> (Scheme 2.15).



**Scheme 2.15.** Synthesis of amines **7.h** and **7.p**. Reagents and conditions: a) DMSO, 75 °C, 2 h; b) H<sub>2</sub>, Pd/C, CH<sub>3</sub>OH, rt, 2 h; c) K<sub>2</sub>CO<sub>3</sub>, DMSO, 90 °C, 3 h; d) Red-Al, THF, 0 °C to rt, 3 h. Yields of isolated compounds are reported in brackets

Amine **7.u** was instead prepared in three steps starting from 4-aminobenzylamine after a careful strategy of protecting groups insertion.<sup>85</sup> In case of the corresponding carbamate **8.u**, the *N*-Boc protection was easily removed in the last synthetic step obtaining **5.u** in very good isolated yields (Scheme 2.16).



**Scheme 2.16.** Synthesis of  $\beta$ -lactam carbamate **5.u**. Reagents and conditions: a) triphosgene, TEA, CH<sub>2</sub>Cl<sub>2</sub>, 0 °C then reflux, 3 h; b) **A**, TiCl<sub>4</sub> (10 mol%), CH<sub>2</sub>Cl<sub>2</sub>, rt, 18 h; c) TFA, CH<sub>2</sub>Cl<sub>2</sub>, 0 °C then rt. Yields of isolated compounds are reported in brackets

### 2.9.2 Antibacterial activity

(in collaboration with Prof. C. E. A. Cocuzza and Dr. R. Musumeci, University of Milano)

Antibacterial activity screening of compounds **5.a-u** was carried out against recent, well-characterized clinical isolates. Gram-positive and Gram-negative bacterial pathogens used for the *in vitro* antimicrobial susceptibility testing included: *Staphylococcus aureus*, *Staphylococcus hominis*, *Staphylococcus epidermidis*, *Enterococcus faecalis* and *Enterococcus faecium* as Gram-positive

species, *Klebsiella pneumoniae*, *Pseudomonas aeruginosa*, and *Escherichia coli* as Gram-negative species, respectively. Some bacterial strains were expressly selected to exhibit a multidrug-resistant phenotype against amoxicillin, linezolid, or vancomycin. Antimicrobial activities of the compounds are listed in Table 2.6, with potency being expressed as minimum inhibitory concentration values (MICs) in mg/L. Only compounds demonstrating MIC values equal to or less than 128 mg/L against corresponding bacterial species were reported.

**Table 2.6.** Antimicrobial activity for new carbamate azetidinones **5.a-u**. Results are expressed as MIC values (mg/L) for compounds **5.a-u**, linezolid (LZD) vancomycin (VA) and cefuroxime (FUR) as reference compounds

Comp.	<i>S. aureus</i>				<i>S. epidermidis</i>	<i>S. hominis</i>	<i>E. faecalis</i>	<i>E. faecium</i>
	ATCC 29213	69856	44674	SAU-1	G1027	$\alpha$ 26	ATCC 29212	VRE2
<b>5.a</b>	16	16	<b>8</b>	<b>8</b>	32	<b>8</b>	>128	>128
<b>5.e</b>	>128	>128	>128	>128	>128	>128	>128	32
<b>5.i</b>	>128	>128	>128	>128	128	<b>8</b>	>128	>128
<b>5.j</b>	128	64	32	128	64	<b>8</b>	>128	>128
<b>5.k</b>	>128	128	128	>128	128	16	>128	>128
<b>5.l</b>	32	32	32	64	16	<b>4</b>	>128	>128
<b>5.m</b>	>128	>128	>128	>128	128	16	>128	>128
<b>5.n</b>	>128	>128	>128	>128	>128	16	>128	>128
<b>5.o</b>	>128	>128	>128	>128	128	<b>8</b> 16	>128	>128
<b>5.p</b>	32	>128	>128	32	>128	16	>128	>128
<b>5.q</b>	128	64	64	128	64	16	>128	>128
<b>5.r</b>	32	>128	>128	16	>128	32	>128	>128
<b>5.s</b>	<b>2</b>	>128	>128	<b>8</b>	>128	>128	>128	>128
<b>5.t</b>	32	>128	>128	<b>4</b>	>128	<b>8</b>	>128	>128
<b>5.u</b>	16	16	<b>8</b>	32	16	<b>2</b>	>128	>128
<b>LZD</b>	2	1	2	16	32	16	2	32
<b>FUR</b>	2	1	8	>128	32	8	>128	>128
<b>VA</b>	0.5	0.5	4	0.5	2	1	2	>128

Also in this case, antibacterial potency was observed only against Gram-positive bacteria, while none of the tested compounds exhibited significant activities against Gram-negative strains (data not shown). Promising potency against Gram-positive pathogens was observed for benzyl- and phenethyl-carbamates, whereas no activity was detected for aniline-carbamates (data not shown). In particular, compounds **5.a** and **5.u** with a benzyl-carbamate residue showed interesting and broad activities over the staphylococcal strains tested, especially for the resistant strains *S. aureus* 44674 and SAU-1 (MICs = 8 mg/L). Moreover, **5.u** demonstrated the best antimicrobial activity against the

multidrug resistant *S. hominis*  $\alpha$ 26 strain showing a MIC value of 2 mg/L. Among alkoxy-benzyl carbamates only compound **5.l** retained some antibacterial activity against *S. aureus* (MICs = 32-64 mg/L), whereas it showed potency against *S. hominis* (MIC = 4 mg/L). Chloro- and fluoro-aryl-substituents lost activity, pointing out a requirement for an electron rich aryl fragment on the benzylamine. Between the compounds with a linezolid-like chain anchored on azetidinones, **5.h**, belonging to the group of aniline-carbamates, was inactive, while **5.p** showed some potency against *S. aureus* and *S. hominis* with MIC = 32 and 16 mg/L, respectively.

As a general trend, the amine fragment of the carbamate considerably impacted on the antibacterial activity: only benzylamine or phenethylamine residues showed potency. A loss of flexibility of an aniline-carbamate compared with a benzyl- or phenethyl-carbamate could be an explanation for this general observation. This argument was supported also by considering the low potency of **5.k** bearing a more steric demanding  $\alpha$ -methyl-benzyl-carbamate and, consequently, a minor flexibility. On extending the chain length between the aryl fragment and the carbamate functional group, as in compounds **5.s** and **5.t**, the activity became more selective against *S. aureus* strains and with a more than valuable potency (MIC = 2 mg/L and 4 mg/L respectively). Notably, **5.s** and **5.t** are more active than cefuroxime and linezolid against *S. aureus* SAU-1, a strain characterized by a MRSA phenotype responsible of resistance to cefuroxime; in addition compounds **5.a**, **5.i**, **5.j**, **5.l**, **5.t** and **5.u** resulted more active than linezolid against *S. hominis*  $\alpha$ 26, another strain possessing an important multidrug resistant (MDR) phenotype and resistant to linezolid.

The working hypothesis on the different activities of benzyl-carbamate vs aniline-carbamate due to different conformations was tentatively investigated by NOESY experiments on compounds **5.d** and **5.j**, chosen for a well-differentiated resonance pattern in the aromatic region. The observed NOE contacts for the two molecules are depicted in Figure 2.24. Azetidinone **5.d** showed few contacts involving exclusively the two -NH groups. On the contrary **5.j** significantly showed more contacts, in particular between the benzyl ester fragment and the *p*-OMe-benzyl carbamate. This data could suggest a different spatial arrangement between the two compounds: **5.j** seemed to prefer a folded conformation in which the two side chains get closer thanks to the more flexible benzyl amine residue, whereas the more rigid aniline carbamate in **5.d** seemed to prevent this possibility.

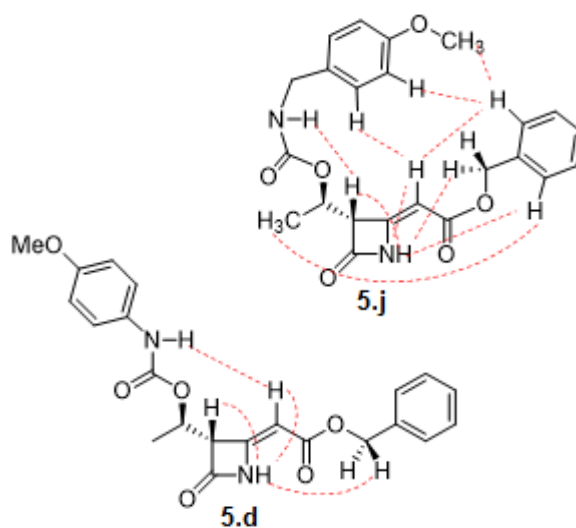


**Figure 2.24.** Structures of azetidinones **5.d** and **5.j**. Dashed red lines indicate the available NOEs. Contacts at a distance less than four bonds were omitted

## 2.10 $\beta$ -lactam based antibacterial biomaterials

### 2.10.1 Biomaterials and hydroxyapatite (HA)

A biomaterial is defined as a substance or a combination of substances able to treat or replace any tissue, organ or body function. The recently developed science of biomaterials is particularly interested in the biological characterization of the new materials, in order to verify, beyond the chemico-physical and mechanical properties, their applications in the biomedical field. From a technological point of view, an ideal biomaterial should have an excellent chemical stability, biocompatibility and biodegradability, absence of toxic/carcinogenic elements and the possibility of being repeatedly sterilized without degradation.

Novel biomaterials<sup>86</sup> could basically arise from:

- a) Materials of biological origin. Materials included in this area can be divided into soft tissues-materials (animal valve prostheses), hard tissues-materials (human bones) and suture materials (fibrin glue). However, the use of biological materials is limited to few applications, due to supply problems.
- b) Artificial materials.<sup>87</sup> Currently, polymeric materials are used in ophthalmology (contact lenses or artificial corneas), but also in pharmacology, with the implementation of macromolecular systems for controlled drug delivery. Interesting applications in the orthopedic field are also found in ceramic materials, such as aluminum oxide or calcium phosphates.
- c) Synthetic production of materials identical to biological materials. This field is still largely in research and experimentation phase; an example is constituted by artificial skin.
- d) Regeneration of biological materials. A possible solution to the reconstruction of organs or parts of body is to provide a support, with an appropriate biomaterial, on which the organism could recreate the missing part.

The increased life expectancy in developed countries has led to a serious rise in the number of age-related musculoskeletal disorders and hence, to an increasing demand of materials for the repair and substitution of damaged tissues, including orthopedic implants for joint replacement. At present, implant premature failures amount to about 10%, a number which will significantly increase in the next future due to the continuous aging of the population.<sup>88</sup> Aseptic loosening and infections represent the main causes of implant failure, and although surgical techniques and prophylactic systemic antibiotic therapy have significantly reduced infections, bacterial colonization of implants and medical devices is still a major problem. After colonization, bacteria may adhere to the surface of the bone or to the orthopedic implant producing a self-protective biofilm, which exhibits remarkable resistance against adverse agents, such as the host immune system and antibiotics.<sup>89</sup> This is also obviously due to the intensive use of antibiotics, which has provoked bacterial resistance to many antimicrobial agents,<sup>90</sup> but on the other hand the systemic administration of very potent antibiotics can provoke irreversible damages to other organs.<sup>91</sup>

The mentioned problem of prosthesis bacterial colonization, which often requires removal of the infected implant, has prompted a number of studies aimed to design and develop antimicrobial surface coatings and biomaterials through functionalization with antibiotics. Most antibacterial agents, such as silver, chlorhexidine and nitric oxide display adverse side effects and/or low efficiency, whereas the antimicrobial resistance of coatings containing classical antibiotics depends on the activity of the

drug on resistant strains and on its side-effects.<sup>92</sup> The development of biomaterials able to act against a wide range of bacteria, including antibiotic resistant bacteria, is therefore of great importance. Due to their excellent biocompatibility and bioactivity, calcium orthophosphates are widely used for the preparation of biomaterials for hard tissues substitution and repair, including coatings for metallic implants, bone cements and scaffolds for regenerative medicine.<sup>93</sup> To this aim, the most employed calcium phosphate is hydroxyapatite (HA), thanks to its similarity to the inorganic phase of bones. Hydroxyapatite is a naturally occurring mineral form of calcium apatite ( $\text{Ca}_5(\text{PO}_4)_3(\text{OH})$ ), usually written as  $\text{Ca}_{10}(\text{PO}_4)_6(\text{OH})_2$  to denote that the crystal unit cell comprises two entities. HA is considered a bioactive, osteo conductive, non toxic and non immunogenic substance since it forms a strong chemical bond with bone tissue, being hence recognized as a good bone graft material. The biological performances of HA can be improved through functionalization with relevant ions and molecules.<sup>94</sup> In particular, HA functionalized with silver nanoparticles, or doped with silver, copper and zinc ions has been reported to display antibacterial activity towards Gram-positive and Gram-negative bacteria.<sup>95</sup> HA has been also proposed as support for classical antibiotics<sup>96</sup> in order to obtain antibacterial materials without possible allergic reactions, due to the presence of metal ions.

According to this, we explored the possibility to functionalize hydroxyapatite nanocrystals with some antibacterial  $\beta$ -lactam compounds with the aim to get new composite materials able to couple the bioactivity of HA with the antimicrobial properties of azetidinones, with relevance against resistant bacteria.<sup>97</sup>

### 2.10.2 Synthesis of azetidinones

Since the efficacy against methicillin resistant *Staphylococcus aureus* of selected azetidinones with an alkylthio-group on the  $\beta$ -lactam nitrogen has been recently reported<sup>39e</sup> (see Paragraph 2.5), we synthesized a series of new monocyclic *N*-thio-substituted  $\beta$ -lactams and studied their loading on hydroxyapatite (Chart 2.3). We chose azetidinones **1.M** and **1.O** as models for *N*-unsubstituted (-NH) compounds, *N*-methylthio-azetidinones (*N*-SCH<sub>3</sub>) **1.N** and **1.P** because they previously showed an interesting antibacterial activity against resistant strains,<sup>17</sup> and *N*-phenylthio-azetidinones (*N*-SPh) **1.V** and **1.W** as *de novo* compounds with an enhanced lipophilic character. It is important to highlight that the OTBS-hydroxyethyl side chain conferred a stronger lipophilic character to **1.O**, **1.P**, and **1.W** compared to **1.M**, **1.N**, and **1.V**.

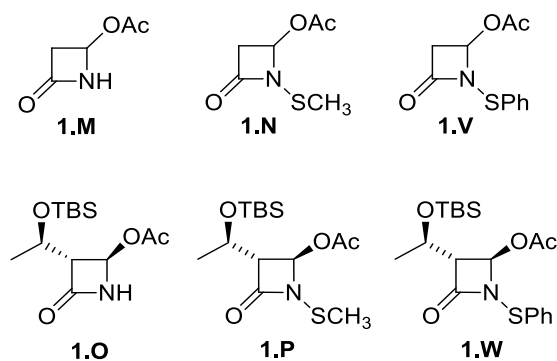
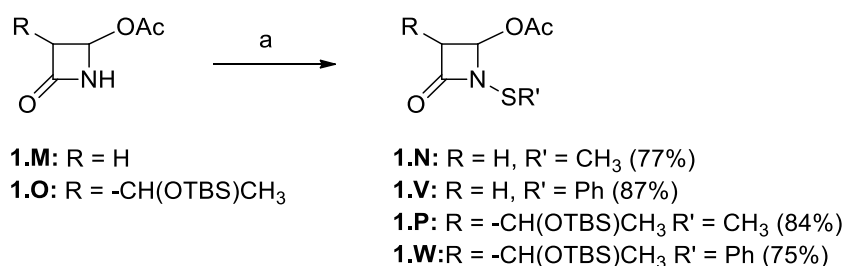


**Chart 2.3.**  $\beta$ -lactams loaded on HA nanocrystals



Azetidinones **1.M** and **1.O** are commercially available, the other compounds were synthesized according to the procedure depicted in Scheme 2.17. Contrary to what previously reported,<sup>17</sup> a new optimized *N*-thiolation procedure was developed using dimethyl- or diphenyl-disulfide in the presence of thionyl chloride and triethylamine in dichloromethane at reflux. These milder reaction conditions allowed to isolate the target compounds after purifications by flash-chromatography from good to very good isolated yields.



**Scheme 2.17.** Synthesis of *N*-thiosubstituted  $\beta$ -lactams **1.N,P,V,W**. Reagents and conditions: a) R'S-SR, SO<sub>2</sub>Cl<sub>2</sub>, TEA, CH<sub>2</sub>Cl<sub>2</sub>, 0 °C then reflux, 4 h. Yields of isolated compounds are reported in brackets

### 2.10.3 Loading of azetidinones on HA

Nanocrystalline HA used as adsorption substrate in this study was synthesized as previously reported<sup>98</sup> in a well-crystallized single phase (cell parameters  $a = 9.428(2)\text{\AA}$ ,  $c = 6.881(1)\text{\AA}$ , Ca/P = 1.66, Surface Area =  $55 \pm 5 \text{ m}^2/\text{g}$ ) with nanocrystals exhibiting mean dimensions of about 200 x 40 nm. The synthesized HA is closer to bone mineral in crystal size and morphology and has been previously shown to promote osteoblast proliferation and differentiation.<sup>99</sup> Moreover, these nanocrystals have been demonstrated to stimulate endothelial cell functions and biochemical pathways, suggesting that they could be successfully employed to promote angiogenesis, and in turn to rouse appropriate osteogenesis.<sup>100</sup>

The adsorption study of azetidinones on HA nanocrystals was performed at first on compounds **1.M-P** chosen as models differentiated for polarity and solubility, and conducted in H<sub>2</sub>O or H<sub>2</sub>O/organic solvent 1:1 mixtures to study the effect of medium. Loading processes were set up in a parallel-synthesis: briefly, HA nanoparticles were suspended in the medium and warmed to 40 °C under magnetic stirring. Azetidinone was then added to the suspension which was heated up to 70 °C. After 4 hours the mixture was centrifugated: the solid functionalized HA-material was oven dried before the analyses, the supernatant aqueous solutions instead were collected and extracted with dichloromethane (DCM). The aqueous and organic phases were separately evaporated and analyzed to quantify the amount of unloaded azetidinones in the two layers. Results are expressed in Figure 2.25 as loading efficiency % back-calculated from the added up residues obtained in DCM and H<sub>2</sub>O in comparison with the amount of azetidinones in the loading solution by means of the equation:

$$LE = \frac{[A - (rw + rDCM)]}{A} * 100$$

where: LE = loading efficiency %; A = amount (g) of azetidinone in the loading solution; rw = residue (g) of azetidinone in water extract; rDCM = residue (g) of azetidinone in dichloromethane extract.

The loading was found to be dependent on the azetidinones and on the medium. Compound **1.M** was efficiently loaded (90%) with H<sub>2</sub>O/ethanol or H<sub>2</sub>O/THF 1:1 mixtures, whereas **1.N** was loaded at a maximum of 56% efficiency in THF or in H<sub>2</sub>O/acetone and H<sub>2</sub>O/CH<sub>3</sub>CN mixtures. Compound **1.O** was efficiently loaded in H<sub>2</sub>O, THF, or in aqueous mixtures as H<sub>2</sub>O/CH<sub>3</sub>CN and H<sub>2</sub>O/acetone; also **1.P** was more efficiently loaded in water or aqueous mixtures. The mixture H<sub>2</sub>O/acetonitrile was chosen as standard solvent to load β-lactams **1.N** and **1.P** despite the good efficiency obtained also with H<sub>2</sub>O/acetone, in order to avoid the possible formation of autocondensation products of acetone promoted by HA.<sup>101</sup> Also the more lipophilic azetidinones **1.V** and **1.W** were loaded in H<sub>2</sub>O/CH<sub>3</sub>CN mixture with good efficiencies, i.e. 88% and 84%, respectively (Figure 2.25).

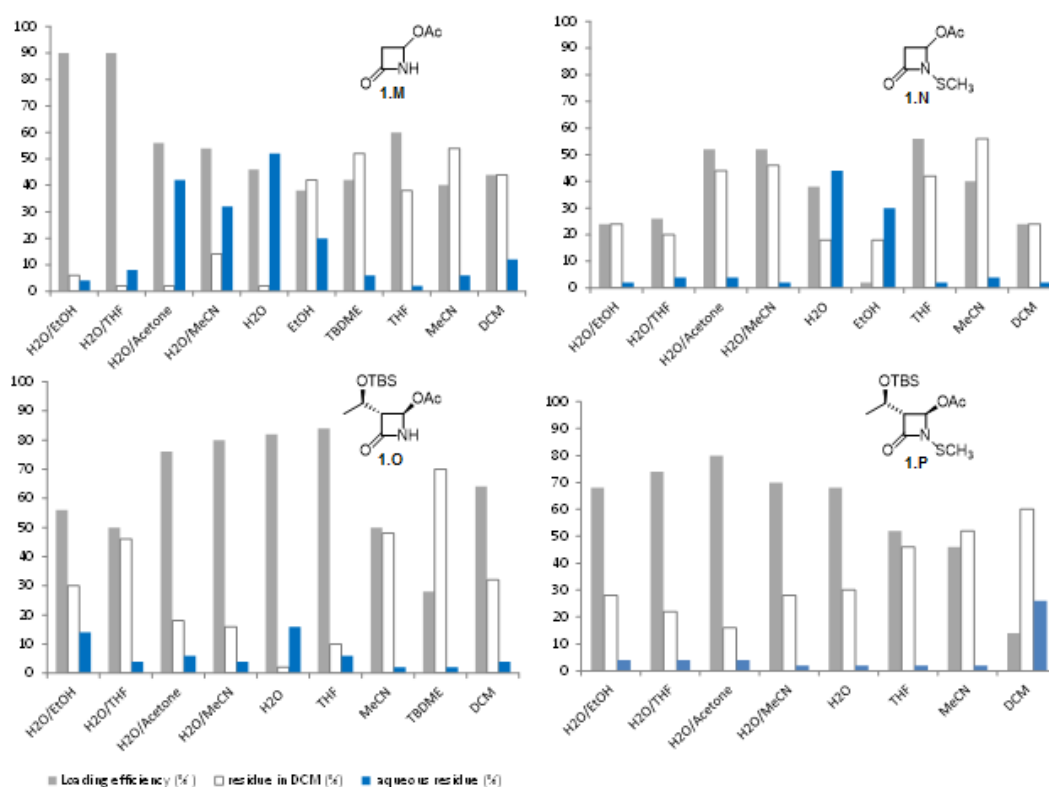


**Figure 2.25.** Medium effect on loading of azetidinones **1.M-P** on HA. Loading efficiency% (grey), azetidinone residue in DCM (white) and in the aqueous layer (blue) are reported

The dependence on concentration and on polarity of the loading solution was investigated on the antibacterial azetidinones **1.N**, **1.P** and **1.V**. Determination of the amount of the azetidinone loaded on HA was assessed by thermogravimetric analysis (TGA) on the dried **1.N-HA**, **1.P-HA**, and **1.V-HA** samples and data are reported in Table 2.7. The loading of **1.N** on HA was higher at 0.14 M (9.5 wt%, entry 1), as indicated by TGA measurement of the corresponding **1.N-HA** sample, but from 0.11 M to 0.06 M it remained almost constant (5.9-5.3 wt%, entries 2-4). Azetidinone **1.V** showed a similar behavior with a 12.7 wt% loading at 0.15 M (entry 6) and 8.5-8.9 wt% at 0.11 and 0.06 M, respectively (entries 7-8). On the contrary, the loading of **1.P** was nearly independent from concentration (5.8-4.8 wt%, entries 10-13).

Variation of the medium polarity was obtained by changing the composition of H<sub>2</sub>O/acetonitrile mixtures in the loading solution. The loading was less affected by the medium polarity for the most

hydrophilic azetidinone **1.N**, which was found to range from 9.5 wt% in a 1:1 mixture of H<sub>2</sub>O/CH<sub>3</sub>CN to 10 wt% in a 7:1 ratio (entries 1 and 5). The loading was instead considerably affected by the medium polarity for the more hydrophobic compounds **1.P** and **1.V** (entries 6 and 9 for **1.V**, entries 11 and 15 for **1.P**). At constant concentration (0.075 M) of **1.P**, the loading on HA was triplicated from acetonitrile alone to H<sub>2</sub>O/acetonitrile 7:1 mixture (from 5.0 to 15.1 wt%, entries 15 and 16). The more favored adsorption of azetidinone **1.P** from a water enriched solution could be explained in terms of effect on the solute solvation: an increase of water content in the loading solution could destabilize the solvation of hydrophobic **1.P** in acetonitrile that, consequently, could be more efficiently taken up by the adsorbent HA.<sup>102</sup> Thanks to this effect, the amount of azetidinone loaded on HA could be properly controlled by changing the polarity of the loading solution, reaching values (up to 17 wt%) higher than other antibacterial agents loaded on apatites, and providing a better covering of the material. On considering that the employed HA has a surface area of 55 m<sup>2</sup>/g, it could be calculated, as an example, that **1.P** could be adsorbed up to 500 μmol/g; this value is significantly higher than those reported for tetracycline (82 μmol/g)<sup>92</sup> and for ampicillin (20 μmol/g)<sup>103</sup> loaded on biomimetic HA.

**Table 2.7.** Effects of solution concentration and polarity on loading of azetidinones **1.N**, **1.P** and **1.V** on HA. Loading was evaluated through TGA analysis

Entry	Comp.	Conc. (M)	Solvent		Loading wt %
			H <sub>2</sub> O/CH <sub>3</sub> CN <sup>a</sup>		
1	<b>1.N</b>	0.14	1:1		9.5
2	<b>1.N</b>	0.11	1:1		5.9
3	<b>1.N</b>	0.07	1:1		5.3
4	<b>1.N</b>	0.06	1:1		5.3
5	<b>1.N</b>	0.17	1.75:0.25		10.0
6	<b>1.V</b>	0.15	1:1		12.7
7	<b>1.V</b>	0.11	1:1		8.5
8	<b>1.V</b>	0.06	1:1		8.9
9	<b>1.V</b>	0.11	1.75:0.25		17.9
10	<b>1.P</b>	0.15	1:1		5.5
11	<b>1.P</b>	0.075	1:1		4.8
12	<b>1.P</b>	0.060	1:1		5.8
13	<b>1.P</b>	0.015	1:1		5.1
14	<b>1.P</b>	0.075	1.5:0.5		11.0
15	<b>1.P</b>	0.075	1.75:0.25		15.1
16	<b>1.P</b>	0.075	0:1		5.0

#### 2.10.4 Characterization of azetidinone-HA samples (in collaboration with Prof. A. Bigi, University of Bologna)

After loading of *N*-thio-azetidinones on hydroxyapatites, a chemical, structural and morphological characterization of the new functionalized biomaterials was performed. In X-ray diffraction (XRD) experiments, all the composite samples showed similar patterns (Figure 2.26) with no peak shifts compared to the starting HA, suggesting that the crystal phase and the structure of the HA material were not affected by the presence of the  $\beta$ -lactam molecules.

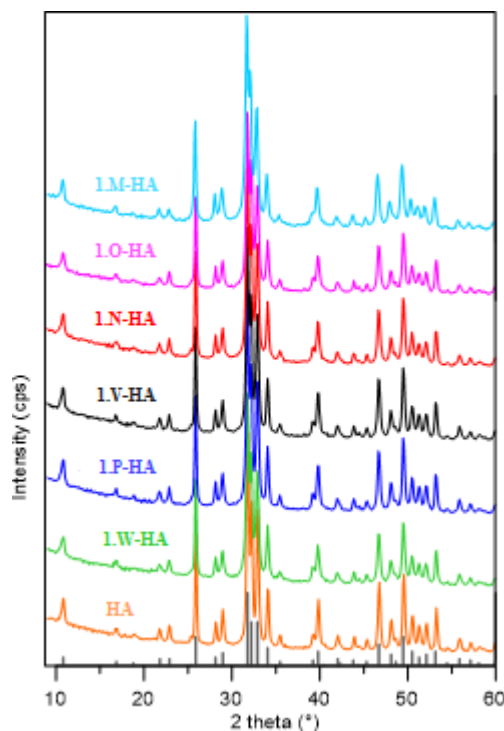


**Figure 2.26.** X-ray diffraction patterns of HA and composite samples **1.M-HA**, **1.N-HA**, **1.O-HA**, **1.P-HA**, **1.V-HA**, **1.W-HA**. The vertical bars at the bottom display the reference pattern of calcium hydroxyapatite

ATR-FTIR spectra of azetidinone-HA samples are reported in Figure 2.27. The spectra displayed the O-H stretching and bending modes of hydroxyapatite at 3572 and 630  $\text{cm}^{-1}$  respectively, the strong bands due to phosphate absorption in the 550-630 and 900-1100  $\text{cm}^{-1}$  regions, and the bands typical of azetidinones whose functional groups could be recognized according to the bands position in the spectra. As an example, the band assignments for sample **1.P-HA** is reported (Figure 2.27, right): aliphatic C-H stretching vibrations in the 2900  $\text{cm}^{-1}$  region, C=O stretching of  $\beta$ -lactam and acetoxy groups at 1790 and 1751  $\text{cm}^{-1}$ , respectively, and O-CO and Si-C stretching in the fingerprint region. Analysis of FT-IR spectra thus revealed that the molecular integrity of the adsorbed azetidinones was fully preserved in the composites and no modification of the bands was observed upon absorption on HA.

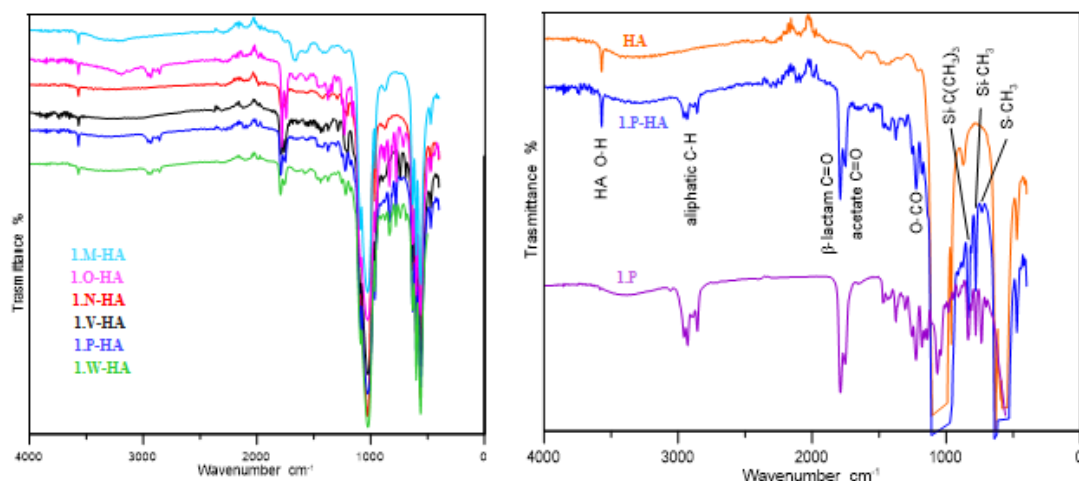


**Figure 2.27.** Left: ATR-FTIR spectra of samples **1.M-HA**, **1.N-HA**, **1.O-HA**, **1.P-HA**, **1.V-HA**, **1.W-HA**. Right: comparison between spectra of **1.P-HA**, **HA**, and **1.P** pure compound; assignments of the main bands are indicated

Also solid state  $^1\text{H}$  and  $^{13}\text{C}$  NMR spectroscopy indicated that loading onto HA did not significantly alter the structure of  $\beta$ -lactams; in fact, resonance signals in  $^1\text{H}$  MAS NMR and  $^{13}\text{C}$  MAS NMR spectra performed for sample **1.P-HA** appeared at the same frequencies as those of **1.P** in solution (data not shown).

TEM images of different samples showed that azetidinone-HA composites were constituted of plate-like crystals, coherently with the typical morphology of HA, which is characterized by crystals elongated along the *c*-axis direction. No significant morphological variation has been observed after azetidinone loading, as shown in Figure 2.28 for samples **1.N-HA** and **1.P-HA** compared with HA alone.

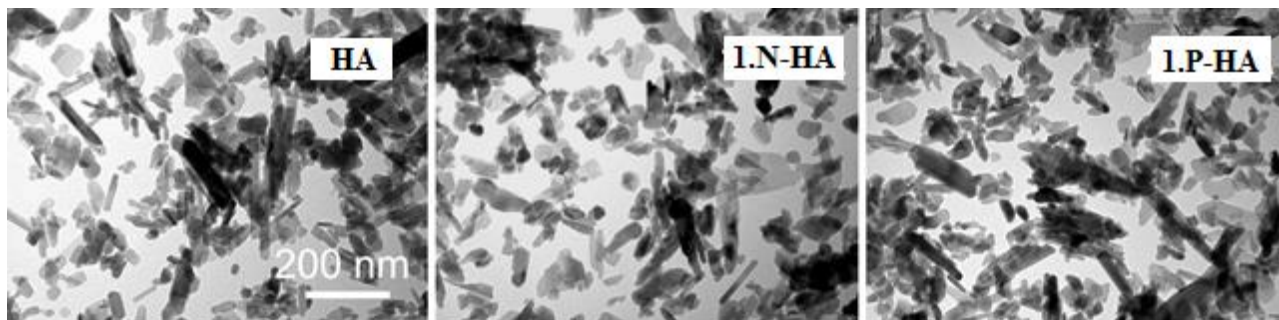


**Figure 2.28.** TEM images of HA, **1.N-HA**, and **1.P-HA** nanocrystals. Scale bar = 200 nm. All images have the same magnification

### 2.10.5 Azetidinone release studies

The *in vitro* release of azetidinones **1.N**, **1.P**, **1.V** and **1.W** from the corresponding functionalized HA samples was evaluated by HPLC analysis. Three aqueous media were tested: deionized water (water MilliQ), phosphate buffer 0.1 M at pH = 7.4 as a model for a physiological pH condition, and acetate buffer 0.1 M at pH = 5.0 to mimic a pathological condition of a bacterial infection with a decreased pH due to the production of acidic metabolites by bacterial strains.<sup>104</sup>

Since early attempts showed scarcely detectable amounts of azetidinones released in the aqueous solutions, which did not increase in the course of time (data not shown), it was observed that only a

refresh of the aqueous solution allowed a new release of the molecules. This fact could be due to the lipophilic character of the compounds that poorly desorbed from apatite because of their low affinity for the aqueous solution.

Results of the *in vitro* release studies of azetidiones-HA samples are reported in Figure 2.29 expressed as cumulative released amounts in mol% over the refresh number. Release profiles of **1.N** and **1.V** in the three aqueous media showed a sort of initial burst release followed by a slower steady profile. **1.N-HA** sample released about 22% of the initial content of **1.N** in the first two refreshes, with a low influence of the pH; interestingly, the release of **1.V** instead was higher in acidic conditions thus affording a favorable pH responsiveness in case of bacterial infections. The initial burst of **1.N-HA** and **1.V-HA** could be related to that portion of molecules adsorbed on the surface in direct contact with the aqueous medium, whereas those molecules that interacted more strongly with HA could be progressively released during the steady state.

On the other hand, the release of azetidiones **1.P** and **1.W** was slower, probably due to their lower hydrophilicity that provided a slow diffusion in the aqueous solutions. It is however important to underline that a low release could be favorable for the maintenance of an active concentration of the molecule on HA, thus supplying an efficient antibacterial activity for a longer period.

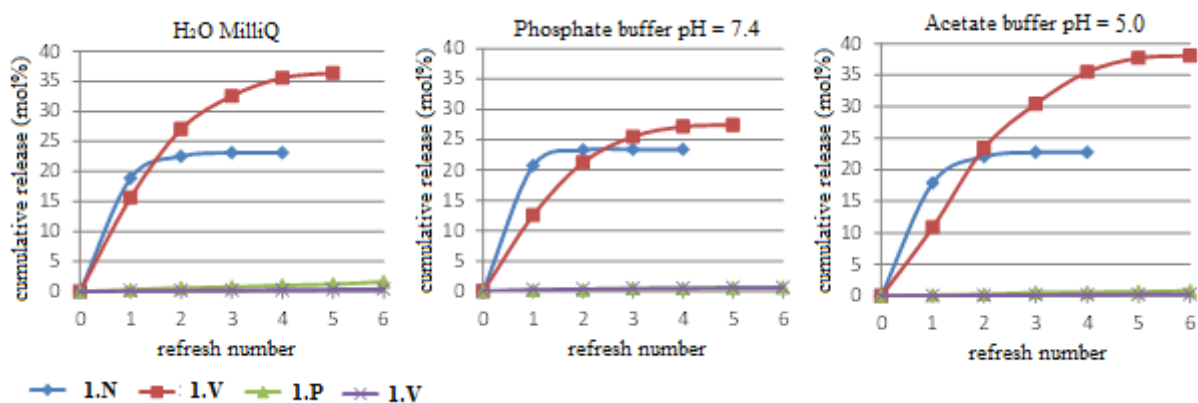


**Figure 2.29.** Release of azetidiones **1.N** (♦ blue), **1.P** (▲ green), **1.V** (■ red), and **1.W** (X violet) from **1.N-HA**, **1.P-HA**, **1.V-HA**, **1.W-HA** in aqueous solution (left), buffer solution at pH = 7.4 (center), buffer solution at pH = 4.5 (right) media. The cumulative release is reported as mol% over the refresh number

### 2.10.6 Antibacterial activity

(in collaboration with Prof. G. A. Gentilomi, University of Bologna)

The *in vitro* antibacterial activity was studied for **1.N-HA**, **1.P-HA**, **1.V-HA** and **1.W-HA** samples (**1.M-HA** and **1.O-HA** were excluded because commercial azetidiones **1.M** and **1.O** alone turned to be inactive as antibacterial agents).<sup>17</sup> The antibacterial activity was examined towards Gram-positive and Gram-negative bacterial strains by KB disk diffusion test, in which the area of clear media around the disk indicates the degree of sensitivity of the strain expressed in millimeters (Table 2.8).

**Table 2.8.** Antibacterial activity of samples **1.N-HA**, **1.P-HA**, **1.V-HA**, **1.W-HA** expressed as diameter of the inhibition zone (in mm)  $\pm$  SD surrounding the azetidinone-HA samples against *S. aureus* and *E. coli* strains. Pure HA disks were used as negative controls; disks containing gentamicin (GMN) were used as positive control

Sample	$\beta$ -lactam content wt %	<i>S. aureus</i> ATCC 25923	<i>E. coli</i> ATCC 25922
<b>1.N-HA</b>	8.1	30 $\pm$ 1	27 $\pm$ 1
<b>1.P-HA</b>	14.0	20 $\pm$ 1	14 $\pm$ 1
<b>1.V-HA</b>	17.0	27 $\pm$ 1	12 $\pm$ 1
<b>1.W-HA</b>	16.5	16 $\pm$ 1	11 $\pm$ 1
HA		NA <sup>a</sup>	NA <sup>a</sup>
GMN		18 $\pm$ 1	19 $\pm$ 1

<sup>a</sup> bacterial-free zone not appearing

All tested azetidinone-HA samples displayed a significant antibacterial activity against both strains, particularly against *S. aureus*. Indeed the inhibition zone for all HA composites was bigger or equal to that of the positive control. All the samples showed activity also against *E. coli* even if they exhibited smaller active diameter values *vs* control, except for **1.N-HA** that remarkably affected *E. coli* growth, yielding an inhibition zone wider than that obtained for gentamicin. The activities of **1.N-HA** and **1.P-HA** against *S. aureus* are in agreement with those exerted by the two molecules alone, which showed MIC ranges of 32-64 mg/L *vs* MRSA. Concerning the activity against Gram-negative bacteria, the free azetidinone **1.N** exhibited a MIC range of 32-64 mg/L, whereas **1.P** was completely inactive.<sup>17</sup> The increased antibacterial activity of the composites **1.N-HA** and **1.P-HA** against *E. coli* could be due to an inherent higher local concentration of the  $\beta$ -lactam on the solid HA, and consequently to a higher efficacy of the new functionalized HA materials.

From antibacterial susceptibility testing against reference bacterial strains, **1.N-HA** emerged as that having the best profile, therefore its antibacterial efficacy was further assayed towards 10 clinical isolates (5 MSSA and 5 MRSA-SCV -small colony variants- strains) obtained from surgical bone biopsies and representative of bacterial strains currently encountered during osteomyelitis. The included strains were the main responsible for chronic and therapy-refractory infections despite systemic antimicrobial treatments, due to their reduced rate of metabolism, intracellular persistence, strong adhesion to implants and host tissues *via* biofilm extracellular matrix formation.<sup>105</sup> Data reported in Table 2.9 indicated that **1.N-HA** strongly inhibited the bacterial growth of both methicillin-resistant and methicillin-susceptible clinical isolates of *S. aureus* from surgical bone biopsies, showing to be a very good candidate as a new functional biomaterial with enhanced antibacterial activity. Moreover, the obtained results for the new **1.N-HA** material confirmed some hypothesis on the mechanism of action of these *N*-thiolated-azetidinones, in particular it excluded the possibility that the Penicillin Binding Protein PBP2a, which is the resistance factor discriminant between MRSA and MSSA, could be the biological target. Nevertheless, it is important to highlight that the loading of **1.N** on HA did not interfere in the mechanism at the root of its antibacterial action, since a similar activity on both MRSA and MSSA strains was previously observed also on the free azetidinone.

**Table 2.9.** Antibacterial activities of **1.N-HA** sample against clinical isolates expressed as diameter of the inhibition zone (in mm)  $\pm$  SD surrounding azetidinone-HA sample; disks containing gentamicin (GMN) were used as positive controls

Clinical isolate	1.N-HA	GMN
<b>MSSA 1</b>	38 $\pm$ 1	30 $\pm$ 1
<b>MSSA 2</b>	28 $\pm$ 1	22 $\pm$ 1
<b>MSSA 3</b>	28 $\pm$ 1	20 $\pm$ 1
<b>MSSA 4</b>	33 $\pm$ 1	22 $\pm$ 1
<b>MSSA 5</b>	30 $\pm$ 1	20 $\pm$ 1
<b>MRSA-SCV 1</b>	30 $\pm$ 1	20 $\pm$ 1
<b>MRSA-SCV 2</b>	28 $\pm$ 1	21 $\pm$ 1
<b>MRSA-SCV 3</b>	34 $\pm$ 1	24 $\pm$ 1
<b>MRSA-SCV 4</b>	25 $\pm$ 1	21 $\pm$ 1
<b>MRSA-SCV 5</b>	30 $\pm$ 1	20 $\pm$ 1

### 2.10.7 Cytotoxicity tests

(in collaboration with P. Torricelli, Istituto Ortopedico Rizzoli, Bologna)

The cytotoxicity of samples **1.N-HA**, **1.P-HA**, **1.V-HA** and **1.W-HA** was tested using MG63 osteoblast-like cell line, widely employed for biomaterial testing; cell proliferation and viability were assessed by colorimetric reagent test. Results at 48 hours and 72 hours of cultures are reported in Figure 2.30a, where values under 70% indicate cytotoxicity of the tested material. **1.P-HA**, **1.V-HA** and **1.W-HA** samples showed significant lower proliferation when compared to negative control (CTR-) at both 48 and 72 h, and their percentage of viability was always under 70%. On the contrary, cells grown in contact with **1.N-HA** showed significant lower values at 48 hours, but at 72 h no significant difference in comparison with CTR- was found and percentage of viability was over 70% both at 48 h and 72 h. In a second test, amount of lactate dehydrogenase (LDH), which is released in culture medium by cells with damaged membranes, was evaluated (Figure 2.31b). The values measured in supernatants showed significant higher release in **1.P-HA**, **1.V-HA** and **1.W-HA** in comparison to CTR- at both experimental times. Also in this case instead, value for **1.N-HA** was higher at 48 h, but it did not differ from CTR- at 72 h, showing an absent cytotoxicity towards MG63 osteoblast-like cell line.



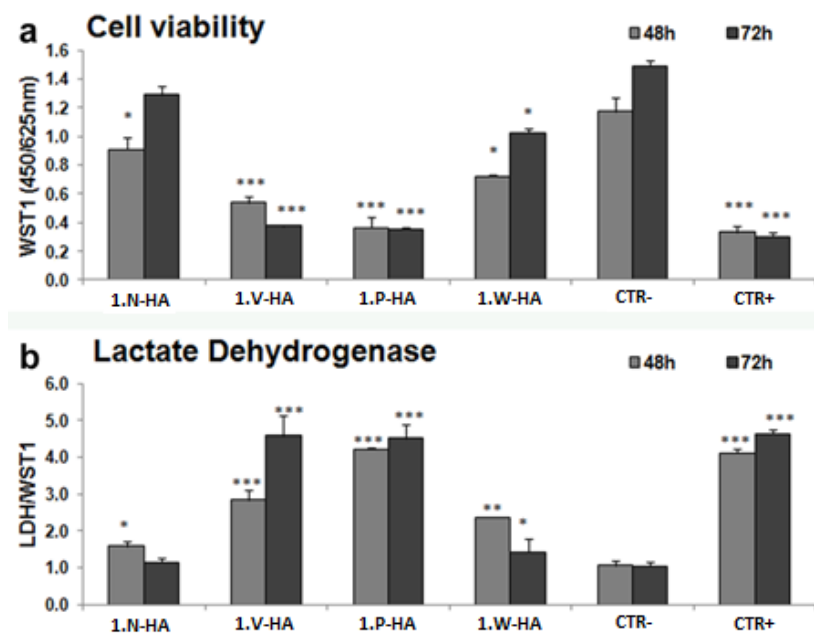


**Figure 2.30.** a) WST1 assay and b) LDH release of MG63 after 48 and 72 h of culture on **1.N-HA**, **1.P-HA**, **1.V-HA**, **1.W-HA**, samples and controls

## 2.11 Other *N*-thio-substituted $\beta$ -lactams

As already widely discussed, *N*-thio-substituted  $\beta$ -lactams have been shown to exhibit an innovative bacteriostatic action mechanism with efficacy also on resistant strains.<sup>17</sup> After the functionalization of hydroxyapatite with a series of *N*-methylthio and *N*-phenylthio-azetidinones resulting in excellent biomaterials with antibacterial activity against resistant pathogens,<sup>97</sup> we decided to expand the library of these compounds for evaluating how diverse thio-substitutions on  $\beta$ -lactam nitrogen could influence and modulate the antibacterial activity. In particular, 12 novel *N*-arylthio- and *N*-alkylthio-azetidinones were designed and synthesized (Chart 2.5) starting from commercially available compounds **1.M** and **1.O**.

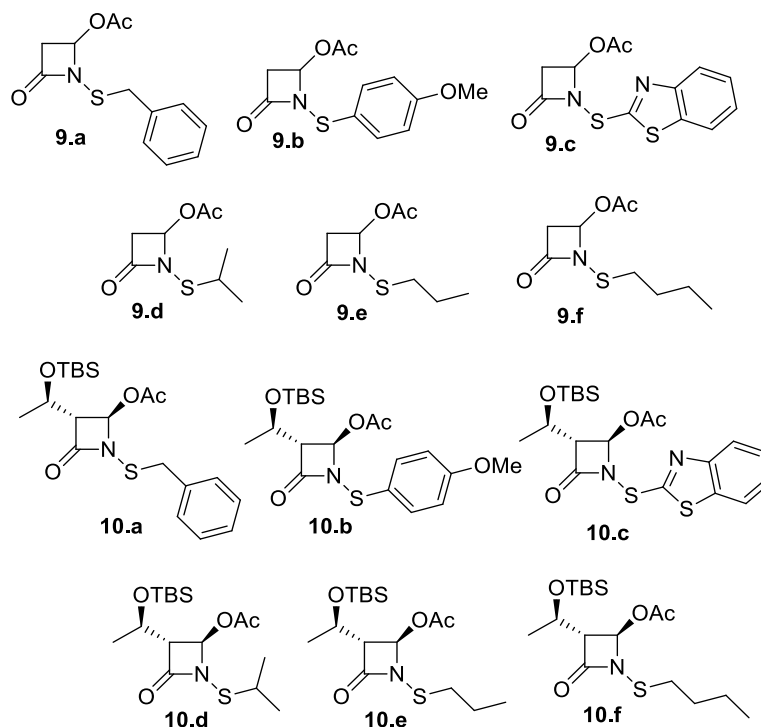
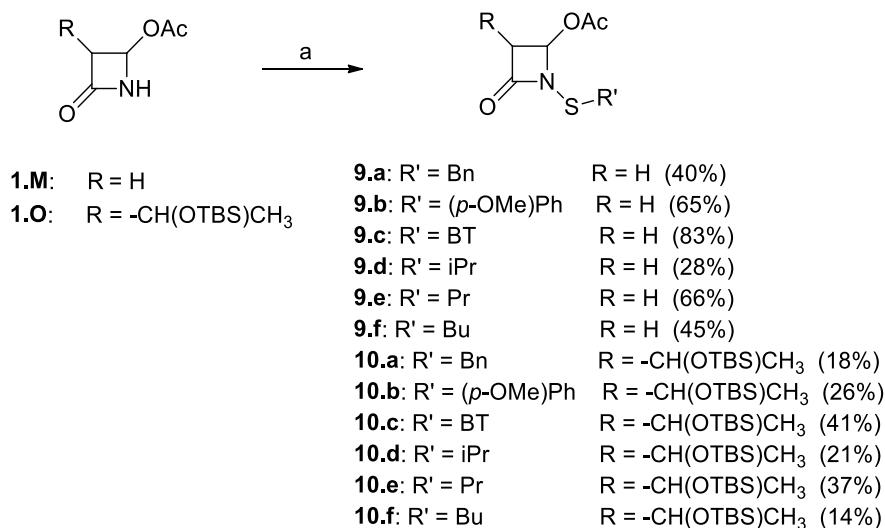


**Chart 2.5.** Novel *N*-thio-substituted  $\beta$ -lactams **9.a-f** and **10.a-f**

### 2.11.1 Synthesis of azetidinones

The novel *N*-thio-substituted  $\beta$ -lactams were prepared according to the procedure already depicted in Paragraph 2.4.2 for compounds **1.N**, **1.P** and **1.V**, **1.W** (Scheme 2.18).



**Scheme 2.18.** Synthesis of *N*-thiosubstituted  $\beta$ -lactams **9a-f** and **10a-f**. Reagents and conditions: a) R'S-SR, SO<sub>2</sub>Cl<sub>2</sub>, TEA, CH<sub>2</sub>Cl<sub>2</sub>, 0 °C then reflux, 4 h. Yields of isolated compounds are reported in brackets

The results reported in Scheme 2.18 appeared rather discordant showing oscillating yields according to the starting substrate and the disulfide. A general worst reactivity emerged when the starting azetidinone **1.O** was used: with the disulfide being equal in fact, yields appeared lower for C3 substituted compounds compared to those obtained starting from azetidinone **1.N** (see **9.a** vs **10.a**,

**9.b** vs **10.b**, **9.c** vs **10.c**, etc..). A hypothesis for this reactivity trend could arise from a partial pyramidalization of the  $\beta$ -lactam nitrogen, supported by computational studies that have been carried out on bicyclic  $\beta$ -lactams and their binding angles.<sup>43</sup> Presuming that a pyramidalization could be present also in compound **1.O**, it would be conceivable a steric hindrance between the -CH(OTBS)CH<sub>3</sub> group in C3 position and the nitrogen lone pair, since the proton of the -NH group should arrange in an intramolecular hydrogen bond with the carbonyl group on the C4 (Figure 2.31).

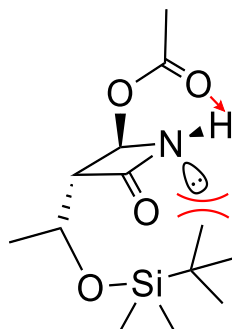


**Figure 2.31.** Spatial arrangement for starting compound **1.O**

This spatial arrangement could hence explain a less availability of the nitrogen lone pair for a nucleophilic attack on the disulfide, causing a lower reactivity of these derivatives compared to those with no substitution on C3. Since a <sup>1</sup>H NMR coupling between -NH hydrogen and that on the C3 position of the ring was observed, these two protons probably dispose on the same side of the lactam plane, supporting the hypothesis that the nitrogen lone-pair and the -OTBS group accordingly point on the other side.

A second observation could account for a different reactivity of the disulphides; in most cases reaction yields are not in accordance with those previously reported for compounds **1.N**, **1.P** and **1.V**, **1.W** obtained from dimethyl or diphenyl disulfide, and even reactants with a similar structure, such as dipropyl disulfide or dibutyl disulfide, furnished in this case very divergent yields (see **9.e** vs **9.f**, **10.e** vs **10.f**). The best results were obtained with *p*-methoxyphenyl disulfide and benzothiazolyl disulfide (48% and 83% starting from substrate **1.M**, 26% and 45% starting from substrate **1.O**, respectively). In addition, in all the performed experiments, a residual presence of starting materials was evidenced: it was therefore hypothesized that the unreacted starting  $\beta$ -lactam could be blocked in the formation of an intermediate *N*-chlorinated compound arising from the presence of reactive chloride ions or radicals in the reaction mixture formed in turn by a degradation of SO<sub>2</sub>Cl<sub>2</sub>. This species could be then decomposed to restore the starting material following an aqueous work-up or silica exposure.

A tentative optimization of the reaction conditions was performed on compounds **9.a** and **10.a** as model substrates (data not shown); the number of equivalents of disulfide, base and sulfonyl chloride were tentatively varied, together with an elongation of reaction times or modification in the heating system (MW irradiation was attempted in neat conditions or in chlorobenzene). Nevertheless, no improvements were detected with the newly employed conditions; even if the yields are in many cases not satisfying, a new library of *N*-thio-substituted  $\beta$ -lactams was obtained with a straightforward one-step protocol starting from commercial available and not expensive azetidinones and disulfides. The novel compounds will be tested to evaluate their antibacterial properties against resistant strains of common pathogens. Moreover, from a preliminary study in collaboration with R. Schnell, Karolinska Institutet Stockholm, compound **1.N** resulted active against a protease of *Mycobacterium*

*tuberculosis*. According to this, other selected *N*-thio-azetidinones are being tested and a further collaboration with P. Dal Monte, University of Bologna, aimed at assaying this class of  $\beta$ -lactam derivatives against *Mycobacterium tuberculosis* from clinical isolates. Results are still being awaited and according to their effectiveness, an optimization procedure for the realization of this compound series could be performed in the future.

## 2.12 Concluding remarks

In this chapter innovative libraries constituted by new  $\beta$ -lactam derivatives were reported, together with their synthesis and biological evaluation. Starting from the already pioneered 4-alkylidene or 4-acetoxy azetidinone scaffolds, different functionalizations on C3 position of the  $\beta$ -lactam ring were examined for modulating the antibacterial activity.

At first, since oxidative stress could contribute to the selection of resistant bacterial strains, we designed some  $\beta$ -lactams armed with phytochemical polyphenolic acids and investigated as dual target antibacterial-antioxidant derivatives. Compounds with a good antibacterial potency against multidrug resistant staphylococcal strains were found (MICs = 2-8 mg/L for the best candidates). Moreover, compounds bearing a catechol moiety on the side chain showed a strong anti-radical capacity against DPPH and ABTS, with TEAC values 2.5 times higher than those known for compounds currently used as antioxidants (Vitamin E, citric acid).<sup>46</sup>

Two of these derivatives were prepared in gram-scale as lead and standard compounds for a preliminary *in vivo* biodistribution study. Molecules were vectorized on solid lipid nanoparticles and the accumulation in mice of the lead compound in its free and vehicular form was evaluated by HPLC-MS-MS of tissues and organs extracts.

We then modified the C3 position with a phenolic benzoic acid linked to a positively charged amine terminus with the scope to partially mimic the amphiphilic behavior of antimicrobial peptides. Also in this case the derivatives were tested against resistant bacteria and found to strongly inhibit bacterial proliferation in *S. aureus* and *S. epidermidis* strains.

In a second project we developed and optimized a two-step protocol for obtaining a new class of monocyclic-alkylidene-azetidinones armed on the C3 hydroxyethyl side chain with aniline-, benzyl- or phenethyl-carbamate moieties. All the new compounds were tested for their antibacterial efficacy against Gram-positive and Gram-negative recent clinical isolates including multidrug-resistant strains and a correlation was found between the biological activity and the *N*-substituent of the carbamate group. In particular, phenethyl-carbamate  $\beta$ -lactams resulted the most active antibacterial agents against some selected strains, comprising linezolid-resistant isolates, with a MIC potency of 2-4 mg/L.<sup>75</sup>

In a parallel study aimed at the realization of novel composite biomaterials possessing antibacterial properties, we performed the loading of some monocyclic *N*-thio-substituted- $\beta$ -lactams with a lipophilic character on nanocrystalline hydroxyapatite (HA). Functionalization of apatites with antibacterial agents active against resistant bacterial strains could be indeed very important for the elaboration of bioactive bone-repair materials. The synthesized azetidinones showed high affinity interactions with HA and could be loaded in good amounts by a proper choice of the polarity of the

loading solution, reaching values up to 17 wt%. The characterization of HA composites revealed the presence of intact  $\beta$ -lactams which could exert their biological activities, and data on cumulative release in aqueous solution showed different trends that can be related to the lipophilicity of the molecules and modulated by suitable groups on azetidinones. What is more important is that all the new  $\beta$ -lactam-HA composites exhibited good antibacterial activity against reference Gram-positive and Gram-negative bacteria with 4-acetoxy-1-(methylthio)-azetidin-2-one-HA sample displaying the best activity and no cytotoxicity.<sup>97</sup> The good results obtained could lead to new functional apatites with enhanced antibacterial properties able to prevent bone infections by resistant pathogens. According to this, novel  $\beta$ -lactams with diverse *N*-thio-substitutions were synthesized and antibacterial tests are in due course.

The most active candidates belonging to each class of the novel derivatives were collected in Figure 2.32 together with their corresponding antibacterial activity<sup>46,75,97</sup> to demonstrate how a structural variability on a fixed monocyclic azetidinone scaffold could give rise to novel promising candidates with strong antimicrobial potency against multidrug resistant strains suitable for a further *in vivo* evaluation.

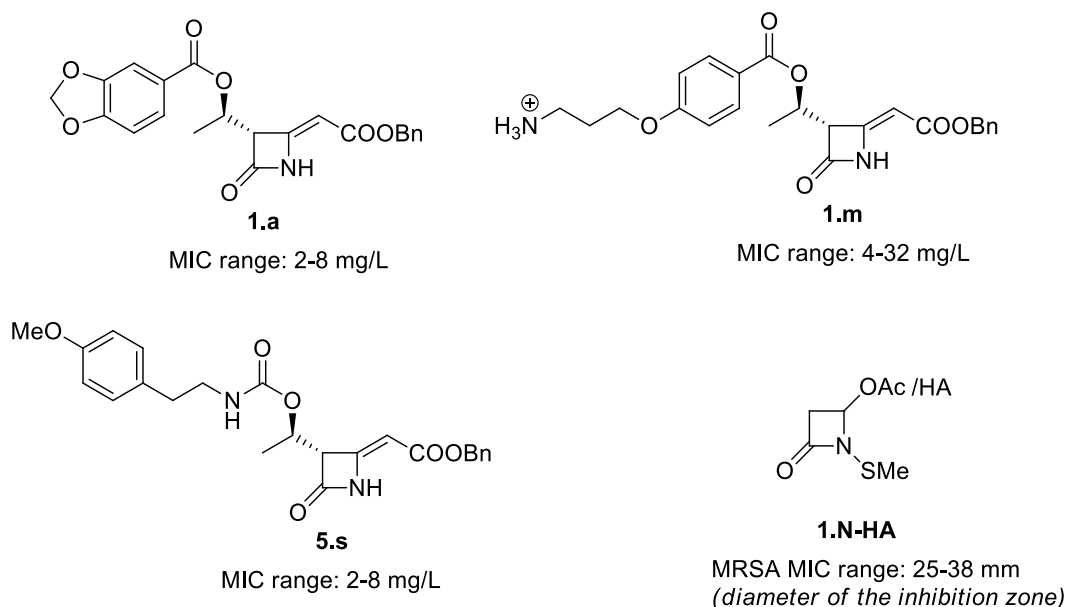


**Figure 2.32.** Best candidate compounds with potent antibacterial activities. MIC ranges in mg/L or in mm diameter inhibition zone toward different bacterial strains are reported<sup>46,75,97</sup>

## 2.13 Experimental Section

### 2.13.1 General information

Commercial reagents (reagent grade, >99%) were used as received without additional purification. Anhydrous solvents were obtained commercially. Deionized water was obtained from a Millipore analytical deionization system (MilliQ). All reactions were performed under an inert atmosphere (N<sub>2</sub>) unless unspecified. TLC: Merck 60 F<sub>254</sub> plates. Column chromatography: Merck silica gel 200-300 mesh. <sup>1</sup>H and <sup>13</sup>C NMR spectra were recorded with an INOVA 400 instrument with a 5 mm probe. 2D NOESY experiments were run using 200 ms mixing time. All chemical shifts are quoted relative to deuterated solvent signals ( $\delta$  in ppm and  $J$  in Hz). Solid state NMR spectra were obtained on a 500MHz Agilent DD<sub>2</sub> spectrometer by using a 22  $\mu$ L rotor. The <sup>13</sup>C and <sup>1</sup>H spectra were recorded at a MAS frequency of 6 kHz. Polarimetric Analyses were conducted on Unipol L 1000 "Schmidt-Haensch" Polarimeter at 598 nm. FTIR spectra: Bruker instrument, measured as films between NaCl plates or CH<sub>2</sub>Cl<sub>2</sub> solutions for solid compounds; wave numbers are reported in cm<sup>-1</sup>. ATR-FTIR spectra: Alpha FT IR Bruker spectrometer with platinum ATR single reflection diamond module. As reference, the background spectrum of air was collected before the acquisition of each sample spectrum. Spectra were recorded with a resolution of 4 cm<sup>-1</sup>, and 32 scans were averaged for each spectrum (scan range 4000–450 cm<sup>-1</sup>). The purities of the target compounds were assessed as being >95% using HPLC-MS. Elemental analysis were performed on a Thermo Flash 2000 CHNS/O Analyzer. HPLC-MS: Agilent Technologies HP1100 instrument, equipped with a ZOBRA-X-Eclipse XDB-C8 Agilent Technologies column; mobile phase: H<sub>2</sub>O/CH<sub>3</sub>CN, 0.4 mL/min, gradient from 30 to 80% of CH<sub>3</sub>CN in 8 min, 80% of CH<sub>3</sub>CN until 25 min, coupled with an Agilent Technologies MSD1100 single-quadrupole mass spectrometer, full scan mode from  $m/z = 50$  to 2600, in positive ion mode, ESI spray voltage 4500 V, nitrogen gas 35psi, drying gas flow 11.5mL/min, fragmentor voltage 20 V. TGA analysis was carried out heating under air stream from 40 °C at 10 °C/min in a TGA7 Perkin Elmer instrument. XRD patterns were collected by using a PANalytical X'PertPro diffractometer equipped with a fast solid state X'Celerator detector and a copper target ( $\lambda = 0.15418$  nm). Data were acquired in the 9 – 60° 2 $\theta$  interval, by collecting data for 50 s at each 0.05° step. For TEM investigations, a small amount of powder was dispersed in ethanol and submitted to ultrasonication. A drop of the calcium phosphate suspension was transferred onto holey carbon foils supported on conventional copper microgrids. A Philips CM 100 transmission electron microscope operating at 80 kV was used.

### 2.13.2 Synthetic general procedures

#### *General procedure for EOM-protection (GP1)*

A solution of the desired methyl ester (1 equiv) in THF (1.5 mL/mmol) was added dropwise to a suspension of NaH (60% in mineral oil) in THF (5 mL/mmol) at 0 °C under inert atmosphere. After 10 min a solution of chloromethylethylether (EOMCl) in THF (2.2 mL/mmol) was added dropwise and the reaction mixture was allowed to warm to room temperature and monitored by TLC. After 2 h the reaction was quenched with a saturated NaHCO<sub>3</sub> solution until pH 10 at 0 °C and extracted with EtOAc (3  $\times$  15 mL). The organic extracts were dried over Na<sub>2</sub>SO<sub>4</sub> and concentrated to obtain the desired EOM-protected compound. The crude was purified by flash-chromatography when specified.

#### *General procedure for hydrolysis of methyl esters (GP2)*

A stirred solution of the desired methyl ester in a mixture of THF/CH<sub>3</sub>OH 4:1 (4 mL/mmol) was treated with 5 M NaOH (1 mL/mmol). The reaction mixture was heated at 40 °C until consumption of the starting material. At completion (4 h, TLC monitoring), EtOAc (10 mL) was added and the organic phase was separated and discarded. The aqueous phase was then cooled to 0 °C, adjusted to pH 5 with HCl 1M and then extracted with

EtOAc (3 × 15 mL). The collected organic layers were dried on Na<sub>2</sub>SO<sub>4</sub> and concentrated to afford the corresponding carboxylic acid.

#### *General procedure for alcohol-acid coupling (GP3)*

To a solution of alcohol **A** (1 equiv) in CH<sub>2</sub>Cl<sub>2</sub> (10 mL/mmol) under inert atmosphere, the desired acid (1.58 equiv) and DMAP (0.2 equiv) were added. The mixture was then cooled to 0 °C and DCC (1.58 equiv) was added; the system was allowed to reach room temperature in 15 min and left under stirring overnight. After 16 h (TLC monitoring) the reaction mixture was quenched with water at 0 °C and extracted with CH<sub>2</sub>Cl<sub>2</sub> (3 × 15 mL). The collected organic phases were dried on Na<sub>2</sub>SO<sub>4</sub> and evaporated. The residue was treated with EtOAc (1 × 20 mL) at 0 °C and filtered to separate dicyclohexylurea precipitate. The solution was then evaporated and purified by flash-chromatography to afford the desired β-lactam functionalized with *O*-protected polyphenolic residue.

#### *General procedure for EOM-deprotection or Boc-deprotection (GP4)*

A stirred solution of the *O*-EOM-protected or *N*-Boc-protected β-lactam (1 equiv) in CH<sub>2</sub>Cl<sub>2</sub> (18.5 mL/mmol) under inert atmosphere was treated with aliquots of trifluoroacetic acid at 0 °C every 60 min. After reaction completion (TLC monitoring), the solvent and the trifluoroacetic acid were evaporated. The crude was triturated with few drops of pentane to obtain the desired deprotected phenolic compound.

#### *General procedure for synthesis of isocyanates (GP5)*

A solution of the desired amine (0.375 mmol, 1 equiv) and triethylamine (105 μL, 0.75 mmol, 2 equiv) in anhydrous CH<sub>2</sub>Cl<sub>2</sub> (3.75 mL) was stirred under inert atmosphere. The mixture was then cooled to 0 °C and bis(trichloromethyl) carbonate (223 mg, 0.75 mmol, 2 equiv) was added in one portion. The mixture was warmed to room temperature and then refluxed. The reaction was monitored through IR spectroscopy (N=C=O stretching at 2274 cm<sup>-1</sup>). After 3 h, the solvent was evaporated under vacuum avoiding any air exposure. The crude isocyanate was washed with anhydrous diethyl ether and filtered under nitrogen (5 × 4 mL) to remove the white precipitate, stored under inert atmosphere and immediately used.

#### *General procedure for synthesis of carbamates (GP6)*

A solution of alcohol **A** (40 mg, 0.15 mmol, 1 equiv) in anhydrous CH<sub>2</sub>Cl<sub>2</sub> (1.5 mL) was stirred under inert atmosphere. The freshly prepared isocyanate (0.375 mmol, 2.5 equiv) diluted in anhydrous CH<sub>2</sub>Cl<sub>2</sub> (1 mL) was then added. After 5 min of stirring, TiCl<sub>4</sub> (1M in CH<sub>2</sub>Cl<sub>2</sub>, 15 μL, 0.015 mmol, 0.1 equiv) was added dropwise. After completion (TLC monitoring, 16 h) the mixture was quenched with water and extracted with CH<sub>2</sub>Cl<sub>2</sub> (3 × 10 mL). The combined organic extracts were dried over Na<sub>2</sub>SO<sub>4</sub>, filtered, concentrated under vacuum and purified by flash-chromatography (CH<sub>2</sub>Cl<sub>2</sub>/acetone 97:3 then 95:5) affording the desired carbamate as a waxy white solid.

#### *General procedure for the synthesis of thio-alkyl and thio-aryl β-lactams (GP7)*

To a solution of the desired disulfide (1-1.25 equiv) in CH<sub>2</sub>Cl<sub>2</sub> (2 mL) under inert atmosphere, a solution of SO<sub>2</sub>Cl<sub>2</sub> (122 μL, 1.5 mmol, 1.5 equiv) in CH<sub>2</sub>Cl<sub>2</sub> (2 mL) was added dropwise at 0 °C. After 10 minutes, the desired azetidinone (1 mmol, 1 equiv) was introduced followed by the dropwise addition of TEA (277 μL, 2 mmol, 2 equiv). The mixture was stirred at reflux for 4 h, then cooled to room temperature, quenched with a saturated aqueous solution of NH<sub>4</sub>Cl (5 mL) and extracted with CH<sub>2</sub>Cl<sub>2</sub> (3 × 15 mL). The combined organic extracts were dried over Na<sub>2</sub>SO<sub>4</sub>, filtered and concentrated in vacuum. The crude was purified by flash-chromatography to yield the desired thio-alkylated or arylated β-lactam.

### 2.13.3 Synthesis of dual active antibacterial-antioxidant $\beta$ -lactams

Starting polyhydroxy benzoic and polyhydroxy cinnamic methyl esters are all known and were prepared according to reported procedures with methanol and sulfuric acid as catalyst.<sup>106</sup> Protected esters **2.a**, **2.b**, **2.e** are known and were prepared by following a literature procedure;<sup>48</sup> acids **3.a**, **3.b**, and **3.e** are known; alcohol **A**, ester **2.h** and acid **3.h** were prepared as previously reported.<sup>39e</sup>

#### *Methyl 4-(ethoxymethoxy)benzoate (2.c)*

Following GP1, *p*-hydroxybenzoic acid methyl ester (395 mg, 2.60 mmol), NaH (208 mg, 5.20 mmol) and EOMCl (482  $\mu$ L, 5.20 mmol) yielded compound **2.c** as a colorless oil (502 mg, 91%). IR (film,  $\text{cm}^{-1}$ ) 2978, 1720, 1607, 1510, 1435, 1279;  $^1\text{H}$  NMR (400 MHz,  $\text{CDCl}_3$ )  $\delta$  (ppm) 1.21 (t,  $J = 7.1$  Hz, 3H), 3.72 (q,  $J = 7.1$  Hz, 2H), 3.87 (s, 3H), 5.26 (s, 2H), 7.05 (d,  $J = 8.9$  Hz, 2H), 7.97 (d,  $J = 8.9$  Hz, 2H);  $^{13}\text{C}$  NMR (100 MHz,  $\text{CDCl}_3$ )  $\delta$  (ppm) 15.0, 51.8, 64.5, 92.8, 115.6, 123.4, 131.4, 161.1, 166.7; ESI-MS ( $R_t = 8.8$  min)  $m/z$  211  $[\text{M}+\text{H}]^+$ .

#### *Methyl 3,4-bis(ethoxymethoxy)benzoate (2.d)*

Following GP1, 3,4-dihydroxy-benzoic acid methyl ester (193 mg, 1.15 mmol), NaH (184 mg, 4.60 mmol) and EOMCl (427  $\mu$ L, 4.60 mmol) yielded compound **2.d** as a colorless oil (163 mg, 50%) after flash-chromatography purification (cyclohexane/EtOAc 75:25). IR (film,  $\text{cm}^{-1}$ ) 2978, 1719, 1602, 1510, 1440, 1290;  $^1\text{H}$  NMR (400 MHz,  $\text{CDCl}_3$ )  $\delta$  (ppm) 1.18 – 1.25 (m, 6H), 3.72 – 3.81 (m, 4H), 3.88 (s, 3H), 5.32 (d,  $J = 9.6$  Hz, 4H), 7.20 (d,  $J = 8.6$  Hz, 1H), 7.66 – 7.71 (m, 1H), 7.80 – 7.83 (m, 1H);  $^{13}\text{C}$  NMR (100 MHz,  $\text{CDCl}_3$ )  $\delta$  (ppm) 15.0, 52.0, 64.5, 64.6, 93.6, 94.1, 115.1, 117.7, 123.9, 124.7, 146.6, 151.5, 166.6; ESI-MS ( $R_t = 9.5$  min)  $m/z$  285  $[\text{M}+\text{H}]^+$ .

#### *(E)-methyl 3-(4-(ethoxymethoxy)phenyl)acrylate (2.f)*

Following GP1, methyl 3-(4-hydroxyphenyl)acrylate (523 mg, 2.93 mmol), NaH (235 mg, 5.88 mmol) and EOMCl (546  $\mu$ L, 5.88 mmol) yielded compound **2.f** as a colorless oil (701 mg, 98%). IR (film,  $\text{cm}^{-1}$ ) 2950, 1714, 1634, 1604, 1511, 1434, 1230;  $^1\text{H}$  NMR (400 MHz,  $\text{CDCl}_3$ )  $\delta$  (ppm) 1.20 (t,  $J = 7.0$  Hz, 3H), 3.70 (q,  $J = 7.0$  Hz, 2H), 3.77 (s, 3H), 5.22 (s, 2H), 6.31 (d,  $J = 16.0$  Hz, 1H), 7.02 (d,  $J = 8.7$  Hz, 2H), 7.44 (d,  $J = 8.7$  Hz, 2H), 7.63 (d,  $J = 16.0$  Hz, 1H);  $^{13}\text{C}$  NMR (100 MHz,  $\text{CDCl}_3$ )  $\delta$  (ppm) 15.0, 51.4, 64.4, 92.8, 115.6, 116.4, 127.9, 129.5, 144.3, 159.1, 167.5; ESI-MS ( $R_t = 10.8$  min)  $m/z$  237  $[\text{M}+\text{H}]^+$ .

#### *(E)-methyl 3-(2-(ethoxymethoxy)phenyl)acrylate (2.g)*

Following GP1, methyl (2*E*)-3-(2-hydroxyphenyl)-2-propenoate (539 mg, 3.03 mmol), NaH (242 mg, 6.06 mmol) and EOMCl (562  $\mu$ L, 6.06 mmol) yielded compound **2.g** as a colorless oil (584 mg, 82%) after flash-chromatography (cyclohexane/EtOAc 70:30). IR (film,  $\text{cm}^{-1}$ ) 2961, 1716, 1636, 1601, 1511, 1448, 1251;  $^1\text{H}$  NMR (400 MHz,  $\text{CDCl}_3$ )  $\delta$  (ppm) 1.22 (t,  $J = 7.1$  Hz, 3H), 3.75 (q,  $J = 7.1$  Hz, 2H), 3.81 (s, 3H), 5.30 (s, 2H), 6.50 (d,  $J = 16.2$  Hz, 1H), 6.99 – 7.03 (m, 1H), 7.19 (dd,  $J = 8.4, 0.8$  Hz, 1H), 7.31 – 7.35 (m, 1H), 7.53 (dd,  $J = 7.7, 1.6$  Hz, 1H), 8.03 (d,  $J = 16.2$  Hz, 1H);  $^{13}\text{C}$  NMR (100 MHz,  $\text{CDCl}_3$ )  $\delta$  (ppm) 15.1, 51.6, 64.6, 93.2, 114.8, 118.3, 121.7, 124.0, 128.4, 131.5, 140.1, 156.2, 167.8; ESI-MS ( $R_t = 9.4$  min)  $m/z$  237  $[\text{M}+\text{H}]^+$ .

#### *(E)-methyl 3-(4-(ethoxymethoxy)-3-methoxyphenyl)acrylate (2.i)*

Following GP1, methyl 3-(4-hydroxy-3-methoxyphenyl)acrylate (139 mg, 0.67 mmol), NaH (67 mg, 1.68 mmol) and EOMCl (124  $\mu$ L, 1.34 mmol) yielded compound **2.i** as a colorless oil (159 mg, 89%). IR (film,  $\text{cm}^{-1}$ ) 2923, 1702, 1637, 1582, 1510, 1461, 1256;  $^1\text{H}$  NMR (400 MHz,  $\text{CDCl}_3$ )  $\delta$  (ppm) 1.17 (t,  $J = 7.1$  Hz, 3H), 3.70 (q,  $J = 7.1$  Hz, 2H), 3.74 (s, 3H), 3.85 (s, 3H), 5.25 (s, 2H), 6.28 (d,  $J = 15.9$  Hz, 1H), 7.01 – 7.13 (m,



3H), 7.58 (d,  $J = 15.9$  Hz, 1H);  $^{13}\text{C}$  NMR (100 MHz,  $\text{CDCl}_3$ )  $\delta$  (ppm) 14.9, 51.4, 55.7, 64.3, 93.7, 110.2, 115.7, 115.8, 122.0, 128.4, 144.5, 148.6, 149.6, 167.3; ESI-MS ( $R_t = 8.7$  min)  $m/z$  267  $[\text{M}+\text{H}]^+$ .

*(E)*-methyl 3-(4-(ethoxymethoxy)-3,5-dimethoxyphenyl)acrylate (**2.j**)

Following GP1, methyl 3-(4-hydroxy-3,5-dimethoxyphenyl)acrylate (470 mg, 1.97 mmol), NaH (197 mg, 4.93 mmol) and EOMCl (366  $\mu\text{L}$ , 3.94 mmol) yielded compound **2.j** as a colorless oil (582 mg, 99%). IR (film,  $\text{cm}^{-1}$ ): 2926, 1714, 1636, 1587, 1505, 1454, 1277;  $^1\text{H}$  NMR (400 MHz,  $\text{CDCl}_3$ )  $\delta$  (ppm) 1.13 (t,  $J = 7.1$  Hz, 3H), 3.72 (s, 3H), 3.79 (s, 6H), 3.81 (q,  $J = 7.1$  Hz, 2H), 5.11 (s, 2H), 6.28 (d,  $J = 15.9$  Hz, 1H), 6.68 (s, 2H), 7.53 (d,  $J = 15.9$  Hz, 1H);  $^{13}\text{C}$  NMR (100 MHz,  $\text{CDCl}_3$ )  $\delta$  (ppm) 14.8, 51.4, 55.8, 64.7, 96.4, 105.0, 116.9, 130.1, 136.5, 144.7, 153.4, 167.1; ESI-MS ( $R_t = 8.2$  min)  $m/z$  297  $[\text{M}+\text{H}]^+$ .

4-(ethoxymethoxy)benzoic acid (**3.c**)

Following GP2, ester **2.c** (210 mg, 1.00 mmol) yielded acid **3.c** as a white solid (121 mg, 62%). Mp 118 – 119  $^\circ\text{C}$ ; IR (film,  $\text{cm}^{-1}$ ) 3418, 2983, 1688, 1603, 1427, 1291;  $^1\text{H}$  NMR (400 MHz,  $\text{CD}_3\text{OD}$ )  $\delta$  (ppm) 1.19 (t,  $J = 7.1$  Hz, 3H), 3.72 (q,  $J = 7.1$  Hz, 2H), 5.30 (s, 2H), 7.08 (d,  $J = 8.8$  Hz, 2H), 7.96 (d,  $J = 8.8$  Hz, 2H);  $^{13}\text{C}$  NMR (100 MHz,  $\text{CD}_3\text{OD}$ )  $\delta$  (ppm) 15.5, 65.5, 93.9, 116.7, 125.0, 132.7, 162.7, 169.7; ESI-MS ( $R_t = 5.9$  min)  $m/z$  195  $[\text{M}-\text{H}]^+$ .

3,4-bis(ethoxymethoxy)benzoic acid (**3.d**)

Following GP2, ester **2.d** (163 mg, 0.57 mmol) yielded acid **3.d** as a waxy white solid (138 mg, 90%). IR (film,  $\text{cm}^{-1}$ ) 3404, 2976, 1687, 1599, 1512, 1443, 1296;  $^1\text{H}$  NMR (400 MHz,  $\text{CDCl}_3$ )  $\delta$  (ppm) 1.18 – 1.24 (m, 6H), 3.72 – 3.80 (m, 4H), 5.31 (s, 2H), 5.34 (s, 2H), 7.22 (d,  $J = 8.6$  Hz, 1H), 7.75 (d,  $J = 8.6$  Hz, 1H), 7.88 (s, 1H);  $^{13}\text{C}$  NMR (100 MHz,  $\text{CDCl}_3$ )  $\delta$  (ppm) 15.0, 64.6, 64.7, 93.6, 94.1, 115.0, 118.2, 123.0, 125.5, 146.6, 152.2, 171.6; ESI-MS ( $R_t = 10.0$  min)  $m/z$  288  $[\text{M}+\text{H}_2\text{O}]^+$ .

*(E)*-3-(4-(ethoxymethoxy)phenyl)acrylic acid (**3.f**)

Following GP2, ester **2.f** (236 mg, 1 mmol) yielded acid **3.f** as a white solid (212 mg, 95%). Mp 152 – 154  $^\circ\text{C}$ ; IR (film,  $\text{cm}^{-1}$ ): 3424, 2973, 1670, 1627, 1603, 1511, 1429, 1264;  $^1\text{H}$  NMR (400 MHz,  $\text{CDCl}_3$ )  $\delta$  (ppm) 1.23 (t,  $J = 7.1$  Hz, 3H), 3.73 (q,  $J = 7.1$  Hz, 2H), 5.26 (s, 2H), 6.33 (d,  $J = 15.9$  Hz, 1H), 7.06 (d,  $J = 8.6$  Hz, 2H), 7.50 (d,  $J = 8.6$  Hz, 2H), 7.74 (d,  $J = 15.9$  Hz, 1H);  $^{13}\text{C}$  NMR (100 MHz,  $\text{CDCl}_3$ )  $\delta$  (ppm) 15.1, 64.5, 92.9, 115.1, 116.5, 127.7, 130.0, 146.6, 159.5, 172.5; ESI-MS ( $R_t = 6.8$  min)  $m/z$  223  $[\text{M}+\text{H}]^+$ .

*(E)*-3-(2-(ethoxymethoxy)phenyl)acrylic acid (**3.g**)

Following GP2, ester **2.g** (236 mg, 1 mmol) yielded acid **3.g** as a waxy white solid (164 mg, 74%). IR (film,  $\text{cm}^{-1}$ ) 3419, 2974, 1677, 1634, 1601, 1510, 1435, 1271;  $^1\text{H}$  NMR (400 MHz,  $\text{CD}_3\text{OD}$ )  $\delta$  (ppm) 1.16 (t,  $J = 7.1$  Hz, 3H), 3.70 (q,  $J = 7.1$  Hz, 2H), 5.27 (s, 2H), 6.49 (d,  $J = 16.2$  Hz, 1H), 6.98 (t,  $J = 7.5$  Hz, 1H), 7.15 (d,  $J = 8.3$  Hz, 1H), 7.30 (t,  $J = 7.8$  Hz, 1H), 7.55 (d,  $J = 7.7$  Hz, 1H), 8.01 (d,  $J = 16.2$  Hz, 1H);  $^{13}\text{C}$  NMR (100 MHz,  $\text{CD}_3\text{OD}$ )  $\delta$  (ppm) 15.4, 65.6, 94.4, 116.0, 119.5, 122.9, 125.1, 129.3, 132.6, 141.4, 157.3, 170.7; ESI-MS ( $R_t = 7.0$  min)  $m/z$  221  $[\text{M}-\text{H}]^+$ .

*(E)*-3-(4-(ethoxymethoxy)-3-methoxyphenyl)acrylic acid (**3.i**)

Following GP2, ester **2.i** (267 mg, 1 mmol) yielded acid **3.i** as a white solid (217 mg, 86%). Mp 131 – 133  $^\circ\text{C}$ ; IR (film,  $\text{cm}^{-1}$ ) 3423, 2904, 1671, 1625, 1583, 1509, 1424, 1254;  $^1\text{H}$  NMR (400 MHz,  $\text{CDCl}_3$ )  $\delta$  (ppm) 1.22 (t,  $J = 7.1$  Hz, 3H), 3.77 (q,  $J = 7.1$  Hz, 2H), 3.91 (s, 3H), 5.32 (s, 2H), 6.33 (d,  $J = 15.9$  Hz, 1H), 7.08 – 7.21 (m, 3H), 7.73 (d,  $J = 15.9$  Hz, 1H);  $^{13}\text{C}$  NMR (100 MHz,  $(\text{CD}_3)_2\text{CO}$ )  $\delta$  (ppm) 15.4, 56.2, 64.9, 94.6, 111.9, 117.3, 117.4, 123.0, 129.8, 145.5, 149.7, 151.4, 167.9; ESI-MS ( $R_t = 5.9$  min)  $m/z$  253  $[\text{M}+\text{H}]^+$ .

*(E)*-3-(4-(ethoxymethoxy)-3,5-dimethoxyphenyl)acrylic acid (**3.j**)

Following GP2, ester **2.j** (237 mg, 0.8 mmol) yielded acid **3.j** as a white solid (187 mg, 83%). Mp 110 – 112 °C; IR (film, cm<sup>-1</sup>) 3423, 2921, 1675, 1627, 1449, 1250; <sup>1</sup>H NMR (400 MHz, (CD<sub>3</sub>)<sub>2</sub>CO) δ (ppm) 1.14 (t, *J* = 7.1 Hz, 3H), 3.85 (q, *J* = 7.1 Hz, 2H), 3.90 (s, 6H), 5.10 (s, 2H), 6.50 (d, *J* = 15.9 Hz, 1H), 7.03 (s, 2H), 7.61 (d, *J* = 15.9 Hz, 1H); <sup>13</sup>C NMR (100 MHz, (CD<sub>3</sub>)<sub>2</sub>CO) δ (ppm) 15.4, 56.2, 64.9, 94.6, 111.9, 117.2, 117.3, 123.0, 129.7, 145.5, 149.7, 151.4, 168.2; ESI-MS (*R*<sub>t</sub> = 6.4 min) *m/z* 283 [M+H]<sup>+</sup>.

*(R)*-1-((*S,Z*)-2-(2-(benzyloxy)-2-oxoethylidene)-4-oxoazetidin-3-yl)ethylbenzo[d][1,3]dioxole-5-carboxylate (**1.a**)

Following GP3, alcohol **A** (55 mg, 0.21 mmol) and acid **3.a** (55 mg, 0.33 mmol) yielded compound **1.a** as a waxy solid (28 mg, 33%) after flash-chromatography purification (CH<sub>2</sub>Cl<sub>2</sub>/acetone 99:1). IR (film, cm<sup>-1</sup>) 3286, 2980, 1820, 1701, 1657, 1489, 1259; [α]<sup>20</sup><sub>D</sub> = -24 (c = 0.8, CH<sub>2</sub>Cl<sub>2</sub>); <sup>1</sup>H NMR (400 MHz, CDCl<sub>3</sub>) δ (ppm) 1.50 (d, *J* = 6.4 Hz, 3H), 4.00 (d, *J* = 6.8 Hz, 1H), 5.14 (d, *J*<sub>AB</sub> = 12.3 Hz, 1H), 5.19 (d, *J*<sub>AB</sub> = 12.3 Hz, 1H), 5.25 (s, 1H), 5.45 (quintet, *J* = 6.4 Hz, 1H), 6.04 (s, 2H), 6.83 (d, *J* = 8.2 Hz, 1H), 7.30 – 7.39 (m, 5H), 7.42 (d, *J* = 1.5 Hz, 1H), 7.62 (dd, *J* = 1.5, 8.2 Hz, 1H), 8.65 (bs, 1H); <sup>13</sup>C NMR (100 MHz, CDCl<sub>3</sub>) δ (ppm) 18.0, 61.6, 66.2, 67.3, 90.6, 101.8, 108.1, 109.5, 123.5, 125.6, 128.2, 128.3, 128.6, 135.7, 147.8, 151.9, 152.1, 164.5, 164.6, 166.6; ESI-MS (*R*<sub>t</sub> = 10.1 min) *m/z* 427 [M+H<sub>2</sub>O]<sup>+</sup>. Found C, 64.72; H, 4.65; N, 3.40 %; C<sub>22</sub>H<sub>19</sub>NO<sub>7</sub> requires C, 64.54; H, 4.68; N, 3.42 %.

*(R)*-1-((*S,Z*)-2-(2-(benzyloxy)-2-oxoethylidene)-4-oxoazetidin-3-yl)ethyl benzo[d][1,3]dioxole-4-carboxylate (**1.b**)

Following GP3, alcohol **A** (35 mg, 0.13 mmol) and acid **3.b** (34 mg, 0.21 mmol) yielded compound **1.b** as a waxy solid (24 mg, 44%) after flash-chromatography purification (CH<sub>2</sub>Cl<sub>2</sub>/acetone 99:1). IR (film, cm<sup>-1</sup>) 3287, 2924, 1820, 1700, 1656, 1457, 1288; [α]<sup>20</sup><sub>D</sub> = -17 (c = 1.2, CH<sub>2</sub>Cl<sub>2</sub>); <sup>1</sup>H NMR (400 MHz, CDCl<sub>3</sub>) δ (ppm) 1.53 (d, *J* = 6.4 Hz, 3H), 3.99 (d, *J* = 6.7 Hz, 1H), 5.17 (s, 2H), 5.29 (s, 1H), 5.46 (quintet, *J* = 6.4 Hz, 1H), 5.97 – 6.01 (m, 2H), 6.85 (t, *J* = 8.0 Hz, 1H), 6.96 (dd, *J* = 1.1, 7.7 Hz, 1H), 7.30 – 7.38 (m, 6H), 8.67 (bs, 1H); <sup>13</sup>C NMR (100 MHz, CDCl<sub>3</sub>) δ (ppm) 18.3, 61.5, 66.1, 67.7, 90.7, 101.8, 112.4, 112.5, 121.3, 122.5, 128.2, 128.3, 128.6, 135.8, 148.7, 148.8, 152.2, 163.2, 164.6, 166.7; ESI-MS (*R*<sub>t</sub> = 10.0 min) *m/z* 427 [M+H<sub>2</sub>O]<sup>+</sup>. Found C, 64.69; H, 4.74; N, 3.37 %; C<sub>22</sub>H<sub>19</sub>NO<sub>7</sub> requires C, 64.54; H, 4.68; N, 3.42 %.

*(R)*-1-((*S,Z*)-2-(2-(benzyloxy)-2-oxoethylidene)-4-oxoazetidin-3-yl)ethyl 4-(ethoxymethoxy)benzoate (**4.c**)

Following GP3, alcohol **A** (39 mg, 0.15 mmol) and acid **3.c** (47 mg, 0.24 mmol) yielded compound **4.c** as a waxy solid (27 mg, 41%) after flash-chromatography purification (CH<sub>2</sub>Cl<sub>2</sub>/acetone 99:1). IR (film, cm<sup>-1</sup>) 3300, 2926, 1821, 1702, 1656, 1606, 1509, 1270; [α]<sup>20</sup><sub>D</sub> = -10 (c = 1.1, CH<sub>2</sub>Cl<sub>2</sub>); <sup>1</sup>H NMR (400 MHz, CDCl<sub>3</sub>) δ (ppm) 1.22 (t, *J* = 7.0 Hz, 3H), 1.51 (d, *J* = 6.3 Hz, 3H), 3.73 (q, *J* = 7.0 Hz, 2H), 4.01 (d, *J* = 6.7 Hz, 1H), 5.15 (d, *J*<sub>AB</sub> = 12.3 Hz, 1H), 5.19 (d, *J*<sub>AB</sub> = 12.3 Hz, 1H), 5.26 (s, 1H), 5.27 (s, 2H), 5.48 (quintet, *J* = 6.3 Hz, 1H), 7.06 (d, *J* = 8.7 Hz, 2H), 7.32 – 7.40 (m, 5H), 7.96 (d, *J* = 8.7 Hz, 2H), 8.67 (bs, 1H); <sup>13</sup>C NMR (100 MHz, CDCl<sub>3</sub>) δ (ppm) 15.0, 18.1, 61.6, 64.6, 66.2, 67.1, 90.6, 92.8, 115.8, 122.9, 128.2, 128.3, 128.6, 131.6, 135.8, 152.2, 161.4, 164.6, 164.9, 166.7; ESI-MS (*R*<sub>t</sub> = 10.9 min) *m/z* 457 [M+H<sub>2</sub>O]<sup>+</sup>.

*(R)*-1-((*S,Z*)-2-(2-(benzyloxy)-2-oxoethylidene)-4-oxoazetidin-3-yl)ethyl-3,4-bis(ethoxymethoxy) benzoate (**4.d**)

Following GP3, alcohol **A** (60 mg, 0.23 mmol) and acid **3.d** (98 mg, 0.36 mmol) yielded compound **4.d** as a yellow oil (44 mg, 37%) after flash-chromatography purification (CH<sub>2</sub>Cl<sub>2</sub>/diethyl ether 95:5). IR (film, cm<sup>-1</sup>) 3287, 2976, 1822, 1704, 1658, 1603, 1509, 1263; [α]<sup>20</sup><sub>D</sub> = -12 (c = 0.6, CH<sub>2</sub>Cl<sub>2</sub>); <sup>1</sup>H NMR (400 MHz, CDCl<sub>3</sub>) δ (ppm) 1.20 (t, *J* = 7.0 Hz, 3H), 1.21 (t, *J* = 7.0 Hz, 3H), 1.51 (d, *J* = 6.4 Hz, 3H), 3.72 – 3.81 (m, 4H), 4.00 (d, *J* = 6.7 Hz, 1H), 5.13 (d, *J*<sub>AB</sub> = 12.3 Hz, 1H), 5.18 (d, *J*<sub>AB</sub> = 12.3 Hz, 1H), 5.26 – 5.33 (m, 5H), 5.43 (quintet,

$J = 6.4$  Hz, 1H), 7.20 (d,  $J = 8.6$  Hz, 1H), 7.30 – 7.35 (m, 5H), 7.65 (dd,  $J = 1.8, 8.6$  Hz, 1H), 7.81 (d,  $J = 1.8$  Hz, 1H), 8.76 (bs, 1H);  $^{13}\text{C}$  NMR (100 MHz,  $\text{CDCl}_3$ )  $\delta$  (ppm) 14.99, 15.01, 18.2, 61.6, 64.5, 64.6, 66.1, 67.3, 90.6, 93.5, 94.0, 115.1, 117.7, 123.3, 124.7, 128.2, 128.3, 128.6, 135.7, 146.7, 151.7, 152.2, 164.7, 164.8, 166.6; ESI-MS ( $R_t = 11.5$  min)  $m/z$  531  $[\text{M}+\text{H}_2\text{O}]^+$ .

*(E)-(R)-1-((S,Z)-2-(2-(benzyloxy)-2-oxoethylidene)-4-oxoazetidin-3-yl)ethyl 3-(benzo[d][1,3]dioxol-5-yl)acrylate (1.e)*

Following GP3, alcohol **A** (67 mg, 0.25 mmol) and acid **3.e** (77 mg, 0.40 mmol) yielded compound **1.e** as a waxy solid (38 mg, 35%) after flash-chromatography purification ( $\text{CH}_2\text{Cl}_2/\text{acetone}$  98:2). IR (film,  $\text{cm}^{-1}$ ) 3286, 2924, 1821, 1704, 1657, 1510, 1256;  $[\alpha]^{20}_{\text{D}} = +9$  ( $c = 1.0, \text{CH}_2\text{Cl}_2$ );  $^1\text{H}$  NMR (400 MHz,  $\text{CDCl}_3$ )  $\delta$  (ppm) 1.46 (d,  $J = 6.4$  Hz, 3H), 3.95 (d,  $J = 6.8$  Hz, 1H), 5.15 (d,  $J_{\text{AB}} = 12.3$  Hz, 1H), 5.18 (d,  $J_{\text{AB}} = 12.3$  Hz, 1H), 5.27 (d,  $J = 0.6$  Hz, 1H), 5.36 (quintet,  $J = 6.4$  Hz, 1H), 6.01 (s, 2H), 6.23 (d,  $J = 15.9$  Hz, 1H), 6.81 (d,  $J = 7.9$  Hz, 1H), 6.98 – 7.03 (m, 2H), 7.32 – 7.37 (m, 5H), 7.59 (d,  $J = 15.9$  Hz, 1H), 8.51 (bs, 1H);  $^{13}\text{C}$  NMR (100 MHz,  $\text{CDCl}_3$ )  $\delta$  (ppm) 18.0, 61.5, 66.2, 66.7, 90.6, 101.6, 106.5, 108.5, 115.2, 124.7, 128.2, 128.3, 128.5, 128.6, 135.7, 145.5, 148.3, 149.8, 152.1, 164.7, 165.9, 166.7; ESI-MS ( $R_t = 10.4$  min)  $m/z$  392  $[\text{M}-43]^+$ . Found C, 66.47; H, 4.89; N, 3.28 %;  $\text{C}_{24}\text{H}_{21}\text{NO}_7$  requires C, 66.20; H, 4.86; N, 3.22 %.

*(E)-(R)-1-((S,Z)-2-(2-(benzyloxy)-2-oxoethylidene)-4-oxoazetidin-3-yl)ethyl-3-(4-ethoxymethoxy)phenyl)acrylate (4.f)*

Following GP3, alcohol **A** (67 mg, 0.25 mmol) and acid **3.f** (89 mg, 0.40 mmol) yielded compound **4.f** as a waxy solid (67 mg, 58%) after flash-chromatography purification (cyclohexane/EtOAc 75:25). IR (film,  $\text{cm}^{-1}$ ) 3286, 2924, 1821, 1704, 1658, 1454, 1256;  $^1\text{H}$  NMR (400 MHz,  $\text{CDCl}_3$ )  $\delta$  (ppm) 1.22 (t,  $J = 7.1$  Hz, 3H), 1.47 (d,  $J = 6.4$  Hz, 3H), 3.73 (q,  $J = 7.1$  Hz, 2H), 3.96 (d,  $J = 6.9$  Hz, 1H), 5.14 (d,  $J_{\text{AB}} = 12.3$  Hz, 1H), 5.18 (d,  $J_{\text{AB}} = 12.3$  Hz, 1H), 5.25 (s, 2H), 5.27 (s, 1H), 5.37 (quintet,  $J = 6.4$  Hz, 1H), 6.29 (d,  $J = 15.9$  Hz, 1H), 7.04 (d,  $J = 8.7$  Hz, 2H), 7.33 – 7.38 (m, 5H), 7.47 (d,  $J = 8.7$  Hz, 2H), 7.65 (d,  $J = 15.9$  Hz, 1H), 8.44 (bs, 1H); ESI-MS ( $R_t = 11.6$  min)  $m/z$  422  $[\text{M}-43]^+$ .

4.2.19. *(E)-(R)-1-((S,Z)-2-(2-(benzyloxy)-2-oxoethylidene)-4-oxoazetidin-3-yl)ethyl 3-(2-(ethoxymethoxy)phenyl)acrylate (4.g)*

Following GP3, alcohol **A** (40 mg, 0.15 mmol) and acid **3.g** (40 mg, 0.18 mmol) yielded compound **4.g** as a waxy solid (45 mg, 65%) after flash-chromatography purification (cyclohexane/EtOAc 75:25). IR (film,  $\text{cm}^{-1}$ ) 3284, 2933, 1821, 1702, 1657, 1631, 1542, 1457, 1264;  $[\alpha]^{20}_{\text{D}} = -16$  ( $c = 1.0, \text{CH}_2\text{Cl}_2$ );  $^1\text{H}$  NMR (400 MHz,  $\text{CDCl}_3$ )  $\delta$  (ppm) 1.21 (t,  $J = 7.1$  Hz, 3H), 1.48 (d,  $J = 6.4$  Hz, 3H), 3.74 (q,  $J = 7.1$  Hz, 2H), 3.97 (d,  $J = 7.0$  Hz, 1H), 5.16 (d,  $J_{\text{AB}} = 12.3$  Hz, 1H), 5.20 (d,  $J_{\text{AB}} = 12.3$  Hz, 1H), 5.29 (s, 3H), 5.38 (quintet,  $J = 6.4$  Hz, 1H), 6.48 (d,  $J = 16.2$  Hz, 1H), 7.01 (t,  $J = 7.5$  Hz, 1H), 7.19 (d,  $J = 8.3$  Hz, 1H), 7.32– 7.36 (m, 6H), 7.53 (d,  $J = 7.7$  Hz, 1H), 8.06 (d,  $J = 16.2$  Hz, 1H), 8.78 (bs, 1H);  $^{13}\text{C}$  NMR (100 MHz,  $\text{CDCl}_3$ )  $\delta$  (ppm) 15.0, 18.1, 61.5, 64.5, 66.1, 66.8, 90.5, 93.2, 114.9, 117.7, 121.7, 123.7, 128.2, 128.3, 128.4, 128.6, 131.7, 135.8, 141.0, 152.3, 156.2, 164.7, 166.1, 166.7; ESI-MS ( $R_t = 11.7$  min)  $m/z$  483  $[\text{M}+\text{H}_2\text{O}]^+$ .

*(E)-(R)-1-((S,Z)-2-(2-(benzyloxy)-2-oxoethylidene)-4-oxoazetidin-3-yl)ethyl-3-(3,4-bis(ethoxy methoxy)phenyl)acrylate (4.h)*

Following GP3, alcohol **A** (65 mg, 0.25 mmol) and acid **3.h** (116 mg, 0.39 mmol) yielded compound **4.h** as a yellow oil (51 mg, 38%) after flash-chromatography purification ( $\text{CH}_2\text{Cl}_2/\text{diethyl ether}$  95:5). IR (film,  $\text{cm}^{-1}$ ) 3266, 2973, 1820, 1701, 1655, 1638, 1510, 1251;  $[\alpha]^{20}_{\text{D}} = +6$  ( $c = 1.0, \text{CH}_2\text{Cl}_2$ );  $^1\text{H}$  NMR (400 MHz,  $\text{CDCl}_3$ )  $\delta$  (ppm) 1.20 – 1.25 (m, 6H), 1.46 (d,  $J = 6.3$  Hz, 3H), 3.73 – 3.80 (m, 4H), 3.96 (d,  $J = 7.0$  Hz, 1H), 5.14 (d,  $J_{\text{AB}} = 12.4$  Hz, 1H), 5.19 (d,  $J_{\text{AB}} = 12.4$  Hz, 1H), 5.27 (s, 1H), 5.30 (s, 2H), 5.31 (s, 2H), 5.37 (quintet,  $J = 6.3$  Hz, 1H), 6.29 (d,  $J = 15.9$  Hz, 1H), 7.12 – 7.19 (m, 2H), 7.32 – 7.37 (m, 6H), 7.61 (d,  $J = 15.9$  Hz, 1H), 8.66 (bs, 1H);  $^{13}\text{C}$  NMR (100 MHz,  $\text{CDCl}_3$ )  $\delta$  (ppm) 15.0, 15.1, 18.0, 61.5, 64.5, 64.6, 66.2, 66.8, 90.6, 93.7, 94.0,

115.5, 115.6, 115.9, 123.1, 123.5, 128.2, 128.3, 128.6, 135.7, 145.5, 147.4, 149.5, 152.1, 164.7, 165.9, 166.7; ESI-MS ( $R_t = 12.1$  min)  $m/z$  557  $[M+H_2O]^+$ .

*(E)-(R)-1-((S,Z)-2-(2-(benzyloxy)-2-oxoethylidene)-4-oxoazetidin-3-yl)ethyl 3-(4-(ethoxymethoxy)-3-methoxyphenyl)acrylate (4.i)*

Following GP3, alcohol **A** (40 mg, 0.15 mmol) and acid **3.i** (61 mg, 0.24 mmol) yielded compound **4.i** as a waxy solid (27 mg, 36%) after flash-chromatography purification ( $CH_2Cl_2$ /acetone 98:2). IR (film,  $cm^{-1}$ ) 3287, 2924, 1821, 1704, 1657, 1510, 1256;  $^1H$  NMR (400 MHz,  $CDCl_3$ )  $\delta$  (ppm) 1.22 (t,  $J = 7.1$  Hz, 3H), 1.47 (d,  $J = 6.4$  Hz, 3H), 3.77 (q,  $J = 7.1$  Hz, 2H), 3.92 (s, 3H), 3.97 (d,  $J = 6.8$  Hz, 1H), 5.14 (d,  $J_{AB} = 12.3$  Hz, 1H), 5.18 (d,  $J_{AB} = 12.3$  Hz, 1H), 5.28 (s, 1H), 5.32 (s, 2H), 5.38 (quintet,  $J = 6.4$  Hz, 1H), 6.29 (d,  $J = 15.9$  Hz, 1H), 7.06 (s, 1H), 7.07 (d,  $J = 8.1$  Hz, 1H), 7.18 (d,  $J = 8.1$  Hz, 1H), 7.33 – 7.37 (m, 5H), 7.64 (d,  $J = 15.9$  Hz, 1H), 8.47 (bs, 1H);  $^{13}C$  NMR (100 MHz,  $(CD_3)_2CO$ )  $\delta$  (ppm) 15.4, 18.4, 56.2, 62.3, 65.0, 66.0, 67.5, 90.4, 94.6, 111.8, 116.5, 117.2, 123.5, 128.8, 129.0, 129.3, 129.5, 137.8, 146.2, 151.4, 153.5, 154.2, 166.2, 166.4, 166.7; ESI-MS ( $R_t = 10.9$  min)  $m/z$  452  $[M-43]^+$ .

*(E)-(R)-1-((S,Z)-2-(2-(benzyloxy)-2-oxoethylidene)-4-oxoazetidin-3-yl)ethyl 3-(4-(ethoxymethoxy)-3,5-dimethoxyphenyl)acrylate (4.j)*

Following GP3, alcohol **A** (40 mg, 0.15 mmol) and acid **3.j** (68 mg, 0.24 mmol) yielded compound **4.j** as a waxy solid (30 mg, 38%) after flash-chromatography purification ( $CH_2Cl_2$ /acetone 98:2). IR (film,  $cm^{-1}$ ) 3289, 2925, 1736, 1649, 1584, 1504, 1454;  $^1H$  NMR (400 MHz,  $CDCl_3$ )  $\delta$  (ppm) 1.21 (t,  $J = 7.1$  Hz, 3H), 1.47 (d,  $J = 6.4$  Hz, 3H), 3.87 (s, 6H), 3.88 (q,  $J = 7.1$  Hz, 2H), 3.97 (d,  $J = 6.7$  Hz, 1H), 5.15 (d,  $J_{AB} = 12.3$  Hz, 1H), 5.18 (d,  $J_{AB} = 12.3$  Hz, 1H), 5.19 (s, 2H), 5.28 (s, 1H), 5.38 (quintet,  $J = 6.4$  Hz, 1H), 6.32 (d,  $J = 15.9$  Hz, 1H), 6.75 (s, 2H), 7.33 – 7.36 (m, 5H), 7.61 (d,  $J = 15.9$  Hz, 1H), 8.56 (bs, 1H);  $^{13}C$  NMR (100 MHz,  $CDCl_3$ )  $\delta$  (ppm) 15.0, 17.9, 56.1, 61.5, 62.1, 65.0, 66.2, 66.8, 90.7, 96.6, 105.3, 116.5, 128.2, 128.4, 128.7, 130.0, 135.7, 136.8, 145.9, 152.0, 153.6, 164.5, 165.7, 166.7; ESI-MS ( $R_t = 11.5$  min)  $m/z$  543  $[M+H_2O]^+$ .

*(R)-1-((S,Z)-2-(2-(benzyloxy)-2-oxoethylidene)-4-oxoazetidin-3-yl)ethyl 4-hydroxybenzoate (1.c)*

Following GP4,  $\beta$ -lactam **4.c** (27 mg, 61  $\mu$ mol) treated with TFA (126  $\mu$ L, 1.68 mmol) yielded compound **1.c** as a yellow oil (23 mg, 99%). IR (film,  $cm^{-1}$ ) 3304, 2982, 1818, 1697, 1662, 1608, 1592, 1269;  $[\alpha]_D^{20} = -5$  ( $c = 1.0$ ,  $CH_2Cl_2$ );  $^1H$  NMR (400 MHz,  $CDCl_3$ )  $\delta$  (ppm) 1.51 (d,  $J = 6.3$  Hz, 3H), 4.02 (d,  $J = 6.5$  Hz, 1H), 5.14 (d,  $J_{AB} = 12.0$  Hz, 1H), 5.19 (d,  $J_{AB} = 12.0$  Hz, 1H), 5.30 (d,  $J = 1.7$  Hz, 1H), 5.47 (quintet,  $J = 6.3$  Hz, 1H), 6.83 (d,  $J = 7.2$  Hz, 2H), 7.31 – 7.40 (m, 5H), 7.89 (d,  $J = 7.2$  Hz, 2H), 8.67 (bs, 1H);  $^{13}C$  NMR (100 MHz,  $CDCl_3$ )  $\delta$  (ppm) 18.0, 61.6, 66.5, 67.1, 91.0, 115.4, 121.5, 128.2, 128.4, 128.7, 132.1, 135.4, 152.1, 160.6, 165.6, 165.7, 167.0; ESI-MS ( $R_t = 8.6$  min)  $m/z$  399  $[M+H_2O]^+$ . Found C, 66.20; H, 4.90; N, 3.58 %  $C_{21}H_{19}NO_6$  requires C, 66.13; H, 5.02; N, 3.67 %.

*(R)-1-((S,Z)-2-(2-(benzyloxy)-2-oxoethylidene)-4-oxoazetidin-3-yl)ethyl 3,4-dihydroxybenzoate (1.d)*

Following GP4,  $\beta$ -lactam **4.d** (36 mg, 70  $\mu$ mol) treated with TFA (210  $\mu$ L, 2.85 mmol) yielded compound as a yellow oil **1.d** (27 mg, 99%). IR (film,  $cm^{-1}$ ) 3356, 2925, 1815, 1694, 1657, 1604, 1524, 1293;  $[\alpha]_D^{20} = -13$  ( $c = 0.9$ ,  $CH_3OH$ );  $^1H$  NMR (400 MHz,  $(CD_3)_2CO$ )  $\delta$  (ppm) 1.48 (d,  $J = 6.4$  Hz, 3H), 4.22 (d,  $J = 6.3$  Hz, 1H), 5.14 (d,  $J_{AB} = 12.4$  Hz, 1H), 5.20 (d,  $J_{AB} = 12.4$  Hz, 1H), 5.25 (s, 1H), 5.42 (quintet,  $J = 6.3$  Hz, 1H), 6.89 (d,  $J = 8.3$  Hz, 1H), 7.29 – 7.50 (m, 7H), 9.89 (bs, 1H);  $^{13}C$  NMR (100 MHz,  $(CD_3)_2CO$ )  $\delta$  (ppm) 18.4, 62.4, 65.9, 67.8, 90.4, 115.8, 117.2, 122.5, 123.4, 128.8, 128.9, 129.2, 137.8, 145.7, 151.1, 154.2, 165.5, 166.3, 166.6; ESI-MS ( $R_t = 8.8$  min)  $m/z$  415  $[M+H_2O]^+$ . Found C, 63.49; H, 4.85; N, 3.56 %;  $C_{21}H_{19}NO_7$  requires C, 63.47; H, 4.82; N, 3.52 %.

*(E)-(R)-1-((S,Z)-2-(2-(benzyloxy)-2-oxoethylidene)-4-oxoazetidin-3-yl)ethyl 3-(4-hydroxyphenyl) acrylate*  
**(1.f)**

Following GP4,  $\beta$ -lactam **4.f** (50 mg, 107  $\mu$ mol) treated with TFA (85  $\mu$ L, 1.13 mmol) yielded compound **1.f** as a yellow oil (43 mg, 99%). IR (film,  $\text{cm}^{-1}$ ) 3405, 3286, 2929, 1819, 1650, 1515, 1453, 1257;  $[\alpha]_{\text{D}}^{20} = +6$  ( $c = 1.0$ ,  $\text{CH}_2\text{Cl}_2$ );  $^1\text{H}$  NMR (400 MHz,  $\text{CDCl}_3$ )  $\delta$  (ppm) 1.46 (d,  $J = 6.4$  Hz, 3H), 3.75 (bs, 1H), 3.97 (d,  $J = 6.6$  Hz, 1H), 5.15 (d,  $J_{\text{AB}} = 12.4$  Hz, 1H), 5.19 (d,  $J_{\text{AB}} = 12.4$  Hz, 1H), 5.28 (s, 1H), 5.37 (quintet,  $J = 6.4$  Hz, 1H), 6.25 (d,  $J = 15.9$  Hz, 1H), 6.84 (d,  $J = 8.5$  Hz, 2H), 7.33 – 7.38 (m, 5H), 7.40 (d,  $J = 8.5$  Hz, 2H), 7.62 (d,  $J = 15.9$  Hz, 1H), 8.53 (bs, 1H);  $^{13}\text{C}$  NMR (100 MHz,  $\text{CDCl}_3$ )  $\delta$  (ppm) 18.0, 61.5, 66.3, 66.6, 90.7, 114.4, 115.9, 126.6, 128.2, 128.4, 128.6, 130.1, 135.7, 145.7, 152.1, 158.4, 164.9, 166.2, 166.7; ESI-MS ( $R_{\text{t}} = 8.9$  min)  $m/z$  364  $[\text{M}-43]^+$ . Found C, 67.71; H, 5.13; N, 3.38 %;  $\text{C}_{23}\text{H}_{21}\text{NO}_6$  requires C, 67.80; H, 5.20; N, 3.44 %.

*(E)-(R)-1-((S,Z)-2-(2-(benzyloxy)-2-oxoethylidene)-4-oxoazetidin-3-yl)ethyl 3-(2-hydroxyphenyl)acrylate*  
**(1.g)**

Following GP4,  $\beta$ -lactam **4.g** (38 mg, 82  $\mu$ mol) treated with TFA (120  $\mu$ L, 1.60 mmol) yielded compound **1.g** as a yellow oil (33 mg, 99%). IR (film,  $\text{cm}^{-1}$ ) 3386, 3282, 2934, 1822, 1702, 1662, 1629, 1604, 1458, 1249;  $[\alpha]_{\text{D}}^{20} = -14$  ( $c = 1.0$ ,  $\text{CH}_2\text{Cl}_2$ );  $^1\text{H}$  NMR (400 MHz,  $(\text{CD}_3)_2\text{CO}$ )  $\delta$  (ppm) 1.45 (d,  $J = 6.3$  Hz, 3H), 4.16 (d,  $J = 6.6$  Hz, 1H), 5.15 (d,  $J_{\text{AB}} = 12.5$  Hz, 1H), 5.19 (d,  $J_{\text{AB}} = 12.5$  Hz, 1H), 5.28 (s, 1H), 5.37 (quintet,  $J = 6.3$  Hz, 1H), 6.64 (d,  $J = 16.1$  Hz, 1H), 6.89 (t,  $J = 7.4$  Hz, 1H), 6.97 (d,  $J = 8.1$  Hz, 1H), 7.26 (t,  $J = 7.4$  Hz, 1H), 7.30 – 7.40 (m, 5H), 7.59 (d,  $J = 7.6$  Hz, 1H), 8.02 (d,  $J = 16.1$  Hz, 1H), 9.84 (bs, 1H);  $^{13}\text{C}$  NMR (100 MHz,  $\text{CDCl}_3$ )  $\delta$  (ppm) 18.0, 61.5, 66.4, 66.8, 90.9, 116.3, 117.0, 120.6, 121.2, 128.2, 128.4, 128.6, 129.1, 131.8, 141.6, 152.1, 155.5, 165.7, 166.9, 167.1; ESI-MS ( $R_{\text{t}} = 11.7$  min)  $m/z$  406  $[\text{M}-\text{H}]^+$ . Found C, 67.99; H, 5.12; N, 3.43 %;  $\text{C}_{23}\text{H}_{21}\text{NO}_6$  requires C, 67.80; H, 5.20; N, 3.44 %.

*(E)-(R)-1-((S,Z)-2-(2-(benzyloxy)-2-oxoethylidene)-4-oxoazetidin-3-yl)ethyl 3-(3,4-dihydroxyphenyl) acrylate*  
**(1.h)**

Following GP4,  $\beta$ -lactam **4.h** (44 mg, 82  $\mu$ mol) treated with TFA (490  $\mu$ L, 6.56 mmol) yielded compound **1.h** as a yellow oil (34 mg, 99%). IR (film,  $\text{cm}^{-1}$ ) 3331, 2925, 1816, 1698, 1657, 1604, 1515, 1260;  $[\alpha]_{\text{D}}^{20} = +11$  ( $c = 0.6$ ,  $\text{CH}_3\text{OH}$ );  $^1\text{H}$  NMR (400 MHz,  $(\text{CD}_3)_2\text{CO}$ )  $\delta$  (ppm) 1.43 (d,  $J = 6.4$  Hz, 3H), 4.14 (d,  $J = 6.5$  Hz, 1H), 5.15 (d,  $J_{\text{AB}} = 12.5$  Hz, 1H), 5.19 (d,  $J_{\text{AB}} = 12.5$  Hz, 1H), 5.26 (s, 1H), 5.33 (quintet,  $J = 6.4$  Hz, 1H), 6.28 (d,  $J = 15.9$  Hz, 1H), 6.87 (d,  $J = 8.2$  Hz, 1H), 7.03 (dd,  $J = 1.6, 8.2$  Hz, 1H), 7.16 (d,  $J = 1.6$  Hz, 1H), 7.30 – 7.40 (m, 5H), 7.56 (d,  $J = 15.9$  Hz, 1H), 9.85 (bs, 1H);  $^{13}\text{C}$  NMR (100 MHz,  $(\text{CD}_3)_2\text{CO}$ )  $\delta$  (ppm) 18.5, 62.3, 66.0, 67.5, 90.4, 115.1, 115.3, 116.4, 122.7, 127.4, 128.8, 129.0, 129.3, 137.8, 146.3, 146.5, 149.0, 154.2, 166.2, 166.4, 166.7; ESI-MS ( $R_{\text{t}} = 8.9$  min)  $m/z$  441  $[\text{M}+\text{H}_2\text{O}]^+$ . Found C, 65.29; H, 5.04; N, 3.23 %;  $\text{C}_{23}\text{H}_{21}\text{NO}_7$  requires C, 65.24; H, 5.00; N, 3.31 %.

*(E)-(R)-1-((S,Z)-2-(2-(benzyloxy)-2-oxoethylidene)-4-oxoazetidin-3-yl)ethyl 3-(4-hydroxy-3-methoxyphenyl)acrylate*  
**(1.i)**

Following GP4,  $\beta$ -lactam **4.i** (20 mg, 40  $\mu$ mol) treated with TFA (150  $\mu$ L, 2.02 mmol) yielded compound **1.i** as a yellow oil (17 mg, 99%). IR (film,  $\text{cm}^{-1}$ ) 3397, 3293, 2930, 1819, 1702, 1659, 1514, 1454, 1267;  $[\alpha]_{\text{D}}^{20} = +13$  ( $c = 1.0$ ,  $\text{CH}_2\text{Cl}_2$ );  $^1\text{H}$  NMR (400 MHz,  $\text{CDCl}_3$ )  $\delta$  (ppm) 1.46 (d,  $J = 6.3$  Hz, 3H), 3.93 (s, 3H), 3.96 (d,  $J = 6.8$  Hz, 1H), 5.14 (d,  $J_{\text{AB}} = 12.4$  Hz, 1H), 5.18 (d,  $J_{\text{AB}} = 12.4$  Hz, 1H), 5.28 (s, 1H), 5.37 (quintet,  $J = 6.3$  Hz, 1H), 6.26 (d,  $J = 15.9$  Hz, 1H), 6.92 (d,  $J = 8.1$  Hz, 1H), 7.03 (s, 1H), 7.06 (d,  $J = 8.1$  Hz, 1H), 7.31 – 7.39 (m, 5H), 7.62 (d,  $J = 15.9$  Hz, 1H), 8.53 (bs, 1H);  $^{13}\text{C}$  NMR (100 MHz,  $\text{CDCl}_3$ )  $\delta$  (ppm) 18.0, 56.0, 61.5, 66.2, 66.7, 90.7, 109.3, 114.6, 114.7, 123.5, 126.7, 128.2, 128.4, 128.7, 146.0, 146.7, 148.2, 152.1, 164.7, 166.1, 166.4, 166.7; ESI-MS ( $R_{\text{t}} = 9.2$  min)  $m/z$  394  $[\text{M}-43]^+$ . Found C, 66.92; H, 5.35; N, 3.15 %;  $\text{C}_{24}\text{H}_{23}\text{NO}_7$  requires C, 65.90; H, 5.30; N, 3.20 %.

(*E*)-(*R*)-1-((*S*,*Z*)-2-(2-(benzyloxy)-2-oxoethylidene)-4-oxoazetidin-3-yl)ethyl dimethoxyphenyl)acrylate (**1.j**)

3-(4-hydroxy-3,5-

Following GP4,  $\beta$ -lactam **4.j** (30 mg, 57  $\mu$ mol) treated with TFA (210  $\mu$ L, 2.85 mmol) yielded compound **1.j** as a yellow oil (26 mg, 99%). IR (film,  $\text{cm}^{-1}$ ) 3398, 3286, 2923, 1819, 1702, 1657, 1514, 1457, 1255;  $[\alpha]_{\text{D}}^{20} = +11$  ( $c = 1.0$ ,  $\text{CH}_2\text{Cl}_2$ );  $^1\text{H NMR}$  (400 MHz,  $\text{CDCl}_3$ )  $\delta$  (ppm) 1.46 (d,  $J = 6.4$  Hz, 3H), 3.92 (s, 6H), 3.97 (d,  $J = 6.8$  Hz, 1H), 5.14 (d,  $J_{\text{AB}} = 12.4$  Hz, 1H), 5.18 (d,  $J_{\text{AB}} = 12.4$  Hz, 1H), 5.28 (s, 1H), 5.38 (quintet,  $J = 6.4$  Hz, 1H), 6.27 (d,  $J = 15.8$  Hz, 1H), 6.77 (s, 2H), 7.33 – 7.36 (m, 5H), 7.60 (d,  $J = 15.8$  Hz, 1H), 8.54 (bs, 1H);  $^{13}\text{C NMR}$  (100 MHz,  $\text{CDCl}_3$ )  $\delta$  (ppm) 18.0, 56.4, 61.6, 62.1, 66.2, 66.6, 90.7, 105.2, 114.9, 125.6, 128.3, 128.4, 128.7, 135.7, 137.3, 146.1, 147.2, 152.1, 160.0, 164.6, 165.9, 166.7; ESI-MS ( $R_{\text{t}} = 9.0$  min)  $m/z$  424  $[\text{M}-43]^+$ . Found C, 64.31; H, 5.41; N, 2.94 %;  $\text{C}_{25}\text{H}_{25}\text{NO}_8$  requires C, 64.23; H, 5.39; N, 3.00 %.

#### 2.13.4 Synthesis of alkylidene- $\beta$ -lactams for vectorization and in vivo biodistribution

Alcohol **A**, compounds **1.K**, **2.K**, **3.K** and **4.K** were prepared as previously reported.<sup>39e</sup> Starting benzoic acid methyl esters are known and were prepared according to reported procedures with methanol and sulfuric acid as catalyst.<sup>106</sup>

##### methyl 4-(ethoxymethoxy)-3-methoxybenzoate (**2.k**)

Following GP1, methyl 4-hydroxy-3-methoxybenzoate (898 mg, 4.93 mmol), NaH (256 mg, 6.4 mmol) and EOMCl (594  $\mu$ L, 6.4 mmol) yielded compound **2.k** as a yellow oil (1.183 g, 99%). IR (film,  $\text{cm}^{-1}$ ) 3409, 2952, 1712, 1598, 1513, 1435, 1293;  $^1\text{H NMR}$  (400 MHz,  $\text{CDCl}_3$ )  $\delta$  (ppm) 1.23 (t,  $J = 14.4$  Hz, 3H), 3.78 (q,  $J = 14.0$  Hz, 2H), 3.90 (s, 3H), 3.94 (s, 3H), 5.35 (s, 2H), 7.21 (d,  $J = 17.2$  Hz, 1H), 7.57 (d,  $J = 4.0$  Hz, 1H), 7.65 (dd,  $J = 3.6, 16.8$  Hz, 1H);  $^{13}\text{C NMR}$  (100 MHz,  $\text{CDCl}_3$ )  $\delta$  (ppm) 14.7, 51.5, 55.6, 64.2, 93.3, 112.2, 114.4, 123.0, 123.5, 148.8, 150.4, 166.3; ESI-MS ( $R_{\text{t}} = 7.4$  min)  $m/z$  241  $[\text{M}+\text{H}]^+$ .

##### 4-(ethoxymethoxy)-3-methoxybenzoic acid (**3.k**)

Following GP2, ester **2.k** (1.183g, 4.93 mmol) yielded acid **3.k** as a white solid (568 mg, 51%). Mp 133 – 135  $^{\circ}\text{C}$ ; IR (film,  $\text{cm}^{-1}$ ) 3396, 3048, 2962, 2901, 1681, 1590, 1458, 1426, 1279;  $^1\text{H NMR}$  (400 MHz,  $\text{CD}_3\text{OD}$ )  $\delta$  (ppm) 1.24 (t,  $J = 7.2$  Hz, 3H), 3.79 (q,  $J = 6.8$  Hz, 2H), 3.96 (s, 3H), 5.38 (s, 2H), 7.25 (d,  $J = 8.4$  Hz, 1H), 7.63 (d,  $J = 1.6$  Hz, 1H), 7.75 (dd,  $J = 1.6, 8.4$  Hz, 1H);  $^{13}\text{C NMR}$  (100 MHz,  $\text{CDCl}_3$ )  $\delta$  (ppm) 15.0, 56.0, 64.7, 93.7, 112.8, 114.6, 122.9, 124.3, 149.1, 151.4, 171.9; ESI-MS ( $R_{\text{t}} = 11.1$  min)  $m/z$  225  $[\text{M}-\text{H}]^-$ .

##### (*R*)-1-((*S*,*Z*)-2-(2-(benzyloxy)-2-oxoethylidene)-4-oxoazetidin-3-yl)ethyl-4-(ethoxymethoxy)-3-methoxybenzoate (**4.k**)

Following GP3, alcohol **A** (83 mg, 0.32 mmol) and acid **3.k** (115 mg, 0.51 mmol) yielded compound **4.k** as a colorless oil (24 mg, 16%) after flash-chromatography purification ( $\text{CH}_2\text{Cl}_2/\text{CH}_3\text{CN}$  from 98:2 to 95:5). IR (film,  $\text{cm}^{-1}$ ) 3295, 2980, 1822, 1704, 1658, 1601, 1511, 1268, 1217;  $[\alpha]_{\text{D}} = +14$  ( $c = 0.4$ ,  $\text{CH}_2\text{Cl}_2$ );  $^1\text{H NMR}$  (400 MHz,  $\text{CD}_3\text{OD}$ )  $\delta$  (ppm) 1.22 (t,  $J = 7.2$  Hz, 3H), 1.52 (d,  $J = 6.4$  Hz, 2H), 3.77 (q,  $J = 7.2$  Hz, 2H), 3.90 (s, 3H), 4.02 (d,  $J = 6.4$  Hz, 1H), 5.15 (d,  $J_{\text{AB}} = 12.4$  Hz, 1H), 5.19 (d,  $J_{\text{AB}} = 12.0$  Hz, 1H), 5.28 (s, 1H), 5.34 (s, 2H), 5.48 (quintet,  $J = 6.4$  Hz, 1H), 7.20 (d,  $J = 8.0$  Hz, 1H), 7.32 – 7.37 (m, 5H), 7.54 (d,  $J = 2.0$  Hz, 1H), 7.61 (dd,  $J = 2.0, 8.8$  Hz, 1H), 8.70 (bs, 1H);  $^{13}\text{C NMR}$  (100 MHz,  $\text{CDCl}_3$ )  $\delta$  (ppm) 15.0, 18.1, 55.9, 61.6, 64.6, 66.1, 67.1, 90.6, 93.6, 112.4, 114.7, 123.2, 123.4, 128.3, 128.5, 135.7, 149.2, 151.0, 152.2, 164.6, 165.0, 166.6; ESI-MS ( $R_{\text{t}} = 10.0$  min)  $m/z$  487  $[\text{M}+\text{H}_2\text{O}]^+$ .

##### (*R*)-1-((*S*,*Z*)-2-(2-(benzyloxy)-2-oxoethylidene)-4-oxoazetidin-3-yl)-ethyl-4-hydroxy-3-methoxybenzoate (**1.k**)

Following GP4,  $\beta$ -lactam **4.k** (22 mg, 47  $\mu$ mol) treated with TFA (83  $\mu$ L, 1.08 mmol) yielded compound **1.k** as a waxy solid (19 mg, 99%). IR (film,  $\text{cm}^{-1}$ ) 3379, 2933, 2852, 1819, 1699, 1659, 1597, 1514, 1282, 1220;  $[\alpha]_{\text{D}} = +11$  ( $c = 0.3$ ,  $\text{CH}_2\text{Cl}_2$ );  $^1\text{H NMR}$  (400 MHz,  $\text{CDCl}_3$ )  $\delta$  (ppm) 1.52 (d,  $J = 6.4$  Hz, 2H), 3.91 (s, 3H), 4.02

(d,  $J = 6.0$  Hz, 1H), 5.15 (d,  $J_{AB} = 12.0$  Hz, 1H), 5.19 (d,  $J_{AB} = 12.0$  Hz, 1H), 5.28 (s, 1H), 5.48 (quintet,  $J = 6.0$  Hz, 1H) 6.94 (d,  $J = 8.4$  Hz, 1H), 7.33-7.37 (m, 5H), 7.51 (s, 1H), 7.60 (d,  $J = 8.4$  Hz, 1H) 8.73 (bs, 1H);  $^{13}\text{C}$  NMR (50 MHz,  $\text{CDCl}_3$ )  $\delta$  (ppm) 18.1, 56.0, 61.7, 66.2, 67.1, 90.6, 111.8, 114.2, 121.7, 124.3, 128.2, 128.3, 128.6, 135.7, 146.4, 150.4, 152.2, 164.7, 165.0, 166.7; ESI-MS ( $R_t = 8.3$  min)  $m/z$  429  $[\text{M}+\text{H}_2\text{O}]^+$ .

### 2.13.5 Synthesis of other antibacterial alkylidene- $\beta$ -lactams

Alcohol **A** was prepared as previously reported.<sup>39c</sup> Starting benzoic acid methyl ester is known and was prepared according to reported procedures with methanol and sulfuric acid as catalyst.<sup>107</sup> *N*-Boc-protected ethanolamine<sup>108</sup> and bromopropylamine<sup>109</sup> were synthesized according to procedures reported in literature. Spectroscopic data are in accordance with those reported.

#### Methyl 4-(2-((*tert*-butoxycarbonyl)amino)ethoxy)benzoate (**2.l**)

To a solution of *N*-Boc-ethanolamine (145 mg, 0.9 mmol, 1 equiv) in THF (6.4 mL) under inert atmosphere, *p*-hydroxybenzoic acid methyl ester (164 mg, 1.08 mmol, 1.2 equiv) and triphenylphosphine (354 mg, 1.35 mmol, 1.5 equiv) were added. The mixture was then cooled to 0 °C and DIAD (0.3 mL, 1.35 mmol, 1.5 equiv) was added; the system was allowed to reach room temperature in 15 min and left under stirring. After 3 h (TLC monitoring) the reaction mixture was quenched with a solution of NaOH 1M and extracted with EtOAc (3  $\times$  10 mL). The collected organic phases were dried on  $\text{Na}_2\text{SO}_4$  and evaporated. The crude was then purified by flash-chromatography ( $\text{CH}_2\text{Cl}_2$ /acetone 90:10) to afford the desired compound **2.l** as a waxy white solid (116 mg, 44%).  $^1\text{H}$  NMR (400 MHz,  $\text{CDCl}_3$ )  $\delta$  (ppm) 7.89 (d,  $J = 8.8$  Hz, 2H), 6.81 (d,  $J = 8.8$  Hz, 2H), 5.22 (bs, 1H), 3.99 (t,  $J = 5.2$  Hz, 2H), 3.79 (s, 3H), 3.47 (d,  $J = 5.0$  Hz, 2H), 1.37 (s, 9H);  $^{13}\text{C}$  NMR (100 MHz,  $\text{CDCl}_3$ )  $\delta$  (ppm) 166.5, 162.1, 155.7, 131.4, 131.1, 122.6, 113.8, 79.3, 67.1, 51.6, 39.7, 28.1; ESI-MS ( $R_t = 9.5$  min)  $m/z$  196  $[\text{M-Boc}+2\text{H}]^+$ .

#### Methyl 4-(3-((*tert*-butoxycarbonyl)amino)propoxy)benzoate (**2.m**)

To a solution of *p*-hydroxybenzoic acid methyl ester (160 mg, 1.05 mmol, 1 equiv) in DMF (2 mL) under inert atmosphere,  $\text{H}_2\text{O}$  (0.2 mL) and  $\text{K}_2\text{CO}_3$  (363 mg, 2.63 mmol, 2.5 equiv) were added. The mixture was stirred at room temperature for 20 minutes and gradually warmed to 45 °C. *N*-Boc-bromopropylamine (377 mg, 1.58 mmol, 1.5 equiv) was then added and the system was left under stirring at rt. After 30 h (TLC monitoring) the reaction mixture was quenched with water extracted with EtOAc (3  $\times$  10 mL). The collected organic phases were dried on  $\text{Na}_2\text{SO}_4$  and evaporated. The crude was then purified by flash-chromatography (cyclohexane/EtOAc 75:25) to afford the desired compound **2.m** as a waxy white solid (182 mg, 56%).  $^1\text{H}$  NMR (400 MHz,  $\text{CDCl}_3$ )  $\delta$  (ppm) 7.92 (dd,  $J = 8.7, 1.1$  Hz, 2H), 6.85 (dd,  $J = 8.7, 1.1$  Hz, 2H), 4.91 (bs, 1H), 4.01 (t,  $J = 5.2$  Hz, 2H), 3.83 (s, 3H), 3.33 – 3.22 (m, 2H), 1.99 – 1.90 (m, 2H), 1.39 (s, 9H);  $^{13}\text{C}$  NMR (100 MHz,  $\text{CDCl}_3$ )  $\delta$  (ppm) 166.7, 162.4, 155.9, 131.4, 122.5, 113.9, 79.0, 65.7, 51.7, 37.6, 29.4, 28.3; ESI-MS ( $R_t = 10.9$  min)  $m/z$  210  $[\text{M-Boc}+2\text{H}]^+$ .

#### 4-(2-((*tert*-butoxycarbonyl)amino)ethoxy)benzoic acid (**3.l**)

Following GP2, ester **2.l** (116 mg, 0.39 mmol) yielded acid **3.l** as a waxy white solid (105 mg, 96%).  $^1\text{H}$  NMR (400 MHz,  $\text{CDCl}_3$ )  $\delta$  (ppm) 8.05 (d,  $J = 8.8$  Hz, 2H), 6.94 (d,  $J = 8.8$  Hz, 2H), 4.98 (bs, 1H), 4.10 (t,  $J = 5.1$  Hz, 2H), 3.57 (d,  $J = 5.0$  Hz, 2H), 1.46 (s, 9H);  $^{13}\text{C}$  NMR (100 MHz,  $\text{CD}_3\text{OD}$ )  $\delta$  (ppm) 169.7, 164.2, 158.6, 132.8, 124.3, 115.2, 80.3, 68.2, 40.9, 28.7; ESI-MS ( $R_t = 7.1$  min)  $m/z$  182  $[\text{M-Boc}+2\text{H}]^+$ .

#### 4-(3-((*tert*-butoxycarbonyl)amino)propoxy)benzoic acid (**3.m**)

Following GP2, ester **2.m** (175 mg, 0.56 mmol) yielded acid **3.m** as a waxy white solid (146 mg, 87%).  $^1\text{H}$  NMR (400 MHz,  $(\text{CD}_3)_2\text{CO}$ )  $\delta$  (ppm) 7.98 (d,  $J = 8.9$  Hz, 2H), 7.01 (d,  $J = 8.8$  Hz, 2H), 6.12 (bs, 1H), 4.14 (t,  $J = 6.4$  Hz, 2H), 3.28 (q,  $J = 6.4$  Hz, 2H), 1.98 (quintet,  $J = 6.4$  Hz, 2H), 1.40 (s, 9H);  $^{13}\text{C}$  NMR (100 MHz,

CDCl<sub>3</sub>)  $\delta$  (ppm) 167.5, 163.8, 156.8, 132.5, 123.6, 115.0, 78.5, 66.6, 38.1, 30.4, 28.6; ESI-MS ( $R_t = 7.8$  min)  $m/z$  196 [M-Boc+2H]<sup>+</sup>.

*(R)-1-((S,Z)-2-(2-(benzyloxy)-2-oxoethylidene)-4-oxoazetidin-3-yl)ethyl 4-(2-((tert-butoxycarbonyl)amino)ethoxy)benzoate (4.l)*

Following GP3, alcohol **A** (63 mg, 0.24 mmol) and acid **3.l** (107 mg, 0.38 mmol) yielded compound **4.l** as a yellow oil (57 mg, 45%) after flash-chromatography purification (CH<sub>2</sub>Cl<sub>2</sub>/diethyl ether 95:5). IR (film, cm<sup>-1</sup>) 2973, 2926, 1820, 1700, 1656, 1605, 1252; [ $\alpha$ ]<sub>D</sub><sup>20</sup> = + 2 (c = 0.9, CH<sub>3</sub>OH); <sup>1</sup>H NMR (400 MHz, CDCl<sub>3</sub>)  $\delta$  (ppm) 8.55 (bs, 1H), 7.95 (d,  $J = 8.9$  Hz, 2H), 7.40 – 7.29 (m, 5H), 6.90 (d,  $J = 8.9$  Hz, 2H), 5.46 (quintet,  $J = 6.4$  Hz, 1H), 5.25 (s, 1H), 5.16 (q,  $J_{AB} = 12.3$  Hz, 2H), 4.98 (bs, 1H), 4.07 (t,  $J = 5.1$  Hz, 2H), 4.01 (d,  $J = 6.8$  Hz, 1H), 3.59 – 3.52 (m, 2H), 1.51 (d,  $J = 6.4$  Hz, 3H), 1.45 (s, 9H); <sup>13</sup>C NMR (100 MHz, CDCl<sub>3</sub>)  $\delta$  (ppm) 166.7, 164.9, 164.7, 162.6, 155.8, 152.2, 135.7, 131.7, 128.6, 128.3, 128.2, 122.3, 114.2, 90.5, 79.7, 67.4, 67.1, 66.1, 61.6, 39.9, 28.3, 18.0; ESI-MS ( $R_t = 11.7$  min)  $m/z$  425 [M-Boc+2H]<sup>+</sup>.

*2-(4-(((R)-1-((S,Z)-2-(2-(benzyloxy)-2-oxoethylidene)-4-oxoazetidin-3-yl)ethoxy)carbonyl)phenoxy)ethanaminium 2,2,2-trifluoroacetate (1.l)*

Following GP4,  $\beta$ -lactam **4.l** (57 mg, 0.11 mmol) treated with TFA (594  $\mu$ L, 5.28 mmol) yielded compound **1.l** as a yellow oil (58 mg, 99%). IR (film, cm<sup>-1</sup>) 3424, 2958, 2926, 1816, 1689, 1656, 1607, 1252; [ $\alpha$ ]<sub>D</sub><sup>20</sup> = + 8 (c = 0.9, CH<sub>3</sub>OH); <sup>1</sup>H NMR (400 MHz, CD<sub>3</sub>OD)  $\delta$  (ppm) 7.96 (d,  $J = 8.3$  Hz, 2H), 7.42 – 7.24 (m, 5H), 7.06 (d,  $J = 8.4$  Hz, 2H), 5.44 (quintet,  $J = 6.3$  Hz, 1H), 5.22 (s, 1H), 5.16 (q,  $J_{AB} = 12.5$  Hz, 2H), 4.30 (t,  $J = 4.6$  Hz, 2H), 4.13 (d,  $J = 5.9$  Hz, 1H), 3.40 (t,  $J = 4.6$  Hz, 1H), 1.47 (d,  $J = 6.3$  Hz, 3H); <sup>13</sup>C NMR (100 MHz, CD<sub>3</sub>OD)  $\delta$  (ppm) 167.9, 167.6, 166.4, 163.5, 154.3, 138.0, 134.0, 132.7, 129.5, 129.1, 129.1, 124.3, 115.5, 91.1, 68.6, 66.6, 65.5, 62.5, 40.1, 18.3; ESI-MS ( $R_t = 2.3$  min)  $m/z$  425 [M-TFA+H]<sup>+</sup>.

*(R)-1-((S,Z)-2-(2-(benzyloxy)-2-oxoethylidene)-4-oxoazetidin-3-yl)ethyl 4-(3-((tert-butoxycarbonyl)amino)propoxy)benzoate (4.m)*

Following GP3, alcohol **A** (50 mg, 0.19 mmol) and acid **3.m** (89 mg, 0.30 mmol) yielded compound **1.m** as a yellow oil (48 mg, 46%) after flash-chromatography purification (CH<sub>2</sub>Cl<sub>2</sub>/diethyl ether 95:5). IR (film, cm<sup>-1</sup>) 2972, 2927, 1821, 1701, 1656, 1606, 1254; [ $\alpha$ ]<sub>D</sub><sup>20</sup> = - 2 (c = 1.0, CH<sub>3</sub>OH); <sup>1</sup>H NMR (400 MHz, CDCl<sub>3</sub>)  $\delta$  (ppm) 8.74 (bs, 1H), 7.94 (d,  $J = 8.8$  Hz, 2H), 7.42 – 7.28 (m, 5H), 6.89 (d,  $J = 8.8$  Hz, 2H), 5.46 (quintet,  $J = 6.4$  Hz, 1H), 5.25 (s, 1H), 5.16 (q,  $J_{AB} = 12.4$  Hz, 2H), 4.77 (bs, 1H), 4.06 (t,  $J = 6.0$  Hz, 2H), 4.01 (d,  $J = 6.8$  Hz, 1H), 3.32 (d,  $J = 6.1$  Hz, 2H), 2.05 – 1.95 (m, 2H), 1.50 (d,  $J = 6.4$  Hz, 3H), 1.44 (s, 9H); <sup>13</sup>C NMR (100 MHz, CDCl<sub>3</sub>)  $\delta$  (ppm) 166.7, 165.0, 164.7, 162.8, 156.0, 152.2, 135.7, 131.7, 128.6, 128.3, 128.2, 122.0, 114.2, 90.5, 79.3, 67.0, 66.1, 65.9, 61.6, 37.8, 29.6, 28.4, 18.1; ESI-MS ( $R_t = 12.0$  min)  $m/z$  439 [M-Boc+2H]<sup>+</sup>.

*3-(4-(((R)-1-((S,Z)-2-(2-(benzyloxy)-2-oxoethylidene)-4-oxoazetidin-3-yl)ethoxy)carbonyl)phenoxy)propan-1-aminium 2,2,2-trifluoroacetate (1.m)*

Following GP4,  $\beta$ -lactam **4.m** (45 mg, 0.09 mmol) treated with TFA (300  $\mu$ L, 2.70 mmol) yielded compound **1.m** as a yellow oil (46 mg, 99%). IR (film, cm<sup>-1</sup>) 3424, 2925, 2855, 1818, 1690, 1664, 1255; [ $\alpha$ ]<sub>D</sub><sup>20</sup> = + 2 (c = 0.7, CH<sub>3</sub>OH); <sup>1</sup>H NMR (400 MHz, CD<sub>3</sub>OD)  $\delta$  (ppm) 7.95 (d,  $J = 8.9$  Hz, 2H), 7.43 – 7.25 (m, 5H), 7.01 (d,  $J = 8.9$  Hz, 2H), 5.43 (dt,  $J = 11.7, 5.9$  Hz, 1H), 5.22 (s, 1H), 5.16 (q,  $J_{AB} = 10.0$  Hz, 1H), 4.19 (t,  $J = 5.6$  Hz, 2H), 4.14 (d,  $J = 5.9$  Hz, 1H), 3.16 (t,  $J = 7.2$  Hz, 2H), 2.17 (dt,  $J = 12.9, 6.3$  Hz, 2H), 1.48 (d,  $J = 6.4$  Hz, 3H); <sup>13</sup>C NMR (100 MHz, CD<sub>3</sub>OD)  $\delta$  (ppm) 167.9, 167.5, 166.5, 164.1, 154.3, 138.0, 132.8, 132.7, 129.5, 129.1, 129.0, 123.7, 115.4, 115.2, 91.1, 68.5, 66.6, 66.4, 62.6, 38.4, 28.2, 18.4; ESI-MS ( $R_t = 2.5$  min)  $m/z$  439 [M-TFA+H]<sup>+</sup>.



### 2.13.6 Synthesis of $\beta$ -lactam carbamates

Isocyanates **6.a-c** and amines **7.a, 7.d-t** are commercial; compounds **A, 7.h, 7.p** and **7.u** were synthesized following already reported procedures.<sup>39e,84,85</sup>

#### *Benzyl(Z)-2-((S)-3-((R)-1-((benzylcarbamoyl)oxy)ethyl)-4-oxo azetidin-2-ylidene)acetate (5.a)*

To a solution of alcohol **A** (29 mg, 0.11 mmol, 1 equiv) in anhydrous  $\text{CH}_2\text{Cl}_2$  (1.1 mL) under inert atmosphere, commercial benzylisocyanate **6.a** (20  $\mu\text{L}$ , 0.17 mmol, 1.5 equiv) and  $\text{TiCl}_4$  (1M in  $\text{CH}_2\text{Cl}_2$ , 11  $\mu\text{L}$ , 0.011 mmol, 0.1 equiv) were added dropwise. The mixture was then refluxed for 6 h. After completion (TLC monitoring) the mixture was quenched with water and extracted with  $\text{CH}_2\text{Cl}_2$  ( $3 \times 10$  mL). The combined organic extracts were dried over  $\text{Na}_2\text{SO}_4$ , filtered, concentrated under vacuum and purified by flash-chromatography (cyclohexane/EtOAc 50:50) affording carbamate **5.a** as a waxy white solid (40 mg, 91%). IR (film,  $\text{cm}^{-1}$ ) 3330, 1818, 1699, 1657;  $[\alpha]_{\text{D}}^{20} = +1$  ( $c = 1.0$ ,  $\text{CH}_2\text{Cl}_2$ );  $^1\text{H}$  NMR (400 MHz,  $\text{CDCl}_3$ )  $\delta$  (ppm) 1.41 (d,  $J = 6.4$  Hz, 3H), 3.89 (d,  $J = 6.4$  Hz, 1H), 4.36 (d,  $J = 5.9$  Hz, 2H), 5.07 (bt,  $J = 5.9$  Hz, 1H), 5.16 (s, 2H), 5.21 (quintet,  $J = 6.4$  Hz, 1H), 5.25 (s, 1H), 7.22 – 7.40 (m, 10H), 8.59 (bs, 1H);  $^{13}\text{C}$  NMR (100 MHz,  $\text{CDCl}_3$ )  $\delta$  (ppm) 18.1, 45.1, 61.7, 66.2, 67.3, 90.6, 127.5, 127.6, 128.3, 128.4, 128.6, 128.7, 135.8, 138.0, 152.0, 155.1, 164.7, 166.7; ESI-MS  $m/z$  412  $[\text{M}+\text{H}_2\text{O}]^+$ . Found C, 67.02; H, 5.63; N, 7.08 %;  $\text{C}_{22}\text{H}_{22}\text{N}_2\text{O}_5$  requires C, 66.99; H, 5.62; N, 7.10 %.

#### *Benzyl(Z)-2-((S)-4-oxo-3-((R)-1-((phenylcarbamoyl)oxy)ethyl) azetidin-2-ylidene)acetate (5.b)*

A mixture of alcohol **A** (27 mg, 0.10 mmol, 1 equiv) and commercial phenylisocyanate **6.b** (16  $\mu\text{L}$ , 0.15 mmol, 1.5 equiv) was subjected to microwave irradiation (400 W, 40 min) under stirring. The crude was directly purified by flash-chromatography (cyclohexane/EtOAc 60:40) affording carbamate **5.b** as a waxy white solid (22 mg, 58%). IR (film,  $\text{cm}^{-1}$ ) 3314, 1815, 1698, 1658;  $[\alpha]_{\text{D}}^{20} = +13$  ( $c = 1.0$ ,  $\text{CH}_2\text{Cl}_2$ );  $^1\text{H}$  NMR (400 MHz,  $\text{CDCl}_3$ )  $\delta$  (ppm) 1.46 (d,  $J = 6.4$  Hz, 3H), 3.96 (d,  $J = 6.0$  Hz, 1H), 5.18 (s, 2H), 5.27 (quintet,  $J = 6.4$  Hz, 1H), 5.29 (s, 1H), 6.72 (bs, 1H), 7.07 (t,  $J = 7.3$  Hz, 1H), 7.28 – 7.40 (m, 9H), 8.61 (bs, 1H);  $^{13}\text{C}$  NMR (100 MHz,  $\text{CD}_3\text{CN}$ )  $\delta$  (ppm) 18.7, 62.5, 66.3, 68.2, 90.6, 119.6, 124.1, 128.9, 129.0, 129.5, 129.8, 137.7, 139.5, 153.6, 154.1, 166.6, 167.2; ESI-MS  $m/z$  337  $[\text{M}-43]^+$ . Found C, 66.39; H, 5.28; N, 7.34 %;  $\text{C}_{21}\text{H}_{20}\text{N}_2\text{O}_5$  requires C, 66.31; H, 5.30; N, 7.36 %.

#### *Benzyl(Z)-2-((S)-4-oxo-3-((R)-1-((o-tolylcarbamoyl)oxy)ethyl) azetidin-2-ylidene)acetate (5.c)*

Following what reported for compound **5.b**, alcohol **A** (21 mg, 0.08 mmol, 1 equiv) and commercial *o*-tolylisocyanate **6.c** (15  $\mu\text{L}$ , 0.12 mmol, 1.5 equiv) yielded carbamate **5.c** as a waxy white solid (15 mg, 48%). IR (film,  $\text{cm}^{-1}$ ) 3293, 1807, 1694, 1640;  $[\alpha]_{\text{D}}^{20} = +28$  ( $c = 1.0$ ,  $\text{CH}_2\text{Cl}_2$ );  $^1\text{H}$  NMR (400 MHz,  $\text{CDCl}_3$ )  $\delta$  (ppm) 1.47 (d,  $J = 6.4$  Hz, 3H), 2.25 (s, 3H), 3.96 (d,  $J = 6.2$  Hz, 1H), 5.18 (s, 2H), 5.24 – 5.31 (m, 2H), 6.43 (bs, 1H), 7.03 – 7.21 (m, 3H), 7.32 – 7.40 (m, 5H), 7.70 – 7.72 (m, 1H), 8.58 (bs, 1H);  $^{13}\text{C}$  NMR (100 MHz,  $\text{CDCl}_3$ )  $\delta$  (ppm) 17.7, 18.0, 61.6, 66.2, 67.7, 90.6, 124.6, 126.8, 128.2, 128.4, 128.6, 130.5, 135.3, 135.8, 151.9, 159.3, 164.6, 166.6; ESI-MS  $m/z$  351  $[\text{M}-43]^+$ . Found C, 66.90; H, 5.63; N, 7.09 %;  $\text{C}_{22}\text{H}_{22}\text{N}_2\text{O}_5$  requires C, 66.99; H, 5.62; N, 7.10 %.

#### *Benzyl(Z)-2-((S)-3-((R)-1-(((4-methoxyphenyl)carbamoyl)oxy) ethyl)-4-oxoazetidin-2-ylidene) acetate (5.d)*

Following GP5 and GP6 carbamate **5.d** was obtained in a 52% yield (32 mg, 0.08 mmol). IR (film) 3054, 1824, 1708, 1656;  $[\alpha]_{\text{D}}^{20} = +23$  ( $c = 1.0$ ,  $\text{CH}_2\text{Cl}_2$ );  $^1\text{H}$  NMR (400 MHz,  $\text{CDCl}_3$ )  $\delta$  (ppm) 1.44 (d,  $J = 6.4$  Hz, 3H), 3.77 (s, 3H), 3.94 (d,  $J = 5.9$  Hz, 1H), 5.18 (s, 2H), 5.25 (quintet,  $J = 6.4$  Hz, 1H), 5.29 (s, 1H), 6.68 (bs, 1H), 6.83 (d,  $J = 8.9$  Hz, 2H), 7.28 – 7.37 (m, 7H), 8.76 (bs, 1H);  $^{13}\text{C}$  NMR (100 MHz,  $\text{CDCl}_3$ )  $\delta$  (ppm) 17.9, 55.5, 61.7, 66.2, 67.6, 90.6, 114.3, 120.7, 128.2, 128.3, 128.6, 130.4, 135.8, 152.0, 152.1, 156.3, 164.8, 166.7; ESI-MS  $m/z$  367  $[\text{M}-43]^+$ . Found C, 64.21; H, 5.46; N, 6.81 %;  $\text{C}_{22}\text{H}_{22}\text{N}_2\text{O}_6$  requires C, 64.38; H, 5.40; N, 6.83 %.

*Benzyl(Z)-2-((S)-3-((R)-1-(((3,5-dimethoxyphenyl)carbamoyl)oxy)ethyl)-4-oxoazetidin-2-ylidene) acetate (5.e)*

Following GP5 and GP6 carbamate **5.e** was obtained in a 53% yield (35 mg, 0.08 mmol). IR (film,  $\text{cm}^{-1}$ ) 3317, 1819, 1699, 1659;  $[\alpha]_{\text{D}}^{20} = +20$  ( $c = 1.0$ ,  $\text{CH}_2\text{Cl}_2$ );  $^1\text{H}$  NMR (400 MHz,  $\text{CD}_3\text{CN}$ )  $\delta$  (ppm) 1.38 (d,  $J = 6.4$  Hz, 3H), 3.72 (s, 6H), 3.99 (d,  $J = 6.1$  Hz, 1H), 5.15 (s, 2H), 5.17 (quintet,  $J = 6.4$  Hz, 1H), 5.27 (s, 1H), 6.19 (t,  $J = 2.2$  Hz, 1H), 6.63 (d,  $J = 1.9$  Hz, 2H), 7.30 – 7.37 (m, 5H), 8.03 (bs, 1H), 9.27 (bs, 1H);  $^{13}\text{C}$  NMR (100 MHz,  $\text{CD}_3\text{CN}$ )  $\delta$  (ppm) 18.5, 55.8, 62.3, 66.3, 68.1, 90.5, 95.9, 97.6, 128.8, 128.9, 129.3, 137.5, 141.2, 153.4, 153.9, 161.9, 166.7, 167.1; ESI-MS  $m/z$  397  $[\text{M}-43]^+$ . Found C, 62.81; H, 5.50; N, 6.34 %;  $\text{C}_{23}\text{H}_{24}\text{N}_2\text{O}_7$  requires C, 62.72; H, 5.49; N, 6.36 %.

*Benzyl(Z)-2-((S)-4-oxo-3-((R)-1-(((4-(trifluoromethyl)phenyl)carbamoyl)oxy)ethyl)azetidin-2-ylidene) acetate (5.f)*

Following GP5 and GP6 carbamate **5.f** was obtained in a 76% yield (51 mg, 0.11 mmol). IR (film,  $\text{cm}^{-1}$ ) 3308, 1809, 1694, 1654;  $[\alpha]_{\text{D}}^{20} = +17$  ( $c = 1.0$ ,  $\text{CH}_2\text{Cl}_2$ );  $^1\text{H}$  NMR (400 MHz,  $\text{CD}_3\text{CN}$ )  $\delta$  (ppm) 1.41 (d,  $J = 6.4$  Hz, 3H), 4.02 (d,  $J = 6.0$  Hz, 1H), 5.22 (quintet,  $J = 6.4$  Hz, 1H), 5.16 (s, 2H), 5.30 (s, 1H), 7.33 – 7.38 (m, 5H), 7.57 – 7.62 (m, 4H), 8.15 (bs, 1H), 9.05 (bs, 1H);  $^{13}\text{C}$  NMR (100 MHz,  $\text{CD}_3\text{CN}$ )  $\delta$  (ppm) 17.8, 61.7, 65.5, 67.8, 89.8, 114.7 (q,  $J = 103$  Hz), 118.3, 126.2 (q,  $J = 3.9$  Hz), 126.3, 128.1, 128.2, 128.7, 136.9, 152.6, 153.2, 165.6, 166.4; ESI-MS  $m/z$  405  $[\text{M}-43]^+$ . Found C, 59.02; H, 4.28; N, 6.24 %;  $\text{C}_{22}\text{H}_{19}\text{F}_3\text{N}_2\text{O}_5$  requires C, 58.93; H, 4.27; N, 6.25 %.

*Benzyl(Z)-2-((S)-3-((R)-1-(((3-fluorophenyl)carbamoyl)oxy)ethyl)-4-oxoazetidin-2-ylidene) acetate (5.g)*

Following GP5 and GP6 carbamate **5.g** was obtained in a 53% yield (32 mg, 0.08 mmol). IR (film,  $\text{cm}^{-1}$ ) 3407, 1810, 1693, 1656;  $[\alpha]_{\text{D}}^{20} = +21$  ( $c = 1.0$ ,  $\text{CH}_2\text{Cl}_2$ );  $^1\text{H}$  NMR (400 MHz,  $\text{CD}_3\text{CN}$ )  $\delta$  (ppm) 1.39 (d,  $J = 6.4$  Hz, 3H), 4.01 (d,  $J = 6.1$  Hz, 1H), 5.16 (s, 2H), 5.19 (quintet,  $J = 6.4$  Hz, 1H), 5.28 (s, 1H), 6.75 – 6.80 (m, 1H), 7.13 (dd,  $J = 8.2, 1.0$  Hz, 1H), 7.25 – 7.38 (m, 7H), 8.14 (bs, 1H), 9.17 (bs, 1H);  $^{13}\text{C}$  NMR (100 MHz,  $\text{CD}_3\text{CN}$ )  $\delta$  (ppm) 18.6, 62.5, 66.4, 68.4, 90.6, 106.3 (d,  $J = 25.9$  Hz), 110.3 (d,  $J = 21.4$  Hz), 115.0, 128.9, 129.0, 129.5, 131.3 (d,  $J = 9.7$  Hz), 137.7, 141.4 (d,  $J = 11.1$  Hz), 153.4, 154.0, 163.9 (d,  $J = 220$  Hz), 166.7, 167.2; ESI-MS  $m/z$  355  $[\text{M}-43]^+$ . Found C, 63.28; H, 4.80; N, 7.01 %;  $\text{C}_{21}\text{H}_{19}\text{FN}_2\text{O}_5$  requires C, 63.31; H, 4.81; N, 7.03 %.

*Benzyl(Z)-2-((S)-3-((R)-1-(((3-fluoro-4-morpholinophenyl)carbamoyl)oxy)ethyl)-4-oxoazetidin-2-ylidene)acetate (5.h)*

Following GP5 and GP6 carbamate **5.h** was obtained in a 72% yield (52 mg, 0.11 mmol). IR (film,  $\text{cm}^{-1}$ ) 3419, 1813, 1719, 1694, 1657;  $[\alpha]_{\text{D}}^{20} = +38$  ( $c = 1.0$ ,  $\text{CH}_3\text{OH}$ );  $^1\text{H}$  NMR (400 MHz,  $\text{CDCl}_3$ )  $\delta$  (ppm) 1.46 (d,  $J = 6.4$  Hz, 3H), 3.09 (s, 4H), 3.87 – 3.93 (m, 4H), 3.97 (d,  $J = 5.9$  Hz, 1H), 5.18 (s, 2H), 5.25 – 5.31 (m, 2H), 6.69 (bs, 1H), 6.96 – 7.01 (m, 2H), 7.34 – 7.41 (m, 6H), 8.51 (bs, 1H);  $^{13}\text{C}$  NMR (100 MHz,  $\text{CDCl}_3$ )  $\delta$  (ppm) 17.9, 51.2, 61.6, 66.2, 66.9, 67.6, 90.8, 107.8, 108.1, 114.6, 119.1, 128.3, 128.4, 128.7, 132.7, 135.7, 151.7, 152.0, 155.6 (d,  $J = 246$  Hz), 164.5, 166.6; ESI-MS  $m/z$  440  $[\text{M}-43]^+$ . Found C, 62.11; H, 5.43; N, 8.67 %;  $\text{C}_{25}\text{H}_{26}\text{FN}_3\text{O}_6$  requires C, 62.10; H, 5.42; N, 8.69 %.

*Benzyl(Z)-2-((S)-3-((R)-1-(((4-methylbenzyl)carbamoyl)oxy)ethyl)-4-oxoazetidin-2-ylidene) acetate (5.i)*

Following GP5 and GP6 carbamate **5.i** was obtained in a 69% yield (42 mg, 0.10 mmol). IR (film,  $\text{cm}^{-1}$ ) 3315, 1810, 1693, 1654;  $[\alpha]_{\text{D}}^{20} = -1$  ( $c = 1.1$ ,  $\text{CH}_2\text{Cl}_2$ );  $^1\text{H}$  NMR (400 MHz,  $\text{CDCl}_3$ )  $\delta$  (ppm) 1.40 (d,  $J = 6.4$  Hz, 3H), 2.31 (s, 3H), 3.88 (d,  $J = 6.4$  Hz, 1H), 4.31 (d,  $J = 5.7$  Hz, 2H), 5.09 (bt,  $J = 5.2$  Hz, 1H), 5.17 (s, 2H), 5.22 (quintet,  $J = 6.4$  Hz, 1H), 5.26 (s, 1H), 7.10 – 7.17 (m, 4H), 7.34 – 7.38 (m, 5H), 8.79 (bs, 1H);  $^{13}\text{C}$  NMR (100 MHz,  $\text{CDCl}_3$ )  $\delta$  (ppm) 18.1, 21.0, 44.8, 61.7, 66.1, 67.2, 90.4, 127.5, 128.2, 128.3, 128.6, 129.3, 135.0, 135.8, 137.2, 152.3, 155.1, 165.0, 166.7; ESI-MS  $m/z$  426  $[\text{M}+\text{H}_2\text{O}]^+$ . Found C, 67.72; H, 5.93; N, 6.85 %;  $\text{C}_{23}\text{H}_{24}\text{N}_2\text{O}_5$  requires C, 67.63; H, 5.92; N, 6.86 %.

*Benzyl(Z)-2-((S)-3-((R)-1-(((4-methoxybenzyl)carbamoyl)oxy) ethyl)-4-oxoazetidin-2-ylidene) acetate (5.j)*

Following GP5 and GP6 carbamate **5.j** was obtained in a 63% yield (40 mg, 0.09 mmol). IR (film,  $\text{cm}^{-1}$ ) 3329, 1811, 1692, 1654;  $[\alpha]_{\text{D}}^{20} = +1$  ( $c = 1.0$ ,  $\text{CH}_2\text{Cl}_2$ );  $^1\text{H}$  NMR (400 MHz,  $\text{CDCl}_3$ )  $\delta$  (ppm) 1.39 (d,  $J = 6.4$  Hz, 3H), 3.77 (s, 3H), 3.88 (d,  $J = 6.3$  Hz, 1H), 4.28 (d,  $J = 5.3$  Hz, 2H), 5.07 (bt,  $J = 5.4$  Hz, 1H), 5.16 (s, 2H), 5.19 (quintet,  $J = 6.5$  Hz, 1H), 5.25 (s, 1H), 6.84 (d,  $J = 8.4$  Hz, 2H), 7.19 (d,  $J = 8.4$  Hz, 2H), 7.32 – 7.37 (m, 5H), 8.73 (bs, 1H);  $^{13}\text{C}$  NMR (100 MHz,  $\text{CDCl}_3$ )  $\delta$  (ppm) 18.1, 44.5, 55.2, 61.7, 66.1, 67.2, 90.4, 114.0, 128.1, 128.3, 128.6, 128.9, 130.2, 135.8, 152.2, 155.1, 159.0, 164.8, 166.6; ESI-MS  $m/z$  442  $[\text{M}+\text{H}_2\text{O}]^+$ . Found C, 65.12; H, 5.71; N, 6.59 %;  $\text{C}_{23}\text{H}_{24}\text{N}_2\text{O}_6$  requires C, 65.08; H, 5.70; N, 6.60 %.

*Benzyl(Z)-2-((3S)-3-((1R)-1-(((1-(4-methoxyphenyl)ethyl) carbamoyl) oxy)ethyl)-4-oxoazetidin-2-ylidene)acetate (5.k)*

Following GP5 and GP6 carbamate **5.k** was obtained in a 69% yield (45 mg, 0.10 mmol). IR (film,  $\text{cm}^{-1}$ ) 3317, 1819, 1698, 1658;  $[\alpha]_{\text{D}}^{20} = -24$  ( $c = 1.2$ ,  $\text{CH}_2\text{Cl}_2$ );  $^1\text{H}$  NMR (400 MHz,  $\text{CDCl}_3$ )  $\delta$  (ppm) 1.41 (d,  $J = 5.6$  Hz, 3H), 1.44 (d,  $J = 7.6$  Hz, 3H), 3.75 (s, 3H), 3.85 (d,  $J = 6.2$  Hz, 1H), 4.77 (bt,  $J = 6.4$  Hz, 1H), 5.07 (d,  $J = 7.2$  Hz, 1H), 5.12 – 5.17 (m, 3H), 5.21 (s, 1H), 6.83 (d,  $J = 8.2$  Hz, 2H), 7.21 (d,  $J = 8.2$  Hz, 2H), 7.29 – 7.38 (m, 5H), 8.82 (bs, 1H);  $^{13}\text{C}$  NMR (100 MHz,  $\text{CDCl}_3$ )  $\delta$  (ppm) 17.9, 22.1, 50.1, 55.2, 61.7, 66.1, 67.0, 90.3, 113.7, 113.9, 126.6, 127.0, 128.1, 128.2, 128.6, 135.2, 135.8, 152.3, 154.3, 158.7, 165.0, 166.7; ESI-MS  $m/z$  456  $[\text{M}+\text{H}_2\text{O}]^+$ . Found C, 65.65; H, 5.96; N, 6.37 %;  $\text{C}_{24}\text{H}_{26}\text{N}_2\text{O}_6$  requires C, 65.74; H, 5.98; N, 6.39 %.

*Benzyl(Z)-2-((S)-3-((R)-1-(((3,4-dimethoxybenzyl)carbamoyl) oxy)ethyl)-4-oxoazetidin-2-ylidene)acetate (5.l)*

Following GP5 and GP6 carbamate **5.l** was obtained in a 75% yield (51 mg, 0.11 mmol). IR (film,  $\text{cm}^{-1}$ ) 3356, 1819, 1700, 1657;  $[\alpha]_{\text{D}}^{20} = +1$  ( $c = 1.0$ ,  $\text{CH}_2\text{Cl}_2$ );  $^1\text{H}$  NMR (400 MHz,  $\text{CDCl}_3$ )  $\delta$  (ppm) 1.39 (d,  $J = 6.4$  Hz, 3H), 3.84 (s, 6H), 3.88 (d,  $J = 6.3$  Hz, 1H), 4.28 (d,  $J = 5.7$  Hz, 2H), 5.09 (bt,  $J = 5.5$  Hz, 1H), 5.12 – 5.18 (m, 2H), 5.20 (quintet,  $J = 6.1$  Hz, 1H), 5.24 (s, 1H), 6.67 – 6.81 (m, 3H), 7.32 – 7.36 (m, 5H), 8.72 (bs, 1H);  $^{13}\text{C}$  NMR (100 MHz,  $\text{CDCl}_3$ )  $\delta$  (ppm) 18.1, 44.9, 55.7, 55.8, 61.7, 66.1, 67.2, 90.4, 110.8, 111.1, 119.8, 128.2, 128.3, 128.6, 130.6, 135.7, 148.4, 149.1, 155.1, 164.9, 152.2, 166.6; ESI-MS  $m/z$  472  $[\text{M}+\text{H}_2\text{O}]^+$ . Found C, 63.55; H, 5.78; N, 6.16 %;  $\text{C}_{24}\text{H}_{26}\text{N}_2\text{O}_7$  requires C, 63.43; H, 5.77; N, 6.16 %.

*Benzyl(Z)-2-((S)-3-((R)-1-(((4-chlorobenzyl)carbamoyl)oxy) ethyl)-4-oxoazetidin-2-ylidene) acetate (5.m)*

Following GP5 and GP6 carbamate **5.m** was obtained in a 69% yield (45 mg, 0.10 mmol). IR (film,  $\text{cm}^{-1}$ ) 3329, 1810, 1691, 1649;  $[\alpha]_{\text{D}}^{20} = +2$  ( $c = 1.1$ ,  $\text{CH}_2\text{Cl}_2$ );  $^1\text{H}$  NMR (400 MHz,  $\text{CDCl}_3$ )  $\delta$  (ppm) 1.39 (d,  $J = 6.3$  Hz, 3H), 3.88 (d,  $J = 6.3$  Hz, 1H), 4.29 (d,  $J = 5.9$  Hz, 2H), 5.16 – 5.20 (m, 4H), 5.24 (s, 1H), 7.17 (d,  $J = 8.0$  Hz, 2H), 7.25 (d,  $J = 8.0$  Hz, 2H), 7.31 – 7.39 (m, 5H), 8.83 (bs, 1H);  $^{13}\text{C}$  NMR (100 MHz,  $\text{CDCl}_3$ )  $\delta$  (ppm) 18.1, 44.3, 61.6, 66.2, 67.4, 90.4, 128.2, 128.3, 128.4, 128.6, 128.8, 133.3, 135.7, 136.7, 152.2, 155.2, 165.0, 166.7; ESI-MS  $m/z$  446  $[\text{M}+\text{H}_2\text{O}]^+$ . Found C, 61.60; H, 4.95; N, 6.52 %;  $\text{C}_{22}\text{H}_{21}\text{ClN}_2\text{O}_5$  requires C, 61.61; H, 4.94; N, 6.53 %.

*Benzyl(Z)-2-((S)-3-((R)-1-(((2-chlorobenzyl)carbamoyl)oxy) ethyl)-4-oxoazetidin-2-ylidene) acetate (5.n)*

Following GP5 and GP6 carbamate **5.n** was obtained in a 59% yield (38 mg, 0.09 mmol). IR (film,  $\text{cm}^{-1}$ ) 3318, 1819, 1699, 1658;  $[\alpha]_{\text{D}}^{20} = +1$  ( $c = 1.0$ ,  $\text{CH}_2\text{Cl}_2$ );  $^1\text{H}$  NMR (400 MHz,  $\text{CDCl}_3$ )  $\delta$  (ppm) 1.39 (d,  $J = 6.4$  Hz, 3H), 3.89 (d,  $J = 6.4$  Hz, 1H), 4.44 (d,  $J = 6.2$  Hz, 2H), 5.16 (s, 2H), 5.19 – 5.26 (m, 3H), 7.19 – 7.21 (m, 2H), 7.33 – 7.37 (m, 7H), 8.67 (bs, 1H);  $^{13}\text{C}$  NMR (100 MHz,  $\text{CDCl}_3$ )  $\delta$  (ppm) 18.1, 43.0, 61.7, 66.2, 67.4, 90.5, 127.1, 128.2, 128.3, 128.6, 129.0, 129.5, 129.7, 133.4, 135.5, 135.8, 152.1, 155.1, 164.8, 166.7; ESI-MS  $m/z$  446  $[\text{M}+\text{H}_2\text{O}]^+$ . Found C, 61.74; H, 4.96; N, 6.52 %;  $\text{C}_{22}\text{H}_{21}\text{ClN}_2\text{O}_5$  requires C, 61.61; H, 4.94; N, 6.53 %.

*Benzyl(Z)-2-((S)-3-((R)-1-(((4-fluorobenzyl)carbamoyl)oxy) ethyl)-4-oxoazetidin-2-ylidene) acetate (5.o)*

Following GP5 and GP6 carbamate **5.o** was obtained in a 69% yield (43 mg, 0.10 mmol). IR (film,  $\text{cm}^{-1}$ ) 3330, 1817, 1697, 1656;  $[\alpha]_{\text{D}}^{20} = +1$  ( $c = 1.0$ ,  $\text{CH}_2\text{Cl}_2$ );  $^1\text{H}$  NMR (400 MHz,  $\text{CDCl}_3$ )  $\delta$  (ppm) 1.40 (d,  $J = 6.4$  Hz, 3H), 3.89 (d,  $J = 6.3$  Hz, 1H), 4.31 (d,  $J = 5.8$  Hz, 2H), 5.08 (bt,  $J = 5.9$  Hz, 1H), 5.16 (s, 2H), 5.20 (quintet,  $J = 6.4$  Hz, 1H), 5.24 (s, 1H), 6.96 – 7.00 (m, 2H), 7.21 – 7.24 (m, 2H), 7.33 – 7.40 (m, 5H), 8.61 (bs, 1H);  $^{13}\text{C}$  NMR (100 MHz,  $\text{CDCl}_3$ )  $\delta$  (ppm) 18.1, 44.4, 61.7, 66.2, 67.4, 90.5, 115.5 (d,  $J = 21.5$  Hz), 128.2, 128.3, 128.6, 129.1 (d,  $J = 9.1$  Hz), 133.9, 135.8, 152.1, 155.1, 162.2 (d,  $J = 240$  Hz), 164.6, 166.6; ESI-MS  $m/z$  430  $[\text{M}+\text{H}_2\text{O}]^+$ . Found C 63.96, H 5.11, N 6.77 %;  $\text{C}_{22}\text{H}_{21}\text{FN}_2\text{O}_5$  requires C 64.07, H 5.13, N 6.79 %.

*Benzyl(Z)-2-((S)-3-((R)-1-(((3-fluoro-4-morpholinobenzyl)carbamoyl)oxy)ethyl)-4-oxoazetidin-2-ylidene)acetate (5.p)*

Following GP5 and GP6 carbamate **5.p** was obtained in a 74% yield (55 mg, 0.11 mmol). IR (film,  $\text{cm}^{-1}$ ) 3329, 1814, 1696, 1658;  $[\alpha]_{\text{D}}^{20} = +4$  ( $c = 1.2$ ,  $\text{CH}_2\text{Cl}_2$ );  $^1\text{H}$  NMR (400 MHz,  $\text{CDCl}_3$ )  $\delta$  (ppm) 1.39 (d,  $J = 6.1$  Hz, 3H), 3.03 (s, 4H), 3.84 (s, 4H), 3.88 (d,  $J = 6.0$  Hz, 1H), 4.26 (s, 2H), 5.13 – 5.28 (m, 5H), 6.86 – 6.94 (m, 3H), 7.16 – 7.35 (m, 5H), 8.80 (bs, 1H);  $^{13}\text{C}$  NMR (100 MHz,  $\text{CDCl}_3$ )  $\delta$  (ppm) 18.0, 44.1, 50.8, 61.6, 66.1, 66.8, 67.3, 90.4, 115.4 (d,  $J = 21.3$  Hz), 118.7 (d,  $J = 3.2$  Hz), 123.4 (d,  $J = 3.0$  Hz), 128.1, 128.3, 128.6, 133.0 (d,  $J = 7.4$  Hz), 135.8, 139.1 (d,  $J = 9.0$  Hz), 152.2, 155.1, 155.5 (d,  $J = 240$  Hz), 164.9, 166.6; ESI-MS  $m/z$  498  $[\text{M}+\text{H}]^+$ . Found C, 62.75; H, 5.68; N, 8.44 %;  $\text{C}_{26}\text{H}_{28}\text{FN}_3\text{O}_6$  requires C, 62.77; H, 5.67; N, 8.45 %.

*Benzyl(Z)-2-((S)-3-((R)-1-(((benzo[d][1,3]dioxol-5-ylmethyl)carbamoyl)oxy)ethyl)-4-oxoazetidin-2-ylidene)acetate (5.q)*

Following GP5 and GP6 carbamate **5.q** was obtained in a 76% yield (50 mg, 0.11 mmol). IR (film,  $\text{cm}^{-1}$ ) 3301, 1819, 1701, 1656;  $[\alpha]_{\text{D}}^{20} = -3$  ( $c = 1.1$ ,  $\text{CH}_2\text{Cl}_2$ );  $^1\text{H}$  NMR (400 MHz,  $\text{CDCl}_3$ )  $\delta$  (ppm) 1.39 (d,  $J = 6.4$  Hz, 3H), 3.88 (d,  $J = 6.3$  Hz, 1H), 4.19 – 4.29 (m, 2H), 5.13 – 5.22 (m, 4H), 5.24 (s, 1H), 5.91 (s, 2H), 6.71 – 6.76 (m, 3H), 7.31 – 7.37 (m, 5H), 8.82 (bs, 1H);  $^{13}\text{C}$  NMR (100 MHz,  $\text{CDCl}_3$ )  $\delta$  (ppm) 18.0, 44.8, 61.6, 66.1, 67.2, 90.4, 101.0, 108.1, 108.2, 120.8, 128.2, 128.3, 128.6, 132.0, 135.8, 146.9, 147.8, 152.3, 155.1, 165.0, 166.7; ESI-MS  $m/z$  456  $[\text{M}+\text{H}_2\text{O}]^+$ . Found C, 63.33; H, 5.08; N, 6.38 %;  $\text{C}_{23}\text{H}_{22}\text{N}_2\text{O}_7$  requires C, 63.01; H, 5.06; N, 6.39 %.

*Benzyl(Z)-2-((S)-3-((R)-1-(((4-nitrobenzyl)carbamoyl)oxy) ethyl)-4-oxoazetidin-2-ylidene) acetate (5.r)*

Following GP5 and GP6 carbamate **5.r** was obtained in a 66% yield (44 mg, 0.10 mmol). IR (film,  $\text{cm}^{-1}$ ) 3322, 1817, 1699, 1657;  $[\alpha]_{\text{D}}^{20} = +5$  ( $c = 1.1$ ,  $\text{CH}_2\text{Cl}_2$ );  $^1\text{H}$  NMR (400 MHz,  $\text{CDCl}_3$ )  $\delta$  (ppm) 1.41 (d,  $J = 6.2$  Hz, 3H), 3.91 (d,  $J = 6.0$  Hz, 1H), 4.45 (d,  $J = 5.9$  Hz, 2H), 5.17 (s, 2H), 5.19 – 5.23 (m, 1H), 5.25 (s, 1H), 5.33 (bt,  $J = 5.6$  Hz, 1H), 7.33 – 7.38 (m, 5H), 7.42 (d,  $J = 8.3$  Hz, 2H), 8.15 (d,  $J = 8.3$  Hz, 2H), 8.71 (bs, 1H);  $^{13}\text{C}$  NMR (100 MHz,  $\text{CDCl}_3$ )  $\delta$  (ppm) 18.1, 44.3, 61.6, 66.2, 67.6, 90.5, 123.9, 127.9, 128.2, 128.4, 128.6, 135.7, 145.7, 147.3, 152.0, 155.3, 164.8, 166.6; ESI-MS  $m/z$  457  $[\text{M}+\text{H}_2\text{O}]^+$ . Found C, 60.04; H, 4.82; N, 9.54 %;  $\text{C}_{22}\text{H}_{21}\text{N}_3\text{O}_7$  requires C, 60.13; H, 4.82; N, 9.56 %.

*Benzyl(Z)-2-((S)-3-((R)-1-(((4-methoxyphenethyl)carbamoyl)oxy)ethyl)-4-oxoazetidin-2-ylidene)acetate (5.s)*

Following GP5 and GP6 carbamate **5.s** was obtained in a 84% yield (55 mg, 0.13 mmol). IR (film,  $\text{cm}^{-1}$ ) 3302, 1819, 1700, 1658;  $[\alpha]_{\text{D}}^{20} = -8$  ( $c = 1.2$ ,  $\text{CH}_2\text{Cl}_2$ );  $^1\text{H}$  NMR (400 MHz,  $\text{CDCl}_3$ )  $\delta$  (ppm) 1.37 (d,  $J = 6.3$  Hz, 3H), 2.74 (t,  $J = 6.8$  Hz, 2H), 3.34 – 3.43 (m, 2H), 3.77 (s, 3H), 3.86 (d,  $J = 6.6$  Hz, 1H), 4.77 (bt,  $J = 5.4$  Hz, 1H), 5.12 – 5.21 (m, 3H), 5.24 (s, 1H), 6.84 (d,  $J = 8.2$  Hz, 2H), 7.09 (d,  $J = 8.2$  Hz, 2H), 7.32 – 7.37 (m, 5H), 8.72 (bs, 1H);  $^{13}\text{C}$  NMR (100 MHz,  $\text{CDCl}_3$ )  $\delta$  (ppm) 18.1, 35.0, 42.3, 55.2, 61.7, 66.2, 67.1, 90.4, 114.0, 128.2, 128.3, 128.6, 129.7, 130.5, 135.8, 152.3, 155.0, 158.2, 164.9, 166.7; ESI-MS  $m/z$  456  $[\text{M}+\text{H}_2\text{O}]^+$ . Found C, 65.82; H, 6.00; N, 6.38 %;  $\text{C}_{24}\text{H}_{26}\text{N}_2\text{O}_6$  requires C, 65.74; H, 5.98; N, 6.39 %.

*Benzyl(Z)-2-((S)-3-((R)-1-(((3,4-dimethoxyphenethyl) carbamoyl)oxy)ethyl)-4-oxoazetidin-2-ylidene)acetate (5.t)*

Following GP5 and GP6 carbamate **5.t** was obtained in a 57% yield (40 mg, 0.09 mmol). IR (film,  $\text{cm}^{-1}$ ) 3355, 1819, 1701, 1657;  $[\alpha]_{\text{D}}^{20} = -5$  ( $c = 1.2$ ,  $\text{CH}_2\text{Cl}_2$ );  $^1\text{H}$  NMR (400 MHz,  $\text{CDCl}_3$ )  $\delta$  (ppm) 1.37 (d,  $J = 6.3$  Hz, 3H), 2.74 (t,  $J = 7.1$  Hz, 2H), 3.38 – 3.43 (m, 2H), 3.83 – 3.87 (m, 7H), 4.79 (bt,  $J = 5.6$  Hz, 1H), 5.13 – 5.19 (m, 3H), 5.23 (s, 1H), 6.69 – 6.80 (m, 3H), 7.32 – 7.36 (m, 5H), 8.67 (bs, 1H);  $^{13}\text{C}$  NMR (100 MHz,  $\text{CDCl}_3$ )  $\delta$  (ppm) 18.1, 35.6, 42.3, 55.7, 55.8, 61.7, 66.2, 67.1, 90.4, 111.4, 111.8, 120.7, 128.2, 128.3, 128.6, 131.0, 135.7, 147.7, 149.0, 152.3, 155.0, 164.9, 166.6; ESI-MS  $m/z$  486  $[\text{M}+\text{H}_2\text{O}]^+$ . Found C, 64.13; H, 6.04; N, 5.87 %;  $\text{C}_{25}\text{H}_{28}\text{N}_2\text{O}_7$  requires C, 64.09; H, 6.02; N, 5.98 %.

*Benzyl(Z)-2-((S)-3-((R)-1-(((4-((tert-butoxycarbonyl)amino)benzyl)carbamoyl)oxy)ethyl)-4-oxoazetidin-2-ylidene)acetate (8.u)*

Following GP5 and GP6 carbamate **8.u** was obtained in a 55% yield (42 mg, 0.08 mmol). IR (film,  $\text{cm}^{-1}$ ) 3334, 1812, 1698, 1657;  $[\alpha]_{\text{D}}^{20} = -3$  ( $c = 1.1$ ,  $\text{CH}_2\text{Cl}_2$ );  $^1\text{H}$  NMR (400 MHz,  $\text{CDCl}_3$ )  $\delta$  (ppm) 1.39 (d,  $J = 6.4$  Hz, 3H), 1.51 (s, 9H), 3.87 (d,  $J = 6.4$  Hz, 1H), 4.27 – 4.29 (m, 2H), 5.05 (bt,  $J = 4.8$  Hz, 1H), 5.16 (s, 2H), 5.20 (quintet,  $J = 6.4$  Hz, 1H), 5.24 (s, 1H), 6.47 (bs, 1H), 7.16 (d,  $J = 8.2$  Hz, 2H), 7.25 (d,  $J = 8.2$  Hz, 2H), 7.32 – 7.40 (m, 5H), 8.62 (bs, 1H);  $^{13}\text{C}$  NMR (100 MHz,  $\text{CDCl}_3$ )  $\delta$  (ppm) 18.2, 28.3, 44.6, 61.7, 66.2, 67.3, 80.6, 90.5, 114.0, 118.7, 128.2, 128.3, 128.6, 132.6, 135.8, 137.8, 152.2, 152.7, 155.1, 164.8, 166.7; ESI-MS  $m/z$  527  $[\text{M}+\text{H}_2\text{O}]^+$ .

*4-((((R)-1-((S,Z)-2-(2-(benzyloxy)-2-oxoethylidene)-4-oxoazetidin-3-yl)ethoxy)carbonyl)amino)methyl)benzenaminium 2,2,2-trifluoroacetate (5.u)*

Following GP4,  $\beta$ -lactam **8.u** (42 mg, 0.08 mmol, 1 equiv) treated with TFA (184  $\mu\text{L}$ , 2.4 mmol) yielded compound **5.u** as a colorless oil (40 mg, 96%). IR (film,  $\text{cm}^{-1}$ ) 3356, 1815, 1701, 1655;  $[\alpha]_{\text{D}}^{20} = -14$  ( $c = 1.0$ ,  $\text{CH}_3\text{OH}$ );  $^1\text{H}$  NMR (400 MHz,  $\text{CD}_3\text{OD}$ )  $\delta$  (ppm) 1.36 (d,  $J = 6.4$  Hz, 3H), 3.95 (d,  $J = 6.7$  Hz, 1H), 4.09 – 4.17 (m, 2H), 5.10 (quintet,  $J = 6.4$  Hz, 1H), 5.17 (s, 2H), 5.24 (s, 1H), 6.64 (d,  $J = 8.1$  Hz, 2H), 7.00 (d,  $J = 8.1$  Hz, 2H), 7.29 – 7.38 (m, 5H);  $^{13}\text{C}$  NMR (100 MHz,  $\text{CD}_3\text{CN}$ )  $\delta$  (ppm) 18.8, 44.6, 62.7, 66.4, 68.1, 90.6, 122.4, 129.0, 129.1, 129.2, 129.4, 129.5, 131.6, 137.8, 154.2, 156.8, 166.8, 167.3; ESI-MS  $m/z$  410  $[\text{M}-\text{TFA}+\text{H}]^+$ . Found C, 55.40; H, 4.63; N 8.00 %;  $\text{C}_{24}\text{H}_{24}\text{F}_3\text{N}_3\text{O}_7$  requires C, 55.07; H, 4.62; N, 8.03 %.

### 2.13.7 Development of $\beta$ -lactam-based antibacterial biomaterials

#### 2.13.7.1 Loading of azetidinones

The loading of azetidinones on HA was conducted in  $\text{H}_2\text{O}$  (method A) or  $\text{H}_2\text{O}$ /organic solvent mixtures (method B). Loading processes were set up in a parallel-synthesis fashion with a Carousel 6 reaction station using two necks round bottom flasks (50 mL) with a water-cooled aluminum head. This apparatus is well suited to keep constant some experimental conditions, such as stirring and warming, important parameters in heterogeneous phase processes, and, moreover, it improved and speeded up optimization steps. *Method A*: 200 mg of HA nanoparticles were suspended in 2 mL of  $\text{H}_2\text{O}$  and warmed at 40 °C under magnetic stirring. Azetidinone (50 mg) was added in one portion to the suspension which was then warmed up to 70 °C. Reaction mixtures were controlled *via* TLC on the supernatant solution for monitoring the starting azetidinone disappearance. After 4 h the mixture was quantitatively transferred with 1 mL of  $\text{H}_2\text{O}/\text{CH}_3\text{CN}$  (1:1) in an open test tube and centrifugated for 1 min at 700 rpm. The solid phase was perfectly separated and the supernatant aqueous phase was collected and extracted with dichloromethane (1  $\times$  3 mL). The aqueous and organic phases were separately evaporated and analyzed to quantify the unloaded azetidinone and its distribution in the two phases. Data were expressed as loading efficiency% back-calculated from the added up residues obtained in DCM and  $\text{H}_2\text{O}$  in comparison with the amount of azetidinones in the loading solution by the equation:

$LE = [A - (rw + rDCM)]A * 100$  where: LE = loading efficiency%; A = amount (g) of azetidinone in the loading solution; rw = residue (g) of azetidinone in water extract; rDCM = residue (g) of azetidinone in dichloromethane (DCM) extract.

The solid functionalized HA material was oven dried at 35 °C for 24 h, and kept in dessicator (CaCl<sub>2</sub>) for 24 h before the analyses. *Method B*: 200 mg of HA nanoparticles were suspended in 1 mL of H<sub>2</sub>O and warmed at 40 °C under magnetic stirring, then azetidinone (50 mg) was solubilized in 1 mL of organic solvent and added to the suspended HA, then the mixture was warmed at 70 °C under stirring for 4 h. Reaction mixtures were controlled *via* TLC on the supernatant solution for monitoring the starting azetidinone disappearance. The work-up procedure was the same as for Method A.

Loading amount of the azetidinone molecules on HA was evaluated through thermogravimetric analysis as difference between the total weight loss measured between 38 and 800 °C for each loaded sample and that measured for pristine HA. Moreover, the determination was also performed through the evaluation of the intensity of the adsorption band of C=O at 1790 cm<sup>-1</sup>.

#### 2.13.7.2 In vitro release

The release profiles of azetidinones loaded on HA were investigated in H<sub>2</sub>O Milli Q, buffer phosphate (0.1 M, pH = 7.4), and buffer acetate (0.1 M, pH = 5.0). Samples of azetidinones **1.N-HA** (8.1% of loaded azetidinone, TGA measurement), **1.V-HA** (12.6 %), **1.P-HA** (15.7 %), and **1.W-HA** (10.9 %) were used for the *in vitro* release study. In a 10 mL test tube an azetidinone-HA sample (50 mg) was suspended in 2.5 mL of the aqueous solutions H<sub>2</sub>O Milli Q, buffer phosphate (0.1 M, pH = 7.4), or buffer acetate (0.1 M, pH = 4.5). Experiments were conducted at 37 °C in thermostat with sampling and refresh of the aqueous solution after 1, 2, 3, 6, 8, 24, 30 h. At each time point, the solution was centrifugated (1 min, 700 rpm), the supernatant was separated and the released concentration of the azetidinone was determined by HPLC-UV analysis. The solid was incubated again with a fresh solution of the specific medium (2.5 mL). The release of samples **1.N-HA** and **1.P-HA** were also studied in buffer acetate at pH = 5.0 by a once-a-day refresh for 9 days with the procedure and analyses above described. Linear calibration curves for the HPLC-UV analysis of azetidinones in supernatant solutions were established at 210 nm (column: Phenomenex Gemini C18, 3 μm, 100 x 3mm, flow 0.4 mL/min, T = 30 °C); parameters for **1.N**: Rt = 3.9 min H<sub>2</sub>O/CH<sub>3</sub>CN = 80:20 in the region of concentration from 3 to 0.15 mM; for **1.V**: Rt = 5.3 min H<sub>2</sub>O/CH<sub>3</sub>CN = 60:40 in the region of concentration from 2.5 to 0.05 mM; for **1.P**: Rt = 12.2 min from H<sub>2</sub>O/CH<sub>3</sub>CN = 80:20 to 20:80 in 8 min, in the region of concentration from 1 to 0.225 mM; for **1.W**: Rt = 7.1 min H<sub>2</sub>O/CH<sub>3</sub>CN = 30:70 in the region of concentration from 1 to 0.05 mM.

#### 2.13.7.3 Synthesis of N-thio-substituted-azetidinones

Azetidinones **1.M** and **1.O** are commercially available.

##### *4-Acetoxy-1-(methylthio)-azetidin-2-one (1.N)*

Following GP7, dimethyldisulfide (113 μL, 1.25 mmol) was reacted with 4-acetoxy-azetidin-2-one **1.M** (129 mg, 1 mmol) yielding compound **1.N** as a yellow oil (169 mg, 77%) after purification by flash-chromatography (cyclohexane/EtOAc 80:20). IR (film, cm<sup>-1</sup>) 3341, 3200, 1790, 1752, 1393, 1213; <sup>1</sup>H NMR (400 MHz, CDCl<sub>3</sub>) δ (ppm) 2.15 (s, 3H), 2.47 (s, 3H), 3.03 (dd, *J* = 15.3, 1.6 Hz, 1H), 3.38 (dd, *J* = 15.3, 4.2 Hz, 1H), 6.10 (dd, *J* = 4.2, 1.6 Hz, 1H); <sup>13</sup>C NMR (100 MHz, CDCl<sub>3</sub>) δ (ppm) 20.9, 22.8, 46.3, 78.8, 167.9, 170.1; ESI-MS (R<sub>t</sub> = 2.3 min) *m/z* 176 [M+H]<sup>+</sup>, 198 [M+Na]<sup>+</sup>.

##### *4-acetoxy-1-(phenylthio)-azetidin-2-one (1.V)*

Following GP7, diphenyldisulfide (218 mg, 1 mmol) was reacted with 4-acetoxy-azetidin-2-one **1.M** (129 mg, 1 mmol) yielding compound **1.V** as a yellow oil (206 mg, 87%) after purification by flash-chromatography

(cyclohexane/EtOAc 80:20). IR (film,  $\text{cm}^{-1}$ ) 3059, 2923, 2850, 1785, 1754, 1585, 1355, 1287;  $^1\text{H}$  NMR (400 MHz,  $\text{CDCl}_3$ )  $\delta$  (ppm) 1.99 (s, 3H), 3.10 (dd,  $J = 1.2, 15.3$  Hz, 1H), 3.42 (dd,  $J = 4.3, 15.3$  Hz, 1H), 6.19 (dd,  $J = 1.2, 4.2$  Hz, 1H), 7.50–7.27 (m, 5H);  $^{13}\text{C}$  NMR (100 MHz,  $\text{CDCl}_3$ )  $\delta$  (ppm) 20.6, 46.2, 78.6, 128.6, 129.2, 136.0, 167.2, 170.0; ESI-MS ( $R_t = 10.2$  min)  $m/z$  238  $[\text{M}+\text{H}]^+$ , 260  $[\text{M}+\text{Na}]^+$ .

#### (2R, 3R)-3-(-1-(*t*-butyldimethylsilyloxy)ethyl)-4-acetoxy-1-(methylthio)-azetidin-2-one (**1.P**)

Following GP7, dimethyldisulfide (90  $\mu\text{L}$ , 1 mmol) was reacted with (2R,3R)-3-((R)-1-((*tert*-butyldimethylsilyloxy)ethyl)-4-oxoazetidin-2-yl acetate **1.O** (287 mg, 1 mmol) yielding compound **1.P** as a yellow oil (280 mg, 84%) after purification by flash-chromatography (cyclohexane/EtOAc 90:10). IR (film,  $\text{cm}^{-1}$ ) 2955, 2929, 2856, 1792, 1751, 1251;  $^1\text{H}$  NMR (400 MHz,  $\text{CDCl}_3$ )  $\delta$  (ppm) 0.03 (s, 3H), 0.05 (s, 3H), 0.84 (s, 9H), 1.26 (d,  $J = 6.4$  Hz, 3H), 2.13 (s, 3H), 2.45 (s, 3H), 3.17 (dd,  $J = 2.9, 1.4$  Hz, 1H), 4.21 (dq,  $J = 6.3, 2.9$  Hz, 1H), 6.21 (d,  $J = 1.3$  Hz, 1H);  $^{13}\text{C}$  NMR (100 MHz,  $\text{CDCl}_3$ )  $\delta$  (ppm) -5.1, -4.5, 17.9, 21.0, 22.2, 22.8, 25.7, 63.9, 66.3, 80.2, 169.3, 169.8; ESI-MS ( $R_t = 12.3$  min)  $m/z$  356  $[\text{M}+\text{Na}]^+$ , 234  $[\text{M}+\text{H}]^+$ .

#### (2R,3R)-3-(-1-(*t*-butyldimethylsilyloxy)ethyl)-4-acetoxy-1-(phenylthio)-azetidin-2-one (**1.W**)

Following GP7, diphenyldisulfide (218 mg, 1 mmol) was reacted with (2R,3R)-3-((R)-1-((*tert*-butyldimethylsilyloxy)ethyl)-4-oxoazetidin-2-yl acetate **1.O** (287 mg, 1 mmol) yielding compound **1.W** as a yellow oil (297 mg, 75%) after purification by flash-chromatography (cyclohexane/EtOAc 90:10). IR (film,  $\text{cm}^{-1}$ ) 2955, 2929, 2856, 1793, 1758, 1472, 1257;  $[\alpha]_D^{20} = -16$  ( $c = 1.0$ ,  $\text{CH}_2\text{Cl}_2$ ).  $^1\text{H}$  NMR (400 MHz,  $\text{CDCl}_3$ )  $\delta$  (ppm) -0.01 (s, 3H), 0.03 (s, 3H), 0.80 (s, 9H), 1.24 (d,  $J = 6.4$  Hz, 1H), 1.94 (s, 3H), 3.26 (dd,  $J = 1.4, 3.3$  Hz, 1H), 4.21 (dq,  $J = 3.4, 6.3$  Hz, 1H), 6.32 (d,  $J = 1.2$  Hz, 1H), 7.24–7.49 (m, 5H);  $^{13}\text{C}$  NMR (100 MHz,  $\text{CDCl}_3$ )  $\delta$  (ppm) -5.13, -4.52, 17.8, 20.6, 22.2, 25.6, 64.1, 66.1, 80.8, 128.2, 128.9, 129.1, 136.3, 169.1, 169.8; ESI-MS ( $R_t = 13.5$  min)  $m/z$  364  $[\text{M}+\text{H}]^+$ , 386  $[\text{M}+\text{Na}]^+$ .

### 2.13.8 Synthesis of other *N*-thio-substituted $\beta$ -lactams

#### 1-(benzylthio)-4-oxoazetidin-2-yl acetate (**9.a**)

Following GP7, dibenzyldisulfide (246 mg, 1 mmol) was reacted with 4-acetoxy-azetidin-2-one **1.M** (129 mg, 1 mmol) yielding compound **9.a** as a yellow oil (100 mg, 40%) after purification by flash-chromatography (cyclohexane/EtOAc 75:25). IR (film,  $\text{cm}^{-1}$ ) 3085, 3061, 2960, 2923, 1779, 1751, 1429, 1225;  $^1\text{H}$  NMR (400 MHz,  $\text{CDCl}_3$ )  $\delta$  (ppm) 7.40–7.27 (m, 5H), 5.62–5.57 (m, 1H), 4.13 (d,  $J = 12.7$  Hz, 1H), 3.93 (d,  $J = 12.7$  Hz, 1H), 3.23 (dd,  $J = 15.3, 4.1$  Hz, 1H), 2.92 (d,  $J = 15.3$  Hz, 1H), 2.04 (s, 3H);  $^{13}\text{C}$  NMR (100 MHz,  $\text{CDCl}_3$ )  $\delta$  (ppm) 169.8, 167.8, 135.2, 129.3, 128.6, 127.7, 78.9, 46.1, 42.9, 20.7; ESI-MS ( $R_t = 7.7$  min)  $m/z$  252  $[\text{M}+\text{H}]^+$ , 269  $[\text{M}+\text{H}_2\text{O}]^+$ .

#### 1-((4-methoxyphenyl)thio)-4-oxoazetidin-2-yl acetate (**9.b**)

Following GP7, *p*-methoxyphenyldisulfide (278 mg, 1 mmol) was reacted with 4-acetoxy-azetidin-2-one **1.M** (129 mg, 1 mmol) yielding compound **9.b** as a yellow oil (174 mg, 65%) after purification by flash-chromatography (cyclohexane/EtOAc 75:25). IR (film,  $\text{cm}^{-1}$ ) 3065, 3008, 2963, 2942, 1780, 1754, 1591, 1493, 1288;  $^1\text{H}$  NMR (400 MHz,  $\text{CDCl}_3$ )  $\delta$  (ppm) 7.58–7.53 (m, 2H), 6.89–6.84 (m, 2H), 6.11 (dd,  $J = 4.2, 1.6$  Hz, 1H), 3.80 (s, 3H), 3.30 (dd,  $J = 15.2, 4.2$  Hz, 1H), 3.00 (dd,  $J = 15.2, 1.6$  Hz, 1H), 2.03 (s, 3H);  $^{13}\text{C}$  NMR (100 MHz,  $\text{CDCl}_3$ )  $\delta$  (ppm) 170.1, 167.4, 160.9, 134.8, 126.2, 114.7, 78.1, 55.4, 45.9, 20.7; ESI-MS ( $R_t = 7.8$  min)  $m/z$  268  $[\text{M}+\text{H}]^+$ .

#### 1-(benzo[d]thiazol-2-ylthio)-4-oxoazetidin-2-yl acetate (**9.c**)

Following GP7, 2,2'-dithiobis(benzothiazole) (333 mg, 1 mmol) was reacted with 4-acetoxy-azetidin-2-one **1.M** (129 mg, 1 mmol) yielding compound **9.c** as a yellow oil (243 mg, 83%) after purification by flash-chromatography (cyclohexane/EtOAc 75:25). IR (film,  $\text{cm}^{-1}$ ) 2925, 2853, 1798, 1755, 1467, 1428, 1279;  $^1\text{H}$

NMR (400 MHz, CDCl<sub>3</sub>)  $\delta$  (ppm) 7.87 (d,  $J$  = 8.1 Hz, 1H), 7.78 (d,  $J$  = 8.1 Hz, 1H), 7.43 (dd,  $J$  = 8.1, 1.2 Hz, 1H), 7.32 (dd,  $J$  = 1.2, 8.1 Hz, 1H), 6.39 (dd,  $J$  = 4.4, 1.8 Hz, 1H), 3.64 (dd,  $J$  = 15.6, 4.4 Hz, 1H), 3.26 (dd,  $J$  = 15.6, 1.8 Hz, 1H), 2.10 (s, 3H); <sup>13</sup>C NMR (100 MHz, CDCl<sub>3</sub>)  $\delta$  (ppm) 20.6, 46.8, 79.0, 121.1, 122.4, 124.9, 126.4, 135.2, 153.5, 166.8, 166.9, 169.8; ESI-MS ( $R_t$  = 8.2 min)  $m/z$  = 295 [M+H]<sup>+</sup>.

#### *1-(isopropylthio)-4-oxoazetidin-2-yl acetate (9.d)*

Following GP7, diisopropyl disulfide (125  $\mu$ L, 1 mmol) was reacted with 4-acetoxy-azetidin-2-one **1.M** (129 mg, 1 mmol) yielding compound **9.d** as a yellow oil (57 mg, 28%) after purification by flash-chromatography (cyclohexane/EtOAc 75:25). IR (film, cm<sup>-1</sup>) 2965, 2927, 1783, 1753, 1373, 1227; <sup>1</sup>H NMR (400 MHz, CDCl<sub>3</sub>)  $\delta$  (ppm) 6.06 (dd,  $J$  = 4.2, 1.6 Hz, 1H), 3.39 (dd,  $J$  = 15.4, 4.2 Hz, 1H), 3.23 (sept,  $J$  = 6.7 Hz, 1H), 3.01 (dd,  $J$  = 15.4, 1.6 Hz, 1H), 2.12 (s, 3H), 1.26 (d,  $J$  = 6.7 Hz, 3H), 1.23 (d,  $J$  = 6.7 Hz, 3H); <sup>13</sup>C NMR (100 MHz, CDCl<sub>3</sub>)  $\delta$  (ppm) 170.0, 168.8, 79.4, 46.1, 41.6, 21.5, 21.1, 20.8; ESI-MS ( $R_t$  = 6.0 min)  $m/z$  204 [M+H]<sup>+</sup>, 226 [M+Na]<sup>+</sup>.

#### *4-oxo-1-(propylthio)azetidin-2-yl acetate (9.e)*

Following GP7, propyl disulfide (141  $\mu$ L, 1 mmol) was reacted with 4-acetoxy-azetidin-2-one **1.M** (129 mg, 1 mmol) yielding compound **9.e** as a yellow oil (134 mg, 66%) after purification by flash-chromatography (cyclohexane/EtOAc 75:25). IR (film, cm<sup>-1</sup>) 2965, 2934, 1785, 1755, 1375, 1290; <sup>1</sup>H NMR (400 MHz, CDCl<sub>3</sub>)  $\delta$  (ppm) 6.04 (dd,  $J$  = 4.1, 1.5 Hz, 1H), 3.36 (dd,  $J$  = 15.3, 4.1 Hz, 1H), 2.99 (dd,  $J$  = 15.3, 1.5 Hz, 1H), 2.78 – 2.64 (m, 2H), 2.11 (s, 3H), 1.70 – 1.59 (m, 2H), 0.99 (t,  $J$  = 7.4 Hz, 3H); <sup>13</sup>C NMR (100 MHz, CDCl<sub>3</sub>)  $\delta$  (ppm) 170.0, 168.4, 79.1, 46.2, 41.0, 21.9, 20.8, 12.9; ESI-MS ( $R_t$  = 6.3 min)  $m/z$  204 [M+H]<sup>+</sup>, 226 [M+Na]<sup>+</sup>.

#### *1-(butylthio)-4-oxoazetidin-2-yl acetate (9.f)*

Following GP7, butyl disulfide (190  $\mu$ L, 1 mmol) was reacted with 4-acetoxy-azetidin-2-one **1.M** (129 mg, 1 mmol) yielding compound **9.f** as a yellow oil (36 mg, 17%) after purification by flash-chromatography (cyclohexane/EtOAc 75:25). IR (film, cm<sup>-1</sup>) 2960, 2931, 1785, 1754, 1374, 1226; <sup>1</sup>H NMR (400 MHz, CDCl<sub>3</sub>)  $\delta$  (ppm) 6.07 – 6.04 (m, 1H), 3.37 (dd,  $J$  = 15.3, 4.1 Hz, 1H), 3.00 (dd,  $J$  = 15.3, 1.4 Hz, 1H), 2.83 – 2.68 (m, 2H), 2.13 (s, 3H), 1.61 (m, 2H), 1.48 – 1.35 (m, 2H), 0.90 (t,  $J$  = 6.7 Hz, 3H); <sup>13</sup>C NMR (100 MHz, CDCl<sub>3</sub>)  $\delta$  (ppm) 170.0, 168.4, 79.2, 46.2, 38.7, 30.6, 21.5, 20.9, 13.5; ESI-MS ( $R_t$  = 7.7 min)  $m/z$  235 [M+H<sub>2</sub>O]<sup>+</sup>.

#### *(2R,3R)-1-(benzylthio)-3-((R)-1-((tert-butyl dimethylsilyl)oxy)ethyl)-4-oxoazetidin-2-yl acetate (10.a)*

Following GP7, dibenzyl disulfide (246 mg, 1 mmol) was reacted with (2R,3R)-3-((R)-1-((tert-butyl dimethylsilyl)oxy)ethyl)-4-oxoazetidin-2-yl acetate **1.O** (287 mg, 1 mmol) yielding compound **10.a** as a yellow oil (74 mg, 18%) after purification by flash-chromatography (cyclohexane/EtOAc 80:20). IR (film, cm<sup>-1</sup>) 2955, 2929, 2886, 2856, 1790, 1754, 1471, 1375, 1222; [ $\alpha$ ]<sub>D</sub><sup>20</sup> = -10 (c = 1.0, CH<sub>2</sub>Cl<sub>2</sub>); <sup>1</sup>H NMR (400 MHz, CDCl<sub>3</sub>)  $\delta$  (ppm) 7.35 – 7.29 (m, 5H), 6.09 (d,  $J$  = 1.4 Hz, 1H), 4.15 – 4.10 (m, 1H), 4.04 (q,  $J_{AB}$  = 12.4 Hz, 2H), 3.14 (dd,  $J$  = 3.8, 1.4 Hz, 1H), 2.03 (s, 3H), 1.22 (d,  $J$  = 6.3 Hz, 3H), 0.84 (s, 9H), 0.05 (s, 3H), 0.02 (s, 3H); <sup>13</sup>C NMR (100 MHz, CDCl<sub>3</sub>)  $\delta$  (ppm) 169.8, 169.2, 134.9, 129.4, 128.6, 127.7, 81.1, 66.3, 64.3, 43.5, 25.6, 22.1, 20.8, 17.8, -4.4, -5.1; ESI-MS ( $R_t$  = 14.4 min)  $m/z$  432 [M+Na]<sup>+</sup>.

#### *(2R,3R)-3-((R)-1-((tert-butyl dimethylsilyl)oxy)ethyl)-1-((4-methoxyphenyl)thio)-4-oxoazetidin-2-yl acetate (10.b)*

Following GP7, *p*-methoxyphenyl disulfide (278 mg, 1 mmol) was reacted with (2R,3R)-3-((R)-1-((tert-butyl dimethylsilyl)oxy)ethyl)-4-oxoazetidin-2-yl acetate **1.O** (287 mg, 1 mmol) yielding compound **10.b** as a yellow oil (111 mg, 26%) after purification by flash-chromatography (cyclohexane/EtOAc 90:10). IR (film, cm<sup>-1</sup>) 2955, 2930, 2895, 2856, 1788, 1757, 1494, 1250; [ $\alpha$ ]<sub>D</sub><sup>20</sup> = -13 (c = 1.0, CH<sub>2</sub>Cl<sub>2</sub>); <sup>1</sup>H NMR (400 MHz, CDCl<sub>3</sub>)  $\delta$  (ppm) 7.58 – 7.55 (m, 2H), 7.00 – 6.78 (m, 2H), 6.25 (d,  $J$  = 1.4 Hz, 1H), 4.16 (qd,  $J$  = 6.3, 3.5 Hz, 1H), 3.80 (s, 3H), 3.18 (dd,  $J$  = 3.5, 1.4 Hz, 1H), 2.01 (s, 3H), 1.20 (d,  $J$  = 6.3 Hz, 3H), 0.76 (s, 9H), 0.01 (s,



3H), -0.05 (s, 3H); <sup>13</sup>C NMR (100 MHz, CDCl<sub>3</sub>) δ (ppm) 170.0, 168.7, 160.8, 134.7, 126.4, 114.6, 80.3, 66.1, 64.0, 55.4, 25.6, 22.2, 20.8, 17.8, -4.6, -5.2; ESI-MS (R<sub>t</sub> = 14.2 min) *m/z* 448 [M+Na]<sup>+</sup>.

*(3R)-1-(benzo[d]thiazol-2-ylthio)-3-((R)-1-((tert-butyldimethylsilyl)oxy)ethyl)-4-oxoazetidin-2-yl acetate (10.c)*

Following GP7, 2,2'-dithiobis(benzothiazole) (333 mg, 1 mmol) was reacted with (2R,3R)-3-((R)-1-((tert-butyldimethylsilyl)oxy)ethyl)-4-oxoazetidin-2-yl acetate **1.O** (287 mg, 1 mmol) yielding compound **10.c** as a yellow oil (187 mg, 41%) after purification by flash-chromatography (cyclohexane/EtOAc 90:10). IR (film, cm<sup>-1</sup>) 3064, 2954, 2929, 2856, 1802, 1762, 1469, 1428, 1255; [α]<sub>D</sub><sup>20</sup> = -5 (c = 0.9, CH<sub>2</sub>Cl<sub>2</sub>); <sup>1</sup>H NMR (400 MHz, CDCl<sub>3</sub>) δ (ppm) 7.87 (d, *J* = 8.0 Hz, 1H), 7.78 (d, *J* = 8.0 Hz, 1H), 7.43 (dd, *J* = 8.0, 1.1 Hz, 1H), 7.32 (dd, *J* = 8.0, 1.1 Hz, 1H), 6.45 (d, *J* = 1.6 Hz, 1H), 4.39 – 4.31 (m, 1H), 3.45 (dd, *J* = 4.1, 1.6 Hz, 1H), 2.07 (s, 3H), 1.31 (d, *J* = 6.3 Hz, 3H), 0.87 (s, 9H), 0.11 (s, 3H), 0.08 (s, 3H); <sup>13</sup>C NMR (100 MHz, CDCl<sub>3</sub>) δ (ppm) 169.6, 168.1, 167.8, 153.7, 135.3, 126.3, 124.7, 122.3, 121.0, 81.3, 66.9, 64.6, 25.6, 22.1, 20.0, 17.8, -4.4, -5.1; ESI-MS (R<sub>t</sub> = 15.2 min) *m/z* 453 [M+H]<sup>+</sup>.

*(2R,3R)-3-((R)-1-((tert-butyldimethylsilyl)oxy)ethyl)-1-(isopropylthio)-4-oxoazetidin-2-yl acetate (10.d)*

Following GP7, isopropyl disulfide (125 μL, 1 mmol) was reacted with (2R,3R)-3-((R)-1-((tert-butyldimethylsilyl)oxy)ethyl)-4-oxoazetidin-2-yl acetate **1.O** (287 mg, 1 mmol) yielding compound **10.d** as a yellow oil (96 mg, 27%) after purification by flash-chromatography (cyclohexane/EtOAc 40:60). IR (film, cm<sup>-1</sup>) 2958, 2929, 2857, 1791, 1754, 1461, 1375, 1222; [α]<sub>D</sub><sup>20</sup> = -18 (c = 1.0, CH<sub>2</sub>Cl<sub>2</sub>); <sup>1</sup>H NMR (400 MHz, CDCl<sub>3</sub>) δ (ppm) 6.21 (d, *J* = 1.4 Hz, 1H), 4.22 (qd, *J* = 6.3, 3.2 Hz, 2H), 3.23 (sept, *J* = 6.7 Hz, 1H), 3.19 (dd, *J* = 3.2, 1.4 Hz, 1H), 2.13 (s, 3H), 1.28 (d, *J* = 6.7 Hz, 3H), 1.24 (d, *J* = 6.3, 3H), 1.23 (d, *J* = 6.7 Hz, 3H), 0.85 (s, 9H), 0.06 (s, 3H), 0.04 (s, 3H); <sup>13</sup>C NMR (100 MHz, CDCl<sub>3</sub>) δ (ppm) 170.2, 169.8, 81.3, 66.4, 64.1, 41.6, 29.7, 25.7, 22.2, 21.8, 21.01, 20.99, 17.9, -4.5, -5.0; ESI-MS (R<sub>t</sub> = 13.6 min) *m/z* 384 [M+Na]<sup>+</sup>.

*(2R,3R)-3-((R)-1-((tert-butyldimethylsilyl)oxy)ethyl)-4-oxo-1-(propylthio)azetidin-2-yl acetate (10.e)*

Following GP7, propyl disulfide (141 μL, 1 mmol) was reacted with (2R,3R)-3-((R)-1-((tert-butyldimethylsilyl)oxy)ethyl)-4-oxoazetidin-2-yl acetate **1.O** (287 mg, 1 mmol) yielding compound **10.e** as a yellow oil (133 mg, 37%) after purification by flash-chromatography (cyclohexane/EtOAc 90:10). IR (film, cm<sup>-1</sup>) 2958, 2931, 2884, 2857, 1790, 1753, 1462, 1362, 1224; [α]<sub>D</sub><sup>20</sup> = -14 (c = 1, CH<sub>2</sub>Cl<sub>2</sub>); <sup>1</sup>H NMR (400 MHz, CDCl<sub>3</sub>) δ (ppm) 6.17 (d, *J* = 1.2 Hz, 1H), 4.19 (qd, *J* = 6.3, 3.2 Hz, 1H), 3.17 – 3.13 (m, 1H), 2.77 – 2.62 (m, 2H), 2.11 (s, 3H), 1.71 – 1.58 (m, 2H), 1.21 (d, *J* = 6.3 Hz, 3H), 0.98 (t, *J* = 7.3 Hz, 3H), 0.83 (s, 9H), 0.04 (s, 3H), 0.01 (s, 3H); <sup>13</sup>C NMR (100 MHz, CDCl<sub>3</sub>) δ (ppm): 169.7, 80.9, 66.3, 64.0, 41.1, 25.6, 22.2, 22.0, 20.9, 17.8, 12.9, -4.6, -5.1; ESI-MS (R<sub>t</sub> = 13.7 min) *m/z* = 384 [M+Na]<sup>+</sup>.

*(2R,3R)-3-((R)-1-((tert-butyldimethylsilyl)oxy)ethyl)-1-(butylthio)-4-oxoazetidin-2-yl acetate (10.f)*

Following GP7, butyl disulfide (190 μL, 1 mmol) was reacted with (2R,3R)-3-((R)-1-((tert-butyldimethylsilyl)oxy)ethyl)-4-oxoazetidin-2-yl acetate **1.O** (287 mg, 1 mmol) yielding compound **10.f** as a yellow oil (51 mg, 14%) after purification by flash-chromatography (cyclohexane/EtOAc 90:10). IR (film, cm<sup>-1</sup>) 2958, 2931, 2858, 1791, 1754, 1463, 1376, 1224; [α]<sub>D</sub><sup>20</sup> = -16 (c = 0.9, CH<sub>2</sub>Cl<sub>2</sub>); <sup>1</sup>H NMR (400 MHz, CDCl<sub>3</sub>) δ (ppm) 6.18 (d, *J* = 1.2 Hz, 1H), 4.20 (qd, *J* = 6.3, 3.2 Hz, 1H), 3.17 – 3.15 (m, 1H), 2.73 (m, 2H), 1.66 – 1.53 (m, 2H), 1.47 – 1.32 (m, 2H), 1.22 (d, *J* = 6.3 Hz, 3H), 0.89 (t, *J* = 7.3 Hz, 4H), 0.83 (s, 9H), 0.04 (s, 3H), 0.02 (s, 3H); <sup>13</sup>C NMR (100 MHz, CDCl<sub>3</sub>) δ (ppm) 169.7, 81.0, 66.4, 64.0, 38.8, 30.6, 25.6, 22.2, 21.5, 20.9, 17.8, 13.5, -4.5, -5.1; ESI-MS (R<sub>t</sub> = 15.1 min) *m/z* = 398 [M+Na]<sup>+</sup>.

## 3. Novel $\beta$ -lactam compounds active as integrin ligands

### 3.1 Multifaceted activities of $\beta$ -lactam compounds

Azetidinone derivatives first attracted attention for their antibacterial properties, but during the last two decades researches convincingly demonstrated that structural modifications of monocyclic  $\beta$ -lactams with specific substituents was an effective procedure for the detection of varied pharmacological effects different from antibacterial activity.<sup>40</sup> In fact, the azetidinone core-structure could be considered a privileged structure having two specific structural features that are of interest with regard to biological activity: *i*) a constrained four-membered cyclic amide which could easily undergo ring-opening reactions by nucleophilic residues in the active sites of enzymes; *ii*) a rigid core structure that, by reducing the conformational degrees of freedom, could favor and actually enhance directional non-covalent bonding for ligand-receptor recognition.<sup>110</sup>

#### 3.1.1 $\beta$ -lactams as enzyme inhibitors

As a matter of fact, over the past few decades diverse azetidinone derivatives demonstrated biological activity as inhibitors of a wide range of enzymes.<sup>111</sup>

For example, 3-chloro-azetidinones were mainly evaluated as antibacterials, as above mentioned, but some derivatives showed activities as anti-inflammatory and analgesic agents.<sup>112</sup> Activities of 3-amino-azetidinones were instead related to the presence of the same substituent of natural penicillins and cephalosporins. They showed to behave as inhibitors of cathepsins,<sup>113</sup> proteasome<sup>114</sup> and vasopressin<sup>115</sup> (Figure 3.1).

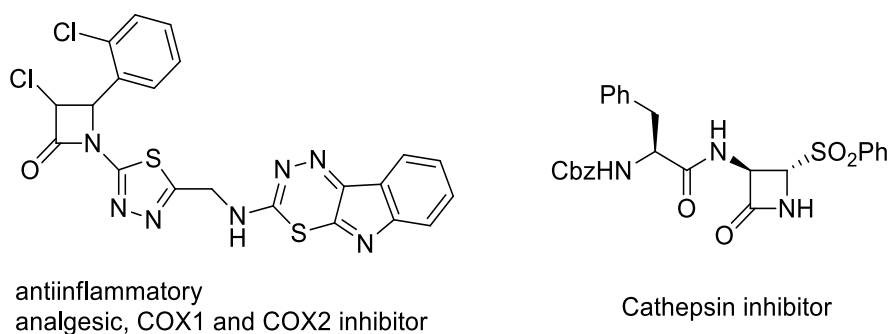


**Figure 3.1.** 3-chloro and 3-amino-azetidinones as enzyme inhibitors<sup>37</sup>

The already described class of 4-alkylidene-azetidinones, besides the aforementioned antibacterial activity, has been investigated against matrix metallo proteases (MMPs) as gelatinases inhibitors and against human leucocyte elastase (HLE)<sup>39a,116</sup> (Figure 3.2).

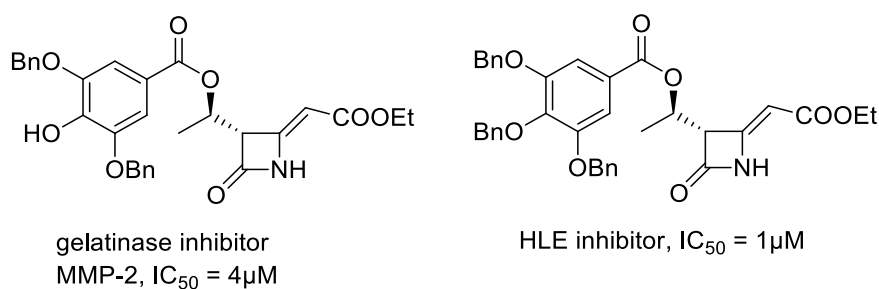


**Figure 3.2.** 4-alkylidene-azetidinones as enzyme inhibitors<sup>40</sup>

Moreover, *N*-acylation of the azetidinone ring represented an effective way to activate monocyclic  $\beta$ -lactams towards nucleophilic ring-opening reactions, gaining enzymatic inhibitors with different biological targets such as porcine pancreas elastase (PPE) and HLE,<sup>117</sup> platelet aggregation,<sup>118</sup> prostate specific antigen,<sup>119</sup> human fatty acid amide hydrolase (hFAAH),<sup>120</sup> and human cytomegalovirus protease (HCMV)<sup>121</sup> (Figure 3.3).

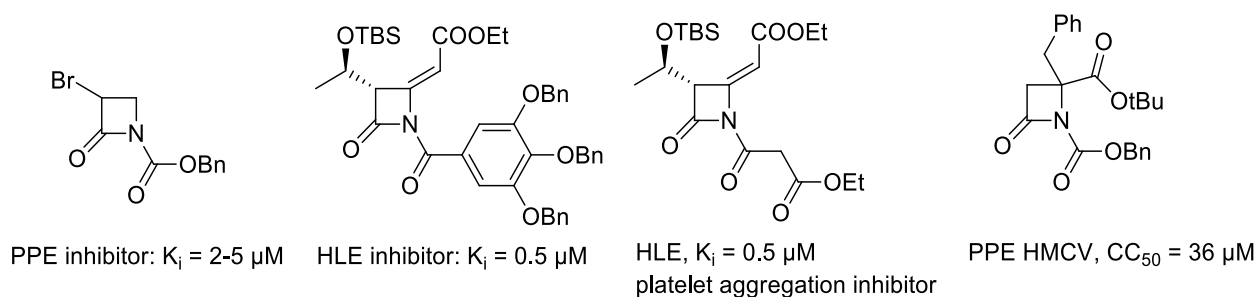


**Figure 3.3.** *N*-acyl-azetidinones as enzyme inhibitors<sup>40</sup>

*N*-thiolated  $\beta$ -lactams, beyond the already described antibacterial activity, were evaluated as antifungal,<sup>122</sup> apoptosis inducers,<sup>123</sup> and selective histone deacetylases (HDAC) inhibitors<sup>124</sup> (Figure 3.4).

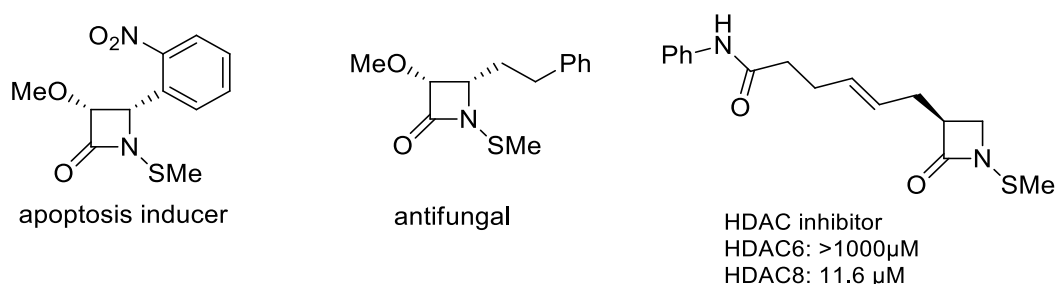


**Figure 3.4.** *N*-thiolated-azetidinones as enzyme inhibitors<sup>40</sup>

More recently, new  $\beta$ -lactam lipopeptides have been described to inhibit a bacterial signal peptidase,<sup>125</sup> and advances have been reported regarding the use of  $\beta$ -lactams as antagonists of cholesterol absorption.<sup>126</sup> Moreover, some azetidinones have been shown to be antagonists of heat shock protein 90,<sup>127</sup> and some of their derivatives were antithrombotic agents.<sup>128</sup>

Among the cited monocyclic azetidinones, some molecules successfully reached an advanced level of preclinical or early clinical studies. It is important to underline that the important biological activities mentioned above were closely linked to the presence of the highly reactive four-membered lactam ring, which, if conveniently substituted on its three positions, could represent a valuable source of molecular diversity.<sup>40</sup>

### 3.1.2 $\beta$ -lactams as integrin ligands

Among receptor ligands that are structurally based on the  $\beta$ -lactam core, only few azetidinones have been shown to exhibit activity against integrins, which are a complex family of cellular receptors.<sup>129</sup>

#### 3.1.2.1 Integrins

Integrins are heterodimeric transmembrane proteins structurally constituted by a non-covalent association of  $\alpha$  and  $\beta$  subunits. Both subunits are type I transmembrane glycoproteins that contain a relatively large extracellular domain, a single transmembrane domain, and a short cytoplasmic tail<sup>130</sup> (Figure 3.5).

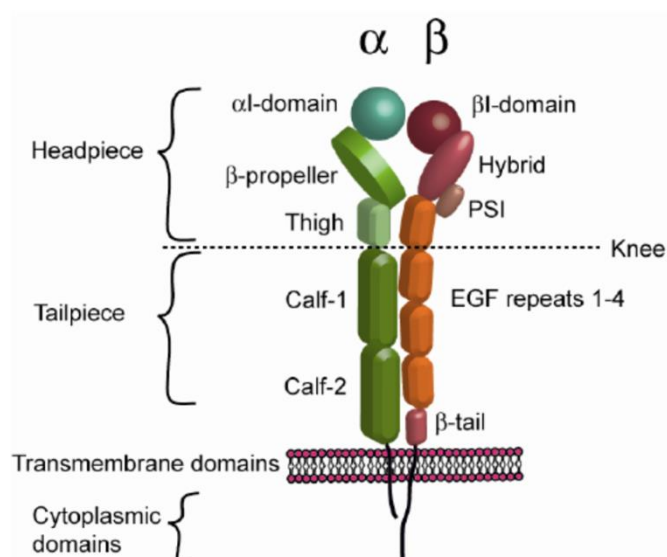


**Figure 3.5.** Integrin structure<sup>131</sup>

In mammals, 18  $\alpha$ -subunits and 8  $\beta$ -subunits assemble into 24 different integrins, each exhibiting a distinct binding affinity to particular ligands<sup>132</sup> (Figure 3.6). The  $\alpha$ -subunits have the greatest influence on ligand-binding specificity and define different integrin families. Integrins may recognize collagen ( $\alpha_1$ ,  $\alpha_2$ ,  $\alpha_{10}$ , and  $\alpha_{11}$ ), laminin ( $\alpha_3$ ,  $\alpha_6$ , and  $\alpha_7$ ), inflammatory ligands ( $\alpha_4$ ,  $\alpha_L$ ,  $\alpha_M$ ,  $\alpha_X$ , and  $\alpha_D$ ) and RGD (arginine-glycine-aspartic acid) motifs ( $\alpha_{IIb}$ ,  $\alpha_V$ ,  $\alpha_5$ , and  $\alpha_8$ ). In particular RGD integrins bind different ECM (extracellular matrix) proteins such as, among the others, vitronectin, fibronectin, fibrinogen and plasminogen.<sup>133</sup> Conversely, leukocyte integrins recognizing inflammatory ligands bind proteins containing LDV (leucine-aspartic acid-valine) or related sequences such as LDT (leucine-aspartic acid-threonine) and IDS (isoleucine-aspartic acid-serine).

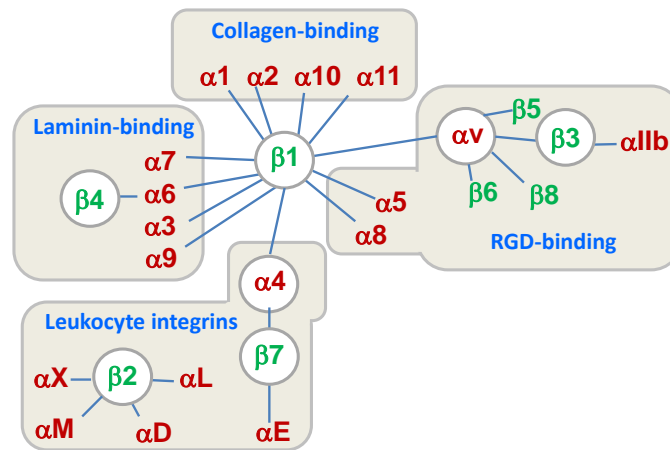


**Figure 3.6.** Classification of the 24 integrin heterodimers according to the combination of  $\alpha$  and  $\beta$  subunits, their specific ligands, or cell type. Figure adapted from ref. <sup>134</sup>

Integrins are basically adhesion receptors that mediate dynamic adhesive cell-cell and cell-matrix interactions,<sup>135</sup> but they can overall regulate crucial aspects of cellular functions, including migration, adhesion, differentiation, growth and survival, by communicating bidirectional signals between the extracellular and intracellular environments.<sup>136</sup> Integrins are normally inactive with low affinity for their endogenous ligands, but they undergo rapid activation upon various stimuli.<sup>137</sup> Activation occurs when membrane-bound proteins increase the affinity of ectodomains for extracellular ligands, promoting cell adhesion and modulating intracellular signalling cascades (inside-out signalling).<sup>138</sup> But as bidirectional receptors, integrins, upon ligand binding in the extracellular matrix, transmit outside-in signals into the cell (Figure 3.7).

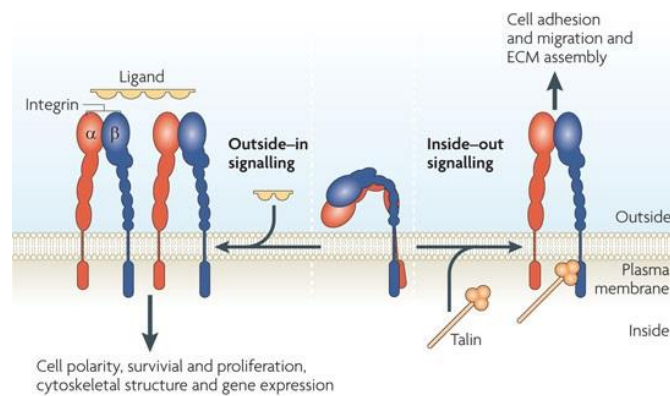


**Figure 3.7.** Integrin outside-in and inside-out signalling. Figure adapted from ref. <sup>139</sup>

The ligand-binding site forms a region at the intersection of  $\alpha$  and  $\beta$  subunits and contains a metal ion-dependent adhesion site (MIDAS), able to bind Asp, Glu, or carboxylic acid residues in ligands. In RGD-binding integrins for example, Arg of RGD binds the  $\alpha$ -subunit while Asp coordinates to the  $Mg^{2+}$  ion in the MIDAS. The binding of endogenous ligands to integrins recruits several cellular components and modulates intracellular signalling cascades, especially those leading to the activation of focal adhesion kinase (FAK) and mitogen-activated protein kinase (MAPK) pathways that play a crucial role in the regulation of numerous cell functions.<sup>140</sup>

The ability of integrins to bind and associate with various components of the ECM or soluble ligands largely depends on the structural conformations of the two subunits  $\alpha$  and  $\beta$ , and distinct conformations are crucial for regulating both inside-out and outside-in cell signalling.<sup>141</sup> Structural studies (crystallography, NMR and electron microscopy) have revealed three possible states for integrins: a bent, an extended-closed, and an extended-open conformations (Figure 3.8), corresponding respectively to a low affinity, an activated, and an activated together with ligand integrin conformers.<sup>142</sup>

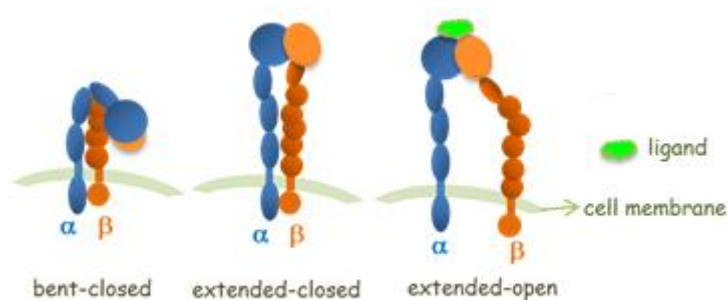


**Figure 3.8.** Three integrin conformational states. Figure adapted from ref. 134

Integrin capacity to activate, integrate and distribute information identifies this family of adhesion receptors as valuable drug targets.<sup>143</sup> In fact, integrins are involved in immune responses, leukocyte traffic, haemostasis, and their potential as a therapeutic target is now widely recognized.<sup>137</sup> In particular, among the integrin superfamily,  $\alpha_v\beta_3$  and  $\alpha_5\beta_1$  classes have been implicated in tumor development playing a pivotal role in the formation of new blood vessels and being overexpressed on activated endothelial cells in physiological and pathological angiogenesis.<sup>144</sup> In addition,  $\alpha_4\beta_{1/7}$  and  $\alpha_{LM}\beta_2$  have been implicated in the regulation of inflammation and immune functions, and  $\alpha_{IIb}\beta_3$  has been involved in platelet aggregation.<sup>133</sup>

### 3.1.2.2 Integrin ligands

The tight regulation of integrin signalling is paramount for normal physiological functions and a mis-regulated integrin activity is associated with several pathological conditions. Therefore, extensive efforts have been made to discover and develop integrin ligands for use in clinical applications.<sup>145</sup> Pharmacologically, ligands can be classified according to their action at the receptor. Agonists are compounds that mimic the signalling of endogenous compounds binding to receptors; antagonists instead block the receptor interaction with endogenous agonists without inducing any activation and signal transduction. In addition, ligands defined partial agonists possess less ability to activate the receptor and the associated signal transduction, while inverse agonists are able to stabilize the receptor in its inactive conformation. A ligand can also be defined allosteric if it modulates receptor activity acting on a topographically distinct position from the site of activity or ligand binding. Recently, it has been recognized that not all agonists behave in the same manner, introducing the hypothesis of biased agonism for integrins.<sup>146</sup>

To date, many researches have focused on the development of small molecules or antibodies able to mainly inhibit integrins and up to now, a large number of peptidic and non-peptidic ligands for  $\alpha_v\beta_3$  and  $\alpha_v\beta_5$  receptor have been developed, which are all related to the minimal recognition motif RGD (Arg-Gly-Asp) present on ECM proteins.<sup>147</sup> Despite the great expectations, antagonists of  $\alpha_v\beta_3$ ,  $\alpha_v\beta_5$

and  $\alpha_5\beta_1$  integrins that have entered clinical trials as antiangiogenic agents for cancer treatment, have generally been unsuccessful. As an example, the well-known Cilengitide (Figure 3.9a), a small RGD-containing cyclic pentapeptide developed by Kessler<sup>148</sup>, has been studied in clinical phase III for glioblastoma and in phase II for other types of cancers. Nevertheless, its addition to temozolomide chemo-radiotherapy failed to be effective with the consequence that this agent was not further developed. Actually, no anticancer drug targeting integrins has been approved yet.

As already mentioned, the interest in developing new integrin antagonists is widely recognized; less attention was instead turned to those ligands that could promote integrin activity, maybe for avoiding a possible activation of angiogenesis and tumor growth. However, several studies have suggested that small molecules that act as integrin agonists may open novel opportunities for therapeutics, which gain benefits to increase rather than decrease integrin-dependent adhesion. These include an agonist of  $\alpha_M\beta_2$  integrin<sup>149</sup> that ameliorates kidney transplantation,<sup>150</sup> an agonist of  $\alpha_L\beta_2$  integrin that inhibits lymphocyte trans-endothelial migration,<sup>151</sup> and an agonist of  $\alpha_4\beta_1$  integrin that induces progenitor cell adhesion.<sup>152</sup> Gupta *et al.* also reported that small agonist molecules could reduce leukocyte migration, tissue accumulation and inflammatory injury.<sup>153</sup> Another important example concerns the chemoresistance in melanoma that involved a loss of integrin-mediated adhesion; in this case, stimulation of integrin signalling by agonists significantly improved the response to chemotherapy.<sup>154</sup> These latter studies suggest that, using small molecules or modifying the sequence of small peptides, an integrin antagonist could be converted to an agonist that could promote cell adhesion and modulate intracellular signalling pathways.

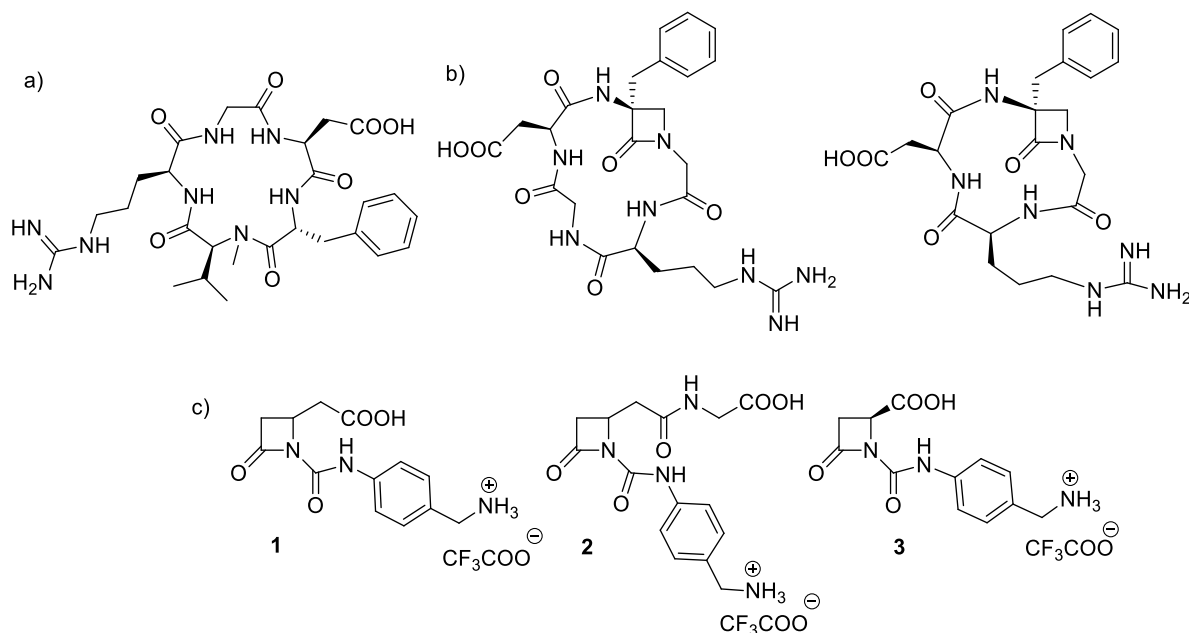


**Figure 3.9.** Previously reported  $\beta$ -lactams as integrin ligands<sup>155</sup>, and Cilengitide (a)

Recent research efforts have tentatively improved the pharmacological parameters of the developed derivatives mainly by altering their polarity and rigidity. Among several heterocyclic structures, Palomo *et al.* and Aizpurua *et al.* embedded an azetidinone scaffold in cyclic peptides or pseudopeptides containing the RGD recognition motif or a RGD-like sequence (Figure 3.9b).<sup>129</sup> The

incorporation of a conformational constrain, such as the introduction of an unsaturated  $\beta$ -amino acid or a  $\beta$ -lactam scaffold in a cyclic structure, was in general intended to enhance selectivity and modulate the affinity toward the receptor. In particular the azetidinone ring, as widely discussed, constitutes *per se* a site of conformational restriction with a  $\beta$ -amino acid moiety in a cyclic structure. According to this, the ability of azetidinones, not inserted into cyclopeptides, to target integrins was recently evaluated by my research group.<sup>155</sup>

A preliminary study on the synthesis of three new azetidinones **1-3** as potential integrin ligands (Figure 3.9c) was reported. The approach used was based on rationalization from known integrin ligands and the novel molecules were designed with the azetidinone as a rigid cyclic central core, with two arms holding a carboxylic acid and a basic moiety, as in the RGD sequence. The 4-amidobenzylamine residue was chosen as a basic terminus that was directly linked to the  $\beta$ -lactam nitrogen atom as in urea derivatives, and a carboxylic acid was located on the C4 side chain and differently spaced from the ring. The C3 position was not substituted in order to mimic the methylene residue of glycine in the RGD peptide. The two side chains anchored on the  $\beta$ -lactam provided a favourable alignment on the receptor, thus meeting the crucial requirements for integrin affinity. When these new molecules were tested on cell lines K562 (human erythroleukemia expressing  $\alpha_5\beta_1$  integrin) and SK-MEL-24 (human malignant melanoma expressing  $\alpha_v\beta_3$  integrin), a concentration-dependent enhancement of fibronectin-mediated adhesion was observed. In particular,  $\beta$ -lactam **1** displayed a higher affinity toward  $\alpha_5\beta_1$  integrin (EC<sub>50</sub> 12 nM) and  $\beta$ -lactam **2** was more selective for integrin  $\alpha_v\beta_3$  (EC<sub>50</sub> 11 nM), both resulting agonist ligands. Compound **3** instead was around 1000 times less effective.<sup>155</sup>

### 3.1.2.3 Integrin activation: internalization, trafficking and endocytosis

The term "integrin activation" defines the transition of integrins from a bent-closed to an extended-open conformation that, as aforementioned, could be induced by both cytoplasmic events (inside-out activation) and extracellular factors such as the interaction with a ligand (outside-in activation).<sup>132b</sup> The interaction with the ligand not only activates the integrin itself, but also induces a series of important processes for cellular activity such as integrin clustering, trafficking and endocytosis.<sup>156</sup> Although extensive research within the integrin field has elucidated key signal transduction pathways as being involved in integrin-mediated cellular behavior, it is only relatively recently that the importance of integrin trafficking in modulating cellular function has been demonstrated.<sup>157</sup>

Integrin clustering is defined as the interaction between adjacent integrins to form hetero-oligomers incited by several factors: inside-out signals that stimulate the recruitment of multivalent protein complexes in the cytoplasmic domain, interaction with ligands in the extracellular domain, homodimerization in the transmembrane domain or release from cytoskeletal constraints, which leads to the diffusion of integrins on the membrane.<sup>139</sup>

Integrin trafficking is regulated by members of the Ras-associated binding (Rab) family of small GTPases, which function as molecular switches regulating vesicular transport in eukaryotic cells.<sup>158</sup> It can be globally defined as a process consisting of a complex intracellular internalization, through which integrin heterodimers are endocytosed into the cytoplasm by modifying the shape of the plasma membrane, and are later exocytosed back to the cell surface.<sup>157</sup>



Endocytosis is in fact characterized by the internalization of protein receptors from the plasma membrane into internal membrane compartments before sorting to different cellular locations. Generally, endocytic processes are classified as clathrin-dependent endocytosis (CDE) or clathrin-independent endocytosis (CIE), whereby CIE describes several distinct endocytic routes (Figure 3.10).<sup>159</sup> Cell surface receptors are endocytosed by one of these routes, but it is also possible that a given type of integrin could follow more than one pathway depending on regions within a cell, cell conditions, and cell type.<sup>160</sup>

Clathrin-mediated endocytosis, the best-characterised internalisation route, involves the recruitment of small vesicles that have a crystalline coat made up of a complex of proteins associated with the cytosolic protein clathrin, called clathrin-coated pit (CCP).<sup>161</sup> In contrast, less is known about the mechanisms involved in CIE, and, in particular, how cargoes are recruited. Caveolae are the most common reported non-clathrin-coated plasma membrane buds which exist on the surface of many, but not all, cell types.<sup>162</sup> Caveolar-mediated endocytosis is mediated by small flask-shaped invaginations, caveolae, in the membrane, consisting of the cholesterol-binding protein caveolin and glycolipids.<sup>163</sup>

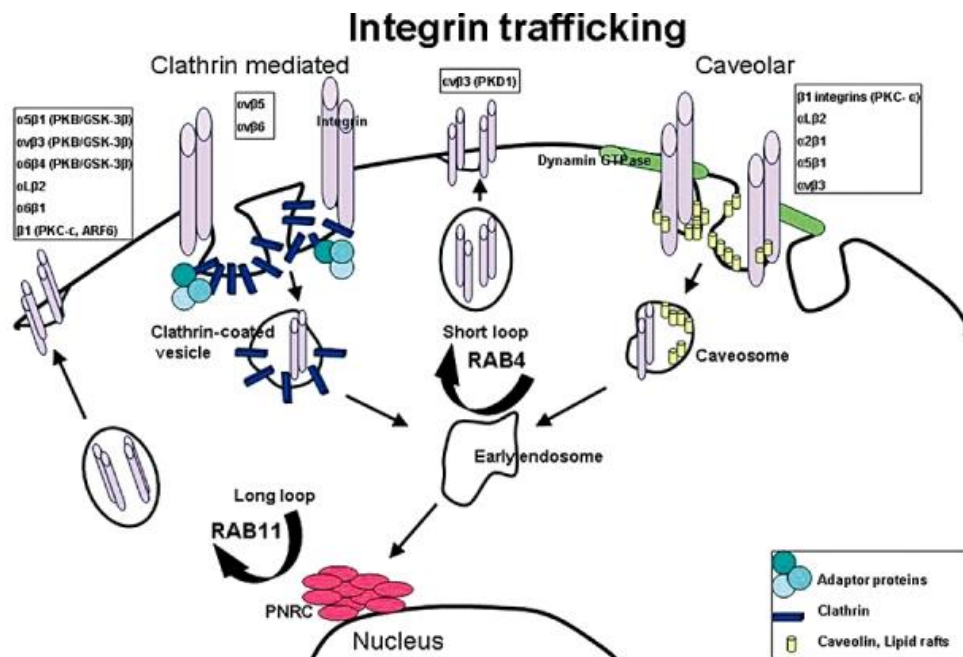


**Figure 3.10.** Integrin trafficking depicting the two main pathways of internalization, clathrin-mediated and caveolar, and the pathways of recycling. Figure adapted from ref <sup>164</sup>

Once internalized, integrins are predominantly recycled back to the plasma membrane. Following endocytosis, integrins travel to early endosomes from which they can either be returned directly to the plasma membrane in a Rab4-dependent manner (the short loop) or further trafficked to the perinuclear recycling compartment (PNRC) before being recycled through Rab11-dependent mechanisms (the long loop)<sup>165</sup> (Figure 3.10). Integrin trafficking therefore provides a constant supply of "new" receptors, regulating integrin population on the cell surface through cycles of endo/exocytosis.<sup>166</sup>

Understanding the molecular mechanisms of integrin trafficking is pivotal for monitoring tumor progression and for the development of anticancer drugs. Several studies indeed demonstrated that tumor cells overexpress integrin receptors and their signal transduction occurs in an anomalous way;<sup>167</sup> an alteration in the mechanisms regulating endocytosis could therefore contribute to the invasive capacity of these cells.<sup>168</sup>

Despite the internalization of integrins regulate many cellular processes, such as migration and adhesion, especially in many pathological conditions,<sup>169</sup> very little is known about the mechanism of internalization of integrin-bound RGD peptides,<sup>170</sup> and if integrin agonists and antagonists could mediate trafficking processes in a different way.

## **3.2 Development of a new integrin-ligand library**

### *3.2.1 Synthesis of azetidiones*

As described in Paragraph 3.1.2.2, my research group recently reported the synthesis of three derivatives, two of which exhibited good affinity and specificity towards  $\alpha_v\beta_3$  and  $\alpha_5\beta_1$  integrin classes being active as agonists at a nanomolar level.<sup>155</sup>

After these first promising biological data, we expanded the scope of the work and developed a library of new monocyclic  $\beta$ -lactam derivatives (Chart 3.1). Similarly to what previously reported, we decided to exploit the possibility of using only a  $\beta$ -lactam core to obtain a constrained molecule that could favor complexation with the receptor, excluding the insertion of an azetidinone ring in cyclic peptides. The novel compounds were specifically designed by a structure-based strategy to target particular classes of integrins.<sup>171</sup> Biological activity, indeed, is always related to the residues present on the  $\beta$ -lactam scaffolds and in this case we suitably modified the amine and the carboxylic acid side chains with a wider structural variability, with the aim to enhance selectivity and to modulate the efficacy against the receptor.

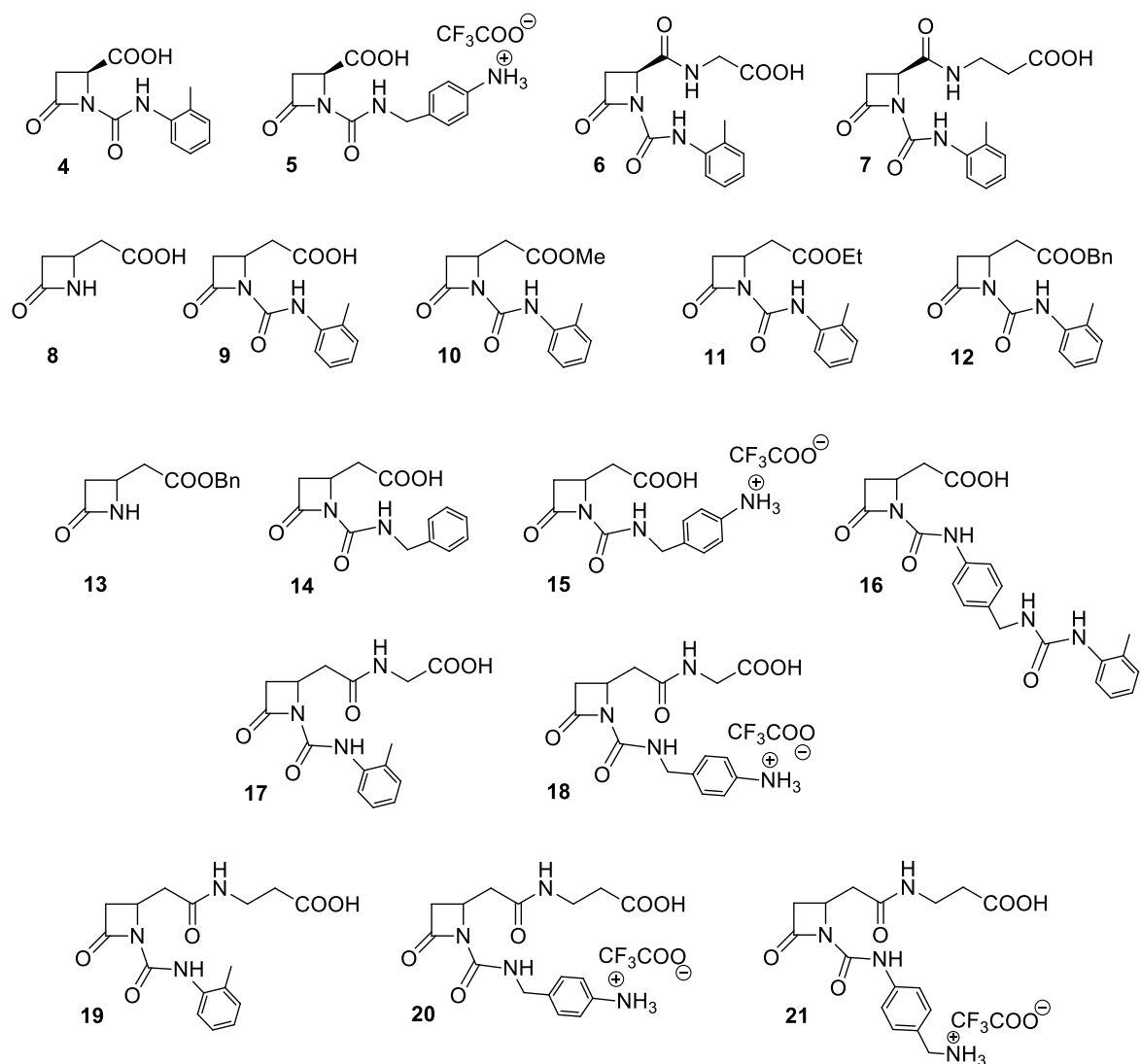


**Chart 3.1.** Novel  $\beta$ -lactam compounds **4-21** designed to target integrins

Of the various integrin ligands explored by others, we were particularly interested in the antagonists reported by Tolomelli *et al.*<sup>172</sup> They found that a 4-aminobenzylamide residue was an effective Arg mimetic with an increased affinity for  $\alpha_v\beta_3$  and  $\alpha_5\beta_1$  integrins, whereas the presence of a 4-[(*N*-2-methylphenyl)ureido]-phenylacetyl (MPUPA) motif greatly enhanced bioactivity and specificity for  $\alpha_4\beta_1$  integrins.<sup>173</sup>

We then chose to install a 4-aminobenzylamido- or its isomeric 4-aminomethylphenylamido- residue on the N1 nitrogen atom of the azetidinone *via* a condensation reaction with isocyanates (Figure 3.11). These two isomeric substitutions were selected to evaluate the influence of the basicity of the amine terminus; in this case we compared benzylamine and aniline residues.<sup>174</sup>

The carboxylic acid function which could coordinate at the metal ion-dependent adhesion site (MIDAS) of the  $\beta$ -subunit of integrins<sup>175</sup> was placed on the C4 side chain of the azetidinone. In detail,  $\beta$ -lactams **4-7** (Chart 3.1) were designed with a C4 carboxylic acid residue, as either a free acid or dipeptide, and compounds **8-21** with a C4 acetic acid residue, as either a free acid, ester or dipeptide. In dipeptide derivatives, two amino acids glycine or  $\beta$ -alanine were chosen for their un-substituted flexible chains and coupled with the azetidinone carboxylic acid.

Essentially, a panel of 18 new azetidinones was synthesized starting from two commercially available compounds, *L*-aspartic acid and 4-acetoxyazetidinone. The general synthetic approach is depicted in Figure 3.11. Compounds **4-7** were prepared starting from *L*-aspartic acid, cyclization to give azetidin-2-one 4-carboxyester, insertion of the imide by condensation with an isocyanate, and C4 side chain elongation *via* a peptide coupling procedure. The C4 acetic acid derivatives **8-21** were synthesized from the commercially available 4-acetoxyazetidinone with a Reformatsky reagent and bromoacetates.<sup>176</sup> Again, the imido group was obtained with the appropriate isocyanate and peptide coupling gave higher molecular weight derivatives.

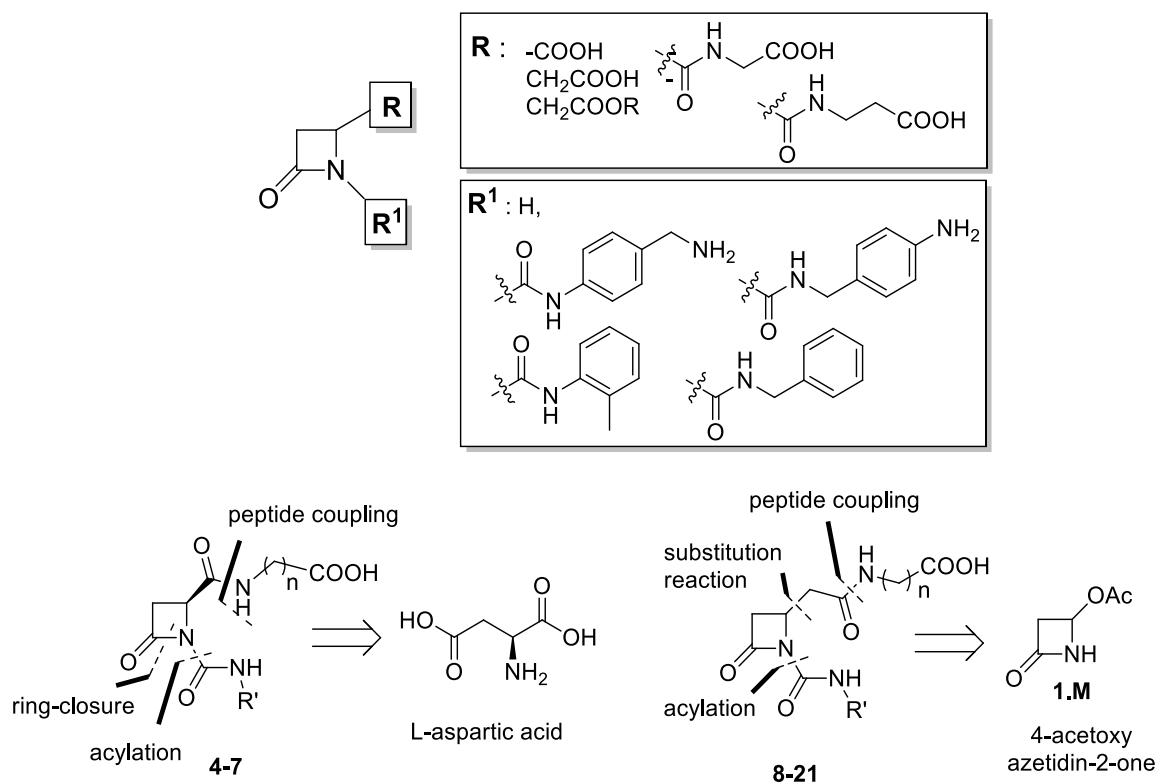
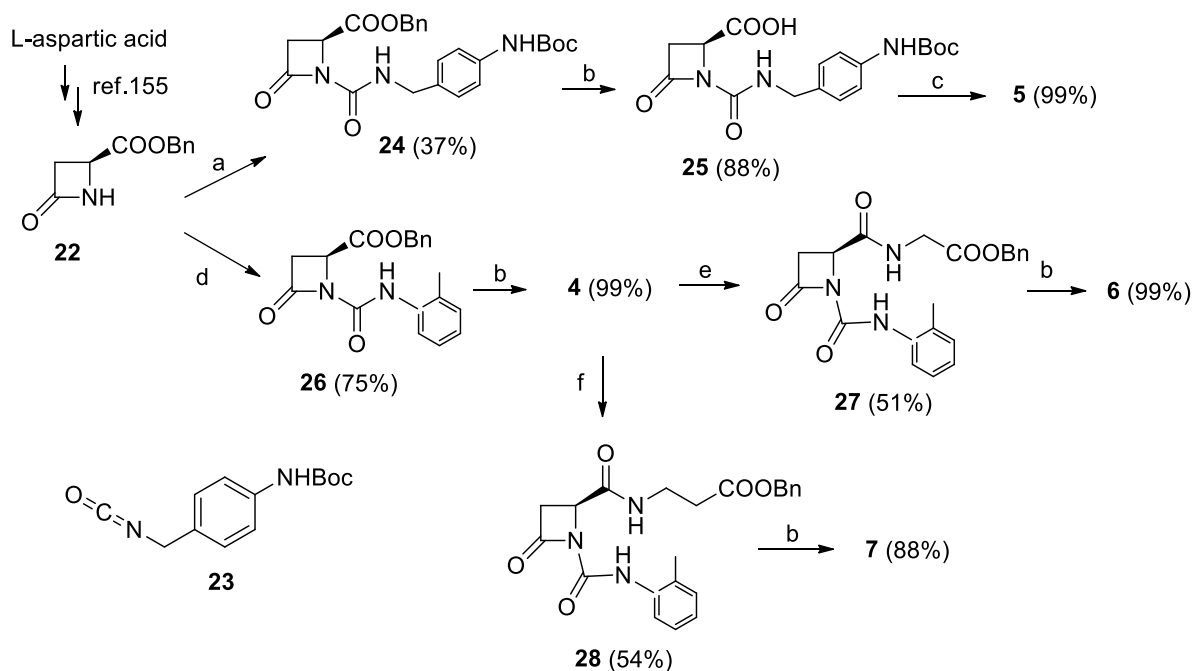


Figure 3.11. Substituent variations and synthetic strategies for  $\beta$ -lactams **4-21**

A careful strategy for protecting the carboxylic acid and the amine terminus was developed in order to preserve the  $\beta$ -lactam ring throughout the synthesis, and in particular in the final deprotection step. Particular attention was paid to specific combinations of temporary or permanent protecting groups to achieve full or partial deprotection depending on the requirements of the synthetic strategy. The synthesis of compounds **4-21** is described in detail in Schemes 3.1-3.4.

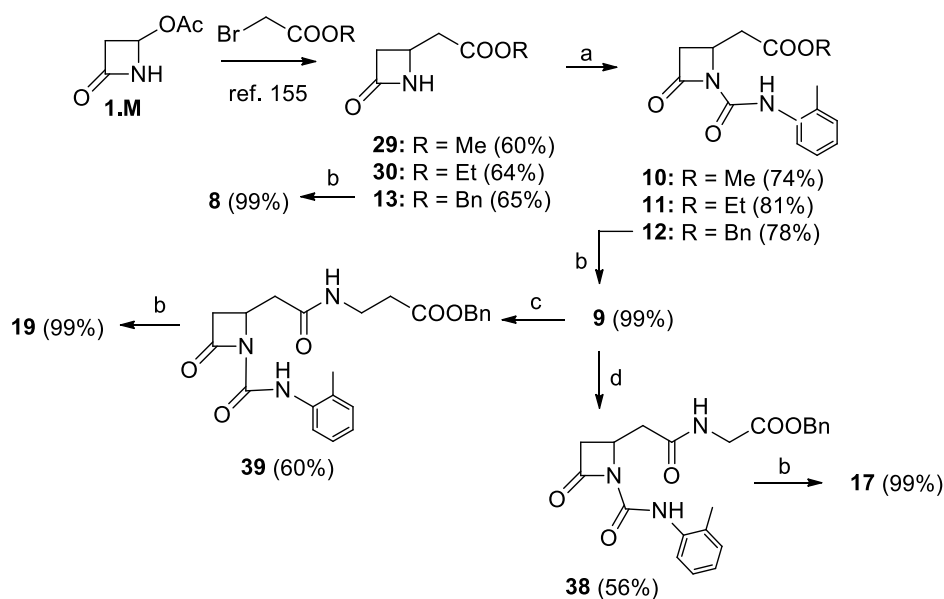
The 4-carboxylic-azetidin-2-one benzyl ester **22** was obtained in a two-step procedure starting from *L*-aspartic acid as previously reported<sup>155</sup> (Scheme 3.1). Treatment of **22** with NaHMDSA in THF at  $-78\text{ }^\circ\text{C}$  and *tert*-butyl(4-(isocyanatomethyl)phenyl)carbamate **23**, freshly prepared with triphosgene, gave **24**. Hydrogenolysis yielded the corresponding acid **25** and final treatment with trifluoroacetic acid furnished compound **5** as a trifluoroacetate salt.

Compound **26** was obtained from **22** with the commercially available *o*-tolyl isocyanate in acetonitrile and potassium carbonate. Subsequent hydrogenolysis gave **4** in good yields. The carboxylic acid **4** was coupled with glycine benzylester or  $\beta$ -alanine benzylester to give compounds **27** and **28**, respectively. Finally, azetidinones **6** and **7** were obtained from **27** and **28** by hydrogenolysis.



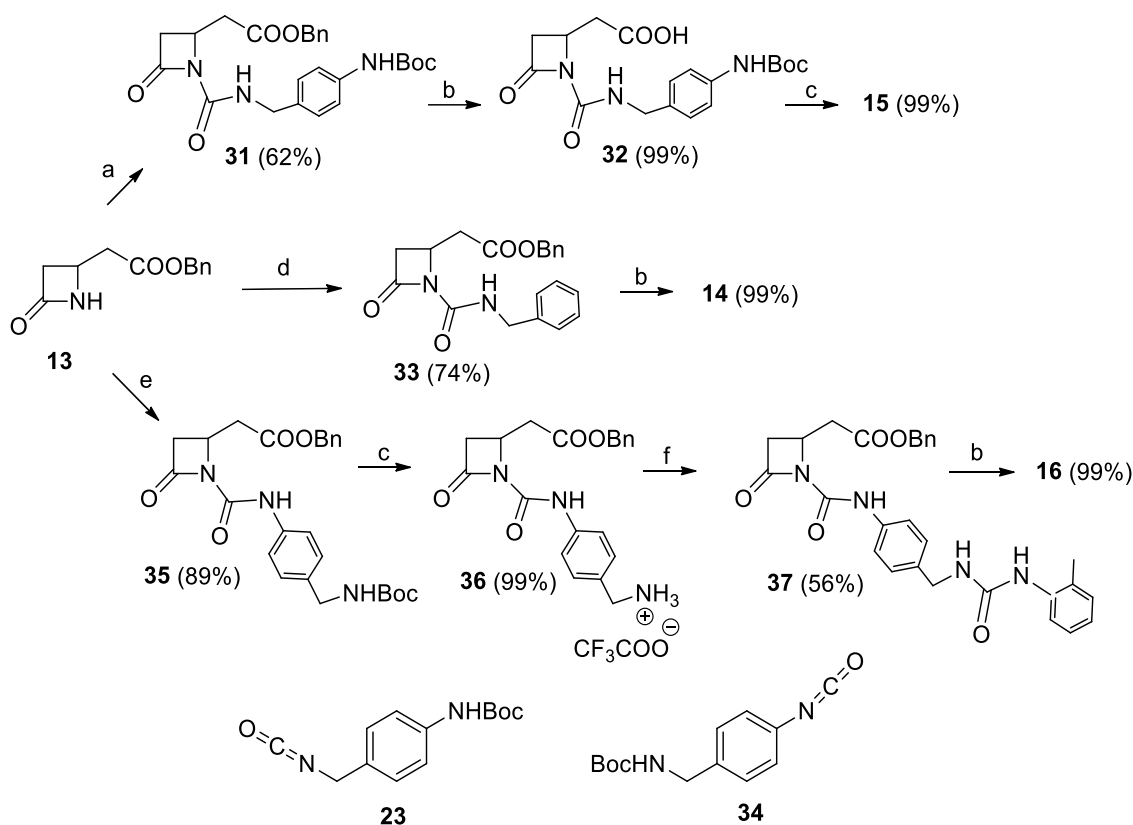
**Scheme 3.1.** Synthesis of  $\beta$ -lactams **4-7**. Reagents and conditions: a) NaHMDSA, *tert*-butyl(4-(isocyanatomethyl)phenyl)carbamate **23**, THF,  $-78\text{ }^{\circ}\text{C}$ , 1 h; b)  $\text{H}_2$ , Pd/C (10%), THF/ $\text{CH}_3\text{OH}$  1:1, rt, 2 h; c) TFA,  $\text{CH}_2\text{Cl}_2$ ,  $0\text{ }^{\circ}\text{C}$  then rt, 24 h; d)  $\text{K}_2\text{CO}_3$ , *o*-tolyl isocyanate,  $\text{CH}_3\text{CN}$ , rt, 2 h; e) oxalylchloride, TEA,  $\text{CH}_2\text{Cl}_2$ , glycine benzylester-HCl, DMAP, rt, 16 h; f) oxalylchloride, TEA,  $\text{CH}_2\text{Cl}_2$ ,  $\beta$ -alanine benzylester-PTSA, DMAP, rt, 16 h. Yields of isolated compounds are reported in brackets

The syntheses of  $\beta$ -lactams **8-21** included a common origin: a substitution reaction on 4-acetoxyazetidinone **1.M** by a Reformatsky reagent as outlined in Scheme 3.2. Methyl-, ethyl-, or benzyl-bromoacetates were treated with an excess of metallic Zn in THF to furnish the corresponding Reformatsky reagents which were then coupled with 4-acetoxyazetidin-2-one to give 4-acetateazetidin-2-one esters **29**, **30**, and **13** in good overall yields after flash-chromatography. Treatment of the three esters with *o*-tolylisocyanate under basic conditions provided the imido-azetidinones **10**, **11**, and **12**.  $\beta$ -lactams **8** and **9** were then obtained by hydrogenolysis from **13** and **12**, respectively. The azetidinone **9** was instead subjected to peptide coupling with glycine benzylester or  $\beta$ -alanine benzylester with 1-ethyl-3-(3-dimethylaminopropyl)carbodiimide (EDC) as coupling reagent, TEA, and a catalytic amount of dimethylaminopyridine (DMAP) to give intermediates **38** and **39**, which were deprotected by hydrogenolysis to give **17** and **19**, respectively (Scheme 3.2).



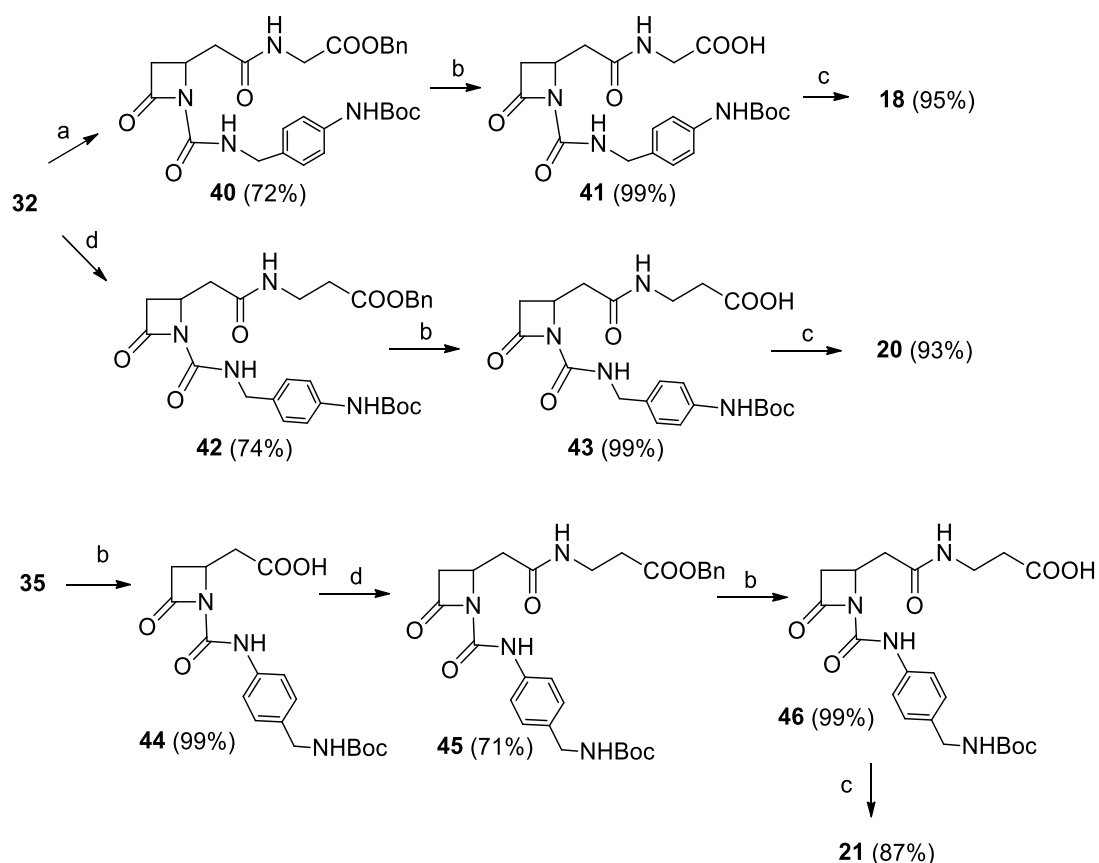
**Scheme 3.2.** Synthesis of  $\beta$ -lactams **8-13**, **17**, and **19**. Reagents and conditions: a)  $\text{K}_2\text{CO}_3$ , *o*-tolyl isocyanate,  $\text{CH}_3\text{CN}$ , rt, 2 h; b)  $\text{H}_2$ ,  $\text{THF}/\text{CH}_3\text{OH}$  1:1, Pd/C (10%), rt, 2 h; c) EDC, TEA, DMAP,  $\beta$ -alanine benzylester-PTSA,  $\text{CH}_2\text{Cl}_2$ , 0 °C then rt, 16 h; d) EDC, TEA, DMAP, glycine benzylester-PTSA,  $\text{CH}_2\text{Cl}_2$ , 0 °C then rt, 16 h. Yields of isolated compounds are reported in brackets

A N1-side chain was inserted on azetidinone **13**, which had been previously deprotonated at  $-78$  °C with sodium hexamethyl disilylamide ( $\text{NaHMDSA}$ ), by means of *tert*-butyl(4-(isocyanatomethyl)phenyl) carbamate **23** (Scheme 3.3), which was obtained in turn from 4-*N*-Boc-aminobenzylamine and triphosgene. Hydrogenolysis of the resulting adduct **31** gave **32**, which in turn provided compound **15** after treatment with trifluoroacetic acid. Azetidinone **36** was obtained by a similar procedure in two steps starting from **13** and *tert*-butyl-4-isocyanatobenzylcarbamate **34**. Treatment of **36** with commercially available *o*-tolylisocyanate and triethylamine gave **37**, which in turn provided azetidinone **16** by hydrogenolysis. Compound **14** was gained in two steps from **13** by condensation with commercially available benzyl isocyanate and hydrogenolysis.



**Scheme 3.3.** Synthesis of  $\beta$ -lactams **14-16**. Reagents and conditions: a) NaHMDSA, *tert*-butyl(4-(isocyanatomethyl)phenyl)carbamate **23**, THF,  $-78\text{ }^{\circ}\text{C}$ , 1 h; b)  $\text{H}_2$ , Pd/C (10%), THF/ $\text{CH}_3\text{OH}$  1:1, rt, 2 h; c) TFA,  $\text{CH}_2\text{Cl}_2$ ,  $0\text{ }^{\circ}\text{C}$  then rt, 24 h; d)  $\text{K}_2\text{CO}_3$ , benzylisocyanate,  $\text{CH}_3\text{CN}$ , rt, 2 h; e) NaHMDSA, *tert*-butyl 4-isocyanatobenzylcarbamate **34**, THF,  $-78\text{ }^{\circ}\text{C}$ , 1 h; f) TEA, *o*-tolylisocyanate,  $0\text{ }^{\circ}\text{C}$  then rt, 2 h. Yields of isolated compounds are reported in brackets

Azetidinones **18** and **20** instead resulted from carboxylic acid **32** by peptide coupling with glycine benzyl ester or  $\beta$ -alanine benzyl ester, respectively (Scheme 3.4). When intermediates **40** and **42** were subjected to a two-step procedure consisting of hydrogenolysis and treatment with TFA for the final deprotection, compounds **18** and **20** were obtained in very good yields. Preliminary hydrogenolysis of compound **35** gave intermediate **44**, which, *via* peptide coupling with  $\beta$ -alanine benzylester, hydrogenolysis and treatment with TFA, yielded the final compound **21** (Scheme 3.4).



**Scheme 3.4.** Synthesis of  $\beta$ -lactams **18**, **20**, and **21**. Reagents and conditions: a) DCC, TEA, DMAP,  $\text{CH}_2\text{Cl}_2$ , glycine benzylester-PTSA,  $0^\circ\text{C}$  to rt, 16 h; b)  $\text{H}_2$ , Pd/C (10%), THF/ $\text{CH}_3\text{OH}$  1:1, rt, 2 h; c) TFA,  $\text{CH}_2\text{Cl}_2$ ,  $0^\circ\text{C}$  then rt, 24 h; d) DCC, TEA, DMAP,  $\beta$ -alanine benzylester-PTSA,  $\text{CH}_2\text{Cl}_2$ ,  $0^\circ\text{C}$  to rt, 16 h. Yields of isolated compounds are reported in brackets

### 3.2.2 Biological evaluations

(in collaboration with Prof. S. M. Spampinato and Dr. M. Baiula, University of Bologna)

#### 3.2.2.1 Cell adhesion and solid-phase binding assays

To investigate the activity and selectivity profiles of the novel  $\beta$ -lactam derivatives, we performed adhesion assays with different cell lines expressing the RGD integrins  $\alpha_v\beta_3$ ,  $\alpha_v\beta_5$ ,  $\alpha_v\beta_6$ ,  $\alpha_5\beta_1$  and  $\alpha_{IIb}\beta_3$  or leukocyte integrins  $\alpha_4\beta_1$  and  $\alpha_L\beta_2$ . In these assays, cells were seeded onto plates coated with specific endogenous substrates (fibronectin, fibrinogen, VCAM-1 or ICAM-1) and allowed to adhere before the number of adherent cells was determined in the presence of increasing concentrations of the tested  $\beta$ -lactams compounds ( $1 \times 10^{-10}$  M -  $1 \times 10^{-4}$  M); their ability to increase or inhibit cell adhesion mediated by the endogenous integrin ligand was evaluated. In particular, those compounds that inhibited cell adhesion were referred to as antagonists, whereas compounds that increased cell adhesion were considered to be agonists.

Compounds **6**, **10**, **11**, **12**, **13**, **16**, and **18** resulted completely inactive in adhesion assays (data not shown); the other  $\beta$ -lactam derivatives resulted effective in cell-adhesion tests and are summarized in Table 3.1, together with the preferential selectivity of each compound for one integrin class over the others assayed. The peptides H-Gly-Arg-Gly-Asp-Thr-Pro-OH (**47**), Ac-Asp-Arg-Leu-Asp-Ser-



OH (**48**),<sup>172a</sup> cyclo(-Arg-Gly-Asp-D-Phe-Val) (**49**),<sup>177</sup> (*N*-[[4-[[[(2-methylphenyl)amino]carbonyl]amino]-phenyl]acetyl]-l-leucyl-l-aspartyl-l-valyl-l-proline (**50**) (BIO-1211)<sup>178</sup> and Tirofiban (**51**)<sup>179</sup> were included as reference ligands for the various integrins assayed.

**Table 3.1.** Effects of active  $\beta$ -lactam compounds on RGD-binding and leukocyte integrin-mediated cell adhesion. Data are presented as EC<sub>50</sub> for agonists (in bold), and as IC<sub>50</sub> for antagonists (nM). Values represent the mean  $\pm$  SD of three independent experiments carried out in quadruplicate

Comp.	RGD-binding integrins					Leukocyte integrins		Preferential selectivity
	SK-MEL-24/ FN $\alpha_v\beta_3$	MCF7/Fg $\alpha_v\beta_5$	HT-29/FN $\alpha_v\beta_6$	K562/FN $\alpha_5\beta_1$	HEL/Fg $\alpha_{IIb}\beta_3$	Jurkat/ VCAM-1 $\alpha_4\beta_1$	Jurkat/ ICAM-1 $\alpha_1\beta_2$	
1	<b>55.0 <math>\pm</math> 0.04<sup>a</sup></b> agonist	<b>5.09 <math>\pm</math> 0.07</b> agonist	<b>167 <math>\pm</math> 6</b> agonist	<b>12.0 <math>\pm</math> 0.02<sup>a</sup></b> agonist	> 5000	> 5000	2410 $\pm$ 64 antagonist	$\alpha_v\beta_5$ and $\alpha_5\beta_1$
2	<b>11.0 <math>\pm</math> 0.03<sup>a</sup></b> agonist	<b>505 <math>\pm</math> 17</b> agonist	> 5000	<b>763 <math>\pm</math> 0.08<sup>a</sup></b> agonist	> 5000	> 5000	> 5000	$\alpha_v\beta_3$
3	> 5000 <sup>a</sup>	> 5000	> 5000	<b>365 <math>\pm</math> 0.05<sup>a</sup></b> agonist	> 5000	> 5000	> 5000	$\alpha_5\beta_1$
5	> 5000	> 5000	> 5000	525.0 $\pm$ 1.2 antagonist	> 5000	8.8 $\pm$ 0.8 antagonist	> 5000	$\alpha_4\beta_1$
15	71.7 $\pm$ 0.5 antagonist	> 5000	> 5000	<b>44.5 <math>\pm</math> 2.6</b> agonist	> 5000	574.0 $\pm$ 1.7 antagonist	0.39 $\pm$ 0.02 antagonist	$\alpha_L\beta_2$ and $\alpha_v\beta_3$
20	> 5000	> 5000	> 5000	1050 $\pm$ 17 antagonist	> 5000	> 5000	> 5000	$\alpha_5\beta_1$
21	> 5000	> 5000	> 5000	<b>6.7 <math>\pm</math> 0.6</b> agonist	1563 $\pm$ 69	> 5000	> 5000	$\alpha_5\beta_1$
8	40.9 $\pm$ 0.8 antagonist	<b>376 <math>\pm</math> 15</b> agonist	> 5000	<b>1031 <math>\pm</math> 35</b> agonist	<b>311 <math>\pm</math> 35</b> agonist	> 5000	1627 $\pm$ 23 antagonist	$\alpha_v\beta_3$
14	> 5000	> 5000	> 5000	417 $\pm$ 6 antagonist	> 5000	> 5000	> 5000	$\alpha_5\beta_1$
4	352 $\pm$ 7 antagonist	> 5000	> 5000	158 $\pm$ 4 antagonist	> 5000	1.39 $\pm$ 0.04 antagonist	> 5000	$\alpha_4\beta_1$
7	active ligand	> 5000	> 5000	> 5000	> 5000	> 5000	> 5000	$\alpha_v\beta_3$
9	> 5000	> 5000	> 5000	> 5000	> 5000	<b>12.9 <math>\pm</math> 0.6</b> agonist	> 5000	$\alpha_4\beta_1$
17	> 5000	> 5000	> 5000	<b>9.9 <math>\pm</math> 0.1</b> agonist	> 5000	> 5000	> 5000	$\alpha_5\beta_1$
19	<b>187 <math>\pm</math> 3</b> agonist	<b>670 <math>\pm</math> 24</b> agonist	44.4 $\pm$ 0.8 antagonist	<b>49.0 <math>\pm</math> 2.9</b> agonist	> 5000	17.4 $\pm$ 0.8 antagonist	> 5000	$\alpha_4\beta_1$
47	925.5 $\pm$ 6.3 antagonist	34.2 $\pm$ 0.7 antagonist	> 5000	0.62 $\pm$ 0.09 antagonist	> 5000	nd	nd	

<b>48</b>	25 ± 3 antagonist	2278 ± 0.07 antagonist	> 5000	> 5000	> 5000	nd	nd
<b>50</b>	nd	nd	nd	nd	nd	8.6 ± 1.5 antagonist	0.84 ± 0.19 antagonist
<b>49</b>	146 ± 43 antagonist	16.0 ± 1.3 antagonist	3696 ± 38 antagonist	nd	nd	nd	nd
<b>51</b>	nd	nd	nd	nd	9.4 ± 0.8 antagonist	nd	nd

<sup>a</sup>Data preliminarily reported in ref 155; nd = not determined.

With regard to  $\alpha_v\beta_3$  integrin, no structural variation improved fibronectin-mediated cell adhesion, and the previously reported<sup>155</sup> compounds **1** and **2** confirmed to be the most active agonists toward this class. Among the new derivatives, azetidinones **15** and **8**, which have either a less basic aniline terminus (**15**) or a carboxylic acid terminus alone (**8**), reduced cell adhesion mediated by  $\alpha_v\beta_3$  integrin, and thus displayed antagonist activity. To notice, compound **7** with an acidic terminus of  $\beta$ -alanine and an ureido MPUPA motif was considered an active ligand but showed a peculiar behavior: at low concentrations ( $10^{-10}$  -  $10^{-7}$  M) it behaved as antagonist while it acted as an agonist at higher concentrations ( $10^{-6}$  -  $10^{-4}$  M). According to this, recently Van Agthoven *et al.* have described a wild type fibronectin (wtFN10) that binds and activates  $\alpha_v\beta_3$  integrin whereas a high-affinity mutant (hFN10), carrying substitutions adjacent to the RGD sequence, behaves as a pure antagonist as it favors an inactive conformation of the integrin.<sup>180</sup>

Interestingly, a shorter acidic side chain, as in compound **4**, acted as a low potent antagonist, whereas a longer one, as in **19**, switched the activity to agonism.

Compounds **1** and **8** acted as agonists in cell adhesion assays towards  $\alpha_v\beta_5$  integrin. With regard to  $\alpha_v\beta_6$  integrin, **1** and **19** were the most effective in cell adhesion assays: **1** behaved as an agonist whereas **19** was an antagonist. This latter compound was the most potent towards  $\alpha_v\beta_6$  integrin albeit it bound to  $\alpha_5\beta_1$  and  $\alpha_4\beta_1$  integrin with similar activities.

With regard to  $\alpha_5\beta_1$  integrin, compounds **1**, **21**, and **17** appeared to be the most potent agonists at promoting cell adhesion, with EC<sub>50</sub> values of 12.0, 6.7 and 9.9 nM, respectively. Moreover, **21** and **17** were relatively selective agonists for  $\alpha_5\beta_1$  over the other integrins assayed. The inhibition of  $\alpha_5\beta_1$ -mediated cell adhesion was observed only at a micromolar range for a few derivatives with a short carboxylic acid terminus on C4, and a less basic or MPUPA residue on the nitrogen atom (**5**, **14**, and **4**). Interestingly, compounds **3** and **5**, despite a low potency for the  $\alpha_5\beta_1$  receptor, showed opposite activities, in that **3** was an agonist whereas **5** was an antagonist of cell adhesion. A similar result was observed for **20** and **21**: the former, with an aniline residue, was a weak antagonist (IC<sub>50</sub> > 1000 nM) whereas the latter, with a benzylamine terminus, was a strong agonist (EC<sub>50</sub> = 6.7 nM).

A more basic amine terminus (benzylamine vs aniline residues) tended to favor agonist behavior (see, for instance, **1**, **2**, and **3** vs **5**, **15**, and **20**), although these  $\beta$ -lactams could act as electrostatic clamps for  $\alpha_5\beta_1$  or  $\alpha_v\beta_3$  integrins, like the RGD peptide (see modeling section at Paragraph 3.2.3). On the other hand, the presence of an acidic terminus alone with a suitable chain length could allow a favorable interaction at the MIDAS, hence affecting cell adhesion. In fact, esters **10**, **11**, **12**, and **13**,

which lacked these characteristics, were completely inactive toward all integrins, as well as compounds **16** and **18** with longer side chains.

All the selected  $\beta$  lactam compounds were inactive for integrin  $\alpha_{11b}\beta_3$ , apart azetidinone **8** that showed only a low affinity in cell adhesion assay ( $EC_{50}$  311 nM), acting as an agonist.

The investigation was extended also to leukocyte integrins  $\alpha_4\beta_1$  and  $\alpha_L\beta_2$ . Compounds **5** and **4** with a short carboxylic acid terminus or either a less basic or no amine residue efficiently interacted with  $\alpha_4\beta_1$  integrin by inhibiting VCAM-1-mediated cell adhesion with  $IC_{50}$  values of 8.8 and 1.39 nM, respectively. Replacing the amine terminus with a MPUPA residue led to an increased activity at a nanomolar level also for derivatives for **9** and **19**. Whilst **19** revealed to be an antagonist, compound **9**, which is a homolog of **4** at the C4 position, was an effective and very selective agonist of cell adhesion mediated by  $\alpha_4\beta_1$  integrin ( $EC_{50}$  = 12.9 nM); this activity was found to decrease with an increase in side chain the length (see compound **9** vs **17**).

In this series of new  $\beta$ -lactam derivatives, it was hard to find a correlation between the activities toward  $\alpha_4\beta_1$  and  $\alpha_5\beta_1$  integrins: most of the  $\beta$ -lactams that were active toward the former integrin were inactive toward the latter. Compound **19** is an exception in this sense, because it showed similar potencies for opposite activities: agonist toward  $\alpha_5\beta_1$  ( $EC_{50}$  = 49 nM), but antagonist toward  $\alpha_4\beta_1$  ( $IC_{50}$  = 17.4 nM).

Concerning  $\beta$ -lactam activity toward  $\alpha_L\beta_2$  integrin, only **15** showed excellent activity as an antagonist at subnanomolar concentrations ( $IC_{50}$  = 0.39 nM), despite it was not selective toward the other integrins assayed.

The abilities of the newly found agonist  $\beta$ -lactams to increase cell adhesion were tested in absence of fibronectin for  $\alpha_5\beta_1$  or VCAM-1 for  $\alpha_4\beta_1$  integrin. For this purpose, the adhesion of K562 and Jurkat E6.1 cells was evaluated in wells that had been previously coated by passive adsorption with each novel agonist under investigation (2-10 mg/L). Regarding  $\alpha_5\beta_1$  integrin,  $\beta$ -lactam agonists **15**, **17**, **19**, and **21** induced a significant concentration-dependent increase in K562 cell adhesion, as observed for fibronectin (Figure 3.12A). Pre-incubation of K562 cells with c(-RGDfV) (**49**) (1 $\mu$ M), a well-known antagonist of RGD integrins,<sup>177a</sup> significantly reduced cell adhesion mediated by azetidinones **15** and **19** but not by **17** and **21** (Figure 3.12A). These results could suggest that  $\beta$ -lactams **15** and **19** may bind the MIDAS site, an effect prevented by c(-RGDfV) (**49**). Conversely, **17** and **21** might bind to an allosteric site since cell adhesion mediated by these compounds was preserved even in the presence of c(-RGDfV) (**49**).

In addition, compound **9**, which is the only  $\alpha_4\beta_1$  agonist, significantly augmented Jurkat E6.1 cell adhesion, similarly to VCAM-1 (Figure 3.12B).

Pre-incubation with a neutralizing antibody against the  $\alpha_5$  or  $\alpha_4$  integrin subunits (10 mg/L) blocked the augmented adhesion of K562 or Jurkat E6.1 cells induced by  $\beta$ -lactam agonists **15**, **17**, **19**, **21**, and **9** respectively (Figure 3.12A and B). These results confirmed that cell adhesion mediated by the new  $\beta$ -lactam agonists effectively and specifically involved  $\alpha_5\beta_1$  and  $\alpha_4\beta_1$  integrins, respectively.

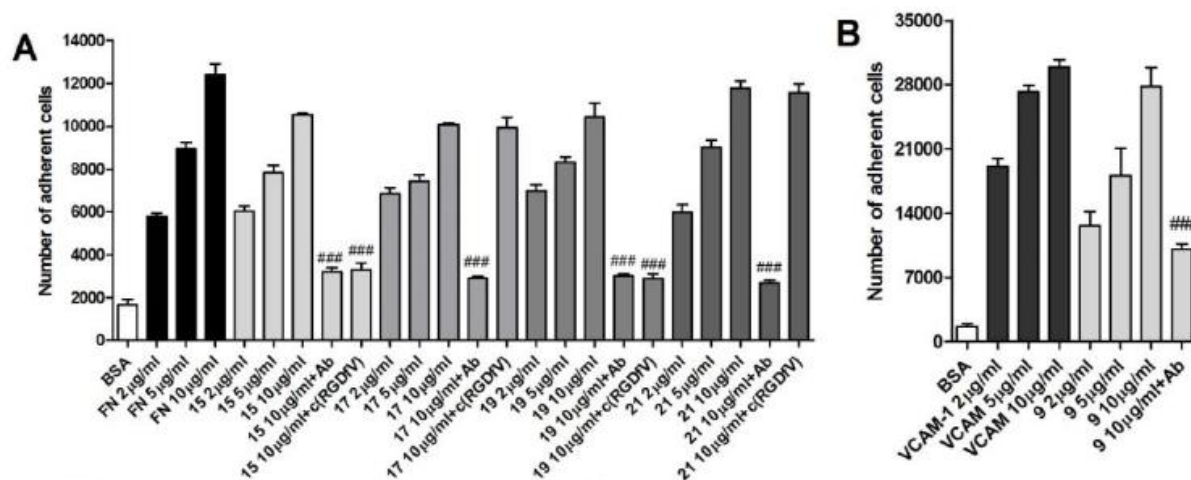


**Figure 3.12.** A) K562 cell adhesion to wells coated with fibronectin (FN) or agonists (**15**, **17**, **19**, **21**) directly coated into wells by passive adsorption is increased in a concentration-dependent manner. Pre-incubation with a neutralizing antibody against the  $\alpha 5$  integrin subunit blocked the augmented adhesion of K562 cells induced by  $\beta$ -lactam agonists. Pre-incubation with a cilengitide analog c-(RGDfV) significantly reduced cell adhesion mediated by **15** and **19** whereas it was not effective to influence cell adhesion induced by **17** and **21**; B) Jurkat E6.1 cell adhesion of VCAM-1 or agonist **9** is significantly increased. Pre-incubation with a neutralizing antibody against the  $\alpha 4$  integrin subunit blocked the augmented adhesion of Jurkat E6.1 cells induced by  $\beta$ -lactam **9**

The most interesting  $\beta$ -lactam compounds behaving as integrin ligands in cell adhesion assays above described, were further characterized in solid-phase competitive integrin binding assays on isolated integrins set up for  $\alpha_v\beta_3$ ,  $\alpha_v\beta_5$ ,  $\alpha_v\beta_6$ ,  $\alpha_5\beta_1$ ,  $\alpha_{IIb}\beta_3$ , and  $\alpha_L\beta_2$ , whereas affinity to  $\alpha_4\beta_1$  was evaluated by a scintillation proximity-binding assay (SPA). Interestingly, the assayed compounds showed affinity values and selectivity that agreed with the data found in cell adhesion assays reported in Table 3.1 (data not shown); an exception was compound **8** that, in comparison to cell adhesion assays, was 20 times more potent vs  $\alpha_v\beta_3$  and 370 times more potent vs  $\alpha_v\beta_5$  in solid-phase binding assays (data not shown).

### 3.2.2.2 Effects of selected $\beta$ -lactams on integrin-mediated ERK phosphorylation

Intracellular signaling generated by the interaction of extracellular matrix components with selected integrins involves second messengers,<sup>181</sup> including extracellular signal-regulated kinases 1 and 2 (ERK1/2). The effects of  $\beta$ -lactams that most strongly affected  $\alpha_5\beta_1$  integrin-mediated cell adhesion were evaluated on ERK1/2 phosphorylation in K562 cells. Selected azetidinones that behaved as agonists in cell adhesion assays, i.e. **15**, **17**, **19**, and **21**, significantly increased ERK1/2 phosphorylation when added alone to cells; moreover, **17**, **19**, and **21** increased ERK1/2 phosphorylation in a concentration-dependent manner (Figure 3.13A and B). Conversely, the  $\alpha_5\beta_1$  integrin antagonist **4** reduced ERK1/2 phosphorylation induced by fibronectin in a concentration-related manner (Figure 3.13C).

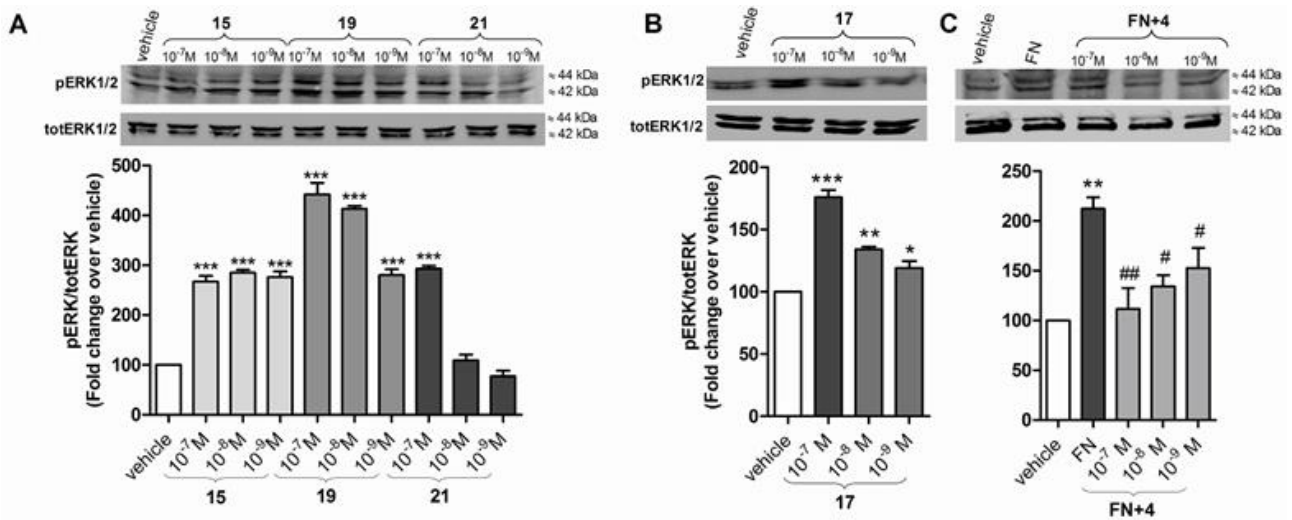


**Figure 3.13.** Effects of selected  $\beta$ -lactams on ERK1/2 phosphorylation mediated by  $\alpha_5\beta_1$  integrin expressed in K562 cells. A), B) Agonists **15**, **17**, **19** and **21** significantly increased ERK1/2 phosphorylation; C) Compound **4** prevented FN-induced phosphorylation of ERK1/2 in a concentration-dependent manner

$\beta$ -lactam **9**, a selective  $\alpha_4\beta_1$  integrin agonist, when added alone to Jurkat E6.1 cells, strongly and significantly increased ERK1/2 phosphorylation in comparison to vehicle-treated cells (Figure 3.14A). In Jurkat E6.1 cells exposed to VCAM-1, a significant increase in ERK1/2 phosphorylation was detected, and pre-incubation with  $\beta$ -lactam antagonists **4**, **5**, and **19** caused a significant decrease in VCAM-1-mediated ERK1/2 phosphorylation (Figure 3.14B and C); moreover, azetidinones **5** and **19** were effective in a concentration-dependent manner.

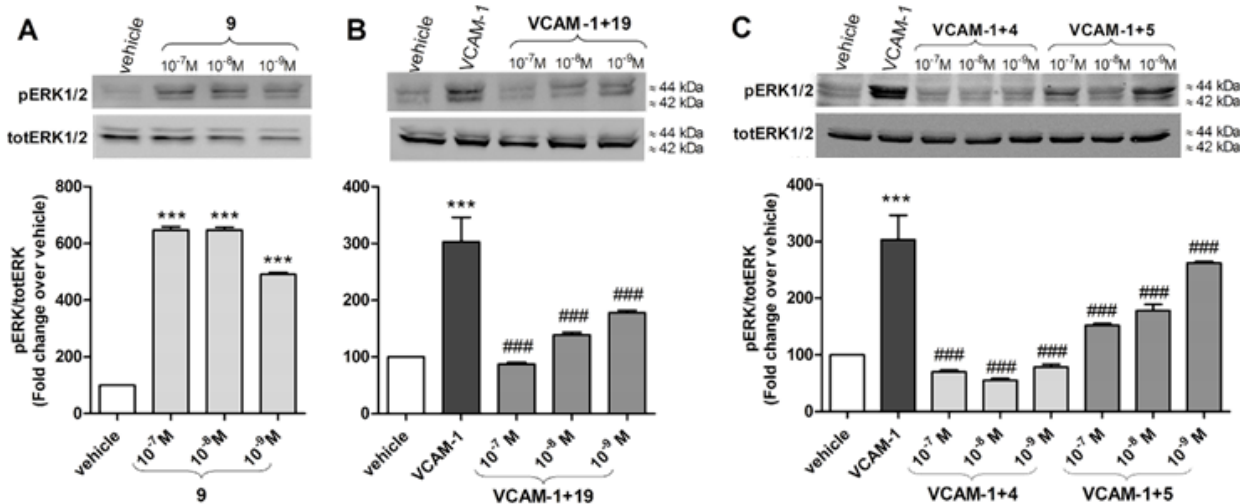


**Figure 3.14.** Effects of selected  $\beta$ -lactams on ERK1/2 phosphorylation mediated by  $\alpha_4\beta_1$  integrin expressed in Jurkat E6.1 cells. A)  $\beta$ -lactam agonist **9** significantly increased ERK1/2 phosphorylation; B), C) Azetidinones **4**, **5**, and **19** prevented VCAM-1-induced phosphorylation of ERK1/2 in a concentration-dependent manner

### 3.2.2.3 Effects on selected $\beta$ -lactams to HUTS-21 epitope exposure

As already mentioned, integrins exist in three major conformations: an inactive or bent conformation, an intermediate-activity conformation and a high-activity open conformation.<sup>182</sup> Conformational changes in integrin subunits can be monitored using conformation-specific antibodies that recognize a specific epitope that is exposed only in a defined structural conformation.<sup>183</sup>

To determine whether the binding of these new  $\beta$ -lactams to  $\alpha_4\beta_1$  integrin could alter its conformation, we used the HUTS-21(PE) monoclonal antibody (mAb), comprising the fluorophore reporter phycoerythrin (PE), that recognizes a LIBS (ligand-induced binding site) epitope masked on inactive integrin but exposed upon agonist binding or partial integrin activation. This mAb was added to the cells, and cells were then analyzed by flow cytometry. As expected, the binding of VCAM-1 induced a conformational rearrangement in the  $\beta_1$  subunit that resulted in exposure of the HUTS-21 epitope and increased antibody binding (Figure 3.15). Similarly, agonist **9** significantly increased HUTS-21 antibody binding in a concentration-dependent manner. Conversely, the  $\alpha_4\beta_1$  antagonist compounds **4** and **5** significantly and in a concentration-related manner reduced the exposure of HUTS-21 epitope measured as mAb binding (Figure 3.15). Taken together, these data suggest that novel  $\beta$ -lactams acting as  $\alpha_4\beta_1$  agonists may induce changes in integrin conformation, leading to its activation, while  $\alpha_4\beta_1$  antagonists may promote inactive or intermediate-activity conformations.

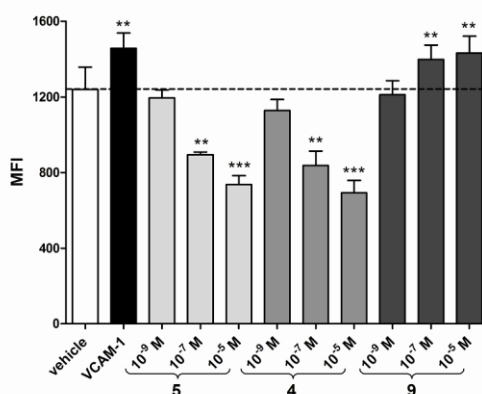


**Figure 3.15.** Binding of HUTS-21 antibody to Jurkat E6.1 cells in the presence of different concentrations of the new  $\beta$ -lactams. Antagonists **4** and **5** significantly reduced exposure of the HUTS-21 epitope, while  $\beta$ -lactam agonist **9** increased the binding of HUTS-21 mAb to Jurkat E6.1 cells in a concentration-dependent manner

### 3.2.3 Molecular Modeling

(in collaboration with Prof. L. Belvisi and Dr. M. Civera, University of Milano)

The binding mode of representative  $\beta$ -lactam derivatives to  $\alpha_v\beta_3$  integrin was investigated by a docking approach that was previously developed and successfully applied to the study of small libraries of cyclic and linear RGD peptidomimetics.<sup>184</sup> The Glide<sup>185</sup> program V4.5 was used for docking calculations and the crystal structure of the extracellular segment of integrin  $\alpha_v\beta_3$  in a complex with the cyclic pentapeptide Cilengitide (PDB code 1L5G)<sup>186</sup> was used as a reference model for interpretation of the results.

The Glide docking protocol was applied to  $\beta$ -lactam derivatives **1** and **15**, which contain the same C4 acetic acid and a benzylamine and aniline basic moiety, respectively, in order to generate computational models of interaction with the ligand-binding site of  $\alpha_v\beta_3$  integrin. Although the specific role of a more basic amine terminus (benzylamine *vs* aniline residues) in favoring agonist behavior on the basis of rigid-protein docking calculations is hard to discuss, it was possible to examine the effect of the basic moiety on the ability of the ligand to form an electrostatic clamp and to reproduce the crystallographic binding mode of Cilengitide.

Docking runs starting from both enantiomers of compound **1** produced poses that conserved the key polar interactions observed in the X-ray complex of Cilengitide-  $\alpha_v\beta_3$  integrin. In the calculated poses, the ligand carboxylate group was coordinated to the metal cation in the MIDAS region of the  $\beta_3$  subunit, and the ligand benzylamine moiety forms salt bridge/H-bond interactions with the negatively charged side chain of Asp218 in the  $\alpha_v$  subunit (Figure 3.16). Further stabilizing interactions occurred in docking poses of compound **1**, involving the formation of hydrogen bonds between the ligand carboxylate group and the backbone amide hydrogen of Asn215 and Tyr122 in the  $\beta$  unit, and between the  $\beta$ -lactam carbonyl and the  $\beta_3$ -Arg214 side chain. Ring-stacking or a T-shaped interaction between the ligand aromatic group and the  $\alpha_v$ -Tyr178 side chain was also observed in the binding modes calculated for compound **1**.

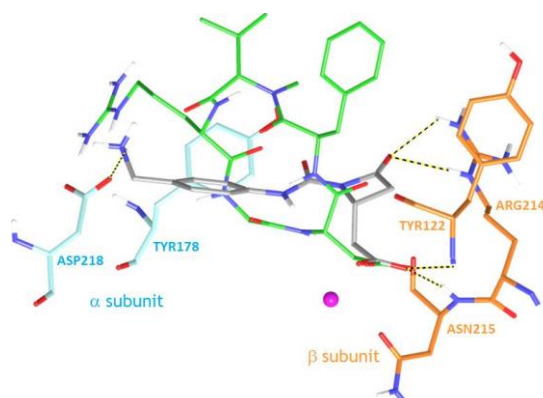


**Figure 3.16.** Docking pose of compound (*R*)-**1** (grey carbon atoms) in the crystal structure of the extracellular domain of  $\alpha_v\beta_3$  integrin ( $\alpha$  unit cyan,  $\beta$  unit orange) overlaid on the bound conformation of Cilengitide (green carbon atoms). Only selected integrin residues involved in interactions with the ligand are shown. The metal ion at MIDAS is shown as a magenta CPK sphere. Intermolecular hydrogen bonds are shown as dashed lines

Docking runs starting from the two enantiomers of compound **15** produced rather different results. In the calculated poses of (*R*)-**15**, the acid and basic pharmacophoric groups acted like an electrostatic clamp and interacted with charged regions of the receptor binding site. Nevertheless, a poor fit with the receptor-bound structure of Cilengitide was observed, mainly for the aniline basic moiety (Figure 3.17), which formed a distorted H-bond with the negatively charged carboxylate of  $\alpha_v$ -Asp218. Similar to what observed for compound **1**, one carboxylate oxygen of (*R*)-**15** was coordinated to the MIDAS metal cation, while the second carboxylate oxygen formed H-bonds with the backbone amides of Asn215 and Tyr122 in the  $\beta$  unit. Further stabilizing interactions observed in the binding modes of (*R*)-**15** involved an H-bond between the  $\beta$ -lactam carbonyl and the  $\beta_3$ -Arg214 side chain, and ring-stacking between the ligand aromatic group and the  $\alpha_v$ -Tyr178 side chain.

In the calculated poses of (*S*)-**15** instead, the electrostatic clamp was often lost and the ligand engaged in interactions only with the  $\beta$ -subunit. In particular, the coordination of the ligand carboxylate to the MIDAS cation was retained, while the aniline moiety moved toward the  $\beta$ -chain, driven by hydrophobic interactions (data not shown).

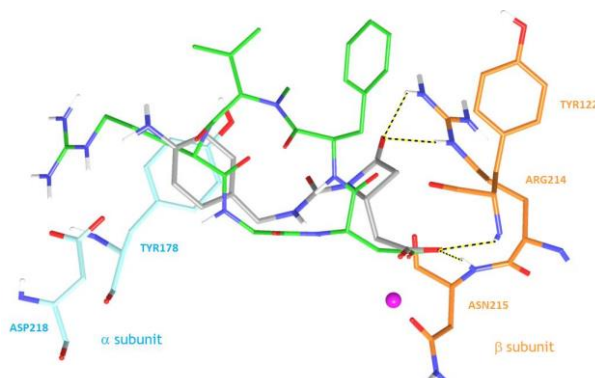


**Figure 3.17.** Docking pose of compound (*R*)-**15** (grey carbon atoms) in the crystal structure of the extracellular domain of  $\alpha_v\beta_3$  integrin ( $\alpha$  unit cyan,  $\beta$  unit orange) overlaid on the bound conformation of Cilengitide (green carbon atoms). Only selected integrin residues involved in interactions with the ligand are shown. The metal ion at MIDAS is shown as a magenta CPK sphere. Intermolecular hydrogen bonds are shown as dashed lines

This latter study highlights how docking poses originated from opposite enantiomers of the same compound produced distinct conformations and consequently distinct binding modes of the molecule on the receptor. This evidence could suggest the need of further investigations on the configuration at C4 position of the  $\beta$ -lactam ring for evaluating how it could be involved in integrin affinity and recognition.

### 3.3 Other $\beta$ -lactam based integrin ligands

As described in detail in the previous Paragraph 3.2, we developed a library of  $\beta$ -lactam derivatives that were specifically designed for targeting RGD-binding and leukocyte integrins. The design of the new compounds revealed to be successful since we obtained selective and potent agonists that could promote cell adhesion, and antagonists that could inhibit integrin functions. In general a benzylamine terminus appeared to favor agonist behavior and this supported the hypothesis that these new  $\beta$ -lactams could act as an electrostatic clamp on the receptor, as suggested by molecular docking studies at  $\alpha_v\beta_3$  integrin.<sup>171</sup> Nevertheless, it was not always immediate to understand how the modifications inserted on the side chains of the  $\beta$ -lactam scaffold could influence the activity on the receptor and a rationalization on agonist or antagonist behaviour of the derivatives was contrived. In fact, an opposite activity was in some cases shown by the same compound according to the class assayed, or between two derivatives differing in their molecular structure for a single carbon atom. For a better formulation of an effective structure activity relationship on these compounds, a series of new derivatives was designed and realized. In particular, the objective of this study was to identify the structural elements that could be considered essential for preserving integrin activity. For realizing this new small library, compounds were deprived from some functional groups or de-structured from their cyclic scaffold compared to those already reported. The novel targets are reported in Chart 3.2.



### 3.3.1 Synthesis of azetidiones

Compounds **52-55** were designed with a single side chain for verifying that both the acid and the amine terminals were needed for an effective activity as integrin ligands. Notably, compounds **52-54** have only an acid residue on the C4 position of the ring with different chain lengths. In compound **53** a C-C double bond was additionally inserted for evaluating the effect of a more rigid structure on the alignment with the receptor. Compound **55** instead lacked the acid terminus carrying only the amine group on the  $\beta$ -lactam nitrogen. In derivatives **56** and **58** we wanted to evaluate if the absence of an *o*-tolylurea group could influence the activity on the receptor and the amine function was hence removed in the N1 side chain. In another case, the  $\beta$ -lactam ring was replaced by a 5-term proline ring (compound **57**) or removed at all (open compounds **59** and **60**), in order to demonstrate if a cyclic rigid scaffold was necessary for integrin recognition. Derivatives **61-64** belonged to a series of enantiomerically pure compounds, synthesized in order to evaluate how the stereocenter on C4 could influence the activity. The stereoselectivity was switched compared to reported compounds of the *L*-series that in most of the cases resulted very potent in cell adhesion assays. As shown from docking studies on compound **15** in fact, different interactions on the receptor were detected for opposite enantiomers of the same compound.<sup>171</sup>

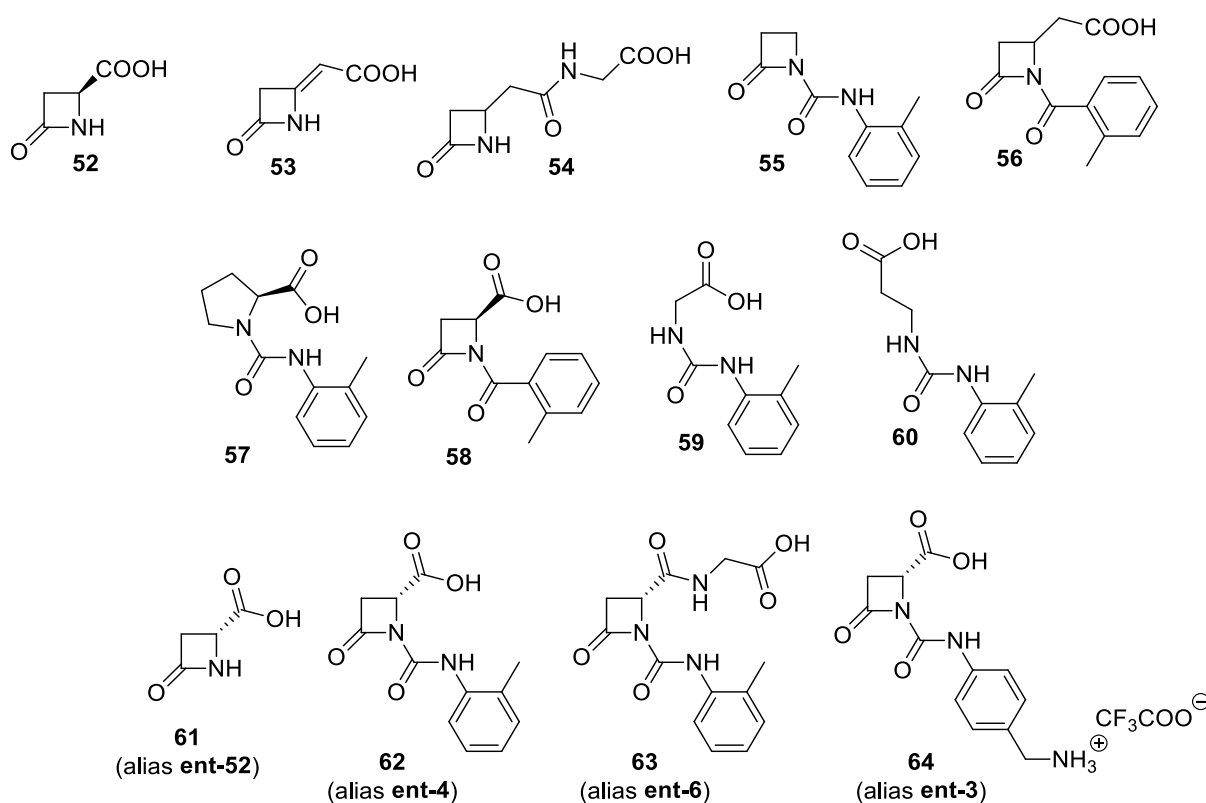
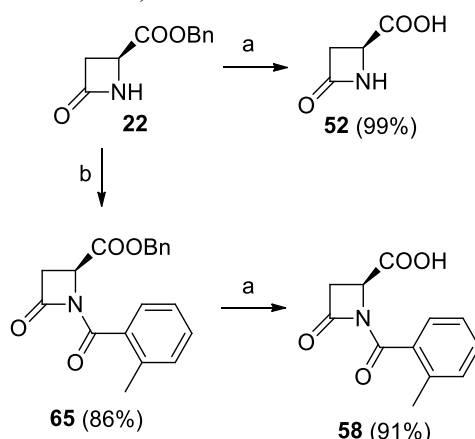


Chart 3.2.  $\beta$ -lactam based integrin ligands **52-64** designed for evaluating the crucial moieties for receptor recognition

The synthetic strategies adopted for the new derivatives are reported in the following Schemes 3.5-3.9. From 4-carboxylic-azetid-2-one benzyl ester **22**, whose synthesis was already discussed in Paragraph 3.2.1, hydrogenolysis in standard conditions yielded the corresponding carboxylic acid **52**. Treatment of **22** with *o*-toluylchloride, TEA and catalytic DMAP instead furnished intermediate **65**

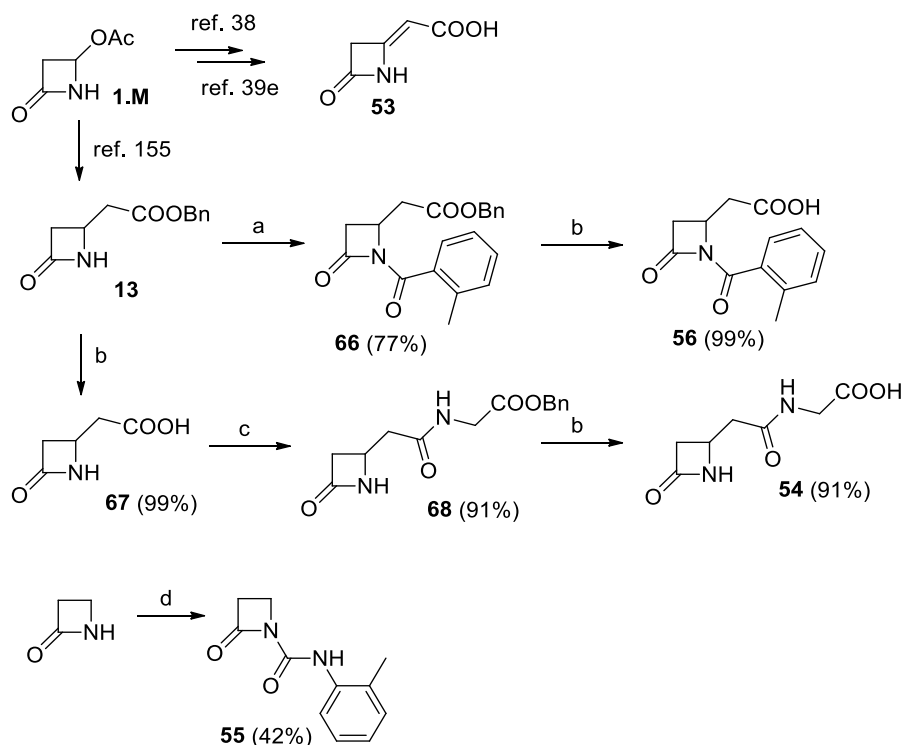
in good yields with a newly inserted amide moiety. It was in turn deprotected to give compound **58** with a free acid functionality (Scheme 3.5).



**Scheme 3.5.** Synthesis of  $\beta$ -lactams **52** and **58**. Reagents and conditions: a)  $\text{H}_2$ , Pd/C (10%), THF/ $\text{CH}_3\text{OH}$  1:1, rt, 2 h; b) *o*-toluoylchloride, TEA, DMAP,  $\text{CH}_2\text{Cl}_2$ , 0 °C then rt, 6 h. Yields of isolated compounds are reported in brackets

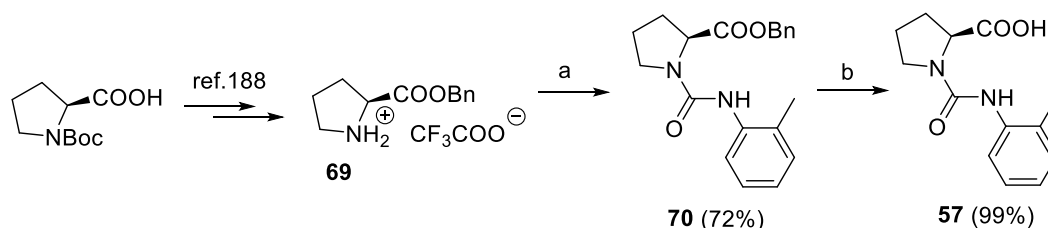
The synthesis of derivatives **53-54** and **56** share 4-acetoxiazetidin-2-one **1.M** as a common substrate (Scheme 3.6). Compound **53** was gained *via* an alkylidene formation mediated by benzyl diazoacetate and stoichiometric titanium tetrachloride followed by a hydrogenolytic procedure.<sup>38,39e</sup> A substitution reaction on 4-acetoxiazetidinone by a Reformatsky reagent gave intermediate **13** as previously outlined.<sup>171</sup> It was then treated with *o*-toluoylchloride in basic conditions to gain the imido group in derivative **66** that was subjected to a hydrogenolysis reaction leading to compound **56**. When a direct hydrogenolysis on **13** was performed, compound **67** was yielded and further reacted with DCC, glycine benzylester, TEA and DMAP to give a side chain elongation on C4. The benzyl ester group on molecule **68** was finally removed in order to obtain derivative **54**.

Target compound **55** was instead realized in a simple one step procedure starting from commercial 2-azetidinone and *o*-tolylisocyanate in basic conditions. Reactions with potassium carbonate or triethylamine were attempted, but a stronger base (NaHMDSA) at low temperature was required for yielding **55**, even if with poor yields (Scheme 3.6).



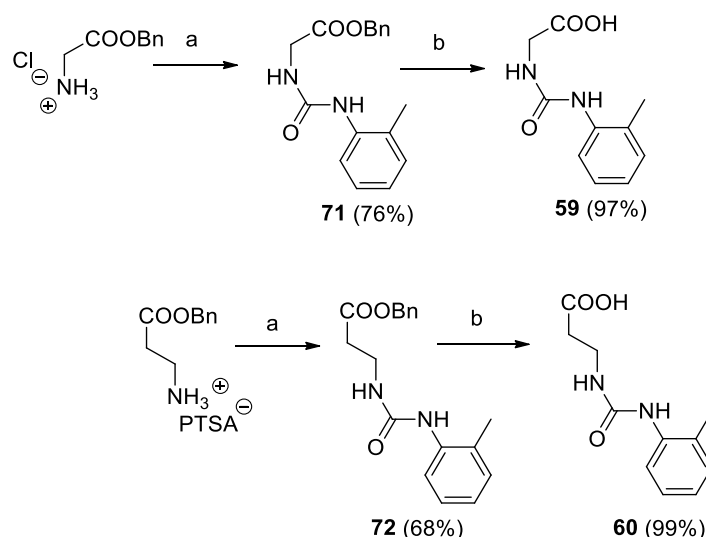
**Scheme 3.6.** Synthesis of  $\beta$ -lactams **53-56**. Reagents and conditions: a) *o*-toluylchloride, TEA, DMAP,  $\text{CH}_2\text{Cl}_2$ ,  $0^\circ\text{C}$  then rt, 18 h; b)  $\text{H}_2$ , Pd/C (10%), THF/ $\text{CH}_3\text{OH}$  1:1, rt, 2 h; c) DCC, TEA, DMAP, glycine benzylester-HCl,  $\text{CH}_2\text{Cl}_2$ ,  $0^\circ\text{C}$  then rt, 16 h; d) *o*-tolylisocyanate, NaHMDSA, THF,  $-78^\circ\text{C}$ , 1 h. Yields of isolated compounds are reported in brackets

Derivative **70** was obtained in good yields from benzyl-*L*-prolinate trifluoroacetate salt **69** after substrate desalification with TEA and reaction with *o*-tolylisocyanate. Compound **69** was in turn obtained after an esterification with benzylic alcohol on commercial *N*-Boc-*L*-proline and a following Boc deprotection with trifluoroacetic acid.<sup>187</sup> A final hydrogenolysis on compound **70** yielded target **57** quantitatively (Scheme 3.7).



**Scheme 3.7.** Synthesis of  $\beta$ -lactam **57**. Reagents and conditions: a) *o*-tolylisocyanate, TEA,  $\text{CH}_2\text{Cl}_2$ , rt, 4 h; b)  $\text{H}_2$ , Pd/C (10%), THF/ $\text{CH}_3\text{OH}$  1:1, rt, 2 h. Yields of isolated compounds are reported in brackets

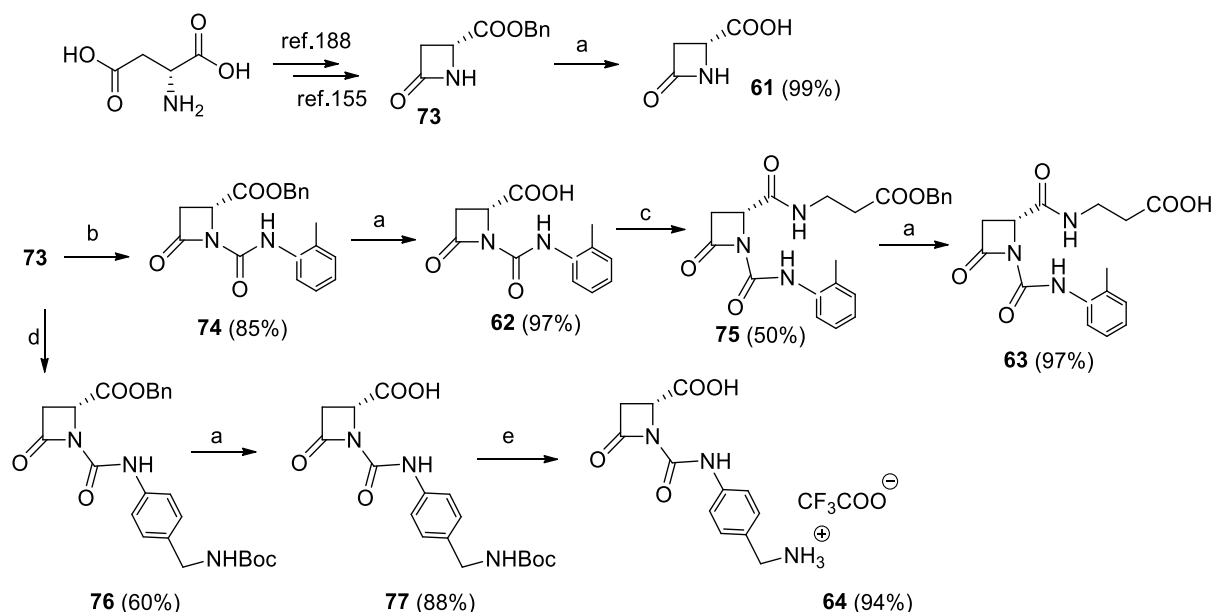
Not cyclic derivatives **59** and **60** were obtained with a two step-protocol after hydrogenolysis on the corresponding benzyl esters **71** and **72**, which were subjected to a nitrogen derivatization mediated by TEA and *o*-tolylisocyanate on the starting glycine or  $\beta$ -alanine benzyl esters. An excess of TEA was utilized for unprotect the amine moiety present as chlorohydrate or trifluoroacetate salt in the commercial formulations of the aminoacids (Scheme 3.8).



**Scheme 3.8.** Synthesis of  $\beta$ -lactams **59-60**. Reagents and conditions: a) *o*-tolylisocyanate, TEA,  $\text{CH}_2\text{Cl}_2$ , rt, 4 h; b)  $\text{H}_2$ , Pd/C (10%), THF/ $\text{CH}_3\text{OH}$  1:1, rt, 2 h. Yields of isolated compounds are reported in brackets

Compounds **61-64** arose from *D*-aspartic acid that, according to a literature procedure, was previously di-benzylated with benzylic alcohol, *p*-toluenesulfonic acid and cyclohexane in a Dean-Stark apparatus.<sup>188</sup> It was then performed a cyclization with *tert*-butylmagnesium chloride after an *in situ* nitrogen atom protection with trimethylsilylchloride and TEA.<sup>155</sup> The so-formed  $\beta$ -lactam **73** was used as a starting material for obtaining the *D*-class  $\beta$ -lactam derivatives as follows: a direct hydrogenolysis on **73** gave acid **61**; treatment with *o*-tolylisocyanate and triethylamine instead furnished compound **74** in good yields. Subsequent hydrogenolysis resulted in target **62** that was further coupled with  $\beta$ -alanine benzylester to yield the higher molecular weight derivative **75**. Azetidinone **63** was then obtained from **75** by hydrogenolysis.

Finally, intermediate **76** was gained through a reaction on compound **73** mediated by NaHMDSA in THF at  $-78\text{ }^\circ\text{C}$  and *tert*-butyl(4-isocyanatobenzylcarbamate) **34**, freshly prepared *in situ* with triphosgene and TEA from the relative amine. Hydrogenolysis gave the corresponding acid **77** and final treatment with trifluoroacetic acid furnished compound **64** as a trifluoroacetate salt (Scheme 3.9).



**Scheme 3.9.** Synthesis of  $\beta$ -lactams **61–64**. Reagents and conditions: a)  $\text{H}_2$ , Pd/C (10%), THF/ $\text{CH}_3\text{OH}$  1:1, rt, 2 h; (b) *o*-tolylisocyanate, TEA,  $\text{CH}_2\text{Cl}_2$ , rt, 4 h; (c) oxalylchloride, TEA,  $\text{CH}_2\text{Cl}_2$ ,  $\beta$ -alanine benzyloxyester-PTSA, DMAP, rt, 16 h; (d) NaHMDSA, *tert*-butyl 4-isocyanatobenzylcarbamate **34**, THF,  $-78^\circ\text{C}$ , 1 h; (e) TFA,  $\text{CH}_2\text{Cl}_2$ ,  $0^\circ\text{C}$  then rt, 6 h. Yields of isolated compounds are reported in brackets

### 3.3.2 Biological evaluations

(in collaboration with Prof. S. M. Spampinato and Dr. M. Baiula, University of Bologna)

The ability of the new ligands to modulate cell adhesion was in this case limited to K562 (expressing  $\alpha_5\beta_1$  integrin), SK-MEL-24 (expressing  $\alpha_v\beta_3$  integrin) and Jurkat E6.1 (expressing  $\alpha_4\beta_1$  integrin) cellular lines to immobilized fibronectin (FN) and vascular cell adhesion molecule-1 (VCAM-1), respectively. Results of cell adhesion assays are reported in Table 3.2. As already discussed these cell models are widely used to investigate potential ligands capable of influencing cell adhesion mediated by the aforementioned integrins.<sup>155</sup> Structure similarity among the already described derivatives<sup>171</sup> and the novel compounds were considered for evaluate how the lack of a structural portion or a  $\beta$ -lactam scaffold modification could have influenced the activity as integrin ligands. For a better comparison, some of the previous described structures are reported in Figure 3.18.

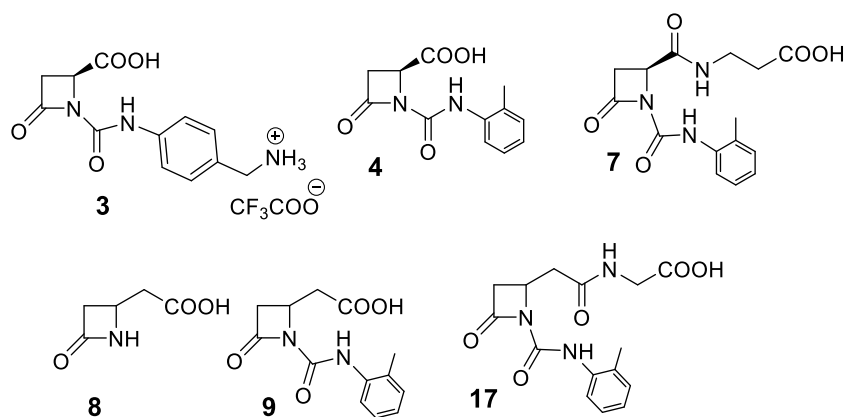


**Figure 3.18.**  $\beta$ -lactam integrin ligands already described and used as a comparison for the newly synthesized derivatives<sup>171</sup>

In compound **53** an alkylidene moiety was inserted for evaluating the effect of a more rigid structure compared to derivative **8** with a single bond on C4.  $\beta$ -lactam **53** displayed a good activity on  $\alpha_v\beta_3$  integrin behaving as an agonist. The same behavior was maintained for  $\alpha_4\beta_1$  but with a lower potency; activity was instead switched to antagonist on  $\alpha_5\beta_1$  class but with a negligible potency. To notice for comparison, compound **8** showed a promotion of cell adhesion toward  $\alpha_5\beta_1$  and an inhibition toward  $\alpha_v\beta_3$ . Derivatives **54** and **55** have a single side chain, the amine moiety for compound **54** and the acid terminus for **55**. Compound **54** showed basically no activity in the adhesion tests: only a low affinity for  $\alpha_4\beta_1$  as an agonist was detected, showing that the acid portion on C4 is fundamental for switching on the recognition with the receptor. Similarly compound **55** displayed a poor potency on  $\alpha_5\beta_1$  class as an antagonist, really lower than that displayed by compound **17** with the same chain on C4 but with an additional amine terminus on N1. Molecules **56** and **58** could be compared respectively with **9** and **4**, being designed with an amide group on N1 position instead of a ureidic functionality. In this case, **58** preserved its ability as an antagonist on  $\alpha_5\beta_1$  but lost potency on  $\alpha_v\beta_3$  and  $\alpha_4\beta_1$  that was instead displayed by **4**. On the other side, compound **56** showed a low potency only toward  $\alpha_5\beta_1$  but lost activity on  $\alpha_4\beta_1$ , in contrast to **9** that was a selective agonist on this latter class. Both the new derivatives were less effective compared to **4** and **9** revealing the importance of an amine group on the side chain for modulate the affinity with the receptor. “Open” derivatives **59** and **60** were planned to be the not-cyclic form of compounds **4** and **9**. Both the new derivatives lost activity on  $\alpha_4\beta_1$  class, toward which the corresponding cyclic  $\beta$ -lactams were selective and potent ligands. Surprisingly, they gained activity toward the RGD-integrin family of  $\alpha_v\beta_3$  (as both strong agonists) and  $\alpha_5\beta_1$  (as weak antagonist for **59** and weak agonist for **60**). In this case the open form of the molecules could be an option for influence the selectivity, but the potency is anyway decreased, probably for the loss of a side chain alignment when a cyclic core structure is missing. The insertion of a proline ring as constrained scaffold (compound **57**) revealed to be promising since it acted as an agonist (conversely to  $\beta$ -lactam **4**) for all the integrin assayed but was overall effective on  $\alpha_4\beta_1$  with a potency of 10 nM, revealing to be the most active compound of this new series.

Opposite enantiomers **52** and **61** derived from a cyclization of *L*- or *D*-aspartic acid respectively, and showed opposite effects also in cell adhesion mediated by  $\alpha_v\beta_3$  integrins, with **52** being an agonist and **61** an antagonist at a micromolar level. Activity was anyway in both cases reduced in comparison with compound **8** with a longer acidic side chain, showing that **52** and **61** were probably too little ligands for interact properly with the integrin binding site. Also compounds **62**, **63** and **64** are

enantiomerically pure at C4 (*R* configuration) deriving from *D*-aspartic acid. To notice, compound **62** displayed no activity at all in cell adhesion tests; its enantiomer **4** was instead an antagonist toward  $\alpha_v\beta_3$ ,  $\alpha_5\beta_1$  and  $\alpha_4\beta_1$  integrin classes. Compound **63** was inactive on  $\alpha_v\beta_3$  integrins unlike its enantiomer **7** that was an active ligand toward this family. While **7** was completely inactive on  $\alpha_5\beta_1$ , derivative **63** showed a discrete selectivity on this class in inhibiting cell adhesion. Also compound **64** completely lacked the activity that was on contrary promoted by its enantiomer **3** as a modest agonist on  $\alpha_5\beta_1$ . In general we could assume that for this series of compounds (**61-64**) the *R* configuration at C4 stereocenter was detrimental for integrin activity and only *S* enantiomers were active in the receptor recognition. Following this consideration, we decided to perform an enzymatic kinetic resolution on some of the racemic C4 acetic acid derivatives (compounds **9** and **17**) for evaluating if the active enantiomer could increase the potency in cell adhesion assays (see Chapter 4).

**Table 3.2.** Effects of  $\beta$ -lactam compounds **52-64** on RGD-binding and leukocyte integrin-mediated cell adhesion. Data are presented as EC<sub>50</sub> for agonists (in bold), and as IC<sub>50</sub> for antagonists (nM). Values represent the mean of three independent experiments carried out in quadruplicate

Comp.	SK-MEL-24/ FN $\alpha_v\beta_3$	K562/FN $\alpha_5\beta_1$	Jurkat/ VCAM-1 $\alpha_4\beta_1$
<b>52</b>	<b>1560</b> agonist	nt	> 5000
<b>53</b>	<b>76</b> agonist	6480 antagonist	<b>255</b> agonist
<b>54</b>	> 5000	1110 antagonist	> 5000
<b>55</b>	> 5000	> 5000	976 agonist
<b>56</b>	> 5000	419 antagonist	> 5000
<b>57</b>	2880 agonist	140 agonist	<b>10</b> agonist
<b>58</b>	> 5000	42 antagonist	> 5000
<b>59</b>	<b>85</b> agonist	3512 antagonist	> 5000
<b>60</b>	<b>30</b> agonist	<b>5760</b> agonist	> 5000
<b>61</b>	1079 antagonist	> 5000	> 5000
<b>62</b>	> 5000	> 5000	> 5000
<b>63</b>	> 5000	97 antagonist	> 5000
<b>64</b>	> 5000	> 5000	> 5000

nt = not tested

Further investigations on the most active  $\beta$ -lactam compounds are planned in order to show if they could influence intracellular signalling activated by endogenous integrin agonists, as described for previously described agonist compounds.<sup>171</sup> Specifically, compound **57** confirmed its agonist behavior since a significant increase in ERK1/2 phosphorylation was detected when added alone to cells (data not shown). Signalling tests on compounds **53**, **58-60** are still in course.

### 3.4 Studies on integrin internalization mediated by $\beta$ -lactam compounds

(in collaboration with Prof. S. M. Spampinato and Dr. M. Baiula, University of Bologna)

As already outlined in Paragraph 3.1.2.3, integrin trafficking and internalization are important mechanisms adopted by cells for regulating integrin-extracellular matrix interactions, but the effects exerted by synthetic integrin ligands on endocytosis mechanisms are still unclear.

Having in hands some novel derivatives active as integrin agonists or antagonists, we decided to investigate how these ligands could eventually promote or inhibit trafficking processes. Therefore, integrin internalization mediated by the developed synthetic  $\beta$ -lactams was evaluated through confocal microscopy analysis using HEK293 cell lines expressing fluorescent  $\alpha_5$  integrin. For these experiments, a plasmid of  $\alpha_5$  integrin fused with an Enhanced Green Fluorescent Protein (EGFP) was transfected in HEK293 cells (Figure 3.19), and its expression was monitored with fluorescence microscopy. Control cells expressed fluorescent  $\alpha_5$  integrin that was localized primarily on cell membrane. Following fibronectin (FN) exposure (10  $\mu\text{g}/\text{mL}$ ), after 15 minutes integrin was internalized into the cytoplasm and consequently the cell appeared completely green-colored (Figure 3.19).

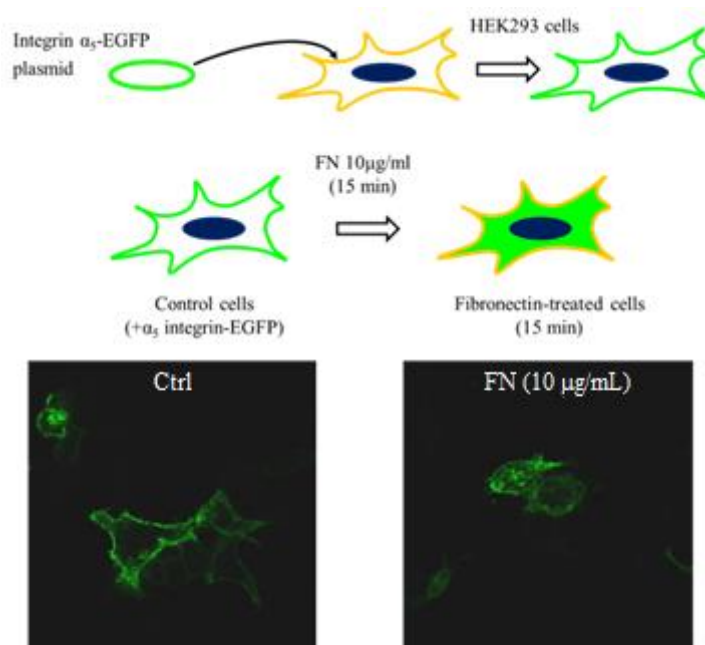


**Figure 3.19.** Plasmid mediated-transfer and expression of  $\alpha_5$  integrin fused with Enhanced Green Fluorescent Protein (EGFP). On the left: Control cells (+ $\alpha_5$  integrin-EGFP); on the right: fibronectin-treated cells (10  $\mu\text{g}/\text{mL}$  - 15 min)

The same behavior was found when the cells were treated with  $\alpha_5\beta_1$  agonist compound **21**, able to promote internalization in a 1  $\mu\text{M}$  concentration. A time course experiment for following the exposure



of **21** from 15 minutes to 4 hours was conducted and demonstrated the evolution of the progressive integrin internalization (Figure 3.20).

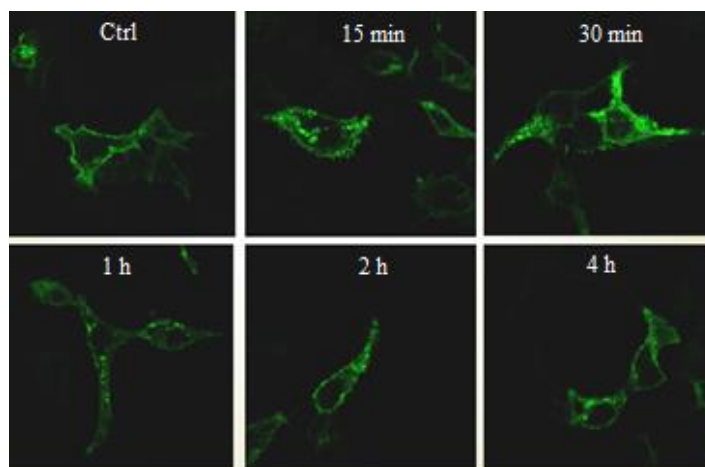


**Figure 3.20.** Confocal microscopy analysis of HEK293 cells expressing fluorescent  $\alpha_5$  integrin: internalization mediated by  $\alpha_5\beta_1$  agonist **21** in time course experiment

Conversely,  $\alpha_5\beta_1$  antagonist compound **4** showed to prevent integrin endocytosis mediated by fibronectin. As shown in Figure 3.21 in fact, the fluorescence remained confined along the cell membrane and the internalization was inhibited, in both absence and presence of fibronectin.

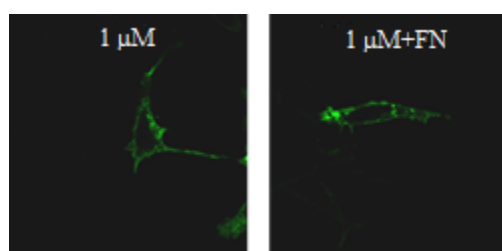


**Figure 3.21.** Confocal microscopy analysis of HEK293 cells expressing fluorescent  $\alpha_5$  integrin: internalization inhibited by  $\alpha_5\beta_1$  antagonist compound **4** (15 min), in absence (left) and in presence (right) of fibronectin (FN – 10  $\mu\text{g}/\text{mL}$ )

### 3.5 Fluorescent $\beta$ -lactam compounds

Since it resulted from fluorescence microscopy that the developed agonist ligands could induce integrin internalization, we decided to better investigate the behavior of these compounds in the trafficking process. Therefore, we developed some novel fluorescent derivatives conjugating the most potent agonists among those discovered with fluorescent tags. In this way their role in internalization processes could be in turn studied with confocal microscopy for evaluating if the ligand itself could be internalized into the cell *via* endocytosis together with the integrin.

### 3.5.1 Imaging and bioimaging

Imaging is a technique that allows to detect an area of an organism or of a cell not visible from the outside, by means of fluorescent molecules present in the sample. Fluorescent molecules are widely used as analytical and diagnostic tools in various research fields, ranging from molecular and cellular biology to biochemistry, biophysics, biotechnology and medicine.<sup>189</sup> This remarkable development is due to their high sensitivity, which allows the visualization of biological compounds in physiological conditions, to their high spatial and temporal resolution, which allows to analyze the dynamic processes of cell signal transduction, and to their non-invasiveness.<sup>190</sup> Fluorescence is in fact useful for cellular monitoring both *in vitro* and *in vivo* permitting for example to investigate the structure and dynamics of proteins, the variation of conformations induced upon ligand binding, the interactions between protein-protein and protein-nucleic acid, the protein trafficking and the enzymatic activity.<sup>191</sup> Fluorescence labelling can be extended over a wide range of wavelengths (non-NIR or NIR – near infrared region) using semiconductor nanocrystals, fluorescent proteins, or organic molecules.<sup>192</sup> One of the main strategy for bioimaging is the conjugation between small fluorophores and a ligand. For a specific and selective detection of the desired target molecule (associated with tumor cells for example), the ligand combined with the fluorescent dye has to be exclusively recognized by such target.<sup>193</sup> Usually, ligands employed for bio-imaging are small molecules, peptides, antibodies and aptamers, able to bind a molecule or a protein with a specific affinity toward cellular receptors, cancer antigens, enzymes or nucleic acids (Figure 3.22).<sup>194</sup>

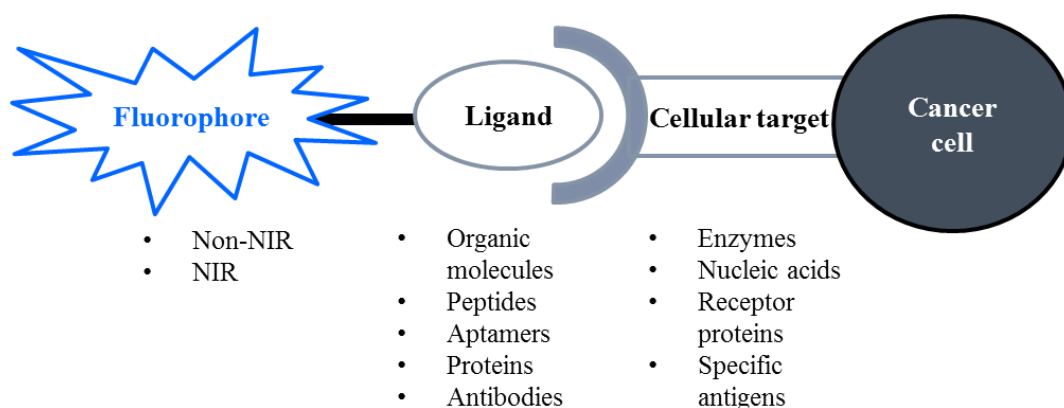


**Figure 3.22.** Conjugation between a fluorophore and a specific ligand for a cellular target, as a suitable model for bio-imaging

### 3.5.2 Fluorophores

In recent years, detection based on fluorescence techniques has received special attention and notable progress has been made in both fluorescence instrumentation and synthesis of new fluorophores. Fluorophores (or fluorochromes) are fluorescent chemical compounds that can re-emit light upon light excitation. They typically are planar or cyclic molecules with many  $\pi$  bonds, and contain several combined aromatic groups.<sup>195</sup> The organic fluorophores are classified according to their increasing absorption and emission wavelengths when conjugated or complexed with an analyte. Compounds providing fluorescence from the near-ultraviolet to approximately 500 nm include oxobenzopyrans, naphthofurans, oligothiophenes, 4,7-phenanthroline-5,6-diones, benzooxadiazoles, dansyl chloride, naphthalene 2,3-dicarboxaldehyde, and 6-propionyl-2-(dimethylamino)naphthalene. Organic

fluorescent labels emitting between 500 nm and the near-infrared (ca. 900 nm) comprise fluoresceins (including biarsenical dyes), rhodamines, 4,4-difluoro-4-bora-3a,4a-diaza-*s*-indacenes (BODIPY dyes), squaraines, and cyanines.<sup>190</sup>

Before selecting a suitable fluorophore, some intrinsic features need to be considered, i.e. their absorption and emission wavelength, their emission intensity (calculated as the product of the molar extinction coefficient  $\epsilon$  and the quantum yield  $\phi$ ), their solubility and stability,<sup>196</sup> and the presence of appropriate chemical functions that could allow a conjugation with small molecules, amino acids, proteins or specific ligands.<sup>197</sup> Another factor to consider when choosing a specific fluorophore is the solvent; the fluorescence of a molecule can in fact be switched on or off according to the different solvent.

For our purpose, we selected two fluorophores among the most employed for bioimaging, i.e. fluorescein isothiocyanate (FITC), with a green light emission<sup>198</sup> and Rhodamine B, with a red light emission<sup>199</sup> (Figure 3.23). Both compounds are commercially available, easy to handle and derivatize, and stable in cellular conditions. FITC is easily accessible and due to its absorption wavelength (492 nm) does not interfere with the absorption of cellular proteins and does not require sophisticated microscopic tools.<sup>200</sup> Rhodamine B in turn is a low-cost fluorophore widely used because of its high photostability and chemostability in aqueous media.<sup>201</sup> Moreover, emitting in the near infrared region, Rhodamine B can be widely exploited for biological applications.<sup>202</sup>

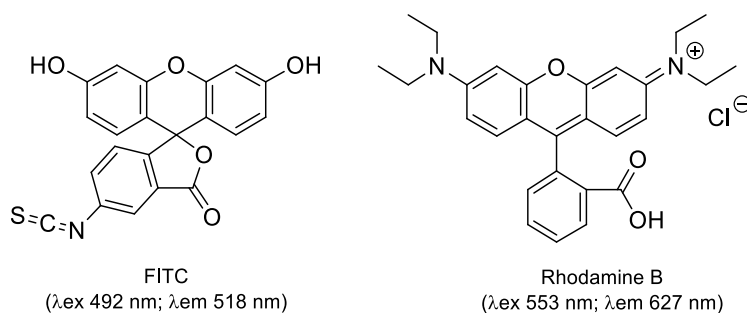


**Figure 3.23.** Structures of FITC and Rhodamine B. Excitation and emission wavelengths are reported

### 3.5.3 Development of $\beta$ -lactam-fluorophore conjugates

#### 3.5.3.1 Synthesis of azetidiones

In our case three novel derivatives bearing a fluorophore moiety (Rhodamine B or FITC) were realized, over-functionalizing the structures of compounds **9** and **17** that resulted the most potent agonists toward  $\alpha_4\beta_1$  and  $\alpha_5\beta_1$  integrin classes, respectively<sup>171</sup> (Figure 3.24).

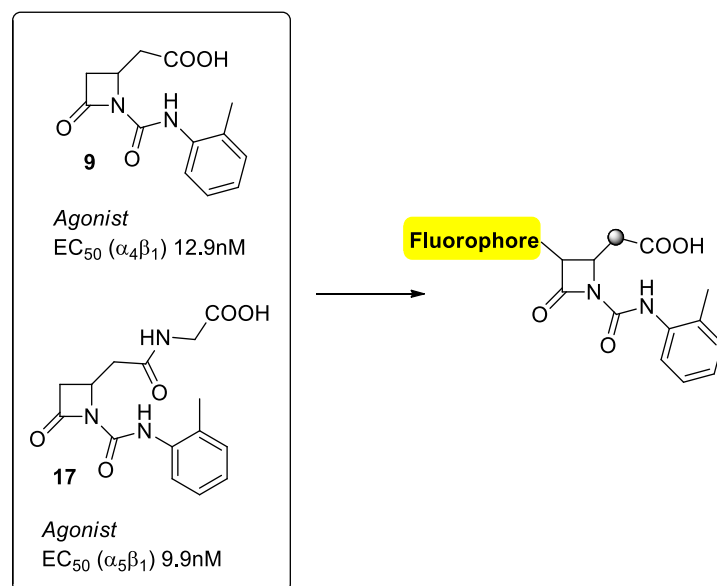
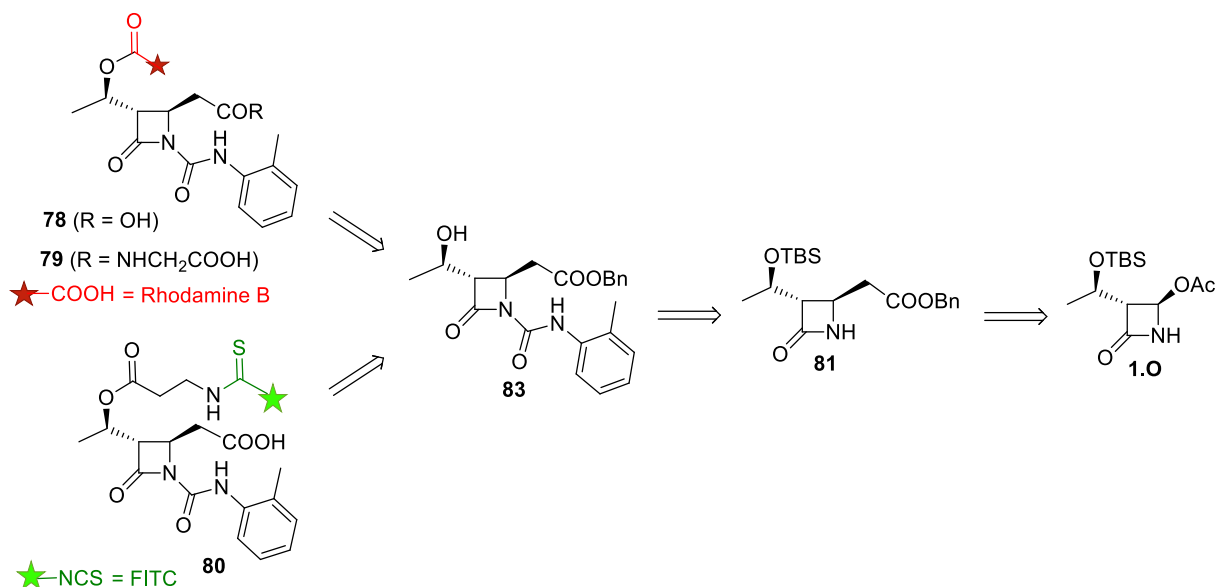


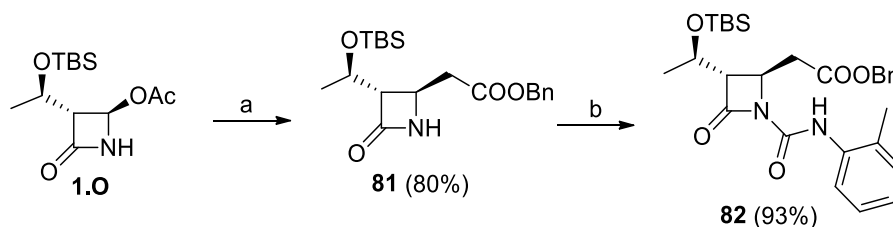
**Figure 3.24.** Design of new fluorescent compounds based on previously reported agonist  $\beta$ -lactams **9** and **17**

For the realization of the new fluorescent derivatives, an appropriate commercial  $\beta$ -lactam (**1.0**) was selected as starting material for having the C3 position of the ring already functionalized with an oxygen protected hydroxyethyl group. This  $\beta$ -lactam scaffold was suitably modified on C4 and N1 for obtaining the acid and the basic terminal functionalities required for preserving the activity toward integrin receptors. The C3 position in the starting material was instead exploited as a useful anchoring point for the conjugation with the selected fluorophores. Rhodamine B (compounds **78** and **79**) was directly inserted on the hydroxyl functionality; in compound **79** the side chain on C4 was strategically elongated with a glycine residue, for hopefully promoting the affinity toward a different integrin class (see compound **17** vs **9**). Compound **80** instead was conjugated with fluoresceine and an extra spacer was inserted, since the derivatization with the isothiocyanate group of FITC required an amine terminal in the molecular scaffold (Scheme 3.10).



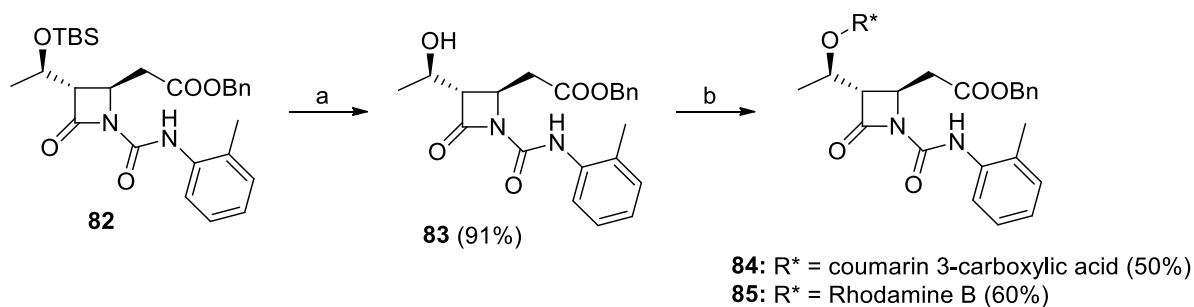
**Scheme 3.10.** Synthetic strategy for compounds **78**, **79** and **80**

The synthesis of all targets called for a nucleophilic substitution reaction on the commercially available  $\beta$ -lactam **1.O**, by a suitable Reformatskj reagent, obtained in turn from benzyl bromoacetate and zinc in excess. The same procedure already described for 4-acetoxiazetidione **1.M** as starting material<sup>171</sup> was followed, obtaining, despite a major hindrance of the substrate, a good reproducibility and even better yields. The resulting compound **81** was then acylated on the  $\beta$ -lactam nitrogen with the commercially available *o*-tolylisocyanate, in order to insert the basic moiety necessary for modulating the affinity toward integrin receptors. The reaction was firstly attempted with the optimized conditions found for the corresponding C3-underivatized  $\beta$ -lactam, i.e. potassium carbonate in CH<sub>3</sub>CN.<sup>171</sup> Since the obtained yields were unsatisfying, the stronger base NaHMDSA in THF at -78 °C was employed, but also in this case the target compound was afforded in yields lower than 30%; much better results were gained with triethylamine in CH<sub>2</sub>Cl<sub>2</sub> at room temperature. Moreover, when the equivalents of isocyanate were increased up to 5 and contextually the solvent volume was reduced, for enhancing the isocyanate concentration, compound **82** was isolated with a 93% yield (Scheme 3.11).



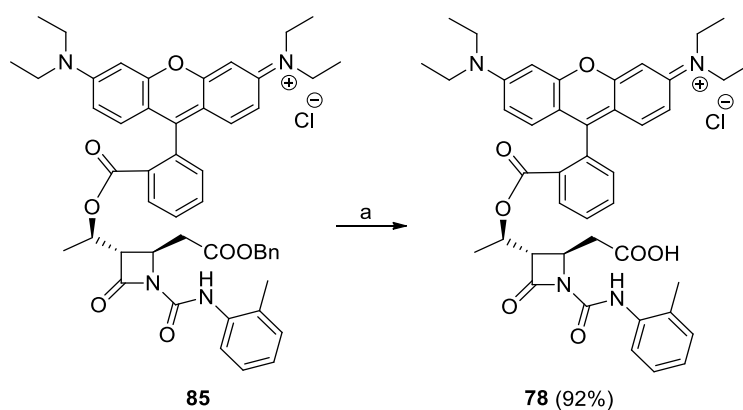
**Scheme 3.11.** Synthesis of  $\beta$ -lactams **81** and **82**; Reagents and conditions: a) 1. Zn, TMSCl, benzylbromoacetate, THF, 30 °C then rt, 3 h; 2. (2*R*,3*R*)-3-((*R*)-1-((*tert*-butyldimethylsilyl)oxy)ethyl)-4-oxazetidine-2-yl acetate, THF, 0 °C then rt, 3 h; b) *o*-tolylisocyanate, TEA, CH<sub>2</sub>Cl<sub>2</sub>, rt, 16 h. Yields of isolated compounds are reported in brackets

Subsequently, the *tert*-butyldimethylsilyl group on the C3 side chain was removed under acidic conditions, using a complex of boron trifluoride diethyl etherate at 0 °C, as already reported in Chapter 2 for alkylidene derivatives.<sup>46</sup> The reaction is fast and selective, and alcohol **83**, obtained in good yields, constituted a common intermediate for achieving the three target fluorescent compounds. For the synthesis of **78** and **79**, the free hydroxyl group of **83** was exploited for the direct insertion of the fluorophore mediated by standard reagents DCC and DMAP. An esterification with the carboxylic acid function of Rhodamine B was planned, but, in order to test the reactivity of the substrate, coumarin 3-carboxylic acid was previously tested as a model with Steglich esterification conditions. The process revealed to be quite efficient, and the same procedure was then repeated with Rhodamine B. In this case, the conversion was never complete, even using the reagents in equimolar ratio or increasing the reaction times. Nevertheless, compound **85** was isolated with a 60% yield after purification by flash-chromatography. The column was conducted with a gradient elution of EtOAc/CH<sub>3</sub>OH mixture for allowing a separation between the target and the starting Rhodamine B, both very polar compounds in the form of sodium salts (Scheme 3.12).



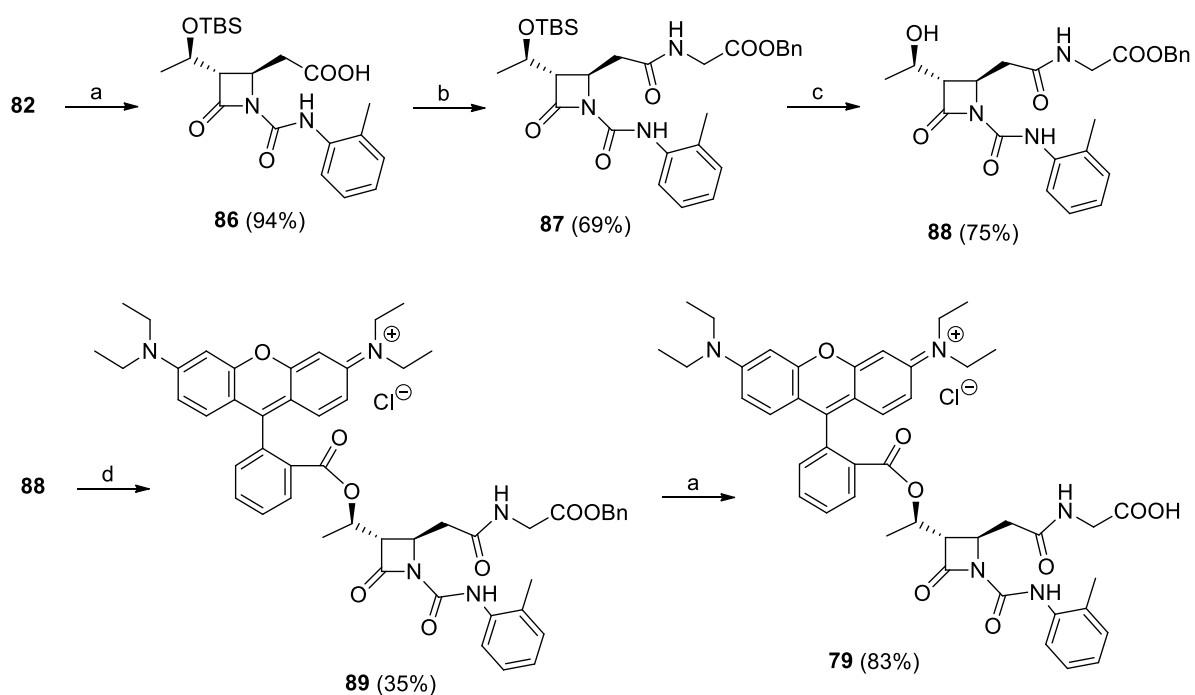
**Scheme 3.12.** Synthesis of  $\beta$ -lactams **84** and **85**; Reagents and conditions: a) boron trifluoride diethyletherate, CH<sub>3</sub>CN, 0 °C then rt, 2 h; b) DCC, TEA, DMAP, coumarin 3-carboxylic acid or Rhodamine B, CH<sub>2</sub>Cl<sub>2</sub>, 0 °C then rt, 16 h. Yields of isolated compounds are reported in brackets

The final synthetic step comprised a standard Pd-catalyzed hydrogenolysis for restoring the terminal acid moiety necessary for the interaction with the integrin receptor (Scheme 3.13).



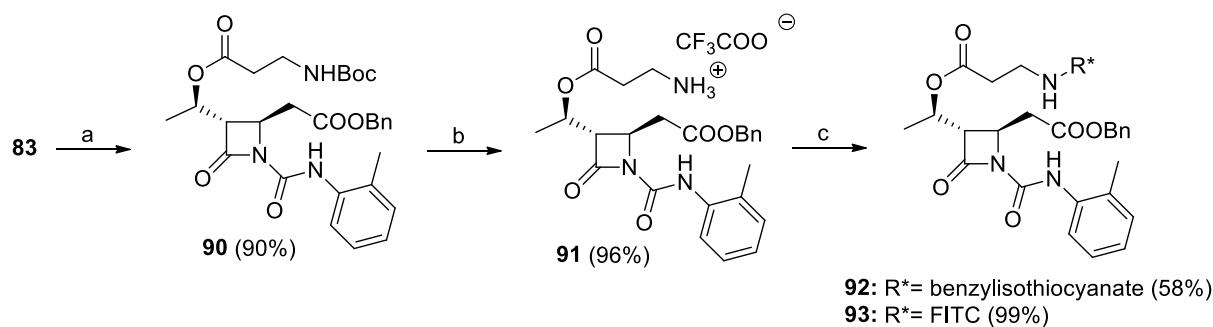
**Scheme 3.13.** Synthesis of target  $\beta$ -lactam **78**. Reagents and conditions: a) H<sub>2</sub>, Pd/C (10%), THF/CH<sub>3</sub>OH 1:1, rt, 2 h. Yields of isolated compound is reported in brackets

Synthesis of target compound **79** (Scheme 3.14) kept in account the elongation of the side chain on C4 position with a glycine residue. Compound **82** was therefore subjected to the deprotection of the benzyl ester function *via* hydrogenolysis yielding **86**, followed by a reaction with glycine benzyl ester under standard peptidic coupling conditions to give intermediate **87**. At this stage of the synthesis, the alcohol group on the C3 side chain was restored with the aforementioned conditions (intermediate **88**), and the coupling with Rhodamine B was performed, this time with lower yields due to poor solubility of the crude. A final hydrogenolysis on compound **89** for removing the C4 benzyl ester yielded the target product **79** in good yields.



**Scheme 3.14.** Synthesis of target  $\beta$ -lactam **79**. Reagents and conditions: a)  $\text{H}_2$ , Pd/C (10%), THF/ $\text{CH}_3\text{OH}$  1:1, rt, 2 h; b) DCC, TEA, DMAP, glycine benzylester-HCl,  $\text{CH}_2\text{Cl}_2$ , 0 °C then rt, 16 h; c) boron trifluoride diethyletherate,  $\text{CH}_3\text{CN}$ , 0 °C then rt, 2 h; d) DCC, TEA, DMAP, Rhodamine B,  $\text{CH}_2\text{Cl}_2$ , 0 °C then rt, 16 h. Yields of isolated compounds are reported in brackets

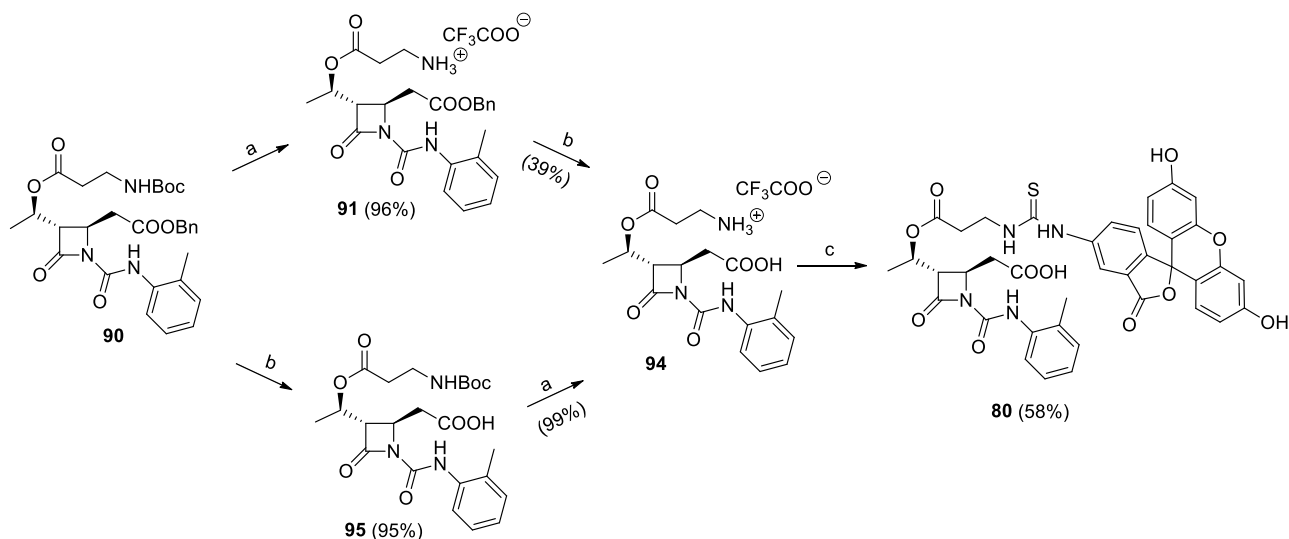
Finally, for the synthesis of compound **80**, attempts of a direct reaction of FITC on the hydroxyl group of alcohol **83**<sup>203</sup> revealed unsuccessful. It is indeed reported that isothiocyanates react nearly exclusively with amine functionalities to give the corresponding thioureas.<sup>204</sup> In order to insert the required terminal amine group, we proceeded with an esterification reaction between alcohol **83** and commercial *N*-Boc- $\beta$ -alanine, and obtained compound **90** in excellent yields. At this stage **90** displayed two orthogonal protecting groups: at first, deprotection of *N*-Boc-amine was carried out with an excess of trifluoroacetic acid (compound **91**). As already discussed for the reaction with Rhodamine B, the coupling was initially tested with a model substrate, benzyl isothiocyanate in this case, in order to verify the reactivity and the operative conditions. The reaction was simply mediated by an excess of TEA and isothiocyanate and proceeded with good yields after flash-chromatography (compound **92**). When the coupling was performed with FITC in the same conditions, the crude mixture resulted difficult to purify, due to the similar retention factors of the target compound **93** and the residual FITC on silica gel. The reaction gave better results when attempted with a substoichiometric amount of isothiocyanate; in this way the purification step was avoided and the target compound **93** was quantitatively yielded (Scheme 3.15).



**Scheme 3.15.** Synthesis of  $\beta$ -lactam **92** and **93**. Reagents and conditions: a) Boc-alanine benzyl ester, DCC, DMAP,  $\text{CH}_2\text{Cl}_2$ ,  $0^\circ\text{C}$  then rt, 16 h; b) TFA,  $\text{CH}_2\text{Cl}_2$ ,  $0^\circ\text{C}$  then rt, 16 h; c) benzylisocyanate or FITC, TEA,  $\text{CH}_2\text{Cl}_2$ , rt, 4 h. Yields of isolated compounds are reported in brackets

The benzyl ester deprotection at C4 was first attempted with classical hydrogenolysis conditions, but the presence of a sulfur atom in the starting material deactivated, as suspected, the palladium catalyst,<sup>205</sup> leading to a null conversion. Also attempts of a remotion in basic conditions (solution of  $\text{NH}_4\text{OH}$  25% in  $\text{CH}_3\text{OH}$ <sup>206</sup> or  $\text{K}_2\text{CO}_3$  in  $\text{CH}_3\text{OH}$ <sup>207</sup>) were unsuccessful.

We then decided to deprotect the benzyl ester group before inserting the fluorophore; when the hydrogenolysis reaction was conducted on intermediate **91**, the corresponding acid **94** was gained with low yields (Scheme 3.16). Therefore we tried a previous hydrogenolysis reaction on intermediate **90** (to give  $\beta$ -lactam **95**), followed by the Boc group deprotection; with this strategy compound **94** was gained with quantitative yields in both steps (Scheme 3.16). The coupling with fluorescein isothiocyanate was finally performed as the last step of the synthesis and the target compound **80** was obtained after an acid work-up and a purification by column chromatography that was required to reach a purity up to 95% to HPLC-MS.



**Scheme 3.16.** Synthesis of target  $\beta$ -lactam **80**. Reagents and conditions: a) TFA,  $\text{CH}_2\text{Cl}_2$ ,  $0^\circ\text{C}$  then rt, 16 h; b)  $\text{H}_2$ , Pd/C (10%), THF/ $\text{CH}_3\text{OH}$  1:1, rt, 2 h; c) FITC, TEA,  $\text{CH}_2\text{Cl}_2$ , rt, 16 h. Yields of isolated compounds are reported in brackets



### 3.5.3.2 Spectrophotometric evaluations

(in collaboration with Prof. P. Ceroni, University of Bologna)

Once that the target compounds were obtained and completely characterized, qualitative fluorescence spectroscopy experiments were conducted in order to verify if the fluorophore properties could be affected by the conjugation with the  $\beta$ -lactam scaffolds. Excitation and emission spectra of compounds **78**, **79** and **80** are reported in Figure 3.25, together with their relative maximum wavelengths. If compared with the values reported for Rhodamine B methyl ester<sup>208</sup> ( $\lambda_{\text{ex}} = 558$  nm,  $\lambda_{\text{em}} = 585$  nm) and for FITC ( $\lambda_{\text{ex}} = 492$  nm,  $\lambda_{\text{em}} = 518$  nm),<sup>209</sup> it was possible to assume that no significant variations in the fluorophore properties could be underlined after the coupling with the synthetic ligands, since the compared values are in all cases in perfect accordance. Considering the molar extinction coefficients, compounds **78** ( $69706 \text{ M}^{-1} \text{ cm}^{-1}$  at 556 nm in methanol) and **79** ( $79901 \text{ M}^{-1} \text{ cm}^{-1}$  at 559 nm in methanol) were comparable to the value reported for Rhodamine B methyl ester ( $83000 \text{ M}^{-1} \text{ cm}^{-1}$  at 555 nm in methanol). To notice, the replacement of the free carboxylate group of Rhodamine B ( $106000 \text{ M}^{-1} \text{ cm}^{-1}$  at 545 nm in ethanol)<sup>210</sup> with a methyl ester decreased the molar extinction coefficient.<sup>211</sup> Compound **80** instead presented a molar extinction coefficient ( $4820 \text{ M}^{-1} \text{ cm}^{-1}$  at 480 nm in methanol) that resulted extremely lower than the value reported for FITC ( $73000 \text{ M}^{-1} \text{ cm}^{-1}$  at 494 nm in aqueous buffer, pH = 9),<sup>212</sup> thus probably causing low fluorescence properties of the molecule that could constitute an issue in the further planned confocal microscopy analyses.

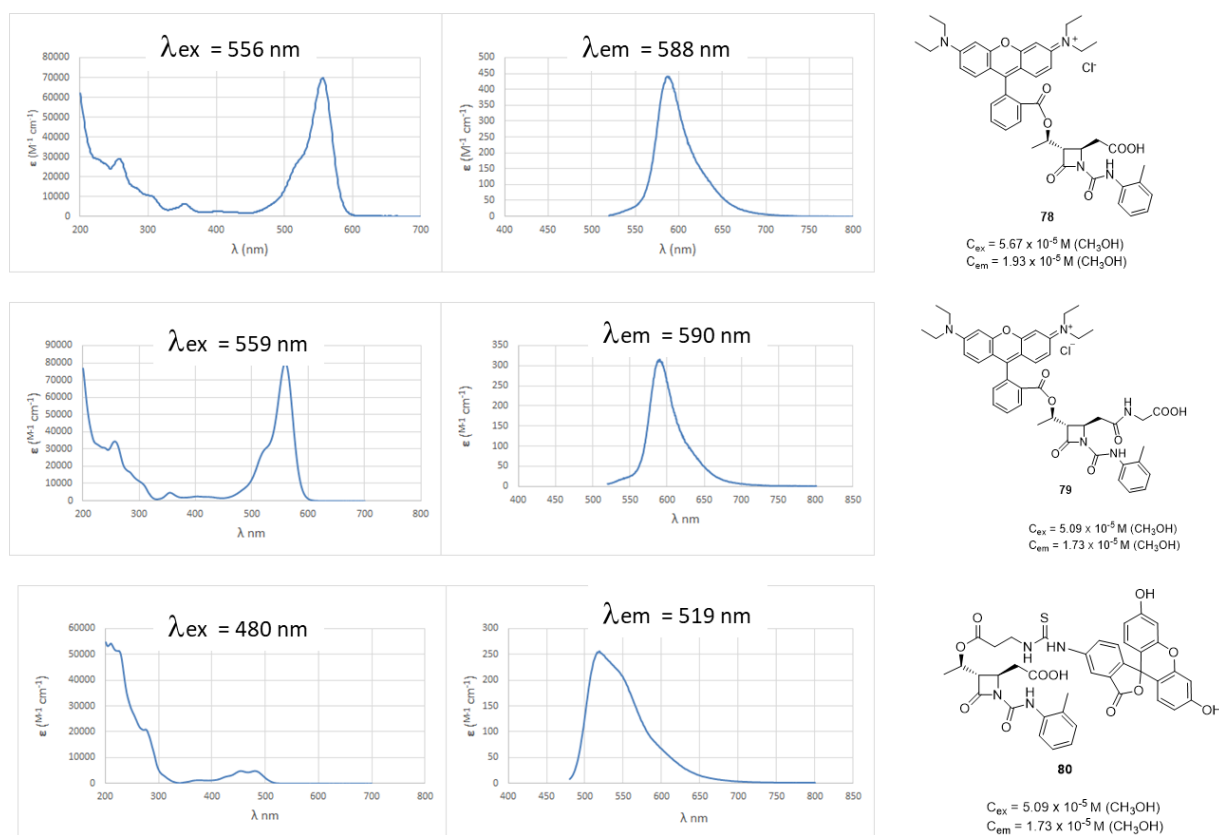


**Figure 3.25.** Excitation and emission spectra of  $\beta$ -lactams **78**, **79** and **80**. Relative concentrations and solvent (in brackets) are reported below the structures

### 3.5.3.3 Biological evaluations

(in collaboration with Prof. S. M. Spampinato and Dr. M. Baiula, University of Bologna)

#### Cell adhesion assays

The ability of the new fluorescent compounds **78**, **79** and **80** to modulate the adhesion of specific integrin-expressing cells has been tested. Interestingly, all the compounds resulted agonist and showed a concentration-dependent enhancement in fibronectin-mediated adhesion of K562 (expressing  $\alpha_5\beta_1$ ) or Jurkat E6.1 (expressing  $\alpha_4\beta_1$ ) cells (Figure 3.26). In particular,  $\beta$ -lactam **78** was the most potent in enhancing cell adhesion toward  $\alpha_4\beta_1$  showing sub-micromolar affinity ( $EC_{50} = 0.55 \mu\text{M}$ ), also displaying a comparable activity on  $\alpha_5\beta_1$  ( $EC_{50} = 0.33 \mu\text{M}$ ). Compound **79** instead showed a preferential selectivity for  $\alpha_5\beta_1$  integrin class, presenting a remarkable nanomolar activity ( $EC_{50} = 20.5 \text{ nM}$ ). The obtained activity trend reflected what was previously described for the relative C3 non-substituted  $\beta$ -lactams. In fact, compound **9** displayed a selectivity toward  $\alpha_4\beta_1$ , while compound **17** with a longer glycine-derived C4 side chain was active only on  $\alpha_5\beta_1$ . Finally, FITC-compound **80** was the less potent in adhesion assays even if anyway displayed some affinity toward  $\alpha_5\beta_1$  and  $\alpha_4\beta_1$  integrins ( $EC_{50} = 11.1 \mu\text{M}$  and  $41.1 \mu\text{M}$  respectively).

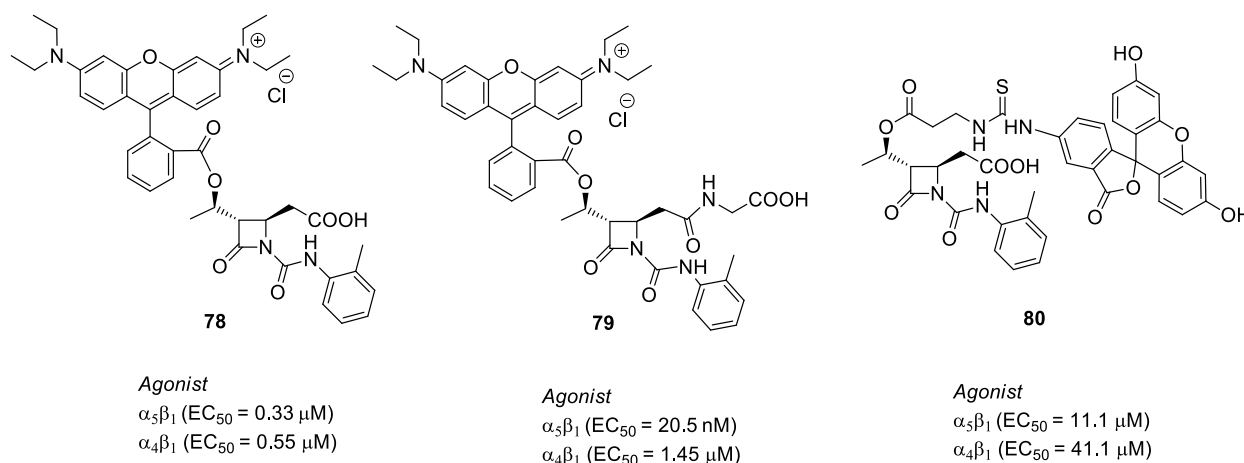


**Figure 3.26.** Structures of target  $\beta$ -lactams **78**, **79** and **80** and results of cell-adhesion assays. Values of  $EC_{50}$  are reported in brackets

Even if the novel fluorescent derivatives generally lacked in adhesion ability compared to their non-fluorescent analogues, switching from nanomolar to micromolar range, it was impressive that they preserved a good activity despite their much increased molecular complexity. Moreover, since an agonist behavior was maintained, the novel compounds were considered promising for investigating the role of the ligands in internalization and other integrin-mediated cellular processes.

#### Confocal microscopy analysis

Studies on the promotion of integrin internalization mediated by the novel synthesized derivatives are in due course by confocal microscopy analyses. Preliminary results on compound **78** that displayed a good activity in promoting cell adhesion toward  $\alpha_5\beta_1$  integrins are reported in Figure 3.27. The experiment was carried out as described in Paragraph 3.4 by means of a green fluorescent  $\alpha_5$

integrin transfected on HEK cells. In this case also the red fluorescence was considered, for monitoring if the Rhodamine-ligand was confined on the cell membrane, visible inside the cell, or not present at all.

Switching on the green light, in non-treated HEK cells the fluorescence originated by  $\alpha_5$  integrin was localized on the membrane surface and in the endoplasmic reticulum (control). In cells treated with compound **78** instead, the green fluorescence was visible inside the cell, clearly showing that the agonist ligand could promote integrin internalization. When the red fluorescence was activated, in non-treated HEK cells fluorescence is absent, as expected. In presence of **78** instead, the red fluorescence diffused inside the cell that appeared completely red-colored, possibly indicating the internalization of the compound into the cytoplasm. Further microscopy images should be recorded in order to have a more clear idea on the effect exerted by our ligand and on its eventual selective internalization into overexpressing-integrin cells. Compounds **79** and **80** should also be tested in confocal microscopy analyses. To notice, molecule **80** with a green fluorophore is not suitable for an experiment conducted with a green integrin, since it would not be possible to discriminate the source of the fluorescence (if arising from the integrin or from the ligand). In this case, the analysis could be performed with non-fluorescent HEK cells (for evaluating the internalization of the ligand alone), or with cells transfected with a red integrin (for evaluating both integrins and ligand internalization).

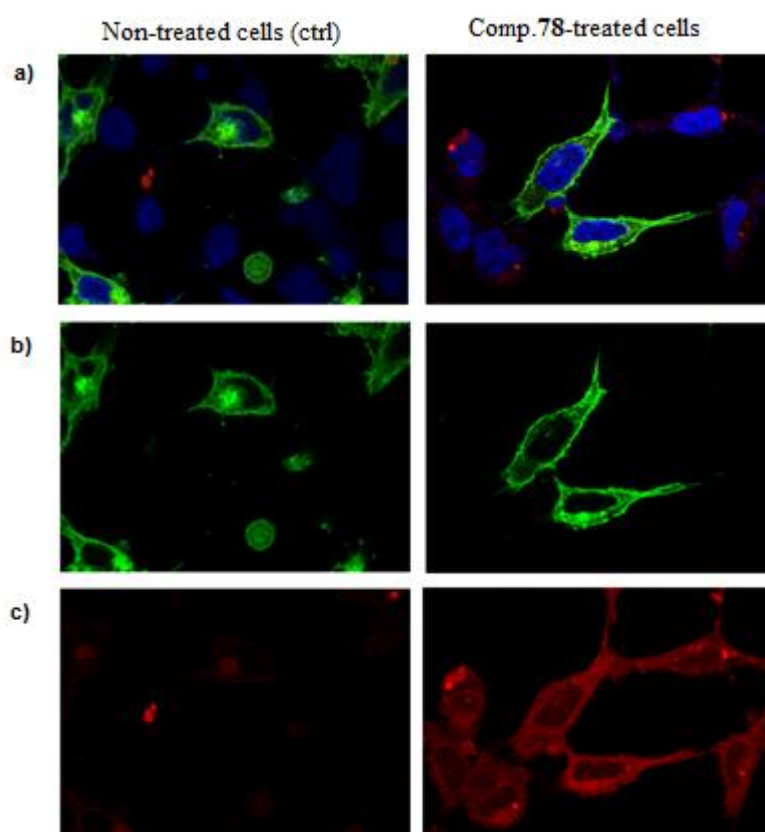


**Figure 3.27.** Confocal microscopy analysis of HEK293 cells expressing fluorescent  $\alpha_5$  integrin. On the left column: control cells (+ $\alpha_5$  integrin-GFP); on the right column: compound **78**-treated cells ( $10^{-6}$  M); a) merge of blue (nuclei), green ( $\alpha_5$  integrin) and red (compound **78**) fluorescence; b) green fluorescence; c) red fluorescence

## 3.6 Cytotoxic $\beta$ -lactam compounds

### 3.6.1 Cytotoxic agents and Targeted drug delivery systems

The term ‘cytotoxic’ refers to any drug able to damage or kill cells through cell division inhibition, and therefore, is potentially useful for anticancer chemotherapy.

Cytotoxic drugs include:

- alkylating agents, which act by forming covalent bonds with DNA and by preventing its replication.
- antimetabolites, which block or alter one or more metabolic pathways involved in DNA synthesis.
- cytotoxic antibiotics, which prevent the division of mammalian cells.
- plant derivatives (vinca alkaloids, taxanes, camptothecins), which act specifically on microtubules.

Antibiotic and antimetabolite classes represent the most employed drugs for chemotherapy.

Cytotoxic antibiotics exert their effect by direct action on DNA. Among them, Doxorubicin (Figure 3.28a), which belongs to the anthracycline family, acts as an intercalating agent, by inserting between the DNA bases and inhibiting their synthesis. The major cytotoxic effect, however, is exerted with an inhibitory action on topoisomerase II, an enzyme whose activity is definitely increased in diseased cells. This enzyme must ensure that, during DNA replication, a rotation occurs around the replicating fork in order to prevent the neo-synthesized DNA to become irreversibly entangled. This rotation occurs by first producing an incision in both DNA strands, and then by restoring their integrity. Doxorubicin stabilizes the DNA-topoisomerase II complex immediately after incision, blocking the following process. In addition to the common side effects, Doxorubicin can cause cumulative and dose-dependent damage to myocardium, provoking arrhythmias and heart failure, probably due to a free radicals formation.<sup>213</sup>

Among the antimetabolite drugs instead, 5-fluoro uracil (5-FU) (Figure 3.28b), thanks to its structural similarity to uracil, can be incorporated into DNA with consequent alterations in its functionalities. 5-FU prevents cell proliferation by irreversible inhibition of the enzyme thymidylase synthetase, responsible for the synthesis of thymidine, essential in turn for DNA formation. Some of its derivatives functionalized in N1 and/or N3 positions of the pyrimidine ring also displayed promising features from both a pharmacokinetic and a pharmacodynamic point of view, being exploited as 5-FU prodrugs.<sup>214</sup> The main undesirable effects of this cytotoxic agent are gastrointestinal epithelial damage and myelotoxicity.

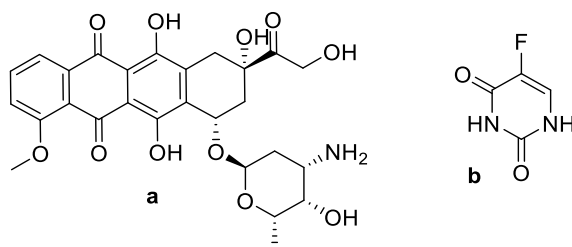


**Figure 3.28.** Examples of cytotoxic agents. a) Doxorubicin; b) 5-fluorouracil

Nowadays conventional anti-cancer therapies, such as chemotherapy, could not guarantee a selectivity towards tumour cells, resulting in numerous side effects and acute toxicities, as described in the aforementioned examples of Doxorubicin and 5-FU. Therefore, the need to develop new

selective therapies that could effectively target tumour cells with the lowest possible toxicity toward healthy cells is urgently required.<sup>215</sup> In the last decade, several research groups have focused on the development of “targeted drug delivery systems (TDDs)”, with the aim of maximizing the effectiveness of the drug whilst minimizing side effects, by means of a selective transport of the drug into the diseased cells. Generally, TDDs consist of a carrier/ligand and a cytotoxic agent, coupled by a suitable linker (Figure 3.29).

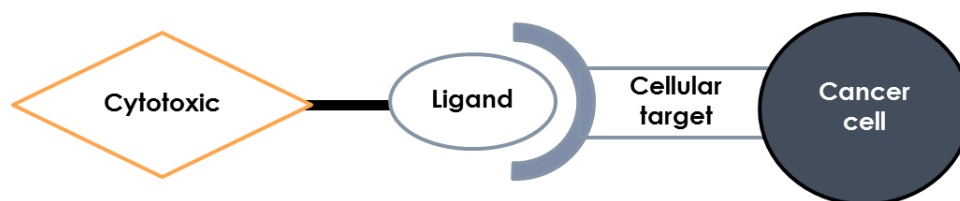


**Figure 3.29.** General structure of a targeted drug delivery system

The carrier is that portion responsible for the selective delivery of the drug inside the diseased cell. Some crucial points such as chemical synthesis, kinetic parameters, avidity of the conjugate to the target cell, and tissue penetration, are necessary for obtaining an efficient carrier. The linker, on the other hand, is a molecular portion that allows an appropriate distance between the cytotoxic and the carrier. The linker is usually coupled to the cytotoxic/carrier portions through amide or ester bonds, even if also ethers, thioethers, triazoles or other groups are frequently employed. In general, amide bonds are less susceptible to hydrolysis under physiological conditions,<sup>216</sup> while ester bonds can be more easily hydrolysed by enzymes such as lipases or esterases. If the stability of the conjugated system is sufficient to approach the biological target, the hydrolysis of the linker can guarantee a controlled release of the drug within sub-cellular compartments. Thus, the linker structure could define the exact cleavage point between the carrier and the cytotoxic agent, mediated by internal or external stimuli. In this way, the drug is inactive during transport, but extremely effective once the diseased cell is reached.<sup>217</sup>

Following this approach, different types of TDDs have been developed, depending on the carrier:

- Cytotoxic conjugates to nanocarriers.

The development of drug delivery systems based on nanoparticles is representing a real revolution in the therapeutic field,<sup>218</sup> due to their large surface area and good morphological variability that lead to excellent pharmacokinetics, good passive accumulation at the site of interest and increased effect of permeation and retention. Moreover, the use of nanocarriers allows an easier uptake by the diseased cells and therefore an increase in the effectiveness of the drug.<sup>219</sup> The most common example arises from magnetic nanoparticles (MNPs), widely used to transport and store the drug in diseased cells by an external magnetic field, without affecting healthy cells. Moreover, their surface can be easily functionalized with bioactive molecules by covalent bonds or by exploiting the presence of pores.

- Cytotoxic conjugates to antibodies.

Monoclonal antibodies are considered a possible vehicle for selective drug transport, since their high binding specificity could favor a selective accumulation of the drug at the affected site. Specifically, the ability to release the cytotoxic agent only near the tumour derives from the presence, on cancer cells, of a specific antigen recognized by the antibody. Even if several factors limit the use of these

conjugates, such as the difficult internalization of the antibodies, recent studies have shown that some antibody-cytotoxic conjugates, while not internalizing, could allow a good transport of the drug in the extracellular space, followed by the internalization of the cytotoxic residue alone. This mechanism also generates a spectator effect in the cells in proximity.<sup>220</sup>

- Cytotoxic conjugates to peptides.

Since many tumour cells have been shown to overexpress peptides-binding receptors, these peptides revealed a promising carrier role in targeted delivery systems. In developing peptide-cytotoxic conjugates, the selected peptide should interact strictly with the precise subtype receptor overexpressed in tumour cells, and the linked cytotoxic drug must not influence the binding properties with the receptor, nor the specificity.<sup>221</sup> The peptide, upon binding with the receptor, is internalized inside the cytoplasm by crossing the cell membrane, and the cytotoxic portion is then released after the cleavage of the linker (Figure 3.30). Favourably, a small amount of the conjugated is required since peptides generally display a very high affinity toward the receptor in the nanomolar range; in addition, the cytotoxic activity of a peptide-conjugate could also be increased by attacking more than one cytotoxic agent to the peptide carrier. The most representative class of peptide-conjugates is based on the RGD sequence, which, as already described, is the smallest ligand recognized by integrin receptors overexpressed in some tumour cells.

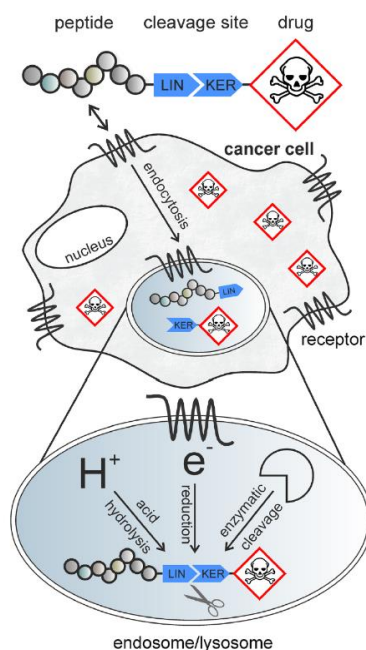


**Figure 3.30.** Mechanism of action of a peptide-cytotoxic conjugate. Figure adapted from ref. 217

### 3.6.2 Development of cytotoxic conjugates

Having in hands some peptide-like (pseudopeptides) derivatives that showed an high affinity toward integrin receptors, and considering the promising fluorescence studies possibly indicating an internalization of our ligands in overexpressing-integrin cells, we decided to realize some ligand-cytotoxic-conjugates using the  $\beta$ -lactam agonist derivatives as carriers. It is important to underline that in this case the compounds were designed as possibly exerting a drug-cargo action in order to

selectively deliver the cytotoxic portion into a cancer cell through integrin internalization. Our scope was then to provoke an endocytosis of the entire drug conjugate upon binding with the integrin receptor without the linker being necessarily cleaved outside or inside the cell to release the free cytotoxic agent. Preliminary studies were then aimed at the realization of the conjugated system; the study of an appropriate linker and its eventual cleavage conditions will be addressed secondly, only if the system as such will not be found to exert a cytotoxic action.

Two novel azetidinone-drug conjugates were therefore designed: commercial 5-fluorouracil and Doxorubicin were selected as suitable cytotoxic agents, and  $\beta$ -lactam **83** was employed as synthetic precursor. The cytotoxic residues were inserted at the  $\beta$ -lactam C3 position, hence replacing the previously inserted fluorophore moieties (Figure 3.31).

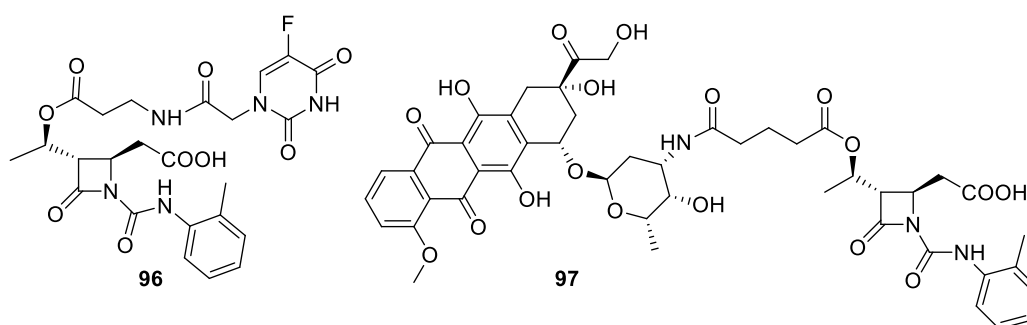
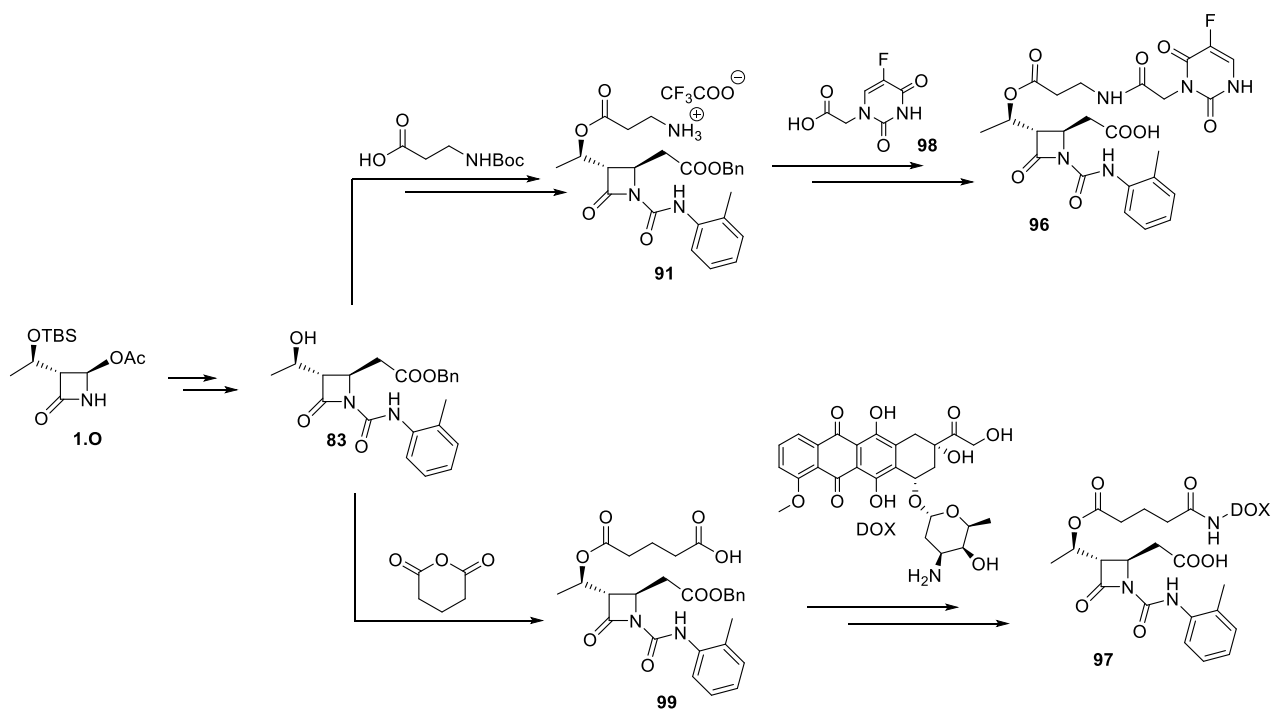


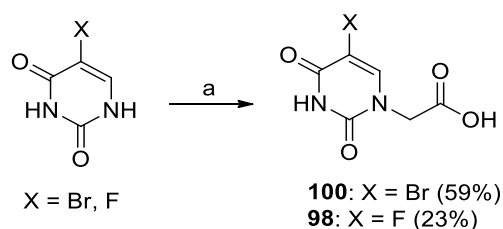
**Figure 3.31.**  $\beta$ -lactam derivatives conjugated with a cytotoxic residue of 5-fluorouracil (**96**) and Doxorubicin (**97**)

The choice of functional groups in the conjugated system was crucial for the incorporation of cytotoxic residues: Doxorubicin was introduced as such, while 5-fluorouracil was further functionalized on the more reactive nitrogen with bromoacetic acid to obtain **98** with an acid terminus easily anchorable on the  $\beta$ -lactam fragment. The 3-hydroxyethyl side chain in compound **83** was derivatized with an appropriate linker for allowing the conjugation with the relative cytotoxic portion. Accordingly, a carboxylic acid and an amine were inserted as two different terminal functional groups for allowing the reaction with Doxorubicin amine terminal and fluorouracil acetic acid, respectively. The amine function was introduced as reported in Paragraph 3.5.3.1 through a simple coupling with *N*-Boc- $\beta$ -alanine and its following deprotection with TFA (compound **91**). The acid portion instead was obtained *via* an esterification with glutaric anhydride (compound **99**). In both cases, after the coupling with cytotoxics, the last synthetic step involved the C4 benzyl ester hydrogenolysis for obtaining the free acid functionality necessary for integrin binding (Scheme 3.17).



**Scheme 3.17.** Synthetic strategy for the synthesis of conjugated  $\beta$ -lactam-cytotoxics **96** and **97**

As already performed for the conjugation with fluorescent tags, also in this case the reactivity of uracils was previously investigated using the available non-cytotoxic 5-bromouracil as a model. Firstly, a *N*-alkylation with bromoacetic acid mediated by potassium hydroxide as a strong base and heating to 60 °C<sup>222</sup> was performed on uracil (Scheme 3.18). After an acid work-up, 5-bromouracil acetic acid precipitated as a white solid and was isolated in a 60% yield. Analogously, the reaction was repeated with 5-fluorouracil, but in this case no precipitate was formed after the acid work up and the product was isolated by lyophilisation followed by flash-chromatography. The purification step greatly affected the yield, probably because the target compound was extremely polar and scarcely eluted from the chromatography column. Different methods have been tested, varying reaction times, temperature and work-ups, but the formation of the product precipitate was never observed.

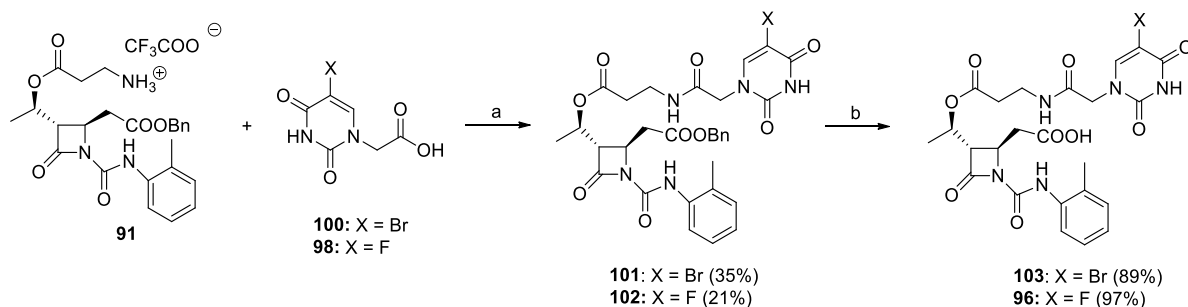


**Scheme 3.18.** Synthesis of uracil derivatives **98** and **100**. Reagents and conditions: a) bromoacetic acid, KOH, H<sub>2</sub>O, 60 °C then rt, 16 h. Yields of isolated compounds are reported in brackets

Once that the uracil partner was obtained, the convergent synthesis proceeded with a peptide coupling between the amine group of intermediate **91** and the acid group of the uracil-compounds **98** or **100**. The reaction was conducted with the already reported Steglich esterification conditions after amine salt deprotection of **91** in basic conditions to give **101** or **102**. Both DCC and EDC have been tested

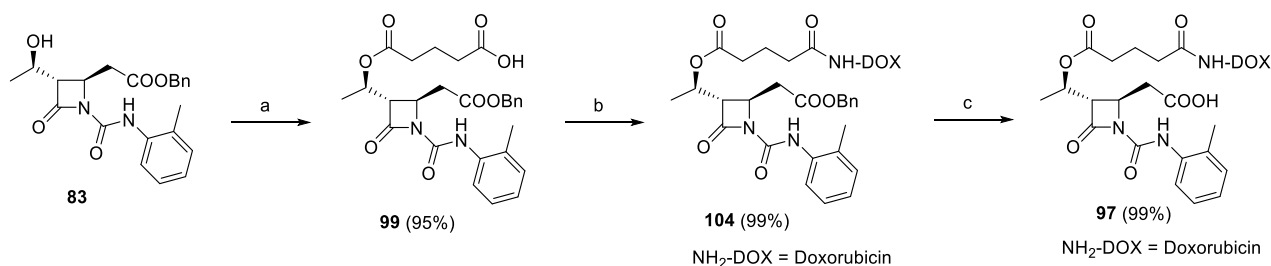


as carboxylic acid activators: the latter furnished slightly better yields, probably for the complete elimination of the resulting ureidic by-product in the extraction work-up. Anyway, due to the very poor solubility of the reaction crude in common organic solvents or solvent mixtures, the yield of this step was poor, and will require a further optimization. The target compounds **96** or **103** were obtained by a final hydrogenolysis reaction in standard conditions, with rather quantitative yields for both bromo- and fluoro-uracil derivatives (Scheme 3.19).



**Scheme 3.19.** Synthesis of  $\beta$ -lactams **96** and **103** conjugated with uracil derivatives. Reagents and conditions: a) EDC, TEA, DMAP,  $\text{CH}_2\text{Cl}_2$ , 0 °C to rt, 16 h; b)  $\text{H}_2$ , Pd/C (10%), THF/ $\text{CH}_3\text{OH}$  1:1, rt, 2 h. Yields of isolated compounds are reported in brackets

Conjugation with cytotoxic Doxorubicin required instead an acid function to be coupled with. Therefore, as already anticipated, a coupling between the alcohol  $\beta$ -lactam **83** and glutaric anhydride was performed under mild conditions in excellent yields. An acid work-up and a liquid-liquid extraction gained the desired acid target **99** without the need of flash-chromatography purification. At this stage the cytotoxic residue was inserted; Doxorubicin (DOX) displays a very intense red colour, due to the high conjugation of its tetracyclic system, and therefore it is also called "red devil" or "red death". The reaction was conducted in a very small scale and Doxorubicin was handled with the appropriate precautions because of its strong cytotoxic character, commonly exploited for chemotherapy treatments. The primary amine function of Doxorubicin was coupled with the carboxylic acid linker previously inserted on the  $\beta$ -lactam scaffold; the reaction occurred in the presence of HBTU (hexafluorophosphate benzotriazole tetramethyl uronium) and DIPEA (*N,N*-diisopropylethylamine). After 16 hours the conversion resulted complete and the target DOX-conjugate **104** was obtained after liquid-liquid extraction in quantitative yields.<sup>223</sup> Finally, hydrogenolysis was performed to give compound **97** with a free acid function for integrin recognition (Scheme 3.20).



**Scheme 3.20.** Synthesis of  $\beta$ -lactam **97** conjugated with Doxorubicin. Reagents and conditions: a) glutaric anhydride, TEA, DMAP,  $\text{CH}_2\text{Cl}_2$ , rt, 16 h; b) Doxorubicin, HBTU, DIPEA,  $\text{CH}_2\text{Cl}_2$ , rt, 16 h; c)  $\text{H}_2$ , Pd/C (10%), THF/ $\text{CH}_3\text{OH}$  1:1, rt, 2 h. Yields of isolated compounds are reported in brackets

### 3.6.3 Biological evaluations

(in collaboration with Prof. S. M. Spampinato and Dr. M. Baiula, University of Bologna)

Unexpected results arised from adhesion and cytotoxicity tests performed on azetidinone-conjugates **96** and **97**. Surprisingly, in cell-adhesion assays both derivatives resulted antagonist on  $\alpha_4\beta_1$  integrins at a micromolar level. An intermediate analogue of this series, compound **95**, bearing the free acid functionality on C4 position and the  $\beta$ -alanine linker protected with a Boc group, was tested as a model. In fact, the three compounds **95**, **96** and **97** share a common (or similar) derivatization at C3 position with a linker coupled to the carrier and to the drug portion with an ester and an amidic group, respectively. Also compound **95** displayed an antagonist behaviour, even if toward  $\alpha_5\beta_1$  integrins (while was inactive on  $\alpha_4\beta_1$ ). Further tests are still in course for studying the adhesion of **96** and **97** on  $\alpha_5\beta_1$  class.

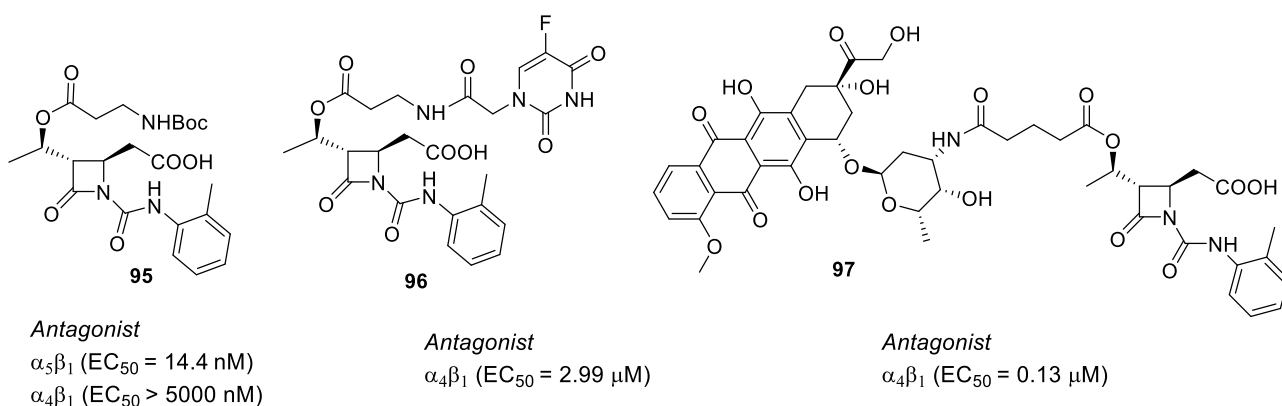


**Figure 3.32.** Structures of compounds **95**, **96** and **97** and results of cell-adhesion assays. Values of  $EC_{50}$  are reported in brackets

The resulting antagonist behaviour of the three compounds was in contrast with that previously detected for the C3 unsubstituted compound **9** and for the fluorescent derivatives **78-80** that demonstrated instead an agonist behaviour on  $\alpha_4\beta_1$  integrins (see Paragraph 3.5.3.3). A comparison of the concentration-response curves showing the different effects of aforementioned compounds on cell adhesion is reported in Figure 3.33. In particular, compounds **9**, **78**, **96**, and **97** were compared, since they share the  $\beta$ -lactam scaffold, and in particular the acid and the *o*-tolyl terminus at C4 and N1 positions, which are thought to be responsible for the interaction with the receptor.

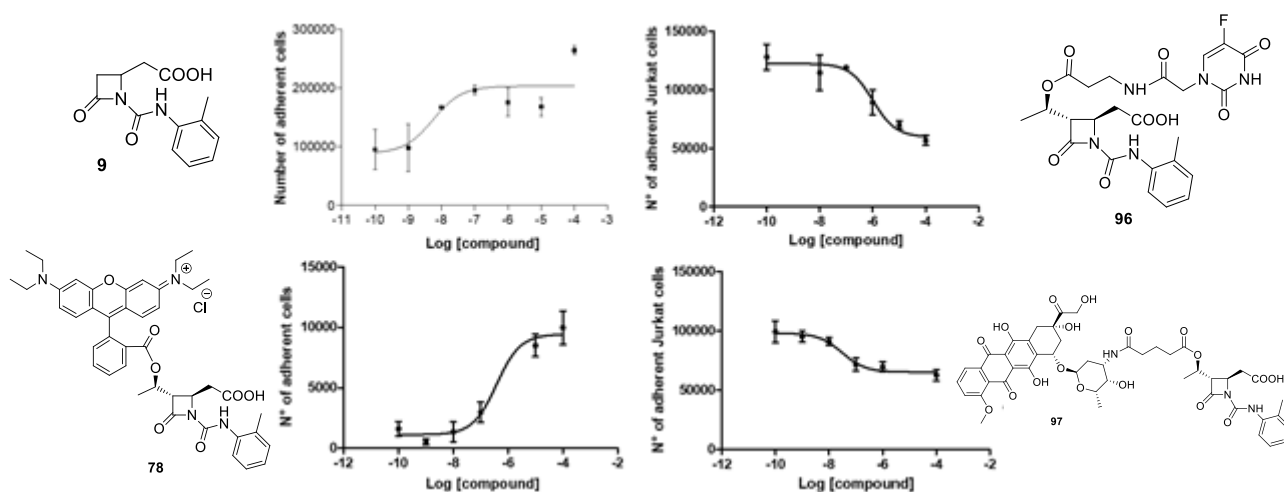


**Figure 3.33.** Compounds **9** and **78** enhanced fibronectin-mediated adhesion to Jurkat E6.1 cells expressing  $\alpha_4\beta_1$  integrin (left column); compounds **96** and **97** diminished fibronectin-mediated adhesion to Jurkat E6.1 cells expressing  $\alpha_4\beta_1$  integrin (right column). Results are expressed as the number of cells attached from quadruplicate wells and repeated at least three times

Nevertheless, an influence of the C3 side chain on integrin activity resulted evident, and, apart compound **9** that had a free C3 position,  $\beta$ -lactam **78** was prepared with an ester bond to link the carrier and the fluorophore. It was therefore thought that the presence of a linker with an amide group could influence integrin activity switching it to antagonist.

According to this, two possible examples of ligands with a minimal linker portion and with an ester-ester linker were designed for a conjugation with 5-fluorouracil to evaluate the veridicity of the aforementioned hypothesis (Figure 3.34). The synthesis of the compounds is still underway. The conjugation with Doxorubicin revealed not suitable for this working method, as it necessarily required an amide bond for linking the primary amine group of the cytotoxic on the carrier.

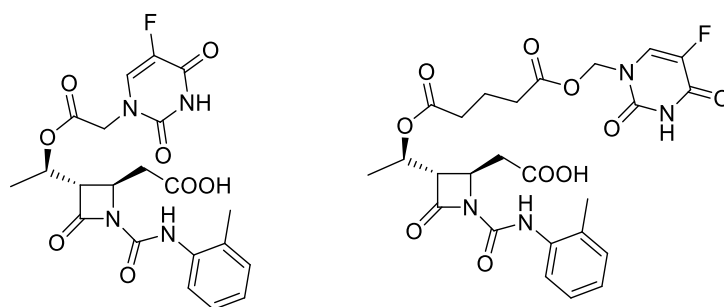


**Figure 3.34.** Structures of conjugated  $\beta$ -lactam-fluorouracil compounds designed to potentially promote an agonist behaviour

Concerning cytotoxic assay, we assessed by cytofluorimetry the percentage of Jurkat cells (overexpressing  $\alpha_4\beta_1$  integrins) in early apoptosis after exposure to different concentrations of conjugated compounds **96** and **97**, or to the reference cytotoxic drug, doxorubicin [doxo] or 5-fluorouracil [5-FU], as a positive control for 72 hours (Figure 3.35). Both target compounds resulted inactive as cytotoxic at any tested concentration, conversely to their relative positive controls. This result is quite unsatisfactory, but in line with the activity displayed by **96** and **97** in cell adhesion tests. In fact, as already demonstrated, an antagonist behaviour implied the inhibition of integrin

internalization process, and consequently internalization of the compound itself. If the conjugates are not able to be internalized in the cell, they could consequently not explicate their cytotoxic potential.

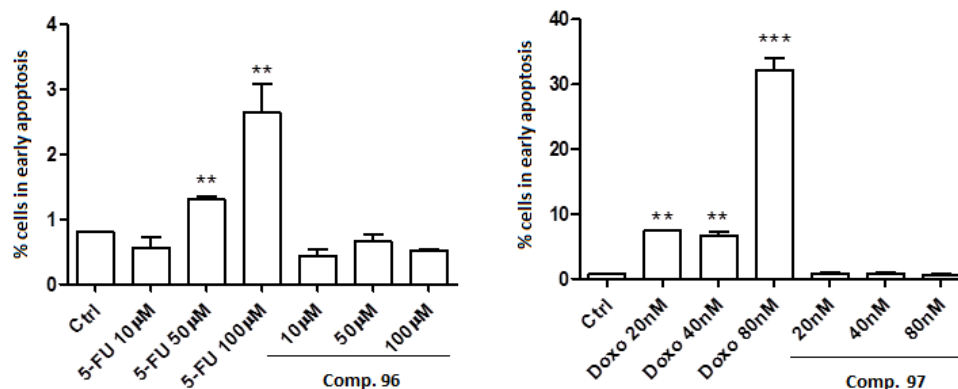


**Figure 3.35.** Cytotoxic assays evaluating the early apoptosis of Jurkat cells upon exposure of compounds **96** and **97**, and relative positive controls (5-Fu and Doxo) for 72 hours

### 3.7 Loading of $\beta$ -lactam integrin ligands on Sr-hydroxyapatite

As already widely discussed, among the library of  $\beta$ -lactams recently developed, some derivatives were found to strongly promote cell adhesion mediated by integrins at a nanomolar level.<sup>171</sup> According to this and to the good results achieved with the realization of novel hydroxyapatite biomaterials with enhanced antibacterial activity<sup>97</sup> (see Paragraph 2.10), we decided to further expand this project by loading some agonist  $\beta$ -lactam derivatives on strontium-enriched hydroxyapatite nanocrystals (Sr-HA) through absorption. This recently initiated study aimed at realizing a functional biomaterial for bone regeneration able to repair bone lesions or to support the implantation of artificial prostheses, stimulating the growth of bone cells in the proximity of the substitution material.

In fact, coating an artificial material with a thin layer of HA resulted an effective approach that provided good biocompatibility and osteoconductivity to the material.<sup>224</sup> Biological tests on different cell lines (mainly human mesenchymal stem cells and osteoblast-like cells) revealed that calcium phosphate coatings could improve cell adhesion, proliferation and differentiation for promoting bone regeneration.<sup>225</sup> Cellular responses to an implanted biomaterial involve highly complex chemico-biological processes linked to different surface properties.<sup>226</sup> Recent studies have shown that cell-substrate interactions are associated with surface topography, porosity, chemical and elemental composition, dissolution behavior, and macro and micro-surface structure.<sup>227</sup> These physico-chemical characteristics can be properly manipulated in order to promote a clinical integration of the implant with the surrounding cells and tissues.<sup>228</sup> An example concerns cationic or anionic substitutions in the apatites, which is possible thanks to their high stability and flexibility. Among divalent cations that can replace calcium in HA structure, strontium has aroused a considerable biologic interest, being present in the mineral phase of the bone and overall being able to increase the number of osteoblasts, reduce bone resorption and stimulate bone formation.<sup>229</sup>

In order to obtain better biological performances, a hydroxyapatite material enriched with a 10% content of strontium cations (Sr-HA) has been synthesized and employed for the loading of suitable

$\beta$ -lactam derivatives. Three agonist azetidiones **1**, **9** and **17** were chosen for their structural variability and for their specificity toward different integrin classes in enhancing cell adhesion; the preferential integrin class and the corresponding EC<sub>50</sub> values in cell-adhesion assays are reported in Figure 3.36. Compound **4** instead, being an antagonist of integrin activity, was evaluated as negative control. The synthesis of the  $\beta$ -lactam derivatives was carried out as described in Paragraph 3.2.1 with excellent reproducibility.<sup>171</sup> An appropriate loading study of the four molecules on Sr-HA was developed, together with an evaluation of the compound release in different aqueous media. A complete characterization of the materials as well as biological tests of the final loaded samples are actually in due course by Prof. A. Bigi, University of Bologna and P. Torricelli, Istituto Ortopedico Rizzoli.

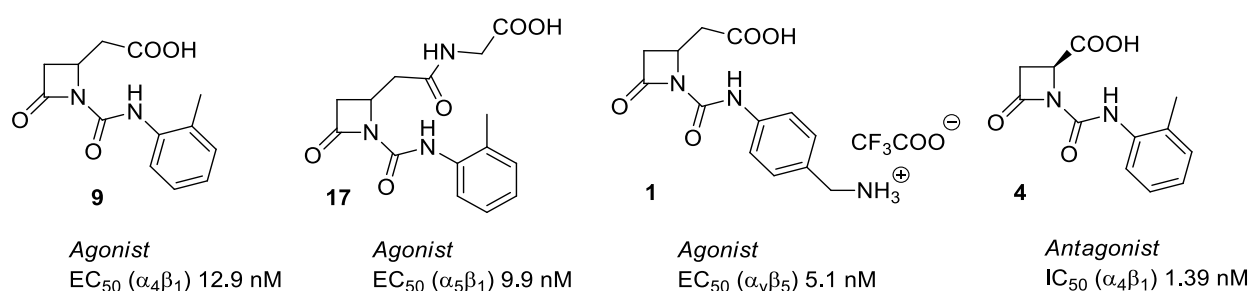


**Figure 3.36.**  $\beta$ -lactam compounds **1**, **4**, **9** and **17** absorbed on Sr-hydroxyapatite. EC<sub>50</sub> or IC<sub>50</sub> values of their activity as agonists or antagonist (of specific integrins) are reported

### 3.7.1 Loading of azetidiones on Sr-HA

The loading of azetidiones on Sr-HA nanocrystals was carried out in H<sub>2</sub>O or H<sub>2</sub>O/organic solvent mixtures to evaluate the medium effect on the loading. H<sub>2</sub>O/acetonitrile mixtures were chosen as standard solvent following the good results obtained in the previously described study with antibacterial  $\beta$ -lactams.<sup>97</sup> The experimental procedure used for the loading process was nearly analogue to that reported for *N*-thioalkylated azetidiones.<sup>97</sup> In brief, the appropriate  $\beta$ -lactam was firstly dissolved in the reaction solvent, then Sr-HA was added. The system was stirred for 4 hours at room temperature, then the reaction mixture was quantitatively transferred and centrifuged: the supernatant was collected to determine the recovery of the unloaded  $\beta$ -lactam, while the solid phase (constituting the functionalized Sr-HA) was oven-dried and further analysed and characterized.

The amount of the loaded  $\beta$ -lactam compounds (as weight %) on Sr-HA was determined through thermogravimetric analysis (TGA). Compounds **1** and **9** were chosen as models due to their different N1 derivatization and consequent lipophilicity. Loading of compounds **4** and **17** was instead performed by far only in the best conditions found for the other derivatives (Table 3.3).

**Table 3.3.** Effects of solution concentration and polarity on loading of azetidinones **1**, **4**, **9** and **17** on Sr-HA. Loading was evaluated through TGA analysis

Entry	Comp.	Solvent	Loading (wt%)
1	<b>9</b>	H <sub>2</sub> O/CH <sub>3</sub> CN 1:3	<b>5.3</b>
3	<b>9</b>	H <sub>2</sub> O/ CH <sub>3</sub> CN 3:1	<b>12.9</b>
4	<b>9</b>	H <sub>2</sub> O/ CH <sub>3</sub> CN 10:1	<b>14.4</b>
5	<b>9</b>	CH <sub>3</sub> CN	<b>9.0</b>
6	<b>9</b>	H <sub>2</sub> O/ CH <sub>3</sub> CN 1:1 (double amount of <b>9</b> )	<b>24.0</b>
7	<b>9</b>	H <sub>2</sub> O/EtOH 3:1	<b>15.1</b>
8	<b>9</b>	H <sub>2</sub> O/THF 3:1	<b>14.3</b>
9	<b>1</b>	H <sub>2</sub> O/ CH <sub>3</sub> CN 1:5	<b>8.4</b>
10	<b>1</b>	H <sub>2</sub> O/ CH <sub>3</sub> CN 1:1	<b>4.5</b>
11	<b>1</b>	H <sub>2</sub> O/ CH <sub>3</sub> CN 1:5 (triple amount of <b>1</b> )	<b>8.1</b>
12	<b>1</b>	H <sub>2</sub> O/ CH <sub>3</sub> CN 1:5 70 °C	<b>4.4</b>
13	<b>1</b>	H <sub>2</sub> O	<b>7.2</b>
14	<b>1</b>	THF	<b>5.8</b>
15	<b>1</b>	H <sub>2</sub> O/EtOH 1:5	<b>6.6</b>
16	<b>4</b>	H <sub>2</sub> O/ CH <sub>3</sub> CN 3:1	<b>6.5</b>
17	<b>17</b>	H <sub>2</sub> O/ CH <sub>3</sub> CN 3:1	<b>9.1</b>
17	<b>17</b>	H <sub>2</sub> O/ CH <sub>3</sub> CN 3:1 60 °C	<b>4.9</b>
18	<b>17</b>	H <sub>2</sub> O/EtOH 3:1 60 °C	<b>4.9</b>

A variation of the medium polarity was obtained by changing the H<sub>2</sub>O/acetonitrile ratio in the loading solution. From the data reported in Table 3.3 it emerged that the loading amount of compound **9** increased at enhancing of solvent polarity (Entries 1-4), with percentages ranging from 5.3% (with H<sub>2</sub>O/ CH<sub>3</sub>CN 1:3) to 14.4% (with H<sub>2</sub>O/ CH<sub>3</sub>CN 10:1). This could be rationalized considering that the molecule is moderately apolar and very affine to acetonitrile, and thus preferentially avoided the binding with HA when the solvent was predominantly composed of the organic phase. However, when the loading was carried out in acetonitrile alone, a good uptake from the solution was observed (9%, entry 5). To notice, a loading experiment of compound **9** in water alone was not conducted due to its total insolubility. An additional test in H<sub>2</sub>O/CH<sub>3</sub>CN 1:1 solution was performed with a doubled amount of  $\beta$ -lactam **9**, and a corresponding tripled loading value compared to the standard condition was obtained (24%, entry 6). A change in the organic solvent was attempted, hence including 3:1

aqueous mixtures with ethanol and tetrahydrofuran (entries 7 and 8, respectively). In both cases no substantial variations in the loading amount of compound **9** were detected in comparison with the corresponding H<sub>2</sub>O/CH<sub>3</sub>CN mixture. The amount of compound **9** adsorbed on Sr-HA could be therefore easily controlled using a water/organic solvent mixture of suitable polarity, permitting both medium-low (5-9%) and high (24%) loadings. In order to assess whether the presence of Sr on HA could influence the loading, an experiment was carried out on Ca-HA using the same conditions reported in entry 3. In this case a loading value of 12.8% was obtained, demonstrating that the replacement of Strontium in Ca-HA did not affect the absorption of the  $\beta$ -lactam compounds.

Conversely with what detected for compound **9**, the loading on Sr-HA of compound **1** settled around medium-low loadings (5-9%) without reaching values superior to 10% in none of the attempted conditions. As a general trend, its loading decreased with the increase of the solvent polarity (entries 9 and 10); in this case indeed, the molecule is more polar and affine to the aqueous medium, and hence preferred to remain in solutions with a higher water content. An increase in the loading value was not observed when the amount of compound **1** was tripled compared to the standard conditions (8.1%, entry 11), and even a tentative to perform the experiment at higher temperatures did not allow to improve the quantity of the absorbed molecule, that was instead decreased to 4.4% (entry 12). The absorption was also carried out using only H<sub>2</sub>O, and a good loading percentage (7.2%) was observed (entry 13). Since it was not possible to conduct an experiment in acetonitrile alone due to the insolubility of compound **1**, tetrahydrofuran was tested (entry 14), but only a relatively low loading (5.8%) was achieved. Finally, on employing the mixture H<sub>2</sub>O/EtOH 1:5 (6.6%, entry 15), the absorbed amount was only slightly increased, and acetonitrile demonstrated in this case to allow the higher loadings.

After these screenings, the loading on Sr-HA was performed also with compounds **4** and **17**. Being structurally similar to **9**, the loading of **4** was carried out with the conditions described in entry 3. Nevertheless, the loading of compound **4** showed a halved value (6.5%, entry 16) compared with that found for compound **9**.

Concerning compound **17** instead, standard H<sub>2</sub>O/CH<sub>3</sub>CN 3:1 conditions (entry 3) did not allow a complete solubilization of the molecule; therefore, data reported in entry 17 simply correspond to a heterogeneous mixture of two solids (Sr-HA and compound **17**) and are negligible. It was then necessary to suitably modify the loading method, and compound **17** was dissolved in a greater quantity of solvent at a higher temperature (60 °C). Different solvent mixtures were attempted, but without showing any loading variations (4.9%, entries 18 and 19).

In conclusion,  $\beta$ -lactam molecules were adsorbed on Sr-HA as a function of their partition coefficient between the solid phase and the loading solvent; Sr-HA in fact competed with the solvent for the recruitment of  $\beta$ -lactams, which was found to be dependant on the solvent mixture polarity.

### 3.7.2 Characterization of azetidinone-Sr-HA samples

The new azetidinone-functionalized Sr-HA composites were characterized by ATR spectroscopy that furnished important informations on the interactions established between the organic molecules and the apatite. In fact, from the comparison between the spectra of the composites and of the pure

molecules, the disappearance of the peaks related to the stretching of the C4 acid group and of the CO of the dimer, typical of carboxylic acids in the solid state, was noticed.

As shown in Figure 3.37A indeed, the spectrum of the functionalized **9-Sr-HA** evidenced that the band corresponding to acid C=O stretching at  $1715\text{ cm}^{-1}$  was no longer observed compared to that of **9** alone, as well as the  $1309\text{ cm}^{-1}$  peak relative to the CO stretching of the dimer. Conversely, two new intense bands at  $1570\text{ cm}^{-1}$  and  $1440\text{ cm}^{-1}$  appeared and were attributed to the asymmetric and symmetric stretching of a carboxylate C=O, respectively. This evidence demonstrated that compound **9** was probably adsorbed on the material through an ionic interaction established between the carboxylic function of the molecule and the cationic species present on HA. The other characteristic signals of compound **9** remained unaltered upon adsorption on HA.

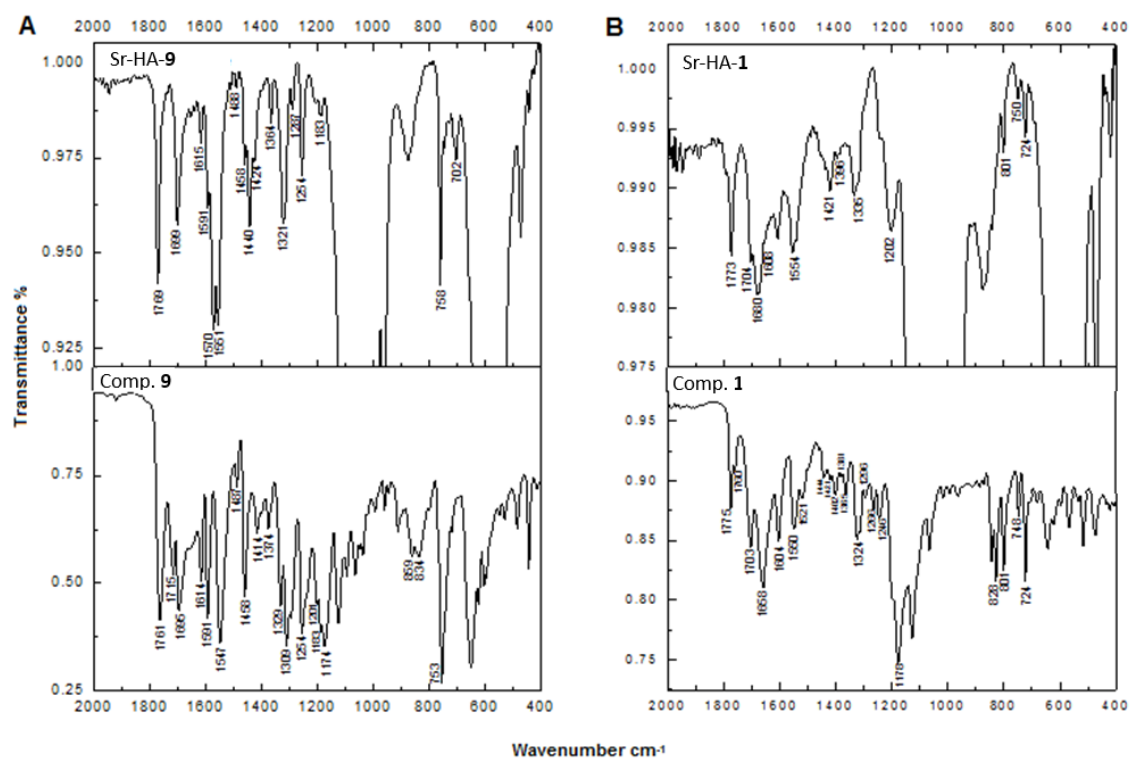


**Figure 3.37.** A) comparison between ATR-spectra of **9-Sr-HA** and **9** pure compound in the region  $2000\text{-}400\text{ cm}^{-1}$ ; B) comparison between ATR-spectra of **1-Sr-HA** and **1** pure compound in the region  $2000\text{-}400\text{ cm}^{-1}$

The other three compounds **1**, **4** and **17** showed only a partial disappearance of the peak related to the carboxylic acid C=O stretching and a partial appearance of bands related to the carboxylate species, probably proving that the binding with Sr-HA was weaker than that existing for compound **9**; this fact could also explain the lower values of loadings detected for compounds **1**, **4** and **17** compared to **9** (see Table 3.3). As an example, ATR spectra of **1-Sr-HA** composite and compound **1** alone were reported in Figure 3.37B. In **1-Sr-HA** spectrum, the peaks corresponding to the acid carbonyl at  $1703\text{ cm}^{-1}$  and to the dimer band at  $1324\text{ cm}^{-1}$  were still present, even if with a lower intensity compared to that displayed for molecule **1** alone. Nevertheless, the band at  $1680\text{ cm}^{-1}$  could be assigned to the C=O ureidic stretching associated with the stretching of a carboxylate species. As a result,  $\beta$ -lactam **1** probably exhibited only a partial carboxylate formation upon absorption on HA, and an interaction



between the ammonium salt function in the molecule and the negatively charged phosphate groups on HA surface had to be also considered.

### 3.7.3 Azetidinone release study

The *in vitro* release of azetidinones from the corresponding functionalized Sr-HA samples was evaluated by HPLC analysis in different aqueous media mimicking the physiological environment. Experiments were conducted at 37 °C in thermostat with sampling and refresh of the solution at set time intervals as already explained in the previously reported study.<sup>97</sup> At each time point, the supernatant was separated and the concentration of the released  $\beta$ -lactam was determined by HPLC-UV analysis, after an appropriate construction of calibration curves for each compound. The HA sample was then incubated again with a fresh solution of the specific medium (refresh). Some of the results were selected and summarized in Figure 3.38, expressed as cumulative release in mol% (of the total loaded amount) over the refresh number.

Since previous evaluations of HA biomaterials demonstrated that an excessive concentration of  $\beta$ -lactam molecules could be cytotoxic (see Paragraph 2.10.7), the release studies were performed on samples displaying a moderate compound loading, i.e. 12.9% for **9-Sr-HA**, 8.4% for **1-Sr-HA**, 6.5% for **4-Sr-HA** and 4.9% for **17-Sr-HA**.

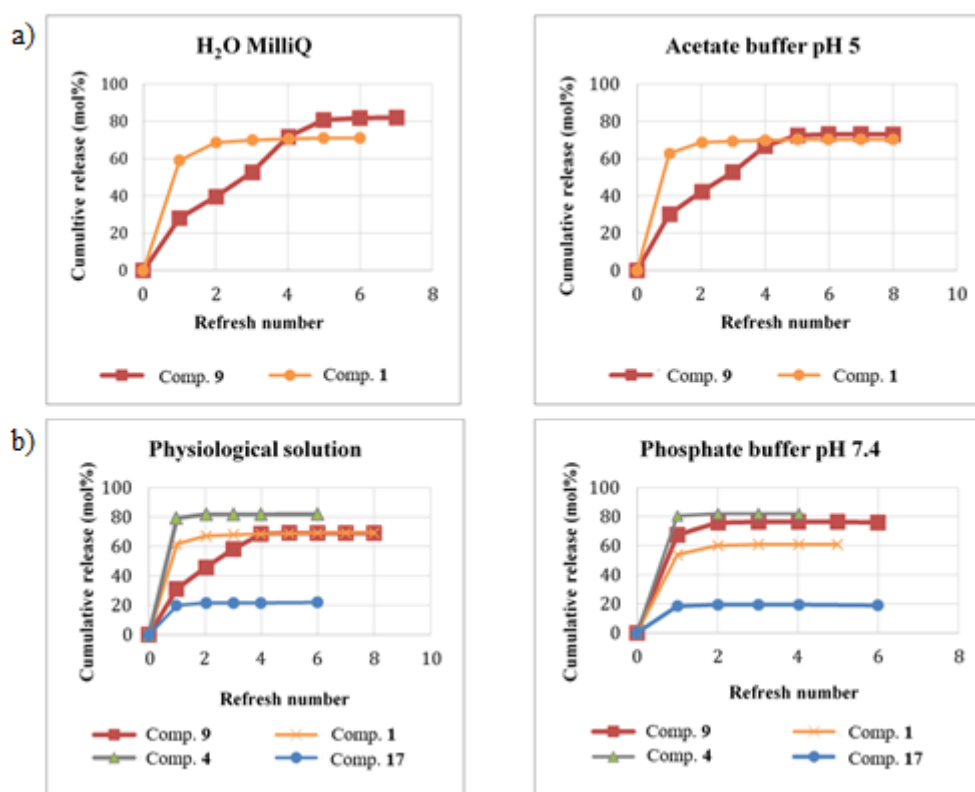


**Figure 3.38.** a) release of azetidinones **9** (■ red) and **1** (● orange) from **9-Sr-HA** and **1-Sr-HA** in aqueous solution (left) and acetate buffer solution at pH 5.0 (right) media; b) release of azetidinones **9** (■ red), **1** (X orange), **4** (▲ grey), and **17** (● blue), from **9-Sr-HA**, **1-Sr-HA**, **4-Sr-HA**, and **17-Sr-HA** in physiological solution (left) and phosphate buffer solution at pH 7.4 (right) media. The cumulative release is reported as mol % over the refresh number and evaluated through HPLC analysis

In general, the release profiles confirmed what was observed in the loading study, showing a dependence between the amount of the released molecule per refresh and its solubility in the medium.

In fact, more hydrophobic molecules showed a slower release (see **9** vs **1** in Figure 3.38a), then allowing to maintain a high concentration of active molecule at a local level. Also the medium composition resulted a determining factor for the release, since ions eventually present in solution could compete with the active sites of hydroxyapatite and accelerate the release process in its initial phase, as detected for phosphate buffer solutions (PBS). Another general observation regarded the incomplete release of the  $\beta$ -lactams from the materials, probably due to a strong interaction between these two species, which could prevent a total deliver of the compounds in the aqueous media.

As already mentioned, the initial release of compound **9** in water, acetate buffer and physiological solution is slower compared to **1**, probably due to the lipophilic nature of **9** and its consequent low affinity for aqueous solutions. The presence of phosphate ions competing with HA in PBS probably prevented this phenomenon (Figure 3.38b, right). Instead, the release profiles of compound **1** in all aqueous media displayed a sort of initial burst release followed by a slower steady profile; also the amount of the delivered molecule was comparable among all the tested solutions, which slightly decreased only in phosphate buffer. In fact, both compounds **1** and **9** were released to a lesser extent in PBS than in MilliQ water, possibly for a worst dissolution of the organic molecules in aqueous solvents with high ionic strength; the same accounted for physiological solution vs MilliQ water.

Compounds **4** and **17** displayed delivery profiles similar to compound **1**, but with higher and lower amounts of released molecules respectively, in accordance with their different solubilities.

Final samples (**1-Sr-HA** with 8.4% of loaded azetidinone and **9-Sr-HA** with 7.3% of loaded azetidinone) were tested in adhesion assays against bone mesenchymal stem cells. The novel biomaterials resulted effective in promoting the adhesion, however resulted cytotoxic leading to cell death in a few days (data not shown). According to this, we planned the preparation of new biocomposites with a lower amount of adsorbed azetidinones (in the order of 3-5% loading value).

### **3.8 Loading of agonist $\beta$ -lactam integrin ligands on PLLA nanofibers**

Targeting strategies for nanomedicines include methods based on the use of monoclonal antibodies or specific peptides, but it is also possible to use integrin-mediated targeting, aptamer-mediated targeting, folate receptor targeting, transferrin receptor targeting, or magnetic nanoparticle drug targeting.<sup>230</sup>

Among these techniques, the loading of bioactive compounds such as drugs, enzymes and antibodies onto polymeric surfaces is a cornerstone of biomaterial and tissue engineering technologies and has been widely investigated in the last decades for applications in medical diagnostics, drug delivery, tissue engineering, bioprocessing and food packaging.<sup>231</sup> Polymeric biomaterials used in regenerative medicine need to be modified to achieve bioactivity and to confer cell signaling properties. In particular, surface modification of polymeric scaffolds with molecules targeting biological functions allows the regulation of cellular processes, promoting adhesion, proliferation, and differentiation.<sup>232</sup>

One method of achieving tailored interactions between cells and material system is indeed to biofunctionalize the latter with ligands that bind integrin receptors present on the cell surface.<sup>233</sup>

Among polymeric biomaterials, bioresorbable polymers such as polyesters have been demonstrated to present excellent biocompatibility jointly to interesting bulk properties.<sup>234</sup>

Poly-(L)-lactic acid (PLLA) is a biocompatible and biodegradable polymer widely employed to fabricate devices for tissue engineering, regenerative medicine and for controlled delivery of small molecules. In this context, electrospinning has been recognized as a powerful technique for fabricating scaffolds with a defined micro/nanoarchitecture.<sup>235</sup> Compared to other fiber fabricating techniques, electrospinning is robust, highly versatile, requires simple operating apparatuses and yields large quantities of products. Drug delivery systems using electrospun nanofibers have been developed in the last number of decades for a wide range of tissue engineering applications, like tissue scaffolds, anti-bacterial sheets, and anti-cancer therapy.<sup>236</sup> Although nanofibers alone have many advantages, such as high surface to volume ratio, porosity, and a structure that mimics the extracellular matrix (ECM) structure, the loading of drugs on flexible sheets has improved the function of nanofibers.<sup>237</sup>

According to these purposes, the nanofibers could constitute a drug delivery carrier or a scaffold. Electrospun nanofiber scaffolds often possess interconnecting pores for allowing cells to attach, migrate/infiltrate, and proliferate, while permitting free exchange of nutrients and wastes.<sup>238</sup> Their inherently high surface-to-volume ratio enhances cell attachment, drug loading, and mass transfer properties.<sup>239</sup> The surface can be modified with bioactive molecules and cell recognizable ligands capable of imitating the natural extracellular matrix.<sup>240</sup>

Some interesting applications for our scope regarded the immobilization of the cell adhesive peptide RGD to electrospun nanofibers of PLGA/PLGA-*b*-PEG-NH<sub>2</sub> for a potential wound dressing device.<sup>241</sup> Moreover, the application of drug surface-modified nanofiber was recently extended to control stem cells differentiation.<sup>242</sup>

Considering these interesting applications, and disposing of some ligands able to strongly promote cell adhesion, we decided to prepare PLLA-nanofiber scaffolds functionalized with our agonist  $\beta$ -lactams by means of electrospinning technique. In fact, Vanderslice *et al.* demonstrated that agonists could enhance the effects of stem cell-based therapies by improving cell retention and engraftment<sup>152</sup>, while Yea *et al.* found that an agonist antibody of the alpha integrin chains could induce human stem cells to become dendritic cells.<sup>243</sup>

An appropriate loading method of  $\beta$ -lactams on PLLA was developed and allowed the preparation of new biocompatible materials functional as promoters of human mesenchimal stem cells (hMSC) adhesion.

The same agonist compounds **1**, **9** and **17** that were successfully absorbed on Sr-HA nanocrystals (see Paragraph 3.8) were selected as candidates for the loading on PLLA electrospun nanofibers (Figure 3.39).

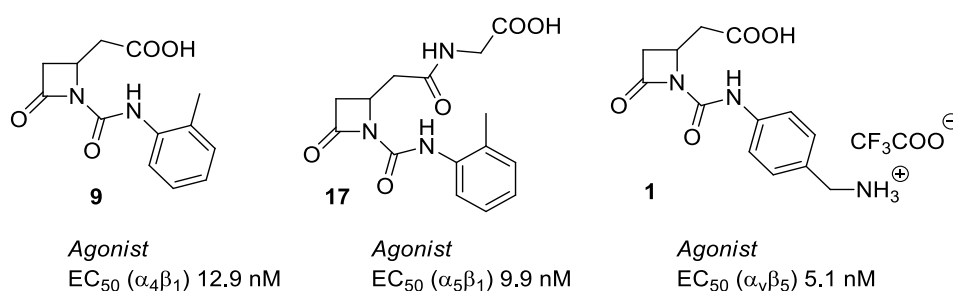


**Figure 3.39.**  $\beta$ -lactam compounds **1**, **9** and **17** loaded on PLLA nanofibers. EC<sub>50</sub> values of their activity as agonists (of specific integrins) are reported

### 3.8.1 Loading of azetidinones on PLLA

The synthesis of the compounds was already described; the loading of  $\beta$ -lactams through electrospinning technique was conducted as previously reported.<sup>231</sup> Briefly, a mixture of PLLA and azetidinone compound was dissolved in a mixed solvent,  $\text{CH}_2\text{Cl}_2$ :DMF = 65:35 v/v at a concentration of 13% w/v. The polymer solution was dispensed through a glass syringe in the electrospinning apparatus after the application of a high voltage power supply; the electrospun fibers were collected over a rotating cylindrical collector, and the so-obtained fibrous electrospun mats were completely characterized and subjected to biological tests after sterilization.

The amount of  $\beta$ -lactams **1**, **9** and **17** loaded on PLLA was quantitatively assessed by complete dissolution of weighted mats of azetidinone-PLLA samples in dichloromethane ( $\text{CH}_2\text{Cl}_2$ , 1 mL), evaporation, extraction with methanol (2 mL) and finally, HPLC-UV quantification. Notably, azetidinones are perfectly soluble in methanol conversely to the polymer. The concentration of the  $\beta$ -lactam in the sample was determined by interpolation with calibration curves. Each analysis was performed in triplicate and three independent experiments were carried out for each azetidinone-PLLA mat. The amount of the  $\beta$ -lactam loaded on each PLLA scaffold was then established through the mean value obtained from three separate experiments. The assessed values (expressed as %w/w of compound/PLLA mat) are 7.48% for **9-PLLA**, 6.18% for **1-PLLA**, and 6.31% for **17-PLLA**. The same values expressed in mol%/weight mat are 0.016% for **9-PLLA**, 0.029% for **1-PLLA**, 0.020% for **17-PLLA**. The amount % of the loaded azetidinones are in accordance with what determined by TGA measurements.

A control experiment in order to confirm the quantification was performed simulating the conditions of a complete release of the compounds from the scaffolds, i.e. a washing with methanol that preserved the integrity of the scaffold but completely dissolved the organic molecules. The amount of the released compounds was again evaluated by HPLC analysis: after three washing with methanol, a complete release of the compound was observed in all cases, confirming the assessed loading % values.

HPLC-MS and  $^1\text{H}$  NMR analysis of the obtained solutions of released azetidinones from PLLA mats established the integrity of the compounds upon loading.

### 3.8.2 Characterization of azetidinones-PLLA-samples (in collaboration with Prof. L. Focarete, University of Bologna)

After functionalization with the  $\beta$ -lactams, the physico-chemical and morphological properties of the electrospun PLLA fibers were evaluated through scanning electron microscopy (SEM), thermogravimetric analysis (TGA), differential scanning calorimetry (DSC) and attenuated total reflectance (ATR) spectroscopy, and compared to those of the untreated fibers.

SEM microscopy experiments were conducted on loaded PLLA scaffolds and on PLLA alone as reference (Figure 3.40). Recorded images allowed to obtain a statistic distribution of the fiber diameters and highlighted that all the scaffolds were characterized by absence of defects along the fiber (beads) and good dimensional homogeneity (average diameters around 500 nm), comparable to those displayed by pristine PLLA. Only **1-PLLA** sample presented a diameter distribution centered at 400 nm.

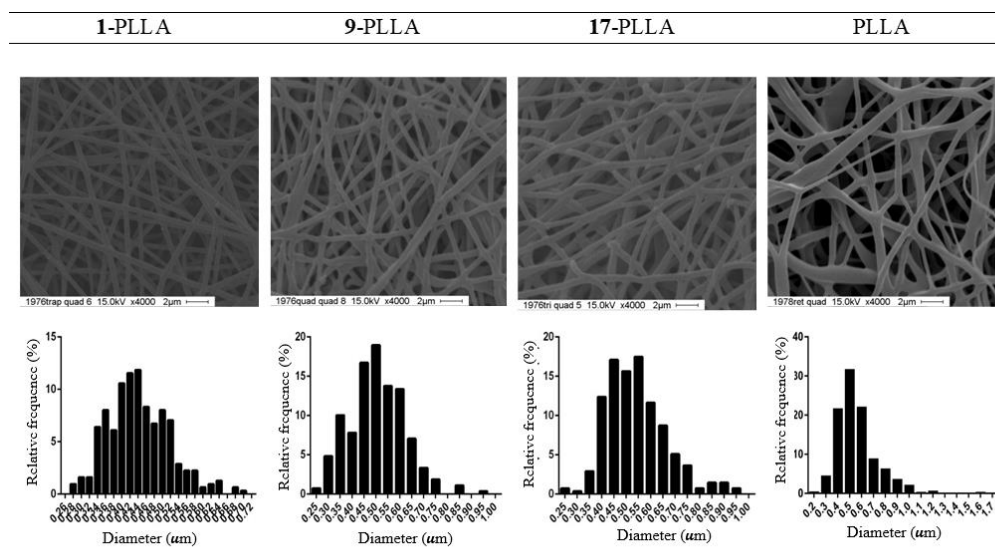


**Figure 3.40.** SEM images (4000x) of **1**-, **9**-, **17**-PLLA samples and PLLA alone. A fiber dimensional analysis is reported

Thermogravimetric analyses were conducted on PLLA, on compounds **1**, **9**, **17**, and on PLLA-loaded scaffolds (Figure 3.41). PLLA itself degraded in a single step between 200 °C and 350 °C while  $\beta$ -lactam compounds were characterized by a less circumscribed thermal degradation with an onset of around 125 °C and residues at 600 °C (in the order of 10-20% weight). PLLA+molecule samples displayed a two-step degradation, a first of low entity, which was attributed to the degradation of the molecules, followed by a more intense peak that was assigned to PLLA degradation. Since the degradation intervals of molecules and PLLA were partially superimposable, only an estimated loading of the  $\beta$ -lactams on PLLA could be calculated by TGA. However, the resulting values of 9-10% weight for all the three samples were in substantial agreement with the nominal loading calculated with HPLC-UV analysis. Moreover, the presence of  $\beta$ -lactams **9** and **17** on electrospun PLLA nanofibers induced a degradation at higher temperatures compared to PLLA alone, thus indicating a stabilization of the material, while this effect was not observed for **1**-PLLA scaffold.

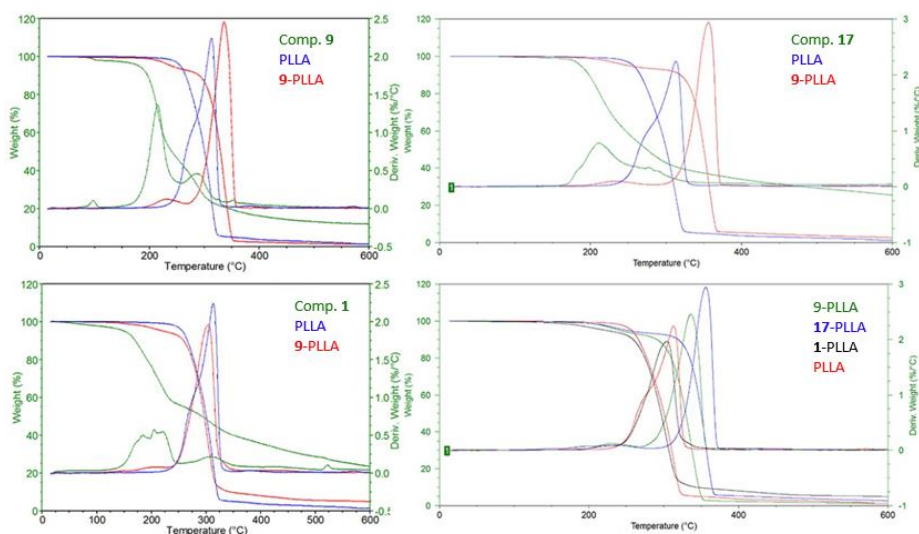


**Figure 3.41.** Thermogravimetric analysis (TGA) of compounds **1**, **9**, **17**, samples of **1**-, **9**-, **17**-PLLA, and PLLA alone

Also DSC analyses were carried out on PLLA-loaded scaffolds and PLLA alone (Figure 3.42). From the obtained calorimetric curves, the loading of the molecules appeared to not affect the thermal properties of PLLA, as the material resulted completely amorphous after the electrospinning process. Considering **9-PLLA** and **17-PLLA** samples, the presence of the organic compound provoked a plasticizing effect on the system leading to a lowering of  $T_g$  compared to PLLA alone. Also a slight decrease of  $\Delta H_c$  and  $T_m$  (melting temperature) was detected, indicating respectively a lower crystallization capacity and the presence of less perfect crystalline systems upon loading of the compounds. In case of **1-PLLA**,  $T_g$  remained constant, while a shift at lower temperatures of the crystallization temperature ( $T_c$ ) led to a narrowing of the crystallization interval without affecting  $\Delta H_c$ ; this could lead to the formation of crystals with faster kinetics in sample **1-PLLA** compared to PLLA alone.

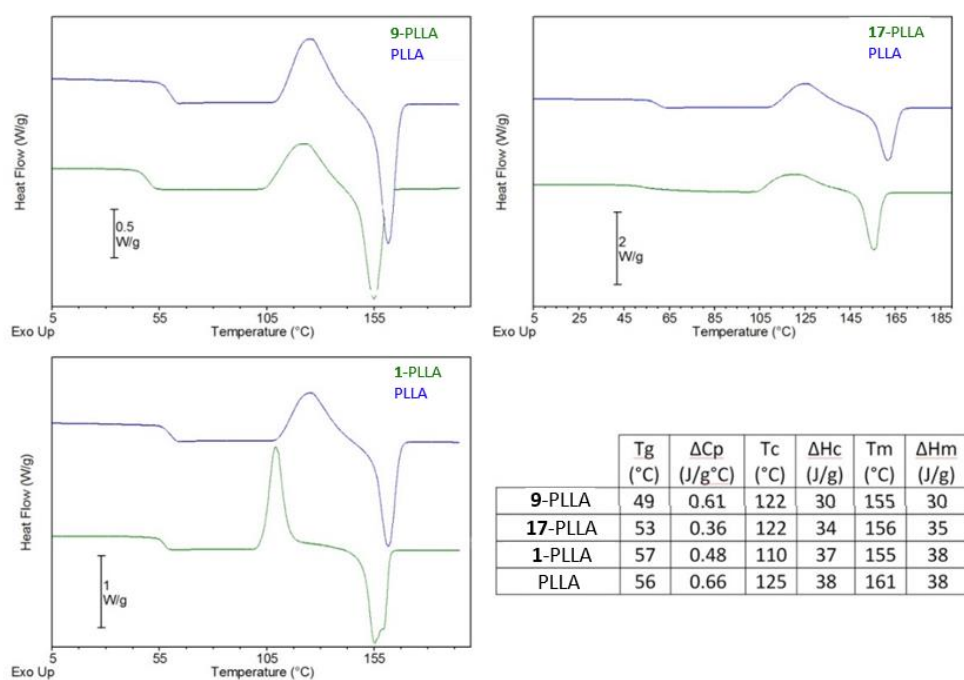


**Figure 3.42.** Differential scanning calorimetry (DSC) analysis of samples of **1-**, **9-**, **17-PLLA**, and PLLA alone

In Figure 3.43 ATR-FTIR spectra of azetidinones-PLLA samples,  $\beta$ -lactams **1**, **9** and **17** alone, and plain PLLA in an enlarged region (from 2100 to 1480  $\text{cm}^{-1}$ ) are reported. From the spectra of the molecules alone, it was possible to identify the typical IR bands of azetidinones with the relative assignments. In the functionalized materials spectra, the three bands belonging to the stretching of the  $\beta$ -lactam carbonyl groups overlapped with the strong peak relative to C=O stretching of the PLLA polymer at 1756  $\text{cm}^{-1}$ . Nevertheless the bands of aromatic C=C stretching and secondary amide NH bending at around 1600 and 1555  $\text{cm}^{-1}$  clearly emerged in the functionalized material spectra without being present in that of PLLA alone. Analysis of the functionalized PLLA spectra thus revealed the molecular integrity of the adsorbed azetidinones, as no modification of the relative bands was observed upon loading. Also PLLA was not affected by the presence of  $\beta$ -lactam molecules since any peak shift compared to plain PLLA was detected.

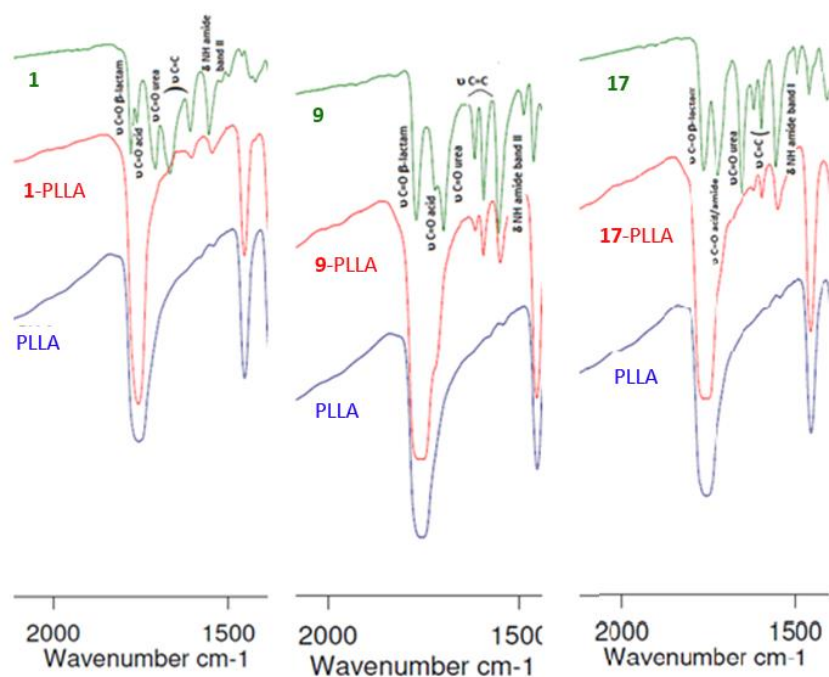


**Figure 3.43.** ATR-FTIR analysis for functionalized materials (red lines) **1-PLLA** (left), **9-PLLA** (center) **17-PLLA** (right), in comparison with pure compounds (green lines) and PLLA alone (blue line). Enlarged and selected parts of ATR-FTIR spectra are reported. Assignments of the main bands are indicated

### 3.8.3 Azetidinone release study

The *in vitro* release profile of azetidinones from the corresponding functionalized PLLA electrospun nanofibers - **1-PLLA** (6.18% of loaded azetidinone), **9-PLLA** (7.48%), and **17-PLLA** (6.31%) - was investigated by HPLC analysis in phosphate buffer solution (PBS) 0.1 M at pH = 7.4.

Experiments were conducted at 37 °C in thermostat with sampling and refresh of the solution at set time intervals for allowing a constant new release of the molecules, according to what previously described. Briefly, in a 10 mL test tube an electrospun azetidinone-PLLA mat was suspended in PBS; at each time point, the supernatant was separated, the released concentration of the azetidinone was determined by HPLC-UV analysis and the PLLA mat was incubated again with a fresh solution of the specific medium (refresh). The results are reported as cumulative release in mol% (of the total loaded amount) over the refresh number.

From the release profiles of the three PLLA samples emerged a different behaviour according to the polarity of the loaded molecule (Figure 3.44). Since  $\beta$ -lactam **1** is soluble in water, more than 50% of the loaded compound was released after the first analysis, reaching a total deliver of 64% in the second refresh. The detected released amount in the following four refreshes was less than 1%. Compound **17** showed a slightly lower affinity for the aqueous solution; the composite material straight released a 30% of the loaded molecule and a compressive amount of around 60% in the first five refreshes. The deliver was monitored for additional 10 refreshes reaching a total value of 64%.

Compound **9** presented an absent desorption from the polymer in the first four refreshes probably due to its higher lipophilic character. After the fifth refresh the compound exhibited a slow sustained release reaching a 48% deliver of the initial content in 15 refreshes. From the collected data, it could be estimated a release of 11  $\mu$ g on average per refresh in the last six analyses.

Notably, in all cases a complete release of the compounds from the scaffolds was never observed; in fact, an amount of the  $\beta$ -lactams ranging from 25 to 50% was hold on the nanofibers, possibly representing that portion of molecules adsorbed on the inner part of the material with a less exposure to aqueous medium.

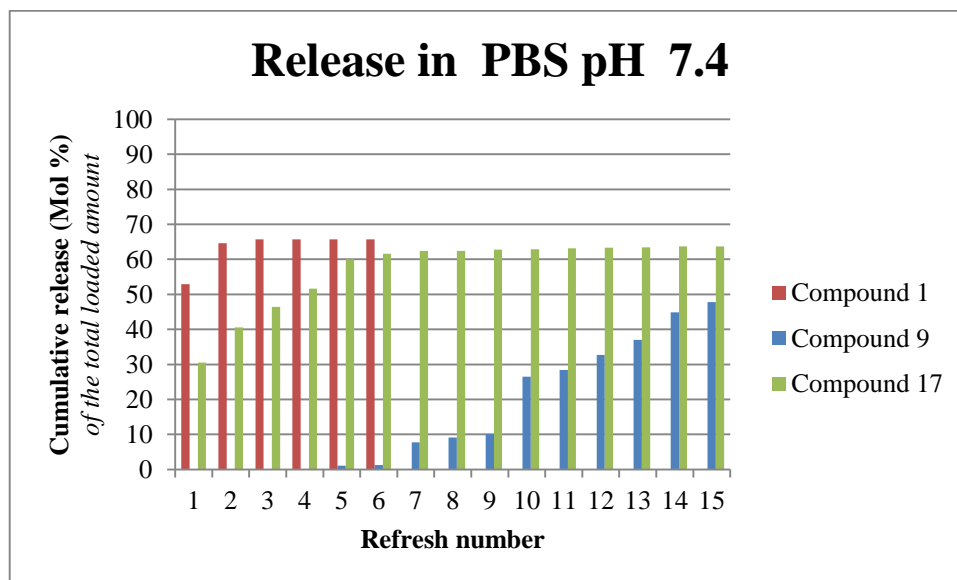


**Figure 3.44.** Release of azetidinones **1** (red), **9** (blue), and **17** (green) from **1-PLLA**, **9-PLLA** and **17-PLLA** in phosphate buffer solution pH 7.4. The scaffolds were used as such for the release studies. The cumulative release is reported as mol% of the total loaded amount of  $\beta$ -lactams over the refresh number

Another set of release experiments was conducted with wet azetidinone-PLLA scaffolds in order to allow a swelling of the mats in the buffer solution. The washing phase consisted in a pre-treatment of the scaffolds that were quickly (2 seconds) immersed in a PBS/ethanol 70:30 solution (wash 1), followed by two subsequent washing in PBS buffer for 5 minutes (wash 2 and 3). The experiments were then conducted as described above for dry-mats and the amount of released  $\beta$ -lactam compounds was evaluated by HPLC-UV analysis.

Compound **1**, due to its affinity to the aqueous medium, was almost totally released during the pre-washing phase (Figure 3.45, wash 1-3), during which up to 80% of the loaded compound was recovered; when subjected to the release experiment in PBS, only traces of the molecule were detected in 6 refreshes. The pre-treatment showed a similar effect also on compound **17**, with a 40% of the molecule released in the washing phase. An additional 20% was instead delivered during the following experiment in PBS (17% in the first analysis and about 3% in the next 14 refreshes).

Despite a considerable amount of molecules **1** and **17** was released during the pre-washing phase, it is worth to mention that also in this case it was never observed a complete release of the compound from the scaffold. Indeed, a residual 20% (for compound **1**) and 40% (for compound **17**) was still present in the material and available for a subsequent slow release.

Conversely, the washing phase did not influence the release of **9** since only traces of the compound were detected after the pre-treatment and its profile was basically in accordance with the corresponding dry release; after the refresh n.15 indeed, in both cases the released amount of the molecule was around 50% of the initial content. The wet-mat analysis was monitored for longer and maintained a constant profile releasing almost the same amount of molecule after each refresh (1.6  $\mu$ g



on average between refreshes 15-30), reaching up to 60% of the total loaded compound after 30 analyses. In this case a slow deliver could be favorable for maintaining an active and constant concentration of the released molecule in the proximal environment, thus enabling a longer efficient activity.

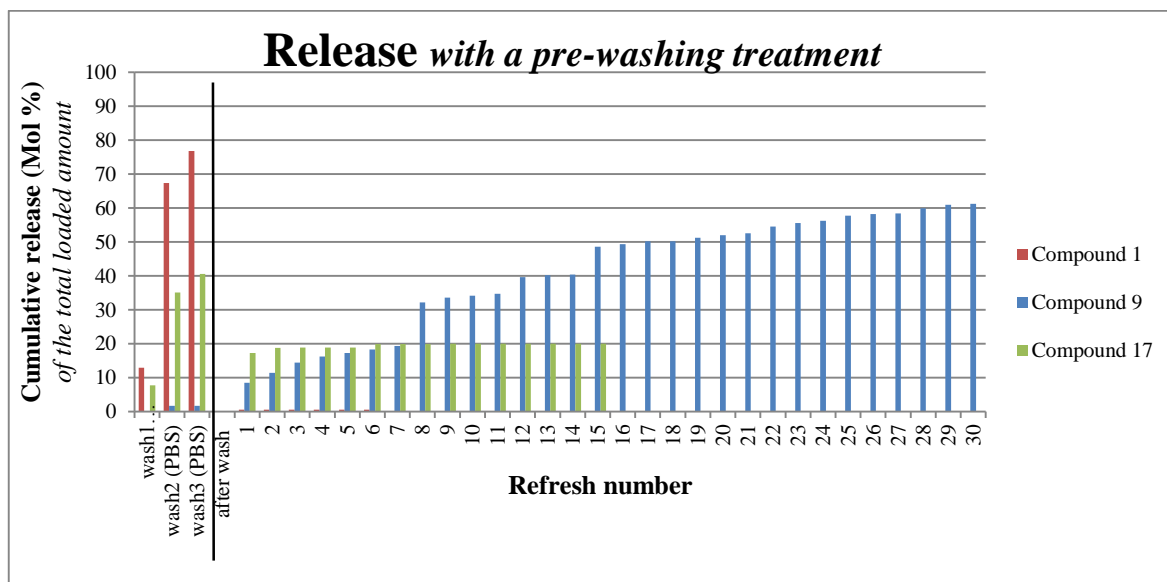


**Figure 3.45.** Release of azetidinones **1** (red), **9** (blue), and **17** (green) from **1-PLLA**, **9-PLLA** and **17-PLLA** in buffer solution at pH 7.4 medium. The scaffolds were subjected to a pre-washing phase before the release studies. The cumulative release is reported as mol% over the refresh number

For this reason, the release of compound **9** was additionally studied in aqueous solution (H<sub>2</sub>O MilliQ) and acetate buffer 0.1 M at pH = 5 with dry-treatment in order to have a complete panel of possible releasing conditions. The release in acetate buffer showed a behaviour similar to that recorded in PBS, with no recover of the  $\beta$ -lactam in the first six refreshes. The evolution of the profile appeared to be then in steady growth but considerably slower than that reported for PBS medium (at refresh n.15 the released amount was barely 10% of the total loaded amount vs 50% detected in PBS). The monitoring of the release was then prolonged for additional 15 refreshes, recording a constant delivery progress that reached up to 75% at the end of the analysis. The release conducted in water turned to be faster than the buffered solutions, with a recover of 45% in the first seven refreshes; it was then observed a slower trend with about 60% of released compound at the end of the experiment (release n. 21).

A comparison among the three different aqueous media studied for the release of compound **9** is reported in Figure 3.46.

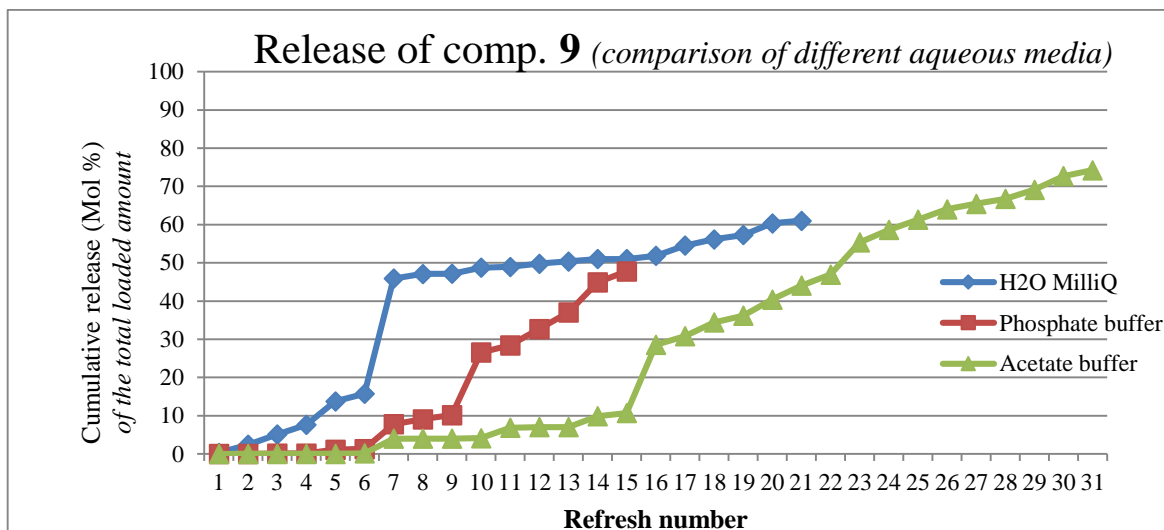


**Figure 3.46.** Release of azetidinone **9** in aqueous solution (♦ blue), buffer solution at pH 7.4 (▪ red), buffer solution at pH 5.0 (▲ green). The scaffolds were used as such for the release studies. The cumulative release is reported as mol% of the total loaded amount of  $\beta$ -lactams over the refresh number

To notice, further SEM experiments were conducted on the scaffolds after the release studies (in PBS medium), both for dry and wet conditions. Also in this case no modification of the fiber morphology was detected by SEM analysis, compared to pre-release samples. The images collected after the deliver experiments confirmed in fact the retention of the fibrous matrix for all the samples, which remained characterized by good homogeneity and absence of defects (Figure 3.47).

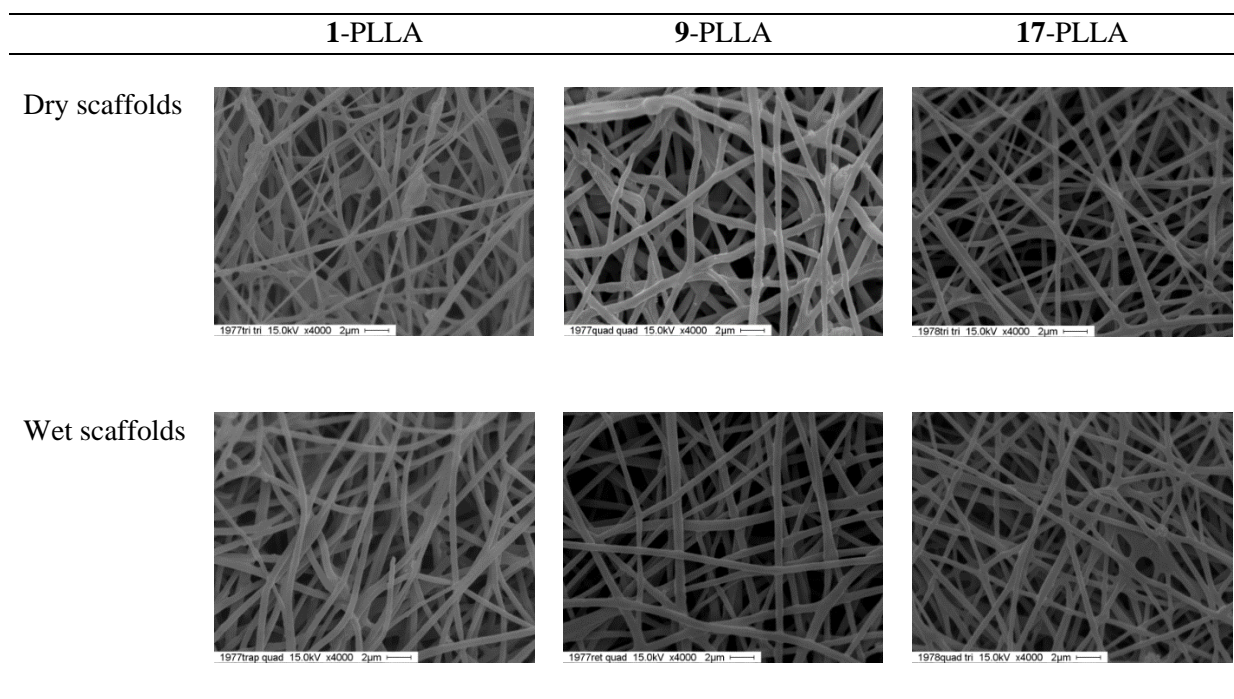


**Figure 3.47.** SEM images (4000x) of 1-, 9-, 17-PLLA samples after release study in dry and wet conditions

### 3.8.4 Biological evaluations

(in collaboration with Prof. L. Visai and Dr. N. Bloise, University of Pavia)

Biological interaction between plain PLLA, agonist containing PLLA and hBM-MSCs (human Bone Marrow-Mesenchymal Stem Cells) were explored by *in vitro* tests as follows.

#### Cell Adhesion: viability and morphology determination

hBM-MSCs adhesion was determined after 2 h from seeding and expressed as percentage of viable cells over the seeded cell number (T0). As shown in Figure 3.48A, a significant increase of cell adhesion was observed in wet-treated samples in comparison with dried counterparts, except for sample **1-PLLA**. However, the agonist-PLLA scaffolds behaved differently both in dry and wet condition. Specifically, a higher cell adhesion was measured in **9** and **17** in comparison with plain PLLA surface. Moreover, **9-PLLA** showed an higher cell adhesion than **1-**, **17-** and plain PLLA scaffolds (Figure 3.48B).

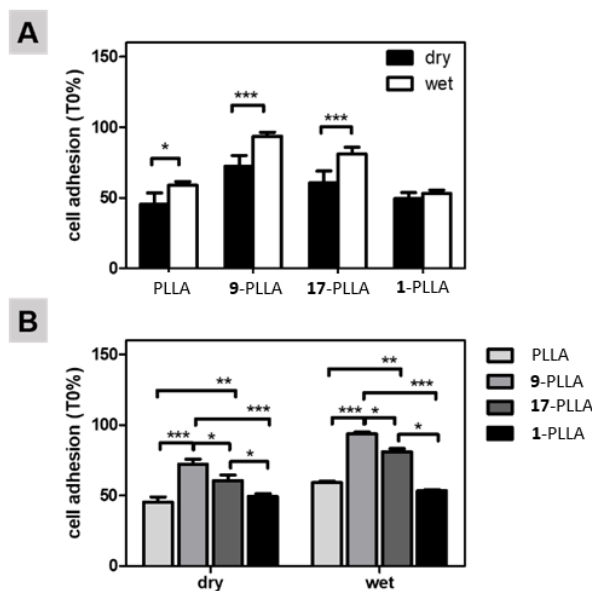


**Figure 3.48.** Cell adhesion of hBM-MSCs cultured on 1-, 9-, 17-PLLA samples and plain PLLA. Cell adhesion is plotted as percentage of viable cells in comparison with initial seeded cell number (T0). Graph (A) showed the differences between all substrates under investigation, graph (B) showed the differences between dry and wet conditions

Cell morphology was analysed by confocal laser scanning microscopy (CLSM), which showed a more homogeneous staining (cells appeared slightly large and had more defined cytoskeleton) in the wet condition in comparison with the dry one (Figure 3.49). Moreover, from this first immunofluorescent analysis it was possible to notice that **9-PLLA** appeared to be the most populated with respect to plain PLLA and **1-**, **17-** agonists. All these results provided evidence that the wet treatment was a necessary step to make the scaffold more suitable for hBM-MSCs adhesion.

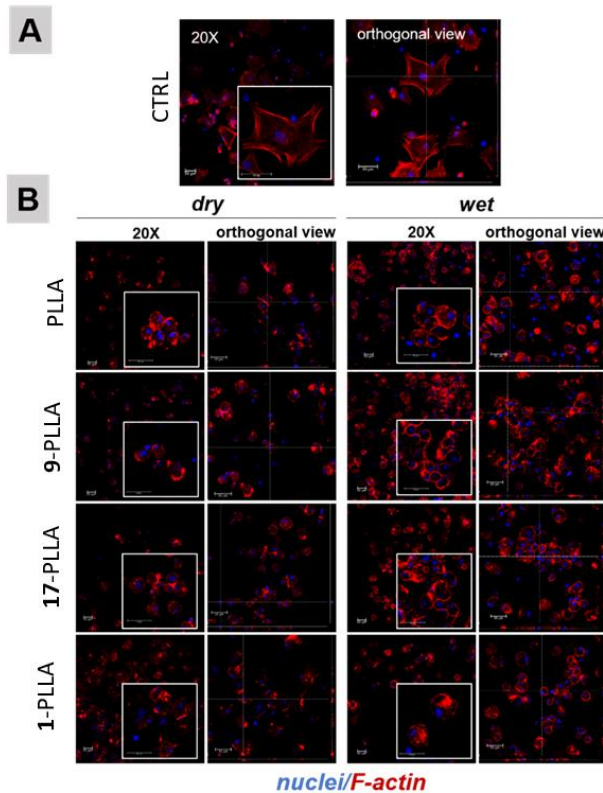


**Figure 3.49.** Cell morphology assessed by Confocal laser microscopy analysis of hBM-MSCs. The cytoskeleton organization was observed by F-actin staining with Phalloidin (red). Nuclei were stained with Hoechst 33342 (blue). Magnified areas of cells are shown in insets. Scale bars: 50  $\mu\text{m}$ . Orthogonal view of images stacks are also shown

### Quantitative analysis of the proteins involved in the adhesive process

The results of the following studies were performed on PLLA samples treated in wet condition, as this was proved to be the most suitable treatment. Immunofluorescence (data not shown) and western blot analyses concerning the expression and activation of some proteins involved in the adhesive process (p-FAK,  $\beta_1$ -integrin, vinculin) showed significant differences between samples. Immunofluorescence revealed the presence of the typical p-FAK “spot” staining, distributed in the cell membrane, mainly in cells adhered on PLLA and **9**- sample in comparison with **1**- and **17**- scaffolds. In addition, the green fluorescence due to the presence of  $\beta_1$ -integrin and vinculin was very marked at level of the membrane of cells seeded on PLLA, **9**- and **17**- in comparison with cells cultured in **1**, in which the fluorescent signal was almost absent (data not shown).

Western blot analysis supported the above results. In fact, the expression of  $\beta_1$ -integrin in the active form was significantly greater in **9**- than in **1**-, **17**- , and PLLA alone. On the contrary, only a slight enhancement in the amount of vinculin and in the activation of p-FAK protein was observed in **9**- sample in comparison with the other surfaces (Figure 3.50).

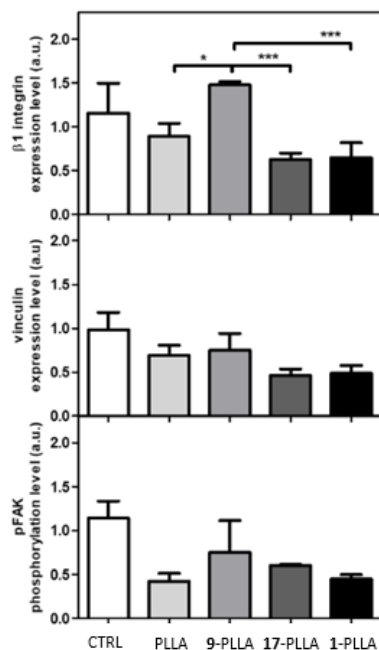


**Figure 3.50.** Quantitative analysis by western blot assay of proteins involved in the adhesive process. Expression levels of  $\beta 1$  integrin and vinculin and the phosphorylation level of P-FAK in hBM-MSCs cells were analysed by Western blot using specific antibodies

### 3.9 Concluding remarks

In this chapter it was reported the recent interest of my research group in targeting integrins with small  $\beta$ -lactam derivatives.

First of all, a novel series of  $\beta$ -lactams that was designed and synthesized to target RGD-binding and leukocyte integrins was described. The compound library was evaluated by investigating the effects on integrin-mediated adhesion and signalling in cell lines expressing  $\alpha_v\beta_3$ ,  $\alpha_v\beta_5$ ,  $\alpha_v\beta_6$ ,  $\alpha_5\beta_1$ ,  $\alpha_{IIb}\beta_3$ ,  $\alpha_4\beta_1$  and  $\alpha_L\beta_2$  integrins. SAR analysis of the new series of azetidiones enabled the recognition of structural elements associated with integrin selectivity and, by adopting this approach, selective and potent agonists toward  $\alpha_v\beta_3$ ,  $\alpha_v\beta_5$ ,  $\alpha_5\beta_1$ , or  $\alpha_4\beta_1$  integrins were obtained, as well as potent antagonists for  $\alpha_v\beta_3$ ,  $\alpha_5\beta_1$ ,  $\alpha_4\beta_1$  and  $\alpha_L\beta_2$  integrins. In particular, the developed  $\beta$ -lactams could bind with good affinity to their target integrins, promoting cell adhesion and inducing cell signalling in case of agonists, or could prevent the binding of endogenous ligands in case of antagonists.<sup>172</sup>

Following these encouraging results, it was synthesized a second library of compounds aimed to highlight the pharmacophore elements necessary for integrin affinity. As a general result, both the presence of a cyclic rigid structure and two duly aligned side chains with amine and acid functions resulted essential for promoting recognition with the integrin receptor. Some novel potential scaffolds emerged from the library, having nanomolar activities as integrin agonists, i.e. a proline-derived compound and two open ligands realized from the conjugation with glycine or  $\beta$ -alanine with *o*-tolylisocyanate.

Only a few studies have focused on the discovery of integrin agonists that may be useful in clinical conditions.<sup>149-152</sup> Nevertheless, agonist behavior could be crucial for the regulation of integrin-involved processes such as trafficking and endocytosis. Confocal microscopy studies conducted with a fluorescent  $\alpha_5$  integrin investigated the effect of our synthetic ligands on integrin trafficking. These analysis highlighted that agonist compounds could induce integrin internalization as well as the endogenous ligand fibronectin; conversely, endocytosis was prevented when integrins were exposed to an antagonist ligand.

According to this, three novel fluorescent compounds were successfully obtained by suitably modifying the  $\beta$ -lactam scaffold in some of the more potent agonist integrin ligands. In particular, a conjugation with two fluorophore molecules (Rhodamine B and FITC) was performed on the C3 position of the azetidinone and the new obtained fluorescent ligands maintained an integrin affinity as agonists at a micromolar level. Exploratory investigations aimed at discovering the fate of these compounds during integrin trafficking were conducted by means of confocal microscopy: so far the reported fluorescence images suggested an internalization of the ligand into the cytoplasm, but more accurate analyses need to be addressed.

However, in this desirable case, the designed structure could be employed as a drug-cargo for selectively carrying a cytotoxic molecule into cancer cells exploiting the process of integrin internalization. A study for the realization of this delivery system was initiated developing some  $\beta$ -lactams armed with 5-fluorouracil and Doxorubicin as cytotoxic compounds. These residues should replace the fluorophore moieties and were successfully introduced on the C3 hydroxyethyl side chain of the  $\beta$ -lactam ring after the insertion of suitable linkers. Nevertheless, the final targets resulted not cytotoxic and antagonist compounds in cell adhesion assays; this behaviour probably avoided the internalization of the ligands into the cells and hence prevented them to exert the cytotoxic activity. Other compounds need therefore to be designed and prepared with the essential requirement to display an agonist activity.

In addition, among the  $\beta$ -lactams found to strongly promote integrin activity, some compounds were selected and loaded on different bio-materials, poly-(*L*)-lactic acid and Sr-hydroxyapatite, in order to develop new biocompatible and biodegradable conjugates for possible tissue engineering applications and/or controlled drug-delivery system of small molecules.

In both cases, the release profiles of the novel biomaterials were deeply investigated. They were also tested in order to verify the desired increased cell adhesion exerted by the materials compared to the molecules alone. In particular, PLLA-azetidinone scaffolds were assayed against human mesenchymal stem cells (hMSCs), showing a higher cell adhesion in PLLA containing agonists in comparison with plain PLLA.

To notice, compound **9** in particular was selected as a really promising integrin ligand, due to the simple three-steps procedure necessary for its preparation and to its selective nanomolar activity as agonist. For these reasons, it was chosen for the realization of novel PLLA- or HA-based biomaterials, and its scaffold was further modified on the C3 position with the insertion of fluorophore and cytotoxic residues for possible cancer cell-targeting applications (Figure 3.51).

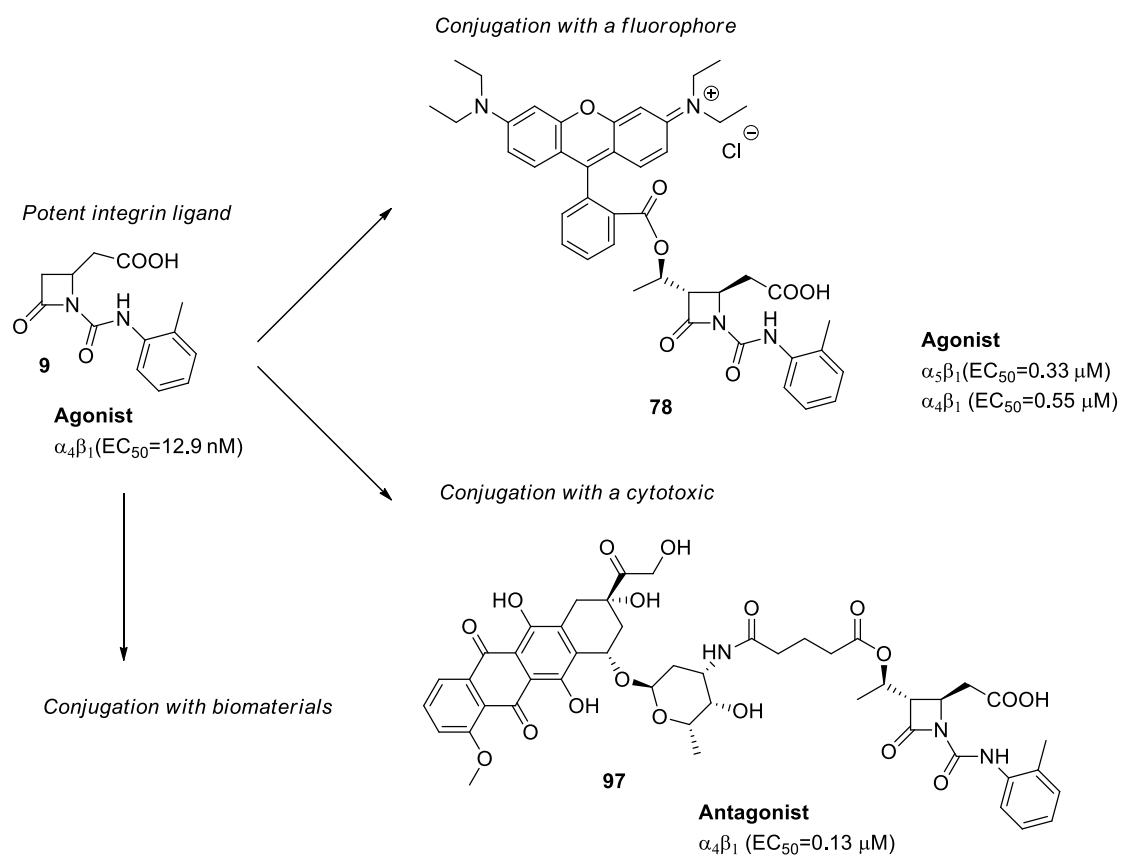


**Figure 3.51.** Compound **9** as strong agonist integrin ligand and applications developed from its molecular structure

## 3.10 Experimental Section

### 3.10.1 General information

See Paragraph 2.13.1

Chiral-HPLC: Agilent Technologies 1200 instrument equipped with a variable wave-length UV detector (reference 210 nm), on Daicel Chiralcel columns (0.46 cm I.D. x 25 cm) with HPLC grade isopropanol and n-hexane as eluting solvents.

### 3.10.2 Synthetic general procedures

#### *General procedure for N-acylation of $\beta$ -lactams (GP1A, GP1B and GP1C)*

**GP1A:** A solution of sodium bis(trimethylsilyl)amide (NaHMDSA) (1M in THF, 1.1 equiv) was added dropwise to a solution of the starting  $\beta$ -lactam (1 equiv) in anhydrous THF (9 mL/mmol) at -78 °C under a nitrogen atmosphere. The mixture was stirred for 15 min, then a solution of the desired isocyanate (1.5 equiv) in anhydrous THF (1 mL) was added dropwise. After completion (TLC monitoring, 30 min) the mixture was quenched with a saturated solution of  $\text{NH}_4\text{Cl}$  and extracted with EtOAc (10 mL) and with  $\text{CH}_2\text{Cl}_2$  ( $2 \times 10$  mL). The combined organic extracts were dried over  $\text{Na}_2\text{SO}_4$ , concentrated in vacuum and purified by flash-chromatography affording the desired derivatives.

**GP1B:** The starting  $\beta$ -lactam (1 equiv) was dissolved in anhydrous  $\text{CH}_3\text{CN}$  (1 mL) under a nitrogen atmosphere. Anhydrous and finely ground  $\text{K}_2\text{CO}_3$  (1.5 equiv) was added, followed by a dropwise addition of the commercially available *o*-tolyl- or benzyl isocyanate (1.2 equiv). The mixture was stirred at room temperature until a complete consumption of the starting  $\beta$ -lactam (about 2 h, TLC monitoring) and then quenched with a saturated solution of  $\text{NH}_4\text{Cl}$ . The solvent was reduced under vacuum and the residual aqueous solution was extracted with  $\text{CH}_2\text{Cl}_2$  ( $3 \times 10$  mL). The organic layers were collected, dried over  $\text{Na}_2\text{SO}_4$ , concentrated in vacuum and purified by flash-chromatography affording the desired *N*-acylated  $\beta$ -lactam.

**GP1C:** The starting  $\beta$ -lactam (1 equiv) was dissolved in anhydrous  $\text{CH}_2\text{Cl}_2$  (11 mL/mmol) under a nitrogen atmosphere. Anhydrous TEA was added dropwise, followed by a dropwise addition of the desired isocyanate or isothiocyanate. The mixture was stirred at room temperature until a complete consumption of the starting  $\beta$ -lactam (16 h, TLC monitoring) and then quenched with a saturated solution of  $\text{NH}_4\text{Cl}$ . The mixture was extracted with  $\text{CH}_2\text{Cl}_2$  ( $3 \times 10$  mL), the organic layers were collected, dried over anhydrous  $\text{Na}_2\text{SO}_4$ , concentrated in vacuum and purified by flash-chromatography affording the desired *N*-acylated compound.

#### *General procedure for hydrogenolysis (GP2)*

A  $\beta$ -lactam benzyl ester (1 equiv) was dissolved in a mixture of THF and  $\text{CH}_3\text{OH}$  (22 mL/mmol, 1:1 v/v) and Pd/C (10% w/w) was added. The solution was then stirred under a  $\text{H}_2$  atmosphere (1 atm) at room temperature. After a complete consumption of the starting material (TLC monitoring, 2 h) the reaction mixture was filtered through celite and concentrated in vacuum. The crude was then triturated with few drops of pentane to afford the desired carboxylic acid.

#### *General procedure for N-Boc-deprotection (GP3)*

A *N*-Boc-protected  $\beta$ -lactam (1 equiv) was dissolved in  $\text{CH}_2\text{Cl}_2$  (18.5 mL/mmol) under a nitrogen atmosphere and trifluoroacetic acid (TFA) (4 equiv) was added dropwise at 0 °C. New TFA aliquots were added each 30 mins at 0 °C until a complete conversion (HPLC or TLC monitoring). The solvent was removed under reduced pressure and the crude was triturated with few drops of pentane to afford the resulting deprotected compound.



### General procedure for peptidic coupling (GP4A and GP4B)

**GP4A:** The starting  $\beta$ -lactam carboxylic acid (1 equiv) was dissolved in  $\text{CH}_2\text{Cl}_2$  (10 mL/mmol) under a nitrogen atmosphere. Oxalyl chloride (1.5 equiv) was added dropwise and the mixture was stirred at room temperature for 1.5 h; then glycine benzylester or  $\beta$ -alanine benzylester (1 equiv) was added, followed by the addition of anhydrous TEA at 0 °C and DMAP (0.2 equiv). The mixture was stirred at room temperature until a complete consumption of the starting  $\beta$ -lactam (16 h, TLC monitoring) and then quenched with a saturated solution of  $\text{NH}_4\text{Cl}$ . The residual aqueous solution was extracted with  $\text{CH}_2\text{Cl}_2$  ( $3 \times 10$  mL). The organic layers were collected, dried over  $\text{Na}_2\text{SO}_4$ , concentrated in vacuum and purified by flash-chromatography to afford the desired coupled  $\beta$ -lactam.

**GP4B:** The starting  $\beta$ -lactam carboxylic acid (1 equiv) was dissolved in  $\text{CH}_2\text{Cl}_2$  (14 mL/mmol) under a nitrogen atmosphere. 1-Ethyl-3-(3-dimethylaminopropyl) carbodiimide (EDC) or  $N,N'$ -dicyclohexylcarbodiimide (DCC) was added at 0 °C; then a previously prepared solution of glycine benzyl ester or  $\beta$ -alanine benzylester (commercially available as chloridrate or *p*-toluenesulfonate salt, 1.5 equiv) and TEA (1.6 equiv) in  $\text{CH}_2\text{Cl}_2$  (12 mL/mmol) was added dropwise. After addition of DMAP, the solution was warmed to rt and left under stirring after complete consumption of the starting material (16 h, TLC monitoring). The mixture was quenched with  $\text{H}_2\text{O}$  and extracted with  $\text{CH}_2\text{Cl}_2$  ( $3 \times 10$  mL). The organic layers were collected, dried over  $\text{Na}_2\text{SO}_4$  and concentrated in vacuum. When DCC was used, the crude was suspended in EtOAc at 0 °C and the solid residual dicyclohexylurea was eliminated by filtration. Purification by flash-chromatography afforded the desired coupled  $\beta$ -lactam.

### 3.10.3 Synthesis of the new integrin ligand library

$\beta$ -lactams **13**, **22**, **35** and **44** were synthesized according to a previously reported procedure.<sup>155</sup> Isocyanate **34** was synthesized according to a previously reported procedure;<sup>155</sup> isocyanate **23** was synthesized according to a reported procedure<sup>155</sup> starting from *tert*-butyl-(4-(aminomethyl)phenyl)carbamate, which in turn was prepared as in ref. 85.

LC-MS and  $^1\text{H}$  NMR monitoring indicated no degradation for all new  $\beta$ -lactam molecules stored as pure compounds at 4 °C for up to 4 months. As models, we studied the stabilities of compounds **2** and **4** in buffered water solutions at pH = 7.4 at 30 °C and in serum at 30 °C, verifying a non-degradation of the compounds up to 24 h.

Any potential cell toxicity of  $\beta$ -lactams under investigations was evaluated by Annexin V-7-AAD assay by flow cytometry. We observed that all compounds ( $10^{-4}$  M) added for three hours to the cell lines used in this study did not cause any cell necrosis and/or apoptosis.

### (*S*)-Benzyl 1-(4-*tert*-butoxycarbonylamino)benzylcarbamoyl)-4-oxoazetidine-2-carboxylate (**24**)

Following GP1A compound **22** (35 mg, 0.17 mmol) was treated with NaHMDSA (375  $\mu\text{L}$ , 0.375 mmol) and isocyanate **23** (64 mg, 0.26 mmol). Purification by flash-chromatography ( $\text{CH}_2\text{Cl}_2$ /diethyl ether 95:5) yielded compound **24** as a colorless oil (69 mg, 37%). IR (film,  $\text{cm}^{-1}$ ) 3358, 1780, 1744, 1731, 1709;  $[\alpha]_D^{20} = -0.4$  ( $c = 0.9$ ,  $\text{CH}_2\text{Cl}_2$ );  $^1\text{H}$  NMR (400 MHz,  $\text{CDCl}_3$ )  $\delta$  (ppm) 1.51 (s, 9H), 3.01 (dd,  $J = 2.8, 15.6$  Hz, 1H), 3.30 (dd,  $J = 6.2, 15.6$  Hz, 1H), 4.38 (dd,  $J = 6.0, 14.8$  Hz, 1H), 4.45 (dd,  $J = 6.0, 14.8$  Hz, 1H), 4.52 (dd,  $J = 2.8, 6.2$  Hz, 1H), 5.22 (d,  $J_{AB} = 12.2$  Hz, 1H), 5.27 (d,  $J_{AB} = 12.2$  Hz, 1H), 6.56 (s, 1H), 6.67 (bt,  $J = 6.0$  Hz, 1H), 7.19 – 7.21 (m, 2H), 7.27 – 7.39 (m, 7H);  $^{13}\text{C}$  NMR (100 MHz,  $\text{CDCl}_3$ )  $\delta$  (ppm) 28.2, 41.0, 43.3, 48.7, 67.6, 80.4, 118.7, 128.2, 128.3, 128.5, 128.6, 129.9, 132.0, 134.7, 137.8, 149.3, 152.6, 164.6, 169.0; ESI-MS  $m/z$  471  $[\text{M}+\text{H}_2\text{O}]^+$ , 476  $[\text{M}+\text{Na}]^+$ .

*(S)*-1-(4-*tert*-butoxycarbonylamino)benzylcarbamoyl)-4-oxoazetidine-2-carboxylic acid (**25**)

Following GP2 compound **24** (51 mg, 0.11 mmol) yielded compound **25** as a waxy white solid (35 mg, 88%). IR (film,  $\text{cm}^{-1}$ ) 3363, 1770, 1699, 1694, 1692;  $[\alpha]_{\text{D}}^{20} = -0.5$  ( $c = 0.6$ ,  $\text{CH}_3\text{OH}$ );  $^1\text{H NMR}$  (400 MHz,  $\text{CD}_3\text{OD}$ )  $\delta$  (ppm) 1.50 (s, 9H), 2.90 (dd,  $J = 2.8, 15.6$  Hz, 1H), 3.27 (dd,  $J = 6.4, 15.6$  Hz, 1H), 4.31 – 4.41 (m, 3H), 7.22 (d,  $J = 8.4$  Hz, 2H), 7.35 (d,  $J = 8.4$  Hz, 2H);  $^{13}\text{C NMR}$  (100 MHz,  $\text{CD}_3\text{OD}$ )  $\delta$  (ppm) 28.7, 41.9, 43.9, 49.2, 80.8, 119.9, 128.9, 130.1, 133.8, 139.7, 150.7, 151.7, 155.2, 166.6; ESI-MS  $m/z$  362  $[\text{M-H}]^-$ .

*(S)*-4-(2-carboxy-4-oxoazetidine-1-carboxamidomethyl) benzenaminium 2,2,2-trifluoroacetate (**5**)

Following GP3, compound **25** (35 mg, 0.96 mmol) was treated with TFA (137  $\mu\text{L}$ , 1.82 mmol, 19 equiv) yielding compound **5** as a waxy solid (36 mg, 99%). IR (film,  $\text{cm}^{-1}$ ) 3362, 1780, 1698, 1677;  $[\alpha]_{\text{D}}^{20} = -3$  ( $c = 0.9$ ,  $\text{CH}_3\text{OH}$ );  $^1\text{H NMR}$  (400 MHz,  $\text{CD}_3\text{OD}$ )  $\delta$  (ppm) 3.04 (dd,  $J = 2.8, 15.8$  Hz, 1H), 3.44 (dd,  $J = 6.4, 15.8$  Hz, 1H), 4.45 – 4.48 (m, 3H), 7.36 (d,  $J = 8.0$  Hz, 2H) 7.49 (d,  $J = 8.0$  Hz, 2H);  $^{13}\text{C NMR}$  (100 MHz,  $\text{CD}_3\text{OD}$ )  $\delta$  (ppm) 42.0, 43.6, 50.2, 118.4 (q,  $J = 300.0$  Hz), 124.2, 130.0, 131.1, 141.2, 151.8, 162.4 (q,  $J = 35.6$  Hz), 166.6, 172.9;  $^{19}\text{F NMR}$  (375 MHz,  $\text{CD}_3\text{OD}$ )  $\delta$  (ppm) -77.1; ESI-MS  $m/z$  264  $[\text{M-TFA+H}]^+$ , 281  $[\text{M-TFA+H}_2\text{O}]^+$ . Found C, 44.44; H, 3.81; N, 10.91 %;  $\text{C}_{14}\text{H}_{14}\text{F}_3\text{N}_3\text{O}_6$  requires C, 44.57; H, 3.74; N, 11.14 %.

*(S)*-Benzyl 4-oxo-(*o*-tolylcarbamoyl)azetidine-2-carboxylate (**26**)

Following GP1B, compound **22** (103 mg, 0.5 mmol) was treated with  $\text{K}_2\text{CO}_3$  (104 mg, 0.75 mmol) and *o*-tolylisocyanate (74  $\mu\text{L}$ , 0.6 mmol). Purification by flash-chromatography (cyclohexane/EtOAc 70:30) yielded compound **26** as a light brown oil (126 mg, 75%). IR (film,  $\text{cm}^{-1}$ ) 3348, 1776, 1751, 1718;  $[\alpha]_{\text{D}}^{20} = -9$  ( $c = 1.2$ ,  $\text{CH}_2\text{Cl}_2$ );  $^1\text{H NMR}$  (400 MHz,  $\text{CDCl}_3$ )  $\delta$  (ppm) 2.30 (s, 3H), 3.12 (dd,  $J = 2.8, 15.8$  Hz, 1H), 3.42 (dd,  $J = 6.2, 15.8$  Hz, 1H), 4.62 (dd,  $J = 2.8, 6.2$  Hz, 1H), 5.25 (d,  $J_{\text{AB}} = 12.2$  Hz, 1H), 5.30 (d,  $J_{\text{AB}} = 12.2$  Hz, 1H), 7.04 – 7.08 (m, 1H), 7.18 – 7.21 (m, 2H), 7.35 – 7.38 (m, 5H), 7.93 (d,  $J = 8.1$  Hz, 1H), 8.28 (bs, 1H);  $^{13}\text{C NMR}$  (100 MHz,  $\text{CDCl}_3$ )  $\delta$  (ppm) 17.3, 41.0, 48.8, 67.5, 120.9, 124.4, 126.6, 127.4, 128.1, 128.4, 128.4, 130.2, 134.6, 134.9, 146.6, 165.1, 168.7; ESI-MS  $m/z$  339  $[\text{M+H}]^+$ , 361  $[\text{M+Na}]^+$ , 699  $[\text{2M+Na}]^+$ .

*(S)*-4-oxo-(*o*-tolylcarbamoyl)azetidine-2-carboxylic acid (**4**)

Following GP2 compound **26** (115 mg, 0.34 mmol) yielded compound **4** as a white solid (83 mg, 99%). IR (film,  $\text{cm}^{-1}$ ) 3339, 1787, 1755, 1737; Mp 121 – 124  $^\circ\text{C}$ ;  $[\alpha]_{\text{D}}^{20} = -15$  ( $c = 1.0$ ,  $\text{CH}_2\text{Cl}_2$ );  $^1\text{H NMR}$  (400 MHz,  $\text{CD}_3\text{OD}$ )  $\delta$  (ppm) 2.30 (s, 3H), 3.13 (dd,  $J = 2.8, 15.8$  Hz, 1H), 3.52 (dd,  $J = 6.4, 15.8$  Hz, 1H), 4.52 – 4.56 (m, 1H) (d,  $J = 3.6$  Hz, 1H), 7.05 – 7.08 (m, 1H), 7.17 – 7.24 (m, 2H), 7.76 (d,  $J = 8.0$  Hz, 1H);  $^{13}\text{C NMR}$  (100 MHz,  $\text{CDCl}_3$ )  $\delta$  (ppm) 17.5, 41.2, 49.3, 121.5, 125.0, 126.7, 128.1, 130.4, 134.5, 147.7, 165.5, 171.8; ESI-MS  $m/z$  247  $[\text{M-H}]^-$ . Found C, 57.97; H, 5.02; N, 11.21 %;  $\text{C}_{12}\text{H}_{12}\text{N}_2\text{O}_4$  requires C, 58.06; H, 4.87; N, 11.29 %.

Benzyl (*S*)-(4-oxo-1-(*o*-tolylcarbamoyl)azetidine-2-carbonyl)glycinate (**27**)

Following GP4A, carboxylic acid **4** (40 mg, 0.16 mmol, 1 equiv) was treated with oxalyl chloride (21  $\mu\text{L}$ , 0.24 mmol, 1.5 equiv), glycine benzylester hydrochloride (32 mg, 0.16 mmol, 1 equiv), TEA (112  $\mu\text{L}$ , 0.8 mmol, 5 equiv) and DMAP (4 mg, 0.032 mmol, 0.2 equiv). Purification by flash-chromatography (cyclohexane/EtOAc 60:40) yielded compound **27** as a white waxy solid (32 mg, 51%). IR (film,  $\text{cm}^{-1}$ ) 3337, 1774, 1750, 1719, 1687;  $[\alpha]_{\text{D}}^{20} = -12$  ( $c = 1.0$ ,  $\text{CH}_2\text{Cl}_2$ );  $^1\text{H NMR}$  (400 MHz,  $\text{CDCl}_3$ )  $\delta$  (ppm) 2.30 (s, 3H), 3.32 (dd,  $J = 6.4, 16.4$  Hz, 1H), 3.53 (dd,  $J = 3.2, 16.4$  Hz, 1H), 4.07 – 4.18 (m, 2H), 4.70 (dd,  $J = 3.2, 6.4$  Hz, 1H), 5.16 (d,  $J_{\text{AB}} = 12.4$  Hz, 1H), 5.20 (d,  $J_{\text{AB}} = 12.4$  Hz, 1H), 7.06 – 7.10 (m, 1H), 7.19 – 7.24 (m, 2H), 7.31 – 7.35 (m, 5H), 7.88 (d,  $J = 8.0$  Hz, 1H), 7.99 (bt,  $J = 5.0$  Hz, 1H), 8.48 (bs, 1H);  $^{13}\text{C NMR}$  (100 MHz,  $\text{CDCl}_3$ )  $\delta$  (ppm) 17.6, 40.4, 41.6, 51.7, 67.2, 121.4, 125.0, 126.8, 128.0, 128.3, 128.5, 128.6, 130.5, 134.6, 135.0, 148.9, 166.8, 167.9, 169.0; ESI-MS  $m/z$  396  $[\text{M+H}]^+$ , 418  $[\text{M+Na}]^+$ .

*(S)*-*(4-oxo-1-(o-tolylcarbamoyl)azetidine-2-carbonyl)glycine* (**6**)

Following GP2 compound **27** (29 mg, 0.70 mmol) yielded compound **6** as a white solid (21 mg, 99%). Mp 190 – 192 °C; IR (film, cm<sup>-1</sup>) 3356, 1778, 1737, 1690, 1674; [ $\alpha$ ]<sub>D</sub><sup>20</sup> = - 11 (c = 1.1, CH<sub>3</sub>OH); <sup>1</sup>H NMR (400 MHz, CD<sub>3</sub>OD)  $\delta$  (ppm) 2.29 (s, 3H), 3.14 (dd, *J* = 2.9, 15.8 Hz, 1H), 3.45 (dd, *J* = 6.2, 15.8 Hz, 1H), 3.93 (d, *J*<sub>AB</sub> = 17.8 Hz, 1H), 4.08 (d, *J*<sub>AB</sub> = 17.8 Hz, 1H), 4.63 (dd, *J* = 2.9, 6.2 Hz, 1H), 7.04 – 7.08 (m, 1H), 7.15 – 7.22 (m, 2H), 7.79 (d, *J* = 8.0 Hz, 1H); <sup>13</sup>C NMR (100 MHz, CD<sub>3</sub>OD)  $\delta$  (ppm) 17.7, 41.9, 42.3, 51.5, 122.9, 126.0, 127.6, 129.9, 131.5, 136.4, 149.4, 167.9, 171.5, 172.5; ESI-MS *m/z* 609 [2M-H]<sup>-</sup>. Found C, 55.21; H, 4.99; N, 13.58 %; C<sub>14</sub>H<sub>15</sub>N<sub>3</sub>O<sub>5</sub> requires C, 55.08; H, 4.95; N, 13.76 %.

*Benzyl (S)*-*3-(4-oxo-1-(o-tolylcarbamoyl)azetidine-2-carboxamido)propanoate* (**28**)

Following GP4A, carboxylic acid **4** (40 mg, 0.16 mmol, 1 equiv) was treated with oxalyl chloride (16  $\mu$ L, 0.19 mmol, 1.2 equiv), beta alanine benzylester *p*-toluenesulfonate salt (56 mg, 0.16 mmol, 1 equiv), TEA (90  $\mu$ L, 0.64 mmol, 4 equiv) and DMAP (4 mg, 0.032 mmol, 0.2 equiv). Purification by flash-chromatography (cyclohexane/EtOAc 60:40) yielded compound **28** as a white waxy solid (35 mg, 54%). IR (film, cm<sup>-1</sup>) 3340, 1774, 1729, 1686, 1683; [ $\alpha$ ]<sub>D</sub><sup>20</sup> = - 11 (c = 1.0, CH<sub>2</sub>Cl<sub>2</sub>); <sup>1</sup>H NMR (400 MHz, CDCl<sub>3</sub>)  $\delta$  (ppm) 2.30 (s, 3H), 2.63 (t, *J* = 6.3 Hz, 2H), 3.28 (dd, *J* = 6.3, 16.3 Hz, 1H), 3.48 (dd, *J* = 3.2, 16.3 Hz, 1H), 3.54 – 3.67 (m, 2H), 4.55 (dd, *J* = 3.2, 6.3 Hz, 1H), 5.12 (s, 2H), 7.05 – 7.09 (m, 1H), 7.19 – 7.22 (m, 2H), 7.30 – 7.35 (m, 5H), 7.71 (bs, 1H), 7.88 (d, *J* = 8.8 Hz, 1H), 8.46 (bs, 1H); <sup>13</sup>C NMR (100 MHz, CDCl<sub>3</sub>)  $\delta$  (ppm) 17.6, 33.9, 35.3, 40.4, 51.8, 66.5, 121.4, 125.0, 126.8, 128.0, 128.2, 128.3, 128.5, 130.5, 134.7, 135.6, 148.7, 166.9, 167.5, 171.6; ESI-MS *m/z* 410 [M+H]<sup>+</sup>, 432 [M+Na]<sup>+</sup>.

*(S)*-*3-(4-oxo-1-(o-tolylcarbamoyl)azetidine-2-carboxamido)propanoic acid* (**7**)

Following GP2 compound **28** (32 mg, 0.80 mmol) yielded compound **7** as a white solid (22 mg, 88%). Mp 161 – 163 °C; IR (film, cm<sup>-1</sup>) 3353, 1781, 1739, 1708, 1649; [ $\alpha$ ]<sub>D</sub><sup>20</sup> = - 7 (c = 1.1, CH<sub>3</sub>OH); <sup>1</sup>H NMR (400 MHz, CD<sub>3</sub>OD)  $\delta$  (ppm) 2.29 (s, 3H), 2.56 (t, *J* = 6.6 Hz, 2H), 3.08 (dd, *J* = 2.9, 15.8 Hz, 1H), 3.39 (dd, *J* = 6.1, 15.8 Hz, 1H), 3.45 – 3.57 (m, 2H), 4.52 (dd, *J* = 2.9, 6.1 Hz, 1H), 7.04 – 7.07 (m, 1H), 7.16 – 7.22 (m, 2H), 7.79 (d, *J* = 8.0 Hz, 1H); <sup>13</sup>C NMR (100 MHz, CD<sub>3</sub>OD)  $\delta$  (ppm) 17.7, 34.4, 36.6, 42.1, 51.6, 122.9, 126.0, 127.6, 129.9, 131.5, 136.4, 149.3, 168.0, 171.0, 175.1; ESI-MS *m/z* 318 [M-H]<sup>-</sup>. Found C, 56.83; H, 5.38; N, 13.02 %; C<sub>15</sub>H<sub>17</sub>N<sub>3</sub>O<sub>5</sub> requires C, 56.42; H, 5.37; N, 13.16 %.

*Methyl 2-(4-oxoazetidin-2-yl)acetate* (**29**)

Zn powder (2.018 g, 31.04 mmol, 7.2 equiv) was suspended in THF (9.7 mL) under nitrogen followed by TMSCl (196  $\mu$ L, 1.552 mmol, 0.1 equiv) addition. After 30 min of stirring the temperature was raised to 30 ÷ 35 °C and a solution of methyl bromoacetate (1.47 mL, 15.52 mmol, 3.6 equiv) in THF (19.4 mL) was added dropwise in 30 min. After 30 min of stirring the mixture was cooled to rt and decanted, providing a limpid grey supernatant that was added dropwise to a solution of commercially available 4-acetoxy-azetidin-2-one (500 mg, 3.88 mmol, 1 equiv) in anhydrous THF (22 mL) at 0 °C. The mixture was stirred at rt for 3 h, quenched with ice and a saturated Seignette salt solution and extracted with EtOAc (5 × 50 mL). The organic layers were dried on Na<sub>2</sub>SO<sub>4</sub>, filtered and concentrated in vacuum. Flash-chromatography (cyclohexane/EtOAc 70:30 then EtOAc 100%) yielded ester **29** as a yellow solid (332 mg, 60%). Mp 60 – 65 °C; IR (film, cm<sup>-1</sup>) 3390, 1760, 1730; <sup>1</sup>H NMR (400 MHz, CDCl<sub>3</sub>)  $\delta$  (ppm) 2.63 (dd, *J* = 8.6, 16.7 Hz, 1H), 2.69 – 2.73 (m 1H), 2.74 (dd, *J* = 5.0, 16.7 Hz, 1H), 3.20 (ddd, *J* = 2.2, 5.0, 15.2 Hz, 1H), 3.70 (s, 3H), 3.96 – 4.02 (m, 1H), 6.77 (bs, 1H); <sup>13</sup>C NMR (100 MHz, CDCl<sub>3</sub>)  $\delta$  (ppm) 39.2, 43.0, 44.6, 52.0, 169.0, 171.0; ESI-MS *m/z* 144 [M+H]<sup>+</sup>.

*Ethyl 2-(4-oxoazetidin-2-yl)acetate (30)*

Following the procedure reported for **29**, commercially available 4-acetoxy-azetidin-2-one (500 mg, 3.88 mmol, 1 equiv) was treated with ethyl bromoacetate (1.72 mL, 15.52 mmol, 3.6 equiv). Purification by flash-chromatography (CH<sub>2</sub>Cl<sub>2</sub>/acetone 80:20) yielded compound **30** as a waxy yellow solid (390 mg, 64%). IR (film, cm<sup>-1</sup>) 3224, 1731, 1725; <sup>1</sup>H NMR (400 MHz, CDCl<sub>3</sub>) δ (ppm) 1.27 (t, *J* = 7.2 Hz, 3H), 2.58 (dd, *J* = 9.0, 16.6 Hz, 1H), 2.66 (dd, *J* = 1.3, 14.9 Hz, 1H), 2.73 (dd, *J* = 4.6, 16.6 Hz, 1H), 3.16 (ddd, *J* = 2.2, 4.8, 14.9 Hz, 1H), 3.92 – 3.95 (m, 1H), 4.17 (q, *J* = 7.1 Hz, 2H), 6.14 (bs, 1H); <sup>13</sup>C NMR (100 MHz, CDCl<sub>3</sub>) δ (ppm) 14.2, 39.9, 43.4, 43.8, 61.0, 167.0, 170.9; ESI-MS *m/z* 158 [M+H]<sup>+</sup>, 180 [M+Na]<sup>+</sup>.

*2-(4-oxoazetidin-2-yl)acetic acid (8)*

Following GP2 compound **13** (130 mg, 0.59 mmol) yielded compound **8** as a white solid (75 mg, 99%). Mp 120 – 125 °C; IR (nujol, cm<sup>-1</sup>) 3230, 1752, 1695; <sup>1</sup>H NMR (400 MHz, CD<sub>3</sub>OD) δ (ppm) 2.61 (dd, *J* = 7.7, 16.8 Hz, 1H), 2.65 (dd, *J* = 2.3, 14.8 Hz, 1H), 2.69 (dd, *J* = 5.8, 16.8 Hz, 1H), 3.10 (dd, *J* = 4.9, 14.8 Hz, 1H), 3.90 – 3.96 (m, 1H); <sup>13</sup>C NMR (100 MHz, CD<sub>3</sub>OD) δ (ppm) 40.5, 43.4, 45.3, 170.7, 174.6. Found C, 46.71; H, 5.59; N, 10.78 %; C<sub>5</sub>H<sub>7</sub>N<sub>3</sub>O<sub>3</sub> requires C, 46.51; H, 5.46; N, 10.85 %.

*Methyl 2-(4-oxo-1-(*o*-tolylcarbamoylethyl)azetidin-2-yl)acetate (10)*

Following GP1B, compound **29** (77 mg, 0.54 mmol) was treated with K<sub>2</sub>CO<sub>3</sub> (112 mg, 0.81 mmol) and *o*-tolylisocyanate (80 μL, 0.65 mmol). Purification by flash-chromatography (CH<sub>2</sub>Cl<sub>2</sub>/diethyl ether 90:10) yielded compound **10** as a waxy yellow solid (110 mg, 74%). IR (film, cm<sup>-1</sup>) 3335, 1766, 1736, 1710; <sup>1</sup>H NMR (400 MHz, CDCl<sub>3</sub>) δ (ppm) 2.30 (s, 3H), 2.74 (dd, *J* = 9.0, 16.6 Hz, 1H), 2.96 (dd, *J* = 2.9, 16.6 Hz, 1H), 3.35 (dd, *J* = 4.6, 12.6 Hz, 1H), 3.40 (dd, *J* = 4.5, 12.6 Hz, 1H), 3.73 (s, 3H), 4.43 – 4.49 (m, 1H), 7.03 – 7.06 (m, 1H), 7.18 – 7.23 (m, 2H), 7.92 (d, *J* = 8.0 Hz, 1H), 8.45 (bs, 1H); <sup>13</sup>C NMR (100 MHz, CDCl<sub>3</sub>) δ (ppm) 17.6, 36.7, 42.7, 47.4, 52.0, 121.0, 124.5, 126.7, 127.5, 130.4, 135.2, 147.8, 166.8, 170.3; ESI-MS *m/z* 277 [M+H]<sup>+</sup>. Found C, 61.12; H, 5.78; N, 9.98 %; C<sub>14</sub>H<sub>16</sub>N<sub>2</sub>O<sub>4</sub> requires C, 60.86; H, 5.84; N, 10.14 %.

*Ethyl 2-(4-oxo-1-(*o*-tolylcarbamoylethyl)azetidin-2-yl)acetate (11)*

Following GP1B compound **30** (65 mg, 0.41 mmol) was treated with K<sub>2</sub>CO<sub>3</sub> (86 mg, 0.62 mmol) and *o*-tolyl isocyanate (61 μL, 0.49 mmol). Purification by flash-chromatography (CH<sub>2</sub>Cl<sub>2</sub>/diethyl ether 80:20) yielded compound **11** as a white solid (110 mg, 81%). Mp 91 – 93 °C; IR (film, cm<sup>-1</sup>) 3340, 1761, 1730, 1714; <sup>1</sup>H NMR (400 MHz, CDCl<sub>3</sub>) δ (ppm) 1.27 (t, *J* = 7.1 Hz, 3H), 2.30 (s, 3H), 2.74 (dd, *J* = 9.0, 16.5 Hz, 1H), 2.96 (dd, *J* = 2.8, 16.5 Hz, 1H), 3.33 (dd, *J* = 3.8, 16.6 Hz, 1H), 3.38 (dd, *J* = 5.7, 16.6 Hz, 1H), 4.18 (q, *J* = 7.1 Hz, 2H), 4.43 – 4.48 (m, 1H), 7.03 – 7.06 (m, 1H), 7.17 – 7.23 (m, 2H), 7.93 (d, *J* = 8.0 Hz, 1H), 8.45 (bs, 1H); <sup>13</sup>C NMR (100 MHz, CDCl<sub>3</sub>) δ (ppm) 14.1, 17.6, 36.8, 42.6, 47.5, 60.9, 120.9, 124.4, 126.7, 127.4, 130.4, 135.2, 147.8, 166.8, 169.8; ESI-MS *m/z* 291 [M+H]<sup>+</sup>, 603 [2M+Na]<sup>+</sup>. Found C, 62.13; H, 6.27; N, 9.41 %; C<sub>15</sub>H<sub>18</sub>N<sub>2</sub>O<sub>4</sub> requires C, 62.06; H, 6.25; N, 9.65 %.

*Benzyl 2-(4-oxo-1-(*o*-tolylcarbamoylethyl)azetidin-2-yl)acetate (12)*

Following GP1B compound **13** (75 mg, 0.34 mmol) was treated with K<sub>2</sub>CO<sub>3</sub> (70 mg, 0.54 mmol) and *o*-tolylisocyanate (51 μL, 0.41 mmol). Purification by flash-chromatography (CH<sub>2</sub>Cl<sub>2</sub>/diethyl ether 90:10) yielded compound **12** as a white solid (110 mg, 74%). Mp 74 – 76 °C; IR (film, cm<sup>-1</sup>) 3338, 1767, 1733, 1713; <sup>1</sup>H NMR (400 MHz, CDCl<sub>3</sub>) δ (ppm) 2.29 (s, 3H), 2.81 (dd, *J* = 8.8, 16.5 Hz, 1H), 2.95 (dd, *J* = 2.8, 16.5 Hz, 1H), 3.36 (dd, *J* = 6.0, 16.4 Hz, 1H), 3.37 (dd, *J* = 4.8, 16.4 Hz, 1H), 4.47 – 4.49 (m, 1H), 5.14 (d, *J*<sub>AB</sub> = 12.6 Hz, 1H), 5.18 (d, *J*<sub>AB</sub> = 12.6 Hz, 1H), 7.03 – 7.06 (m, 1H), 7.17 – 7.23 (m, 2H), 7.32 – 7.37 (m, 5H), 7.92 (d, *J* = 8.1 Hz, 1H), 8.42 (bs, 1H); <sup>13</sup>C NMR (100 MHz, CDCl<sub>3</sub>) δ (ppm) 17.7, 37.0, 42.6, 47.5, 66.8, 121.0, 124.4,

126.8, 127.5, 128.3, 128.4, 128.6, 130.4, 135.2, 135.3, 147.8, 166.7, 169.7; ESI-MS  $m/z$  353 [M+H]<sup>+</sup>, 375 [M+Na]<sup>+</sup>, 727 [2M+Na]<sup>+</sup>. Found C, 68.43; H, 5.88; N, 7.80 C<sub>20</sub>H<sub>20</sub>N<sub>2</sub>O<sub>4</sub> requires C, 68.17; H, 5.72; N, 7.95 %.

*2-(4-oxo-(o-tolylcarbamoyl)azetidin-2-yl) acetic acid (9)*

Following GP2 compound **12** (88 mg, 0.25 mmol) yielded compound **9** as a white solid (65 mg, 99%). Mp 114 – 117 °C; IR (film, cm<sup>-1</sup>) 3344, 1766, 1708; <sup>1</sup>H NMR (400 MHz, (CD<sub>3</sub>)<sub>2</sub>CO)  $\delta$  (ppm) 2.27 (s, 3H), 2.90 (dd,  $J$  = 9.1, 16.7 Hz, 1H), 3.08 (dd,  $J$  = 2.9, 16.0 Hz, 1H), 3.26 (dd,  $J$  = 3.7, 16.7 Hz, 1H), 3.42 (dd,  $J$  = 5.7, 16.0 Hz, 1H), 4.42 – 4.46 (m, 1H), 7.00 – 7.04 (m, 1H), 7.17 – 7.23 (m, 2H), 7.99 (d,  $J$  = 8.1 Hz, 1H), 8.55 (bs, 1H); <sup>13</sup>C NMR (100 MHz, (CD<sub>3</sub>)<sub>2</sub>CO)  $\delta$  (ppm) 17.6, 36.6, 43.1, 48.4, 121.2, 124.7, 127.4, 127.7, 131.2, 136.9, 148.8, 168.4, 171.7; ESI-MS  $m/z$  263 [M+H]<sup>+</sup>, 285 [M+Na]<sup>+</sup>, 547 [2M+Na]<sup>+</sup>. Found C, 59.24; H, 5.56; N, 10.44 %; C<sub>13</sub>H<sub>14</sub>N<sub>2</sub>O<sub>4</sub> requires C, 59.54; H, 5.38; N, 10.68 %.

*Benzyl 2-(1-(4-tert-butoxycarbonylaminobenzylcarbamoyl)-4-oxoazetidin-2-yl) acetate (31)*

Following GP1A compound **13** (57 mg, 0.26 mmol) was treated with NaHMDSA (325  $\mu$ L, 0.325 mmol) and isocyanate **23** (97 mg, 0.39 mmol). Purification by flash-chromatography (CH<sub>2</sub>Cl<sub>2</sub>/diethyl ether 95:5) yielded compound **31** as a colorless oil (75 mg, 62%). IR (film, cm<sup>-1</sup>) 3365, 1769, 1730, 1703, 1697; <sup>1</sup>H NMR (400 MHz, CDCl<sub>3</sub>)  $\delta$  (ppm) 1.51 (s, 9H), 2.71 (dd,  $J$  = 9.0, 16.5 Hz, 1H), 2.84 (dd,  $J$  = 2.9, 16.2 Hz, 1H), 3.26 (dd,  $J$  = 5.6, 16.2 Hz, 1H), 3.34 (dd,  $J$  = 4.0, 16.5 Hz, 1H), 4.31 – 4.43 (m, 3H), 5.12 (d,  $J_{AB}$  = 12.2 Hz, 1H), 5.16 (d,  $J_{AB}$  = 12.2 Hz, 1H), 6.46 (bs, 1H), 6.77 (bt,  $J$  = 5.7 Hz) 7.20 – 7.22 (m, 2H), 7.30 – 7.39 (m, 7H); <sup>13</sup>C NMR (100 MHz, CDCl<sub>3</sub>)  $\delta$  (ppm) 28.2, 37.0, 42.5, 43.0, 47.1, 66.6, 80.5, 118.7, 128.2, 128.3, 128.5, 132.2, 135.3, 137.8, 150.2, 152.6, 166.1, 169.7; ESI-MS  $m/z$  468 [M+H]<sup>+</sup>, 485 [M+H<sub>2</sub>O]<sup>+</sup>, 490 [M+Na]<sup>+</sup>, 506 [M+K]<sup>+</sup>.

*2-(1-(4-tert-butoxycarbonylaminobenzylcarbamoyl)-4-oxoazetidin-2-yl) acetic acid (32)*

Following GP2 compound **31** (39 mg, 0.80 mmol) yielded compound **32** as a white solid (30 mg, 99%). Mp 78 – 81 °C; IR (film, cm<sup>-1</sup>) 3355, 1769, 1731, 1707, 1695; <sup>1</sup>H NMR (400 MHz, CD<sub>3</sub>OD)  $\delta$  (ppm) 1.51 (s, 9H), 2.73 (dd,  $J$  = 8.9, 16.5 Hz, 1H), 2.91 (dd,  $J$  = 2.6, 16.0 Hz, 1H), 3.13 (dd,  $J$  = 2.4, 16.5 Hz, 1H), 3.28 (dd,  $J$  = 5.6, 16.0 Hz, 1H), 4.28 – 4.31 (m, 1H), 4.34 – 4.36 (m, 2H), 7.21 (d,  $J$  = 8.4 Hz; 2H), 7.35 (d,  $J$  = 8.3 Hz; 2H); <sup>13</sup>C NMR (100 MHz, CD<sub>3</sub>OD)  $\delta$  (ppm) 28.7, 37.3, 43.2, 43.7, 43.8, 80.8, 119.9, 128.9, 133.9, 139.7, 152.4, 155.2, 168.1, 173.5; ESI-MS  $m/z$  376 [M-H]<sup>-</sup>.

*4-(2-(carboxymethyl)-4-oxoazetidine-1-carboxamidomethyl) benzenaminium trifluoroacetate (15)*

Following GP3 compound **32** (14 mg, 0.37 mmol) was treated with TFA (19.3  $\mu$ L, 0.259 mmol, 7 equiv) yielding compound **15** as a yellow oil (14 mg, 99%). IR (film, cm<sup>-1</sup>) 3365, 1771, 1703, 1679; <sup>1</sup>H NMR (400 MHz, CD<sub>3</sub>OD)  $\delta$  (ppm) 2.75 (dd,  $J$  = 8.7, 16.6 Hz, 1H), 2.93 (dd,  $J$  = 3.0, 16.1 Hz, 1H), 3.11 (dd,  $J$  = 3.7, 16.6 Hz, 1H), 3.27 (dd,  $J$  = 5.8, 16.1 Hz, 1H), 4.28 – 4.33 (m, 1H), 4.44 – 4.46 (m, 2H), 7.29 (d,  $J$  = 8.4 Hz, 2H), 7.45 (d,  $J$  = 8.4 Hz, 2H); <sup>13</sup>C NMR (100 MHz, CD<sub>3</sub>OD)  $\delta$  (ppm) 37.3, 43.2, 43.5, 48.6, 123.9, 130.1, 131.4, 141.2, 152.6, 168.1, 173.5; <sup>19</sup>F NMR (375 MHz, CD<sub>3</sub>OD)  $\delta$  (ppm) -77.0; ESI-MS  $m/z$  278 [M-TFA+H]<sup>+</sup>. Found C, 46.32; H, 3.98; N, 10.56 %; C<sub>15</sub>H<sub>16</sub>F<sub>3</sub>N<sub>3</sub>O<sub>6</sub> requires C, 46.04; H, 4.12; N, 10.74 %.

*Benzyl 2-(1-(benzylcarbamoyl)-4-oxoazetidin-2-yl)acetate (33)*

Following GP1B compound **13** (80 mg, 0.37 mmol) was treated with K<sub>2</sub>CO<sub>3</sub> (77 mg, 0.56 mmol) and benzylisocyanate (54  $\mu$ L, 0.44 mmol). Purification by flash-chromatography (CH<sub>2</sub>Cl<sub>2</sub>/diethyl ether 90:10) yielded compound **33** as a light yellow oil (96 mg, 74%). IR (film, cm<sup>-1</sup>) 3367, 1767, 1732, 1694; <sup>1</sup>H NMR (400 MHz, CDCl<sub>3</sub>)  $\delta$  (ppm) 2.69 (dd,  $J$  = 9.0, 16.5 Hz, 1H), 2.81 (dd,  $J$  = 2.9, 16.2 Hz, 1H), 3.22 (dd,  $J$  = 5.6, 16.2 Hz, 1H), 3.30 (dd,  $J$  = 4.0, 16.5 Hz, 1H), 4.31 – 4.36 (m, 1H), 4.37 – 4.46 (m, 2H), 5.09 (d,  $J_{AB}$  = 12.3 Hz, 1H), 5.13 (d,  $J_{AB}$  = 12.3 Hz, 1H), 6.82 (bt,  $J$  = 5.6 Hz, 1H), 7.22 – 7.36 (m, 10H); <sup>13</sup>C NMR (100 MHz,

CDCl<sub>3</sub>)  $\delta$  (ppm) 37.0, 42.4, 43.4, 47.0, 66.6, 127.4, 127.5, 128.2, 128.3, 128.5, 128.6, 135.3, 137.7, 150.3, 166.1, 169.6; ESI-MS  $m/z$  353 [M+H]<sup>+</sup>.

*2-(1-(benzylcarbamoyl)-4-oxoazetidin-2-yl)acetic acid (14)*

Following GP2 compound **33** (69 mg, 0.20 mmol) yielded compound **14** as a white solid (52 mg, 99%). Mp 100 – 103 °C; IR (film, cm<sup>-1</sup>) 3356, 1767, 1734, 1698; <sup>1</sup>H NMR (400 MHz, CDCl<sub>3</sub>)  $\delta$  (ppm) 2.65 (dd,  $J$  = 8.9, 16.8 Hz, 1H), 2.82 (dd,  $J$  = 2.3, 16.3 Hz, 1H), 3.21 – 3.29 (m, 2H), 4.31 – 4.34 (m, 1H), 4.37 – 4.47 (m, 2H), 6.92 (bt,  $J$  = 5.8 Hz, 1H), 7.23 – 7.32 (m, 5H), 7.50 (bs, 1H); <sup>13</sup>C NMR (100 MHz, CDCl<sub>3</sub>)  $\delta$  (ppm) 36.8, 42.6, 43.5, 47.1, 127.5, 127.6, 128.6, 137.5, 150.6, 166.4, 173.7; ESI-MS  $m/z$  261 [M-H]<sup>-</sup>. Found C, 59.41; H, 5.32; N, 10.59 %; C<sub>13</sub>H<sub>14</sub>N<sub>2</sub>O<sub>4</sub> requires C, 59.54; H, 5.38; N, 10.68 %.

*4-(2-(2-(benzyloxy)-2-oxoethyl)-4-oxoazetidine-carboxamido)phenyl methanaminium 2,2,2-trifluoroacetate (36)*

Following GP3 compound **35** (133 mg, 0.28 mmol) was treated with TFA (322  $\mu$ L, 4.32 mmol, 15.2 equiv) yielding compound **36** as a waxy white solid (136 mg, 99%). IR (film, cm<sup>-1</sup>) 3336, 1771, 1704, 1680; <sup>1</sup>H NMR (400 MHz, CDCl<sub>3</sub>)  $\delta$  (ppm) 2.81 (dd,  $J$  = 8.6, 16.5 Hz, 1H), 2.96 (dd,  $J$  = 2.6, 16.4 Hz, 1H), 3.30 – 3.38 (m, 2H), 4.25 (bs, 2H), 4.44 – 4.50 (m, 1H), 5.16 (s, 2H), 7.21 – 7.23 (m, 2H), 7.33 – 7.35 (m, 5H), 7.39 – 7.41 (m, 2H), 8.45 (bs, 1H), 8.77 (bs, 3H); <sup>13</sup>C NMR (100 MHz, CDCl<sub>3</sub>)  $\delta$  (ppm) 36.7, 42.5, 43.0, 47.6, 66.8, 120.4, 127.9, 128.2, 128.4, 128.5, 129.8, 135.2, 137.3, 147.9, 166.8, 169.9; ESI-MS  $m/z$  351 [M-TFA-NH<sub>3</sub>+H]<sup>+</sup>, 735 [2M-2TFA+H]<sup>+</sup>.

*Benzyl 2-(4-oxo-(4-(3-*o*-tolylureidomethyl)phenylcarbamoyl)azetidin-2-yl) acetate (37)*

Following GP1C, compound **36** (136 mg, 0.28 mmol, 1 equiv) in THF (2.4 mL) was treated with TEA (43  $\mu$ L, 0.31 mmol, 1.1 equiv) and *o*-tolylisocyanate (38  $\mu$ L, 0.31 mmol, 1.1 equiv). Purification by flash-chromatography (CH<sub>2</sub>Cl<sub>2</sub>/EtOAc 90:10 then 70:30) yielded compound **37** as a white solid (79 mg, 56%). Mp 184 – 187 °C; IR (film, cm<sup>-1</sup>) 3319, 1771 1712; <sup>1</sup>H NMR (400 MHz, CDCl<sub>3</sub>)  $\delta$  (ppm) 2.25 (s, 3H), 2.79 (dd,  $J$  = 8.8, 16.5 Hz, 1H), 2.94 (dd,  $J$  = 2.6, 16.3 Hz, 1H), 3.32 – 3.37 (m, 2H), 4.40 (bs, 2H), 4.42 – 4.47 (m, 1H), 5.15 (s, 2H), 6.21 (bs, 1H), 7.13 – 7.41 (m, 13H), 8.41 (bs, 1H); <sup>13</sup>C NMR (100 MHz, CDCl<sub>3</sub>)  $\delta$  (ppm) 17.8, 36.8, 42.7, 44.0, 47.5, 66.8, 119.9, 125.7, 126.3, 127.2, 128.2, 128.3, 128.4, 128.5, 128.6, 131.1, 132.2, 134.9, 135.3, 136.1, 156.6, 166.6, 169.6, 174.2; ESI-MS  $m/z$  501 [M+H]<sup>+</sup>, 523 [M+Na]<sup>+</sup>, 1001 [2M+H]<sup>+</sup>.

*2-(4-oxo-(4-(3-*o*-tolylureidomethyl)phenylcarbamoyl)azetidin-2-yl) acetic acid (16)*

Following GP2 compound **37** (79 mg, 0.158 mmol) yielded compound **16** as a white solid (64 mg, 99%). Mp 160 – 162 °C; IR (film, cm<sup>-1</sup>) 3319, 1774, 1707, 1629; <sup>1</sup>H NMR (400 MHz, CD<sub>3</sub>CN)  $\delta$  (ppm) 2.21 (s, 3H), 2.76 (dd,  $J$  = 6.0, 16.5 Hz, 1H), 2.93 (d,  $J$  = 16.0 Hz, 1H), 3.13 (d,  $J$  = 16.5 Hz, 1H), 3.28 (d,  $J$  = 16.0 Hz, 1H), 4.31 – 4.36 (m, 3H), 5.76 (bs, 1H), 6.68 (bs, 1H), 6.95 – 6.99 (m, 1H), 7.12 – 7.17 (m, 2H), 7.29 (d,  $J$  = 8.9 Hz, 2H), 7.44 (d,  $J$  = 7.6 Hz, 2H), 7.68 (d,  $J$  = 7.8 Hz, 1H), 8.45 (bs, 1H), 9.38 (bs, 1H); <sup>13</sup>C NMR (100 MHz, CD<sub>3</sub>OD)  $\delta$  (ppm) 18.0, 37.3, 43.3, 44.2, 49.3, 121.1, 124.9, 125.4, 127.4, 129.0, 131.4, 131.7, 137.1, 137.5, 138.1, 149.7, 158.8, 168.6, 173.5; ESI-MS  $m/z$  411 [M+H]<sup>+</sup>, 433 [M+Na]<sup>+</sup>, 821 [2M+H]<sup>+</sup>. Found C, 61.33; H, 5.35; N, 13.48 %; C<sub>21</sub>H<sub>22</sub>N<sub>4</sub>O<sub>5</sub> requires C, 61.46; H, 5.40; N, 13.65 %.

*Benzyl 2-(2-(4-oxo-(*o*-tolylcarbamoyl)azetidin-2-yl) acetamido) acetate (38)*

Following GP4B, compound **9** (98 mg, 0.374 mmol, 1 equiv) was treated with EDC (72 mg, 0.374 mmol, 1 equiv), glycine benzyl ester *p*-toluenesulfonate salt (189 mg, 561  $\mu$ mol, 1.5 equiv), TEA (84  $\mu$ L, 0.598 mmol, 1.6 equiv) and DMAP (46 mg, 0.374 mmol, 1 equiv). Purification by flash-chromatography (CH<sub>2</sub>Cl<sub>2</sub>/CH<sub>3</sub>CN 95:5 then 80:20) yielded compound **38** as a light yellow solid (85 mg, 56%). Mp 174 – 176 °C; IR (film, cm<sup>-1</sup>)

<sup>1</sup>) 3321, 1767, 1723, 1708, 1645; <sup>1</sup>H NMR (400 MHz, CDCl<sub>3</sub>)  $\delta$  (ppm) 2.30 (s, 3H), 2.78 (dd,  $J = 7.9, 14.9$  Hz, 1H), 3.14 – 3.21 (m, 2H), 3.34 (dd,  $J = 5.4, 16.4$  Hz, 1H), 4.02 (dd,  $J = 4.8, 18.4$  Hz, 1H), 4.11 (dd,  $J = 5.4, 18.4$  Hz, 1H), 4.43 – 4.48 (m, 1H), 5.16 (s, 2H), 6.43 (bt,  $J = 5.8$  Hz, 1H), 7.04 – 7.07 (m, 1H), 7.18 – 7.23 (m, 2H), 7.32 – 7.39 (m, 5H), 7.89 (d,  $J = 7.9$  Hz, 1H), 8.51 (bs, 1H); <sup>13</sup>C NMR (100 MHz, CDCl<sub>3</sub>)  $\delta$  (ppm) 17.7, 38.2, 41.3, 42.6, 48.4, 67.2, 121.2, 124.6, 126.7, 127.8, 128.4, 128.5, 128.6, 130.5, 135.0, 135.1, 148.5, 167.2, 169.2, 169.4; ESI-MS  $m/z$  410 [M+H]<sup>+</sup>, 432 [M+Na]<sup>+</sup>.

*2-(2-(4-oxo-(o-tolylcarbamoyl)azetidin-2-yl)acetamido) acetic acid (17)*

Following GP2 compound **38** (85 mg, 0.208 mmol) yielded compound **17** as a white solid (66 mg, 99%). Mp 182 – 185 °C; IR (film, cm<sup>-1</sup>) 3300, 1764, 1720, 1649; <sup>1</sup>H NMR (400 MHz, CD<sub>3</sub>OD)  $\delta$  (ppm) 2.28 (s, 3H), 2.74 (dd,  $J = 8.5, 14.8$  Hz, 1H), 3.08 – 3.16 (m, 2H), 3.29 – 3.37 (m, 1H), 3.88 (d,  $J_{AB} = 17.4$  Hz, 1H), 3.94 (d,  $J_{AB} = 17.4$  Hz, 1H), 4.39 – 4.47 (m, 1H), 7.03 – 7.07 (m, 1H), 7.16 – 7.22 (m, 2H), 7.81 (d,  $J = 7.5$  Hz, 1H), 8.63 (bs, 1H) <sup>13</sup>C NMR (100 MHz, CD<sub>3</sub>OD)  $\delta$  (ppm) 17.8, 38.8, 41.8, 43.1, 54.8, 122.9, 125.8, 127.6, 129.8, 131.5, 136.6, 150.0, 168.9, 172.3, 172.8; ESI-MS  $m/z$  318 [M-H]<sup>-</sup>, 637 [2M-H]<sup>-</sup>. Found C, 56.13; H, 5.51; N, 12.98 %; C<sub>15</sub>H<sub>17</sub>N<sub>3</sub>O<sub>5</sub> requires C, 56.42; H, 5.37; N, 13.16 %.

*Benzyl 3-(2-(4-oxo-(o-tolylcarbamoyl)azetidin-2-yl)acetamido) propanoate (39)*

Following GP4B, compound **9** (63 mg, 0.240 mmol, 1 equiv) was treated with EDC (46 mg, 0.240 mmol, 1 equiv), beta alanine benzylester *p*-toluenesulfonate salt (127 mg, 0.360 mmol, 1.5 equiv), TEA (54  $\mu$ L, 0.384 mmol, 1.6 equiv) and DMAP (29 mg, 0.240 mmol, 1 equiv). Purification by flash-chromatography (CH<sub>2</sub>Cl<sub>2</sub>/EtOAc 80:20 then 70:30) yielded compound **39** as a white waxy solid (61 mg, 60%). IR (film, cm<sup>-1</sup>) 3334, 1765, 1732, 1712, 1656; <sup>1</sup>H NMR (400 MHz, CDCl<sub>3</sub>)  $\delta$  (ppm) 2.29 (s, 3H), 2.51 – 2.64 (m, 3H), 3.07 (dd,  $J = 3.8, 15.1$  Hz, 1H), 3.12 (dd,  $J = 3.0, 16.4$  Hz, 1H), 3.32 (dd,  $J = 5.6, 16.4$  Hz, 1H), 3.48 – 3.57 (m, 2H), 4.36 – 4.41 (m, 1H), 5.06 (d,  $J_{AB} = 12.4$  Hz, 1H), 5.10 (d,  $J_{AB} = 12.4$  Hz, 1H), 6.44 (bs, 1H) 7.02 – 7.06 (m, 1H), 7.17 – 7.22 (m, 2H), 7.31 – 7.39 (m, 5H), 7.92 (d,  $J = 7.9$  Hz, 1H), 8.50 (bs, 1H); <sup>13</sup>C NMR (100 MHz, CDCl<sub>3</sub>)  $\delta$  (ppm) 17.6, 33.8, 34.8, 38.4, 42.6, 48.3, 66.4, 120.9, 124.4, 126.7, 127.5, 128.1, 128.3, 128.5, 130.4, 135.1, 135.5, 148.2, 167.2, 168.8, 172.0; ESI-MS  $m/z$  424 [M+H]<sup>+</sup>, 446 [M+Na]<sup>+</sup>.

*3-(2-(4-oxo-(o-tolylcarbamoyl)azetidin-2-yl)acetamido) propanoic acid (19)*

Following GP2 compound **39** (61 mg, 0.14 mmol) yielded compound **19** as a white solid (47 mg, 99%). Mp 175 – 178 °C; IR (film, cm<sup>-1</sup>) 3300, 1769, 1700, 1638; <sup>1</sup>H NMR (400 MHz, CD<sub>3</sub>OD)  $\delta$  (ppm) 2.27 (s, 3H), 2.47 – 2.56 (m, 2H), 2.64 (dd,  $J = 8.3, 14.7$  Hz, 1H), 3.00 – 3.08 (m, 2H), 3.29 – 3.36 (m, 1H), 3.40 – 3.48 (m, 2H), 4.38 – 4.43 (m, 1H), 7.03 – 7.06 (m, 1H), 7.16 – 7.22 (m, 2H), 7.81 (d,  $J = 8.0$  Hz, 1H), 8.19 (bs, 1H); <sup>13</sup>C NMR (100 MHz, CD<sub>3</sub>OD)  $\delta$  (ppm) 17.8, 34.5, 36.4, 39.3, 43.1, 49.8, 122.8, 125.8, 127.6, 129.7, 131.5, 136.6, 150.1, 159.4, 168.9, 172.1; ESI-MS  $m/z$  332 [M-H]<sup>-</sup>, 665 [2M-H]<sup>-</sup>. Found C, 57.58; H, 5.80; N, 12.45 %; C<sub>16</sub>H<sub>19</sub>N<sub>3</sub>O<sub>5</sub> requires C, 57.65; H, 5.75; N, 12.61 %.

*Benzyl 2-(2-(4-tert-butoxycarbonylamino)benzylcarbamoyl)-4-oxoazetidin-2-yl acetamido) acetate (40)*

Following GP4B, compound **32** (27 mg, 0.72 mmol, 1 equiv) was treated with DCC (16 mg, 0.79 mmol, 1.1 equiv), glycine benzylester *p*-toluenesulfonate salt (38 mg, 0.108 mmol, 1.5 equiv), TEA (16  $\mu$ L, 0.115 mmol, 1.6 equiv) and DMAP (2 mg, 0.014 mmol, 0.2 equiv). Purification by flash-chromatography (CH<sub>2</sub>Cl<sub>2</sub>/CH<sub>3</sub>CN 95:5 then 80:20) yielded compound **40** as a light yellow solid (27 mg, 72%). Mp 64 – 66 °C; IR (film, cm<sup>-1</sup>) 3355, 1766, 1724, 1707, 1691, 1671; <sup>1</sup>H NMR (400 MHz, CDCl<sub>3</sub>)  $\delta$  (ppm) 1.50 (s, 9H), 2.69 (dd,  $J = 8.0, 15.0$  Hz, 1H), 3.05 (dd,  $J = 3.0, 16.4$  Hz, 1H), 3.10 (dd,  $J = 3.8, 15.0$  Hz, 1H), 3.22 (dd,  $J = 5.6, 16.4$  Hz, 1H), 3.99 (dd,  $J_{AB} = 5.4, 18.2$  Hz, 1H), 4.05 (dd,  $J_{AB} = 5.5, 18.2$  Hz; 1H), 4.30 – 4.41 (m, 3H), 5.16 (s, 2H), 6.54 (bs, 1H), 6.66 (bs, 1H), 6.90 (bt,  $J = 5.9$  Hz, 1H), 7.17 – 7.22 (m, 2H), 7.28 – 7.39 (m, 7H); <sup>13</sup>C NMR (100 MHz,

CDCl<sub>3</sub>)  $\delta$  (ppm) 28.3, 38.4, 41.3, 42.6, 43.1, 48.0, 67.2, 80.6, 118.8, 128.3, 128.4, 128.5, 128.6, 132.2, 135.1, 137.8, 150.9, 152.7, 166.7, 169.3, 169.5; ESI-MS  $m/z$  525 [M+H]<sup>+</sup>, 542 [M+H<sub>2</sub>O]<sup>+</sup>, 547 [M+Na]<sup>+</sup>, 563 [M+K]<sup>+</sup>.

2-(2-(1-(4-*tert*-butoxycarbonylamino)benzyl)carbamoyl)-4-oxoazetidin-2-yl) acetamido) acetic acid (**41**)

Following GP2 compound **40** (22 mg, 0.042 mmol) yielded compound **41** as a white solid (18 mg, 99%). Mp 100 – 103 °C; IR (film, cm<sup>-1</sup>) 3350, 1768, 1717, 1694, 1682; <sup>1</sup>H NMR (400 MHz, CD<sub>3</sub>OD)  $\delta$  (ppm) 1.51 (s, 9H), 2.65 (dd,  $J$  = 8.6, 14.6 Hz, 1H), 2.95 – 3.03 (m, 1H), 3.05 – 3.14 (m, 1H), 3.24 (dd,  $J$  = 5.4, 16.0 Hz, 1H), 3.86 (d,  $J_{AB}$  = 19.9 Hz, 1H), 3.91 (d,  $J_{AB}$  = 19.9 Hz, 1H), 4.27 – 4.39 (m, 3H), 7.21 (d,  $J$  = 7.8 Hz, 2H), 7.35 (d,  $J$  = 7.8 Hz, 2H), 8.86 (bs, 1H); <sup>13</sup>C NMR (100 MHz, CDCl<sub>3</sub>)  $\delta$  (ppm) 28.7, 30.7, 39.1, 43.0, 43.8, 49.3, 80.8, 119.9, 129.0, 134.0, 139.8, 152.5, 155.3, 168.1, 172.3, 173.0; ESI-MS  $m/z$  435 [M+H]<sup>+</sup>, 457 [M+Na]<sup>+</sup>.

4-(2-(1-carboxymethyl-amidomethyl)-4-oxoazetidine-1-carboxamidomethyl) benzenaminium 2,2,2-trifluoroacetate (**18**)

Following GP3 compound **41** (19 mg, 0.044 mmol) was treated with TFA (23  $\mu$ L, 0.306 mmol, 7 equiv) yielding compound **18** as a yellow oil (18.5 mg, 95%). IR (film, cm<sup>-1</sup>) 3356, 1793, 1782, 1736, 1712, 1698; <sup>1</sup>H NMR (400 MHz, CD<sub>3</sub>OD)  $\delta$  (ppm) 2.68 (dd,  $J$  = 8.3, 14.8 Hz, 1H), 3.01 (dd,  $J$  = 2.8, 16.1 Hz, 1H), 3.07 (dd,  $J$  = 4.0, 14.8 Hz, 1H), 3.24 (dd,  $J$  = 5.7, 16.1 Hz, 1H), 3.85 – 3.94 (m, 2H), 4.31 – 4.38 (m, 1H), 4.43 (d,  $J_{AB}$  = 15.8 Hz, 1H), 4.48 (d,  $J_{AB}$  = 15.8 Hz, 1H), 7.33 (d,  $J$  = 8.3 Hz, 2H), 7.47 (d,  $J$  = 8.3 Hz, 2H); <sup>13</sup>C NMR (100 MHz, CD<sub>3</sub>OD)  $\delta$  (ppm) 30.7, 38.9, 42.9, 43.5, 49.3, 123.8, 130.1, 131.8, 141.0, 152.6, 168.1, 172.3, 172.8; <sup>19</sup>F NMR (375 MHz, CD<sub>3</sub>OD)  $\delta$  (ppm) -77.0; ESI-MS  $m/z$  335 [M-TFA+H]<sup>+</sup>. Found C, 45.28; H, 4.51; N, 12.35 %; C<sub>17</sub>H<sub>19</sub>F<sub>3</sub>N<sub>4</sub>O<sub>7</sub> requires C, 45.54; H, 4.27; N, 12.50 %.

Benzyl 3-(2-(1-(4-((*tert*-butoxycarbonyl)amino)benzyl)carbamoyl)-4-oxoazetidin-2-yl) acetamido)propanoate (**42**)

Following GP4B, compound **32** (62 mg, 0.164 mmol, 1 equiv) was treated with DCC (32 mg, 0.181 mmol, 1.1 equiv), beta alanine benzylester *p*-toluenesulfonate salt (86 mg, 0.246 mmol, 1.5 equiv), TEA (37  $\mu$ L, 0.262 mmol, 1.6 equiv) and DMAP (4 mg, 0.033 mmol, 0.2 equiv). Purification by flash-chromatography (EtOAc/CH<sub>2</sub>Cl<sub>2</sub> 70:30) yielded compound **42** as a light yellow waxy solid (65 mg, 74%). IR (film, cm<sup>-1</sup>) 3434, 1767, 1726, 1698, 1665; <sup>1</sup>H NMR (400 MHz, CDCl<sub>3</sub>)  $\delta$  (ppm) 1.50 (s, 9H), 2.49 – 2.61 (m, 3H), 2.96 – 3.02 (m, 2H), 3.19 (dd,  $J$  = 5.6, 16.3 Hz, 1H), 3.41 – 3.55 (m, 2H), 4.25 – 4.28 (m, 1H), 4.32 (dd,  $J$  = 5.8, 14.8 Hz, 1H), 4.37 (dd,  $J$  = 5.2, 14.8 Hz, 1H), 5.11 (s, 2H), 6.57 (bt,  $J$  = 5.8 Hz, 1H), 6.66 (bs, 1H), 6.88 (bt,  $J$  = 5.9 Hz, 1H), 7.18 (d,  $J$  = 8.4 Hz, 2H), 7.29 – 7.37 (m, 7H); <sup>13</sup>C NMR (100 MHz, CDCl<sub>3</sub>)  $\delta$  (ppm) 28.3, 33.9, 34.9, 38.7, 42.6, 43.1, 48.0, 66.5, 80.5, 118.8, 128.2, 128.3, 128.4, 128.6, 132.2, 135.5, 137.8, 150.7, 152.7, 166.7, 169.0, 172.0; ESI-MS  $m/z$  539 [M+H]<sup>+</sup>, 561 [M+Na]<sup>+</sup>.

3-(2-(1-(4-((*tert*-butoxycarbonyl)amino)benzyl)carbamoyl)-4-oxoazetidin-2-yl)acetamido) propanoic acid (**43**)

Following GP2 compound **42** (22 mg, 0.040 mmol) yielded compound **43** as a white solid (18 mg, 99%). Mp 77 – 79 °C; IR (film, cm<sup>-1</sup>) 3370, 1768, 1696, 1614; <sup>1</sup>H NMR (400 MHz, CD<sub>3</sub>OD)  $\delta$  (ppm) 1.51 (s, 9H), 2.49 (t,  $J$  = 6.6 Hz, 2H), 2.56 (dd,  $J$  = 8.4, 14.7 Hz, 1H), 2.92 (dd,  $J$  = 2.9, 16.1 Hz, 1H), 2.99 (dd,  $J$  = 4.3, 14.7 Hz, 1H), 3.23 (dd,  $J$  = 5.7, 16.1 Hz, 1H), 3.41 (t,  $J$  = 6.6 Hz, 2H), 4.27 – 4.30 (m, 1H), 4.33 – 4.39 (m, 2H), 7.21 (d,  $J$  = 8.5 Hz, 2H), 7.35 (d,  $J$  = 8.5 Hz, 2H); <sup>13</sup>C NMR (100 MHz, CD<sub>3</sub>OD)  $\delta$  (ppm) 28.7, 34.8, 36.4, 39.4, 43.0, 43.8, 49.4, 81.0, 119.9, 129.0, 134.0, 139.8, 152.4, 155.3, 168.1, 171.9; ESI-MS  $m/z$  449 [M+H]<sup>+</sup>, 471 [M+Na]<sup>+</sup>.



*4-((2-(2-((2-carboxyethyl)amino)-2-oxoethyl)-4-oxoazetidine-1-carboxamido)methyl) benzenaminium 2,2,2-trifluoroacetate (20)*

Following GP3 compound **43** (19 mg, 0.044 mmol) was treated with TFA (56  $\mu$ L, 0.756 mmol, 18 equiv) yielding compound **20** as a yellow oil (18 mg, 93%). IR (film,  $\text{cm}^{-1}$ ) 3406, 1768, 1676, 1655, 1648;  $^1\text{H}$  NMR (400 MHz,  $\text{CD}_3\text{OD}$ )  $\delta$  (ppm) 2.49 (t,  $J = 6.7$  Hz, 2H), 2.59 (dd,  $J = 8.1, 14.6$  Hz, 1H), 2.92 – 2.98 (m, 2H), 3.24 (dd,  $J = 5.7, 16.1$  Hz, 1H), 3.40 (t,  $J = 6.7$  Hz, 2H), 4.28 – 4.33 (m, 1H), 4.43 (d,  $J_{\text{AB}} = 15.5$  Hz, 1H), 4.48 (d,  $J_{\text{AB}} = 15.5$  Hz, 1H), 7.32 (d,  $J = 8.3$  Hz, 2H), 7.47 (d,  $J = 8.3$  Hz, 2H);  $^{13}\text{C}$  NMR (100 MHz,  $\text{CD}_3\text{OD}$ )  $\delta$  (ppm) 34.5, 36.3, 39.3, 42.9, 43.6, 49.4, 123.0, 129.7, 130.1, 139.7, 152.5, 168.1, 171.9, 175.2;  $^{19}\text{F}$  NMR (375 MHz,  $\text{CD}_3\text{OD}$ )  $\delta$  (ppm) -77.0; ESI-MS  $m/z$  461  $[\text{M}-\text{H}]^-$ . Found C, 46.89; H, 4.38; N, 12.00 %;  $\text{C}_{18}\text{H}_{21}\text{F}_3\text{N}_4\text{O}_7$  requires C, 46.76; H, 4.58; N, 12.12 %.

*Benzyl 3-(2-(1-(4-(((tert-butoxycarbonyl)amino)methyl)phenyl)carbamoyl)-4-oxoazetidin-2-yl)acetamido)propanoate (45)*

Following GP4B compound **44** (86 mg, 0.23 mmol, 1 equiv) was treated with DCC (52 mg, 0.25 mmol, 1.1 equiv), beta alanine benzylester *p*-toluenesulfonate salt (123 mg, 0.35 mmol, 1.5 equiv), TEA (52  $\mu$ L, 0.37 mmol, 1.6 equiv) and DMAP (6 mg, 0.046 mmol, 0.2 equiv) Purification by flash-chromatography ( $\text{CH}_2\text{Cl}_2/\text{EtOAc}$  80:20 then 50:50) yielded compound **45** as a light yellow waxy solid (88 mg, 71%). IR (film,  $\text{cm}^{-1}$ ) 3333, 1767, 1710, 1661, 1604;  $^1\text{H}$  NMR (400 MHz,  $\text{CDCl}_3$ )  $\delta$  (ppm) 1.44 (s, 9H), 2.54 – 2.60 (m, 3H), 3.04 (dd,  $J = 3.5, 14.8$  Hz, 1H), 3.08 (dd,  $J = 3.1, 16.3$  Hz, 1H), 3.28 (dd,  $J = 5.7, 16.4$  Hz, 1H), 3.50 (q,  $J = 6.1$  Hz, 2H), 4.21 – 4.25 (m, 2H), 4.33 – 4.38 (m, 1H), 4.89 (bt,  $J = 6.0$  Hz, 1H), 5.06 (s, 2H), 6.50 (bt,  $J = 5.8$  Hz, 1H), 7.20 (d,  $J = 8.3$  Hz, 2H), 7.30 – 7.35 (m, 5H), 7.39 (d,  $J = 8.3$  Hz, 1H), 8.48 (bs, 1H);  $^{13}\text{C}$  NMR (100 MHz,  $\text{CDCl}_3$ )  $\delta$  (ppm) 28.3, 33.9, 34.9, 38.5, 42.7, 44.1, 48.4, 66.5, 79.4, 119.9, 128.2, 128.2, 128.4, 128.6, 135.0, 135.5, 136.0, 148.0, 155.8, 167.1, 168.8, 172.1; ESI-MS  $m/z$  539  $[\text{M}+\text{H}]^+$ , 561  $[\text{M}+\text{Na}]^+$ .

*3-(2-(1-(4-(((tert-butoxycarbonyl)amino)methyl)phenyl)carbamoyl)-4-oxoazetidin-2-yl)acetamido)propanoic acid (46)*

Following GP2 compound **45** (79 mg, 0.150 mmol) yielded compound **46** as a waxy white solid (67 mg, 99%). IR (film,  $\text{cm}^{-1}$ ) 3346, 1773, 1740, 1710, 1688, 1655;  $^1\text{H}$  NMR (400 MHz,  $\text{CD}_3\text{OD}$ )  $\delta$  (ppm) 1.45 (s, 9H), 2.50 (t,  $J = 6.6$  Hz, 2H), 2.62 (dd,  $J = 14.8, 8.2$  Hz, 1H), 3.01 (ddd,  $J = 19.3, 15.5, 3.7$  Hz, 2H), 3.30 (dd,  $J = 5.8$  Hz, 1H), 3.43 (t,  $J = 6.7$  Hz, 2H), 4.18 (s, 2H), 4.34 – 4.43 (m, 1H), 7.23 (d,  $J = 8.4$  Hz, 2H), 7.43 (d,  $J = 8.4$  Hz, 2H);  $^{13}\text{C}$  NMR (100 MHz,  $\text{CD}_3\text{OD}$ )  $\delta$  (ppm) 28.8, 34.8, 36.5, 39.4, 43.1, 44.5, 49.6, 84.3, 121.1, 128.8, 136.9, 137.4, 149.7, 163.7, 168.5, 171.9, 175.6; ESI-MS  $m/z$  561  $[\text{M}+\text{TFA}-\text{H}]^-$ .

*(4-(2-(2-((2-carboxyethyl)amino)-2-oxoethyl)-4-oxoazetidine-1-carboxamido)phenyl) methanaminium 2,2,2-trifluoroacetate (21)*

Following GP3 compound **46** (60 mg, 0.13 mmol) was treated with TFA (174  $\mu$ L, 2.34 mmol, 18 equiv) yielding compound **21** as a white solid (51 mg, 87%). Mp 121 – 124  $^\circ\text{C}$ ; IR (film,  $\text{cm}^{-1}$ ) 3060, 1781, 1753, 1699, 1685, 1655;  $^1\text{H}$  NMR (400 MHz,  $\text{CD}_3\text{OD}$ )  $\delta$  (ppm) 2.52 (t,  $J = 6.7$  Hz, 2H), 2.66 (dd,  $J = 7.9, 14.9$  Hz, 1H), 2.98 – 3.04 (m, 2H), 3.33 – 3.35 (m, 1H), 3.43 (t,  $J = 6.7$  Hz, 2H), 4.08 (s, 2H), 4.39 – 4.42 (m, 1H), 7.41 (d,  $J = 8.5$  Hz, 2H), 7.59 (d,  $J = 8.5$  Hz, 2H), 8.88 (bs, 1H);  $^{13}\text{C}$  NMR (100 MHz,  $\text{CD}_3\text{OD}$ )  $\delta$  (ppm) 34.6, 36.4, 39.3, 43.1, 43.9, 49.8, 121.3, 121.4, 129.9, 130.9, 139.6, 149.5, 168.5, 172.1, 175.2;  $^{19}\text{F}$  NMR (375 MHz,  $\text{CD}_3\text{OD}$ )  $\delta$  (ppm) -77.0; ESI-MS  $m/z$  461  $[\text{M}-\text{H}]^-$ . Found C, 46.58; H, 4.76; N, 11.84 %;  $\text{C}_{18}\text{H}_{21}\text{F}_3\text{N}_4\text{O}_7$  requires C, 46.76; H, 4.58; N, 12.12 %.

### 3.10.4 Synthesis of other $\beta$ -lactam based integrin ligands

Compounds **34** and **53** were synthesized according to previously reported procedures by our research group.<sup>155,39f</sup> Compounds **52**, **61**, **69**, **73** are known and were synthesized according to reported procedures;<sup>155,188,189,244,245</sup> spectroscopic data are in accordance to those reported in literature. Optical purity of compounds synthesized from *D*-aspartic acid was assessed by chiral-HPLC analysis on compound **74** chosen as a model using a Chiralpack IA column, eluent: isopropanol/*n*-hexane 50:50, flow = 0.5 mL/min, temperature = 40 °C.

#### *Benzyl (S)-1-(2-methylbenzoyl)-4-oxoazetidine-2-carboxylate (65)*

Benzyl (*S*)-4-oxoazetidine-2-carboxylate (62 mg, 0.30 mmol, 1 equiv) was dissolved in anhydrous CH<sub>2</sub>Cl<sub>2</sub> (1.5 mL) under nitrogen. TEA (135  $\mu$ L, 0.96 mmol, 3.2 equiv), DMAP (4 mg, 0.03 mmol, 0.1 equiv) were then added, followed by dropwise addition of *o*-toluoylchloride (78  $\mu$ L, 0.6 mmol, 2 equiv) at 0 °C. After 10 minutes, the solution was warmed and stirred at room temperature until a complete consumption of the starting  $\beta$ -lactam (6 h, TLC monitoring). The mixture was quenched with a saturated solution of NH<sub>4</sub>Cl and extracted with CH<sub>2</sub>Cl<sub>2</sub> (3  $\times$  10 mL). The organic layers were collected, dried over Na<sub>2</sub>SO<sub>4</sub>, concentrated in vacuum and purified by flash-chromatography (cyclohexane/EtOAc 70:30), yielding compound **65** as a colorless oil (100 mg, 93%). IR (film, cm<sup>-1</sup>) 3031, 2962, 2928, 1805, 1746, 1684, 1490; [ $\alpha$ ]<sub>D</sub><sup>20</sup> = -78 (c = 1.2, CH<sub>2</sub>Cl<sub>2</sub>); <sup>1</sup>H NMR (400 MHz, CDCl<sub>3</sub>)  $\delta$  (ppm) 7.52 (d, *J* = 7.5 Hz, 1H), 7.44 – 7.35 (m, 6H), 7.26 (t, *J* = 7.2 Hz, 2H), 5.30 (d, *J*<sub>AB</sub> = 12.2 Hz, 1H), 5.26 (d, *J*<sub>AB</sub> = 12.1 Hz, 1H), 4.68 (dd, *J* = 6.8, 3.5 Hz, 1H), 3.34 (dd, *J* = 16.1, 6.8 Hz, 1H), 3.07 (dd, *J* = 16.1, 3.5 Hz, 1H), 2.41 (s, 3H); <sup>13</sup>C NMR (100 MHz, CDCl<sub>3</sub>)  $\delta$  (ppm) 169.0, 165.8, 161.3, 137.4, 134.7, 132.1, 131.6, 130.8, 128.7, 128.64, 128.57, 128.4, 125.4, 67.7, 48.7, 40.4, 19.5; ESI-MS (R<sub>t</sub> = 10.2 min) *m/z* 324 [M+H]<sup>+</sup>.

#### *(S)-1-(2-methylbenzoyl)-4-oxoazetidine-2-carboxylic acid (58)*

Following GP2, compound **65** (80 mg, 0.25 mmol) yielded compound **58** as a waxy solid (53 mg, 91%). IR (film, cm<sup>-1</sup>) 2967, 2930, 1806, 1728, 1686, 1603; [ $\alpha$ ]<sub>D</sub><sup>20</sup> = -81 (c = 1.0, CH<sub>2</sub>Cl<sub>2</sub>); <sup>1</sup>H NMR (400 MHz, CD<sub>3</sub>OD)  $\delta$  (ppm) 7.49 (d, *J* = 7.7 Hz, 1H), 7.39 (t, *J* = 7.5 Hz, 1H), 7.27 – 7.21 (m, 2H), 4.59 (dd, *J* = 7.0, 3.4 Hz, 1H), 3.41 (dd, *J* = 16.1, 7.0 Hz, 1H), 3.05 (dd, *J* = 16.1, 3.4 Hz, 1H), 2.40 (s, 3H); <sup>13</sup>C NMR (100 MHz, CD<sub>3</sub>OD)  $\delta$  (ppm) 172.9, 167.7, 164.0, 138.1, 134.4, 132.2, 131.7, 129.4, 126.5, 50.4, 41.5, 19.5; ESI-MS (R<sub>t</sub> = 6.3 min) *m/z* 234 [M+H]<sup>+</sup>.

#### *Benzyl 2-(1-(2-methylbenzoyl)-4-oxoazetidin-2-yl)acetate (66)*

Following the procedure reported for **65**, compound **13** (50 mg, 0.23 mmol, 1 equiv) was treated with TEA (103  $\mu$ L, 0.73 mmol, 3.2 equiv), DMAP (3 mg, 0.023 mmol, 0.1 equiv) and *o*-toluoylchloride (60  $\mu$ L, 0.46 mmol, 2 equiv). Purification by flash-chromatography (cyclohexane/EtOAc 70:30) yielded compound **66** as a colorless oil (60 mg, 77%). IR (film, cm<sup>-1</sup>) 2958, 2929, 1796, 1734, 1676, 1511, 1456; <sup>1</sup>H NMR (400 MHz, CDCl<sub>3</sub>)  $\delta$  (ppm) 7.44 – 7.32 (m, 7H), 7.25 – 7.22 (m, 2H), 5.19 (d, *J*<sub>AB</sub> = 12.3 Hz, 1H), 5.15 (d, *J*<sub>AB</sub> = 12.2 Hz, 1H), 4.56 – 4.50 (m, 1H), 3.37 – 3.25 (m, 2H), 2.94 (dd, *J* = 16.6, 3.6 Hz, 1H), 2.85 (dd, *J* = 16.3, 8.4 Hz, 1H), 2.40 (s, 3H); <sup>13</sup>C NMR (100 MHz, CDCl<sub>3</sub>)  $\delta$  (ppm) 169.7, 166.8, 163.0, 137.0, 135.3, 132.7, 131.3, 130.8, 128.6, 128.58, 128.45, 128.36, 125.4, 66.8, 46.6, 42.1, 36.8, 19.6; ESI-MS (R<sub>t</sub> = 7.6 min) *m/z* 338 [M+H]<sup>+</sup>.

#### *2-(1-(2-methylbenzoyl)-4-oxoazetidin-2-yl)acetic acid (56)*

Following GP2, compound **66** (32 mg, 0.09 mmol) yielded compound **56** as a waxy solid (22 mg, 99%). IR (film, cm<sup>-1</sup>) 2960, 2857, 1795, 1704, 1677, 1430; <sup>1</sup>H NMR (400 MHz, CD<sub>3</sub>OD)  $\delta$  (ppm) 7.45 (d, *J* = 7.7 Hz, 1H), 7.39 (t, *J* = 7.5 Hz, 1H), 7.24 (dd, *J* = 14.4, 7.3 Hz, 2H), 4.47 (ddd, *J* = 10.2, 7.6, 3.6 Hz, 1H), 3.30 (dd, *J* = 16.1, 6.4 Hz, 1H), 3.13 (dd, *J* = 16.3, 3.7 Hz, 1H), 3.01 (dd, *J* = 16.3, 3.7 Hz, 1H), 2.85 (dd, *J* = 16.3, 8.3 Hz,

1H), 2.38 (s, 3H); <sup>13</sup>C NMR (100 MHz, CD<sub>3</sub>OD) δ (ppm) 174.0, 168.7, 165.6, 137.7, 135.0, 132.0, 131.6, 129.4, 126.5, 48.6, 43.0, 37.2, 19.5; ESI-MS (R<sub>t</sub> = 5.1 min) *m/z* 248 [M+H]<sup>+</sup>.

#### *Benzyl (2-(4-oxoazetidin-2-yl)acetyl)glycinate (68)*

Following GP4B compound **67** (76 mg, 0.59 mmol, 1 equiv) was treated with DCC (16 mg, 0.79 mmol, 1.1 equiv), glycine benzylester chloridrate salt (179 mg, 0.89 mmol, 1.5 equiv), TEA (132 μL, 0.94 mmol, 1.6 equiv) and DMAP (14 mg, 0.12 mmol, 0.2 equiv). Purification by flash-chromatography (CH<sub>2</sub>Cl<sub>2</sub>/EtOAc 60:40 then EtOAc 100%) yielded compound **68** as a colorless oil (68 mg, 42%). IR (film, cm<sup>-1</sup>) 3300, 2954, 1742, 1657, 1562, 1411. <sup>1</sup>H NMR (400 MHz, CDCl<sub>3</sub>) δ (ppm) 7.37 – 7.31 (m, 5H), 6.99 (bs, 1H), 6.72 (bs, 1H), 5.16 (d, *J* = 12.3 Hz, 1H), 5.12 (d, *J* = 12.3 Hz, 1H), 4.15 (dd, *J* = 18.1, 6.1 Hz, 1H), 3.97 – 3.95 (m, 1H), 3.91 (dd, *J* = 18.1, 5.0 Hz, 1H), 3.09 (dd, *J* = 14.8, 3.2 Hz, 1H), 2.68 – 2.55 (m, 2H), 2.45 (dd, *J* = 14.4, 9.4 Hz, 1H); <sup>13</sup>C NMR (100 MHz, CDCl<sub>3</sub>) δ (ppm) 170.7, 170.1, 167.5, 134.9, 128.6, 128.5, 128.3, 67.2, 44.8, 43.3, 41.5, 41.1; ESI-MS (R<sub>t</sub> = 10.5 min) *m/z* 277 [M+H]<sup>+</sup>.

#### *(2-(4-oxoazetidin-2-yl)acetyl)glycine (54)*

Following GP2, compound **68** (68 mg, 0.25 mmol) yielded compound **54** as a waxy solid (42 mg, 91%). IR (film, cm<sup>-1</sup>) 3316, 2927, 1730, 1636, 1534, 1476; <sup>1</sup>H NMR (400 MHz, CD<sub>3</sub>OD) δ (ppm) 3.98 – 3.94 (m, 1H), 3.93 (d, *J* = 18.0, 1H), 3.89 (d, *J* = 18.0 Hz, 1H), 3.10 (dd, *J* = 15.0, 4.9 Hz, 1H), 2.69 (dd, *J* = 15.0, 1.9 Hz, 1H), 2.66 – 2.55 (m, 2H); <sup>13</sup>C NMR (100 MHz, CD<sub>3</sub>OD) δ (ppm) 173.23, 173.21, 170.4, 45.9, 43.6, 42.1, 41.8.

#### *2-oxo-N-(o-tolyl)azetidine-1-carboxamide (55)*

Following GP1A, 2-azetidinone (50 mg, 0.7 mmol, 1 equiv) was treated with NaHMDSA (1M in THF, 875 μL, 1.25 equiv) and *o*-tolylisocyanate (108 μL, 0.875 mmol, 1.25 equiv) for 30 minutes. Purification by flash-chromatography (cyclohexane/EtOAc 60:40) yielded compound **55** as a colorless oil (60 mg, 42%). IR (film, cm<sup>-1</sup>) 3298, 2919, 1762, 1710, 1614, 1552, 1459; <sup>1</sup>H NMR (400 MHz, CDCl<sub>3</sub>) δ (ppm) 8.44 (bs, 1H), 7.95 (d, *J* = 8.0 Hz, 1H), 7.23 – 7.17 (m, 2H), 7.04 (t, *J* = 7.4 Hz, 1H), 3.72 (t, *J* = 4.8 Hz, 2H), 3.12 (t, *J* = 4.8 Hz, 2H), 2.30 (s, 3H); <sup>13</sup>C NMR (100 MHz, CDCl<sub>3</sub>) δ (ppm) 167.4, 147.9, 135.3, 130.3, 127.4, 126.7, 124.3, 121.0, 37.3, 36.0, 17.6; ESI-MS (R<sub>t</sub> = 6.8 min) *m/z* 205 [M+H]<sup>+</sup>.

#### *Benzyl (o-tolylcarbamoyl)-L-prolinate (70)*

Following GP1C, benzyl-*L*-prolinate trifluoroacetate salt **69** (82 mg, 0.26 mmol, 1 equiv) was treated with TEA (73 μL, 0.52 mmol, 2 equiv) and *o*-tolylisocyanate (36 μL, 0.29 mmol, 1.1 equiv). Purification by flash-chromatography (cyclohexane/EtOAc 50:50) yielded compound **70** as a colorless oil (63 mg, 72%). IR (film, cm<sup>-1</sup>) 3313, 2971, 1743, 1640, 1524, 1455; [α]<sub>D</sub><sup>20</sup> = – 56 (*c* = 1.1, CH<sub>2</sub>Cl<sub>2</sub>); <sup>1</sup>H NMR (400 MHz, CDCl<sub>3</sub>) δ (ppm) 7.73 (d, *J* = 8.0 Hz, 1H), 7.36 – 7.29 (m, 5H), 7.18 – 7.12 (m, 2H), 6.99 (t, *J* = 7.4 Hz, 1H), 6.34 (bs, 1H), 5.22 (d, *J*<sub>AB</sub> = 12.4 Hz, 1H), 5.14 (d, *J*<sub>AB</sub> = 12.4 Hz, 1H), 4.55 (dd, *J* = 8.1, 2.3 Hz, 1H), 3.61 – 3.48 (m, 2H), 2.20 (s, 3H), 2.16 – 1.99 (m, 4H); <sup>13</sup>C NMR (100 MHz, CDCl<sub>3</sub>) δ (ppm) 172.6, 154.1, 136.7, 135.5, 130.1, 128.4, 128.24, 128.16, 128.0, 126.5, 123.7, 122.4, 66.8, 59.3, 46.1, 29.6, 24.4, 17.6; ESI-MS (R<sub>t</sub> = 9.4 min) *m/z* 338 [M+H]<sup>+</sup>.

#### *(o-tolylcarbamoyl)-L-proline (57)*

Following GP2, compound **70** (60 mg, 0.18 mmol) yielded compound **57** as a waxy solid (44 mg, 99%). IR (film, cm<sup>-1</sup>) 3423, 2927, 1720, 1709, 1639, 1527, 1457; [α]<sub>D</sub><sup>20</sup> = – 47 (*c* = 1.0, CH<sub>3</sub>OH). <sup>1</sup>H NMR (400 MHz, CD<sub>3</sub>OD) δ (ppm) 7.38 (d, *J* = 7.8 Hz, 1H), 7.17 (d, *J* = 7.5 Hz, 1H), 7.12 (t, *J* = 7.4 Hz, 1H), 7.02 (t, *J* = 7.3 Hz, 1H), 4.31 (t, *J* = 5.9 Hz, 1H), 3.61 – 3.56 (m, 2H), 2.27 (s, 3H), 2.17 – 1.91 (m, 4H); <sup>13</sup>C NMR (100 MHz,

CD<sub>3</sub>OD)  $\delta$  (ppm) 177.0, 157.6, 138.1, 134.9, 131.3, 127.5, 127.1, 126.6, 60.8, 47.5, 31.0, 25.4, 18.2; ESI-MS ( $R_t = 3.3$  min)  $m/z$  249 [M+H]<sup>+</sup>.

*Benzyl (o-tolylcarbamoyl)glycinate (71)*

Following GP1C, glycine benzylester chlorohydrate salt (70 mg, 0.35 mmol, 1 equiv) was treated with TEA (108  $\mu$ L, 0.77 mmol, 2.2 equiv) and *o*-tolylisocyanate (43  $\mu$ L, 0.35 mmol, 1 equiv), yielding compound **71** without further purification as a waxy solid (71 mg, 68%). IR (film, cm<sup>-1</sup>) 3339, 3307, 2957, 1736, 1719, 1636, 1567, 1447; <sup>1</sup>H NMR (400 MHz, CD<sub>3</sub>CN)  $\delta$  (ppm) 7.61 (d,  $J = 8.0$  Hz, 1H), 7.42 – 7.30 (m, 5H), 7.19 – 7.12 (m, 2H), 7.00 (t,  $J = 7.2$  Hz, 1H), 6.83 (bs, 1H), 5.70 (bs, 1H), 5.16 (s, 2H), 3.94 (d,  $J = 5.9$  Hz, 2H), 2.22 (s, 3H); <sup>13</sup>C NMR (100 MHz, CD<sub>3</sub>CN)  $\delta$  (ppm) 172.8, 156.5, 138.4, 137.3, 131.1, 130.0, 129.3, 128.9, 128.8, 127.1, 124.2, 123.4, 66.7, 36.5, 18.0; ESI-MS ( $R_t = 8.3$  min)  $m/z$  299 [M+H]<sup>+</sup>.

*(o-tolylcarbamoyl)glycine (59)*

Following GP2, compound **71** (70 mg, 0.23 mmol) yielded compound **59** as a waxy solid (47 mg, 99%). IR (film, cm<sup>-1</sup>) 3411, 3263, 2988, 1707, 1614, 1598, 1459; <sup>1</sup>H NMR (400 MHz, CD<sub>3</sub>OD)  $\delta$  (ppm) 7.50 (d,  $J = 7.9$  Hz, 1H), 7.18 – 7.11 (m, 2H), 7.01 (t,  $J = 7.4$  Hz, 1H), 3.92 (s, 2H), 2.26 (s, 3H); <sup>13</sup>C NMR (100 MHz, CD<sub>3</sub>CN)  $\delta$  (ppm) 172.8, 157.2, 136.6, 130.4, 130.0, 126.0, 124.0, 123.5, 35.3, 16.6; ESI-MS ( $R_t = 2.5$  min)  $m/z$  209 [M+H]<sup>+</sup>.

*Benzyl 3-(3-(o-tolyl)ureido)propanoate (72)*

Following GP1C, beta alanine benzylester *p*-toluenesulfonate salt (70 mg, 0.2 mmol, 1 equiv) was treated with TEA (56  $\mu$ L, 0.4 mmol, 2 equiv) and *o*-tolylisocyanate (27  $\mu$ L, 0.22 mmol, 1.1 equiv). Purification by flash-chromatography (cyclohexane/EtOAc 60:40) yielded **72** as a colorless oil (47 mg, 76%). IR (film, cm<sup>-1</sup>) 3308, 3066, 2954, 1727, 1632, 1566, 1456; <sup>1</sup>H NMR (400 MHz, CD<sub>3</sub>CN)  $\delta$  (ppm) 7.63 (d,  $J = 8.0$  Hz, 1H), 7.37 – 7.31 (m, 5H), 7.16 – 7.10 (m, 2H), 6.96 (t,  $J = 7.0$  Hz, 1H), 6.79 (bs, 1H), 5.68 (bs, 1H), 5.11 (s, 2H), 3.43 (q,  $J = 6.4$  Hz, 2H), 2.56 (t,  $J = 6.4$  Hz, 2H), 2.25 (s, 3H); <sup>13</sup>C NMR (100 MHz, CD<sub>3</sub>CN)  $\delta$  (ppm) 173.0, 156.7, 138.5, 137.4, 131.2, 130.2, 129.5, 129.04, 128.95, 127.2, 124.4, 123.6, 66.9, 36.6, 35.7, 18.2; ESI-MS ( $R_t = 8.4$  min)  $m/z$  313 [M+H]<sup>+</sup>.

*3-(3-(o-tolyl)ureido)propanoic acid (60)*

Following GP2, compound **72** (45 mg, 0.14 mmol) yielded compound **60** as a waxy solid (30 mg, 97%). IR (film, cm<sup>-1</sup>) 3303, 3032, 2954, 1715, 1632, 1573, 1418; <sup>1</sup>H NMR (400 MHz, CD<sub>3</sub>OD)  $\delta$  (ppm) 7.48 (d,  $J = 7.9$  Hz, 1H), 7.16 – 7.11 (m, 2H), 7.00 (t,  $J = 7.8$  Hz, 1H), 3.45 (t,  $J = 6.3$  Hz, 2H), 2.53 (t,  $J = 6.3$  Hz, 2H), 2.23 (s, 3H); <sup>13</sup>C NMR (100 MHz, CD<sub>3</sub>OD)  $\delta$  (ppm) 175.8, 158.8, 138.1, 131.9, 131.4, 127.4, 125.4, 125.0, 36.8, 35.6, 18.0; ESI-MS ( $R_t = 2.6$  min)  $m/z$  223 [M+H]<sup>+</sup>.

*Benzyl (R)-4-oxo-1-(o-tolylcarbamoyl)azetidine-2-carboxylate (74)*

Following GP1C, compound **73** (80 mg, 0.39 mmol, 1 equiv) was treated with TEA (66  $\mu$ L, 0.47 mmol, 1.2 equiv) and *o*-tolylisocyanate (58  $\mu$ L, 0.47 mmol, 1.2 equiv). Purification by flash-chromatography (CH<sub>2</sub>Cl<sub>2</sub>/diethyl ether 95:5) yielded **74** as a waxy solid (112 mg, 85%). IR (film, cm<sup>-1</sup>) 3346, 3031, 2924, 1776, 1751, 1718, 1614, 1593, 1387; [ $\alpha$ ]<sub>D</sub><sup>20</sup> = + 96 (c = 1.0, CH<sub>2</sub>Cl<sub>2</sub>); <sup>1</sup>H NMR (400 MHz, CDCl<sub>3</sub>)  $\delta$  (ppm) 8.29 (bs, 1H), 7.93 (d,  $J = 8.0$  Hz, 1H), 7.41 – 7.31 (m, 5H), 7.25 – 7.15 (m, 2H), 7.07 (t,  $J = 7.4$  Hz, 1H), 5.30 (d,  $J_{AB} = 12.2$  Hz, 1H), 5.25 (d,  $J_{AB} = 12.2$  Hz, 1H), 4.62 (dd,  $J = 6.2, 2.9$  Hz, 1H), 3.40 (dd,  $J = 15.8, 6.2$  Hz, 1H), 3.11 (dd,  $J = 15.8, 2.9$  Hz, 1H), 2.31 (s, 3H); <sup>13</sup>C NMR (100 MHz, CDCl<sub>3</sub>)  $\delta$  (ppm) 168.8, 165.2, 146.8, 135.0, 134.7, 130.4, 128.65, 128.61, 128.3, 127.7, 126.8, 124.7, 121.2, 67.8, 48.9, 41.2, 17.6; ESI-MS ( $R_t = 10.5$  min)  $m/z$  339 [M+H]<sup>+</sup>.

*(R)*-4-oxo-1-(*o*-tolylcarbamoyl)azetidine-2-carboxylic acid (**62**)

Following GP2, compound **74** (105 mg, 0.31 mmol) yielded compound **62** as a white solid (74 mg, 97%). Mp 121 – 123 °C; IR (film, cm<sup>-1</sup>) 3344, 3024, 2966, 2962, 1775, 1717, 1615, 1593, 1459; [ $\alpha$ ]<sub>D</sub><sup>20</sup> = + 114 (c = 1.2, CH<sub>2</sub>Cl<sub>2</sub>); <sup>1</sup>H NMR (400 MHz, CDCl<sub>3</sub>)  $\delta$  (ppm) 8.37 (bs, 1H), 8.19 (bs, 1H), 7.86 (d, *J* = 8.4 Hz, 1H), 7.18 – 7.15 (m, 2H), 7.05 (t, *J* = 7.4 Hz, 1H), 4.59 (dd, *J* = 6.2, 2.2 Hz, 1H), 3.37 (dd, *J* = 16.0, 6.2 Hz, 1H), 3.20 (dd, *J* = 16.0, 2.2 Hz, 1H), 2.28 (s, 3H); <sup>13</sup>C NMR (100 MHz, CDCl<sub>3</sub>)  $\delta$  (ppm) 172.0, 165.7, 147.9, 134.6, 130.5, 128.0, 126.8, 125.1, 121.5, 49.7, 41.3, 17; ESI-MS (R<sub>t</sub> = 5.9 min) *m/z* 249 [M+H]<sup>+</sup>.

*Benzyl (R)*-3-(4-oxo-1-(*o*-tolylcarbamoyl)azetidine-2-carboxamido)propanoate (**75**)

Following GP4A, compound **62** (69 mg, 0.28 mmol, 1 equiv) was treated with oxalyl chloride (29  $\mu$ L, 0.34 mmol, 1.2 equiv), beta alanine benzylester *p*-toluenesulfonate salt (98 mg, 0.28 mmol, 1 equiv), TEA (157  $\mu$ L, 1.12 mmol, 4 equiv) and DMAP (7 mg, 0.056 mmol, 0.2 equiv). Purification by flash-chromatography (cyclohexane/EtOAc 60:40), yielded **75** as a colorless oil (56 mg, 50%). IR (film, cm<sup>-1</sup>) 3339, 2957, 1773, 1730, 1678, 1615, 1593, 1459; [ $\alpha$ ]<sub>D</sub><sup>20</sup> = + 102 (c = 0.9, CH<sub>2</sub>Cl<sub>2</sub>); <sup>1</sup>H NMR (400 MHz, CDCl<sub>3</sub>)  $\delta$  (ppm) 8.46 (bs, 1H), 7.89 (d, *J* = 8.4 Hz, 1H), 7.73 (bs, 1H), 7.35 – 7.29 (m, 5H), 7.22 – 7.18 (m, 2H), 7.07 (t, *J* = 7.4 Hz, 1H), 5.11 (s, 2H), 4.54 (dd, *J* = 6.1, 3.1 Hz, 1H), 3.66 – 3.54 (m, 2H), 3.46 (dd, *J* = 16.3, 3.1 Hz, 1H), 3.26 (dd, *J* = 16.3, 6.1 Hz, 1H), 2.63 (t, *J* = 6.2 Hz, 2H), 2.30 (s, 3H); <sup>13</sup>C NMR (100 MHz, CDCl<sub>3</sub>)  $\delta$  (ppm) 171.6, 167.5, 166.8, 148.6, 135.5, 134.7, 130.5, 128.5, 128.22, 128.16, 128.0, 126.7, 124.9, 121.4, 66.5, 51.7, 40.3, 35.3, 33.9, 17.6; ESI-MS (R<sub>t</sub> = 9.2 min) *m/z* 410 [M+H]<sup>+</sup>.

*(R)*-3-(4-oxo-1-(*o*-tolylcarbamoyl)azetidine-2-carboxamido)propanoic acid (**63**)

Following GP2, compound **75** (46 mg, 0.11 mmol) yielded compound **63** as a waxy solid (34 mg, 97%). IR (film, cm<sup>-1</sup>) 3352, 1779, 1734, 1708, 1648, 1595, 1550, 1458; [ $\alpha$ ]<sub>D</sub><sup>20</sup> = + 57 (c = 0.7, CH<sub>3</sub>OH); <sup>1</sup>H NMR (400 MHz, CDCl<sub>3</sub>)  $\delta$  (ppm) 8.46 (bs, 1H), 7.83 – 7.81 (m, 2H), 7.21 – 7.18 (m, 2H), 7.07 (t, *J* = 7.4 Hz, 1H), 4.59 (dd, *J* = 6.0, 3.1 Hz, 1H), 3.63 – 3.52 (m, 2H), 3.44 (dd, *J* = 16.2, 3.1 Hz, 1H), 3.24 (dd, *J* = 16.2, 6.0 Hz, 1H), 2.59 (t, *J* = 5.6 Hz, 2H), 2.29 (s, 3H); <sup>13</sup>C NMR (100 MHz, CD<sub>3</sub>OD)  $\delta$  (ppm) 175.3, 171.0, 168.0, 149.4, 136.4, 131.5, 129.9, 127.6, 126.0, 123.0, 51.6, 42.1, 36.7, 34.5, 17.7; ESI-MS (R<sub>t</sub> = 4.3 min) *m/z* 320 [M+H]<sup>+</sup>.

*Benzyl (R)*-1-((4-(((*tert*-butoxycarbonyl)amino)methyl)phenyl)carbamoyl)-4-oxoazetidine-2-carboxylate (**76**)

Following GP1C, compound **73** (70 mg, 0.34 mmol, 1 equiv) was treated with TEA (84  $\mu$ L, 0.60 mmol, 1.5 equiv) and the freshly prepared isocyanate **34** (1.5 equiv). Purification by flash-chromatography (cyclohexane/EtOAc 50:50) yielded compound **76** as a colorless oil (110 mg, 60%). IR (film, cm<sup>-1</sup>) 3344, 2975, 1777, 1751, 1708, 1603, 1542, 1317; [ $\alpha$ ]<sub>D</sub><sup>20</sup> = + 62 (c = 0.8, CH<sub>2</sub>Cl<sub>2</sub>); <sup>1</sup>H NMR (400 MHz, CDCl<sub>3</sub>)  $\delta$  (ppm) 8.27 (bs, 1H), 7.42 (d, *J* = 8.4 Hz, 2H), 7.33 – 7.28 (m, 5H), 7.23 (d, *J* = 8.4 Hz, 2H), 5.28 (d, *J*<sub>AB</sub> = 12.2 Hz, 1H), 5.23 (d, *J*<sub>AB</sub> = 12.2 Hz, 1H), 4.86 (bs, 1H), 4.59 (dd, *J* = 6.2, 2.9 Hz, 1H), 4.27 – 4.25 (m, 2H), 3.38 (dd, *J* = 15.8, 6.2 Hz, 1H), 3.08 (dd, *J* = 15.8, 2.9 Hz, 1H), 1.45 (s, 9H); <sup>13</sup>C NMR (400 MHz, CDCl<sub>3</sub>)  $\delta$  (ppm) 168.8, 165.0, 155.8, 146.6, 135.8, 135.1, 134.7, 128.64, 128.62, 128.3, 128.2, 119.9, 79.4, 67.8, 48.9, 44.1, 41.2, 28.4; ESI-MS (R<sub>t</sub> = 10.4 min) *m/z* 471 [M+H]<sup>+</sup>.

*(R)*-1-((4-(((*tert*-butoxycarbonyl)amino)methyl)phenyl)carbamoyl)-4-oxoazetidine-2-carboxylic acid (**77**)

Following GP2, compound **76** (110 mg, 0.24 mmol) yielded compound **77** as a waxy solid (78 mg, 88%). IR (film, cm<sup>-1</sup>) 3341, 2978, 2932, 1776, 1707, 1604, 1544, 1417; [ $\alpha$ ]<sub>D</sub><sup>20</sup> = + 45 (c = 1.0, CH<sub>2</sub>Cl<sub>2</sub>); <sup>1</sup>H NMR (400 MHz, CD<sub>3</sub>OD)  $\delta$  (ppm) 7.43 (d, *J* = 8.4 Hz, 2H), 7.23 (d, *J* = 8.4 Hz, 2H), 4.51 (dd, *J* = 6.4, 2.9 Hz, 1H), 4.19 – 4.17 (m, 2H), 3.45 (dd, *J* = 15.8, 6.4 Hz, 1H), 3.08 (dd, *J* = 15.8, 2.9 Hz, 1H), 1.45 (s, 9H); <sup>13</sup>C NMR (100 MHz, CD<sub>3</sub>OD)  $\delta$  (ppm) 173.3, 167.3, 158.4, 149.0, 137.2, 137.0, 128.8, 121.2, 80.2, 50.8, 44.5, 42.1, 28.8; ESI-MS (R<sub>t</sub> = 7.1 min) *m/z* 381 [M+H<sub>2</sub>O]<sup>+</sup>, 386 [M+Na]<sup>+</sup>.

*(R)*-(4-(2-carboxy-4-oxoazetidine-1-carboxamido)phenyl)methanaminium 2,2,2-trifluoroacetate (**64**)

Following GP3, compound **77** (72 mg, 0.19 mmol, 1 equiv) was treated with TFA (261  $\mu$ L, 3.42 mmol, 18 equiv), yielding compound **64** as a waxy solid (67 mg, 94%). IR (film,  $\text{cm}^{-1}$ ) 3417, 3301, 2969, 1781, 1743, 1708, 1666, 1604, 1549, 1421;  $[\alpha]_{\text{D}}^{20} = +96$  ( $c=1.1$ ,  $\text{CH}_3\text{OH}$ );  $^1\text{H}$  NMR (400 MHz,  $\text{CD}_3\text{OD}$ )  $\delta$  (ppm) 7.57 (d,  $J = 8.4$  Hz, 2H), 7.41 (d,  $J = 8.4$  Hz, 2H), 4.61 – 4.59 (m, 1H), 4.08 – 4.06 (m, 2H), 3.50 (dd,  $J = 15.7$ , 5.6 Hz, 1H), 3.12 (d,  $J = 15.7$  Hz, 1H);  $^{13}\text{C}$  NMR (100 MHz,  $\text{CD}_3\text{OD}$ )  $\delta$  (ppm) 171.9, 167.1, 148.8, 139.4, 130.9, 130.2, 121.5, 43.8, 43.6, 42.1;  $^{19}\text{F}$  NMR (375 MHz,  $\text{CD}_3\text{OD}$ )  $\delta$  (ppm) -76.7; ESI-MS ( $R_t = 1.3$  min)  $m/z$  247  $[\text{M}+\text{H}]^+$ .

### 3.10.5 Synthesis of fluorescent $\beta$ -lactam compounds

*Benzyl 2-((2R,3S)-3-((R)-1-((tert-butyldimethylsilyl)oxy)ethyl)-4-oxoazetidin-2-yl)acetate (81)*

Following the procedure reported for **13**, commercially available (2R,3R)-3-((R)-1-((tert-butyldimethylsilyl)oxy)ethyl)-4-oxoazetidin-2-yl acetate **1.O** (250 mg, 0.87 mmol, 1 equiv) was treated with benzyl bromoacetate (0.56 mL, 3.48 mmol, 4 equiv). Purification by flash-chromatography (cyclohexane/EtOAc 75:25 then 70:30) yielded compound **81** as a white solid (258 mg, 79%). Spectroscopic data are in accordance with those reported in literature.<sup>246</sup> Mp 91 – 92  $^{\circ}\text{C}$ ;  $^1\text{H}$  NMR (400 MHz,  $\text{CDCl}_3$ )  $\delta$  (ppm) 7.40 – 7.28 (m, 5H), 6.01 (bs, 1H), 5.13 (s, 2H), 4.20 – 4.13 (m, 1H), 4.01 – 3.94 (m, 1H), 2.79 (d,  $J = 3.4$  Hz, 1H), 2.75 (d,  $J = 3.7$  Hz, 1H), 2.59 (dd,  $J = 16.4$ , 9.9 Hz, 1H), 1.17 (d,  $J = 6.3$  Hz, 3H), 0.85 (s, 9H), 0.05 (d,  $J = 1.1$  Hz, 6H); ESI-MS ( $R_t = 12.5$  min)  $m/z$  378  $[\text{M}+\text{H}]^+$ .

*Benzyl 2-((2R,3S)-3-((R)-1-((tert-butyldimethylsilyl)oxy)ethyl)-4-oxo-1-(o-tolylcarbamoyl)azetidin-2-yl)acetate (82)*

Following GP1C compound **81** (80 mg, 0.21 mmol, 1 equiv) was treated with TEA (148  $\mu$ L, 1.05 mmol, 5 equiv) and *o*-tolylisocyanate (130  $\mu$ L, 1.05 mmol, 5 equiv). Purification by flash-chromatography (cyclohexane/EtOAc 90:10) yielded compound **82** as a colorless oil (100 mg, 93%). IR (film,  $\text{cm}^{-1}$ ) 3341, 2955, 2930, 2857, 1766, 1737, 1718, 1548, 1459;  $[\alpha]_{\text{D}}^{20} = -72$  ( $c = 1.0$ ,  $\text{CH}_2\text{Cl}_2$ );  $^1\text{H}$  NMR (400 MHz,  $\text{CDCl}_3$ )  $\delta$  (ppm) 8.41 (bs, 1H), 7.91 (d,  $J = 8.1$  Hz, 1H), 7.38 – 7.29 (m, 5H), 7.20 (dd,  $J = 14.3$ , 7.3 Hz, 2H), 7.05 (t,  $J = 7.3$  Hz, 1H), 5.16 (s, 2H), 4.61 – 4.58 (m, 1H), 4.35 – 4.29 (m, 1H), 3.22 (dd,  $J = 15.6$ , 3.9 Hz, 2H), 2.93 (dd,  $J = 15.5$ , 7.7 Hz, 1H), 2.27 (s, 3H), 1.20 (d,  $J = 6.3$  Hz, 3H), 0.84 (s, 9H), 0.08 (s, 3H), 0.06 (s, 3H);  $^{13}\text{C}$  NMR (100 MHz,  $\text{CDCl}_3$ )  $\delta$  (ppm) 169.7, 168.2, 147., 135.4, 135.3, 130.3, 128.5, 128.4, 128.3, 127.5, 126.7, 124.3, 121.1, 66.7, 64.7, 62.6, 49.5, 36.9, 25.5, 22.0, 17.8, 17.6, -4.2, -5.3; ESI-MS ( $R_t = 18.1$  min)  $m/z$  511  $[\text{M}+\text{H}]^+$ .

*Benzyl 2-((2R,3S)-3-((R)-1-hydroxyethyl)-4-oxo-1-(o-tolylcarbamoyl)azetidin-2-yl)acetate (83)*

$\text{BF}_3 \cdot \text{OEt}_2$  (35  $\mu$ L, 0.28 mmol, 1.15 equiv) was added to a solution of  $\beta$ -lactam **82** (124 mg, 0.24 mmol, 1 equiv) in  $\text{CH}_3\text{CN}$  (5 mL) at 0  $^{\circ}\text{C}$  under nitrogen atmosphere. After 30 minutes, the reaction was allowed to warm to room temperature and stirred until a complete consumption of the starting material (2 h, TLC monitoring). The mixture was then quenched with phosphate buffer (0.1M, pH 7.4, 10 mL) and extracted with  $\text{CH}_2\text{Cl}_2$  ( $3 \times 15$  mL). The organic layers were collected, dried over  $\text{Na}_2\text{SO}_4$  and concentrated in vacuum. The crude was purified by flash-chromatography (cyclohexane/EtOAc 70:30) yielding compound **83** as a colorless oil (76 mg, 91%). IR (film,  $\text{cm}^{-1}$ ) 3475, 3340, 2971, 1764, 1735, 1715, 1548, 1459;  $[\alpha]_{\text{D}}^{20} = -81$  ( $c = 1.0$ ,  $\text{CH}_2\text{Cl}_2$ );  $^1\text{H}$  NMR (400 MHz,  $\text{CDCl}_3$ )  $\delta$  (ppm) 8.43 (bs, 1H), 7.93 (d,  $J = 7.9$  Hz, 1H), 7.41 – 7.28 (m, 5H), 7.20 (dd,  $J = 15.0$ , 7.2 Hz, 2H), 7.04 (t,  $J = 7.5$  Hz, 1H), 5.19 (d,  $J_{\text{AB}} = 12.2$  Hz, 1H), 5.16 (d,  $J_{\text{AB}} = 12.2$  Hz, 1H), 4.38 (dt,  $J = 9.8$ , 3.2 Hz, 1H), 4.21 (dq,  $J = 12.7$ , 6.3 Hz, 1H), 3.52 (dd,  $J = 17.1$ , 3.6 Hz, 1H), 3.12 (dd,  $J = 7.9$ , 2.6 Hz, 1H), 2.77 (dd,  $J = 17.1$ , 9.8 Hz, 1H), 2.28 (s, 3H), 1.37 (d,  $J = 6.3$  Hz, 3H);  $^{13}\text{C}$  NMR (100 MHz,  $\text{CDCl}_3$ )  $\delta$  (ppm) 171.2, 166.9, 147.7, 135.2, 135.0, 130.4, 128.6, 128.5, 128.4, 127.3, 126.8, 124.5, 120.8, 67.2, 65.8, 63.5, 51.9, 36.4, 21.1, 17.6. ESI-MS ( $R_t = 10.0$  min)  $m/z$  397  $[\text{M}+\text{H}]^+$ .

*(R)-1-((2R,3S)-2-(2-(benzyloxy)-2-oxoethyl)-4-oxo-1-(o-tolylcarbamoyl)azetidin-3-yl)ethyl 2-oxo-2H-chromene-3-carboxylate (84)*

To a solution of alcohol **83** (60 mg, 0.15 mmol, 1 equiv) in CH<sub>2</sub>Cl<sub>2</sub> (2.5 mL) under nitrogen atmosphere, coumarin 3-carboxylic acid (46 mg, 0.24 mmol, 1.6 equiv) and DMAP (4 mg, 0.03 mmol, 0.2 equiv) were added. The mixture was then cooled to 0 °C and DCC (50 mg, 0.24 mmol, 1.6 equiv) was added; the system was allowed to reach room temperature in 15 minutes and left under stirring overnight. After 24 h (TLC monitoring) the reaction mixture was filtered washing with CH<sub>2</sub>Cl<sub>2</sub> (5 mL) and evaporated. The crude was suspended in EtOAc and the solid residual dicyclohexylurea was eliminated by filtration. The organic layer was concentrated in vacuum and purified by flash-chromatography (cyclohexane/EtOAc 70:30) yielding compound **84** as a colorless oil (50 mg, 59%). IR (film, cm<sup>-1</sup>) 3341, 3036, 2956, 2925, 2854, 1766, 1736, 1710, 1611, 1593, 1458; [α]<sub>D</sub><sup>20</sup> = -46 (c = 1.1, CH<sub>2</sub>Cl<sub>2</sub>); <sup>1</sup>H NMR (400 MHz, CDCl<sub>3</sub>) δ (ppm) 8.50 (s, 1H), 8.38 (bs, 1H), 7.94 (d, *J* = 8.1 Hz, 1H), 7.63 (t, *J* = 7.9 Hz, 1H), 7.55 (d, *J* = 7.8 Hz, 1H), 7.37 – 7.26 (m, 6H), 7.24 – 7.12 (m, 2H), 7.04 (t, *J* = 7.5 Hz, 1H), 5.54 (quintet, *J* = 6.4 Hz, 1H), 5.13 (s, 2H), 4.64 – 4.54 (m, 1H), 3.54 (dd, *J* = 6.4, 1.9 Hz, 1H), 3.36 (dd, *J* = 16.3, 3.6 Hz, 1H), 2.99 (dd, *J* = 16.3, 7.9 Hz, 1H), 2.25 (s, 3H), 1.52 (d, *J* = 6.4 Hz, 3H); <sup>13</sup>C NMR (100 MHz, CDCl<sub>3</sub>) δ (ppm) 169.6, 166.2, 162.2, 156.2, 155.2, 149.1, 147.6, 135.3, 135.2, 134.5, 130.3, 129.6, 128.5, 128.34, 128.27, 127.4, 126.7, 124.8, 124.4, 121.0, 117.8, 117.7, 16.7, 69.1, 66.7, 59.8, 51.5, 36.3, 18.2, 17.6; ESI-MS (R<sub>t</sub> = 12.1 min) *m/z* 569 [M+H]<sup>+</sup>.

*N-(9-(2-(((R)-1-((2R,3S)-2-(2-(benzyloxy)-2-oxoethyl)-4-oxo-1-(o-tolylcarbamoyl)azetidin-3-yl)ethoxy)carbonyl)phenyl)-6-(diethylamino)-3H-xanthen-3-ylidene)-N-ethylethanaminium chloride (85)*

Following the procedure reported for **84**, alcohol **83** (57 mg, 0.14 mmol, 1 equiv) was treated with Rhodamine B (67 mg, 0.14 mmol, 1 equiv), DMAP (3.4 mg, 0.03 mmol, 0.2 equiv) and DCC (29 mg, 0.14 mmol, 1 equiv). Purification by column chromatography (CH<sub>2</sub>Cl<sub>2</sub>:EtOAc 50:50 then EtOAc 100% then EtOAc:CH<sub>3</sub>OH 80:20) yielded compound **85** as a purple solid (72 mg, 60%). IR (film, cm<sup>-1</sup>) 3338, 3062, 2976, 2929, 2855, 1766, 1720, 1647, 1592, 1548, 1413; <sup>1</sup>H NMR (400 MHz, CDCl<sub>3</sub>) δ (ppm) 8.27 (bs, 1H), 8.20 (d, *J* = 7.8 Hz, 1H), 7.83 (t, *J* = 8.6 Hz, 2H), 7.70 (t, *J* = 7.7 Hz, 1H), 7.36 – 7.27 (m, 6H), 7.23 – 7.15 (m, 2H), 7.10 – 7.01 (m, 3H), 6.90 – 6.82 (m, 3H), 6.79 (d, *J* = 9.5 Hz, 1H), 5.30 – 5.22 (m, 1H), 5.07 (s, 2H), 4.17 – 4.11 (m, 1H), 3.68 – 3.53 (m, 8H), 3.31 (dd, *J* = 6.2, 2.7 Hz, 1H), 3.15 (dd, *J* = 16.3, 4.0 Hz, 1H), 2.77 (dd, *J* = 16.4, 8.2 Hz, 1H), 2.18 (s, 3H), 1.29 (t, *J* = 6.9 Hz, 12H), 1.14 (d, *J* = 6.4 Hz, 3H); <sup>13</sup>C NMR (100 MHz, CDCl<sub>3</sub>) δ (ppm) 169.2, 165.8, 164.0, 158.0, 157.6, 157.5, 155.5, 155.3, 147.3, 142.1, 135.2, 134.9, 133.5, 133.3, 131.1, 131.03, 131.01, 130.44, 130.38, 130.37, 129.7, 128.5, 128.4, 128.2, 127.4, 126.7, 124.6, 122.7, 120.9, 114.4, 114.1, 113.34, 113.30, 96.3, 68.3, 66.7, 59.9, 51.2, 46.1, 36.3, 17.7, 17.5, 12.6; ESI-MS (R<sub>t</sub> = 9.1 min) *m/z* 821 [M-Cl]<sup>+</sup>.

*N-(9-(2-(((R)-1-((2R,3S)-2-(carboxymethyl)-4-oxo-1-(o-tolylcarbamoyl)azetidin-3-yl)ethoxy)carbonyl)phenyl)-6-(diethylamino)-3H-xanthen-3-ylidene)-N-ethylethanaminium chloride (78)*

Following GP2 compound **85** (38 mg, 0.04 mmol) yielded compound **78** as a purple solid (31 mg, 92%). IR (film, cm<sup>-1</sup>) 3341, 2975, 2931, 1765, 1716, 1648, 1590, 1339; <sup>1</sup>H NMR (400 MHz, CD<sub>3</sub>OD) δ (ppm) 8.25 (d, *J* = 7.7 Hz, 1H), 7.83 (t, *J* = 7.5 Hz, 1H), 7.74 (dd, *J* = 15.2, 7.7 Hz, 2H), 7.43 (d, *J* = 7.4 Hz, 1H), 7.20 – 7.14 (m, 3H), 7.09 – 6.98 (m, 6H), 5.34 – 5.28 (m, 1H), 3.93 – 3.90 (m, 1H), 3.70 – 3.60 (m, 8H), 3.32 – 3.30 (m, 1H), 2.94 (dd, *J* = 14.9, 3.6 Hz, 1H), 2.45 (dd, *J* = 14.9, 8.7 Hz, 1H), 2.17 (s, 3H), 1.32 – 1.28 (m, 12H), 0.99 (d, *J* = 6.4 Hz, 3H); <sup>13</sup>C NMR (100 MHz, CD<sub>3</sub>OD) δ (ppm) 171.0, 167.1, 166.4, 164.6, 157.6, 157.5, 155.6, 155.4, 138.5, 135.1, 132.7, 131.5, 131.1, 130.9, 130.5, 130.3, 129.8, 129.2, 127.4, 126.6, 124.3, 124.2, 120.8, 114.8, 114.1, 113.4, 113.2, 106.0, 96.7, 69.5, 61.0, 55.2, 52.4, 46.8, 34.7, 17.7, 17.5, 12.8; ESI-MS (R<sub>t</sub> = 8.0 min) *m/z* 731 [M-Cl]<sup>+</sup>.

*2-((2R,3S)-3-((R)-1-((tert-butyldimethylsilyl)oxy)ethyl)-4-oxo-1-(o-tolylcarbamoyl)azetid-2-yl)acetic acid (86)*

Following GP2 compound **82** (88 mg, 0.17 mmol) yielded compound **86** as a colorless oil (67 mg, 94%). IR (film,  $\text{cm}^{-1}$ ) 3335, 2956, 2930, 2857, 1768, 1741, 1716, 1550, 1253;  $[\alpha]_{\text{D}}^{20} = -52$  ( $c = 1.0$ ,  $\text{CH}_3\text{OH}$ );  $^1\text{H}$  NMR (400 MHz,  $\text{CDCl}_3$ )  $\delta$  (ppm) 8.44 (bs, 1H), 7.87 (d,  $J = 8.0$  Hz, 1H), 7.19 (dd,  $J = 13.1, 7.2$  Hz, 2H), 7.05 (t,  $J = 7.4$  Hz, 1H), 4.61 – 4.53 (m, 1H), 4.34 (dd,  $J = 6.2, 3.0$  Hz, 1H), 3.25 (dd,  $J = 16.1, 4.4$  Hz, 1H), 3.21 – 3.19 (m, 1H), 2.90 (dd,  $J = 16.1, 7.6$  Hz, 1H), 2.28 (s, 3H), 1.25 (d,  $J = 6.3$  Hz, 3H), 0.84 (s, 9H), 0.08 (s, 3H), 0.06 (s, 3H);  $^{13}\text{C}$  NMR (100 MHz,  $\text{CDCl}_3$ )  $\delta$  (ppm) 174.9, 168.3, 148.1, 135.1, 130.4, 127.9, 126.8, 124.6, 121.4, 64.7, 62.8, 49.3, 36.8, 25.6, 22.0, 17.8, 17.6, -4.2, -5.3; ESI-MS ( $R_t = 5.9$  min)  $m/z$  421  $[\text{M}+\text{H}]^+$ .

*Benzyl 2-(2-((2R,3S)-3-((R)-1-((tert-butyldimethylsilyl)oxy)ethyl)-4-oxo-1-(o-tolylcarbamoyl)azetid-2-yl)acetamido)acetate (87)*

Following GP4B compound **86** (111 mg, 0.26 mmol, 1 equiv) was treated with DCC (56 mg, 0.27 mmol, 1.1 equiv), glycine benzylester chloridrate salt (79 mg, 0.39 mmol, 1.5 equiv), TEA (59  $\mu\text{L}$ , 0.42 mmol, 1.6 equiv) and DMAP (6 mg, 0.052 mmol, 0.2 equiv). Purification by flash-chromatography (cyclohexane/EtOAc 70:30) yielded compound **7** as a colorless oil (94 mg, 69%). IR (film,  $\text{cm}^{-1}$ ) 3333, 2955, 2930, 2857, 1764, 1748, 1714, 1678, 1548, 1460;  $[\alpha]_{\text{D}}^{20} = -36$  ( $c = 1.0$ ,  $\text{CH}_2\text{Cl}_2$ );  $^1\text{H}$  NMR (400 MHz,  $\text{CDCl}_3$ )  $\delta$  (ppm) 8.52 (bs, 1H), 7.85 (d,  $J = 8.0$  Hz, 1H), 7.38 – 7.27 (m, 5H), 7.21 – 7.17 (m, 2H), 7.05 (t,  $J = 7.4$  Hz, 1H), 6.72 (bt,  $J = 4.8$  Hz, 1H), 5.15 (d,  $J_{\text{AB}} = 12.5$  Hz, 1H), 5.11 (d,  $J_{\text{AB}} = 13.2$  Hz, 1H), 4.56 (dd,  $J = 7.5, 5.0$  Hz, 1H), 4.33 (dd,  $J = 6.2, 2.8$  Hz, 1H), 4.10 (dd,  $J = 18.2, 5.9$  Hz, 1H), 3.94 (dd,  $J = 18.2, 5.2$  Hz, 1H), 3.50 (t,  $J = 2.8$  Hz, 1H), 3.00 – 2.89 (m, 2H), 2.28 (s, 3H), 1.23 (d,  $J = 6.3$  Hz, 3H), 0.84 (s, 9H), 0.08 (s, 3H), 0.06 (s, 3H);  $^{13}\text{C}$  NMR (100 MHz,  $\text{CDCl}_3$ )  $\delta$  (ppm) 169.3 (2C), 168.6, 148.8, 135.2, 135.1, 130.4, 128.5, 128.4, 128.3, 128.1, 126.6, 124.5, 121.4, 67.1, 64.7, 62.1, 50.1, 41.3, 38.3, 25.6, 21.9, 17.8, 17.6, -4.2, -5.3; ESI-MS ( $R_t = 12.0$  min)  $m/z$  568  $[\text{M}+\text{H}]^+$ .

*Benzyl 2-(2-((2R,3S)-3-((R)-1-hydroxyethyl)-4-oxo-1-(o-tolylcarbamoyl)azetid-2-yl)acetamido)acetate (88)*

Following the procedure reported for **83**,  $\beta$ -lactam **87** (94 mg, 0.17 mmol, 1 equiv) was treated with  $\text{BF}_3 \cdot \text{OEt}_2$  (25  $\mu\text{L}$ , 0.20 mmol, 1.15 equiv). Purification by column chromatography ( $\text{CH}_2\text{Cl}_2/\text{EtOAc}$  50:50) yielded compound **88** as a white solid (58 mg, 75%). IR (film,  $\text{cm}^{-1}$ ) 3442, 3289, 2968, 2922, 2855, 1741, 1705, 1636, 1498;  $[\alpha]_{\text{D}}^{20} = -54$  ( $c = 1.0$ ,  $\text{CH}_2\text{Cl}_2$ );  $^1\text{H}$  NMR (400 MHz,  $\text{CDCl}_3$ )  $\delta$  (ppm) 8.48 (bs, 1H), 7.90 (d,  $J = 8.0$  Hz, 1H), 7.35 (m, 5H), 7.20 (dd,  $J = 11.9, 7.6$  Hz, 2H), 7.05 (t,  $J = 7.4$  Hz, 1H), 6.51 (d,  $J = 5.4$  Hz, 1H), 5.18 (s, 2H), 4.34 (dt,  $J = 10.3, 2.9$  Hz, 1H), 4.18 (dq,  $J = 9.3, 6.0$  Hz, 2H), 4.07 (dd,  $J = 5.4, 2.1$  Hz, 2H), 3.48 (dd,  $J = 16.2, 3.2$  Hz, 1H), 3.19 (dd,  $J = 9.0, 2.7$  Hz, 1H), 2.65 (dd,  $J = 16.1, 10.3$  Hz, 1H), 2.29 (s, 3H), 1.38 (d,  $J = 6.1$  Hz, 3H);  $^{13}\text{C}$  NMR (100 MHz,  $\text{CDCl}_3$ )  $\delta$  (ppm) 170.3, 169.3, 167.1, 148.2, 135.1, 134.9, 130.5, 128.7, 128.6, 128.4, 127.6, 126.8, 124.6, 121.0, 67.4, 66.2, 64.0, 53.0, 41.4, 37.3, 21.3, 17.6; ESI-MS ( $R_t = 8.8$  min)  $m/z$  454  $[\text{M}+\text{H}]^+$ .

*N-(9-(2-(((R)-1-((2R,3S)-2-(2-((2-benzyloxy)-2-oxoethyl)amino)-2-oxoethyl)-4-oxo-1-(o-tolylcarbamoyl)azetid-3-yl)ethoxy)carbonyl)phenyl)-6-(diethylamino)-3H-xanthen-3-ylidene)-N-ethylethanaminium chloride (89)*

Following the procedure reported for **84**, alcohol **88** (77 mg, 0.17 mmol, 1 equiv) was treated with Rhodamine B (81 mg, 0.17 mmol, 1 equiv), DMAP (4 mg, 0.034 mmol, 0.2 equiv) and DCC (35 mg, 0.19 mmol, 1.1 equiv). Purification by column chromatography ( $\text{CH}_2\text{Cl}_2/\text{EtOAc}$  50:50 then EtOAc 100% then EtOAc: $\text{CH}_3\text{OH}$  80:20) yielded compound **89** as a purple solid (55 mg, 35%). IR (film,  $\text{cm}^{-1}$ ) 3339, 3059, 2978, 2932, 1762, 1717, 1648, 1590, 1414;  $^1\text{H}$  NMR (400 MHz,  $\text{CDCl}_3$ )  $\delta$  (ppm) 8.92 (bt,  $J = 5.8$  Hz, 1H), 8.33 (bs, 1H), 8.17 (dd,  $J = 7.8, 1.1$  Hz, 1H), 7.83 (d,  $J = 7.3$  Hz, 1H), 7.69 (td,  $J = 7.5, 1.4$  Hz, 1H), 7.63 (td,  $J = 7.7, 1.3$  Hz, 1H), 7.30 – 7.21 (m, 6H), 7.14 – 7.05 (m, 4H), 6.96 (td,  $J = 7.5, 1.1$  Hz, 1H), 6.85 – 6.79 (m, 3H), 6.75 (d,  $J = 2.4$



H<sub>z</sub>, 1H), 5.19 (dt, *J* = 12.2, 6.2 Hz, 1H), 5.03 (s, 2H), 3.95 – 3.88 (m, 3H), 3.68 (dd, *J* = 5.3, 2.7 Hz, 1H), 3.61 – 3.50 (m, 8H), 3.14 (dd, *J* = 14.4, 3.4 Hz, 1H), 2.91 (dd, *J* = 14.4, 9.0 Hz, 1H), 2.16 (s, 3H), 1.29 – 1.19 (m, 12H), 0.98 (d, *J* = 6.4 Hz, 3H); <sup>13</sup>C NMR (100 MHz, CDCl<sub>3</sub>) δ (ppm) 169.6, 169.6, 166.6, 164.3, 158.0, 157.6, 157.4, 155.5, 155.3, 147.4, 135.5, 135.3, 132.8, 132.6, 131.3, 131.1, 130.8, 130.5, 130.4, 130.2, 129.9, 128.3, 128.0, 127.4, 126.5, 124.1, 120.9, 114.5, 114.2, 113.3, 113.2, 105.9, 96.4, 96.3, 68.5, 66.4, 59.2, 52.1, 46.0, 45.9, 41.1, 37.2, 17.5, 17.3, 12.4; ESI-MS (*R*<sub>t</sub> = 8.8 min) *m/z* 878 [M-Cl]<sup>+</sup>.

*N*-(9-(2-(((*R*)-1-((2*R*,3*S*)-2-(2-((carboxymethyl)amino)-2-oxoethyl)-4-oxo-1-(*o*-tolylcarbamoyl)azetidin-3-yl)ethoxy)carbonyl)phenyl)-6-(diethylamino)-3*H*-xanthen-3-ylidene)-*N*-ethylethanaminium chloride (**79**)

Following GP2 compound **89** (55 mg, 0.06 mmol) yielded compound **79** as a purple solid (44 mg, 83%). IR (film, cm<sup>-1</sup>) 3337, 3063, 2977, 2931, 1764, 1716, 1748, 1550, 1462; <sup>1</sup>H NMR (400 MHz, CD<sub>3</sub>OD) δ (ppm) 8.22 (d, *J* = 7.6 Hz, 1H), 7.84 (t, *J* = 7.2 Hz, 1H), 7.74 (dd, *J* = 14.5, 7.6 Hz, 2H), 7.43 (d, *J* = 7.3 Hz, 1H), 7.20 – 6.92 (m, 9H), 5.33 – 5.27 (m, 1H), 3.91 – 3.81 (m, 3H), 3.68 – 3.60 (m, 8H), 3.48 – 3.44 (m, 1H), 3.00 (dd, *J* = 14.5, 3.6 Hz, 1H), 2.61 (dd, *J* = 14.5, 8.7 Hz, 1H), 2.15 (s, 3H), 1.29 (t, *J* = 6.8 Hz, 12H), 0.92 (d, *J* = 6.4 Hz, 3H); <sup>13</sup>C NMR (100 MHz, CDCl<sub>3</sub>) δ (ppm) 169.2, 166.5, 164.5, 157.9, 157.7, 157.5, 155.6, 155.4, 147.4, 138.4, 135.2, 132.8, 131.5, 131.2, 130.9, 130.6, 130.4, 130.3, 130.0, 127.5, 126.6, 124.3, 120.9, 114.6, 114.3, 113.4, 113.2, 106.0, 96.6, 96.5, 68.5, 59.8, 54.5, 52.4, 46.0, 38.0, 17.5, 17.4, 12.5; ESI-MS (*R*<sub>t</sub> = 7.7 min) *m/z* 788 [M-Cl]<sup>+</sup>.

(*R*)-1-((2*R*,3*S*)-2-(2-(benzyloxy)-2-oxoethyl)-4-oxo-1-(*o*-tolylcarbamoyl)azetidin-3-yl)ethyl 3-((*tert*-butoxycarbonyl)amino)propanoate (**90**)

Following the procedure reported for **84**, alcohol **83** (98 mg, 0.25 mmol, 1 equiv) was treated with Boc-β-alanine (76 mg, 0.4 mmol, 1.6 equiv), DMAP (6 mg, 0.05 mmol, 0.2 equiv) and DCC (83 mg, 0.4 mmol, 1.6 equiv). Purification by flash-chromatography (cyclohexane/EtOAc 80:20) yielded compound **90** as a colorless oil (127 mg, 89%). IR (film, cm<sup>-1</sup>) 3344, 2977, 2932, 1766, 1736, 1718, 1594, 1546, 1459; [α]<sub>D</sub><sup>20</sup> = -25 (c = 0.6, CH<sub>2</sub>Cl<sub>2</sub>); <sup>1</sup>H NMR (400 MHz, CDCl<sub>3</sub>) δ (ppm) 8.38 (bs, 1H), 7.92 (d, *J* = 8.0 Hz, 1H), 7.38 – 7.28 (m, 5H), 7.20 (dd, *J* = 15.0, 7.6 Hz, 2H), 7.05 (t, *J* = 7.4 Hz, 1H), 5.39 – 5.29 (m, 1H), 5.16 (d, *J* = 2.0 Hz, 1H), 5.15 (d, *J* = 2.0 Hz, 1H), 5.08 (bs, 1H), 4.46 – 4.39 (m, 1H), 3.45 – 3.28 (m, 4H), 2.86 (dd, *J* = 15.3, 7.4 Hz, 1H), 2.52 (t, *J* = 4.5 Hz, 2H), 2.28 (s, 3H), 1.43 (s, 9H), 1.38 (d, *J* = 4.3 Hz, 3H); <sup>13</sup>C NMR (100 MHz, CDCl<sub>3</sub>) δ (ppm) 171.1, 169.5, 166.2, 155.8, 147.5, 135.3, 135.1, 130.4, 128.6, 128.5, 128.3, 127.4, 126.8, 124.6, 120.9, 79.3, 67.4, 66.9, 60.1, 51.5, 36.5, 36.0, 34.7, 28.3, 18.1, 17.6; ESI-MS (*R*<sub>t</sub> = 12.0 min) *m/z* 468 [M-Boc+H]<sup>+</sup>.

2,2,2-trifluoroacetaldehyde, 3-((*R*)-1-((2*R*,3*S*)-2-(2-(benzyloxy)-2-oxoethyl)-4-oxo-1-(*o*-tolylcarbamoyl)azetidin-3-yl)ethoxy)-3-oxopropan-1-aminium salt (**91**)

Following GP3 compound **90** (59 mg, 0.10 mmol, 1 equiv) was treated with TFA (138 μL, 1.8 mmol, 18 equiv) yielding compound **91** as a colorless oil (56 mg, 96%). IR (film, cm<sup>-1</sup>) 3342, 3064, 2930, 2856, 1767, 1733, 1680, 1594, 1460; [α]<sub>D</sub><sup>20</sup> = -16 (c = 0.9, CH<sub>2</sub>Cl<sub>2</sub>); <sup>1</sup>H NMR (400 MHz, CD<sub>3</sub>CN) δ (ppm) 8.36 (bs, 1H), 7.82 (d, *J* = 8.1 Hz, 1H), 7.40 – 7.32 (m, 3H), 7.26 – 7.17 (m, 2H), 7.07 (td, *J* = 7.5, 1.2 Hz, 3H), 5.42 – 5.34 (m, 1H), 5.16 (d, *J* = 12.4 Hz, 1H), 5.12 (d, *J* = 12.4 Hz, 1H), 4.39 (ddd, *J* = 8.1, 4.0, 2.7 Hz, 1H), 3.46 (dd, *J* = 7.3, 2.7 Hz, 1H), 3.26 – 3.17 (m, 3H), 3.08 – 2.82 (m, 3H), 2.71 (t, *J* = 6.3 Hz, 2H), 2.25 (s, 3H), 1.36 (d, *J* = 6.4 Hz, 3H); <sup>13</sup>C NMR (100 MHz, CDCl<sub>3</sub>) δ (ppm) 171.1, 170.4, 165.8, 148.2, 135.0, 134.4, 130.6, 128.64, 128.61, 128.5, 128.0, 126.8, 125.4, 121.8, 68.8, 67.1, 60.6, 51.9, 36.5, 36.1, 30.6, 17.9, 17.4; ESI-MS (*R*<sub>t</sub> = 1.7 min) *m/z* 468 [M-TFA]<sup>+</sup>.

*(R)*-1-((2*R*,3*S*)-2-(2-(benzyloxy)-2-oxoethyl)-4-oxo-1-(*o*-tolylcarbamoyl)azetidin-3-yl)ethyl 3-(3-benzylthioureido)propanoate (**92**)

Following GP1C, compound **91** (61 mg, 0.11 mmol, 1 equiv) was treated with TEA (46  $\mu$ L, 0.33 mmol, 3 equiv) and benzylisothiocyanate (43  $\mu$ L, 0.33 mmol, 3 equiv). Purification by flash-chromatography (cyclohexane/EtOAc 50:50) yielded compound **92** as a colorless oil (39 mg, 58%). IR (film,  $\text{cm}^{-1}$ ) 3345, 3062, 3031, 2934, 1766, 1732, 1707, 1621, 1547, 1459;  $[\alpha]_{\text{D}}^{20} = -18$  ( $c = 1.0$ ,  $\text{CH}_2\text{Cl}_2$ );  $^1\text{H}$  NMR (400 MHz,  $\text{CDCl}_3$ )  $\delta$  (ppm) 8.26 (bs, 1H), 7.85 (d,  $J = 8.1$  Hz, 1H), 7.34 – 7.24 (m, 10H), 7.20 – 7.09 (m, 2H), 7.02 (tt,  $J = 7.4$ , 1.3 Hz, 1H), 6.47 (bs, 1H), 6.38 (bs, 1H), 5.26 (hept,  $J = 6.2$  Hz, 1H), 5.07 (s, 2H), 4.56 (bs, 2H), 4.39 – 4.26 (m, 1H), 3.95 – 3.74 (m, 2H), 3.32 – 3.30 (m, 1H), 3.29 – 3.23 (m, 1H), 2.75 (ddd,  $J = 16.4$ , 8.6, 1.1 Hz, 1H), 2.60 (td,  $J = 6.3$ , 4.8 Hz, 2H), 2.19 (s, 3H), 1.33 (dd,  $J = 6.4$ , 1.0 Hz, 3H);  $^{13}\text{C}$  NMR (100 MHz,  $\text{CDCl}_3$ )  $\delta$  (ppm) 171.8, 169.7, 166.3, 147.5, 135.1, 134.9, 130.5, 128.8, 128.6, 128.5, 128.3, 127.8, 127.57, 127.52, 126.8, 124.8, 121.1, 67.7, 67.0, 60.00, 51.6, 48.1, 40.1, 36.5, 33.9, 18.0, 17.5; ESI-MS ( $R_t = 11.9$  min)  $m/z$  617  $[\text{M}+\text{H}]^+$ .

*(R)*-1-((2*R*,3*S*)-2-(2-(benzyloxy)-2-oxoethyl)-4-oxo-1-(*o*-tolylcarbamoyl)azetidin-3-yl)ethyl 3-(3-(3',6'-dihydroxy-3-oxo-3*H*-spiro[isobenzofuran-1,9'-xanthen]-5-yl)thioureido)propanoate (**93**)

Following GP1C, compound **91** (60 mg, 0.10 mmol, 1 equiv), TEA (42  $\mu$ L, 0.30 mmol, 3 equiv) and fluorescein isothiocyanate (35 mg, 0.09 mmol, 0.9 equiv) yielded compound **93** without further purification as an orange solid (85 mg, 99%). IR (film,  $\text{cm}^{-1}$ ) 3335, 2923, 2825, 1766, 1733, 1594, 1546, 1460;  $^1\text{H}$  NMR (400 MHz,  $\text{CD}_3\text{OD}$ )  $\delta$  (ppm) 8.11 (d,  $J = 1.7$  Hz, 1H), 7.71 – 7.65 (m, 2H), 7.32 – 7.18 (m, 5H), 7.16 – 7.05 (m, 3H), 6.98 (t,  $J = 7.5$  Hz, 1H), 6.72 – 6.59 (m, 4H), 6.52 – 6.48 (m, 2H), 5.38 – 5.30 (m, 1H), 5.11 (d,  $J = 12.2$  Hz, 1H), 5.07 (d,  $J = 12.2$  Hz, 1H), 4.42 – 4.38 (m, 1H), 3.93 – 3.77 (m, 2H), 3.47 (dd,  $J = 7.0$ , 2.9 Hz, 1H), 3.17 – 3.11 (m, 1H), 2.91 (dd,  $J = 16.3$ , 7.9 Hz, 1H), 2.77 – 2.59 (m, 2H), 2.17 (s, 3H), 1.33 (d,  $J = 6.4$  Hz, 3H);  $^{13}\text{C}$  NMR (100 MHz,  $\text{CDCl}_3$ )  $\delta$  (ppm) 182.8, 172.9, 171.4, 171.1, 167.9, 161.6, 160.4, 154.2, 149.5, 142.1, 138.5, 137.2, 136.4, 131.5, 130.3, 129.9, 129.5, 129.4, 129.3, 127.6, 126.0, 125.9, 123.0, 113.8, 113.7, 111.5, 111.4, 103.6, 69.0, 67.8, 61.3, 52.9, 41.1, 37.2, 34.5, 18.5, 17.8; ESI-MS ( $R_t = 10.8$  min)  $m/z$  857  $[\text{M}+\text{H}]^+$ .

2-((2*R*,3*S*)-3-((*R*)-1-((3-((*tert*-butoxycarbonyl)amino)propanoyl)oxy)ethyl)-4-oxo-1-(*o*-tolylcarbamoyl)azetidin-2-yl)acetic acid (**95**)

Following GP2 compound **90** (107 mg, 0.19 mmol) yielded compound **95** as a colorless oil (86 mg, 95%). IR (film,  $\text{cm}^{-1}$ ) 3343, 2979, 2936, 1766, 1738, 1714, 1615, 1593, 1548, 1460;  $[\alpha]_{\text{D}}^{20} = -45$  ( $c = 1.0$ ,  $\text{CH}_2\text{Cl}_2$ );  $^1\text{H}$  NMR (400 MHz,  $\text{CD}_3\text{OD}$ )  $\delta$  (ppm) 7.74 (d,  $J = 7.9$  Hz, 1H), 7.14 (dd,  $J = 14.7$ , 7.6 Hz, 2H), 7.01 (t,  $J = 7.4$  Hz, 1H), 5.36 – 5.27 (m, 1H), 4.42 – 4.35 (m, 1H), 3.48 (dd,  $J = 6.3$ , 2.1 Hz, 1H), 3.29 – 3.23 (m, 1H), 3.21 – 3.17 (m, 1H), 2.79 (dd,  $J = 15.9$ , 8.4 Hz, 1H), 2.48 (t,  $J = 6.7$  Hz, 2H), 2.22 (s, 3H), 1.37 (s, 9H), 1.35 (d,  $J = 6.4$  Hz, 3H);  $^{13}\text{C}$  NMR (100 MHz,  $\text{CD}_3\text{OD}$ )  $\delta$  (ppm) 172.5, 168.2, 158.0, 149.6, 136.4, 131.5, 130.0, 127.6, 126.0, 123.0, 80.2, 68.9, 61.3, 53.1, 37.3, 35.6, 28.7, 18.5, 17.8; ESI-MS ( $R_t = 9.6$  min)  $m/z$  378  $[\text{M}-\text{Boc}+\text{H}]^+$ .

2,2,2-trifluoroacetaldehyde, 3-((*R*)-1-((2*R*,3*S*)-2-(carboxymethyl)-4-oxo-1-(*o*-tolylcarbamoyl)azetidin-3-yl)ethoxy)-3-oxopropan-1-aminium salt (**94**)

Following GP3 compound **95** (51 mg, 0.11 mmol, 1 equiv) was treated with TFA (185  $\mu$ L, 2.42 mmol, 22 equiv) yielding compound **94** as a colorless oil (54 mg, 99%). IR (film,  $\text{cm}^{-1}$ ) 3340, 3067, 2940, 1771, 1733, 1726, 1718, 1678, 1594, 1461;  $[\alpha]_{\text{D}}^{20} = -34$  ( $c = 1.0$ ,  $\text{CH}_2\text{Cl}_2$ );  $^1\text{H}$  NMR (400 MHz,  $\text{CD}_3\text{CN}$ )  $\delta$  (ppm) 8.39 (bs, 1H), 7.83 (d,  $J = 8.1$  Hz, 1H), 7.25 – 7.17 (m, 2H), 7.07 (t,  $J = 7.5$  Hz, 1H), 6.43 (bs, 3H), 5.51 – 5.39 (m, 1H), 4.36 (dt,  $J = 9.7$ , 3.1 Hz, 1H), 3.40 (dd,  $J = 8.6$ , 2.6 Hz, 1H), 3.29 (d,  $J = 3.4$  Hz, 2H), 3.23 (dd,  $J = 16.3$ , 4.5 Hz, 1H), 2.78 – 2.67 (m, 3H), 2.25 (s, 3H), 1.40 (d,  $J = 6.4$  Hz, 3H);  $^{13}\text{C}$  NMR (100 MHz,  $\text{CD}_3\text{CN}$ )  $\delta$  (ppm) 173.2, 171.3, 167.1, 149.0, 136.4, 131.3, 129.2, 127.5, 125.5, 122.2, 69.3, 61.4, 53.4, 36.8, 36.6, 31.8, 18.6, 17.6; ESI-MS ( $R_t = 9.6$  min)  $m/z$  378  $[\text{M}-\text{TFA}]^+$ .

*2-((2R,3S)-3-((R)-1-((3-(3-(3',6'-dihydroxy-3-oxo-3H-spiro[isobenzofuran-1,9'-xanthen]-5-yl)thioureido)propanoyl)oxy)ethyl)-4-oxo-1-(o-tolylcarbamoyl)azetidin-2-yl)acetic acid (80)*

Following GP1C compound **94** (46 mg, 0.09 mmol, 1 equiv) was treated with TEA (50  $\mu$ L, 0.36 mmol, 4 equiv) and FITC (32 mg, 0.08 mmol, 0.9 equiv). After complete consumption of the starting  $\beta$ -lactam (4 h), the solvent was evaporated in vacuum and the crude was re-dissolved in CH<sub>3</sub>OH (1 mL), then water and HCl (1M) were added until pH = 3 to litmus. The aqueous solution was extracted with EtOAc (3  $\times$  10 mL). The organic layers were collected, dried over Na<sub>2</sub>SO<sub>4</sub> and concentrated in vacuum. Purification by flash-chromatography (EtOAc/CH<sub>3</sub>OH 80:20 then 70:30) yielded compound **80** as an orange solid (38 mg, 55%). IR (film, cm<sup>-1</sup>) 3374, 2972, 2936, 1764, 1710, 1688, 1594, 1545, 1460; <sup>1</sup>H NMR (400 MHz, CD<sub>3</sub>OD)  $\delta$  (ppm) 8.18 (s, 1H), 7.74 (d, *J* = 1.5 Hz, 1H), 7.71 (d, *J* = 7.7 Hz, 1H), 7.16 – 7.05 (m, 3H), 6.99 (t, *J* = 7.4 Hz, 1H), 6.70 – 6.60 (m, 4H), 6.51 (dd, *J* = 8.7, 2.3 Hz, 2H), 5.42 – 5.33 (m, 1H), 4.43 (dd, *J* = 5.8, 3.1 Hz, 1H), 3.90 – 3.80 (m, 2H), 3.47 (dd, *J* = 7.2, 2.4 Hz, 1H), 3.14 (dd, *J* = 15.3, 3.6 Hz, 1H), 2.70 (t, *J* = 6.2 Hz, 2H), 2.63 (dd, *J* = 15.3, 9.1 Hz, 1H), 2.21 (s, 3H), 1.39 (d, *J* = 6.4 Hz, 3H); <sup>13</sup>C NMR (100 MHz, CD<sub>3</sub>OD)  $\delta$  (ppm) 182.8, 175.9, 172.9, 171.4, 168.4, 162.3, 154.5, 149.7, 148.4, 142.3, 136.3, 131.5, 130.4, 130.2, 129.5, 127.6, 126.03, 125.98, 123.2, 120.4, 119.6, 116.7, 114.2, 111.8, 103.6, 69.2, 61.5, 54.0, 41.0, 39.1, 34.6, 18.6, 17.8; ESI-MS (*R*<sub>t</sub> = 8.4 min) *m/z* 767 [M+H]<sup>+</sup>.

### 3.10.6 Synthesis of cytotoxic $\beta$ -lactam compounds

Compounds **83** and **91** were synthesized as previously described (see Paragraph 3.10.5)

*2-(5-bromo-2,4-dioxo-3,4-dihydropyrimidin-1(2H)-yl)acetic acid (100)*

Following the procedure reported in ref. 223, 5-bromouracile (150 mg, 0.79 mmol, 1 equiv), KOH (176 mg, 3.14 mmol, 4 equiv) and bromoacetic acid (143 mg, 1.03 mmol, 1.3 equiv) yielded 5-bromouracilacetic acid **100** as a white solid (106 mg, 59%). Spectroscopic data are in accordance with those reported in literature. Mp 244 °C; IR (film, cm<sup>-1</sup>) 3187, 1708, 1687, 1654; <sup>1</sup>H NMR (400 MHz, DMSO-d<sub>6</sub>)  $\delta$  (ppm) 11.89 (s, 1H), 8.00 (s, 1H), 4.43 (s, 2H); <sup>13</sup>C-NMR (100 MHz, DMSO-d<sub>6</sub>)  $\delta$  (ppm) 48.8, 94.6, 145.7, 150.4, 159.7, 169.3; ESI-MS (*R*<sub>t</sub> = 10.0 min) *m/z* 397 [M+H]<sup>+</sup>.

*2-(5-fluoro-2,4-dioxo-3,4-dihydropyrimidin-1(2H)-yl)acetic acid (98)*

Following the procedure reported in ref. 223, 5-fluorouracile (150 mg, 1.15 mmol, 1 equiv), KOH (258 mg, 4.61 mmol, 4 equiv) and bromoacetic acid (207 mg, 1.50 mmol, 1.3 equiv) yielded 5-fluorouracilacetic acid **98** as a white solid (50 mg, 23%) after purification by flash-chromatography (EtOAc/CH<sub>3</sub>OH 90:10) of the evaporated water extract. Spectroscopic data are in accordance with those reported in literature. Mp 276 – 277 °C; <sup>1</sup>H NMR (400 MHz, DMSO-d<sub>6</sub>)  $\delta$  (ppm) 11.90 (s, 1H), 8.00 (d, *J* = 6.8 Hz, 1H), 4.30 (s, 1H); <sup>13</sup>C NMR (100 MHz, DMSO-d<sub>6</sub>)  $\delta$  (ppm) 169.2, 157.4, 149.6, 138.4, 130.5, 48.6; ESI-MS *m/z* 189 [M+H]<sup>+</sup>.

*(R)-1-((2R,3S)-2-(2-(benzyloxy)-2-oxoethyl)-4-oxo-1-(o-tolylcarbamoyl)azetidin-3-yl)ethyl 3-(2-(5-bromo-2,4-dioxo-3,4-dihydropyrimidin-1(2H)-yl)acetamido)propanoate (101)*

Compound **91** (80 mg, 0.14 mmol, 1.2 equiv) was dissolved in CH<sub>2</sub>Cl<sub>2</sub> (1.2 mL) under a nitrogen atmosphere. TEA (42  $\mu$ L, 0.30 mmol, 2.2 equiv) was added dropwise, followed by the addition of EDC (17 mg, 0.11 mmol, 1 equiv) and of a solution of 5-bromouracilacetic acid **100** (26 mg, 0.11 mmol, 1 equiv) in CH<sub>2</sub>Cl<sub>2</sub> (1.6 mL) at 0 °C. After addition of DMAP (13 mg, 0.11 mmol, 1 equiv), the solution was warmed to rt and left under stirring after complete consumption of the starting material (16 h, TLC monitoring). The mixture was quenched with H<sub>2</sub>O and extracted with CH<sub>2</sub>Cl<sub>2</sub> (3  $\times$  10 mL). The organic layers were collected, dried over Na<sub>2</sub>SO<sub>4</sub> and concentrated in vacuum. Purification by flash-chromatography (CH<sub>2</sub>Cl<sub>2</sub>/EtOAc 90:10) yielded compound **101** as a waxy solid (24 mg, 35%). IR (film, cm<sup>-1</sup>) 3426, 3000, 2915, 1661, 1437; [ $\alpha$ ]<sub>D</sub><sup>20</sup> = – 12 (c = 1.1, DMSO);

<sup>1</sup>H NMR (400 MHz, DMSO-d<sub>6</sub>) δ (ppm) 11.80 (bs, 1H), 8.52 (bs, 1H), 8.29 (bs, 1H), 8.11 (s, 1H), 7.73 (d, *J* = 8.0 Hz, 1H), 7.41 – 7.27 (m, 5H), 7.21 (dd, *J* = 20.0, 7.6 Hz, 2H), 7.06 (t, *J* = 7.4 Hz, 1H), 5.57 (d, *J* = 8.0 Hz, 1H), 5.35 – 5.23 (m, 1H), 5.12 (s, 2H), 4.36 (d, *J* = 2.9 Hz, 1H), 4.30 (s, 2H), 3.59 (dd, *J* = 6.3, 2.6 Hz, 1H), 3.39 – 3.25 (m, 2H), 3.13 (dd, *J* = 16.3, 4.3 Hz, 1H), 3.04 (dd, *J* = 16.3, 7.6 Hz, 1H), 2.46 (t, *J* = 7.0 Hz, 2H), 2.20 (s, 3H), 1.29 (d, *J* = 6.3 Hz, 3H); <sup>13</sup>C NMR (100 MHz, DMSO-d<sub>6</sub>) δ (ppm) 170.3, 169.7, 166.6, 166.3, 159.8, 150.4, 147.5, 146.2, 135.8, 135.3, 130.4, 128.5, 128.4, 128.1, 128.1, 126.4, 124.5, 121.6, 94.3, 67.0, 65.9, 61.5, 49.6, 46.7, 35.8, 34.8, 33.8, 17.8, 17.2; ESI-MS (*R*<sub>t</sub> = 7.5 min) *m/z* 699 [M+H]<sup>+</sup>.

*(R)*-1-((2*R*,3*S*)-2-(2-(benzyloxy)-2-oxoethyl)-4-oxo-1-(*o*-tolylcarbamoylethyl)azetididin-3-yl)ethyl 3-(2-(5-fluoro-2,6-dioxo-2,3-dihydropyrimidin-1(6*H*)-yl)acetamido)propanoate (**102**)

Following what reported for compound **101**, compound **91** (40 mg, 0.07 mmol, 1.1 equiv), TEA (20 μL, 0.14 mmol, 2.2 equiv), 5-fluoroacetic acid **98** (11 mg, 0.1 mmol, 1 equiv), EDC (12 mg, 0.06 mmol, 1 equiv) and DMAP (7 mg, 0.06 mmol, 1 equiv) yielded compound **102** as a colorless oil (7 mg, 21%) after purification by flash-chromatography (cyclohexane/EtOAc 20:80). IR (film, cm<sup>-1</sup>) 3341, 3070, 2927, 2853, 1765, 1719, 1666, 1616, 1593, 1547, 1460, 1379, 1339, 1249; [α]<sub>D</sub><sup>20</sup> = -35 (*c* = 1.0, CH<sub>2</sub>Cl<sub>2</sub>); <sup>1</sup>H NMR (400 MHz, CDCl<sub>3</sub>) δ (ppm) 9.48 (d, *J* = 3.8 Hz 1H), 8.35 (bs, 1H), 7.91 (d, *J* = 8.1 Hz, 1H), 7.37 - 7.30 (m, 6H), 7.20 (dd, *J* = 15.3, 7.5 Hz, 2H), 7.06 (t, *J* = 7.6 Hz, 1H), 6.92 (bt, *J* = 6.1 Hz, 1H), 5.42 – 5.32 (m, 1H), 5.14 (s, 2H), 4.44 – 4.38 (m, 1H), 4.22 (dd, *J* = 41.2, 15.6 Hz, 2H), 3.57 – 3.47 (m, 2H), 3.38 (dd, *J* = 16.3, 3.6 Hz, 1H), 3.32 (dd, *J* = 7.8, 2.1 Hz, 1H), 2.79 (dd, *J* = 16.2, 9.1 Hz, 1H), 2.62 – 2.45 (m, 2H), 2.28 (s, 3H), 1.39 (d, *J* = 6.3 Hz, 3H); <sup>13</sup>C NMR (100 MHz, CDCl<sub>3</sub>) δ (ppm) 171.4, 169.9, 166.2, 166.0, 157.1 (d, *J* = 26.5 Hz), 149.6, 147.7, 135.2, 134.9, 130.5, 129.2, 128.9, 128.6, 128.5, 128.3, 127.6, 126.9, 124.8, 121.2, 67.8, 67.0, 60.3, 51.6, 50.8, 36.8, 35.1, 33.6, 18.2, 17.6.

2-((2*R*,3*S*)-3-((*R*)-1-((3-(2-(5-bromo-2,4-dioxo-3,4-dihydropyrimidin-1(2*H*)-yl)acetamido)propanoyloxy)ethyl)-4-oxo-1-(*o*-tolylcarbamoylethyl)azetididin-2-yl)acetic acid (**103**)

Following GP2, compound **101** (29 mg, 0.05 mmol) yielded compound **103** as a colorless oil (22 mg, 89%). IR (film, cm<sup>-1</sup>) 3396, 2949, 2837, 1594, 1547, 1451; [α]<sub>D</sub><sup>20</sup> = -18 (*c* = 1.0, CH<sub>2</sub>Cl<sub>2</sub>); <sup>1</sup>H NMR (400 MHz, CD<sub>3</sub>OD) δ (ppm) 7.77 (d, *J* = 8.0 Hz, 1H), 7.48 (d, *J* = 7.9 Hz, 1H), 7.19 (dd, *J* = 17.5, 7.9 Hz, 2H), 7.09 – 7.04 (m, 1H), 5.65 (d, *J* = 7.9 Hz, 1H), 5.37 (dt, *J* = 13.0, 6.3 Hz, 1H), 4.41 (s, 2H), 3.55 – 3.44 (m, 3H), 3.25 – 3.15 (m, 1H), 2.84 (dd, *J* = 16.1, 8.6 Hz, 1H), 2.58 (dd, *J* = 10.2, 6.4 Hz, 2H), 2.27 (s, 3H), 1.41 (d, *J* = 6.6 Hz, 3H); <sup>13</sup>C NMR (100 MHz, CD<sub>3</sub>OD) δ (ppm) 170.9, 168.0, 166.8, 159.4, 151.3, 148.3, 146.4, 145.7, 135.0, 130.1, 128.8, 126.2, 124.7, 121.8, 100.8, 67.6, 60.0, 51.8, 49.7, 35.0, 33.4, 29.2, 17.0, 16.3.

2-((2*R*,3*S*)-3-((*R*)-1-((3-(2-(5-fluoro-2,6-dioxo-2,3-dihydropyrimidin-1(6*H*)-yl)acetamido)propanoyloxy)ethyl)-4-oxo-1-(*o*-tolylcarbamoylethyl)azetididin-2-yl)acetic acid (**96**)

Following GP2, compound **102** (10 mg, 0.02 mmol) yielded compound **96** as a waxy white solid (8 mg, 97%). IR (film, cm<sup>-1</sup>) 3305, 2954, 2925, 2854, 1764, 1711, 1665, 1643, 1592, 1459, 1379. <sup>1</sup>H NMR (400 MHz, CD<sub>3</sub>OD) δ (ppm) 7.81 – 7.71 (m, 1H), 7.61 (d, *J* = 7.7 Hz, 1H), 7.22 – 7.14 (m, 2H), 7.11 – 6.99 (m, 1H), 5.43 – 5.31 (m, 1H), 4.47 – 4.37 (m, 3H), 3.54 – 3.38 (m, 4H), 2.68 (dd, *J* = 15.3, 8.9 Hz, 1H), 2.59 (dd, *J* = 10.9, 6.0 Hz, 1H), 2.28 (s, 3H), 1.41 (d, *J* = 7.4 Hz, 3H).

5-((*R*)-1-((2*R*,3*S*)-2-(2-(benzyloxy)-2-oxoethyl)-4-oxo-1-(*o*-tolylcarbamoylethyl)azetididin-3-yl)ethoxy)-5-oxopentanoic acid (**99**)

Compound **83** (49 mg, 0.12 mmol, 1.0 equiv) was dissolved in CH<sub>2</sub>Cl<sub>2</sub> (3.5 mL) under a nitrogen atmosphere. Glutaric anhydride (28 mg, 0.24 mmol, 2.0 equiv), DMAP (3 mg, 0.024 mmol, 0.2 equiv) and TEA (34 μL, 0.24 mmol, 2 equiv) were then added. The solution was left under stirring after complete consumption of the

starting material (16 h, TLC monitoring). The mixture was quenched with H<sub>2</sub>O (1 mL) and HCl 2N (2 mL) and extracted with CH<sub>2</sub>Cl<sub>2</sub> (3 × 10 mL). The organic layers were collected, dried over Na<sub>2</sub>SO<sub>4</sub> and concentrated in vacuum to afford compound **99** as a colorless oil (60 mg, 95%). IR (film, cm<sup>-1</sup>) 3344, 3055, 2984, 2928, 2855, 1769, 1736, 1719, 1710, 1614, 1593, 1459, 1382; [α]<sub>D</sub><sup>20</sup> = -36 (c = 1.0, CH<sub>2</sub>Cl<sub>2</sub>); <sup>1</sup>H NMR (400 MHz, CDCl<sub>3</sub>) δ (ppm) 8.38 (bs, 1H), 7.92 (d, *J* = 8.0 Hz, 1H), 7.37 -7.29 (m, 5H), 7.20 (dd, *J* = 14.3, 7.4 Hz, 1H), 7.10 – 6.98 (m, 1H), 5.38 – 5.29 (m, 1H), 5.15 (s, 2H), 4.48 – 4.41 (m, 1H), 3.35 (dd, *J* = 6.3, 2.6 Hz, 1H), 3.29 (dd, *J* = 16.1, 3.9 Hz, 1H), 2.88 (dd, *J* = 16.1, 8.2 Hz, 1H), 2.39 (t, *J* = 7.2 Hz, 4H), 2.27 (s, 3H), 1.98 – 1.87 (m, 2H), 1.36 (d, *J* = 6.4 Hz, 3H); <sup>13</sup>C NMR (100 MHz, CDCl<sub>3</sub>) δ (ppm) 177.5, 171.8, 169.5, 166.3, 147.6, 135.3, 135.1, 130.4, 128.6, 128.4, 128.4, 127.4, 126.8, 124.5, 120.9, 67.1, 66.9, 60.1, 51.4, 36.6, 33.1, 32.6, 19.7, 18.1, 17.6; ESI-MS (R<sub>t</sub> = 10.1 min) *m/z* 511 [M+H]<sup>+</sup>.

*(R)*-1-((2*R*,3*S*)-2-(2-(benzyloxy)-2-oxoethyl)-4-oxo-1-(*o*-tolylcarbamoyl)azetidin-3-yl)ethyl 5-((3-hydroxy-2-methyl-6-((3,5,12-trihydroxy-3-(2-hydroxyacetyl)-10-methoxy-6,11-dioxo-1,2,3,4,6,11-hexahydrotetracen-1-yl)oxy)tetrahydro-2*H*-pyran-4-yl)amino)-5-oxopentanoate (**104**)

Doxorubicin (5 mg, 0.009 mmol, 1 equiv) was dissolved in CH<sub>2</sub>Cl<sub>2</sub> (1 mL) under a nitrogen atmosphere. Compound **99** (5 mg, 0.009 mmol, 1 equiv) and HBTU (11 mg, 0.03 mmol, 3.3 equiv) diluted in CH<sub>2</sub>Cl<sub>2</sub> (2 mL) were then added dropwise. Finally DIPEA (13 μL, 0.08 mmol, 8.5 equiv) was added and the solution was left under stirring after complete consumption of the starting material (16 h, TLC monitoring). The mixture was quenched with H<sub>2</sub>O (3 mL) and extracted with CH<sub>2</sub>Cl<sub>2</sub> (3 × 10 mL). The organic layers were collected, dried over Na<sub>2</sub>SO<sub>4</sub> and concentrated in vacuum to afford compound **104** as a red solid (10 mg, 99%).

Due to its low supply and molecular complexity, an appropriate characterization of compound **104** is still on course.

2-((2*R*,3*S*)-3-((1*R*)-1-((5-((3-hydroxy-2-methyl-6-((3,5,12-trihydroxy-3-(2-hydroxyacetyl)-10-methoxy-6,11-dioxo-1,2,3,4,6,11-hexahydrotetracen-1-yl)oxy)tetrahydro-2*H*-pyran-4-yl)amino)-5-oxopentanoyl)oxy)ethyl)-4-oxo-1-(*o*-tolylcarbamoyl)azetidin-2-yl)acetic acid (**97**)

Following GP2, compound **104** (10 mg, 0.009 mmol) yielded compound **97** as an orange solid (8 mg, 99%).

Due to its low supply and molecular complexity, an appropriate characterization of compound **97** is still on course.

### 3.10.7 Loading of β-lactam compounds on Sr-HA

Azetidinones **1**, **4**, **9** and **17** were synthesized as described in Paragraph 3.10.2.

Stability tests were conducted for compounds **1** and **9** in PBS (0.1M pH = 7.4) at 30 °C and in physiological solution (NaCl 0.9% 0.15M) at 30 °C, verifying a non-degradation of the compounds up to 10 days upon detection at HPLC-UV.

#### 3.10.7.1 Loading of azetidinones

The loading of azetidinones **1**, **4** and **9** on Sr-HA was conducted as follows: azetidinone (10 mg) was diluted in a 10 mL flask in the appropriate reaction mixture (0.6 mL), then Sr-HA nanoparticles (60 mg) were added. The suspension was left under stirring at room temperature. After 4 h the mixture was quantitatively transferred with 1 mL of H<sub>2</sub>O in an open test tube and centrifugated for 5 mins at 1200 rpm. The solid phase was separated, oven dried at 48 °C for 48 h, and kept in dessicator (CaCl<sub>2</sub>) for 24 h before the analyses.

The loading of azetidinone **17** was conducted as follows: azetidinone (10 mg) was diluted in a 10 mL flask in the appropriate organic solvent (0.4 mL). The system was heated to 60 °C for allowing a perfect substrate

solubilisation, following by the dropwise addition of previously heated H<sub>2</sub>O (1.2 mL). Finally, Sr-HA nanoparticles (60 mg) were added. The suspension was left under stirring at room temperature. After 4 h the mixture was quantitatively transferred with 1 mL of H<sub>2</sub>O in an open test tube and centrifugated for 5 mins at 1200 rpm. The solid phase was separated, oven dried at 48 °C for 48 h, and kept in dessicator (CaCl<sub>2</sub>) for 24 h before the analyses.

Loading amounts of the azetidinone molecules on Sr-HA were evaluated through thermogravimetric analysis as difference between the total weight loss measured between 38 and 800 °C for each loaded sample and that measured for pristine Sr-HA.

#### 3.10.7.2 In vitro release

Samples of **1**-Sr-HA, **4**-Sr-HA, **9**-Sr-HA and **17**-Sr-HA were evaluated for the release study. In a 10 mL test tube an azetidinone-Sr-HA sample (25 mg) was suspended in 1.25 mL of the relative aqueous medium (MilliQ water, physiological solution NaCl 0.9%, 0.15M, acetate buffer 0.1M pH 5.0, phosphate buffer 0.1M pH 7.4). Experiments were conducted at 37 °C in thermostat with sampling and refreshing of the solution at set time intervals. At each time point, the supernatant was separated after centrifugation for 5 mins at 1200 rpm and the released concentration of the azetidinone was determined by HPLC-UV analysis. The Sr-HA sample was incubated again with a fresh solution of the relative medium (1.25 mL).

#### 3.10.7.3 HPLC analysis parameters

Linear calibration curves for the HPLC-UV analysis of azetidinones were established at 254 nm. Samples for the construction of calibration curves were diluted in a 1:1 solution H<sub>2</sub>O+TFA 0.08% - CH<sub>3</sub>CN + TFA 0.08%. Column: Zorbax-Eclipse XDB-C18 (4.6 x 150 mm, 5 micron), flow 0.5 mL/min, 30 °C.

Elution conditions:

- **1**: from 100% H<sub>2</sub>O+TFA 0.08% to 30% H<sub>2</sub>O+TFA 0.08% – 70% CH<sub>3</sub>CN + TFA 0.08% in 12 min; retention time: 8.0 min
- **4**: from 70% H<sub>2</sub>O+TFA 0.08% – 30% CH<sub>3</sub>CN + TFA 0.08% to 30% H<sub>2</sub>O+TFA 0.08% – 70% CH<sub>3</sub>CN + TFA 0.08% in 15 min; retention time: 9.0 min
- **9**: from 70% H<sub>2</sub>O+TFA 0.08% – 30% CH<sub>3</sub>CN + TFA 0.08% to 30% H<sub>2</sub>O+TFA 0.08% – 70% CH<sub>3</sub>CN + TFA 0.08% in 15 min; retention time: 9.5 min
- **17**: from 70% H<sub>2</sub>O+TFA 0.08% – 30% CH<sub>3</sub>CN + TFA 0.08% to 30% H<sub>2</sub>O+TFA 0.08% – 70% CH<sub>3</sub>CN + TFA 0.08% in 15 min; retention time: 7.5 min

#### *3.10.8 Loading of β-lactam compounds on PLLA*

Azetidinones **1**, **9**, **17** were synthesized as described in Paragraph 3.10.2.

The electrospinning apparatus was composed of a high voltage power supply (Spellman, SL 50 P 10/CE/230), a syringe pump (KD Scientific 200 series), a glass syringe, a stainless-steel blunt-ended needle (inner diameter: 0.84 mm) connected with the power supply electrode, and a rotating cylindrical collector (50 mm diameter; 120 mm length). PLLA was dissolved in a mixed solvent, CH<sub>2</sub>Cl<sub>2</sub>:DMF = 65:35 v/v at a concentration of 13% w/v. The polymer solution was dispensed, through a teflon tube, to the needle with a flow rate of 0.02 mL/min. The electrospinning process was performed by applying a potential of 20 kV, at rt with a relative humidity of 50%, collecting the electrospun fibers over a rotating cylindrical collector (40 rpm) placed at a distance of 20 cm from the needle. The obtained PLLA electrospun fibrous mats were kept under vacuum over P<sub>2</sub>O<sub>5</sub> at room temperature overnight in order to remove residual solvents.

Fiber morphology was observed with a Philips 515 scanning electron microscope (SEM) at an accelerating voltage of 15 kV. Prior to SEM analysis, samples were sputter-coated with gold. The distribution of fiber diameters was determined through the measurement of about 250 fibers by means of an acquisition and image analysis software (EDAX Genesis).

#### 3.10.8.1 Quantification of azetidinones loaded on PLLA

The amount of azetidinones loaded on PLLA mats was evaluated by HPLC-UV analysis. An electrospun azetidinone-PLLA mat (1-3 mg) was dissolved in 1 mL of CH<sub>2</sub>Cl<sub>2</sub> in a glass vial, the solvent was evaporated under reduced pressure and the residue was diluted in methanol (4 x 0.5 mL). The methanol solution was analysed by HPLC-UV in triplicate; three independent experiments were carried out for each azetidinone-PLLA.

#### 3.10.8.2 *In vitro* release

Samples of **1**-PLLA, **9**-PLLA and **17**-PLLA were evaluated for the release study. In a 10 mL test tube an electrospun azetidinone-PLLA mat (1-3 mg) was suspended in 0.5 mL of the relative solution (methanol or buffer phosphate 0.1M pH 7.4). Experiments were conducted at 37 °C in thermostat (if in PBS) or at room temperature (if in methanol) with sampling and refreshing of the solution at set time intervals. At each time point, the supernatant was separated and the released concentration of the azetidinone was determined by HPLC-UV analysis. The PLLA mat was incubated again with a fresh solution of the relative medium (0.5 mL). Experiments in PBS medium (dry-mat release and wet-mat release) were conducted as described above (dry-mat release) or with a pre-washing phase (wet-mat release). The washing phase consisted in immersing the azetidinone-PLLA mat in: 1) 0.5 mL of a PBS/ethanol 70:30 solution (2 sec); 2) 0.5 mL of PBS buffer (5min) and 3) 0.5 mL of PBS buffer (5min). The wet mat was then used for the release study as described above, the amount of azetidinone released during the washing phase was determined by HPLC-UV analysis.

Linear calibration curves for the HPLC-UV analysis of azetidinones in supernatant solutions were established at 254 nm. For sample **9**-PLLA the release study was established also in MilliQ water and in acetate buffer 0.1M pH = 5. For HPLC analysis parameters, see Paragraph 3.10.7.3.

## 4. Biocatalysis as a promising synthetic strategy

### 4.1 Biocatalysis and enzymes

Biocatalysis involves the use of isolated enzymes or whole cells as catalysts in chemical transformations. Enzymes are globular proteins containing, among the others, two fundamental structural portions: the active site, in which the catalysis actually takes place, and the recognition pockets (binding sites), where the substrate binds and orients properly with a complementary interaction.<sup>247</sup>

Following the official nomenclature, enzymes are numerically categorized with an EC (Enzyme Commission) classification in six classes according to their catalyzed reaction (Figure 4.1).<sup>248</sup>

Class	Reaction type	Examples of enzymes
• Oxidoreductase	Oxidation/reduction of C-H, C-C or C=C bonds	Dehydrogenase, oxidase
• Transferase	Transfer of functional groups such as an amino group, acetyl group or phosphate group.	Transaminase, kinase
• Hydrolase	Hydrolysis/formation of esters, amides, lactones, lactams, epoxides, nitriles, anhydrides and glycosides.	Lipase, amilase, protease
• Lyase	Addition/elimination of small molecules on C=C, C=N and C=O bonds.	Decarboxylase
• Isomerase	Isomerization including epimerization and racemization.	Glucose isomerase, mutase
• Ligase	Formation/breaking of C-O, C-S, C-N, C-C bonds together with triphosphates breaking	Synthetase

**Figure 4.1.** Enzymatic classes according to the International Union of Biochemistry and Molecular Biology

The applicative interest for enzymes in industrial processes and organic synthesis arises from their intrinsic high catalytic power, which allows an increase in the reaction rate of  $10^{8-12}$  times compared to the non-catalyzed processes. Moreover, enzymes are in most cases highly selective, in terms of chemo-, regio- and stereoselectivity,<sup>249</sup> and specific toward substrates and reactions, with by-products being only rarely observed.<sup>250</sup> A further advantage over the traditional catalysis concerns the facility in the biocatalytic conditions control (pH range 4-9, temperature from 0 to 50 °C, atmospheric pressure and aqueous solvents).

For all these reasons biocatalysis is nowadays widespread in the synthesis of chemical compounds and offers multiple advantages such as the reduction of waste, reaction times and number of synthetic steps.<sup>251</sup> Processes involving the use of enzymes operate in mild conditions, do not require protections of functional groups, avoid the use of hazardous materials, reduce the energy demanding - as enzymes rarely perform endo- or exothermic processes - and require catalytic amounts rather than



stoichiometric. In addition, deriving from natural sources, enzymes are renewable, biocompatible, biodegradable and not toxic. Consequently, biocatalytic methods are environmentally attractive and therefore more sustainable, according to the 12 principles of Green Chemistry.<sup>252</sup>

Although the first commercial enzyme preparations dated back to early 1900s, the development of biocatalysis blossomed only in the last decades of the twentieth century; in fact, for a long time the use of enzymes on an industrial scale was greatly limited by their cost, availability, stability, and in some cases excessive selectivity.

As already mentioned, enzymes normally work in water environments, but not all substrates are soluble in aqueous solvents, especially high molecular weight organic compounds. According to this, in the last few years several studies demonstrated the possibility for some enzyme classes to work in organic solvents or biphasic systems (medium engineering).<sup>253</sup> The stability of the enzymes was also increased thanks to immobilization techniques, which allowed an easier separation of the enzyme from the reaction medium and consequently facilitated its recycling. Their high specificity also represents a limitation since many enzymes exclusively accept natural substrates; in this case, the use of biotechnology and the development of genetic engineering allowed an increase in their applicability.<sup>254</sup>

In some cases, the use of enzymes implies the need for a stoichiometric cofactor (e.g. FADH or NADH) and could present a not-negligible cost depending on the form in which it is used: isolated enzymes are the most expensive, followed by whole cells and cell cultures. However, thanks to the development of recombinant DNA technology it is possible to produce different enzymes in large quantities at affordable prices. Moreover, since enzymes often require the same reaction conditions, the opportunity to combine several enzymatic steps in cascade (cascade biocatalysis) was developed<sup>255</sup>, thus allowing to avoid intermediate isolation and separation procedures.

Biocatalysis has now become a standard technology applied to the industrial production of both bulk and fine chemicals; biocatalytic systems are today exploited not only in organic synthesis, but also in textile, food and paper industries, as well as in the production of biosensors. The development of new biocatalytic routes or their integration into existing industrial processes also displays the advantage of using raw materials from renewable sources. Biocatalysts and microorganisms can indeed be used to obtain building blocks for chemical industry from plants and waste materials derived from agriculture. However, the pharmaceutical sector is that involving the major number of biocatalytic process; this reflects the compelling need of pharma-industry to synthesize enantiomerically pure drugs.<sup>256</sup> Two enantiomers of the same molecule could in fact display different spatial distributions on the same receptor or even bind two diverse receptors being responsible of other biological pathways.<sup>257</sup> This inevitably may result in a less or no efficacy of the drug, or in totally different pharmacological effects exerted by the two enantiomers, as in the dramatic case of Thalidomide. This drug was sold in 1950s in its racemic form against nausea and sickness in pregnant women; whilst one enantiomer had the desired effect, the other possessed the capacity of binding the protein cereblon (CRBN) leading to teratogenic effects and many severe birth defects as phocomelia.<sup>258</sup>

Biotransformations operating on already enantiomerically pure precursors represent the most employed biocatalytic technique, followed by kinetic resolutions of racemic mixtures and asymmetric synthesis. Relying on different enzymatic classes, hydrolases are the most studied enzymes, followed by oxido-reductases, while less than 15% involves the other categories.<sup>259</sup> To notice, asymmetric

synthesis is predominantly carried out by lyases or oxide-reductases while kinetic resolutions are mainly performed by hydrolases (Figure 4.2).

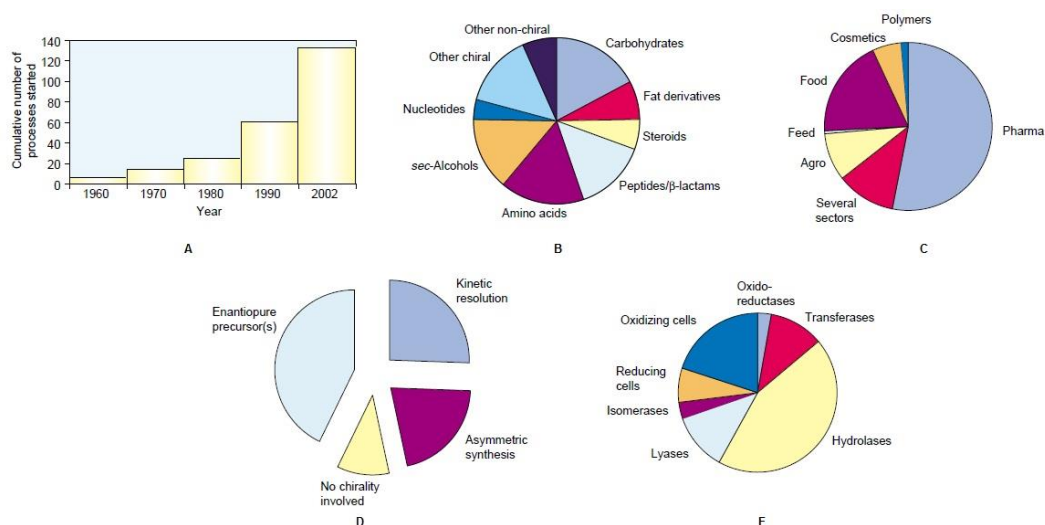


**Figure 4.2.** Industrial biotransformations. Figure adapted from ref. 259

#### 4.1.1 Hydrolases and Lipases

Hydrolases are enzymes able to cleave C-O, C-N and C-C bonds in the presence of water molecules.<sup>260</sup> Their biological role concerns the degradation of nutrients as proteins, fatty acids and polysaccharides in smaller units. For example, proteases are able to cleave the amide bond of a protein affording smaller peptides and amino acids, while glycosidases break the glycoside bond and lead to two glycoside units.

Hydrolases are largely used in organic chemistry because of their stability, their no need of cofactors, and ability to work in pure organic solvents or in co-solvents as acetone, dimethylsulfoxide (DMSO), tetrahydrofuran (THF), and *N,N*-dimethylformamide (DMF). In addition, these enzyme are commercially available and exploitable not only for hydrolysis or alcoholysis, but also for the reverse condensation reaction. In particular, lipases (EC 3.1.1.3), an esterase sub-class, have gained attention in the world of organic chemistry due to their robustness, wide tolerance to different substrates, stability to organic solvents and high temperatures (their activity is maintained at up to 100 °C in certain solvents). Moreover, lipases are inexpensive and available from multiple sources, mainly of microbial origin. Submerged culture and solid state fermentation are widely used methods for production of commercial lipases,<sup>261</sup> but they can also derive from animal sources, after extraction and purification, or simple crude extraction.

Most of the known lipases displays a serine-depending mechanism performed by a serine, aspartic acid and histidine catalytic triad. Histidine acts as proton shuttle between serine and aspartic acid residues, allowing the enzyme active site to maintain its three-dimensional conformation. The active site is covered by a peptide lid that remains closed in the absence of substrate to be processed. Conversely, when the lipase is in contact with a lipid-water interface, the lid undergoes conformational changes letting the active site open and accessible for the substrate (lid effect, Figure 4.3).<sup>262</sup>

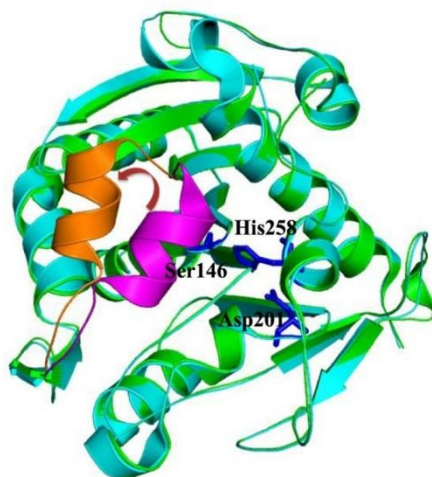
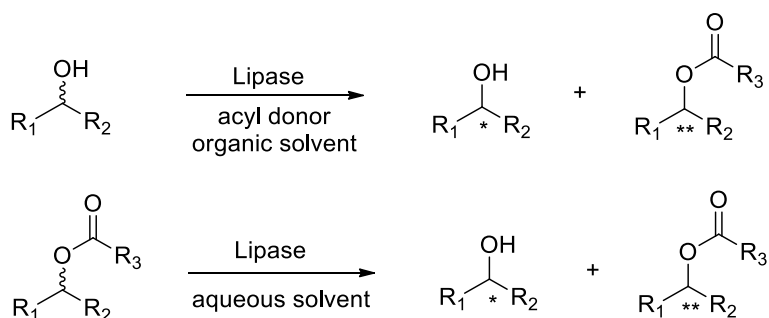


**Figure 4.3.** Lipase active site and lid effect (superimposition of close and open conformations of *Thermomyces lanuginosus* lipase).  
Figure adapted from ref. <sup>263</sup>

## 4.2 Kinetic resolutions with lipases

As aforementioned, one of the most important application of enzymes in organic synthesis is certainly represented by kinetic resolution of racemic compounds. Lipases, in particular conditions, could catalyze both the formation and the hydrolysis of ester bonds, discriminating a particular enantiomer within a racemic mixture (Scheme 4.1).



**Scheme 4.1.** Kinetic resolution mediated by lipases in esterification (above) and in hydrolysis (below) reactions

Since the enzymatic active site is chiral, an enantiomer of the racemic mixture could better fit than the other, hence being converted with a higher reaction rate. The ideality occurs when the reaction rates for the two enantiomers conversion is so different that only one is processed by the enzyme at reasonable times, thus obtaining the maximum 50% yield and elevate enantiomeric excesses (ee). In this desirable case, the enzyme possesses a high enzymatic selectivity ( $E$ ), a dimensionless parameter corresponding to the ratio of the relative rate constants for the single enantiomers.  $E$  values superior to 20 are excellent, while values between 10 and 15 are considered satisfactory.<sup>264</sup> When  $E$  is below 10, the biocatalytic process is not selective and leads to negligible enantiomeric excesses (Figure 4.4).

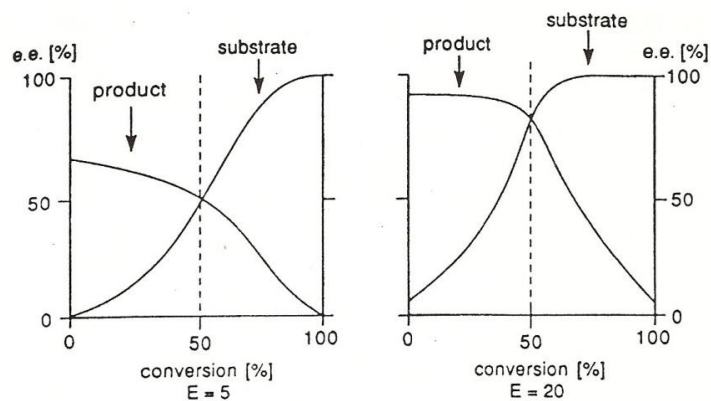


**Figure 4.4.** Curves of conversion vs ee in kinetic resolutions, when  $E=5$  (left) and when  $E=20$  (right)

If a kinetic resolution shows only a moderate selectivity, better results could be eventually achieved considering two consequent steps (Figure 4.5). In this case the reaction has to be stopped when the product displays the maximum enantiomeric excess and yield, i.e. in a range of conversion of around 40% (step I). The product is then isolated and the residual substrate, with a low enantiomeric excess, is re-processed in the same reaction until a total conversion of about 60% is reached (step II). At this point also the substrate could be isolated with its maximum enantiomeric excess and yield. Nevertheless, with this method, at least 20% yield of the second step compound is lost.

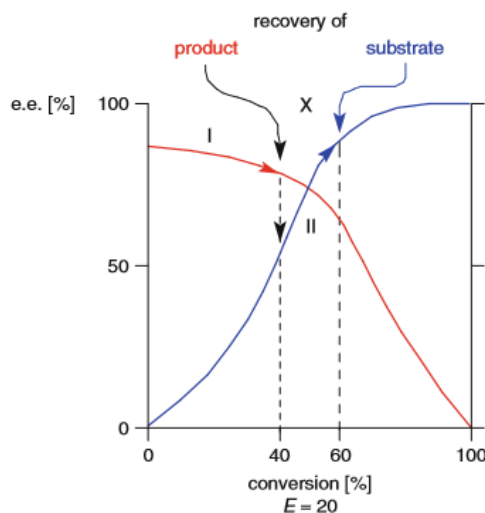
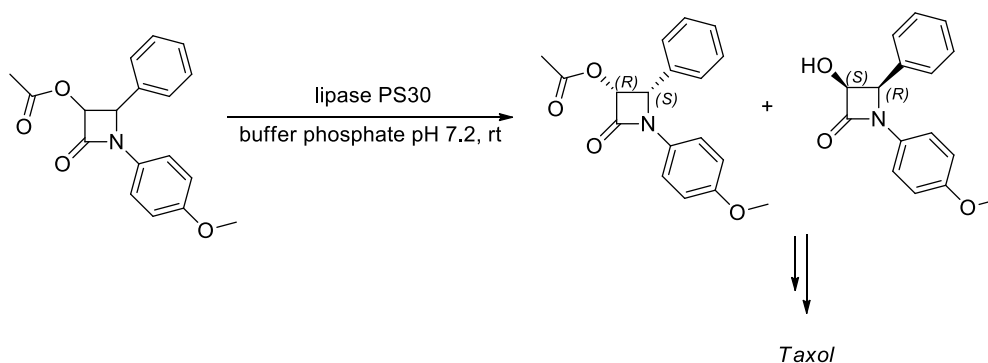


**Figure 4.5.** Two-steps kinetic resolution

Among different substrates that were exploited for kinetic resolution studies,  $\beta$ -lactam compounds found their own niche, due to the presence of defined stereogenic centers on the ring that rendered them attractive for the synthesis of enantiopure intermediates. Generally, enantiomerically pure  $\beta$ -lactams arise from the use of chiral auxiliaries or catalysts in asymmetric syntheses;<sup>265</sup> the use of biocatalytic methods for the formation of enantiopure  $\beta$ -lactams exploits instead kinetic resolutions of racemic mixtures.

An important example reported by Brieva *et al.* described an enzymatic process mediated by lipases for the resolution of a racemic mixture of  $\beta$ -lactam derivatives.<sup>266</sup> In particular, an enantioselective hydrolysis on a racemic 3-acetoxy-4-phenyl  $\beta$ -lactam furnished the corresponding diastereomeric products that were in turn used as intermediates for the synthesis of Taxol (Scheme 4.2).



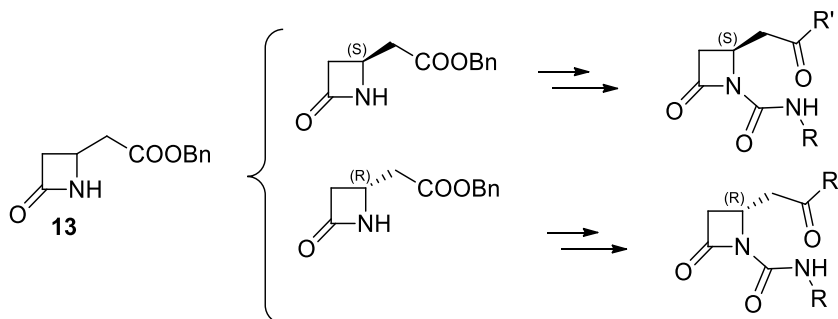
**Scheme 4.2.** Kinetic resolution of  $\beta$ -lactam derivatives mediated by lipases<sup>266</sup>

#### 4.2.1 Development of enantiomerically pure $\beta$ -lactam integrin ligands

As illustrated in Chapter 3, diverse libraries of  $\beta$ -lactam based compounds showed a good affinity toward different integrin families. Most of these compounds were assayed in their racemic form, as they were prepared starting from a commercial racemic azetidinone (4-acetoxy-azetidin-2-one). The stereochemical outcome of the ligands, and in particular the configuration at C4 position of the  $\beta$ -lactam ring, could be discriminant for the interaction with the receptor. It was already demonstrated in fact, both from docking simulations and from *in vitro* tests of ligands with opposite configuration (see Paragraphs 3.2.3 and 3.3.2), how two enantiomers could have opposite activities, or one could display affinity with the other resulting completely inactive.

By far these considerations were evaluated only for those derivatives arising from enantiomerically pure starting materials (*L*- or *D*- aspartic acid), whose configuration at C4 was preserved in the target materials during all the synthetic steps. It could now be interesting to evaluate the role of the enantiopurity also on the ligands arising from the racemic library, and a biocatalytic approach could represent a successful strategy.

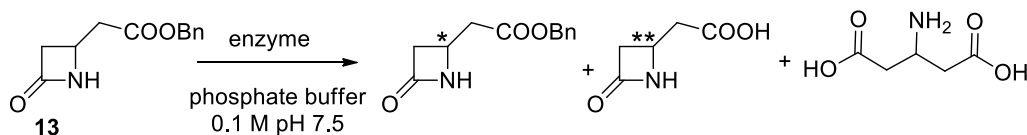
In particular, since  $\beta$ -lactam **13** is a common building block for the synthesis of all the racemic derivatives, it was studied a strategy for obtaining both its enantiomers. In this way, subsequent functionalizations on these intermediates with opposite stereochemistry could provide target integrin ligands presenting a specific optical configuration. It could hence be evaluated their biological effect compared to their previously synthesized racemic analogues (Scheme 4.3).



**Scheme 4.3.** Strategy for the synthesis of enantiomerically pure  $\beta$ -lactam derivatives

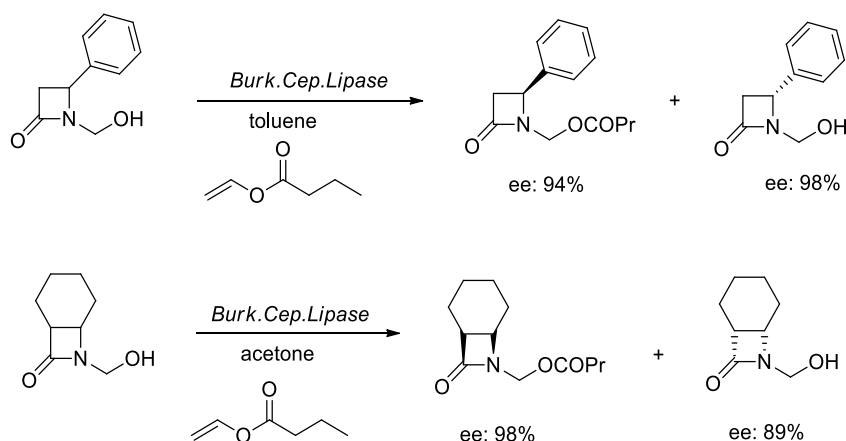
Some previous studies were taken in account for developing the biocatalytic strategy for the synthesis of enantiomers of azetidinone **13**. In particular, an attempt of performing a kinetic resolution directly

on **13**, exploiting its benzyl ester functionality, was previously conducted with a small panel of lipases and esterases (CAL-A, CAL-B, Pig liver esterase). The enzymatic selectivity on this hydrolysis was not satisfactory, leading to the opening of  $\beta$ -lactam ring as by-process and to a maximum enantiomeric excesses of around 75% of the corresponding resolved benzyl ester compound. (Scheme 4.4).



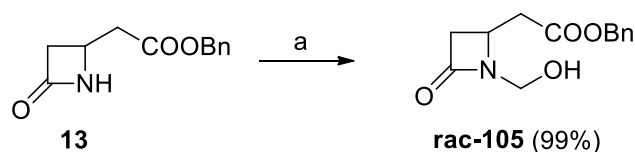
**Scheme 4.4.** Kinetic resolution on compound **13** mediated by lipases or esterases

We were therefore inspired by a work of Fulop *et al.*<sup>267</sup> concerning the kinetic resolution of azetidinones bearing an oxymethylene moiety on the  $\beta$ -lactam -NH; the method comprised an esterification mediated by *Burkolderia Cepacea Lipase* and vinyl butyrate as acyl donor (Scheme 4.5).



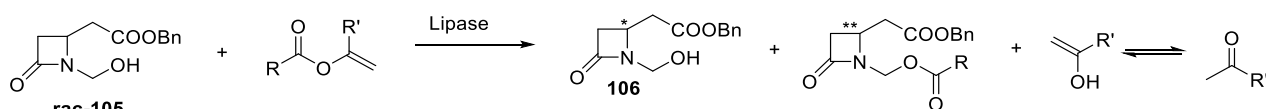
**Scheme 4.5.** Kinetic resolutions of azetidinones mediated by lipases<sup>267</sup>

Since the reported transesterification reactions showed good results in terms of enantiomeric excesses, we evaluated as well the possibility of an alcoholic partner as substrate for an enzymatic kinetic resolution. According to this, compound **13**, whose synthesis has been already discussed, was functionalized with an oxymethylene function on the  $\beta$ -lactam nitrogen by means of paraformaldehyde, catalytic potassium carbonate and sonication<sup>268</sup> (Scheme 4.6).



**Scheme 4.6.** Oxymethylation reaction on  $\beta$ -lactam **13**. Reagents and conditions: a) paraformaldehyde,  $K_2CO_3$ , THF/ $H_2O$  11:1, sonication, 4 h. Yield of isolated product is reported in brackets

With the newly inserted alcoholic function, compound **rac-105** represented an adapt substrate for the enzymatic study. The kinetic resolution was carried out using a catalysis by lipases, with the aim of obtaining the starting compound **106**, i.e. the enantiomeric species not recognized by the enzyme active site, and, simultaneously, the ester product, both in their optically pure form (Scheme 4.7). Different enzyme preparations were screened in order to determine those displaying the best selectivity and reaction rate. Other parameters were consequently considered, such as solvent, temperature and acyl donors. The use of vinyl esters (vinyl acetate, vinyl butyrate and isopropenyl acetate) as acyl donors allowed to prevent the formation of competitive reactions, since the vinyl alcohol co-product tautomerized to aldehyde or ketone with a shift toward product formation, hence avoiding hydrolysis or nucleophilic attack on the newly formed ester.



**Scheme 4.7.** Generic scheme for kinetic resolution on  $\beta$ -lactam **rac-105**

The biocatalytic screenings were monitored through chiral HPLC analysis, thus requiring a preliminary study on the determination of the most suitable analytical conditions. For our purpose, a single analysis should reveal both the reaction conversion and the enantiomeric excesses of the residual substrate and the formed product. Accordingly, acetic and butyric ester products of the biocatalytic process (deriving from the use of vinyl and isopropenyl acetate, or vinyl butyrate respectively) were chemically synthesized by a classic nucleophilic substitution of alcohol **rac-105** on acetic or butyric anhydrides mediated by TEA (data not shown). Once that a perfect separation of the single species in exam was detected, mechanic mixtures of substrate **rac-105** and acetic or butyric esters were prepared and injected in chiral HPLC to simulate a chromatographic run arising from the biocatalytic reaction. The following conditions resulted the best instrumental parameters: column: Daicel Chiralpak IC  $\text{\textcircled{R}}$ , solvent: hexane/isopropanol 50:50, flow: 0.5 mL/min from 0 to 18 min, 1 mL/min from 19 min, temperature: 40  $^{\circ}\text{C}$ . As an example, chromatogram of alcohol **rac-105** and ester **rac-107** is reported in Figure 4.6.

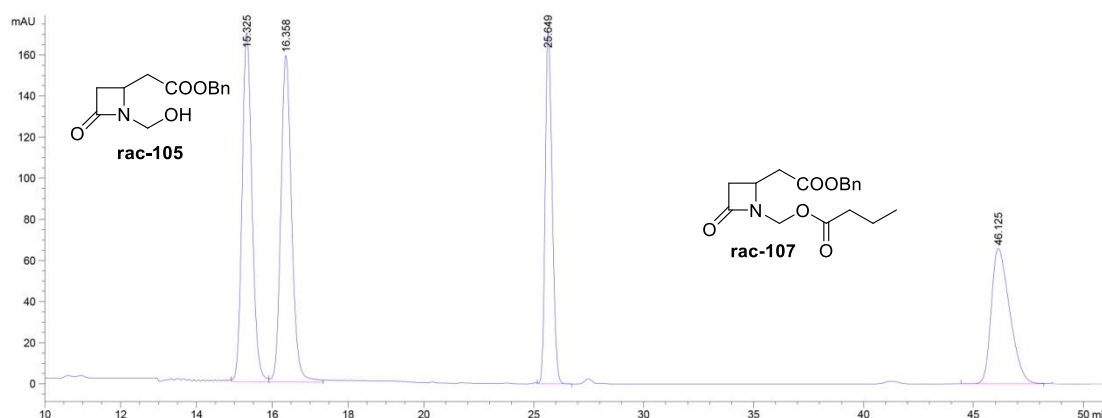


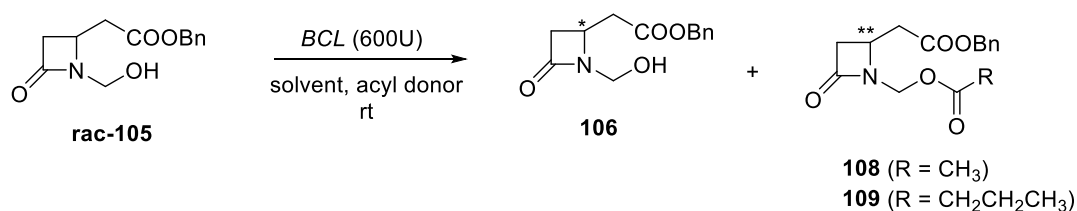
**Figure 4.6.** Chromatographic analysis of a mixture of  $\beta$ -lactams **rac-105** and **rac-107** with the optimized chiral HPLC parameters

With the optimized analytic conditions in hand, the biocatalytic screening was performed. A preliminary study was carried out with *Burkholderia Cepacia Lipase* (BCL), an enzyme widely used

for the kinetic resolution of  $\beta$ -lactam compounds, as reported, among others, by Fulop *et al.*<sup>267</sup> Different anhydrous solvents were screened among those commonly reported in the literature for this type of enzymatic reactions, such as toluene, *tert*-butylmethyl ether (TBME), acetone and THF.<sup>267,269</sup> As already mentioned, vinyl acetate (VA), isopropenyl acetate (IA) and vinyl butyrate (VB) were tested as acyl donors (Table 4.1).

The explorative reactions were simultaneously conducted in dark closed vials. The substrate was diluted in the appropriate anhydrous solvent, then acyl donor in excess and enzyme were introduced. According to the literature,<sup>270</sup> the same amount of enzyme and substrate (in weight) has been added. The vials were placed under orbital shaking at room temperature. The reactions were monitored by sampling and analysis of the mixture at set time intervals with chiral HPLC. To evaluate the conversion, a chromatographic analysis was conducted also at time 0, i.e. before inserting the enzyme into the reaction; areas of the substrate chromatographic peaks at time 0 were then compared with those, progressively decreased, found over the time.

**Table 4.1.** Kinetic resolution of  $\beta$ -lactam **rac-105** mediated by BCL



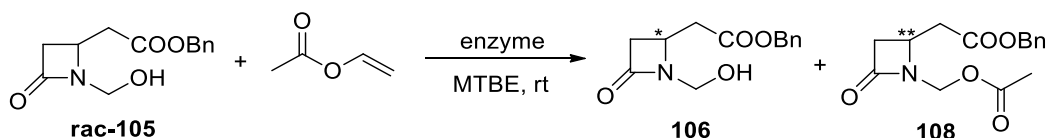
Entry	Solvent	Acyl donor	Time	Conv. (%)	ee <sub>s</sub> (%)	ee <sub>p</sub> (%)
1	Toluene	IA	1 week	< 1	3	-
2	Toluene	VA	1 week	<1	3	-
3	Toluene	VB	1 week	<1	-	-
4	TBME	IA	4 days	13	17	90
5	TBME	VA	4 days	50	89	68
6	TBME	VB	4 days	41	61	90
7	Acetone	VA	1 week	<1	2	-
8	THF	VA	1 week	<1	2	-

From the first screening emerged that toluene (entry 1-3) was totally inefficient in promoting the esterification reaction since the conversion of alcohol **rac-105** was less than 1% after a week, with all the tested acyl donors. On the contrary, the use of TBME (entries 4-6) was much more efficient; in this case conversions and enantiomeric excesses were found to depend on the acyl donor. Isopropenyl acetate provided lower conversions than vinyl acetate and vinyl butyrate (entry 4 vs 5-6), moreover showing an insufficient selectivity, since the enantiomeric excess of the product should have been higher at so low conversions. Vinyl acetate and vinyl butyrate, on the other hand, showed better results in terms of conversion, with VA resulting faster in promoting the reaction. In both cases the enantiomeric excesses are satisfactory, but at around 40-50% conversion the enzyme did not show an ideal selectivity, allowing to give only an enantiomerically enriched species between substrate and



product, and not both simultaneously. Acetone and THF were then tested with VA (entries 7 and 8) but, as found for toluene, the reactions were completely ineffective with basically no conversion after a week. TBME resulted therefore the only promising solvent, and the coupling with vinyl acetate furnished the best reaction rates (entry 5). With these conditions, a wide panel of lipases was screened, in order to find the best enzyme in terms of activity and selectivity (Table 4.2).

**Table 4.2.** Screening of lipases in the kinetic resolution of  $\beta$ -lactam **rac-105** with vinyl acetate and TBME



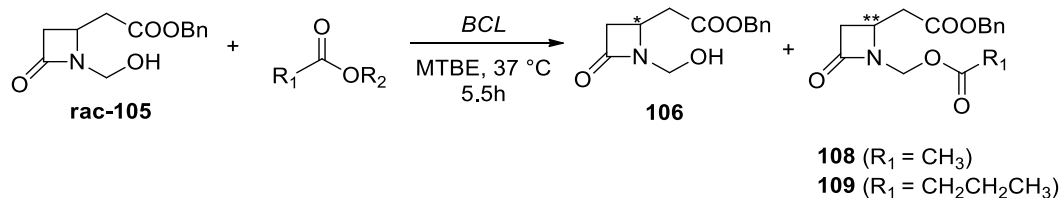
Entry	Enzyme	Unit	Time	Conv. (%)	ee <sub>s</sub> (%)	ee <sub>p</sub> (%)
1	lipase A from <i>Candida Antarctica</i> CLEA	30 U	1 h	43	28	29
2	lipase acrylic resin from <i>Candida Antarctica</i>	150 U	1 h	8	3	44
3	lipase from porcine pancreas (crude type II)	800 U	44 h	<5	-	-
4	lipase from <i>Rhizopus niveus</i>	17 U	24 h	< 1	-	-
5	lipase from <i>Candida lipolytica</i>	11 U	4 d	< 1	-	-
6	lipase from wheat germ	1 U	4 d	< 1	-	-
7	lipase from <i>Mucor javanicus</i>	60 U	4 d	6	6	79
8	lipase from <i>Penicillium roqueforti</i>	6.5 U	4 d	7	6	62
9	lipase from <i>Aspergillus niger</i>	4.5 U	24 h	10	8	59
10	lipase from <i>Rhizopus arrhizus</i>	22 U	24 h	14	17	77
11	lipase from <i>Mucor miehei</i>	14 U	24 h	18	24	87
12	lipase from <i>Candida cylindracea</i>	28 U	24 h	19	13	44
13	lipase from hog pancreas	135 U	24 h	19	18	79
14	lipase from <i>Chromobacterium viscosum</i>	2962 U	4 d	26	20	39
15	lipase from <i>Aspergillus oryzae</i>	200 U	4 d	57	45	75
16	lipase from <i>Burkholderia cepacia</i> (Amano PS)	30 U	4 d	50	89	68
17	lipase from <i>Pseudomonas fluorescens</i>	180 U	24 h	70	91	31
18	$\alpha$ -chymotripsine from bovine pancreas	300 U	7 d	< 1	-	-
19	esterase from pig liver (crude)	380 U	7 d	< 1	-	-
20	acylase from porcine kidney	300 U	44 h	15	21	84

All the screened enzymes belonged to basic or extended commercial kits of lipases, each sample having a different unit value. Lipases from *Candida Antarctica* (entries 1 and 2) showed a really high reaction rate compared to other enzymes, but losing in selectivity: after 1h already, in entry 1 the conversion was at 43% with no selectivity at all; in entry 2 instead, the enzyme already started to process both enantiomers of the substrate at 8% conversion. On the contrary, many of the tested lipases showed no activity at all (entries 3-6). Others displayed only a moderate action on the substrate, with low conversions after 4 days (entries 7-8) or after 24 hours (entries 9-14). Among these entries, lipase from *Mucor miehei* displayed the best value of product enantiomeric excess (entry 11). Lipase from *Aspergillus oryzae* displayed a 57% conversion in 4 days (entry 15), but at the same time *Burkholderia cepacia* lipase (entry 16) afforded higher enantiomeric excess values for the substrate. In this case, a potential interruption of the reaction at around 40% conversion could give rise to a two-step kinetic resolution with better enantiomeric excesses also for the ester product. Lipase from *Pseudomonas fluorescens* (entry 17) displayed a higher conversion in shorter times (24 h vs 4 days), demonstrating a high affinity for the substrate but a worst selectivity.

To notice, besides all the tested lipases, the reaction was also attempted with  $\alpha$ -chymotrypsin (entry 18), a protease that was found to catalyze the synthesis of ester bonds in particular substrates, an esterase (entry 19), known for performing transesterification reactions involving short chain esters, and an acylase (entry 20), an enzyme acting on carbon-nitrogen bonds. Unfortunately,  $\alpha$ -chymotrypsin and the crude esterase did not show any activity; the acylase instead showed some activity but with a scarce reaction rate.

From this screening, *Burkholderia cepacia* emerged as the most promising enzyme, and was further tested with other conditions. An increase in the reaction temperature was attempted for obtaining a parallel enhancement in the reaction rate and different acyl donors were thus tested at 37 °C (Table 4.3). Compared to the first screening (Table 4.1), isopropenyl acetate was no further considered due to its worse efficiency, but acetic anhydride and butyric anhydride were included as acyl donors. Anhydrides are not so commonly used in kinetic resolutions but some literature works reported the use of these compounds as acyl donors in the resolution of primary and secondary alcoholic racemic mixtures.<sup>271</sup> All the reactions were conducted in thermostat and stopped after a fixed time of 5.5 hours.

**Table 4.3.** Kinetic resolution of  $\beta$ -lactam **rac-105** with different acyl donors in TBME at 37 °C



Entry	Acyl donor	Conv. (%)	ee <sub>s</sub> (%)	ee <sub>p</sub> (%)
1	Vinyl acetate	64	88	61
2	Acetic anhydride	12	26	74
3	Vinyl butyrate	46	61	90
4	Butyric anhydride	53	91	87

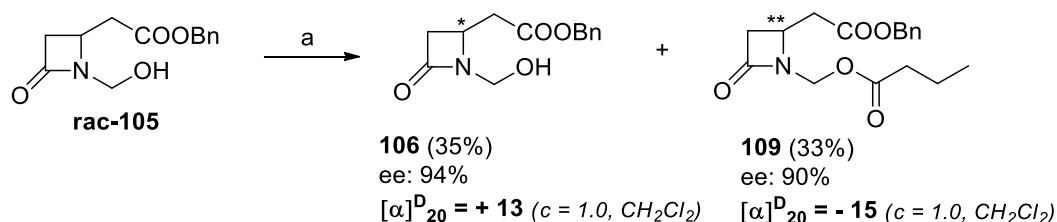
As expected, conversions increased with enhance of temperature to 37 °C. A 64% conversion was in fact obtained with vinyl acetate in 5.5 hours (entry 1), while a lower value (50%) was obtained in 4 days at room temperature. Moreover, as already demonstrated, vinyl acetate provided higher reaction rate compared to vinyl butyrate (entry 1 vs 3), maybe for a less hindrance in the enzyme active site; on the other hand, the enantiomeric excess in the product was not so promising. The worst selectivity could arise from the nature of the enzyme itself, which is a promoter of the hydrolysis of long chain esters (triglycerides).

Acetic anhydride instead displayed too low conversion values for being further considered (entry 2). Interestingly, vinyl butyrate and butyric anhydride showed very good results in terms of both selectivity and reaction rate. Vinyl butyrate (entry 3) appeared as a good candidate for performing a two-step kinetic resolution, since stopping the reaction at around 40% conversion should provide a good product ee. With the second step then, the reaction could be further promoted until a good enantiomeric excess of the substrate is reached (around 60% conversion for a maximum yield).

Using butyric anhydride instead, a classic kinetic resolution could be performed: stopping the reaction at half conversion should be sufficient to obtain good, even if not excellent, enantiomeric excesses for both substrate and product (entry 4), together with the maximum yield possible (50%).

Probably, only with a two-step kinetic resolution, the achievement of ee around or superior to 90% could be possible for both substrate and product.

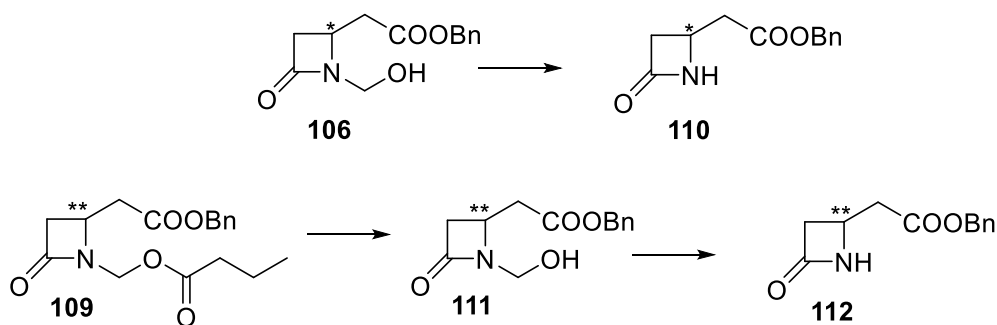
A scale-up experiment was therefore carried out with vinyl butyrate in order to isolate a large amount of both the unreacted substrate and the ester product with the highest possible ee values (Scheme 4.8).



**Scheme 4.8.** Two step kinetic resolution on  $\beta$ -lactam **rac-105**. Reagents and conditions: a) *BCL*, vinyl butyrate, TBME, 37 °C. Yields of isolated compounds are reported in brackets; values of ee and specific optical power are reported for compounds **106** and **109**

As already explained, the first step was interrupted at 38% conversion, the mixture was subjected to work-up and isolation of the product by flash-chromatography with a 90% ee. The substrate was then re-processed in the same conditions until a 67% conversion was reached. Again, the mixture was purified to isolate also the substrate with a good enantiomeric excess (94%). Notably, yields were partially affected by the two step procedure, and arranged around 30-35%. When the scale-up reaction was performed with butyric anhydride as acyl donor, better yields but lower enantiomeric excesses were obtained for both substrate and product (data not shown).

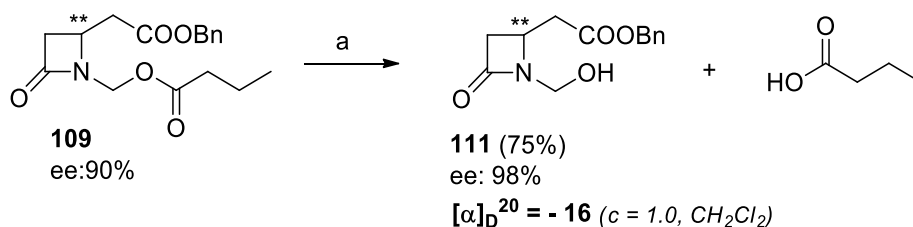
The obtained enriched compounds were then further manipulated for obtaining the two enantiomers **110** and **112**, common intermediates for the synthesis of integrin ligands (Scheme 4.9).



**Scheme 4.9.** Strategy for the synthesis of enantiomerically pure  $\beta$ -lactams **110** and **112**

In particular, ester **109** presented both a benzylic and an alkylic ester functionality; in our case only the butyryl moiety should be selectively hydrolyzed (Scheme 4.9). All the chemical strategies attempted ( $K_2CO_3$  in methanol, TEA under MW irradiation,<sup>272</sup> trifluoroacetic acid in  $CH_2Cl_2$ <sup>273</sup>) resulted in no selectivity, with detection of the partial hydrolysis of benzylic ester or formation of byproducts.

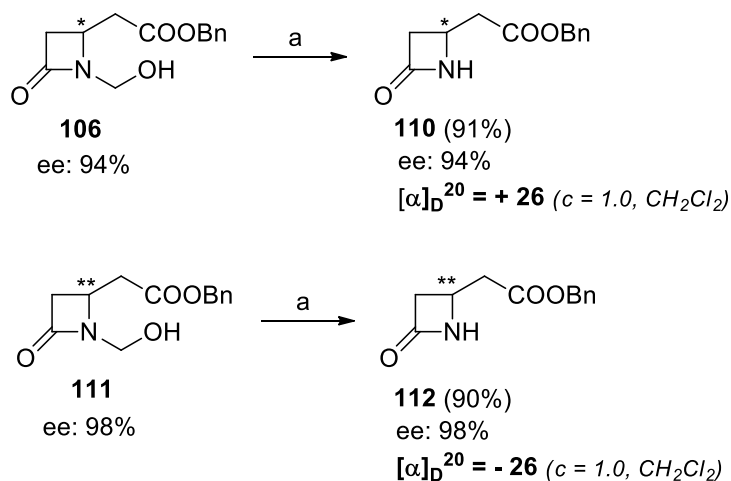
It was then decided to exploit also in this case a biocatalytic strategy, and the same conditions employed for the reverse transesterification reaction were adopted (37 °C and *Burkholderia cepacia lipase*). In this case the presence of an aqueous medium resulted necessary for promoting the hydrolysis, hence the process was carried out in MilliQ water with a minimal amount of acetonitrile to dissolve the substrate. The progress of the reaction was again monitored through chiral HPLC, and the conversion was evaluated as previously explained. When firstly conducted on the racemic ester, after 4 hours one enantiomer of the substrate was completely converted, while the other was partially processed. As expected, the system showed a perfect selectivity toward the aliphatic ester vs the benzylic one. When the reaction was repeated on the enriched ester, in an hour the desired enantiomer was converted into the product, and a further increase in the enantiomeric excess of the target alcohol was obtained. A 100% enantiomeric excess could be ideally obtained by stopping the reaction just before the major enantiomer is completely processed, but obviously this parameter is not so immediate to control. At the end of the reaction, a purification by flash-chromatography resulted necessary in order to eliminate the butanoic acid deriving from the hydrolysis reaction (Scheme 4.10).



**Scheme 4.10.** Enzymatic hydrolysis of  $\beta$ -lactam **109**. Reagents and conditions: a) *BCL*,  $H_2O/CH_3CN$  11:1, 37 °C, 1 h. Yields of isolated compound is reported in brackets; value of ee and specific optical power is reported for compound **111**

Once obtained both enantiomers **106** and **111**, whose different configuration was confirmed by the opposite signs of the specific optical power values, the deprotection of the  $\beta$ -lactam nitrogen was studied. After an attempt in basic conditions with aq.  $NH_4OH$  25% in  $CH_3OH$ ,<sup>268</sup> we turned to an oxidation strategy of the alcoholic group to the corresponding carboxylic acid that spontaneously

should decarboxylate to give the desired target. Diverse oxidative conditions were tested (NaClO/NaClO<sub>2</sub>, TEMPO/NaIO<sub>4</sub>, Laccase), and finally the desired free -NH compound was obtained with an oxidation mediated by classic KMnO<sub>4</sub>, following a literature procedure<sup>274</sup> that was optimized on substrate **rac-105**. In this case the reaction resulted effective, with complete conversions and excellent yields afforded in 16 hours without necessity of crude purification (Scheme 4.11).



**Scheme 4.11.** Oxidation reaction on enantiomers **106** and **111**. Reagents and conditions: a) KMnO<sub>4</sub>, CH<sub>3</sub>CN, 0 °C then rt, 16 h. Yields of isolated compounds are reported in brackets; values of ee and specific optical power are reported for compounds **110** and **112**

Enantiomeric excesses of the substrates were preserved in the target β-lactams **110** and **112**, and anyway verified through chiral HPLC analysis, after detection of suitable separation conditions (Figure 4.7).

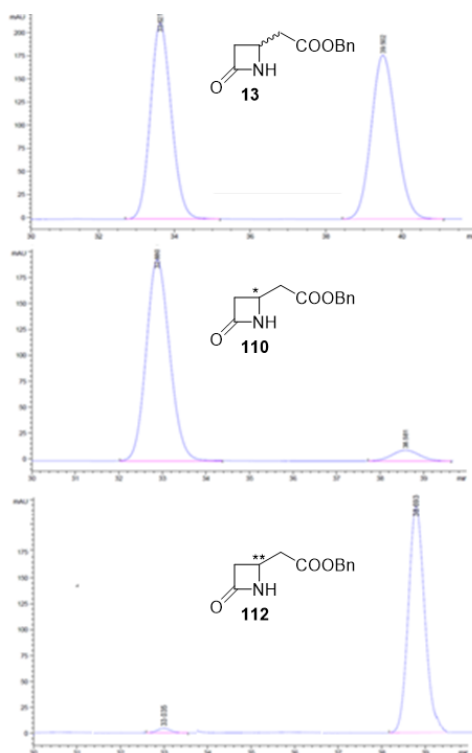


**Figure 4.7.** Chromatographic analysis of β-lactams **13**, **110** and **112** with the optimized chiral HPLC parameters

The absolute configuration of C4 stereocenter could be identified at this stage relying on a reported literature compound<sup>275</sup> that is the corresponding carboxylic acid of **110** or **112**, and whose (*S*)-configuration was assigned (Figure 4.8a). This derivative could therefore be easily obtained, and its synthesis was performed starting from  $\beta$ -lactams **110** and **112** with a simple hydrogenolysis reaction (Figure 4.8b). Comparing the specific rotation power signs, it was possible to assign the configurations of the resulting acids **113** and **114** and, consequently, of their corresponding benzylic precursors **110** and **112**.

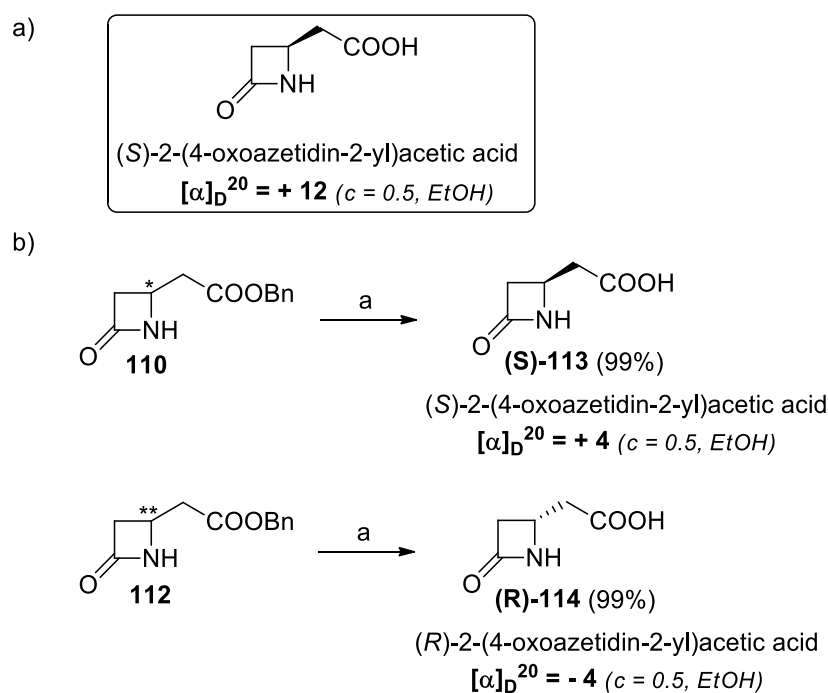
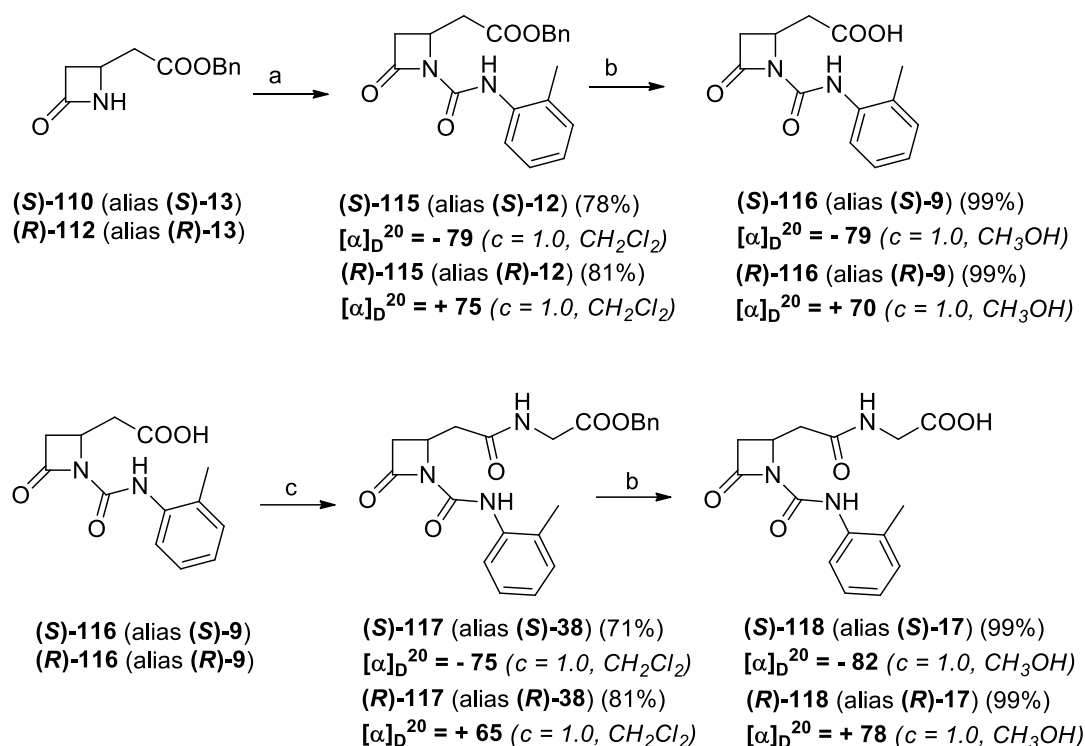


**Figure 4.8.** a) (*S*)-2-(4-oxoazetidin-2-yl)acetic acid and its specific optical power, used for the assignment of absolute configurations in the new enantiomerically enriched derivatives; b) Hydrogenolysis of  $\beta$ -lactams **110** and **112** and assignment of absolute configurations in the target acids **113** and **114**. Reagents and conditions:  $\text{H}_2$ , Pd/C (10%), THF/ $\text{CH}_3\text{OH}$  1:1, rt, 2 h. Yields of isolated compounds are reported in brackets; values of specific optical power are reported for compounds (*S*)-**113** and (*R*)-**114**

Starting from compounds (*S*)-**110** and (*R*)-**112**, further functionalizations were performed in order to obtain the couple of enantiomers **116** and **118** of two selected integrin ligands (**9** and **17**, respectively), both active at nanomolar level toward different classes. The synthetic strategies were successfully repeated from those described for the corresponding racemic compounds in Paragraph 3.1 (Scheme 4.12). The optical purity of the target compounds were also in this case preserved from their starting materials, since no chemical modification affected the C4 stereocenter, and anyway verified through chiral HPLC analysis for compounds **115** and **117**, after detection of the suitable separation conditions (data not shown).



**Scheme 4.12.** Synthesis of enantiomerically enriched  $\beta$ -lactams **116** and **118**. Reagents and conditions: a)  $\text{K}_2\text{CO}_3$ , *o*-tolylisocyanate,  $\text{CH}_3\text{CN}$ , rt, 2 h; b)  $\text{H}_2$ , Pd/C (10%),  $\text{THF}/\text{CH}_3\text{OH}$  1:1, rt, 2 h; c) EDC, TEA, DMAP, glycine benzylester-PTSA,  $\text{CH}_2\text{Cl}_2$ , 0 °C then rt, 16 h. Yields of isolated compounds are reported in brackets; values of specific optical power are reported for compounds **115-118**

#### 4.2.2 Biological evaluations

(in collaboration with Prof. S. M. Spampinato and Dr. M. Baiula, University of Bologna)

The two enantiomeric couples of  $\beta$ -lactam derivatives **116** and **118** were tested in adhesion assays as previously described (Table 4.4). In this case only cell lines expressing leukocyte integrin  $\alpha_4\beta_1$  or RGD integrin  $\alpha_5\beta_1$  were adopted for the biological evaluation, since the corresponding racemic derivatives **9** and **17** resulted selective agonists on  $\alpha_4\beta_1$  and  $\alpha_5\beta_1$  respectively. As reported in the Table, only (*S*)-enantiomers were active in promoting cell adhesion, whilst the opposite (*R*)-compounds resulted completely inactive, demonstrating how the stereoconfiguration at C4 is a fundamental requisite for switching on the activity toward the receptor. This evidence was also proofed for (*S*)-compounds deriving from *L*-aspartic acid vs *R*-series deriving from *D*-aspartic acid (see Paragraph 3.3.2). Values of activity of (**S**)-**116** and (**S**)-**118** are in accordance with those found for their analogue racemic compounds **9** and **17** (see Table 4.4), even if slightly decreased in the potency for the enantiomers vs the racemates, maybe due to a certain variability of cellular tests or for a not complete optical purity (94% ee for the (*S*)-series). However, the activity in the racemic compounds seemed to be not affected by the inactive enantiomer (*R*), since these derivatives simply displayed the value of activity arising from the (*S*)-enantiomer.

**Table 4.4.** Effects of  $\beta$ -lactams **116** and **118** on  $\alpha_4\beta_1$  and  $\alpha_5\beta_1$  integrin-mediated cell adhesion. Activity of the relative racemic compounds **9** and **17** were also included in the Table. Data are presented as EC<sub>50</sub> (nM). Values represent the mean of three independent experiments carried out in quadruplicate

Comp.	Jurkat/ VCAM-1	K562/FN
	$\alpha_4\beta_1$	$\alpha_5\beta_1$
(S)-116	21.2 agonist	n.t.
(R)-116	> 5000	n.t.
<b>9</b>	12.9 agonist	>5000
(S)-118	n.t.	35.3 agonist
(R)-118	n.t.	>5000
<b>17</b>	>5000	9.9 agonist

n.t. = not tested

### 4.3 Oxidation reactions

Oxidation chemistry plays a central role in organic synthesis and many industrial processes rely on oxidations as key steps. In a reality where the main source of chemicals is still fossil (oil, natural gas, fossil fuels), oxidative processes allow to obtain more reactive species from saturated hydrocarbons. Oxidation reactions are indeed an important tool for the interconversion of functional groups and largely exploited for alkane or alcohol transformations.<sup>276</sup>

Despite their broad applicability, oxidation reactions generally involve the use of stoichiometric and not selective high molecular weight oxidizing agents, based on metals such as Cr (VI) and Mn (VII), or on perchlorates. The use of these agents leads to the production of large quantities of waste, often containing very toxic or carcinogenic species. Other oxidants commonly used are peroxides and nitric acid, involving an additional danger in transport, storage and use. Such processes are therefore not sustainable from an environmental safety point of view, possessing an extremely poor atom economy (AE). For these reasons, in recent years there has been great interest in the study and development of more eco-sustainable synthetic strategies based on new catalytic oxidative processes that could comply with the principles of Green Chemistry. Moreover, pressure from society and regulation is placing important restrictions on industrial oxidation technology, with emphasis on the need for sustainable and environmentally friendly processes.

#### 4.3.1 Amine oxidation

Oxidation of amines has been less explored but it can afford a large panel of products (Figure 4.9), with some oxidations aiming at the nitrogen atom, other at both nitrogen and carbon atoms. Thus, selective reagents and controlled conditions are required to get a specific functional group. The oxidation of amines to get aldehydes is a particularly interesting transformation and despite its efficiency, the most common protocols suffer from the required use of stoichiometric amounts of toxic metal-containing reagents, such as KMnO<sub>4</sub>,<sup>277</sup> argentic picolinate,<sup>278</sup> ZnCr<sub>2</sub>O<sub>7</sub>,<sup>279</sup> and



nicotinium dichromate,<sup>280</sup> or palladium-,<sup>281</sup> copper-,<sup>282</sup> and ruthenium-based<sup>283</sup> catalysts. In addition, these methodologies are sometimes affected by over oxidation of aldehydes to carboxylic acids. The synthesis of imines *via* oxidative coupling of primary amines or oxidation of secondary amines were recently explored using metals or metal-complexes as catalysts.<sup>284</sup> Recently, photocatalysts such as titanium or niobium salts by UV irradiation, and mesoporous-C<sub>3</sub>N<sub>4</sub>,<sup>285</sup> Au-Pd/ZrO<sub>2</sub>,<sup>286</sup> conjugated and hollow microporous organic networks<sup>287</sup> by visible irradiation have been reported as active and highly selective catalysts for this oxidation. However, pure oxygen at high pressure is required.

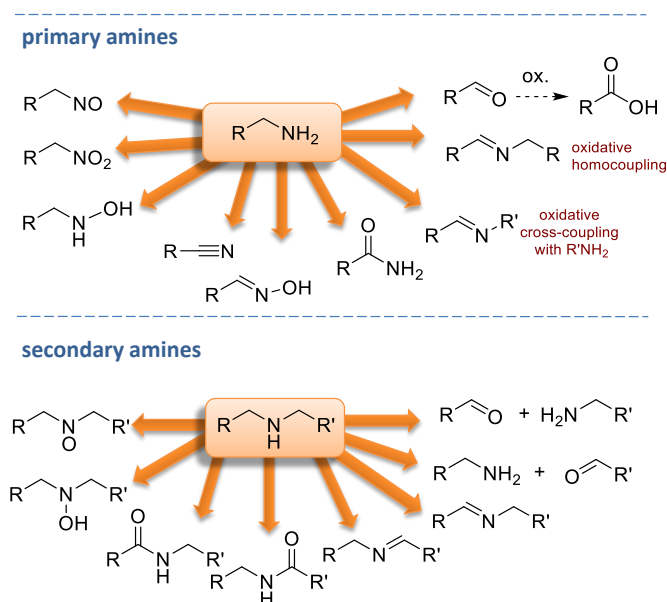


**Figure 4.9.** Functional group diversity generated by oxidation of primary or secondary amines

Many of these oxidation systems still require harsh reaction conditions and produce metal-containing wastes.<sup>288</sup> Therefore, as an improvement, some metal-free methodologies were studied. Recently, synthetic quinone-based catalysts for the efficient aerobic oxidation of amines to imines were reviewed.<sup>289</sup> These methods have been inspired by copper amine oxidases, a family of metallo-enzymes, which selectively converts primary amines into aldehydes, using molecular oxygen through the cooperation of a quinone-based cofactor. Relying on the bio-oxidation of amines, Contente *et al.* reported an application of a flow-based biocatalysis in the oxidation of amines to aldehydes by an immobilized transaminase with sodium pyruvate as co-oxidant.<sup>290</sup>

Concerning the use of inorganic metal-free oxidants, De Souza *et al.* reported a selective synthesis of imines and amides by oxidative coupling of amines using NaOCl.<sup>291</sup> Hypochlorite indeed is a widely used and cheap oxidant but its solutions liberate toxic gases such as chlorine when acidified or heated. Moreover, when chlorine-based oxidants are used in conjunction with organic compounds, the formation of potentially harmful organo-chlorine compounds is often an inevitable side reaction (chloramines, dioxines, etc), thus favoring the development and use of chlorine-free oxidant systems.<sup>292</sup>

From this point of view, NaIO<sub>4</sub> can be considered a promising oxidative agent, since it is a relatively cheap reagent, exploitable in water or aqueous solvents. Moreover, it is active at neutral pH and under mild conditions, which is compatible with a wide range of functionalities; for this reason this agent has been extensively used in oxidation reactions for organic synthetic applications. Sodium periodate has also been often employed in combination with other more expensive oxidants, in this case the use

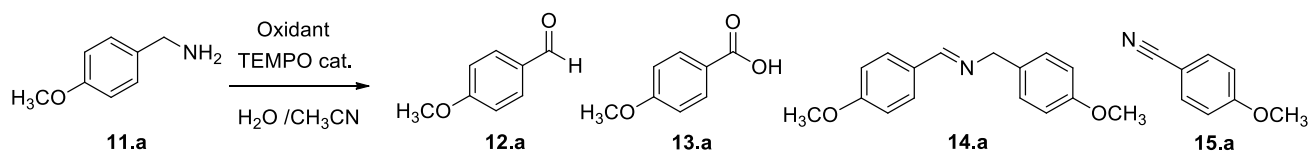
of periodates in stoichiometric amounts as primary oxidants allows the use of these expensive oxidants in catalytic amounts.<sup>293</sup>

#### 4.3.2 Amine oxidation with Sodium periodate/TEMPO system

As an ongoing interest in sustainable oxidation methodologies, we performed a study aimed at the development of a metal-free oxidation protocol for oxidizing amines into the corresponding aldehydes using TEMPO as catalyst.<sup>294</sup> Stable nitroxyl radical TEMPO (2,2,6,6-tetramethylpiperidine-1-oxyl) plays a salient role as catalyst in metal-, organo- or bio-catalysed oxidation processes and significant progress in terms of catalytic efficiency and substrate applicability has been achieved,<sup>295</sup> including oxidation of amines.<sup>296</sup>

Some inorganic oxidants were initially investigated for a selective amine oxidation. To increase the sustainability of the process, a homogeneous aqueous-organic mixture able to dissolve both the starting amine and the oxidant was chosen as reaction solvent, with mixtures of water and acetonitrile turning out to be suitable. For a preliminary study, *p*-OMe-benzylamine **11.a** was selected as model substrate in H<sub>2</sub>O/CH<sub>3</sub>CN (v/v = 2:1). Some inorganic oxidants were then screened, i.e. NaClO, NaClO<sub>2</sub>/NaClO (cat), NaClO/NaBr (cat) following the Anelli-Montanari protocol,<sup>297</sup> Na<sub>2</sub>S<sub>2</sub>O<sub>8</sub>, and NaIO<sub>4</sub>. Data in Table 4.5 illustrate the effect of some reaction parameters on the efficiency and on the distribution of the oxidation products.

**Table 4.5.** Screening of TEMPO catalyzed oxidation systems for *p*-OMe-benzylamine **11.a**



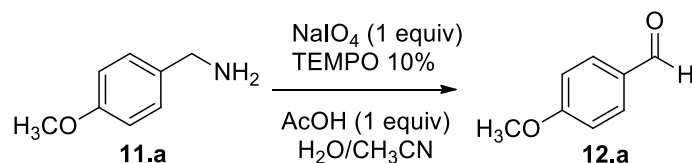
Entry	Oxidant	TEMPO (mol %)	Additive	Time (h)	Conv. (%)	Product (Yield %) <sup>a</sup>
1	NaClO <sub>2</sub> (2 eq)/NaClO (0,05 eq)	10		96	15	<b>14.a</b> (12)
2	NaClO <sub>2</sub> (2 eq)/NaClO (0,05 eq)	10	AcOH, 1 eq	144	98	<b>12.a</b> (10), <b>13.a</b> (40), <b>15.a</b> (50)
3	NaClO (1 eq)	10	AcOH, 1 eq	20	>99	<b>12.a</b> (23), <b>15.a</b> (71)
4	NaClO (1 eq)/NaBr (0.15 eq)	2	AcOH, 1 eq	72	44	<b>12.a</b> (27)
5	NaClO (1 eq)/NaBr (0.15 eq)	10	AcOH, 1 eq	72	80	<b>12.a</b> (73)
6	NaClO (1 eq)/NaBr (0.15 eq)	20	AcOH, 1 eq	72	84	<b>12.a</b> (77)
7	Na <sub>2</sub> S <sub>2</sub> O <sub>8</sub> (1 eq)	-		48	50	<b>12.a</b> (33)
8	Na <sub>2</sub> S <sub>2</sub> O <sub>8</sub> (1 eq)	10	AcOH, 1 eq	72	76	<b>12.a</b> (70)
9	NaIO <sub>4</sub> (1 eq)	-		24	63	<b>12.a</b> (42), <b>14.a</b> (16)
10	NaIO <sub>4</sub> (1 eq)	2		72	75	<b>12.a</b> (45), <b>14.a</b> (49)
11	NaIO <sub>4</sub> (1 eq)	10		24	86	<b>12.a</b> (73)
12	NaIO <sub>4</sub> (1 eq)	-	AcOH, 1 eq	20	13	<b>12.a</b> (12)
13	NaIO <sub>4</sub> (1 eq)	10	AcOH, 1 eq	20	>99	<b>12.a</b> (92)

<sup>a</sup> isolated yields by solvent extraction after acid work-up

The aqueous reaction medium brought an initial drawback deriving from a basic pH resulting on dissolution of amine **11.a** in the aqueous-organic solvent mixture (observed pH = 12). This basicity deactivated in some cases the oxidation system, thus giving low conversions and yields (entries 1, 7, and 9). To overcome this problem, the addition of one equivalent of acetic acid was successful in decreasing the initial pH to 7 and afforded a substantial improvement on both conversions and yields (entries 2, 3, 5, and 8). The radical TEMPO showed to be an effective organocatalyst in promoting the reaction with almost all the oxidants, with an optimized amount of 10 mol% to increase both yields and selectivity (for NaClO/NaBr see entries 4-6, for Na<sub>2</sub>S<sub>2</sub>O<sub>8</sub> see entries 7-8, for NaIO<sub>4</sub> see entries 12 and 13). Concerning the effect of the oxidation system on products selectivity, NaClO<sub>2</sub>/NaClO or NaClO alone are efficient but poorly selective, affording almost complete conversions but a mixture of products: aldehyde/acid/nitrile with NaClO<sub>2</sub>/NaClO, and an aldehyde/nitrile 1:3 mixture with NaClO (entries 2 and 3). NaClO/NaBr and Na<sub>2</sub>S<sub>2</sub>O<sub>8</sub> are very selective oxidants with an exclusive formation of the aldehyde **12.a** but do not reach complete conversions. NaIO<sub>4</sub> alone or with TEMPO 2 mol% gave mixtures of aldehyde and imine (entries 9 and 10), but on increasing the amount of TEMPO to 10% the aldehyde alone was obtained. Finally, NaIO<sub>4</sub> in the presence of 1 equiv. of acetic acid and 10% TEMPO gave complete conversion with an excellent isolated yield of **12.a** (entry 13). Thus, from this initial screening, the system NaIO<sub>4</sub>/TEMPO/AcOH emerged as the most efficient and selective method to oxidize the model amine **11.a** to the aldehyde **12.a**.

After selection of NaIO<sub>4</sub> as the best oxidant, the influence on conversions and yields of the solvent mixture and the amount of TEMPO was examined (Table 4.6).

**Table 4.6.** Optimization of reaction conditions with NaIO<sub>4</sub>/TEMPO oxidation system



Entry	H <sub>2</sub> O/CH <sub>3</sub> CN	Volume (mL)	Time (h)	Conv. (%)	Yield (%) <sup>a</sup>
<b>1</b>	2/1	15	20	>99	92
<b>2</b>	2/1	15	6	44	43
<b>3</b>	2/1	10	6	96	86
<b>4</b>	2/1	5	6	95	92 <sup>c</sup>
<b>5</b>	1/1	10	6	86	86
<b>6</b>	1/2	10	6	60	58
<b>7</b>	CH <sub>3</sub> CN	10	6	27	25
<b>8</b>	H <sub>2</sub> O	10	6	34	10

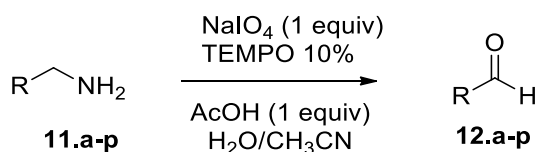
<sup>a</sup>isolated yields of **12.a** as single compound by solvent extraction after acid work-up

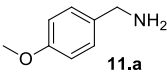
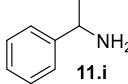
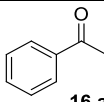
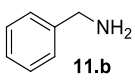
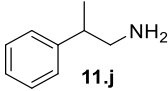
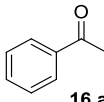
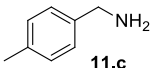
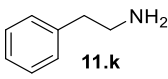
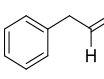
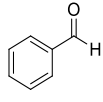
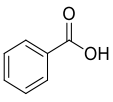
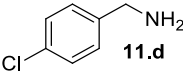
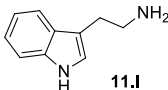
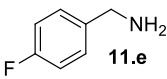
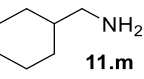
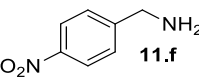
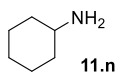
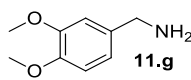
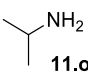
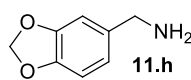
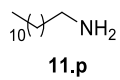
The mixture H<sub>2</sub>O/CH<sub>3</sub>CN 2:1 gave the best result, but on shortening the reaction time, the efficiency decreased (entries 1 and 2). On increasing the concentration of **11.a** by diminishing the total solvent

volume, the system recovered efficiency with good conversions and isolated yields in a shorter reaction time (entries 3 and 4). An increase of the relative amount of CH<sub>3</sub>CN in H<sub>2</sub>O was not efficient (entries 5 and 6) and worse results were obtained either in pure CH<sub>3</sub>CN because of the insolubility of NaIO<sub>4</sub>, or in H<sub>2</sub>O alone because of the insolubility of the starting amine **11.a** (entries 7 and 8).

With the optimized conditions in hand, the oxidation protocol with NaIO<sub>4</sub>/TEMPO/AcOH was applied to a series of commercial aldehydes to test the substrate scope (Table 4.7). Benzylamines **11.a-f** with different substituents on the aromatic ring were selectively and efficiently oxidized to the corresponding benzaldehydes **12.a-f**; both electron donating and electron-withdrawing substituents on the phenyl ring were well tolerated, giving access to the corresponding aldehydes in good to excellent isolated yields. 1-phenylethylamine **11.i** gave acetophenone **16.a** as expected, whereas its structural isomer 2-phenylethylamine **11.k** afforded a mixture of products: 2-phenylacetaldehyde **12.k** isolated in low yields (10%), benzaldehyde **12.b** as the main product (40%) derived from an oxidative C-C cleavage of **12.k**,<sup>298</sup> and traces of benzoic acid as over-oxidation of benzaldehyde. 2-Phenylpropylamine **11.j** yielded acetophenone **16.a** as the only product. Compound **16.a** probably derived from an initial oxidation of **11.j** to 2-phenyl-propanal which underwent an oxidative C-C cleavage to **16.a** as previously observed for phenylpropionic aldehydes.<sup>299</sup> Tryptamine **11.l** provided only polymerized products; moreover any tested cyclic or linear aliphatic amine not underwent a successful oxidation (entries 13-16), thus revealing a strong selectivity towards the oxidation of benzylic moiety.

**Table 4.7.** Scope of primary amine oxidation with NaIO<sub>4</sub>/TEMPO

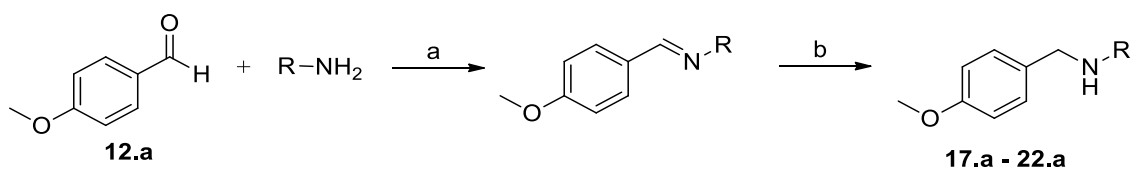


Entry	Starting amine	Yield (%) <sup>a</sup>	Entry	Starting amine	Yield (%) <sup>a</sup>
1	 11.a	92	9	 11.i	 65%
2	 11.b	85	10	 11.j	 40%
3	 11.c	90	11	 11.k	 12.k, 10%  12.b, 40%  13.b, traces
4	 11.d	90	12	 11.l	polymerized products
5	 11.e	93	13 <sup>b</sup>	 11.m	-
6	 11.f	97	14 <sup>b</sup>	 11.n	-
7	 11.g	75	15 <sup>b</sup>	 11.o	-
8	 11.h	81	16 <sup>b</sup>	 11.p	traces

<sup>a</sup> isolated yields by solvent extraction after acid work-up; <sup>b</sup> an equivalent of trifluoroacetic acid (TFA) was added in the basic organic extract

In order to exploit the reaction selectivity toward benzylic amines, a series of *N*-benzyl secondary amines were synthesized for possibly obtaining a selective removal of *p*MeO-benzylic group. The secondary amines were prepared *via* reduction of the corresponding imines or *via* a one-step reductive amination starting from the corresponding aldehydes and amines (Table 4.8).

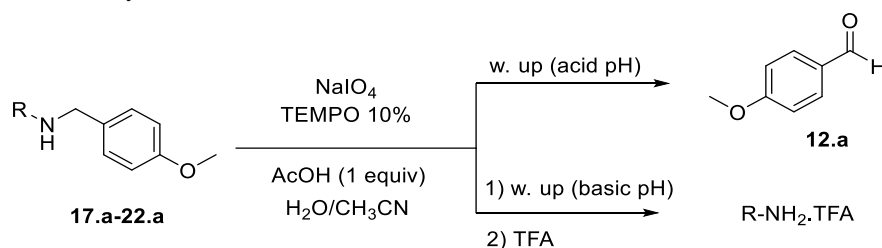
**Table 4.8.** Synthesis of secondary amines **17.a-22.a**<sup>a</sup>



Entry	Amine	Imine	Yield imine (%)	Secondary amine	Yield secondary amine (%)
1			99		90
2			97		83
3			83		86
4			99		92
5			96		83
6 <sup>b</sup>					89

<sup>a</sup> Reagents and conditions: a) aldehyde (1 equiv), amine (from 1 to 2 equiv), MgSO<sub>4</sub> (4 equiv), CH<sub>2</sub>Cl<sub>2</sub> (10 mL), rt, 24 h; b) imine (1 equiv), NaBH<sub>4</sub> (2 equiv), CH<sub>3</sub>OH (5 mL), rt, 24 h; b) Reagents and conditions: aldehyde (1 equiv), amine (1.5 equiv), NaBH(OAc)<sub>3</sub> (2 equiv), AcOH (1.5 equiv), CH<sub>2</sub>Cl<sub>2</sub> (10 mL), rt, 24 h

The optimized oxidative protocol was then applied to the developed *N*-benzyl secondary amines **17.a-22.a** (Table 4.9). Oxidation of symmetrical bis-*p*-methoxy-benzylamine **17.a** exclusively gave aldehyde **12.a** in good yields with 2.2 equiv. of periodate (entry 2). In the presence of 1 equiv. of NaIO<sub>4</sub> (entry 1) only traces of amine **11.a**, intermediate of the first oxidation step, were obtained. This could be due to a slower reactivity of secondary amine **17.a** than primary amine intermediate **11.a**, similarly to the oxidation with TEMPO of secondary alcohols compared to primary ones.<sup>35</sup> Unsymmetrical amines **18.a-22.a** were selectively oxidized only on the benzyl moiety, consequently yielding *p*OMe-benzaldehyde **12.a** and the aliphatic amine that were easily separated *via* liquid-liquid acid-base extraction as pure products in satisfactory to excellent yields. As a general observation, the yield of aldehyde **12.a** was in all cases increased by doubling the equivalents of sodium periodate (entries 1-8). The developed protocol could be then used to obtain selective deprotection of benzylic groups on secondary amines.

**Table 4.9.** Oxidation of secondary amines with NaIO<sub>4</sub>/TEMPO

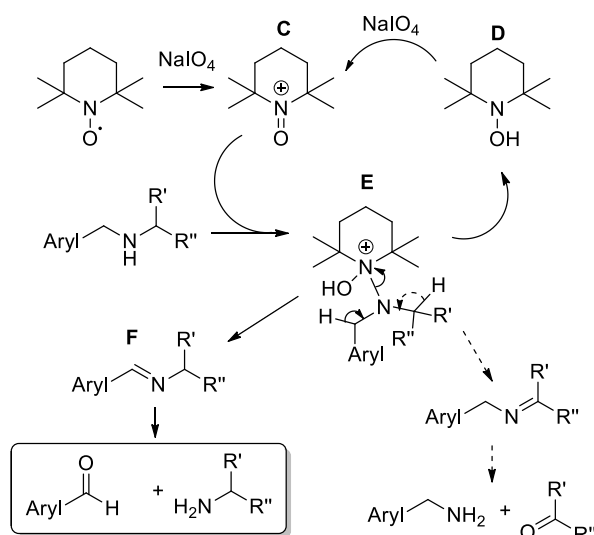
Entry	Starting amine	NaIO <sub>4</sub> (equiv)	R-NH <sub>2</sub> (Y %)	12.a (Y %) <sup>a</sup>	Entry	Starting amine	NaIO <sub>4</sub> (equiv)	R-NH <sub>2</sub> (Y %)	12.a (Y %) <sup>a</sup>
1		1	traces	39	6		1.5	92 <sup>b</sup>	98
2		2.2	8	80	7		1	51 <sup>b</sup>	46
3		1	60 <sup>b</sup>	75	8		2	59 <sup>b</sup>	69
4		2	43 <sup>b</sup>	85	9		1.5	15 <sup>b</sup>	22
5		1	88 <sup>b</sup>	95	10		1.5	80 <sup>b</sup>	92

<sup>a</sup> isolated as single compound by solvent extraction after acid work-up;

<sup>b</sup> amines were isolated as ammonium salts in the basic organic extract by adding an equivalent of trifluoroacetic acid (TFA)

A tentative analysis of TEMPO-mediated oxidation pathway could account for the observed selectivity. TEMPO is a stable nitroxide radical that undergoes a one-electron oxidation to the active oxidizing agent, the oxammonium cation **C** (Scheme 4.13). The oxidation process provides the reduced form as the neutral hydroxylamine **D**. Nitroxide radicals can be used in catalytic amount in the presence of a terminal oxidant and it has been already demonstrated the ability of sodium periodate to behave as terminal oxidant in alcohol oxidations with TEMPO as catalyst.<sup>300</sup> Considering the mechanism proposed for alcohol oxidation by oxammonium cation,<sup>301</sup> a tentative mechanism for the selective oxidation of secondary amines in aqueous medium could be formulated.

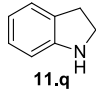
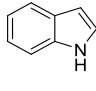
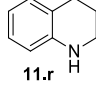
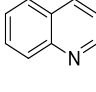
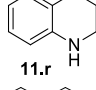
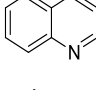
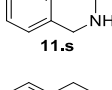
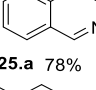
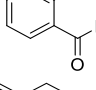
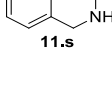
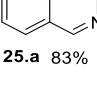
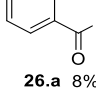
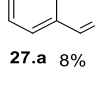
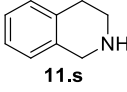
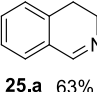
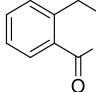
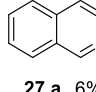
The reaction is initiated by the attack of the amine on **C** leading to the complex **E**,  $\beta$ -hydrogen elimination then produces two possible imines as intermediates and the hydroxylamine **D**, which is re-oxidized to oxammonium **C** by periodate. The H elimination selectively addressed the benzylic hydrogen rather than the aliphatic one probably on account of a lower C-H bond dissociation energy of the benzylic position.<sup>302</sup> In the aqueous medium the aryl-conjugated imine **F** underwent hydrolysis to give the target aryl-aldehyde and amine.



**Scheme 4.13.** Proposed mechanism for selectivity in secondary amine oxidation with NaIO<sub>4</sub>/TEMPO

Finally, three aromatic bicyclic amines **11.q-s** were evaluated as substrates of the oxidative protocol (Table 4.10). Amine **11.q** underwent oxidative aromatization and quantitatively gave indole **23.a** (entry 1), as well as **11.r** provided quinoline **24.a** in 74% isolated yield with 2 equiv. of sodium periodate and 1 equiv. of acetic acid (entry 3). 1,2,3,4-Tetrahydroisoquinoline **11.s** with 1 equiv. of periodate gave imine **25.a** as main product (78% yield) and small amounts of amide **26.a** (entry 4), but on enhancing the equivalents of periodate, increased amounts of **26.a** and the formation of isoquinoline **27.a** were detected (entries 5 and 6). Amide **26.a** could derive from an initial H<sub>2</sub>O addition to imine **25.a** and further oxidation of the intermediate aminol to amide, as recently reported in  $\alpha$ -oxygenation of amines to amides catalyzed by gold nanoparticles in H<sub>2</sub>O.<sup>303</sup>

**Table 4.10.** Oxidation of cyclic amines with NaIO<sub>4</sub>/TEMPO (10 mol%)

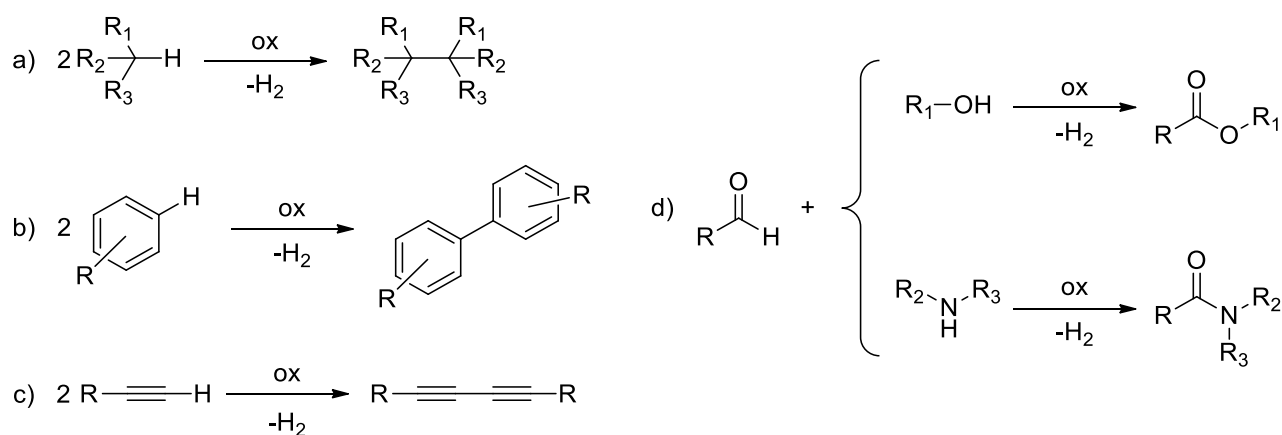
Entry	Amine	NaIO <sub>4</sub> (equiv)	AcOH (equiv)	Product, Yield % <sup>a</sup>
1	 <b>11.q</b>	1	-	 <b>23.a</b> 92%
2	 <b>11.r</b>	1	-	 <b>24.a</b> 48%
3	 <b>11.r</b>	2	1	 <b>24.a</b> 74%
4	 <b>11.s</b>	1	1	 <b>25.a</b> 78%  <b>26.a</b> 5%
5	 <b>11.s</b>	2	1	 <b>25.a</b> 83%  <b>26.a</b> 8%  <b>27.a</b> 8%
6	 <b>11.s</b>	3	1	 <b>25.a</b> 63%  <b>26.a</b> 27%  <b>27.a</b> 6%

<sup>a</sup> Isolated yields by solvent extraction after acid and basic work-up; the yield ratios of products **25.a**:**26.a**:**27.a** were determined via <sup>1</sup>H NMR analysis



### 4.3.3 Oxidative couplings

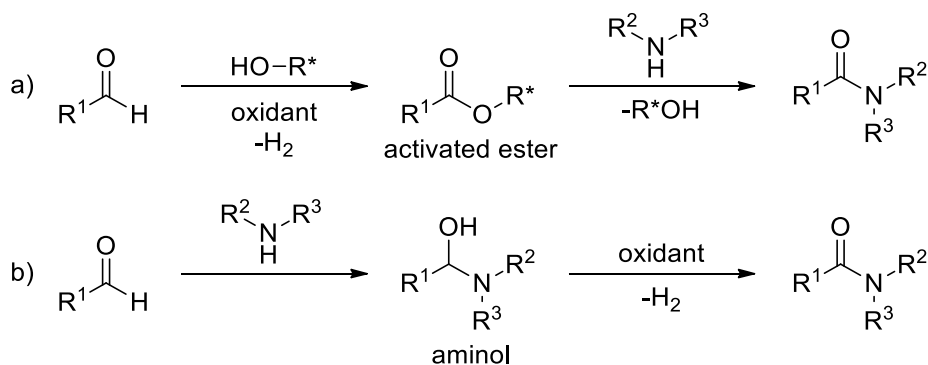
Oxidative couplings play an important role among the oxidation reactions. An important aspect of these processes concerns the possibility of forming C-C bonds by reaction of two C-H bonds under oxidative conditions without the need to enhance their reactivity with further functionalizations. Oxidative couplings display a wide reaction scope as they can occur on  $sp$ ,  $sp^2$  and  $sp^3$  C-H bonds, between bonds of the same type or between a C-H bond and a nitrogen or oxygen nucleophile, being hence applicable for the synthesis of C-C, C-N and C-O bonds (Scheme 4.14). Different oxidant agents could promote these couplings, such as high valence metals, halides,  $O_2$  and  $H_2O_2$ . Catalysts are instead based on Pd, Cu, Ru and Rh.<sup>304</sup>



Scheme 4.14. Scope of oxidative coupling reactions

Oxidative coupling between an aldehyde and an amine has emerged as an alternative method for the synthesis of amides because of its advantages in terms of atom economy, costs, and reagents availability. Amides are of pivotal importance both in nature, being present in many natural molecules (i.e. peptides and proteins) and in organic chemistry,<sup>305</sup> since amide bond is largely found in pharmaceutical products and polymers because of its high stability, polarity, and conformational diversity.

Traditional synthetic pathways for the synthesis of amides often lead to production of high quantities of waste as they require the use of coupling agents (i.e. carbodiimides) or activated reagents (acyl halides or anhydrides). An alternative process instead concerns a one-pot oxidative coupling reaction that can proceed in two ways: either the aldehyde is oxidized to an activated ester which then reacts with the amine (Scheme 4.15a) or aldehyde and amine react to form an aminol which is then oxidized to amide (Scheme 4.15b).<sup>306</sup>



**Scheme 4.15.** Oxidative coupling between: a) aldehydes and alcohols, and b) aldehydes and amines

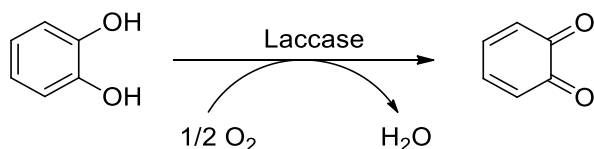
Despite a great expectation about this synthetic strategy, its development has been hindered by the limited applicability of the method, by the need to use chloroamines in order to avoid a self-oxidation, and by the poor reactivity of the C-H bond, often requiring the use of expensive ligands and toxic metal transition catalysts. Although many progresses have been made in the improvement of oxidative amidation reactions, developing metal-free or wide-applicable syntheses,<sup>307</sup> many processes still present sustainability problems, being conducted in organic solvents or with more than one co-catalyst or oxidizing agent.

#### 4.3.4 Biocatalytic oxidation reaction: laccases

A valid alternative to chemical oxidants is the use of biocatalytic systems: enzymes catalyzing oxidation-reduction reactions belong to EC category 1.x.x.x (oxidoreductase). These enzymes are particularly useful in organic synthesis, since they allow to operate in less drastic conditions, (i.e. in water and at room temperature), and in many cases guarantee a better chemo-, regio- and stereoselectivity, avoiding the need of protective groups. These enzymes are also enantioselective and able to generate enantiopure products from prochiral compounds. Industrially, oxidoreductases are employed to functionalize C-H bonds, to enantioselectively reduce carbonyl compounds, to degrade pollutants and are also used in the polymer and biosensor industry.<sup>308</sup> Oxidoreductases are divided into four sub-categories according to the substrate to oxidize: dehydrogenases, oxigenases, peroxidases and oxidases.

Oxidases in particular catalyze the oxidation of alcohols, phenols or amines, reducing O<sub>2</sub> to water or hydrogen peroxide. They also promote oxidative ring closure reactions and oxidative decarboxylation.

Among the oxidases, laccases (EC 1.10.3.2) play a very important role. These enzymes belong to the class of copper-dependent proteins and naturally catalyze the oxidation of phenol-type substrates to the corresponding quinones by reducing molecular oxygen to water (Scheme 4.16); they are ubiquitous enzymes in nature, mainly found in fungi and plants (where they are involved in the formation and degradation of lignin), but also in some bacteria and insects.



**Scheme 4.16.** Catechol oxidation with laccases

From a structural point of view, laccases are glycoproteins and their active site consists of four copper atoms (Figure 4.10).<sup>309</sup> Due to their relatively low oxidation-reduction potentials (less than 0.8 V), laccases use oxygen from air as a terminal oxidant and their action is limited to phenolic substrates whose redox potential is in the range 0.5-1 V.

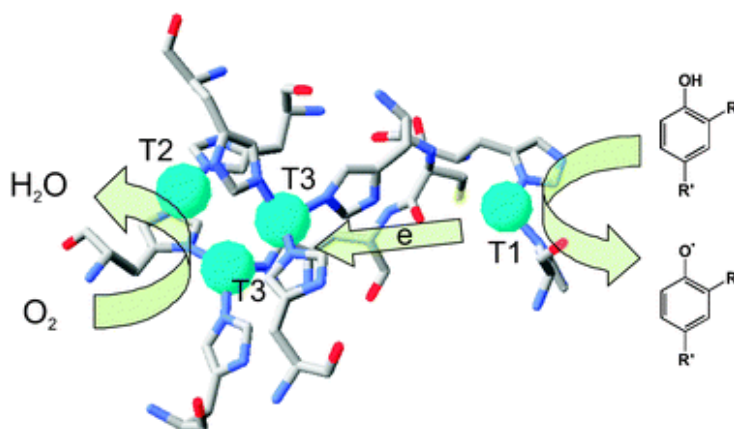


**Figure 4.10.** Laccase active site, the four copper atoms are depicted in light blue. Figure adapted from ref. <sup>310</sup>

The substrate scope of laccases can however be expanded using a mediator, a molecule able to promote the electronic transfer from the substrate to the enzyme, thus allowing the oxidation of non-natural substrates. The coupling of a laccase with a mediator is defined Laccase Mediator System (LMS) (Figure 4.11).<sup>311</sup>

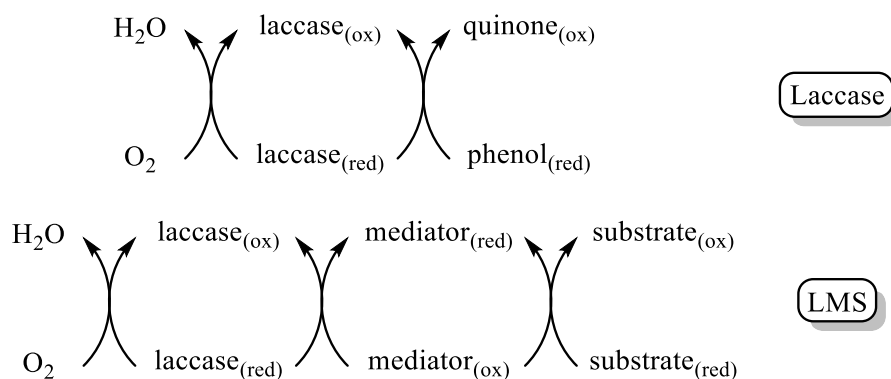


**Figure 4.11.** Mechanism of Laccase and Laccase Mediator System (LMS) oxidation

A perfect mediator is defined as a low molecular weight compound capable of producing stable radicals not interfering with the enzyme activity and able to conduct different catalytic cycles without degrading.<sup>312</sup> Mediators can be divided into synthetic (Figure 4.12a) and natural (Figure 4.12b).

Natural mediators are phenolic compounds such as syringic acid and its derivatives, but also synthetic mediators such as 2,2,6,6 tetramethyl-1-piperidiniloxy (TEMPO) and 2,2'-azino-bis-(3-ethylbenzothiazoline-6-sulphonic acid) (ABTS) have been employed with success.

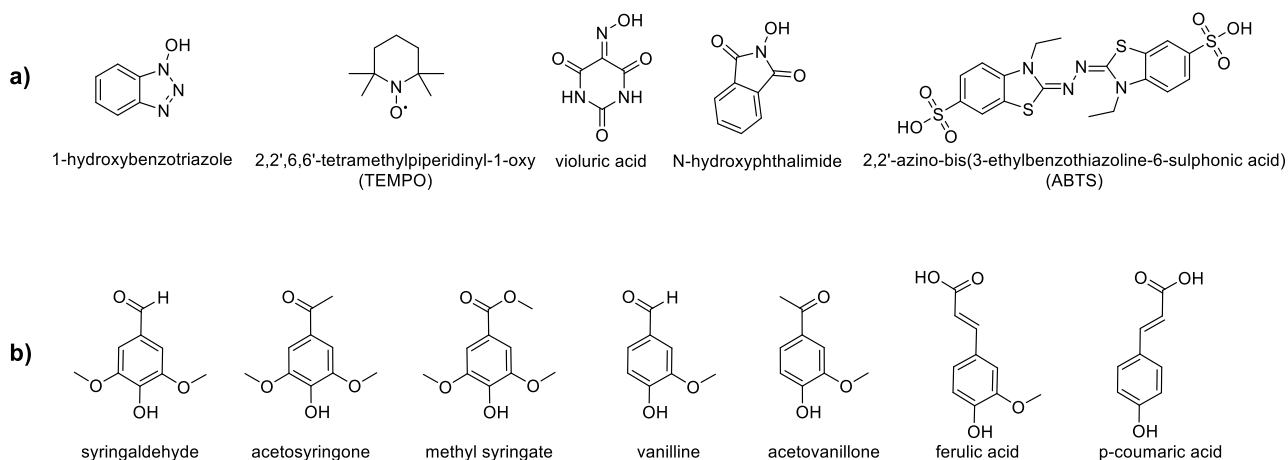
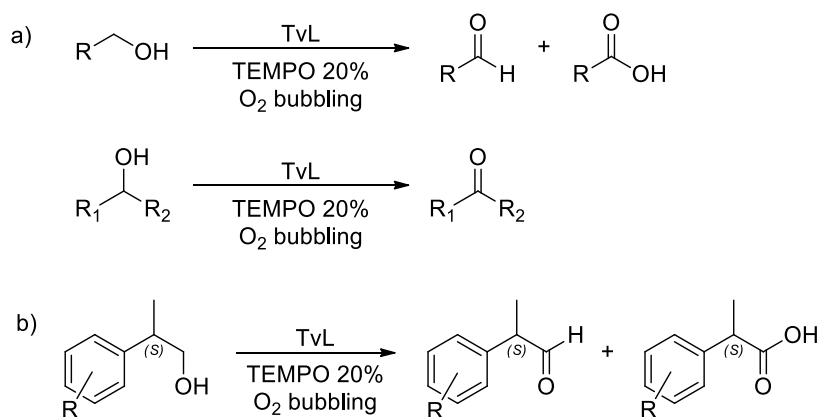


**Figure 4.12.** Examples of laccase mediators: a) synthetic, b) natural

Laccases are used in different industrial fields such as in paper, food and textile industries, as well as in the production of polymeric materials and cosmetic field. Laccases have also received increasing attention in recent years from organic chemistry and are used in pharmaceutical industry for the production of antibiotics, antifungals and antineoplastic drugs,<sup>313</sup> as they can promote clean and selective oxidations with water as the only by-product.

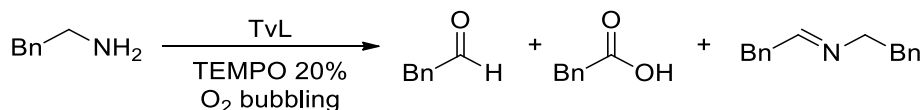
My research group has recently studied oxidative processes promoted by Laccase Mediator System for the biocatalytic transformation of key molecules in synthetic chemistry. In particular, the oxidation of primary alcohols to aldehydes or carboxylic acids and of secondary alcohols to ketones was performed through a catalysis mediated by Laccase from *Trametes versicolor* (TvL) coupled with the synthetic mediator TEMPO (Scheme 4.17a).<sup>314</sup> The reaction was also promoted by oxygen insufflation; the best solvent turned to be water in a pH 4.5 buffered or unbuffered medium; excellent results were also obtained in aqueous solvent with small amounts of acetone.

The system was applicable with excellent results to benzyl alcohols substituted with EW groups on the aromatic ring and to heteroaromatic alcohols, while was not suitable for aliphatic alcohols. This method was also successfully extended to the oxidation of (*S*)-prophenols to the corresponding bioactive (*S*)-prophenes (Scheme 4.17b) with excellent yields and configuration retention.<sup>314</sup>



**Scheme 4.17.** Oxidation of a) primary or secondary alcohols and b) prophenols catalysed by LMS.

In a second work, the same optimised protocol was employed for amine oxidation, a reaction in which laccases generally find a poor application. The laccase/TEMPO system was exploited to oxidise benzyl amines to aldehydes, carboxylic acids or imines (Scheme 4.18).<sup>315</sup> The reaction took place in a buffered aqueous environment for avoiding the enzyme inactivation due to the basic pH generated by the starting amine; the pH control constituted the main factor for selectively obtaining a single product. The protocol was successfully applied to primary, secondary and cyclic benzyl amines, with yields that were not affected by the electronic effects of the ring substituents.



**Scheme 4.18.** Oxidation of benzyl amines catalysed by LMS

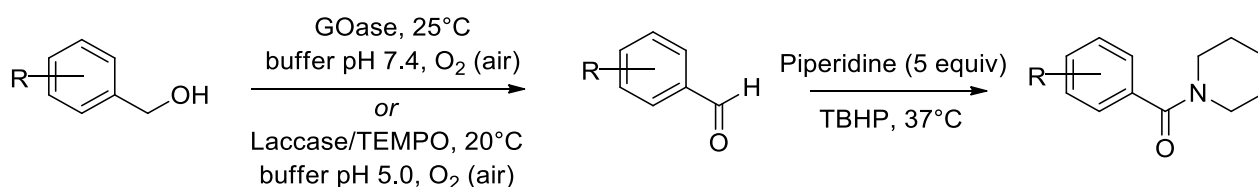
#### 4.3.5 Development of the oxidative amidation

As already described, there is a great interest toward the development of oxidative coupling reactions for the synthesis of amides that could proceed under mild conditions and adopt clean oxidizing agents such as O<sub>2</sub> and renewable catalysts.

Biocatalysis fulfills these requirements and the number of enzyme-mediated processes used in industry has been growing over the past decades due to low environmental impact, low waste production, and high efficiency in terms of stereo-, regio- and chemo-selectivity. However, biocatalysis has not been applied yet to oxidative amidation reactions.

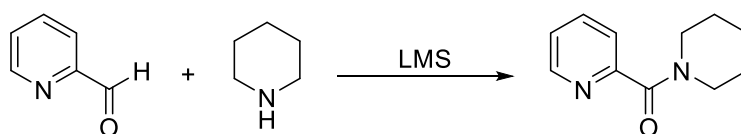
After the good results recently obtained by the research group concerning the oxidation of alcohols or amines to the corresponding carboxylic acids or aldehydes mediated by laccase/TEMPO system,<sup>314,315</sup> we decided to evaluate a possible oxidative amidation reaction promoted by a Laccase Mediator System (LMS).

A recent paper by Bechi *et al.* reported a one-pot two-step process for the conversion of differently substituted aryl alcohols and piperidine into amides: the first step involved the transformation of alcohol into aldehyde *via* enzymatic catalysis mediated by Laccase/TEMPO system or galactose oxidase (GOase); the second step proceeded with the oxidative coupling by addition of piperidine (5 equiv) and *tert*-butyl hydroperoxide (TBHP) (Scheme 4.19).<sup>316</sup>



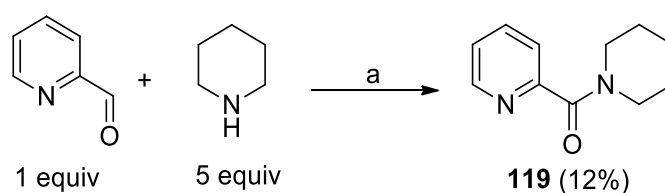
**Scheme 4.19.** One-pot two step amidation reaction<sup>316</sup>

In our case, a direct one-step protocol was adopted starting with an aldehyde as a substrate, and in particular 2-pyridinecarboxaldehyde and piperidine were selected as oxidative coupling partners for preliminary screenings (Scheme 4.20).



**Scheme 4.20.** Model reaction for the amidation oxidative coupling

Commercially available Laccase from *Trametes Versicolor* (TvL) was used and combined with TEMPO (28%) as a mediator. The reaction was performed in unbuffered water under mild conditions (37 °C), and with molecular oxygen (bubbled for 30 secs) as terminal oxidant. To notice, the strong basicity induced by the excess of piperidine avoided the maintenance of the desired pH in the presence of a buffer solution, and even the tentative addition of CH<sub>3</sub>COOH in the reaction mixture for reaching a neutral pH induced solubility issues due to the formation of the corresponding ammonium salt. The presence of a small amount of acetonitrile as a co-solvent allowed instead to obtain a better solubility of the mixture. After 48 h, the conversion resulted complete and the desired amide **119** was isolated, even if with a very low yield (Scheme 4.21).



**Scheme 4.21.** Oxidative coupling of 2-pyridinecarboxaldehyde and piperidine. Reagents and conditions: a) Laccase Tv (5 mg), TEMPO 28%, H<sub>2</sub>O/CH<sub>3</sub>CN, O<sub>2</sub> bubbling (30 secs), 37 °C, 48 h. Yield of isolated compound is reported in brackets

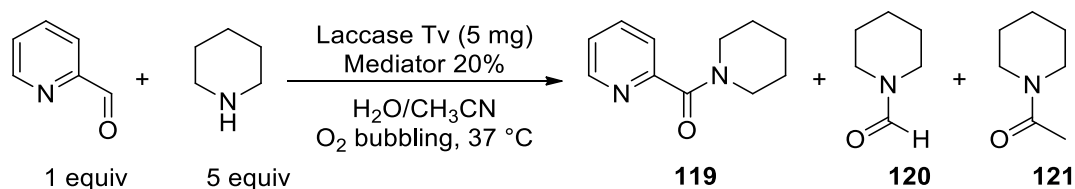
An enhancement of the enzyme amount (30 mg) did not improve the reaction yield. Concerning the oxidizing atmosphere, better results were obtained bubbling O<sub>2</sub> in the mixture than performing the reaction under air or inert gas. Also a reaction starting from the corresponding alcoholic partner (2-pyridine-methanol) was attempted according to what suggested by Bechi *et al.*,<sup>316</sup> but the target amide was not detected.

Following the conditions reported in Scheme 4.21, other substrates were tested. Concerning the aldehydes, isomers of 2-pyridinecarboxaldehyde, benzaldehyde and *para*-substituted benzaldehydes were screened, always leading to a null conversion. Only 4-pyridinecarboxaldehyde provided the corresponding amide with a 7% yield after 6 days (data not shown).

Different amine substrates were then tested and when primary amines such as butylamine or cyclohexylamine were employed, only imines deriving from the starting aldehyde were detected in the crude reaction mixtures (data not shown).

Finally, several mediators, both natural and synthetic, were screened, as reported in Table 4.11.

**Table 4.11.** Mediator screening on amidative oxidation



Entry	Mediator	Time (days)	119 (Yield %) <sup>a</sup>	Ratio 119:120:121 <sup>b</sup>
1	Methyl syringate	4	33	Traces of 120 and 121
2	Syringic acid	7	11	1:0.4:0.5
3	Methyl vanillate	6	5	1:1.3:1.1
4	Syringaldehyde	6	10.5	1:0.9:0.5
5	Acetosyringone	6	9.5	1:0.4:0.5
6	<i>N</i> -hydroxysuccinimide	4	17	1:0.3:0.3
7	1-hydroxybenzotriazole	4	10.5	1:0.4:0.4
8	<i>N</i> -hydroxyphthalimide	4	9.5	1:0.2:0.2

<sup>a</sup> isolated yield after flash-chromatography

<sup>b</sup> Ratios of products **119:120:121** were determined *via* <sup>1</sup>H NMR analysis after work-up

In general, from NMR spectra of the crude reactions, two by-products were detected beside the desired amide **119**, i.e. *N*-formyl piperidine (**120**) and *N*-acetyl piperidine (**121**); their structures were confirmed through HPLC-MS analysis. As depicted in Table 4.11, the best results were obtained with methyl syringate, which led to an encouraging 33% yield (entry 1). The other natural mediators (methyl ester of vanillic acid, syringic acid, syringaldehyde and acetosyringone, entries 2-5) provided comparable or worse results than TEMPO. Among the synthetic mediators instead, *N*-hydroxysuccinimide provided a 17% yield (entry 6), while 1-hydroxybenzotriazole and *N*-hydroxyphthalimide were in line with results obtained with TEMPO (entries 7-8).

Considering the reported results, the subsequent oxidative coupling tests were carried out using methyl syringate; the amount of the mediator was then varied to determine its influence on the reaction yield. Furthermore, with this mediator, the number of piperidine equivalents was tentatively decreased, since an extremely basic environment was undoubtedly harmful for the enzyme (Table 4.12).

**Table 4.12.** Oxidative couplings with methyl syringate

C1=CC=C(C=C1)C(=O)C2=CC=NC=C2 + C1CCNCC1  $\xrightarrow[\text{O}_2 \text{ bubbling, } 37^\circ\text{C}]{\text{Laccase Tv (5 mg), Methyl syringate}}$  C1=CC=C(C=C1)C(=O)N2CCCCC2

1 equiv  **119**

Entry	Methyl syringate (%)	Time (days)	Piperidine (equiv)	Yield % <sup>a</sup>
1	20	4	5	33
2	10	4	5	22
3	20	4	2.5	18
4	20	7	1.5	6

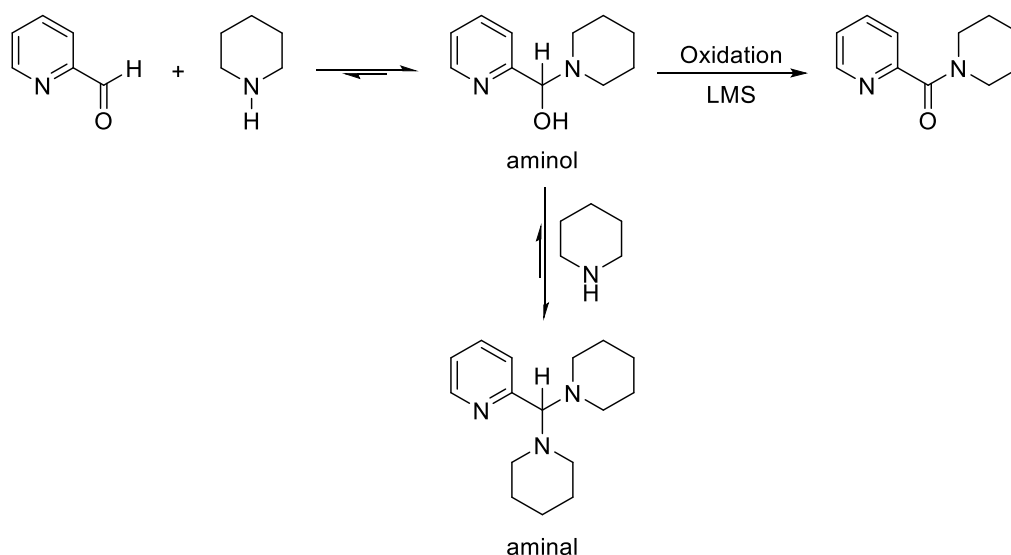
<sup>a</sup>isolated yield after flash-chromatography

From the data reported in Table 4.12 it was clear that both the use of 20% mediator and 5 equivalents of amine were required for obtaining better reaction yields, as a decrease in methyl syringate or piperidine led to a drop in efficacy (entry 1 vs 2, 3, 4). Since no better conditions were detected, a screening in starting aldehydes and amines was performed. Both isomers of 2-pyridinecarboxaldehyde and different *para*-substituted benzaldehydes were tested, but unfortunately none of them resulted active in the oxidative amidation reaction, and only traces of products were detected in all cases (5% yield obtained with 4-pyridinecarboxaldehyde).

Similarly, concerning the amine screening, only pyrrolidine provided the desired product in 30% yield, while morpholine and dipropylamine gained the target amide in 3% and 10% yield, respectively; other acyclic secondary amines achieved only traces of the desired product (data not shown).

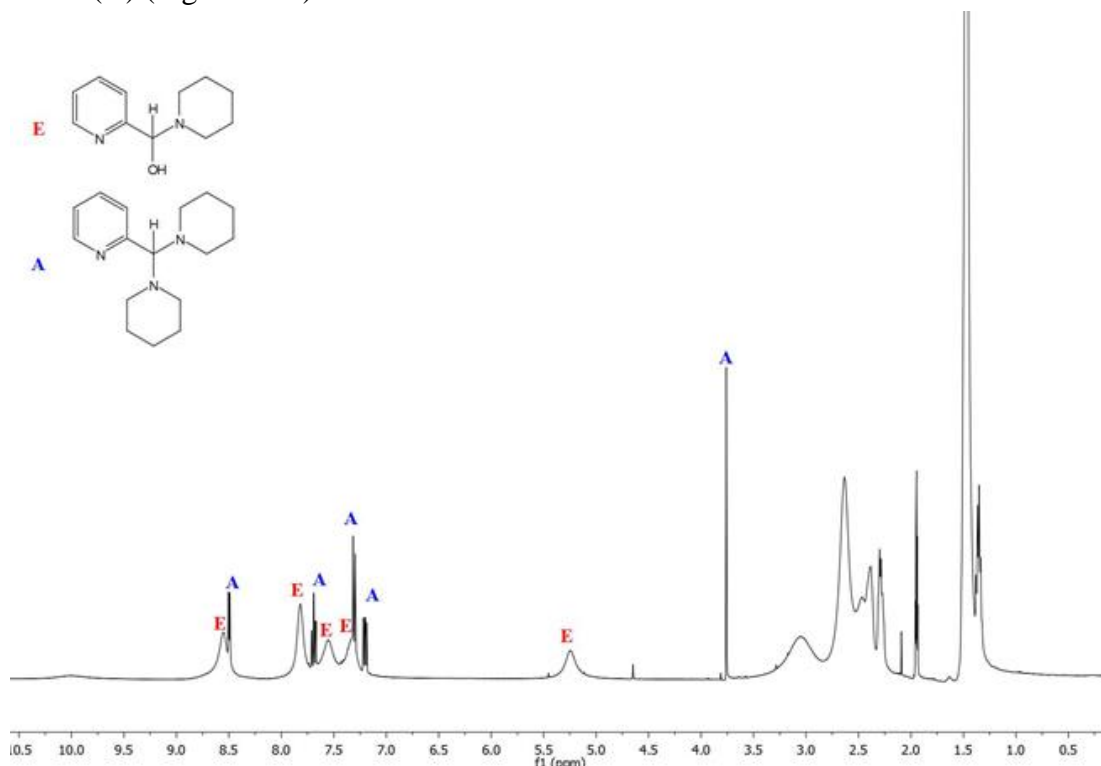
In most of the performed reactions however, the conversion of the aldehyde resulted complete. <sup>1</sup>H-NMR experiments were performed in order to highlight the equilibria established in the reaction mixture and to tentatively understand the reaction mechanism. It was observed that a premixing of aldehyde (1 equiv) and amine (1.5 equiv) in a D<sub>2</sub>O/CD<sub>3</sub>CN mixture gave a hemiaminal intermediate (aminol). Probably, a complete shift of the equilibrium toward the aminol species occurred, hence explaining the complete disappearance of the aldehyde from the reaction mixture. (Scheme 4.22).





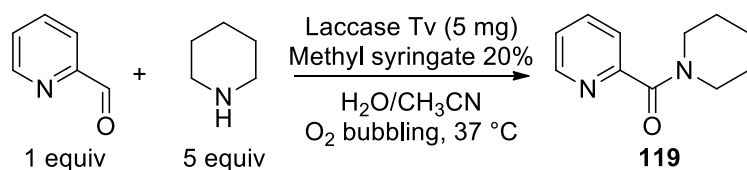
**Scheme 4.22** Possible established equilibria and involved species in the oxidative amidation

Although the aldehyde was completely converted to aminol, the further oxidation to amide was not quantitative; it was then hypothesized that the aminol (E) was engaged in a side reaction. NMR analysis of 2-pyridinecarboxaldehyde and piperidine in  $\text{CD}_3\text{CN}$  showed in fact that, after 30 minutes of reagents mixing, the aminol species was irreversibly captured in a non-productive aminal intermediate (A) (Figure 4.13).



**Figure 4.13.**  $^1\text{H}$  NMR spectrum of 2-pyridinecarboxaldehyde and piperidine in  $\text{CD}_3\text{CN}$  after 30 minutes of reagent mixing

To evaluate the product formation along the time, the reaction was monitored every 24 hours (Table 4.13).

**Table 4.13.** Kinetic study on the product formation

Entry	Time (days)	Yield % <sup>a</sup>
1	1	13
2	2	25
3	3	29
4	4	32

<sup>a</sup> isolated yield after flash-chromatography

The reaction proceeded faster in the first 48 hours, doubling the yield from 24 to 48 hours (entries 1-2). This increase was instead much less pronounced in the following 48 hours (entries 3-4). However, also in this case, a complete conversion of the starting material was observed.

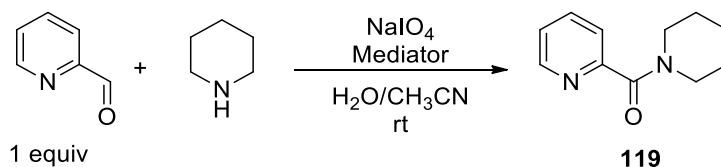
Another possible issue for the non-quantitative oxidation of the hemiaminal intermediate concerned the degradation of the mediator, which in the reaction environment (pH = 12) was unstable and hydrolysed to the corresponding carboxylic acid. The activity of syringic acid in the oxidative amidation reaction had already been evaluated (Table 4.11), resulting to be less effective than the relative ester. A study on the stability of methyl syringate was then performed with the best reaction conditions, without inserting the aldehyde and the enzyme. The evaluation through HPLC monitoring confirmed that already in the first 48 hours the amount of ester in the reaction environment underwent a significant drop; the calculated half-life of the mediator resulted in fact of 36 hours. These results were consistent with the kinetic study of product formation that highlighted how the oxidative coupling was more effective in the first 48 hours of reaction, thus when the mediator was still present in the mixture. After 4 days, hydrolysis of the methyl ester was almost completed, consequently the oxidative reaction could not proceed or proceeded very slowly. It was then attempted a portioned addition of methyl syringate, which was introduced in a 20% amount at the beginning, followed by a subsequent 10% after 24 hours. In this way a 40% yield of amide **119** was obtained after 4 days.

The oxidative amination was then investigated in the absence of both enzyme and mediator, showing that only the atmospheric oxygen could partially promote the process, leading to a 11% yield. Also tests conducted in the absence of enzyme revealed lower yields than those obtained with laccases, demonstrating that the enzyme was necessary for a mediator recycle. However, laccase was probably soon deactivated because of the basic pH of the reaction mixture.

It was finally observed that one equivalent of methyl syringate allowed to obtain the amide in 46% yield, showing only a slight improvement despite the stoichiometric amount of the mediator. A comparable result was obtained with a 60% amount of the mediator; it was therefore hypothesized that the hemiaminal intermediate (Scheme 4.22) could reach an equilibrium stage and consequently its oxidation could not proceed further, despite the mediator availability in the reaction environment. Finally, for comparing the biocatalytic amidative oxidation of 2-pyridinecarboxaldehyde and piperidine with a chemical process, the reaction was tested in the presence of stoichiometric sodium

periodate, according to the good results explicated by this agent in the oxidation of amines to aldehydes (see Paragraph 4.3.2).<sup>294</sup> The oxidative amidation promoted by NaIO<sub>4</sub> was screened under different conditions (H<sub>2</sub>O/CH<sub>3</sub>CN ratios, number of periodate and piperidine equivalents) and some tests were also carried out in the presence of acetic acid in order to decrease the pH in the reaction environment (Table 4.14).

**Table 4.14.** Oxidative amidation promoted by NaIO<sub>4</sub>



Entry	Mediator (%)	Piperidine (equiv)	NaIO <sub>4</sub> (equiv)	H <sub>2</sub> O:CH <sub>3</sub> CN	Time (days)	Yield % <sup>a</sup>	Notes
1	-	5	1	2:1	1	9.5	-
2	-	5	1	2:1	1	traces	5equiv AcOH
3	TEMPO (10%)	5	1	2:1	3	traces	5equiv AcOH
4	-	1	1.2	2:1	1	4	-
5	Methyl siringate (10%)	5	1	2:1	4	traces	-
6	-	5	1	11:1	4	15	-
7	-	5	1.5	11:1	4	traces	5equiv AcOH

<sup>a</sup> isolated yield after flash-chromatography

The best results were obtained using a 11:1 H<sub>2</sub>O/CH<sub>3</sub>CN solvent mixture with 1 equiv of periodate and without acetic acid (entry 6, 15% yield). The reaction carried out under the same conditions in a 2:1 H<sub>2</sub>O/CH<sub>3</sub>CN ratio gave a slightly lower result (entry 1, 9.5%). The addition of acetic acid was totally detrimental (entries 2, 3 and 6); also the tentative decrease of piperidine equivalents led to very poor yields (entry 4), as well as the use of TEMPO or methyl syringate as mediators (entries 3 and 5). It was then concluded that the biocatalytic process globally revealed to be a more efficient methodology for oxidative amidation.

## 4.4 Enzymatic carboxylation of biphenyl compounds

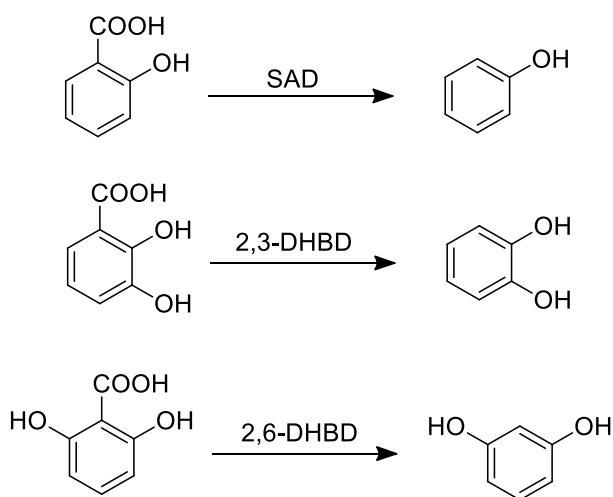
### 4.4.1 (De)carboxylases

The use of CO<sub>2</sub> as a C1 carbon source for the synthesis of organic compounds and polymeric materials has become very attractive,<sup>317</sup> although the high demand of energy required for the activation of carbon dioxide represents a tough challenge for its synthetic utilization, explaining why only a limited number of carboxylation processes runs on industrial scale.<sup>318</sup>

In recent years, numerous chemical carboxylation strategies based on (transition) metal catalysis have been developed, predominantly replacing harsh reaction conditions by eco-friendly catalytic processes.<sup>319</sup> In contrast, nature provides a vast variety of enzymatic CO<sub>2</sub>-fixation reactions that play a vital role in all living organisms. Unfortunately, most of the biosynthetic CO<sub>2</sub>-fixing enzymes are

highly substrate specific, which severely limits the chances to employ them for non-natural substrates. On the other hand, unspecific CO<sub>2</sub>-fixation occurs in biodegradation pathways, which serve as detoxification of electron-rich (hetero)aromatics to enhance the water-solubility of toxic phenols.<sup>320</sup> Whereas the oxidative degradation of aromatics predominantly involving mono-oxygenases has been well studied, only limited data is available on the anaerobic counterpart catalysed by carboxylases. In fact, enzymatic carboxylation of phenolic substances is a common detoxification pathway in anaerobic environments and hence the corresponding enzymes are expected to possess a relaxed substrate tolerance.<sup>321</sup> However, in order to ensure fast turnovers and facile biochemical assays, the majority of enzymatic CO<sub>2</sub>-fixation reactions have been biochemically investigated in the energetically favoured decarboxylation direction and the respective enzymes were commonly denoted as ‘decarboxylases’ rather than ‘carboxylases’.<sup>322</sup> Nevertheless, the carboxylation of (hetero)aromatic and phenolic compounds is a convenient method to obtain aromatic carboxylic acids used as pharmaceuticals and building blocks for organic synthesis,<sup>323</sup> but the traditional chemical (Kolbe–Schmitt) carboxylation process performed on an industrial scale requires high pressure and temperature (~90 bar, 120–300 °C) and often suffers from incomplete regioselectivities resulting in product mixtures.<sup>324</sup> In order to circumvent these limitations, the use of (de)carboxylases in the (reverse) carboxylation direction represents a novel attractive biocatalytic alternative.<sup>322</sup>

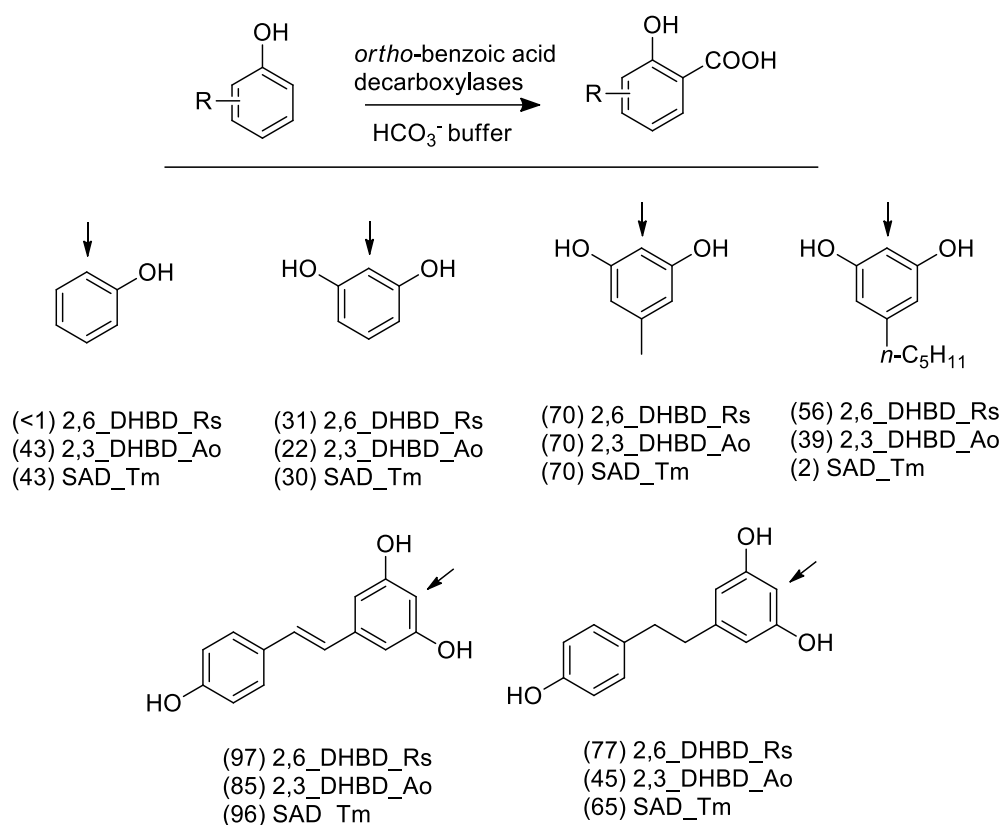
Decarboxylases in general are defined as enzymes, which add or remove a carboxyl group from organic compounds.<sup>325</sup> Some examples among the *ortho*-benzoic acid decarboxylases class are: salicylic acid decarboxylase (SAD), 2,3-dihydroxybenzoic acid decarboxylase (2,3-DHBD), and 2,6-dihydroxybenzoic acid decarboxylases (2,6-DHBD), which naturally catalyse a decarboxylation reaction on salicylic acid, 2,3-dihydroxybenzoic acid and 2,6-dihydroxybenzoic acid respectively (Scheme 4.23).



**Scheme 4.23.** Reactions of salicylic acid decarboxylase (SAD), 2,3-dihydroxybenzoic acid decarboxylase (2,3-DHBD) and 2,6-dihydroxybenzoic acid decarboxylases (2,6-DHBD) with their natural substrates

To date, a biocatalytic toolbox for the regioselective *ortho*-carboxylation of phenols has been established employing decarboxylases at ambient temperature in the reverse carboxylation direction and bicarbonate buffer as CO<sub>2</sub> source.<sup>326</sup> The method was successfully extended by Faber group to

the *o*-carboxylation of polyphenols and flavouring agents.<sup>322,327</sup> The reactions proceeded in a highly regioselective fashion yielding the corresponding *ortho*-hydroxybenzoic acids exclusively. The decarboxylases employed for the studies were: 2,3-DHBD\_Ao=2,3-dihydroxybenzoic acid decarboxylase from *Aspergillus oryzae*, 2,6-DHBD\_Rs=2,6-dihydroxybenzoic acid decarboxylase from *Rhizobium sp.* and SAD\_Tm=salicylic acid decarboxylase from *Trichosporon moniliiforme*. The applicability of the regioselective carboxylation is shown in Scheme 4.24 with a small panel of examples of the substrate scope.<sup>322,327</sup>



**Scheme 4.24.** Regioselective enzymatic carboxylation of (poly)-phenolic substrates. Reagents and conditions: phosphate buffer (pH 8.5, 100 mM), whole lyophilized cells of *E. coli* containing the corresponding overexpressed enzyme (30 mg/mL), substrate (10 mM),  $\text{KHCO}_3$  (3M), 30 °C, 120 rpm, 24 h; Conversions (%) were determined by reversed-phase HPLC and reported in brackets.

Arrows indicate the carboxylation site<sup>322,327</sup>

As shown in Scheme 4.24, two hydroxyl groups are usually required on the aromatic ring for converting the substrate into the carboxylated product, and enzyme 2,6-DHBD displayed in general the best performances by inserting a carboxyl between the two hydroxyl groups. Nevertheless, phenol itself was accepted as a substrate by 2,3-DHBD and SAD (not by 2,6-DHBD); resorcinol instead reacted with all enzymes yet with moderate conversions; in general, *para*-substituents like a methyl group improved the conversions and also a longer alkyl chain was well tolerated by all of the tested decarboxylases. Also the flavonoid derivative resveratrol was converted in good yields enabling an additional electronic activation towards carboxylation, and its analogue bearing a not conjugated system led anyway to discrete conversions.<sup>327</sup>

#### 4.4.2 Stereorecognition in biphenyl compounds

In order to expand the scope of the reaction, we decided to probe the stereorecognition of the enzymatic carboxylation on biphenyl compounds, which are particularly interesting for their property of potentially displaying atropisomerism. In fact, there are many well-documented atropisomeric pharmaceuticals, whose utility as effective drugs or leads have been demonstrated. Worth mentioning among them, is the almost cliched example of bioactive atropisomerism, vancomycin – the well-known glycopeptide antibiotic, often used as a drug of last resort for penicillin-resistant bacterial infections.<sup>328</sup> Atropisomerism is a particular form of axial chirality resulting from the non-planar arrangement of four groups in pairs about the aryl–aryl bond. The steric strain causes an incapacity to undergo torsional isomerization along the chiral axis and when the activation barrier of this process is greater than approximately 80-100 kJ/mol, the different conformers that arise from the hindered rotation can be separated at room temperature.<sup>329</sup> Atropisomers are hence involved in a chemical equilibrium that is thermally controlled, and often have bulky substituents in *ortho* position to the bond joining the aryl rings that cause a significant steric repulsion hindering the rotation about the bond.<sup>330</sup> For instance, an *ortho* di-substitution with chlorine or trifluoromethyl groups on the two biphenyls causes a hindrance sufficient for displaying atropisomerism at room temperature, while a di-substitution with smaller substituents, such as fluorine or carboxylic acids, gives biphenyls that are achiral. In this case, an *ortho* tetra-substitution is required for getting chirality (Figure 4.14).

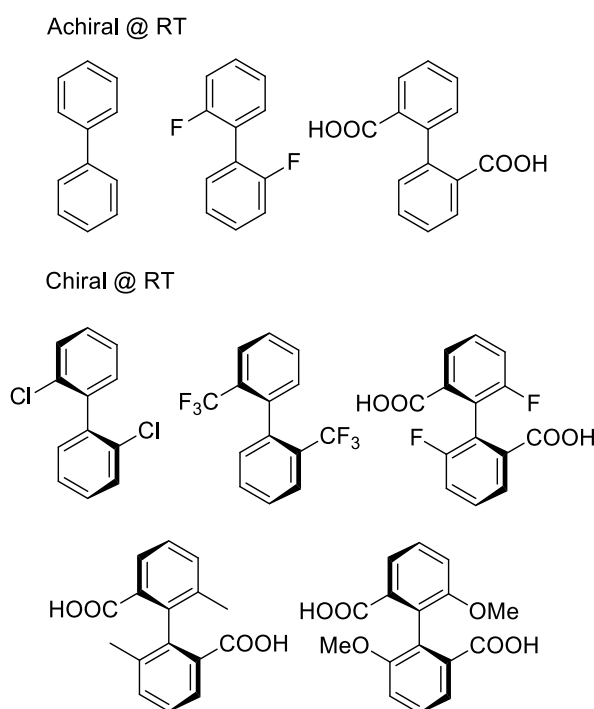
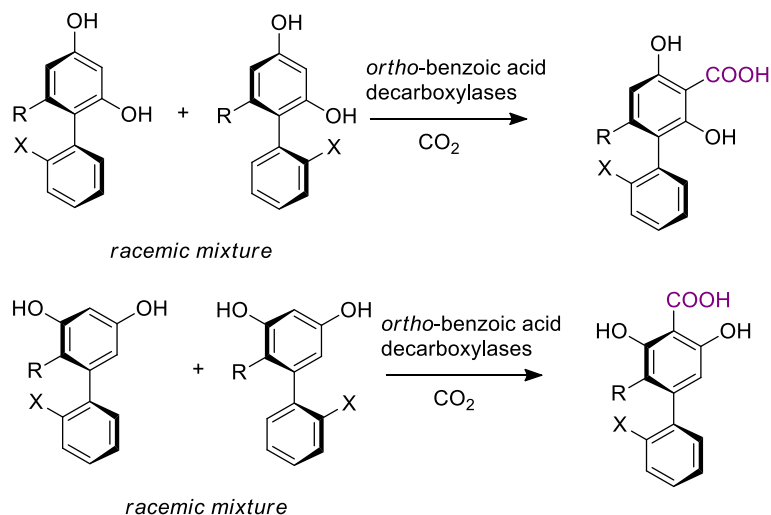


**Figure 4.14.** Examples of achiral and chiral biphenyl compounds at room temperature<sup>330</sup>

In view of this, our aim was to perform an enantioselective synthesis of biphenyl atropisomers by means of the described *ortho*-carboxylation reaction promoted by decarboxylase enzymes. Therefore, the starting biphenyls need to have at least one, or preferably two phenolic groups, a free position in *ortho* to these hydroxyls for allowing the biocatalytic insertion of the carboxyl group, and substituents *ortho* to the biphenyl bond for having the chance to display atropisomerism.

Three main approaches are possible for reaching the goal of this project:

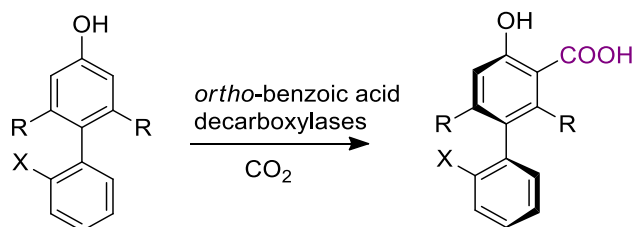
- A kinetic resolution (KR) starting from a racemic mixture of atropisomeric biphenyls that cannot interconvert at room temperature. In this case the enzyme should perform the carboxylation on a single enantiomer to obtain an enantiomerically pure product (Scheme 4.25).



**Scheme 4.25.** Possible approaches for a biocatalytic KR on biphenyl compounds

A second simple strategy could be also attempted:

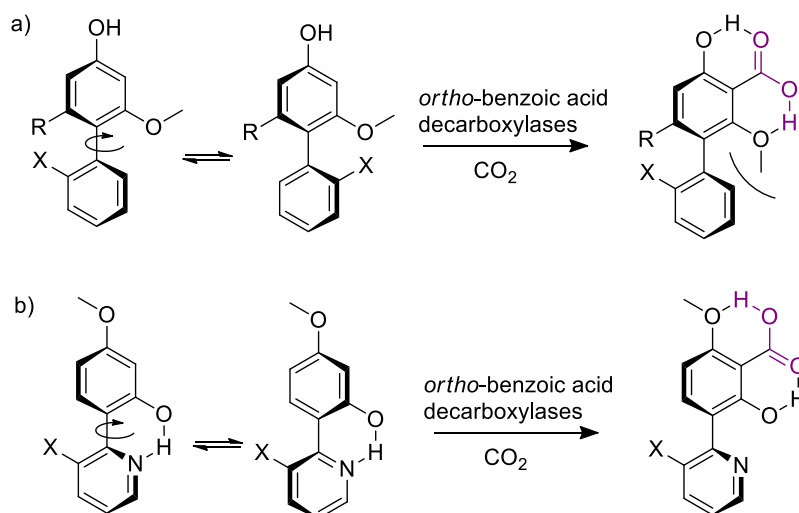
- Desymmetrization of a *meso* biphenyl compound upon the insertion of the carboxyl group by the decarboxylase (Scheme 4.26).



**Scheme 4.26.** Possible approach for the desymmetrization of a *meso* biphenyl compound

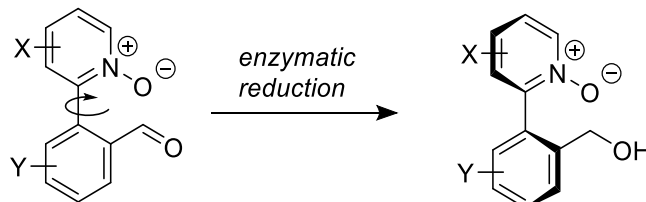
A third thinkable (but difficult to realize) procedure could arise from:

- A dynamic kinetic resolution (DKR): in this case, the enantioselective transformation must take place more slowly than the racemization of the starting materials but faster than the racemization of the products<sup>331</sup>, and the carboxylation reaction should provoke itself the hindered rotation about the aryl-aryl bond. This could possibly occur with the formation of a hydrogen bond between the carboxylic group and the substituents on the ring (Scheme 4.25a), or with the destabilization of a planar transition state by the loss of a hydrogen bond interaction (Scheme 4.27b). In both cases, the insertion of the carboxyl group should be performed in the *meta*-position to the biphenyl bond.



**Scheme 4.27.** Possible approaches for a biocatalytic DKR on biphenyl compounds

The example reported in Scheme 4.27b was suggested by Staniland *et al.*,<sup>332</sup> who recently reported a biocatalytic DKR with a ketoreductase reducing an aldehyde to form a configurationally stable atropisomeric alcohol (Scheme 4.28). In this process the higher rotational barrier in the product arises from the loss of a bonding interaction between the *N*-oxide and the aldehyde and from the interconversion of a small, planar substituent, such as an aldehyde, into a larger, tetrahedral substituent like an alcohol.<sup>333</sup>



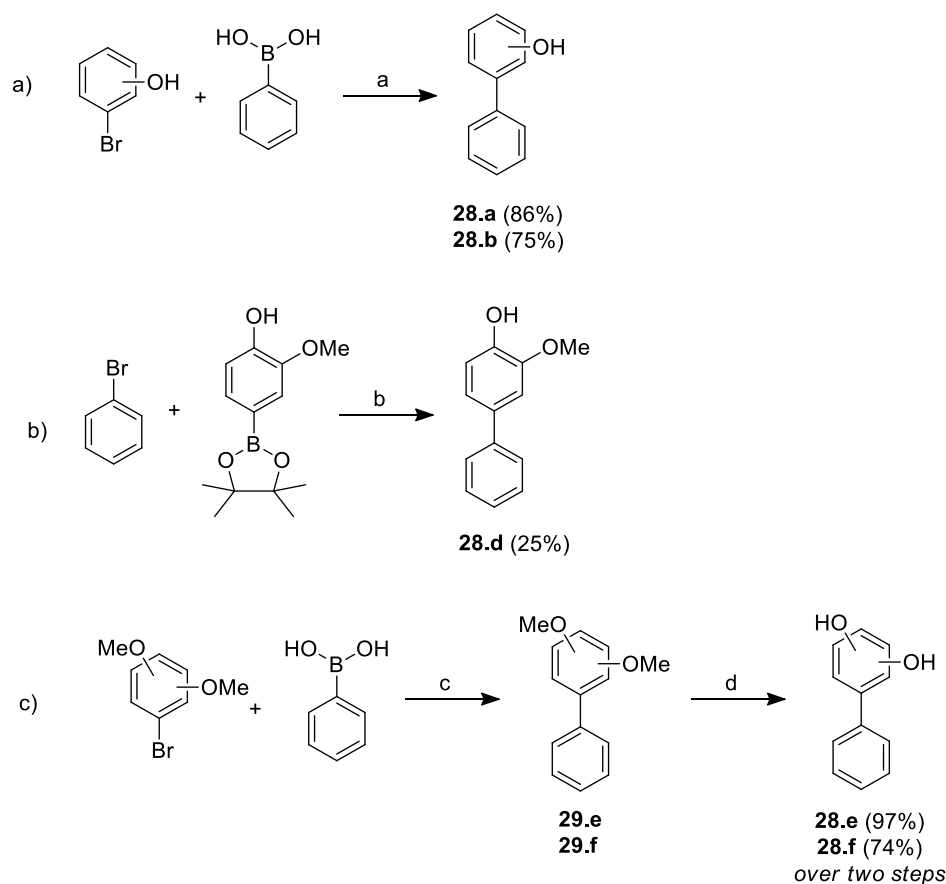
**Scheme 4.28.** Atropselective dynamic kinetic resolution performed by Staniland *et al.*<sup>332</sup>

This latter approach immediately appeared the most challenging; therefore, efforts were focused on the other two strategies.

A panel of model biphenyl compounds was synthesized to perform a first biocatalytic screening and consequently evaluating the general reactivity of the decarboxylases on these particular substrates, whose conversion was unknown so far. Firstly, 3- and 4-phenylphenol (**28.a** and **28.b**) were synthesized in order to evaluate if a single hydroxyl group on one of the rings is accepted and converted by the enzymes (2-phenylphenol **28.c** was available). The reactions were performed with the corresponding bromophenols and boronic acid under Suzuki coupling conditions in water providing good yields<sup>334</sup> (Scheme 4.29a). Secondly, biphenyls with a methoxy and a hydroxyl group (**28.d**) or with two phenolic groups (**28.e** and **28.f**) were prepared for achieving more activated compounds. Biphenyl **28.d** was synthesized starting from bromobenzene and the available corresponding boronic acid pinacol ester, but was obtained in low yields even attempting different solvent systems, equivalents or higher temperature (Scheme 4.29b). Suzuki reaction instead did not occur when the synthesis of compounds **28.e** and **28.f** started from the relative bromoresorcinols; a



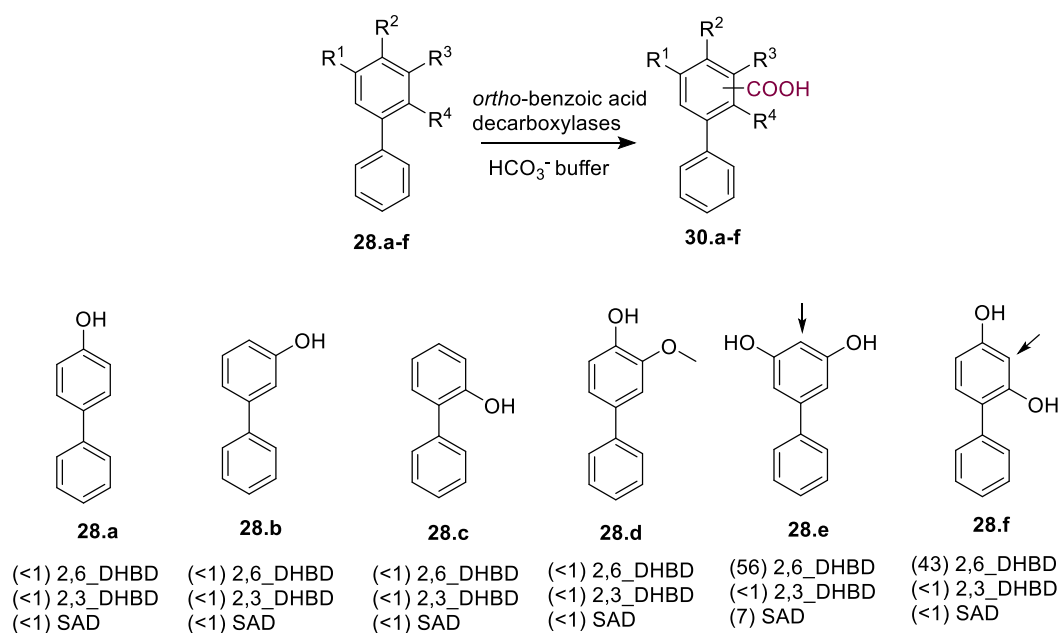
methoxy group-protected starting material was indeed required, together with a following deprotection step with boron tribromide<sup>335</sup> on the relative biphenyls **29.e** and **29.f**, easily performed in good yields over two steps (Scheme 4.29c).



**Scheme 4.29.** Synthesis of the model (poly)phenol-phenols **28.a-f**. Reagents and conditions: a) Pd(OAc)<sub>2</sub> (5%), K<sub>2</sub>CO<sub>3</sub>, H<sub>2</sub>O, rt, 3 h; b) Pd(OAc)<sub>2</sub> (5%), K<sub>2</sub>CO<sub>3</sub>, H<sub>2</sub>O/acetone 1:1, 35 °C, 2 h; c) Pd(OAc)<sub>2</sub> (5%), K<sub>2</sub>CO<sub>3</sub>, H<sub>2</sub>O/EtOH 1:1, 80 °C, 4 h; d) BBr<sub>3</sub>, CH<sub>2</sub>Cl<sub>2</sub>, 0 °C then rt, 16 h. Yields of isolated compounds are reported in brackets

With substrates **28.a-f** in hand, the biocatalytic transformations with the three already reported decarboxylase enzymes (2,3-DHBD\_Ao, SAD\_Tm, 2,6-DHBD\_Rs) were conducted under the conditions optimized in literature.<sup>327</sup> The screening was performed with lyophilized *E. coli* BL21 (DE3) whole cells containing the heterologously expressed decarboxylase enzymes. Activity tests were performed for controlling the specific enzyme activities in the natural decarboxylation reaction from 2,6-dihydroxybenzoic acid (2,6-DHBA) to resorcinol using 10 mg enzyme cells in PBS 50 mM pH 7.0 at four time intervals. The specific activities of fresh enzyme preparations resulted: SAD\_Tm = 5.02 U/mg, 2,3-DHBD\_Ao = 11.8 U/mg, 2,6-DHBD\_Rs = 26.2 U/mg, where 1 Unit = amount of catalyst for conversion of 1 μmol 2,6-DHBA to resorcinol per min.

The outcome of the *ortho*-carboxylation reactions was monitored by HPLC-UV analysis and the conversion was evaluated by <sup>1</sup>H NMR spectroscopy of the crude reaction mixtures by comparing the integral peak areas of the substrate and the carboxylated product (Scheme 4.30).



**Scheme 4.30.** Library of the model biphenyl compounds **28.a-f** and their biotransformation reactions. Reagents and conditions: phosphate buffer (pH 8.5, 100 mM), whole lyophilized cells of *E. coli* containing the corresponding overexpressed enzyme (30 mg/mL), substrate (10 mM),  $\text{KHCO}_3$  (3M), 30 °C, 120 rpm, 24 h. Conversions (%) were determined by  $^1\text{H}$  NMR and reported in brackets. Arrows indicate the carboxylation site

Only the most activated substrates (**28.e** and **28.f**) bearing two phenolic groups were accepted and converted to **30.e** and **30.f**. In particular, 2,6-DHBD turned out to be the most promising enzyme with good conversion for both substrates. Docking studies revealed how the natural substrate of 2,6-DHBD (2,6-dihydroxybenzoic acid) is perfectly accommodated in the active site of the enzyme. However, when a simulation with a hypothetical *ortho*-substituted biphenyl compound (2'-chloro-4-hydroxy-2-methoxy-[1,1'-biphenyl]-3-carboxylic acid) was performed, a poor fitting resulted due to steric hindrance, with a biphenyl ring inevitably crashing into an amino acid residue at the active site entrance (Phe23) (Figure 4.15). In order to further improve the conversion rate, and according to the biotransformation to be tested in future with more bulky biphenyl compounds, we evaluated the possibility to perform enzyme engineering on 2,6-DHBD. In fact, incomplete conversions in the energetically disfavoured uphill direction were improved through reaction engineering in previous works.<sup>326c,336</sup> We hence attempted a site-directed mutagenesis by substitution of Phe23 residue with a less bulky Gly or Ala, for allowing a better fitting of the biphenyl in the active site. The corresponding primers were designed and several site directed mutagenesis approaches were attempted but so far none of them has been successful and the enzyme mutation strategy was abandoned (data not shown).

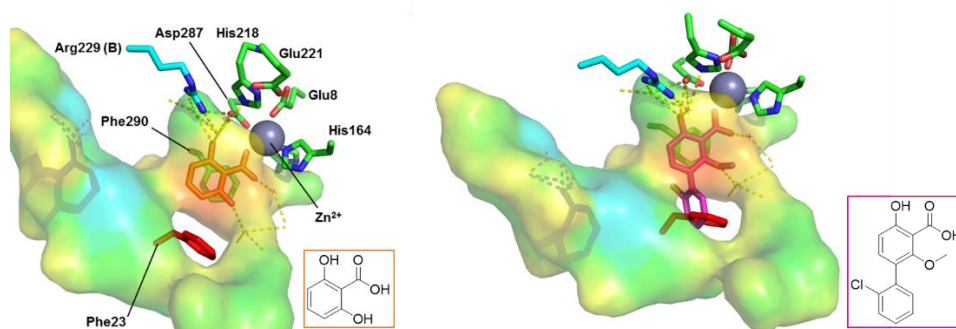


**Figure 4.15.** Active site representation of 2,6-DHBD\_Rs. On the left: Crystal structure of 2,6-DHBD\_Rs (PDB-Code: 2DVU) with 2,6-dihydroxybenzoic acid (orange) in the active site. On the right: Crystal structure of 2,6-DHBD\_Rs (PDB-Code: 2DVU) with 2'-chloro-4-hydroxy-2-methoxy-[1,1'-biphenyl]-3-carboxylic acid (purple) in the active site. Figures were prepared by using PyMOL<sup>337</sup>

Once the behaviour of decarboxylases toward the di-substituted hydroxy biphenyls was detected, a panel of suitable biphenyl compounds can be designed (Figure 4.16). The substrates should hence present a resorcinol moiety in a phenyl ring for being recognized and converted by the enzymes, and contextually at least an *ortho*-bis substitution with bulky groups for allowing a possible kinetic resolution (or a *meso* desymmetrization). Naturally, the first two examples emerged as the synthetically simplest, since only an *ortho*-bis-substitution needed to be inserted. In this case, it has also to be considered that a less bulky substrate could represent an advantage for a good fitting in the enzyme active site, but at the same time is a disadvantage if the substituents are not bulky enough to cause atropisomerism.

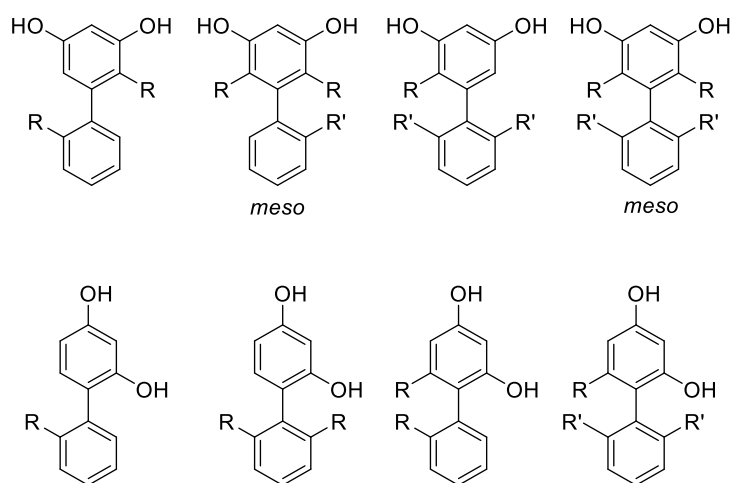
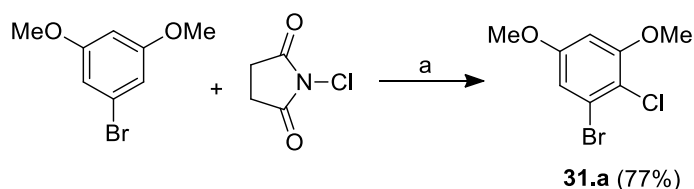


**Figure 4.16.** Possible biphenyl substrates for obtaining an enantioselective KR (or *meso* desymmetrization)

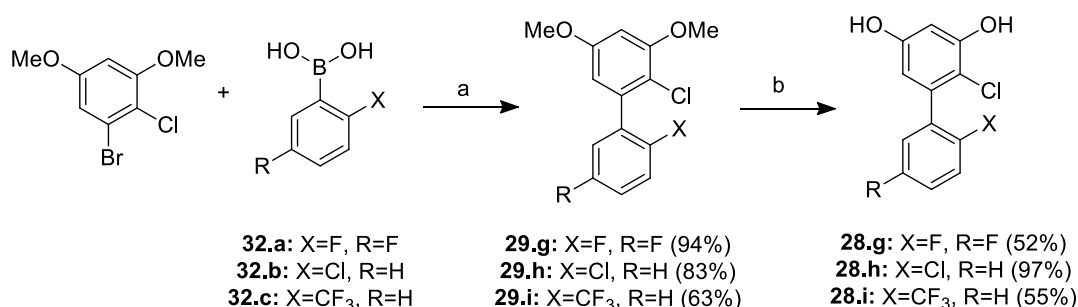
As a preliminary part of the project, only the first two cases were considered for the biocatalytic screening, and accordingly, some feasible biphenyls were designed and synthesized. Bulky chlorine or trifluoromethyl groups were introduced in the *ortho* position to generate atropisomerism as reported in Figure 4.14.

A chlorine group was inserted on 1-bromo-3,5-dimethoxybenzene with *N*-chlorosuccinimide and catalysis promoted by  $\text{TMSCl}$ <sup>338</sup> (Scheme 4.31).



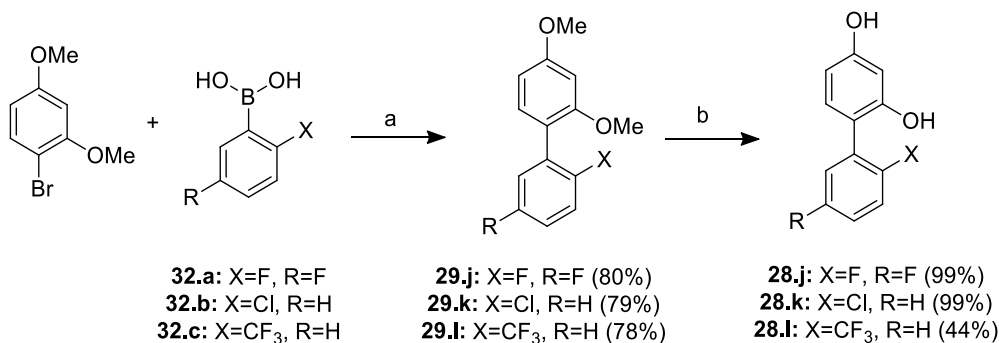
**Scheme 4.31.** Synthesis of compound **31.a**. Reagents and conditions: a) TMSCl, CH<sub>3</sub>CN, rt, 16 h. Yield of isolated compound is reported in brackets

The resulting 1-bromo-2-chloro-3,5-dimethoxybenzene **31.a** was subjected to Suzuki coupling conditions with different *ortho*-substituted phenyl boronic acids. The enhanced steric hindrance in coupling partners required harsher conditions (high temperature) and longer reaction times. Different palladium catalysts were screened, such as Pd(OAc)<sub>2</sub>, Pd(PPh<sub>3</sub>)<sub>4</sub>, Pd(dppf)Cl<sub>2</sub>, with only the latter resulting efficient in promoting the formation of the desired biphenyls **29.g-i** in good to excellent yields. The developed conditions comprised a mixture of 1,4-dioxane and water, Pd(dppf)Cl<sub>2</sub> as catalyst, potassium phosphate tribasic, and heating at 95 °C.<sup>339</sup> Reactions were monitored through GC-MS and reagents were added portionwise at set time intervals until complete conversion. The deprotection step of the methoxy groups was conducted with BBr<sub>3</sub> as previously described to give target biphenyls **28.g-i** (Scheme 4.32).



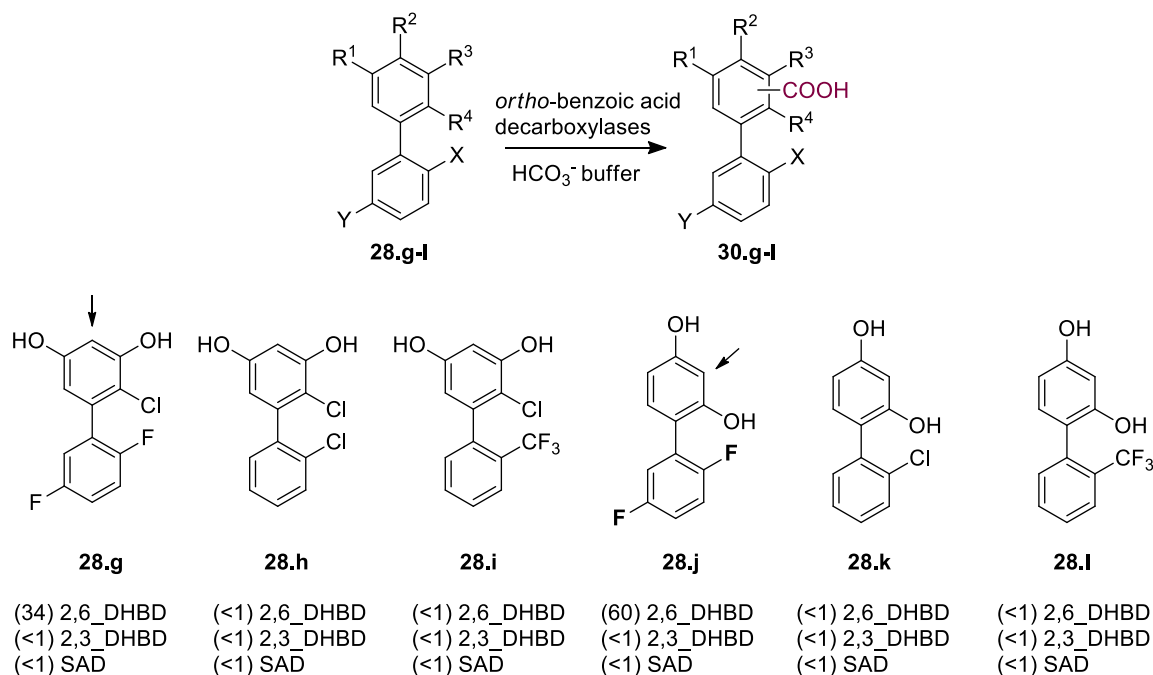
**Scheme 4.32.** Synthesis of 3,5-dihydroxy biphenyl compounds **28.g-i**. Reagents and conditions: a) Pd(dppf)Cl<sub>2</sub> (2.5-5%), K<sub>3</sub>PO<sub>4</sub>, 1,4-dioxane/H<sub>2</sub>O 5:1, 95 °C, 5-6 days; b) BBr<sub>3</sub>, CH<sub>2</sub>Cl<sub>2</sub>, 0 °C then rt, 16 h. Yields of isolated compounds are reported in brackets

With the optimized conditions in hand, synthesis of 2,4-dihydroxy biphenyl compounds **29.j-l** was then performed starting directly from 1-bromo-2,4-dimethoxybenzene and the previously employed boronic acids, and again the deprotection step yielded targets **28.j-l** (Scheme 4.33).



**Scheme 4.33.** Synthesis of 2,4-dihydroxy biphenyl compounds **28.j-l**. Reagents and conditions: a) Pd(dppf)Cl<sub>2</sub> (2.5-5%), K<sub>3</sub>PO<sub>4</sub>, 1,4-dioxane/H<sub>2</sub>O 5:1, 95 °C, 5-6 days; b) BBr<sub>3</sub>, CH<sub>2</sub>Cl<sub>2</sub>, 0 °C then rt, 16 h. Yields of isolated compounds are reported in brackets

The small library of *ortho*-disubstituted biphenyl compounds **28.g-l** was subsequently tested in the biotransformation reactions with the aforementioned conditions (Scheme 4.34).



**Scheme 4.34.** Library of the target *ortho*-substituted biphenyl compounds **28.g-l** and their biotransformation reactions. Reaction conditions: phosphate buffer (pH 8.5, 100 mM), whole lyophilized cells of *E. coli* containing the corresponding overexpressed enzyme (30 mg/mL), substrate (10 mM), KHCO<sub>3</sub> (3M), 30 °C, 120 rpm, 24 h. Conversions (%) were determined by <sup>1</sup>H NMR and reported in brackets. Arrows indicate the carboxylation site

Also in this case, the outcome of the biotransformations was monitored by HPLC-UV and the eventual conversion was evaluated by <sup>1</sup>H NMR spectroscopy. According to the data reported in Scheme 4.34, less hindered biphenyls **28.g** and **28.j** showed some conversions, and were accepted only by 2,6-DHBD (conversion of 34% and 60% respectively) to give the corresponding carboxylated products **30.g** and **30.j**. As an example, <sup>1</sup>H NMR spectra of starting compound **28.g** and of the enzymatic crude reaction mixture with 2,6-DHBD are reported in Figure 4.16 in order to highlight the formation of the carboxylated product **30.g**.

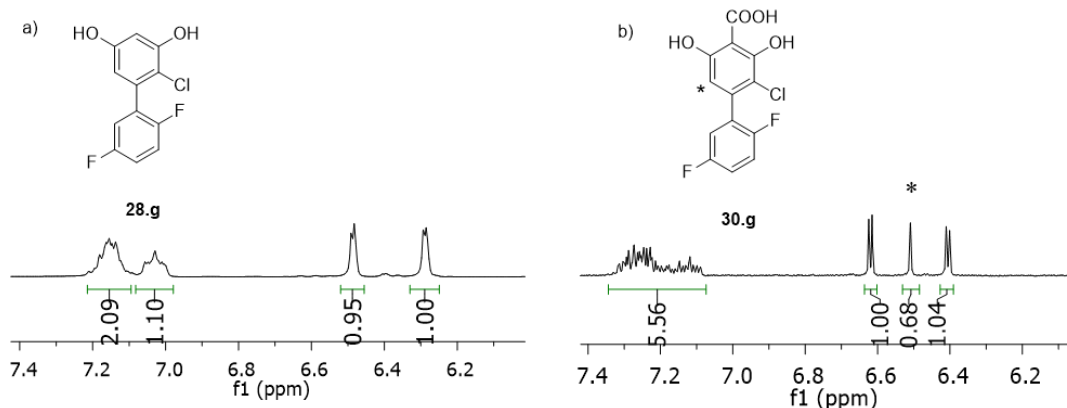


**Figure 4.16.** <sup>1</sup>H NMR spectra of: a) compound **28.g**, b) crude reaction mixture of enzymatic biotransformation on **28.g** with 2,6-DHBD, in an enlarged region of 6.0-7.4 ppm (300 MHz, CD<sub>3</sub>OD). Asterisk indicates a peak belonging to the carboxylated product **30.g**

However, compounds **28.g** and **28.j** did not display atropisomerism due to the presence of a small fluorine substituent in *ortho* position, and the enzyme therefore could not perform a kinetic resolution. In fact, attempts of separating compounds **28.g** and **28.j** through chiral HPLC revealed unsuccessful. More promising compounds **28.h**, **28.i**, **28.k** and **28.l** with chlorine and trifluoromethyl *ortho*-substituents that could potentially display atropisomerism, were however too hindered for being accepted by the enzyme.

Nevertheless, even if a proof of stereorecognition could be achieved in the end, the first enzymatic carboxylation reaction on biphenyl compounds to date was demonstrated with *ortho*-substituted derivatives. Further studies are in course for developing suitable axially chiral biphenyl substrates that could be recognized by the enzyme, serving as proof of concept.

## 4.5 Concluding remarks

In this chapter we evaluated the use of biocatalytic approaches as an alternative and valuable synthetic strategy compared to standard chemical catalysts, especially in terms of eco-sustainability of the process.

Having in hands a series of  $\beta$ -lactam compounds being active as integrin ligands, many of which are racemic at the C4 position of the ring, we were intrigued by the understanding of how different enantiomers could differently interact with the receptor and how the activity could be modulated by choosing a specific enantiomeric ligand. According to this, we performed a study aimed at synthesizing some new enantiomerically pure integrin ligands starting from our developed racemic compounds. The adopted strategy provided to obtain, through a kinetic resolution approach, the couple of enantiomers of a key intermediate of the library, which was further functionalized with different side chains for achieving a structural variability of the ligands. *Burkholderia Cepacia Lipase* (*BCL*) was selected as a suitable and highly performing enzyme for the kinetic resolution. Different integrin ligands with opposite configurations and excellent enantiomeric excesses were obtained and subjected to cell adhesion assays in order to evaluate if their biological activity as integrin ligands was preserved and which enantiomer displayed the greatest activity. We found that the activity was fully maintained only in case of (*S*)-enantiomers, while (*R*)-derivatives resulted completely inactive in the interaction with the receptor, thus revealing an important requirement for further developing new integrin ligands.

A second study regarded the selective oxidation of amines to aldehydes; in this case a biocatalytic approach was already developed within the research group.<sup>315</sup> Therefore we attempted a different synthetic metal-free protocol for promoting oxidation of amines in aqueous-organic medium. Among the tested inorganic metal-free oxidants, NaIO<sub>4</sub> and TEMPO as catalyst emerged as the most efficient and selective system for oxidation of differently substituted benzyl amines to the corresponding benzaldehydes without overoxidation. In addition, unsymmetrical secondary amines underwent selective oxidation only at the benzylic position thus realising an oxidative deprotection of a benzylic group with easy aldehydes and amines isolation.<sup>294</sup>

In the same field, and starting from already reported oxidative screenings of alcohols and amines mediated by laccases, we turned our attention on oxidative coupling reactions for the synthesis of amides, which have emerged as valid alternative strategies to traditional synthetic pathways.

An oxidative coupling process catalysed by a biocatalytic system based on the Laccase mediator system (LMS) was hence studied between an aldehyde and an amine for the synthesis of amides in an aqueous medium, using oxygen as terminal oxidant. The combination of two green catalysts such as Laccase and TEMPO offered multiple advantages such as the mild reaction conditions, the high atom economy of the process and also avoided the use of metals and the production of toxic waste. The study of the oxidative amidation process involved the use of various substrates, and natural and synthetic mediators; however, 2-pyridinecarboxydehyde resulted by far the only substrate able to produce appreciable yields, while for amines good results were obtained only with pyrrolidine.

In general, low yields and narrow applicability of the method resulted a limiting factor, and the process is surely to be further optimized, at least consisting in the first described laccase-catalysed oxidative amidation.

Finally, a three months project developed under the supervision of Prof. Kurt Faber at Graz University regarded a study toward a biocatalytic kinetic resolution on different biphenyl compounds mediated by *ortho*-benzoic acid decarboxylases. The aim of the project was to perform an enantioselective synthesis of atropoisomers through carboxylation of *ortho*-substituted biphenyls. Different model substrates and suitable biphenyls were obtained, but the enzyme demonstrated stereorecognition only for less hindered biphenyls that do not display atropoisomerism. A tentative enzyme engineering procedure was also performed for allowing the enzymatic active site to accept the desired bulky substrates, resulting unsuccessful by far and requiring further studies.

## 4.6 Experimental Section

### 4.6.1 General information

See Paragraph 3.10.1

### 4.6.2 Synthesis of enantiomerically pure $\beta$ -lactams

Compounds **13**, **113-118** were synthesized as described in Paragraph 3.9.3.

#### General procedure for kinetic resolution (GP 1)

In a glass vial with a screw cap, to a solution of alcol **rac-105** (20 mg, 1 equiv), acyl donor (6 equiv) and anhydrous solvent (4 mL), the desired enzyme (20 mg) was added. The mixture was stirred at room temperature under orbital shaking (300 rpm). The reaction was monitored at set time intervals with chiral HPLC (reaction times specified in Tables 4.1, 4.2, 4.3) for evaluate the substrate conversion and the enantiomeric excesses of unreacted alcohol **106** and ester products **108** or **109**.

**106**: IR (film,  $\text{cm}^{-1}$ ) 3406, 3033, 2953, 1736, 1397, 1175;  $^1\text{H}$  NMR (400 MHz,  $\text{CDCl}_3$ )  $\delta$  (ppm) 7.41 – 7.28 (m, 5H), 5.15 (s, 2H), 4.64 (d,  $J_{\text{AB}} = 11.6$  Hz, 1H), 4.60 (d,  $J_{\text{AB}} = 11.6$  Hz, 1H), 4.16 – 4.04 (m, 1H), 3.15 – 3.08 (dd,  $J = 5.3, 15.0$  Hz 1H), 2.86 – 2.71 (m, 2H), 2.70 – 2.64 (dd,  $J = 2.4, 15.0$  Hz, 1H);  $^{13}\text{C}$  NMR (100 MHz,  $\text{CDCl}_3$ )  $\delta$  (ppm) 171.1, 166.6, 135.2, 128.6, 128.5, 128.3, 66.9, 64.1, 47.0, 42.6, 38.7; ESI-MS ( $R_t = 4.4$  min)  $m/z$  232  $[\text{M-OH}]^+$ .

**108**: IR (film,  $\text{cm}^{-1}$ ) 2966, 2877, 1773, 1736, 1456, 1393, 1314, 1248;  $^1\text{H}$  NMR (400 MHz,  $\text{CDCl}_3$ )  $\delta$  (ppm) 7.40 – 7.31 (m, 5H), 5.15 (d,  $J_{\text{AB}} = 11.4$  Hz, 1H), 5.14 (s, 2H), 5.07 (d,  $J_{\text{AB}} = 11.4$  Hz, 1H), 4.08 (dddd,  $J = 7.1, 5.9, 5.4, 2.7$  Hz, 1H), 3.19 (dd,  $J = 15.4, 5.4$  Hz, 1H), 2.94 (dd,  $J = 16.2, 5.9$  Hz, 1H), 2.76 (dd,  $J = 15.4, 2.7$  Hz, 1H), 2.68 (dd,  $J = 16.2, 7.1$  Hz, 1H), 2.26 (t,  $J = 7.3$  Hz, 2H), 1.69 – 1.56 (m, 2H), 0.93 (t,  $J = 7.4$  Hz, 3H);  $^{13}\text{C}$  NMR (100 MHz,  $\text{CDCl}_3$ )  $\delta$  (ppm) 173.3, 170.0, 166.7, 135.3, 128.7, 128.5, 128.4, 66.8, 63.4, 48.6, 43.4, 38.1, 35.8, 18.1, 13.6; ESI-MS ( $R_t = 8.9$  min)  $m/z$  232  $[\text{M-OBu}]^+$ , 342  $[\text{M+Na}]^+$ .

**109**: IR (film,  $\text{cm}^{-1}$ ) 3034, 2959, 1773, 1737, 1498, 1439, 1393, 1366, 1318, 1219;  $^1\text{H}$  NMR (400 MHz,  $\text{CDCl}_3$ )  $\delta$  (ppm) 7.40 – 7.30 (m, 5H), 5.14 (s, 2H), 5.14 (d,  $J_{\text{AB}} = 11.4$  Hz, 1H), 5.07 (d,  $J_{\text{AB}} = 11.4$  Hz, 1H), 4.13 – 4.05 (m, 1H), 3.18 (dd,  $J = 15.4, 5.4$  Hz, 1H), 2.92 (dd,  $J = 16.3, 6.1$  Hz, 1H), 2.76 (dd,  $J = 15.4, 2.7$  Hz, 1H), 2.69 (dd,  $J = 16.3, 7.0$  Hz, 1H), 2.02 (s, 3H);  $^{13}\text{C}$  NMR (100 MHz,  $\text{CDCl}_3$ )  $\delta$  (ppm) 170.6, 169.9, 166.6, 135.3, 128.6, 128.5, 128.4, 66.8, 63.5, 48.5, 43.4, 38.1, 20.7; ESI-MS ( $R_t = 7.1$  min)  $m/z$  232  $[\text{M-OAc}]^+$ , 309  $[\text{M+H}_2\text{O}]^+$ .

#### Preparative scale

With the best conditions (TBME as solvent, *BCL* as enzyme, vinyl butyrate as acyl donor), the kinetic resolution was repeated in a preparative scale. Following the aforementioned conditions, alcohol **rac-105** (150 mg, 0.6 mmol, 1 equiv), vinyl butyrate (457  $\mu\text{L}$ , 3.6 mmol, 6 equiv), TBME (15 mL) and *BCL* (150 mg) were reacted at room temperature in a 30 mL vial with a screw cap. At 38% conversion (chiral HPLC monitoring), solvent was evaporated and the crude was directly purified by flash-chromatography (cyclohexane/EtOAc 40:60) to separate target ester **109** as a colorless oil (60 mg, 33%, ee = 90%,  $[\alpha]_{\text{D}}^{20} = -15$  ( $c = 1.0, \text{CH}_2\text{Cl}_2$ )) and residual alcohol **106**, which was re-processed in the same reaction conditions. At 67% conversion, work-up and purification were carried out as described above, and alcohol **106** was isolated as a colorless oil (51 mg, 35%, ee = 94%,  $[\alpha]_{\text{D}}^{20} = +13$  ( $c = 1.0, \text{CH}_2\text{Cl}_2$ )).



#### *General procedure for hydrolysis with BCL (GP2)*

In a 10 mL vial with a screw cap, to a solution of ester **rac-107** or **109**, CH<sub>3</sub>CN and MilliQ H<sub>2</sub>O (1:11 ratio, 63 mL/mmol), *Burkholderia Cepacia* lipase was added (with the same weight amount of the substrate). The mixture was stirred at 37 °C in thermostat. At completion (1 h, chiral HPLC monitoring), the aqueous mixture was extracted with EtOAc (3 × 10 mL). The collected organic phases were dried over Na<sub>2</sub>SO<sub>4</sub>, filtered and concentrated under vacuum. The crude was purified by flash-chromatography (cyclohexane/EtOAc 40:60) to yield target alcohol **rac-105** or **111** as a colorless oil.

**111**: 75%, ee = 98%, [ $\alpha$ ]<sub>D</sub><sup>20</sup> = - 16 (c = 1.0, CH<sub>2</sub>Cl<sub>2</sub>)

#### *General procedure for oxidation with KMnO<sub>4</sub> (GP3)*

To a solution of the desired alcoholic compound **rac-105**, **106** or **111** (1 equiv) in CH<sub>3</sub>CN (30 mL/mmol), KMnO<sub>4</sub> (6 equiv) was added portionwise at 0 °C. The system was then warmed to room temperature and left under stirring overnight. At completion (16 h, TLC monitoring), the reaction mixture was quenched with a saturated solution of Na<sub>2</sub>S<sub>2</sub>O<sub>5</sub> until complete decoloring. The mixture was then filtered and the acetonitrile evaporated under reduced pressure. The residual aqueous solution was then extracted with EtOAc (3 × 10 mL), dried on anhydrous Na<sub>2</sub>SO<sub>4</sub>, filtered and concentrated. The desired product **13**, **110** or **112** was obtained without further purification as a white solid.

**13**: 99%

**110**: 91%, ee = 94%, [ $\alpha$ ]<sub>D</sub><sup>20</sup> = + 26 (c = 1.0, CH<sub>2</sub>Cl<sub>2</sub>)

**112**: 90%, ee = 98%, [ $\alpha$ ]<sub>D</sub><sup>20</sup> = - 26 (c = 1.0, CH<sub>2</sub>Cl<sub>2</sub>)

#### *Benzyl 2-(1-(hydroxymethyl)-4-oxoazetidin-2-yl)acetate (**rac-105**)*

To a solution of compound **13** (55 mg, 0.25 mmol, 1 equiv) in THF (0.55 mL), paraformaldehyde (11 mg, 0.38 mmol, 1.5 equiv), K<sub>2</sub>CO<sub>3</sub> (2 mg, 0.01 mmol, 0.3 equiv) and water (22  $\mu$ L) were added. The system was sonicated at room temperature. At completion (4 h, TLC monitoring), the reaction mixture was diluted with EtOAc (2.5 mL), dried on anhydrous Na<sub>2</sub>SO<sub>4</sub>, filtered and concentrated. The crude was purified by flash-chromatography (cyclohexane/EtOAc 35:65) yielding compound **rac-105** as a colorless oil (62 mg, 99%).

#### *(2-(2-(benzyloxy)-2-oxoethyl)-4-oxoazetidin-1-yl)methyl butyrate (**rac-107**)*

To a solution of compound **rac-105** (207 mg, 0.83 mmol, 1 equiv) in CH<sub>2</sub>Cl<sub>2</sub> (7.5 mL) under nitrogen atmosphere, butyric anhydride (272  $\mu$ L, 1.6 mmol, 2 equiv) and anhydrous TEA (231  $\mu$ L, 1.6 mmol, 2 equiv) were added dropwise at 0 °C. The system was then warmed to room temperature and left under stirring. At completion (4 h, TLC monitoring), the reaction mixture was quenched with a saturated solution of NH<sub>4</sub>Cl. The aqueous solution was extracted with CH<sub>2</sub>Cl<sub>2</sub> (3 × 10 mL), dried on anhydrous Na<sub>2</sub>SO<sub>4</sub>, filtered and concentrated. The crude was purified by flash-chromatography (cyclohexane/EtOAc 35:65) yielding compound **rac-107** as a colorless oil (100 mg, 76%).

Similarly, compound **rac-105** (213 mg, 0.86 mmol, 1 equiv), acetic anhydride (116  $\mu$ L, 1.7 mmol, 2 equiv) and anhydrous TEA (238  $\mu$ L, 1.7 mmol, 2 equiv) yielded benzyl 2-(1-(acetoxymethyl)-4-oxoazetidin-2-yl)acetate as a colorless oil (61 mg, 70%) after purification by flash-chromatography (cyclohexane/EtOAc 35:65).

## Integrin ligands and synthetic intermediates:

- (*S*)-**113**: 99%, ee = 94%,  $[\alpha]_{\text{D}}^{20} = +4$  (c = 0.5, EtOH)  
(*R*)-**114**: 99%, ee = 98%,  $[\alpha]_{\text{D}}^{20} = -4$  (c = 0.5, EtOH)  
(*S*)-**115**: 78%, ee = 94%,  $[\alpha]_{\text{D}}^{20} = -79$  (c = 1.0, CH<sub>2</sub>Cl<sub>2</sub>)  
(*R*)-**115**: 81%, ee = 98%,  $[\alpha]_{\text{D}}^{20} = +75$  (c = 1.0, CH<sub>2</sub>Cl<sub>2</sub>)  
(*S*)-**116**: 99%, ee = 94%,  $[\alpha]_{\text{D}}^{20} = -79$  (c = 1.0, CH<sub>3</sub>OH)  
(*R*)-**116**: 99%, ee = 98%,  $[\alpha]_{\text{D}}^{20} = +70$  (c = 1.0, CH<sub>3</sub>OH)  
(*S*)-**117**: 71%, ee = 94%,  $[\alpha]_{\text{D}}^{20} = -75$  (c = 1.0, CH<sub>2</sub>Cl<sub>2</sub>)  
(*R*)-**117**: 81%, ee = 98%,  $[\alpha]_{\text{D}}^{20} = +65$  (c = 1.0, CH<sub>2</sub>Cl<sub>2</sub>)  
(*S*)-**118**: 99%, ee = 94%,  $[\alpha]_{\text{D}}^{20} = -82$  (c = 1.0, CH<sub>3</sub>OH)  
(*R*)-**118**: 99%, ee = 98%,  $[\alpha]_{\text{D}}^{20} = +78$  (c = 1.0, CH<sub>3</sub>OH)

### 4.6.2.1 Chiral HPLC parameters

Chiral HPLC-UV analysis of azetidinones were established at 210 nm. Samples for HPLC injection were prepared as follows:

- for transesterification reactions, 0.5 mL of the reaction mixture was filtered through regenerated cellulose syringe filters (diameter = 25 mm, pore diameter = 0.2 μm); the organic solvent was dried, re-suspended in a solution of *n*-hexane/isopropanol 1:1 and directly injected in chiral HPLC
- for hydrolysis reaction, 0.5 mL of the reaction mixture was extracted with EtOAc (0.5 mL); the organic solvent was dried, re-suspended in a solution of hexane/isopropanol 1:1 and directly injected in chiral HPLC

Elution conditions:

Compound **rac-105**, **106** and **111**:

Column: Chiralpak IC, solvent: *n*-hexane/isopropanol 50:50, flow: 0.5 mL/min from 0 to 18 min, 1 mL/min from 19 min, temperature: 40 °C.

Compounds **13**, **110** and **112**:

Column: Chiralpak IC, solvent: *n*-hexane/isopropanol 60:40, flow: 0.5 mL/min, temperature: 40 °C.

Compounds **115** and **117**:

Column: Chiralpak IA, solvent: *n*-hexane/isopropanol 50:50, flow: 0.5 mL/min, temperature: 40 °C.

### 4.6.3 Synthesis for amine oxidation with Sodium periodate/TEMPO system

Starting amines **11.a-11.t** are commercially available; synthesized imines **14.a**, **14.n**, **14.o**, **14.t** and secondary amines **17.a-21.a** are known. The obtained oxidation products: aldehydes **12.a-12.k**, acids **13.a-13.b**, nitrile **15.a**, compounds **16.a**, **23.a-27.a** are known. Structures and purities of all the obtained known compounds were assessed by <sup>1</sup>H NMR and HPLC-MS analysis or by <sup>1</sup>H NMR and GC-MS analysis for compounds **23.a-27.a** and were fully consistent with data reported in databases.

#### General procedure for *p*-methoxybenzylamine oxidation (GP4)

*p*-methoxybenzylamine **11.a** (0.4 mmol, 1 equiv) was dissolved in the corresponding solvent or solvent mixture (see Tables 4.5 and 4.6). AcOH (if specified), TEMPO (if specified) and the oxidant were then added according to what reported in Tables 4.5 and 4.6. The mixture was then quenched (reaction time specified in Tables 4.5 and 4.6) with HCl 1M and extracted with EtOAc (3 × 10 mL). The collected organic layers were

dried on anhydrous Na<sub>2</sub>SO<sub>4</sub>, filtered and concentrated to isolate *p*-anisaldehyde **12.a** (or compounds **13.a**, **14.a**, and **15.a** if specified). The aqueous phase was then basified with NaOH 1M and extracted with EtOAc (3 × 10 mL). The organic layers were dried on anhydrous Na<sub>2</sub>SO<sub>4</sub>, filtered and concentrated to isolate the starting amine **11.a**, if present. The amount of the residual **11.a** allowed the determination of conversion %.

*General procedure for amines oxidation to aldehydes with sodium periodate (GP5)*

AcOH (0.4 mmol, 1 equiv), TEMPO (0.04 mmol, 0.1 equiv) and NaIO<sub>4</sub> (0.4 mmol, 1 equiv) were added to a solution of the desired amine **11.a-11.p** (0.4 mmol, 1 equiv) in a 2:1 ratio of H<sub>2</sub>O/CH<sub>3</sub>CN (15 mL) (see Table 4.7). After 20 h the mixture was quenched with HCl 1M and extracted with EtOAc or diethyl ether (3 × 10 mL). The collected organic layers were dried on anhydrous Na<sub>2</sub>SO<sub>4</sub>, filtered and concentrated to isolate the corresponding aldehydes **12.a-k** or compounds **16.a** and **13.b** where specified. The aqueous phase was then basified with NaOH 1M and extracted with EtOAc or diethyl ether (3 × 10 mL). The organic layers were dried on anhydrous Na<sub>2</sub>SO<sub>4</sub>, filtered and concentrated to isolate the residual starting amines **11.a-11.l**, if present. The residual aliphatic amines **11.m-11.p** were isolated as ammonium salts in the basic organic extract by adding one equivalent of trifluoroacetic acid (TFA) just before the final solvent evaporation.

*General procedure for secondary amines oxidation with sodium periodate (GP6)*

AcOH (0.4 mmol, 1equiv), TEMPO (0.04 mmol, 0.1 equiv) and NaIO<sub>4</sub> (as specified in Table 4.9) were added to a solution of the desired secondary amine **17.a-22.a** (0.4 mmol, 1 equiv) in a 2:1 ratio of H<sub>2</sub>O/CH<sub>3</sub>CN (10 mL) (see Table 4.9). After 20 h the mixture was quenched with HCl 1M and extracted with EtOAc or diethyl ether (3 × 10 mL). The collected organic layers were dried on anhydrous Na<sub>2</sub>SO<sub>4</sub>, filtered and concentrated to isolate *p*-anisaldehyde **12.a**. The aqueous phase was then basified with NaOH 1M and extracted with EtOAc or diethyl ether (3 × 10 mL). The organic layers were dried on anhydrous Na<sub>2</sub>SO<sub>4</sub>, filtered and concentrated to isolate amines RNH<sub>2</sub> (**11.a**, **11.j**, **11.m**, **11.n**, **11.o**, and **11.t**, see Table 4.9). When specified, amines were isolated as ammonium salts in the basic organic extract by adding one equivalent of trifluoroacetic acid (TFA) just before the final solvent evaporation.

*General procedure for cyclic amines oxidation with sodium periodate (GP7)*

AcOH (0.4 mmol, 1equiv, if specified in Table 4.10), TEMPO (0.04 mmol, 0.1 equiv) and NaIO<sub>4</sub> (0.4 mmol, as specified in Table 4.10) were added to a solution of the desired amine **11.q-11.s** (0.4 mmol, 1 equiv) in a 2:1 ratio of H<sub>2</sub>O/CH<sub>3</sub>CN (10 mL). After 20h the mixture was quenched with HCl 1M and extracted with EtOAc or diethyl ether (3 × 10 mL). The collected organic layers were dried on anhydrous Na<sub>2</sub>SO<sub>4</sub>, filtered and concentrated to isolate the oxidation products **23.a**, **25.a** (in its protonated form) or **26.a** (see Table 4.10). The aqueous phase was then basified with NaOH 1M and extracted with EtOAc or diethyl ether (3 × 10 mL). The organic layers were dried on anhydrous Na<sub>2</sub>SO<sub>4</sub>, filtered and concentrated to isolate the starting amines **11.q-11.s** if present, and the oxidation products **24.a**, **25.a** and **27.a** (see Table 4.10).

*General procedure for synthesis of imines 14.a, 14.m, 14.n, 14.o and 14.t (GP8)*

*p*-anisaldehyde **12.a** and the desired amine (**11.a**, **11.m**, **11.n**, **11.o** or **11.t**) were diluted in anhydrous CH<sub>2</sub>Cl<sub>2</sub> (10 mL) under nitrogen atmosphere; MgSO<sub>4</sub> was added and the solution was stirred overnight. After completion (TLC monitoring, 24 h), the mixture was filtered on celite under vacuum and the solvent evaporated under reduced pressure. The desired imines **14.a**, **14.m**, **14.n**, **14.o** and **14.t** were obtained as yellow oils without further purification.

*General procedure for synthesis of secondary amines (GP9)*

Imines **14.a**, **14.m**, **14.n**, **14.o**, or **14.t** (1 equiv) were diluted in anhydrous CH<sub>3</sub>OH (5 mL) and NaBH<sub>4</sub> (2 equiv) was added under nitrogen atmosphere; the solution was stirred overnight. After completion (TLC monitoring, 24 h), the mixture was quenched with water and HCl 6M until pH = 2 and left 30 minutes under stirring. The

organic solvent was then evaporated under reduced pressure and the mixture was basified until pH = 11 with NaOH 5M. The precipitate was filtered out under vacuum, the aqueous phase was extracted with EtOAc (3 × 10 mL). The collected organic layers were dried on anhydrous Na<sub>2</sub>SO<sub>4</sub>, filtered and concentrated to afford the corresponding amines **17.a-21.a** as yellow oils without further purification. Spectroscopic data of amines were consistent with those reported in the literature and in the NMR spectroscopy database (SDBS).

*N*-(4-methoxybenzyl)-1-(4-methoxyphenyl)methanimine (**14.a**)

Following GP8, *p*-anisaldehyde **12.a** (248 μL, 2 mmol, 1 equiv), *p*-methoxybenzylamine **11.a** (266 μL, 2 mmol, 1 equiv) and MgSO<sub>4</sub> (963 mg, 8 mmol, 4 equiv) yielded imine **14.a** (506 mg, 99%).

*N*-(cyclohexylmethyl)-1-(4-methoxyphenyl)methanimine (**14.m**)

Following GP8, *p*-anisaldehyde **12.a** (248 μL, 2 mmol, 1 equiv), cyclohexylmethylamine **11.m** (265 μL, 2 mmol, 1 equiv) and MgSO<sub>4</sub> (963 mg, 8 mmol, 4 equiv) yielded imine **14.m** (447 mg, 97%). IR (film, cm<sup>-1</sup>) 2923, 2849, 1698, 1649, 1606, 1579, 1253; <sup>1</sup>H NMR (400 MHz, CDCl<sub>3</sub>) δ (ppm) 8.14 (s, 1H), 7.66 (d, *J* = 8.7 Hz, 2H), 6.91 (d, *J* = 8.7 Hz, 2H), 3.82 (s, 3H), 3.41 (d, *J* = 6.4 Hz, 2H), 1.79 – 1.65 (m, 6H), 1.31 – 1.11 (m, 3H), 1.02 – 0.93 (m, 2H); <sup>13</sup>C NMR (100MHz, CDCl<sub>3</sub>) δ (ppm) 161.4, 160.1, 131.9, 129.5, 113.9, 68.6, 55.3, 39.0, 31.5, 26.6, 26.1; ESI-MS (*R*<sub>t</sub> = 1.7 min) *m/z* 232 [M+H]<sup>+</sup>.

*N*-cyclohexyl-1-(4-methoxyphenyl)methanimine (**14.n**)

Following GP8, *p*-anisaldehyde **12.a** (248 μL, 2 mmol, 1 equiv), cyclohexylamine **11.n** (299 μL, 2.6 mmol, 1 equiv) and MgSO<sub>4</sub> (1.20 g, 10 mmol, 5 equiv) yielded imine **14.n** (362 mg, 83%).

*N*-isopropyl-1-(4-methoxyphenyl)methanimine (**14.o**)

Following GP8, *p*-anisaldehyde **12.a** (310 μL, 2.5 mmol, 1 equiv), isopropylamine **11.o** (677 μL, 7.5 mmol, 2 equiv) and MgSO<sub>4</sub> (1.81 g, 15 mmol, 6 equiv) yielded imine **14.o** (437 mg, 99%).

*N*-butyl-1-(4-methoxyphenyl)methanimine (**14.t**)

Following GP8, *p*-anisaldehyde **12.a** (248 μL, 2 mmol, 1 equiv), butylamine **11.t** (300 μL, 3 mmol, 1.5 equiv) and MgSO<sub>4</sub> (1.69 g, 14 mmol, 7 equiv) yielded imine **14.t** (369 mg, 96%).

*bis*(4-methoxybenzyl)amine (**17.a**)

Following GP9, imine **14.a** (510 mg, 2 mmol) yielded the secondary amine **17.a** (463 mg, 90%).

*1*-cyclohexyl-*N*-(4-methoxybenzyl)methanamine (**18.a**)

Following GP9, imine **14.m** (447 mg, 1.9 mmol) yielded the secondary amine **18.a** (366 mg, 83%).

*N*-(4-methoxybenzyl)cyclohexanamine (**19.a**)

Following GP9, imine **14.n** (359 mg, 1.65 mmol) yielded the secondary amine **19.a** (315 mg, 87%).

*N*-(4-methoxybenzyl)propan-2-amine (**20.a**)

Following GP9, imine **14.o** (437 mg, 2.5 mmol) yielded the secondary amine **20.a** (408 mg, 92%).

*N*-(4-methoxybenzyl)butan-1-amine (**21.a**)

Following GP9, imine **14.t** (365 mg, 1.9 mmol) yielded the secondary amine **21.a** (307 mg, 83%).

#### *N*-(4-methoxybenzyl)pentan-2-amine (**22.a**)

2-aminopentane **11.j** (366  $\mu$ L, 3 mmol, 1.5 equiv) and acetic acid (172  $\mu$ L, 3 mmol, 1.5 equiv) were added to a solution of *p*-anisaldehyde **12.a** (248  $\mu$ L, 2 mmol, 1 equiv) in anhydrous CH<sub>2</sub>Cl<sub>2</sub> (5 mL) under nitrogen atmosphere. The mixture was left 15 minutes under stirring, then NaBH(OAc)<sub>3</sub> (874 mg, 4 mmol, 2 equiv) was added at 0 °C and the solution was diluted with 2 mL of anhydrous CH<sub>2</sub>Cl<sub>2</sub> and stirred overnight. After completion (TLC monitoring, 24 h), the mixture was quenched with HCl 6M and left 30 minutes under stirring. The mixture was then diluted with water and basified until pH = 11 with NaOH 5M. The aqueous phase was extracted with CH<sub>2</sub>Cl<sub>2</sub> (1  $\times$  10 mL) and diethyl ether (2  $\times$  10 mL), the collected organic layers were dried on anhydrous Na<sub>2</sub>SO<sub>4</sub>, filtered and concentrated to afford the target amine **22.a** as a yellow oil without further purification (370 mg, 89%). IR (film, cm<sup>-1</sup>) 2958, 2930, 2870, 1612, 1512, 1463, 1299, 1246; <sup>1</sup>H NMR (400 MHz, CDCl<sub>3</sub>)  $\delta$  (ppm) 7.23 (d, *J* = 8.5 Hz, 2H), 6.85 (d, *J* = 8.5 Hz, 2H), 3.78 (s, 3H), 3.76 (d, *J*<sub>AB</sub> = 12.7 Hz, 1H), 3.67 (d, *J*<sub>AB</sub> = 12.7 Hz, 1H), 2.69 – 2.65 (m, 1H), 1.47 – 1.31 (m, 4H), 1.07 (d, *J* = 6.2 Hz, 3H), 0.90 (t, *J* = 6.9 Hz, 3H); <sup>13</sup>C NMR (100MHz, CDCl<sub>3</sub>)  $\delta$  (ppm) 158.5, 133.0, 129.2, 113.7, 55.2, 52.1, 50.7, 39.3, 20.2, 19.1, 14.2; ESI-MS (*R*<sub>t</sub> = 2.0 min) *m/z* 208 [M+H]<sup>+</sup>.

#### 4.6.4 Synthesis for oxidative amidation

Starting aldehydes and amines are commercially available; mediators are commercially available. Target amides piperidin-1-yl(pyridin-2-yl)methanone **119**, piperidin-1-yl(pyridin-4-yl)methanone, piperidin-1-yl(pyridin-2-yl)methanone, morpholino(pyridin-2-yl)methanone, *N,N*-dipropyl-2-pyridinecarboxamide are known. Byproducts *N*-formylpiperidine **120** and *N*-acetyl piperidine **121** are known. Structures and purities of all the obtained known compounds were assessed by <sup>1</sup>H NMR and HPLC-MS analysis and were fully consistent with data reported in databases.

#### General procedure for oxidative coupling with Laccase/mediator system (GP10)

In a 10 mL vial with a screw cap, CH<sub>3</sub>CN (0.5 mL), 2-pyridinecarboxaldehyde (0.5 mmol, 1 equiv), H<sub>2</sub>O MilliQ (5.5 mL) and piperidine (2.5 mmol, 5 equiv) were stirred at 37 °C in thermostat for 30 minutes. As specified in Table 4.11, mediator (0.1 mmol, 0.2 equiv) or TEMPO (0.14 mmol, 0.28 equiv), and Laccase Tv (5 mg) were added. O<sub>2</sub> was bubbled for 30 seconds and the vial was closed. The solution was stirred at 37 °C in thermostat; when specified in Table 4.11 (after TLC monitoring), the aqueous solution was extracted with CH<sub>2</sub>Cl<sub>2</sub> (3  $\times$  10 mL). The collected organic phases were dried over Na<sub>2</sub>SO<sub>4</sub>, filtered and concentrated under vacuum. The crude was purified by flash-chromatography (CH<sub>2</sub>Cl<sub>2</sub>/CH<sub>3</sub>OH 98:2) to yield target amide **119** or byproducts **120** and **121**.

General procedure GP10 was used in the screening of starting aldehydes and starting amines with TEMPO as a mediator; in the screening of mediator portioned additions, mediator equivalents, piperidine equivalents, starting aldehydes and amines and reaction times with methyl syringate as a mediator. GP10 was followed also in reactions performed without enzyme or without enzyme and mediator. When the enzymatic process was performed under nitrogen atmosphere, a 25 mL 2-neck-flask was employed as reaction vessel.

#### General procedure for oxidative coupling with sodium periodate (GP11)

In a 25 mL flask, CH<sub>3</sub>CN (as specified in Table 4.14), 2-pyridinecarboxaldehyde (0.5 mmol, 1 equiv), H<sub>2</sub>O MilliQ (as specified in Table 4.14) and piperidine (as specified in Table 4.14) were stirred at room temperature for 10 minutes. Total reaction volume was 6 mL. Then AcOH (if specified), mediator (if specified) and NaIO<sub>4</sub> (as specified in Table 4.14) were added. When specified in Table 4.14 (after TLC monitoring), the aqueous solution was extracted with CH<sub>2</sub>Cl<sub>2</sub> (3  $\times$  10 mL). The collected organic phases were dried over Na<sub>2</sub>SO<sub>4</sub>, filtered and concentrated under vacuum. The crude was purified by flash-chromatography (CH<sub>2</sub>Cl<sub>2</sub>/CH<sub>3</sub>OH 98:2) to yield target amide **119**.

## 4.6.5 Enzymatic ortho-carboxylations

### 4.6.5.1 General information

TLCs were run on silica plates (Merck, silica gel 60, F<sub>254</sub>), for column chromatography silica gel 60 from Merck was used, compounds were visualized using UV (254 nm) and cerium ammonium molybdate. NMR spectra were acquired on a Bruker Avance III 300 MHz spectrometer using a 5 mm BBO probe with z-axis gradients at 300 K. Chemical shifts ( $\delta$ ) are reported in ppm and coupling constants ( $J$ ) are given in Hz. HPLC analysis: HPLC/UV analysis was performed on an HPLC Agilent 1260 Infinity system with a diode array detector and a reversed phase Phenomenex Luna column C18 (100 Å, 250 mm × 4.6 mm, 5 mm, column temperature 24 °C). All compounds were spectrophotometrically detected at 280 nm. Analytic method was run over 22 min with H<sub>2</sub>O/TFA (0.1%) as the mobile phase (flow rate 1 mL/min) and a CH<sub>3</sub>CN/TFA (0.1%) gradient (0–2 min 5%, 2–15 min 5–100%, 15–17 min 100%, 17–22 min 100–5%). All GC-MS measurements were carried out on an Agilent 7890A GC system, equipped with an Agilent 5975C mass-selective detector (electron impact, 70 eV) and a HP-5-MS column (30 m×0.25 mm×0.25 mm film) using He as carrier gas at a flow of 0.55 mL/min. The following temperature program was used for all GC-MS measurements: initial temperature 100 °C, hold for 0.5 min, 10 °C/min to 300 °C.

### 4.6.5.2 Site-directed mutagenesis

All mutants were constructed using the Quik-Change Site-Directed Mutagenesis PCR Kit from Stratagene. The mutagenic primers used to introduce the amino acid changes were the following (FP=forward primer, RP=reverse primer). The free energy resulting from self-dimer formation is given in parentheses.

1a) 2,6-DHBD\_Rs Phe23Gly ( $\Delta G$ : -7.05 kcal/mol)

FP: 5'- ATA ATC ACC TGG AAC ACC ACC TGC ACT ATC CTG -3'  
RP: 5'- CAG GAT AGT GCA GGT GGT GTT CCA GGT GAT TAT -3'

1b) 2,6-DHBD\_Rs Phe23Gly ( $\Delta G$ : -9.89 kcal/mol)

FP: 5'- CA ATA ATC ACC AGG AAC ACC ACC TGC TCT ATC CTG -3'  
RP: 5'- CAG GAT AGC GCA GGT GGT GTT CCG GGT GAT TAT TG-3'

2a) 2,6-DHBD\_Rs Phe23Ala ( $\Delta G$ : -9.89 kcal/mol)

FP: 5'- CA ATA ATC ACC CGG AAC AGC ACC TGC GCT ATC CTG -3'  
RP: 5'- CAG GAT AGC GCA GGT GCT GTT CCG GGT GAT TAT TG -3'

2b) 2,6-DHBD\_Rs Phe23Ala ( $\Delta G$ : -7.05 kcal/mol)

FP: 5'- ATA ATC ACC TGG AAC AGC ACC TGC ACT ATC CTG -3'  
RP: 5'- CAG GAT AGT GCA GGT GCT GTT CCA GGT GAT TAT -3'

### 4.6.5.3 Heterologous expression of (De)carboxylases in *E. coli*

2,3-Dihydroxybenzoic acid decarboxylase from *Aspergillus oryzae* (2,3-DHBD\_Ao), salicylic acid decarboxylase from *Trichosporon moniliiforme* (SAD\_Tm) and 2,6-dihydroxybenzoic acid decarboxylase from *Rhizobium species* (2,6-DHBD\_Rs) were synthesized and ligated into a pET 21a (+) as described in the literature.<sup>326c</sup> Their DNA sequences were identified by sequence comparison in the NCBI Genebank (GI: 94730373 for 2,3-DHBD\_Ao, GI: 225887918 for SAD\_Tm and GI: 116667102 for 2,6-DHBD\_Rs).

Plasmids containing the (de)carboxylase genes were transformed into chemically competent *Escherichia coli* BL21 (DE3) cells and heterologous overexpression was performed as follows: for preculturing 500 mL LB medium [Trypton (10 g/L Oxoid L0042), yeast extract (5 g/L Oxoid L21), NaCl (5 g/L Roth 9265.1)] supplemented with the appropriate antibiotics [ampicillin (100 µg/mL Sigma Aldrich)] were inoculated with 3 mL ONC (overnight starter culture) and incubated at 37 °C and 120 rpm until an OD<sub>600</sub> of 0.6–1.0 was reached. Then IPTG [450 µg/mL, 2 mM (for 2,3-DHBD\_Ao) or 175 µg/mL, 0.5 mM (for the other decarboxylases) Peqlab] was added for induction and the cells left over night at 20 °C and 120 rpm. The next day the cells were harvested by centrifugation (20 min, 5900 rcf, 4 °C), washed with phosphate buffer (5 mL, 50 mM, pH 7.5) and re-centrifuged under the same conditions to obtain a cell pellet. To obtain lyophilized cells the cell pellet was re-suspended in phosphate buffer (5 mL, 50 mM, pH 7.5), shock frozen in liquid nitrogen followed by lyophilization.

Successful overexpression of soluble enzyme was obtained for all decarboxylases. In order to check whether the enzymes are soluble, cells were disrupted using ultrasonication and the separated supernatant and remaining pellet were analysed by SDS-PAGE.

#### 4.6.5.4 Synthesis of biphenyl compounds

Phenyl boronic acids, substituted bromobenzenes, bromophenols are commercial. Compounds **28.a-f**, **29.e-f** and **31.a** are known and spectroscopic data are in accordance with those found in literature.<sup>335,340</sup>

##### *General procedure for the synthesis of phenylphenols (GP12)*

A solution of the desired bromophenol (0.5 mmol, 1 equiv), phenylboronic acid (0.5 mmol, 1 equiv), K<sub>2</sub>CO<sub>3</sub> (1.5 mmol, 3 equiv), Pd(OAc)<sub>2</sub> (5%) and HPLC-water (2 mL) was stirred at room temperature for 3 hours. After complete conversion (TLC monitoring) the slurry mixture was quenched with HCl 1M until acidic to litmus. The resulting precipitate was filtered under vacuum and washed with water. The obtained solid was re-diluted in diethyl ether, dried over Na<sub>2</sub>SO<sub>4</sub>, filtered and concentrated under vacuum. The desired phenylphenol was obtained as a white solid without further purifications.

##### *General procedure for the synthesis of dimethoxy-biphenyls (GP13)*

To a solution of the desired bromodimethoxybenzene (1 equiv), phenylboronic acid (1.5 equiv), and ethanol (2.5 mL/mmol), K<sub>2</sub>CO<sub>3</sub> (3 equiv), Pd(OAc)<sub>2</sub> (5%) and water (2.5 mL/mmol) were added. The mixture was stirred at 80 °C for 4 hours. After complete conversion (TLC monitoring) the system was cooled to room temperature and extracted with EtOAc (3 × 10 mL). The organic phase was washed with water, dried over Na<sub>2</sub>SO<sub>4</sub>, filtered and concentrated under vacuum. The desired product was obtained as a colourless oil without further purifications and used straight for the next step.

##### *General procedure for methoxy-group deprotection (GP14)*

Boron tribromide solution (1M in CH<sub>2</sub>Cl<sub>2</sub>, 4 equiv) was added dropwise at 0 °C to a solution of the desired methoxy-substituted compound (1 equiv) in CH<sub>2</sub>Cl<sub>2</sub> (20 mL/mmol) under nitrogen. After 10 minutes, the system was warmed to room temperature and stirred overnight. After complete conversion (TLC monitoring, 16 h), the mixture was cooled to 0° C, quenched with water dropwise and extracted with EtOAc (3 × 15 mL). The collected organic phase was dried over Na<sub>2</sub>SO<sub>4</sub>, filtered and concentrated under vacuum. The crude was purified by flash-chromatography to afford the desired phenolic compound.

##### *General procedure for the synthesis of ortho-(bis)-substituted-biphenyls (GP15)*

In an oven-dried crimp-cap glass vial, the desired substituted bromobenzene (1 equiv), the desired boronic acid (1.5 equiv) and Pd(dppf)Cl<sub>2</sub> (2%) were dissolved in degassed 1,4-dioxane (3.3 mL/mmol). The mixture was

stirred for 10 minutes, then  $K_3PO_4$  (1.7 mmol) and degassed water (0.7 mL/mmol) were added. The system was stirred at 95 °C until complete conversion. Portions of boronic acid,  $Pd(dppf)Cl_2$  and  $K_3PO_4$  were added every 12 hours until complete conversion. At completion, (GC-MS monitoring) the system was cooled to room temperature. The mixture was diluted with EtOAc (5 mL), dried over  $Na_2SO_4$ , filtered and concentrated under vacuum. The crude was purified by flash-chromatography to afford the desired biphenyl compound.

#### *General procedure for enzymatic ortho-carboxylation (GP16)*

Lyophilized whole cells (30 mg *E. coli* host cells, containing the corresponding overexpressed enzyme) were resuspended in phosphate buffer (900  $\mu$ L, pH 5.5, 100 mM) and rehydrated for 30 min under shaking (30 °C, 700 rpm). The substrate (10 mM final concentration, dissolved in 100  $\mu$ L isopropanol) was added to the enzyme solution (1 mL final volume and 10 mM final concentration). The cell suspension was transferred to a glass vial containing  $KHCO_3$  (3M, 300 mg, final pH 8.5). The vials were immediately tightly sealed with screw caps and were shaken for 24 h (30 °C, 120 rpm). After 24 h the vial was sonicated for 5 minutes and 100  $\mu$ L of the mixture were diluted in 900  $\mu$ L of  $H_2O/CH_3CN/TFA$  (50:50:3) to quench the reaction and precipitate the enzyme. The sample was centrifugated (10 min, 14000 rpm) to remove the enzyme and the resulting clear supernatant was directly used for conversion measurements on a reversed-phase HPLC. All screening experiments were carried out at least in triplicate. The absence of undesired side-activities by the host cells was verified in independent control experiments using lyophilized empty *E. coli* host cells.

#### *3-phenylphenol (28.a)*

Following GP12, 3-bromophenol (82 mg, 0.5 mmol) yielded 3-phenylphenol as a white solid (73 mg, 86%).

#### *4-phenylphenol (28.b)*

Following GP12, 4-bromophenol (82 mg, 0.5 mmol) yielded 4-phenylphenol as a white solid (64 mg, 75%).

#### *3-methoxy-[1,1'-biphenyl]-4-ol (28.d)*

A solution of bromobenzene (47  $\mu$ L, 0.45 mmol, 1.5 equiv), 2-methoxy-4-(4,4,5,5-tetramethyl-1,3,2-dioxaborolan-2-yl)phenol (75 mg, 0.3 mmol, 1 equiv), acetone (0.7 mL),  $K_2CO_3$  (83 mg, 0.6 mmol, 3 equiv), water (0.7 mL) and  $Pd(OAc)_2$  (3.4 mg, 0.015 mmol, 5%) was stirred at 35 °C for 4 hours. After complete conversion (TLC monitoring) the system was cooled to room temperature and extracted with EtOAc (3  $\times$  10 mL). The organic phase was washed with water, dried over  $Na_2SO_4$ , filtered and concentrated under vacuum. The crude was purified by flash-chromatography (cyclohexane/EtOAc 70:30) to afford compound **28.d** as a white solid (15 mg, 25%).

#### *[1,1'-biphenyl]-3,5-diol (28.e)*

Following GP13 and GP14, 1-bromo-3,5-dimethoxybenzene (130 mg, 0.6 mmol) yielded compound **28.e** as a white solid (108 mg, 97% over two steps) after flash-chromatography purification (cyclohexane/EtOAc 60:40).

#### *[1,1'-biphenyl]-2,4-diol (28.f)*

Following GP13 and GP14, 1-bromo-2,4-dimethoxybenzene (43  $\mu$ L, 0.3 mmol) yielded compound **28.f** as a white solid (40 mg, 72% over two steps) after flash-chromatography purification (cyclohexane/EtOAc 60:40).

#### *1-bromo-2-chloro-3,5-dimethoxybenzene (31.a)*

1-bromo-3,5-dimethoxybenzene (109 mg, 0.5 mmol, 1 equiv) was dissolved in  $CH_3CN$  (1 mL); then *N*-chlorosuccinimide (NCS) (73 mg, 0.55 mmol, 1.1 equiv) and  $TMSCl$  (7  $\mu$ L, 0.05 mmol, 0.1 equiv) were added. The mixture was left under stirring at room temperature overnight. After complete conversion (16 h, TLC monitoring) the mixture was diluted with cyclohexane and evaporated. The crude was purified by flash-chromatography (cyclohexane/EtOAc 90:10) to afford compound **31.a** as a white solid (97 mg, 77%).



*2-chloro-2',5'-difluoro-3,5-dimethoxy-1,1'-biphenyl (29.g)*

Following GP15, 1-bromo-2-chloro-3,5-dimethoxybenzene **31.a** (38 mg, 0.15 mmol, 1 equiv), (2,5-difluorophenyl)boronic acid **32.a** (47 mg, 0.30 mmol, 2 equiv), Pd(dppf)Cl<sub>2</sub> (2.7 mg, 0.00375 mmol, 2.5%) and K<sub>3</sub>PO<sub>4</sub> (80 mg, 0.375 mmol, 2.3 equiv) yielded after 5 days compound **29.g** as a colorless oil (40 mg, 94%) after flash-chromatography purification (cyclohexane/EtOAc 60:40). <sup>1</sup>H NMR (300 MHz, CDCl<sub>3</sub>) δ (ppm) 7.15 – 6.97 (m, 3H), 6.57 (d, *J* = 2.7 Hz, 1H), 6.45 (d, *J* = 2.7 Hz, 1H), 3.92 (s, 3H), 3.81 (s, 3H); <sup>13</sup>C NMR (75 MHz, CDCl<sub>3</sub>) δ (ppm) 158.6, 156.0, 135.4, 118.0 (d, *J* = 3.6 Hz), 117.6 (d, *J* = 3.6 Hz), 116.8 (d, *J* = 8.8 Hz), 116.5 (d, *J* = 8.8 Hz), 116.3 (d, *J* = 8.4 Hz), 115.9 (d, *J* = 8.4 Hz), 114.0, 107.0, 99.9, 56.3, 55.6.

*2,2'-dichloro-3,5-dimethoxy-1,1'-biphenyl (29.h)*

Following GP15, 1-bromo-2-chloro-3,5-dimethoxybenzene **31.a** (50 mg, 0.2 mmol, 1 equiv), (2-chlorophenyl)boronic acid **32.b** (63 mg, 0.40 mmol, 2 equiv), Pd(dppf)Cl<sub>2</sub> (3.7 mg, 0.005 mmol, 2.5%) and K<sub>3</sub>PO<sub>4</sub> (98 mg, 0.46 mmol, 2.3 equiv) yielded after 6 days compound **29.h** as a colorless oil (47 mg, 83%) after flash-chromatography purification (cyclohexane/EtOAc 90:10). <sup>1</sup>H NMR (300 MHz, CDCl<sub>3</sub>) δ (ppm) 7.51 – 7.44 (m, 1H), 7.39 – 7.22 (m, 3H), 6.57 (d, *J* = 2.7 Hz, 1H), 6.42 (d, *J* = 2.7 Hz, 1H), 3.93 (s, 3H), 3.81 (s, 3H); <sup>13</sup>C NMR (75 MHz, CDCl<sub>3</sub>) δ (ppm) 158.5, 155.8, 139.9, 138.5, 133.3, 130.9, 129.4, 129.1, 126.5, 113.9, 106.7, 99.4, 56.2, 55.6.

*2'-chloro-3,5-dimethoxy-2-(trifluoromethyl)-1,1'-biphenyl (29.i)*

Following GP15, 1-bromo-2-chloro-3,5-dimethoxybenzene **31.a** (50 mg, 0.2 mmol, 1 equiv), (2-(trifluoromethyl)phenyl)boronic acid **32.c** (152 mg, 0.80 mmol, 4 equiv), Pd(dppf)Cl<sub>2</sub> (7.9 mg, 0.01 mmol, 5.4%) and K<sub>3</sub>PO<sub>4</sub> (195 mg, 0.92 mmol, 4.6 equiv) yielded after 8 days compound **29.i** as a colorless oil (40 mg, 63%) after flash-chromatography purification (cyclohexane/EtOAc 90:10). <sup>1</sup>H NMR (300 MHz, CDCl<sub>3</sub>) δ (ppm) 7.76 (d, *J* = 7.3 Hz, 1H), 7.61 – 7.46 (m, 2H), 7.29 (d, *J* = 7.3 Hz, 1H), 6.56 (d, *J* = 2.7 Hz, 1H), 6.42 (d, *J* = 2.7 Hz, 1H), 3.92 (s, 3H), 3.79 (s, 3H); <sup>13</sup>C NMR (75 MHz, CDCl<sub>3</sub>) δ (ppm) 158.0, 155.5, 139.6, 138.2, 131.6, 131.3, 130.1, 127.9, 126.0 (q, *J* = 5.1 Hz), 113.8, 109.4, 107.1, 99.4, 56.2, 55.6.

*2',5'-difluoro-2,4-dimethoxy-1,1'-biphenyl (29.j)*

Following GP15, 1-bromo-2,4-dimethoxybenzene (36 μL, 0.25 mmol, 1 equiv), (2,5-difluorophenyl)boronic acid **32.a** (99 mg, 0.625 mmol, 2.5 equiv), Pd(dppf)Cl<sub>2</sub> (6.0 mg, 0.00825 mmol, 3.3%) and K<sub>3</sub>PO<sub>4</sub> (149 mg, 0.70 mmol, 2.8 equiv) yielded after 40 hours compound **29.j** as a colorless oil (50 mg, 80%) after flash-chromatography purification (cyclohexane/EtOAc 90:10). <sup>1</sup>H NMR (300 MHz, CDCl<sub>3</sub>) δ (ppm) 7.21 – 7.18 (m, 1H), 7.11 – 6.92 (m, 3H), 6.61 – 6.55 (m, 2H), 3.86 (s, 3H), 3.80 (s, 3H); <sup>13</sup>C NMR (75 MHz, CDCl<sub>3</sub>) δ (ppm) 161.1, 157.7, 131.6 (d, *J* = 1.9 Hz), 118.5 (d, *J* = 4.0 Hz), 118.1 (d, *J* = 4.0 Hz), 116.5, 116.4 (d, *J* = 9.0 Hz), 116.0 (d, *J* = 9.0 Hz), 114.9 (d, *J* = 8.6 Hz), 114.5 (d, *J* = 8.6 Hz), 104.5, 98.8, 55.6, 55.4.

*2'-chloro-2,4-dimethoxy-1,1'-biphenyl (29.k)*

Following GP15, 1-bromo-2,4-dimethoxybenzene (36 μL, 0.25 mmol, 1 equiv), (2-chlorophenyl)boronic acid **32.b** (98 mg, 0.625 mmol, 2.5 equiv), Pd(dppf)Cl<sub>2</sub> (6.0 mg, 0.00825 mmol, 3.3%) and K<sub>3</sub>PO<sub>4</sub> (149 mg, 0.70 mmol, 2.8 equiv) yielded after 40 hours compound **29.k** as a white solid (49 mg, 79%) after flash-chromatography purification (cyclohexane/EtOAc 90:10). Mp 72 – 74 °C; <sup>1</sup>H NMR (300 MHz, CDCl<sub>3</sub>) δ (ppm) 7.49 – 7.43 (m, 1H), 7.33 – 7.24 (m, 3H), 7.15 – 7.10 (m, 1H), 6.60 – 6.55 (m, 2H), 3.87 (s, 3H), 3.78 (s, 3H); <sup>13</sup>C NMR (75 MHz, CDCl<sub>3</sub>) δ (ppm) 160.8, 157.7, 137.5, 134.2, 132.0, 131.3, 129.3, 128.3, 126.3, 121.3, 104.1, 98.7, 55.6, 55.4.

*2-chloro-2',5'-difluoro-[1,1'-biphenyl]-3,5-diol (28.g)*

Following GP14, compound **29.g** (33 mg, 0.12 mmol) yielded compound **28.g** as a white solid (16 mg, 52%) after flash-chromatography purification (cyclohexane/EtOAc 60:40). Mp 139 – 141 °C; <sup>1</sup>H NMR (300 MHz, CDCl<sub>3</sub>) δ (ppm) 7.18 – 6.96 (m, 3H), 6.61 (d, *J* = 2.9 Hz, 1H), 6.41 (d, *J* = 2.9 Hz, 1H), 5.72 (bs, 1H), 4.94 (bs, 1H); <sup>13</sup>C NMR (75 MHz, CD<sub>3</sub>OD) δ (ppm) 157.8, 155.4, 136.6, 118.8 (d, *J* = 3.9 Hz), 118.5 (d, *J* = 4.0 Hz), 117.9 (d, *J* = 9.1 Hz), 117.5 (d, *J* = 9.1 Hz), 117.1 (d, *J* = 8.7 Hz), 116.8 (d, *J* = 8.7 Hz), 111.8, 110.4, 104.6.

*2,2'-dichloro-[1,1'-biphenyl]-3,5-diol (28.h)*

Following GP14, compound **29.h** (43 mg, 0.15 mmol) yielded compound **28.h** as a waxy solid (37 mg, 97%) after flash-chromatography purification (cyclohexane/EtOAc 70:30). <sup>1</sup>H NMR (300 MHz, CDCl<sub>3</sub>) δ (ppm) 7.53 – 7.42 (m, 1H), 7.39 – 7.28 (m, 2H), 7.27 – 7.19 (m, 1H), 6.61 (d, *J* = 2.9 Hz, 1H), 6.37 (d, *J* = 2.9 Hz, 1H), 5.75 (bs, 1H), 5.29 (bs, 1H); <sup>13</sup>C NMR (75 MHz, CDCl<sub>3</sub>) δ (ppm) 154.8, 152.3, 139.4, 137.6, 133.2, 130.8, 129.5, 129.4, 126.6, 111.6, 110.3, 102.9.

*2'-chloro-2-(trifluoromethyl)-[1,1'-biphenyl]-3,5-diol (28.i)*

Following GP14, compound **29.i** (38 mg, 0.12 mmol) yielded compound **28.i** as a yellow oil (19 mg, 55%) after flash-chromatography purification (cyclohexane/EtOAc 75:25). <sup>1</sup>H NMR (300 MHz, (CD<sub>3</sub>)<sub>2</sub>CO) δ (ppm) 7.83 (d, *J* = 7.8 Hz, 1H), 7.75 – 7.69 (m, 2H), 7.36 (d, *J* = 7.8 Hz, 1H), 6.62 (d, *J* = 2.7 Hz, 1H), 6.35 (d, *J* = 2.7 Hz, 1H).

*2',5'-difluoro-[1,1'-biphenyl]-2,4-diol (28.j)*

Following GP14, compound **29.j** (18 mg, 0.07 mmol) yielded compound **28.j** as a white solid (16 mg, 99%) after flash-chromatography purification (cyclohexane/EtOAc 60:40). Mp 110 – 112 °C; <sup>1</sup>H NMR (300 MHz, (CD<sub>3</sub>)<sub>2</sub>CO) δ (ppm) 8.46 (bs, 1H), 8.44 (bs, 1H), 7.21 – 7.12 (m, 2H), 7.11 – 7.02 (m, 2H), 6.53 (d, *J* = 2.4 Hz, 1H), 6.45 (dd, *J* = 8.3, 2.4 Hz, 1H); <sup>13</sup>C NMR (75 MHz, CD<sub>3</sub>OD) δ (ppm) 159.8, 156.8, 132.8 (d, *J* = 2.2 Hz), 119.5 (d, *J* = 4.8 Hz), 119.1 (d, *J* = 4.8 Hz), 117.5 (d, *J* = 10.1 Hz), 117.1 (d, *J* = 10.1 Hz), 115.4 (d, *J* = 9.2 Hz), 115.1 (d, *J* = 9.2 Hz), 114.8, 107.8, 103.7.

*2'-chloro-[1,1'-biphenyl]-2,4-diol (28.k)*

Following GP14, compound **29.k** (46 mg, 0.18 mmol) yielded compound **28.k** as a white solid (39 mg, 98%) after flash-chromatography purification (cyclohexane/EtOAc 60:40). <sup>1</sup>H NMR (300 MHz, CDCl<sub>3</sub>) δ (ppm) 7.56 – 7.47 (m, 1H), 7.38 – 7.31 (m, 3H), 7.06 – 6.99 (m, 1H), 6.53 – 6.47 (m, 2H), 5.34 (bs, 1H), 4.94 (bs, 1H); <sup>13</sup>C NMR (75 MHz, CDCl<sub>3</sub>) δ (ppm) 156.9, 153.6, 135.3, 134.4, 132.4, 131.5, 130.1, 129.5, 127.3, 118.7, 107.9, 102.9.

*2,4-dimethoxy-2'-(trifluoromethyl)-1,1'-biphenyl (29.l)*

Following GP15, 1-bromo-2,4-dimethoxybenzene (36 μL, 0.25 mmol, 1 equiv), (2-trifluoromethylphenyl)boronic acid **32.c** (119 mg, 0.625 mmol, 2.5 equiv), Pd(dppf)Cl<sub>2</sub> (6.0 mg, 0.00825 mmol, 3.3%) and K<sub>3</sub>PO<sub>4</sub> (149 mg, 0.70 mmol, 2.8 equiv) yielded after 40 hours compound **29.l** as a colorless oil (55 mg, 78%) after flash-chromatography purification (cyclohexane/EtOAc 90:10). <sup>1</sup>H NMR (300 MHz, CDCl<sub>3</sub>) δ (ppm) 7.74 (d, *J* = 7.5 Hz, 1H), 7.54 (t, *J* = 7.5 Hz, 1H), 7.45 (t, *J* = 7.5 Hz, 1H), 7.30 (d, *J* = 7.5 Hz,

1H), 7.08 (d,  $J = 9.1$  Hz, 1H), 6.59 – 6.49 (m, 2H), 3.87 (s, 3H), 3.72 (s, 3H).  $^{13}\text{C}$  NMR (75 MHz,  $\text{CDCl}_3$ )  $\delta$  (ppm) 160.7, 157.8, 137.5 (q,  $J = 2.2$  Hz), 132.7, 131.0, 129.7, 129.3, 127.1, 126.0 (q,  $J = 5.1$  Hz), 122.4, 121.3, 103.5, 98.4, 55.5, 55.3.

*2'-(trifluoromethyl)-[1,1'-biphenyl]-2,4-diol (28.i)*

Following GP14, compound **29.i** (33 mg, 0.12 mmol) yielded compound **28.i** as a pinkish solid (20 mg, 44%) after flash-chromatography purification (cyclohexane/EtOAc 60:40). Mp 220 – 222 °C;  $^1\text{H}$  NMR (300 MHz,  $(\text{CD}_3)_2\text{CO}$ )  $\delta$  (ppm) 8.28 – 8.21 (m, 2H), 8.13 (d,  $J = 8.7$  Hz, 1H), 7.89 (ddd,  $J = 15.4, 7.3, 1.4$  Hz, 1H), 7.58 (ddd,  $J = 15.2, 7.4, 1.1$  Hz, 1H), 6.92 (dd,  $J = 8.7, 2.5$  Hz, 1H), 6.81 (d,  $J = 2.4$  Hz, 1H);  $^{13}\text{C}$  NMR (75 MHz,  $(\text{CD}_3)_2\text{CO}$ )  $\delta$  (ppm) 160.5, 159.7, 152.8, 135.4, 135.0, 129.9, 127.6, 124.6, 121.4, 119.8, 112.9, 110.2, 103.1.

*3,5-dihydroxy-[1,1'-biphenyl]-4-carboxylic acid (30.e)*

Following GP16, [1,1'-biphenyl]-3,5-diol **28.e** and 2,6-DHBD\_Rs yielded compound **30.e** with a 56% conversion detected from  $^1\text{H}$  NMR.  $^1\text{H}$  NMR (300 MHz,  $(\text{CD}_3)_2\text{CO}$ )  $\delta$  (ppm) 7.71 – 7.66 (m, 2H), 7.59 – 7.44 (m, 3H), 6.61 (d,  $J = 2.2$  Hz, 2H).

*2,4-dihydroxy-[1,1'-biphenyl]-3-carboxylic acid (30.f)*

Following GP16, [1,1'-biphenyl]-2,4-diol **28.f** and 2,6-DHBD\_Rs yielded compound **30.f** with a 43% conversion detected from  $^1\text{H}$  NMR.  $^1\text{H}$  NMR (300 MHz,  $(\text{CD}_3)_2\text{CO}$ )  $\delta$  (ppm) 7.57 – 7.50 (m, 5H), 7.44 (d,  $J = 8.6$  Hz, 1H), 6.57 (d,  $J = 8.6$  Hz, 1H).

*2-chloro-2',5'-difluoro-3,5-dihydroxy-[1,1'-biphenyl]-4-carboxylic acid (30.g)*

Following GP16, 2-chloro-2',5'-difluoro-[1,1'-biphenyl]-3,5-diol **28.g** and 2,6-DHBD\_Rs yielded compound **30.g** with a 34% conversion detected from  $^1\text{H}$  NMR.  $^1\text{H}$  NMR (300 MHz,  $\text{CD}_3\text{OD}$ )  $\delta$  (ppm) 7.25 – 6.97 (m, 3H), 6.45 (s, 1H).

*2',5'-difluoro-2,4-dihydroxy-[1,1'-biphenyl]-3-carboxylic acid (30.j)*

Following GP16, 2',5'-difluoro-[1,1'-biphenyl]-2,4-diol and 2,6-DHBD\_Rs yielded compound **28.j** with a 60% conversion detected from  $^1\text{H}$  NMR.  $^1\text{H}$  NMR (300 MHz,  $\text{CD}_3\text{OD}$ )  $\delta$  (ppm) 7.29 (dd,  $J = 8.6, 1.1$  Hz, 1H), 7.17 – 7.05 (m, 3H), 6.49 (d,  $J = 8.6$  Hz, 1H).

# References

---

1. S. A. Waksman, *Mycologia*, **1947**, 39 (5), 565–569
2. J. Pogliano, N. Pogliano, J. A. Silverman, *J. Bacteriol.*, **2012**, 194 (17), 4494–4504
3. K. L. Leach, S. J. Brickner, *Ann. N. Y. Acad. Sci.*, **2011**, 1222, 49–54
4. D. J. Diekema, R. N. Jones, *Lancet*, **2001**, 358, 1975–1982
5. R. Sykes, *Bull. World Health Organ.*, **2001**, 79 (8), 778–779
6. a) ESAC: European Surveillance of Antimicrobial Consumption, *Final Management Report 2009 – 2010*, July; b) ECOC: European Centre for Disease Prevention and Control, *Annual Epidemiological Report on Communicable Diseases in Europe*, **2010**
7. a) C. Walsh, *Nature*, **2000**, 406, 775–781; b) C. M. Cimarusti, R. B. Sykes, *Med. Res. Rev.*, **1984**, 4, 1–24
8. R. B. Sykes, D. P. Bonner, K. Bush, N. H. Georgopapadakou, *Antimicrob. Agents Chemother.*, **1982**, 21, 85–92
9. A. O. Mascaretti, C. E. Boschetti, G. O. Danelon, E. G. Mata, O. A. Roveri, *Curr. Med. Chem.*, **1995**, 1, 441–470
10. [www.creative-proteomics.com/services/peptidoglycan-structure-analysis](http://www.creative-proteomics.com/services/peptidoglycan-structure-analysis)
11. G. Martelli, D. Giacomini, *Eur. J. Med. Chem.*, **2018**, 158, 91–105
12. S. Reardon, *Nature news*, 21 december **2015**; Source: CDDEP ResistanceMap
13. World Health Organization (WHO), *Global action plan on antimicrobial resistance*, **2014**
14. E. Turos, T. E. Long, M. I. Konaklieva, C. Coates, J. Y. Shim, S. Dickey, D. V. Lim, A. Cannons, *Bioorg. Med. Chem. Lett.*, **2002**, 12, 2229–2231
15. P. Courvalin, *Clin. Infect. Dis.*, **2006**, 42, Suppl 1:S25–S34
16. P. A. Bradford, *Clin. Microbiol. Rev.*, **2001**, 14, 933–951
17. P. Galletti, C. E. A. Cocuzza, M. Pori, A. Quintavalla, R. Musumeci, D. Giacomini, *ChemMedChem*, **2011**, 6, 1919–1927
18. EMEA: European Medicines Agency, *The Bacterial Challenge: Time to React*, Technical Report EMEA/576176/2009, London, **2009**
19. World Health Organization (WHO), *Global action plan on antimicrobial resistance*, **2015**
20. Infectious Diseases Society of America, *Clin. Infect. Diseases*, **2010**, 50, 1081–1083
21. European commission. *A european one health action plan against antimicrobial resistance (AMR)*, **2017**
22. M. R. Mulvey, A. E. Simor, *CMAJ*, **2009**, 180 (4), 408–415

- 
23. L. B. Rice, D. F. Sahn, R. A. Bonomo, *Manual of Clinical Microbiology* (8th edition), **2003**, ASM Press, Washington DC
  24. P. Courvalin, *J. Intern. Med.*, **2008**, *264*, 4–16
  25. H. C. Neu, *Science*, **1992**, *257*, 1064–1073
  26. P. Courvalin, *Antimicrob. Agents Chemother.*, **1994**, *38*, 1447–1451
  27. D. Lim, N. C. J. Strynadka, *Nature Struct. Biol.*, **2002**, *9* (11), 870–876
  28. M. A. Webber, L. J. V. Piddock, *J. Antimicrob. Chemother.*, **2003**, *51*, 9–11
  29. A. Cavalli, M. L. Bolognesi, A. Minarini, M. Rosini, V. Tumiatti, M. Recanatini, C. Melchiorre, *J. Med. Chem.*, **2008**, *51* (3), 347–372
  30. T. Bishop, P. Sham, *Analysis of Multifactorial Diseases*, **2000**, Academic Press: New York, 1–320
  31. A. Agis-Torres, M. Sölhuber, M. Fernandez, J. M. Sanchez-Montero, *Curr. Neuropharmacol.*, **2014**, *12* (1), 2–36
  32. M. J. Oset-Gasque, J. Marco-Contelles, *ACS Chem. Neurosci.*, **2018**, *9*, 401–403
  33. A. G. Ziady, J. Hansen, *Int. J. Biochem. Cell. Biol.*, **2014**, *52*, 113–123
  34. L. Spicuzza, G. F. Parisi, L. Tardino, N. Ciancio, R. Nenna, F. Midulla, S. Leonardi, *J. Breath Res.*, **2018**, *12*, 026010
  35. F. Galli, A. Battistoni, R. Gambari, A. Pompella, A. Bragonzi, F. Pilolli, L. Iuliano, M. Piroddi, M. C. Dechecchi, G. Cabrini, *Biochim. Biophys. Acta*, **2012**, *1822*, 690–713
  36. W. C. Rutter, D. R. Burgess, D. S. Burgess, *Microb. Drug Resist.*, **2017**, *23*, 51–55
  37. a) C. H. Goss, M. S. Muhlebach, *J. Cystic Fibrosis*, **2011**, *10*, 298–306; b) N. S. Harik, G. Com, X. Tang, M. Melguizo Castro, M. E. Stemper, J. L. Carroll, *Am. J. Infect. Contr.*, **2016**, *44*, 409–415; c) S. Razvi, L. Quittell, A. Sewall, H. Quinton, B. Marshall, L. Saiman, *Chest*, **2009**, *136*, 1554–1560
  38. G. Cainelli, D. Giacomini, P. Galletti, A. Quintavalla, *Eur. J. Org. Chem.*, **2003**, *9*, 1765–1774
  39. a) G. Cainelli, P. Galletti, S. Garbisa, D. Giacomini, L. Sartor, A. Quintavalla, *Bioorg. Med. Chem.*, **2003**, *11*, 5391–5399; b) G. Cainelli, D. Giacomini, P. Galletti, A. Quintavalla, *Tetrahedron Lett.*, **2003**, *44*, 6269–6272; c) F. Broccolo, G. Cainelli, G. Caltabiano, C. E. A. Cocuzza, C. G. Fortuna, P. Galletti, D. Giacomini, G. Musumarra, R. Musumeci, A. Quintavalla, *J. Med. Chem.*, **2006**, *49*, 2804–2811; d) G. Cainelli, C. Angeloni, R. Cervellati, P. Galletti, D. Giacomini, S. Hrelia, R. Sinisi, *Chem. Biodivers.*, **2008**, *5*, 811–829; e) R. Cervellati, P. Galletti, E. Greco, C. E. A. Cocuzza, R. Musumeci, L. Bardini, F. Paolucci, M. Pori, R. Soldati, D. Giacomini, *Eur. J. Med. Chem.*, **2013**, *60*, 340–349
  40. P. Galletti, D. Giacomini, *Curr. Med. Chem.*, **2011**, *18* (28), 4265–4283
  41. S. Gérard, M. Galleni, G. Dive, J. Marchand-Brynaert, *Bioorg. Med. Chem.*, **2004**, *12*, 129–138
  42. a) R. C. Moellering Jr., G. M. Eliopoulos, D. E. Sentochnik, *J. Antimicrob. Chemother.*, **1989**, *24*, Suppl A:1–7. b) K. M. Papp-Wallace, A. Endimiani, M. A. Taracila, R. A. Bonomo, *Antimicrob. Agents Chemother.*, **2011**, *55* (11), 4943–4960

- 
43. a) E. Turos, M. I. Konaklieva, R. X. F. Ren, H. C. Shi, J. Gonzalez, S. Dickey, D. V. Lim, *Tetrahedron*, **2000**, *56*, 5571–5578
44. K. D. Revell, B. Heldreth, T. E. Long, S. Jang, E. Turos, *Bioorg. Med. Chem.*, **2007**, *15*, 2453–2467
45. D. Giacomini, R. Musumeci, C. E. A. Cocuzza, *unpublished results*
46. D. Giacomini, R. Musumeci, P. Galletti, G. Martelli, L. Assennato, G. Sacchetti, A. Guerrini, E. Calaresu, M. Martinelli, C. E. A. Cocuzza, *Eur. J. Med. Chem.*, **2017**, *140*, 604–614
47. a) M. Drăgan, C. D. Stan, A. Iacob, L. Profire, *Farmacía*, **2016**, *64* (5), 717–721; b) M. Andrade, S. Benfeito, P. Soares, D. Magalhães e Silva, J. Loureiro, A. Borges, F. Borges, M. Simões, *RSC Adv.*, **2015**, *5*, 53915–53925; c) J. Guzman, *Molecules*, **2014**, *19*, 19292–19349
48. A. Alam, Y. Takaguchi, H. Ito, T. Yoshida, S. Tsuboi, *Tetrahedron*, **2005**, *61*, 1909–1918
49. B. Neises, W. Steglich, *Angew. Chem. Int. Ed. Engl.*, **1978**, *17*, 522–524
50. a) I. K. Schalk, G. L. A. Mislin, *J. Med. Chem.*, **2017**, *60*, 4573–4576; b) C. Ji, R. E. Juárez-Hernández, M. J. Miller, *Future Med. Chem.*, **2012**, *4*, 297–313
51. R. M. Uppu, S. N. Murthy, W. A. Pryor, N. L. Parinandi, *Free Radicals and Antioxidant Protocols, Methods in Molecular Biology* (2nd Edition), **2010**, Humana Press,
52. A. Cilla, L. Bosch, R. Barberá, A. Alegría, *J. Food Compos. Anal.*, **2017**, *68*, 3–15
53. S. Yin, B. Jiang, G. Huang, Y. Gong, B. You, Z. Yang, Y. Chen, J. Chen, Z. Yuan, M. Li, F. Hu, Y. Zhao, Y. Peng, *Front. Microbiol.*, **2017**, *8*: 1191
54. P. M. Roundtree, B. M. Freeman, *Med. J. Aust.*, **1956**, *42*, 157–161
55. E. Tacconelli, E. Carrara, A. Savoldi, S. Harbarth, M. Mendelson, D. L. Monnet, C. Pulcini, G. Kahlmeter, J. Kluytmans, Y. Carmeli, M. Oueltte, K. Outterson, J. Patel, M. Cavalieri, E. M. Cox, C. R. Houchens, M. L. Grayson, P. Hansen, N. Singh, U. Theuretzbacher, N. Magrini, *Lancet Infect. Dis.*, **2018**, *18*, 318–327
56. H. F. Chambers, F. R. Deleo, *Nat. Rev. Microbiol.*, **2009**, *7*, 629–641
57. H. F. C. Liu, A. Bayer, S. E. Cosgrove, R. S. Daum, S. K. Fridkin, R. J. Gorwitz, S. L. Kaplan, A. W. Karchmer, D. P. Levine, B. E. Murray, M. J. Rybak, D. A. Talan, H. F. Chambers, *Clin. Infect. Dis.*, **2011**, *52*, 1–38
58. P. O. Lewis, E. L. Heil, K. L. Covert, D. B. Cluck, *J. Clin. Pharm. Ther.*, **2018**, 1–12
59. B. C. Kahl, *Infect. Genet. Evol.*, **2014**, *21*, 515–522
60. K. Nahar, N. Gupta, R. Gauvin, S. Absar, B. Patel, V. Gupta, A. Khademhosseini, F. Ahsan, *Eur. J. Pharm. Sci.*, **2013**, *49*, 805–818
61. J. S. Patton, C. S. Fishburn, J. G. Weers, *Proc. Am. Thorac. Soc.*, **2004**, *1*, 338–344
62. a) R. Dal Magro, F. Ornaghi, I. Cambianica, S. Beretta, F. Re, C. Musicanti, R. Rigolio, E. Donzelli, A. Canta, E. Ballarini, G. Cavaletti, P. Gasco, G. Sancini, *J. Control. Release*, **2017**, *249*, 103–110; b) C. Musicanti, P. Gasco, Solid Lipid-Based Nanoparticles, in *Encyclopedia of Nanotechnology*, **2012**, Springer Netherlands: Dordrecht, 2487–2487

- 
63. a) F. Farina, G. Sancini, P. Mantecca, D. Gallinotti, M. Camatini, and P. Palestini, *Toxicol. Lett.*, **2011**, *202* (3), 209–217; b) F. Farina, G. Sancini, E. Longhin, P. Mantecca, M. Camatini, P. Palestini, *Biomed. Res. Int.*, **2013**; *2013*: 583513
64. M. Zasloff, *Nature*, **2002**, *415*, 389–395
65. R. E. W. Hancock, H-G. Sahl, *Nat. Biotechnol.*, **2006**, *24*, 1551–1557
66. H. Jenssen, P. Hamill, R. E. W. Hancock, *Clin. Microbiol. Rev.*, **2006**, *19*, 491–511
67. A. Marr, W. Gooderham, R. E. W. Hancock, *Curr. Opin. Pharmacol.*, **2006**, *6*, 468–472
68. S. Rotem, A. Mor, *Biochim. Biophys. Acta Biomembr.*, **2009**, *1788*, 1582–1592
69. A. Som, S. Vemparala, I. Ivanov, G. N. Tew, *Biopolymers*, **2008**, *90*, 83–93
70. C. D. Fjell, J. A. Hiss, R. E. W. Hancock, G. Schneider, *Nat. Rev. Drug Discov.*, **2012**, *11* (1), 37–51
71. H. D. Thaker, A. Cankaya, R. W. Scott, G. N. Tew, *ACS Med. Chem. Lett.*, **2013**, *4*, 481–485
72. H. D. Thaker, A. Som, F. Ayaz, D. Lui, W. Pan, R. W. Scott, J. Anguita, G. N. Tew, *J. Am. Chem. Soc.*, **2012**, *134*, 11088–11091
73. O. Mitsunobu, Y. Yamada, *BCSJ*, **1967**, *40* (10), 2380–2382
74. A. Williamson, *Philosophical Magazine*, **1850**, *37* (251), 350–356
75. D. Giacomini, G. Martelli, M. Picciché, E. Calaresu, C. E. A. Cocuzza, R. Musumeci, *ChemMedChem.*, **2017**, *12* (18), 1525–1533
76. a) S. Ray, S. R. Pathak, D. Chaturvedi, *Drugs Fut.*, **2005**, *30*, 161–180; b) S. M. Rahmanthullan, R. R. Tidwell, S. K. Jones, J. E. Hall, D. W. Boykin, *Eur. J. Med. Chem.*, **2008**, *43*, 174–177
77. a) C. Borrel, S. Thoret, X. Cachet, D. Guenard, F. Tillequin, M. Koch, S. Michel, *Bioorg. Med. Chem.* **2005**, *13*, 3853–3864; b) D. Chaturvedi, *Tetrahedron*, **2012**, *68*, 15–45
78. M. D. Stephens, N. Yodsanit, C. Melander, *Org. Biomol. Chem.* **2016**, *14*, 6853–6856
79. H. Yoshizawa, T. Kubota, H. Itani, K. Minami, H. Miwa, Y. Nishitani, *Bioorg. Med. Chem.*, **2004**, *12*, 4221–4231
80. S. Yan, M. J. Millera, T. A. Wenczewicz, U. Möllmann, *Medchemcomm.*, **2010**, *1*, 145–148
81. P. Adams, F. A. Baron, *Chem. Rev.*, **1965**, *65*, 567–602
82. R. S. Varma, *Green Chem.*, **1999**, *1*, 43–55
83. M. Feledziak, C. Michaux, D. M. Lambert, J. Marchand-Brynaert, *Eur. J. Med. Chem.*, **2013**, *60*, 101–111
84. R. P. Tangallapally, R. Yendapally, R. E. Lee, A. J. M. Lenaerts, R. E. Lee, *J. Med. Chem.*, **2005**, *48*, 8261–8269
85. J. Lee, M-K. Jin, S-U. Kang, S. Y. Kim, J. Lee, M. Shin, J. Hwang, S. Cho, Y-S. Choi, H-K. Choi, S-E. Kim, Y-G. Suh, Y-S. Lee, Y-H. Kim, H-J. Ha, A. Toth, L. V. Pearce, R. Tran, T. Szabo, J. D. Welter, D. J. Lundberg, Y. Wang, J. Lazar, V. A. Pavlyukovets, M. A. Morgan, P. M. Blumberg, *Bioorg. Med. Chem. Lett.*, **2005**, *15*, 4143–4150

- 
86. J. Park, R. S. Lakes, *Biomaterials: an introduction*, **2007**, Springer Science & Business Media
87. M. Szycher, R. Valdez., *J. Clin. Eng.*, **1983**, *8*, 234
88. J. Raphael, M. Holodniy, S. B. Goodman, S. C. Heilshorn, *Biomaterials*, **2016**, *84*, 301–314
89. T. Bjarnsholt, O. Ciofu, S. Molin, M. Givskov, N. Høiby, *Nat. Rev. Drug Discov*, **2013**, *12*, 791–808
90. a) L. Sandegren, *Ups. J. Med. Sci.*, **2014**, *119*, 103–107; b) M. Rai, K. Kon, A. Ingle, N. Duran, S. Galdiero, M. Galdiero, *Appl. Microbiol. Biotechnol.*, **2014**, *98*, 1951–1961
91. H. Qu, C. Knabe, S. Radin, J. Garino, P. Ducheyne, *Biomaterials*, **2015**, *62*, 95–105
92. a) F. Costa, I. F. Carvalho, R. C. Montelaro, P. Gomes, M. C. L. Martins, *Acta Biomater.*, **2011**, *7*, 1431–1440; b) F. Paladini, M. Pollini, A. Sannino, L. Ambrosio, *Biomacromolecules*, **2015**, *16*, 1873–1885; c) S. Cazalbou, G. Bertrand, C. Drouet, *J. Phys. Chem. B*, **2015**, *119*, 3014–3024
93. a) R. A. Surmenev, M. A. Surmeneva, A. A. Ivanova, *Acta Biomater.*, **2014**, *10*, 557–559; b) J. Zhang, W. Liu, V. Schnitzler, F. Tancret, J. M. Bouler, *Acta Biomater.*, **2014**, *10*, 1035–1049; c) S. V. Dorozhkin, *Materials Science & Engineering C*, **2015**, *55*, 272–326
94. a) A. Bigi, E. Boanini, M. Gazzano, *Biomaterialization and Biomaterials Fundamentals and applications*, **2015**, Woodhead Publishing, 235–266; b) V. Uskoković, D. P. Uskoković, *J. Biomed. Mater. Res. Part B: Appl. Biomater.*, **2011**, *96*, 152–191
95. a) E. Boanini, P. Torricelli, M. C. Cassani, G. A. Gentilomi, B. Ballarin, K. Rubini, F. Bonvicini, A. Bigi, *RSC Adv.*, **2014**, *4*, 645–652; b) G. A. Fielding, M. Roy, A. Bandyopadhyay, S. Bose, *Acta Biomater.*, **2012**, *8*, 3144–3152; c) E. S. Thian, T. Konishi, Y. Kawanobe, P. N. Lim, C. Choong, B. Ho, M. Aizawa, *J. Mater. Sci. Mater. Med.*, **2013**, *24*, 437–445
96. a) S. Leprêtre, *Biomaterials*, **2009**, *30*, 6086–6089; b) C. A. Soriano-Souza, A. L. Rossi, E. Mavropoulos, M. A. Hausen, M. N. Tanaka, M. D. Calasans-Maia, J. M. Granjeiro, M. H. M. Rocha-Lea, A. M. Rossi, *J. Mater. Sci. Mater. Med.*, **2015**, *26*: 166; c) S. Ghosh, V. Wu, S. Pernal, V. Uskoković, *ACS Appl. Mater. Interfaces*, **2016**, *8*, 7691–7708
97. D. Giacomini, P. Torricelli, G. A. Gentilomi, E. Boanini, M. Gazzano, F. Bonvicini, E. Benetti, R. Soldati, G. Martelli, K. Rubini, A. Bigi, *Sci. Rep.*, **2017**, *7*, 2712
98. A. Bigi, E. Boanini, M. Gazzano, M. A. Kojdecki, K. Rubini, *J. Mater. Chem.*, **2004**, *14*, 274–279
99. E. Boanini, P. Torricelli, M. Gazzano, R. Giardino, A. Bigi, *Biomaterials*, **2008**, *29*, 790–796
100. S. Pezzatini, L. Morbidelli, R. Solito, E. Paccagnini, E. Boanini, A. Bigi, M. Ziche, *Bone*, **2007**, *41*, 523–534
101. M. Gruselle, *J. Organomet. Chem.*, **2015**, *793*, 93–101
102. a) C. O. Ania, B. Cabal, J. B. Parra, A. Arenillas, B. Arias, J. J. Pis, *Adsorption*, **2008**, *14*, 343–355; b) B. N. Bhadra, K. H. Cho, N. A. Khan, D. Y. Hong, S. H. Jung, *J. Phys. Chem. C*, **2015**, *119*, 26620–26627
103. A. C. Queiroz, J. D. Santos, F. J. Monteiro, I. R. Gibson, J. C. Knowles, *Biomaterials*, **2001**, *22*, 1393–1400



- 
104. L. J. Liermann, A. S. Barnes, B. E. Kalinowski, X. Zhou, S. L. Brantley, *Chem. Geol.*, **2000**, *171*, 1–16
105. L. Tuchscher, C. A. Kreis, V. Hoerr, L. Flint, M. Hachmeister, J. Geraci, S. Bremer-Streck, M. Kiehntopf, E. Medina, M. Kribus, M. Raschke, M. Pletz, G. Peters, B. Löffler, *J. Antimicrob. Chemoth.*, **2016**, *71*, 438–448
106. C. Spatafora, V. Barresi, V. M. Bhusainahalli, S. Di Micco, N. Musso, R. Riccio, G. Bifulco, D. Condorelli, C. Tringali, *Org. Biomol. Chem.*, **2014**, *12*, 2686–2701
107. C. Zhu, R. Wang, J. R. Falck, *Org. Lett.*, **2012**, *14* (13), 3494–3497
108. A. G. Chittiboyina, M. S. Venkatraman, C. S. Mizuno, P. V. Desai, A. Patny, S. C. Benson, C. I. Ho, T. W. Kurtz, H. A. Pershadsingh, M. A. Avery, *J. Med. Chem.*, **2006**, *49* (14), 4072–4084
109. A. Y-T. Huang, C-H. Tsai, H-Y. Chen, H-T. Chen, C-Y. Lu, Y-T. Lin, C-L Kao, *Chem. Commun.*, **2013**, *49*, 5784–5786
110. B. Alcaide, P. Almendros, C. Aragoncillo, *Curr. Opin. Drug Di. De.*, **2010**, *13*, 685–697
111. a) N. Arya, A. Y. Jagdale, T. A. Patil, S. S. Yeramwar, S. S. Holikatti, J. Dwivedi, C. J. Shishoo, K. S. Jain, *Eur. J. Med. Chem.*, **2014**, *74*, 619–656; b) P. D. Mehta, N. P. S. Sengar, A. K. Pathak, *Eur. J. Med. Chem.*, **2010**, *45*, 5541–5560
112. a) S. K. Bhati, A. Kumar, *Eur. J. Med. Chem.*, **2008**, *43*, 2323–2330; b) K. F. Ansari, C. Lal, *Eur. J. Med. Chem.*, **2009**, *44*, 2294–2299
113. N. E. Zhou, D. Guo, G. Thomas, A. V. N. Reddy, J. Kaleta, E. Purisima, R. Menard, R. G. Micetich, R. Singh, *Bioorg. Med. Chem. Lett.*, **2003**, *13*, 139–141
114. P. Imbach, M. Lang, C. García-Echeverría, V. Guagnano, M. Noorani, J. Roesel, F. Bitsch, G. Rihs, P. Furet, *Bioorg. Med. Chem. Lett.*, **2007**, *17*, 358–362
115. C. D. Guillon, G. A. Koppel, M. J. Brownstein, M. O. Chaney, C. F. Ferris, S. Lu, K. M. Fabio, M. J. Miller, N. D. Heindel, D. C. Hunden, R. D. G. Cooper, S. W. Kaldor, J. J. Skelton, B. A. Dressman, M. P. Clay, M. I. Steinberg, R. F. Bruns, N. G. Simon, *Bioorg. Med. Chem.*, **2007**, *15*, 2054–2080
116. G. Cainelli, P. Galletti, S. Garbisa, D. Giacomini, L. Sartor, A. Quintavalla, *Bioorg. Med. Chem.*, **2005**, *13*, 6120–6132
117. a) S. Gerard, G. Dive, B. Clamot, R. Touillaux, J. Marchand-Brynaert, *Tetrahedron*, **2002**, *58*, 2423–2433; b) S. Gerard, G. Nollet, J. V. Put, J. Marchand-Brynaert, *J. Bioorg. Med. Chem.*, **2002**, *10*, 3955–3964
118. G. Cainelli, A. Folda, G. Scutari, R. Deana, M. Pavanetto, A. Zarpellon, D. Giacomini, P. Galletti, A. Quintavalla, *Platelets*, **2007**, *18*, 357–364
119. P. Singh, S. A. Williams, M. H. Shah, T. Lectka, G. J. Pritchard, J. T. Isaacs, S. R. Denmead, *Proteins: Struct., Funct., Bioinfo.*, **2008**, *70*, 1416–1428
120. M. Feledziak, A. Urbach, G. G. Muccioli, J. Marchand-Brynaert, G. Labar, M. L. Didier, C. Michaux, *J. Med. Chem.*, **2009**, *52*, 7054–7068
121. a) G. Gerona-Navarro, M. Vega, M. T. Garcia-Lopez, G. Andrei, R. Snoeck, J. Balzarini, E. De Clercq, R. Gonzalez-Muniz, *Bioorg. Med. Chem. Lett.*, **2004**, *14*, 2253–2256; b) G. Gerona-Navarro, M. Vega, M. T. Garcia-Lopez, G. Andrei, R. Snoeck, E. De Clercq, J. Balzarini, R. Gonzalez-Muniz, *J. Med. Chem.*, **2005**, *48*, 2612–2621

- 
122. M. O'Driscoll, K. Greenhalgh, A. Young, E. Turos, S. Dickey, D. V. Lim, *Bioorg. Med. Chem.*, **2008**, *16*, 7832–7837
123. A. Kazi, R. Hill, T. E. Long, D. J. Kuhn, E. Turos, Q. Dou, *P. Biochem. Pharmacol.*, **2004**, *67*, 365–374
124. P. Galletti, A. Quintavalla, C. Ventrici, G. Giannini, W. Cabri, S. Penco, G. Gallo, S. Vincenti, D. Giacomini, *ChemMedChem*, **2009**, *4*, 1–12
125. C. Crauste, M. Froeyen, J. Anné, P. Herdewijn, *Eur. J. Org. Chem.* **2011**, *19*, 3437–3449
126. T. Dražić, V. Sachdev, C. Leopold, J. V. Patankar, M. Malnar, S. Hećimović, S. Levak-Frank, I. Habuš, D. Kratky, *Bioorg. Med. Chem.*, **2015**, *23*, 2353–2359
127. N. M. O'Boyle, A. J. S. Knox, T. T. Price, D. C. Williams, D. M. Zisterer, D.G. Lloyd, M. J. Meegan, *Bioorg. Med. Chem.*, **2011**, *19*, 6055–6068
128. P. C Wong, E. J. Crain, C. A. Watson, W.A. Schumacher, *J. Thromb. Thrombolysis*, **2011**, *32*, 129–137
129. a) J. M. Aizpurua, J. I. Ganboa, C. Palomo, I. Loinaz, J. Oyarbide, X. Fernandez, E. Balentova, R. M. Fratila, A. Jimenez, J. I. Miranda, A. Laso, S. Avila, J. L. Castrillo, *ChemBioChem*, **2011**, *12*, 401–405; b) J. M. Aizpurua, J. Oyarbide, X. Fernandez, J. I. Miranda, J. I. Ganboa, S. Avila, J. L. Castrillo, *Eur. Pat. Appl.*, **2012**, EP 2407478 A1 20120118; c) J. M. Aizpurua, J. I. Ganboa, C. Palomo, I. Loinaz, J. I. Miranda, *PCT Int. Appl.*, **2006**, WO 2006048473 A1 20060511
130. M. J. Humphries, *Biochem. Soc. Trans.*, **2000**, *28*, 311–339
131. Adapted from: C. G. Gahmberg, S. C. Fagerholm, S. M. Nurmi, T. Chavakis, S. Marchesan, M. Grönholm, *Biochim. Biophys. Acta*, **2009**, *1790*, 431–444
132. a) J. D. Humphries, A. Byron, M. J. Humphries, *J. Cell. Science*, **2006**, *119*, 3901–3903; b) I. D. Campbell, M. J. Humphries, *Cold Spring Harb. Perspect. Biol.* **2011**, *3* (3), a004994
133. E. F Plow, T. A. Haas, L. Zhang, J. Loftus, J.W. Smith, *J. Biol. Chem.*, **2000**, *275*, 21785–21788
134. A. Tolomelli, P. Galletti, M. Baiula, D. Giacomini, *Cancers* **2017**, *9* (7), 78
135. a) H. Wolfenson, I. Lavelin, B. Geiger, *Dev. Cell*, **2013**, *24*, 447–458; b) M. Barczyk, S. Carracedo, D. Gullberg, *Cell Tissue Res.*, **2010**, *339*, 269–280; c) M. A. Arnaout, S. L. Goodman, J-P. Xiong, *Curr. Op. Cell Biol.*, **2007**, *19*, 495–507; d) N. J. Anthis, I. D. Campbell, *Trends Biochem. Sci.*, **2011**, *36*, 191–198; e) R. Zaidel-Bar, B. Geiger, *J. Cell. Science*, **2010**, *123*, 1385–1388; f) M. A. Arnaout, B. Mahalingam, J. P. Xiong, *Ann. Rev. Cell. Dev. Biol.*, **2005**, *21*, 381–410
136. R. O. Hynes, *Cell*, **2002**, *110*, 673–687
137. S. L. Goodman, M. Picard, *Trends Pharmacol. Sci.*, **2012**, *33*, 405–412
138. S-H. Kim, J. Turnbull, S. Guimond, *J. Endocrinol.* **2011**, *209*, 139–151
139. Adapted from: S. J. Shattil, C. Kim, M. H. Ginsberg, *Nat. Rev. Mol. Cell Biol.*, **2010**, *11* (4), 288–300
140. K. L. Yee, V. M. Weaver, D. A. Hammer, *IET Syst. Biol.*, **2008**, *2*, 8–15

- 
141. B-H. Luo, C. V. Carman, T. A. Springer, *Annu. Rev. Immunol.* **2007**, *25*, 619–647
142. N. Beglova, S. C. Blacklow, J. Takagi, T. A. Springer, *Nat. Struct. Biol.*, **2002**, *9*, 282–287
143. a) K. Ley, J. Rivera-Nieves, W. J. Sandborn, S. Shattil, *Nat. Rev. Drug Discov.*, **2016**, *15*, 173–183; b) S. E. Winograd-Katz, R. Fassler, B. Geiger, K. R. Legate, *Nat. Rev. Mol. Cell Biol.*, **2014**, *15*, 273–288
144. C. Rüegg, A. Margotti, *Cell. Mol. Life Sci.*, **2003**, *60*, 1135–1157
145. a) H. M. Sheldrake, L. H. Patterson, *J. Med. Chem.* **2014**, *57*, 6301–6315; b) U. K. Marelli, F. Rechenmacher, T. R. Sobahi, C. Mas-Moruno, H. Kessler, *Front. Oncol.*, **2013**, *3*, 1–12
146. D. I. Simon, *Circ. Res.*, **2011**, *109*, 1199–1201
147. F. Danhier, A. Le Breton, V. Pr eat, *Mol. Pharmaceutics*, **2012**, *9*, 2961–2973
148. C. Mas-Moruno, F. Rechenmeier, H. Kessler, *Anticancer Agents Med. Chem.*, **2010**, *10* (10), 753–768
149. E. Celik, M. H. Faridi, V. Kumar, S. Deep, V. T. Moy, V. Gupta, *Biophys. J.*, **2013**, *105*, 2517–2727
150. S. Q. Khan, L. Guo, D. J. Cimbaluk, H. Elshabrawy, M. H. Faridi, M. Jolly, J. F. George, A. Agarwal, V. A. Gupta, *Front. Med.*, **2014**, *1*, 1–11
151. W. Yang, C. V. Carman, M. Kim, A. Salas, M. Shimaoka, T. A. Springer, *J. Biol. Chem.*, **2006**, *281*, 37904–37912
152. P. Vanderslice, R. J. Biediger, D. G. Woodside, W. S. Brown, S. Khounlo, N. D. Warier, C. W. Gundlach, A. R. Caivano, W. G. Bornmann, D. S. Maxwell, B.W. McIntyre, J. T. Willerson, R. A. Dixon, *J. Biol. Chem.*, **2013**, *288*, 19414–19428
153. M. H. Faridi, M. M. Altintas, C. Gomez, J. C. Duque, R. I. Vazquez-Padron, V. Gupta, *Biochim. Biophys. Acta*, **2013**, *1830*, 3696–3710
154. M. A. Schwartz, K. McRoberts, M. Coyner, K. L. Andarawewa, H. F. Frierson, Jr., J. M. Sanders, S. Swenson, F. Markland, M. R. Conaway, D. Theodorescu, *Clin. Cancer Res.*, **2008**, *14*, 6193–6197
155. P. Galletti, R. Soldati, M. Pori, M. Durso, A. Tolomelli, L. Gentilucci, S. D. Dattoli, M. Baiula, S. M. Spampinato, D. Giacomini, *Eur. J. Med. Chem.*, **2014**, *83*, 284–293
156. C. Margadant, H. N. Monsuur, J. C. Norman, A. Sonnenberg, *Curr. Opin. Cell Biol.*, **2011**, *23* (5), 607–614
157. A. G. Ramsay, J. F. Marshall, I. R. Hart, *Cancer Metastasis Rev.*, **2007**, *26*, 567–578
158. a) W. J. Chia, B. L. Tang, *Biochim. Biophys. Acta -Reviews on Cancer*, **2009**, *1795* (2), 110–116; b) H. Stenmark, *Nat. Rev. Mol. Cell Biol.*, **2009**, *10* (8), 513–525
159. C. Le Roy, J. L. Wrana, *Nat. Rev. Mol. Cell Biol.*, **2005**, *6*, 112–126
160. a) P. T. Caswell, S. Vadrevu, J. C. Norman, *Nat. Rev. Mol. Cell Biol.*, **2009**, *10* (12), 843–853; b) P. Caswell, J. Norman, *Trends Cell Biol.*, **2008**, *18* (6), 257–263; c) P. T. Caswell, J. C. Norman, *Traffic*, **2006**, *7*, 14–21
161. G. J. Doherty, H. T. McMahon, *Annu. Rev. Biochem.*, **2009**, *78*, 857–902
162. S. Shin, L. Wolgamott, S-O. Yoon, *Int. J. Cell Biol.*, **2012**, 2012:516789

- 
163. Y. Mosesson, G. B. Mills, Y. Yarden, *Nat. Rev. Cancer.*, **2008**, 8 (11), 835–850
164. Adapted from: S. Fortin, M. Le Mercier, I. Camby, S. Spiegl-Kreinecker, W. Berger, F. Lefranc, R. Kiss, *Brain Pathology*, **2010**, 20 (1), 39–49
165. R. E. Bridgewater, J. C. Norman, P. T. Caswell, *J. Cell Sci.*, **2012**, 125, 3695–3701
166. Y. Zhen, H. Stenmark, *J. Cell Sci.*, **2015**, 128, 3171–3176
167. W. Guo, Y. Pylayeva, A. Pepe, T. Yoshioka, W. J. Muller, G. Inghirami, F. G. Giancotti, *Cell*, **2006**, 126 (3), 489–502
168. X. Wu, B. Gan, Y. Yoo, J-L. Guan, *Dev. Cell*, **2005**, 9 (2), 185–196
169. E. Rainero, J. D. Howe, P. T. Caswell, N. B. Jamieson, K. Anderson, D. R. Critchley, L. Machesky, J. C. Norman, *Cell Rep.*, **2015**, S2211-1247, (14)01066-3
170. S. Castel, R. Pagan, F. Mitjans, J. Piulats, S. Goodman, A. Jonczyk, F. Huber, S. Vilarò, M. Reina, *Lab. Investig.*, **2001**, 81, 1615–1626
171. M. Baiula, P. Galletti, G. Martelli, R. Soldati, L. Belvisi, M. Civera, S. D. Dattoli, S. M. Spampinato, D. Giacomini, *J. Med. Chem.*, **2016**, 59 (21), 9721–9742
172. a) A. Tolomelli, L. Gentilucci, E. Mosconi, A. Viola, S. D. Dattoli, M. Baiula, S. M. Spampinato, L. Belvisi, M. Civera, *ChemMedChem*, **2011**, 6, 2264–2272; b) A. Tolomelli, M. Baiula, L. Belvisi, A. Viola, L. Gentilucci, S. Troisi, S. D. Dattoli, S. M. Spampinato, M. Civera, E. Juaristi, *Eur. J. Med. Chem.*, **2013**, 66, 258–268; c) F. Benfatti, G. Cardillo, S. Fabbroni, P. Galzerano, L. Gentilucci, R. Juris, A. Tolomelli, M. Baiula, A. Sparta, S. M. Spampinato, *Bioorg. Med. Chem.*, **2007**, 15, 7380–7390; d) A. Tolomelli, M. Baiula, A. Viola, L. Ferrazzano, L. Gentilucci, S. D. Dattoli, S. M. Spampinato, E. Juaristi, M. Escudero, *ACS Med. Chem. Lett.*, **2015**, 6, 701–706
173. K. C. Lin, H. S. Ateeq, S. H. Hsiung, L. T. Chong, C. N. Zimermann, A. Castro, W. C. Lee, C. E. Hammond, S. Kalkunte, L. L. Chen, R. B. Pepinsky, D. R. Leone, A. G. Sprague, W. M. Abraham, A. Gill, R. R. Lobb, S. P. Adams, *J. Med. Chem.*, **1999**, 42, 920–934
174. W. J. Pitts, J. Wityak, J. M. Smallheer, A. E. Tobin, J. W. Jetter, J. S. Buynitsky, P. P. Harlow, K. A. Solomon, M. H. Corjay, S. A. Mousa, R. R. Wexler, P. K. Jadhav, *J. Med. Chem.*, **2000**, 43, 27–40
175. T. A. Springer, J-H. Wang, *Adv. Protein Chem.*, **2004**, 68, 29–63
176. Y. Ito, S. Terashima, *Tetrahedron Lett.* **1987**, 28, 6625–6628
177. a) M. Gurrath, G. Müller, H. Kessler, M. Aumailley, R. Timpl, *Eur. J. Biochem.* **1992**, 210, 911–921; b) C. Mas-Moruno, F. Rechenmacher, H. Kessler, *Anticancer Agents Med. Chem.* **2010**, 10 (10), 753–768
178. A. R. Qasem, C. Bucolo, M. Baiula, A. Spartà, P. Govoni, A. Bedini, D. Fascì, S. Spampinato, *Biochem. Pharmacol.*, **2008**, 76, 751–762
179. R. A. Bednar, S. L. Gaul, T. G. Hamill, M. S. Egbertson, J. A. Shafer, G. D. Hartman, R. J. Gould, B. Bednar, *J. Pharmacol. Exp. Ther.*, **1998**, 285, 1317–1326
180. J. F. Van Agthoven, J. P. Xiong, J. L. Alonso, X. Rui, B. D. Adair, S. L. Goodman, M. A. Arnaut, *Nat. Struct. Mol. Biol.*, **2014**, 21, 383–388
181. B. D. Cox, M. Natarajan, M. R. Stettner, C. L. Gladson, *J. Cell Biochem.* **2006**, 99, 35–52

- 
182. a) B. H. Luo, T. A. Springer, *Curr. Opin. Cell Biol.*, **2006**, *18*, 579–586; b) C. Margadant, H. N. Monsuur, J. C. Norman, A. Sonnenberg, *Curr. Opin. Cell Biol.*, **2011**, *23*, 607–614
183. M. W. Johansson, D. F. Mosher, *Front Pharmacol.*, **2013**, *4* (33), 1–9
184. a) L. Manzoni, L. Belvisi, D. Arosio, M. Civera, M. Pilkington-Miksa, D. Potenza, A. Caprini, E. M. V. Araldi, E. Monferini, M. Mancino, F. Podestà, C. Scolastico, *ChemMedChem*, **2009**, *4*, 615–632; b) M. Marchini, M. Mingozzi, R. Colombo, I. Guzzetti, L. Belvisi, F. Vasile, D. Potenza, U. Piarulli, D. Arosio, C. C. Gennari, *Chem. Eur. J.*, **2012**, *18*, 6195–6207
185. Glide, version 4.5, **2007**, Schrödinger, LLC, New York, NY (USA)
186. J. P. Xiong, T. Stehle, R. Zhang, A. Joachimiak, M. French, S. L. Goodman, M. A. Arnaout, *Science*, **2002**, *296*, 151–155
187. C. Choi, J-H. Li, M. Vaal, C. Thomas, D. Limburg, Y-Q. Wu, Y. Chen, R. Soni C. Scott, D. T. Ross, H. Guo, P. Howorth, H. Valentine, S. Liang, D. Spicer, M. Fuller, J. Steine, G. S. Hamilton, *Bioorg. Med. Chem. Lett.*, **2002**, *12* (10), 1421–1428
188. C. Bolchi, E. Valoti, L. Fumagalli, V. Straniero, P. Ruggeri, M. Pallavicini, *Org. Process Res. Dev.*, **2015**, *19* (7), 878–883
189. A. T. Krueger, B. Imperiali, *ChemBioChem*, **2013**, *14* (7), 788–799
190. T. Terai, T. Nagano, *Pflugers Arch.*, **2013**, *465* (3), 347–359
191. J. Eng, R. M. Lynch, R. S. Balaban, *Biophys. J.*, **1989**, *55* (4), 621–630
192. M. S. Gonçalves, *Chem. Rev.*, **2009**, *109* (1), 190–212
193. I. Atallah, C. Milet, J-L. Coll, E. Reyt, C. A. Righini, A. Hurbin, *Eur. Arch. Otorhinolaryngol.*, **2015**, *272* (10), 2593–2600
194. Y. Ha, H. K. Choi, *Chem. Biol. Interact.*, **2016**, *248*, 36–51
195. J. C. Stockert, A. Blázquez-Castro, *Fluorescence Microscopy in Life Sciences*, **2017**, Bentham Science Publishers, 61–95
196. B. Valeur, M. N. Berberan-Santos, *Molecular fluorescence: principles and applications* (2nd edition), **2012**, Wiley VCH
197. Y. Wang, L. Chen, *Nanomedicine: Nanotechnol. Biol. Med.*, **2011**, *7* (4), 385–402
198. M. P. Cook, S. Ando, K. Koide, *Tetrahedron Lett.*, **2012**, *53* (39), 5284–5286
199. P. Gobbo, P. Gunawardene, W. Luo, S. Workenti, *Synlett*, **2015**, *26* (9), 1169–1174
200. E. Riva, M. Mattarella, S. Borrelli, M. S. Christodoulou, D. Cartelli, M. Main, S. Faulkner, D. Sykes, G. Cappelletti, J. S. Snaith, D. Passarella, *ChemPlusChem*, **2013**, *78* (3), 222–226
201. X. Chen, Q. Wu, L. Henschke, G. Weber, T. Weil, *Dyes and Pigments*, **2012**, *94* (2), 296–303
202. X. Yi, F. Wang, W. Qin, X. Yang, J. Yuan, *Int. J. Nanomedicine*, **2014**, *9*, 1347–1365

- 
203. S. G. Young, O. U. Taek., K. H. Doo, L. J. Woo, P. H. Geun, P. Y. Ho, Y. J. Bum, *US2003/203944 A1*, **2003**
204. G. Kaupp, J. Schmeyers, J. Boy, *Tetrahedron*, **2000**, *56* (36), 6899–6911
205. P. G. M. Wuts, T. W. Greene, *Greene's protective groups in organic synthesis* (4th edition), **2006**, John Wiley & Sons
206. G. Tasnádi, E. Forró, F. Fülöp, *Tetrahedron Asymmetry*, **2007**, *18* (23), 2841–2844
207. E. J. Corey, N. M. Weinshenker, T. K. Schaaf, W. Huber, *J. Am. Chem. Soc.*, **1969**, *91* (20), 5675–5677
208. R. L. Halterman, J. L. Moore, L. M. Mannel *J. Org. Chem.* **2008**, *73*, 3266–3269
209. <https://www.sigmaaldrich.com/catalog/product/sigma/f7250>
210. L. F. Mottram, S. Forbes, B. D. Ackley, B. R. Peterson, *Beilstein J. Org. Chem.*, **2012**, *8*, 2156–2165
211. J. M. Dixon, M. Taniguchi, J. S. Lindsey, *Photochem. Photobiol.*, **2005**, *81*, 212–213
212. L. Josephson, C-H. Tung, A. Moore, R. Weissleder, *Bioconjugate Chem.*, **1999**, *10* (2), 186–191
213. Y. Octavia, C. G. Tocchetti, K. L. Gabrielson, S. Janssens, H. J. Crijns, A. L. Moens, *J. Mol. Cell. Cardiol.*, **2012**, *52* (6), 1213–1225
214. S. Thysiadis, S. Katsamakakos, P. Dalezis, T. Chatzidisideri, D. Trafalis, V. Sarli, *Future Med. Chem.*, **2017**, *9* (18), 2181–2196
215. A. A. P. Mansur, S. M. Carvalho, Z. I. P. Lobato, M. de Fátima Leite, A. da Silva Cunha, Jr., H. S. Mansur, *Bioconjugate Chem.*, **2018**, *29*, 1973–2000
216. P. Hassanzadeh, F. Atyabi, R. Dinarvand, *J. control. release*, **2018**, *270*, 260–267
217. F. Kratz, I. Muller, C. Ryppa, A. Warnecke, *ChemMedChem*, **2008**, *3*, 20–53
218. Q. Hu, Q. Chen, Z. Gu, *Biomaterials*, **2018**, *178*, 546–558
219. Z. Pourmanouchehri, M. Jafarzadeh, S. Kakaei, E. Sattarzadeh-Khameneh, *J. Inorg. Organomet. Polym. Mater.*, **2018**, *28*, 1980–1990
220. G. Casi, D. Neri, *J. Med. Chem.*, **2015**, *58*, 8751–8761
221. D. Böhme, A. G. Beck-Sickinger, *J. Pep. Sci.*, **2015**, *21*, 186–200
222. a) D-Z. Li; *Eur. J. Med. Chem.*, **2017**, *125*, 1235–1246; b) Z. Liu, Q. Lin, Q. Huang, H. Liu, C. Bao, W. Zhang, X. Zhong, L. Zhu, *Chem. Comm.*, **2011**, *47*, 1482–1484
223. B.S. Chhikara, N. S. Jean, D. Mandal, A. Kumar, K. Parang, *Eur. J. Med. Chem.*, **2011**, *46* (6), 2037–2042
224. A. Oyane, X. Wang, Y. Sogo, A. Ita, H. Tsurushima, *Acta biomater.*, **2012**, *8* (6), 2034–2046
225. R. A. Surmenev, M. A. Surmeneva, A. A. Ivanova, *Acta biomater.*, **2014**, *10*, 557–579

- 
226. B. Feng, J. Weng, B. C. Yang, S. X. Qu, X. D. Zhang, *Biomaterials*, **2004**, *25*, 3421–3428
227. Y. C. Chai, S. Truscetto, S. Van Bael, F. P. Luyten, J. Vleugels, J. Schrooten, *Acta biomater.*, **2011**, *7*, 2310–2319
228. S. Yu, Z. Yu, G. Wang, J. Han, X. Ma, M. S. Dargusch, *Coll. Surf. B: Biointerfaces*, **2011**, *85* (2), 103–115
229. A. Bigi, E. Boanini, C. Capuccini, M. Gazzano, *Inorg. Chim. Acta*, **2007**, *360* (3), 1009–1016
230. K. Ulbrich, K. Holá, V. Šubr, A. Bakandritsos, J. Tuček, R. Zbořil, *Chem. Rev.*, **2016**, *116*, 5338–5431
231. L. S. Dolci, A. Liguori, A. Merlettini, L. Calzà, M. Castellucci, M. Gherardi, V. Colombo, M. L. Focarete, *J. Phys. D: Appl. Phys.*, **2016**, *49*, 274003
232. a) F. Rossi, M. Griensven, *Tissue Eng. A*, **2014**, *20*, 15–16; b) S. Bierbaum, V. Hintze, D. Scharnweber, *Biomatter*, **2012**, *2*, 132–141
233. F. Karimi, A. J. O'Connor, G. G. Qiao, D. E. Heath, *Adv Healthc. Mater.*, **2018**, *7* (12):1701324
234. Y-P. Jiao, F-Z. Cui, *Biomed. Mater.*, **2007**, *2*, R24
235. C. Gualandi, N. Bloise, N. Mauro, P. Ferruti, A. Manfredi, M. Sampaolesi, A. Liguori, R. Laurita, M. Gherardi, V. Colombo, L. Visai, M. L. Focarete, E. Ranucci, *Macromol. Biosci.*, **2016**, *16*, 1533–1544
236. a) J. Lee, J. J. Yoo, A. Atala, S. J. Lee, *Biomaterials*, **2012**, *33*, 6709–6720; b) A. Tambralli, B. Blakeney, J. Anderson, M. Kushwaha, A. Andukuri, D. Dean, H. W. Jun, *Biofabrication*, **2009**, *1*: 025001; c) Y. Wang, Y. Zhang, B. Wang, Y. Cao, Q. Yu, T. Yin, *J. Nanopar. Res.*, **2013**, *15*, 1726–1738
237. Y. J. Son, W. J. Kim, H. S. Yoo, *Arch. Pharm. Res.*, **2014**, *37* (1), 69–78
238. X. Xin, M. Hussain, J. J. Mao, *Biomaterials*, **2007**, *28* (2), 316–325
239. Z-M. Huang, Y-Z. Zhang, M. Kotaki, S. Ramakrishna, *Compos. Sci. Technol.*, **2003**, *63* (15), 2223–2253
240. L. Weng, J. Xie, *Curr. Pharm. Des.*, **2015**, *21* (15), 1944–1959
241. T. G. Kim, T. G. Park, *Tissue Engineering*, **2006**, *12*, 221–233
242. a) X. Zhang, X. Gao, L. Jiang, J. Qin, *Langmuir*, **2012**, *28*, 10026–10032; b) Y. Zhu, Z. Mao, C. Gao, *Biomacromolecules*, **2012**, *14*, 342–349
243. K. Yea, H. Zhang, J. Xie, T. M. Jones, G. Yang, B. Doo Song, R. A. Lerner, *PNAS*, **2013**, *110*, 14966–14971
244. J. E. Baldwin, R. M. Adlington, A. T. Russell, M. L. Smith, *Tetrahedron*, **1995**, *51* (16), 4733–4762
245. Abbott Laboratories - *US6103911*, **2000**, A1
246. H. Ishibashi, K. Kodama, C. Kameoka, H. Kawanami, M. Ikeda, *Tetrahedron*, **1996**, *52* (44), 13867–13880
247. T. Palmer (editor), *Understanding Enzymes* (3rd edition), **1991**, Ellis Horwood Ltd
248. R. de Regil, G. Sandoval, *Biomolecules*, **2013**, *3* (4), 812–847

- 
249. J. M. Choi, S. S. Han, H. S. Kim, *Biotechnology Advances*, **2015**, 33 (7), 1443–1454
250. D. Voet, J. G. Voet, C. W. Pratt, *Fundamentals of Biochemistry: Life at the Molecular Level*, **2012**, Wiley-VCH
251. R. A. Sheldon, I. W. C. E. Arends, U. Hanefeld, *Green Chemistry and Catalysis*, **2007**, Wiley-VCH
252. a) R. Sheldon, J. Woodley, *Chem. Rev.*, **2018**, 118 (2), 801–838; b) United States Environmental Protection Agency, *Green Chemistry*, **2006-06-28**
253. A. Dhar, K. Kanwar, S. S. Arora, P. Kumar, *Biological Procedures Online*, **2006**, 18, 2–11
254. M. Adamczak, S. H. Krishna, *Food Technol. Biotechnol.*, **2004**, 42 (4), 251–264
255. A. Wells, H-P. Meyer, *ChemCatChem*, **2014**, 6, 918–920
256. R. A. Sheldon, P. C. Pereira, *Chem. Soc. Rev.*, **2017**, 46, 2678–2691
257. J. L. Katz, E. Tirelli, J.M. Witkin, *Behav. Pharmacol.*, **1990**, 1, 347–353
258. a) T. Mori, T. Ito, S. Liu, *Sci. Rep.*, **2018**, 8:1294; b) T. Ito, H. Ando, T. Suzuki, *Science*, **2010**, 327 (5971), 1345–1350
259. A. J. J. Straathof, S. Panke, A. Schmid, *Curr. Opin. Biotechnol.*, **2002**, 13, 548–556
260. *International union of Biochemistry and Molecular Biology*
261. R. Gupta, N. Gupta, P. Rathi, *Appl. Microbiol. Biotechnol.*, **2004**, 64 (6), 763–781
262. A. Guldhe, B. Singh, T. Mutanda, *Renew. Sustain. Energy Rev.*, **2015**, 41, 1447–1464
263. F. I. Khan, D. Lan, R. Durrani, W. Huan, Z. Zhao, Y. Wang, *Front. Bioeng. Biotechnol.*, **2017**, 5:16
264. K. Faber, *Biotransformations in Organic Chemistry* (5th edition), **2004**, Springer
265. B. K. Banik,  *$\beta$ -lactams: Unique Structures of Distinction for Novel Molecules*, **2013**, Springer
266. R. Brieva, J. Z. Crich, C. J. Sih, *J. Org. Chem.*, **1993**, 58, 1068–1075
267. J. Kaman, E. Forrò, F. Fulop, *Tetrahedron: Asymmetry*, **2000**, 1, 1593–1600
268. E. Forrò, F. Fulop, *Tetrahedron: Asymmetry*, **2001**, 12, 2351–2358
269. X-G. Li, L. T. Kanerva, *Adv. Synth. Cat.*, **2006**, 348, 197–205
270. IUPAC “Compendium of Chemical Terminology” Gold Book (Version 2.3.3), **2014**
271. T. Miyazawa, E. Kaito, T. Yukawa, *J. Mol. Cat. B-Enzym.*, **2005**, 37, 63–67
272. L. Meier, G. C. Monteiro, R. A. M. Baldissera, M. Mandolesi Sá, *J. Braz. Chem. Soc.*, **2010**, 21 (5), 859–866
273. A. E. Sutton, J. Clardy, *Org. Lett.*, **2000**, 2 (3), 319–321
274. X-G. Li, L. T. Kanerva, *Tetrahedron: Asymmetry*, **2007**, 18, 2468–2472
275. N. Ikota, H. Shibata, K. Koga, *Chem. Pharm. Bull.*, **1985**, 33, 3299–3306



- 
276. a) J. H. Teles, I. Hermans, G. Franz, R. A. Sheldon, *Oxidation, Ullmann's Encyclopedia of Industrial Chemistry*, **2015**, Wiley-VCH, b) F. Cavani, J. H. Teles, *ChemSusChem*, **2009**, 2, 508–534
277. S. S. Rawalay, H. Shechter, *J. Org. Chem.*, **1967**, 32, 3129–3131
278. R. G. R. Bacon, W. J. W. Hanna, *J. Chem. Soc.*, **1965**, 4962–4968
279. S. Sobhani, M. F. Maleki, *Synlett*, **2010**, 3, 383–386
280. S. Sobhani, S. Aryanejad, M. F. Maleki, *Helv. Chim. Acta*, **2012**, 95, 613–617
281. S. Chandrasekhar, G. P. K. Reddy, C. Nagesh, C. R. Reddy, *Tetrahedron Lett.*, **2007**, 48, 1269–1271
282. a) J. Srogl, S. Voltrova, *Org. Lett.*, **2009**, 11, 843–845; b) S. Naya, T. Niwa, R. Negishi, H. Kobayashi, H. Tada, *Angew. Chem. Int. Ed.*, **2014**, 53, 13894–13897
283. N. Iqbal, E. J. Cho, *Adv. Synth. Catal.*, **2015**, 357, 2187–2192
284. a) R. Tang, S. E. Diamond, N. Neary, F. Mares, *J. Chem. Soc. Chem. Commun.*, **1978**, 13, 562–562; b) A. J. Bailey, B. R. James, *Chem. Commun.*, **1996**, 20, 2343–2344; c) K. Yamaguchi, N. Mizuno, *Angew. Chem. Int. Ed.*, **2003**, 42, 1480–1483; d) L. Aschwanden, T. Mallat, F. Krumeich, A. Baiker, *J. Mol. Catal. A: Chem.*, **2009**, 309, 57–62; e) M. H. So, Y. Liu, C. M. Ho, C. M. Che, *Chem. Asian J.*, **2009**, 4, 1551–1561; f) M. LARGERON, *Eur. J. Org. Chem.*, **2013**, 24, 5225–5235; g) H. Yu, Y. Zhai, G. Dai, S. Ru, S. Han, Y. Wei, *Chem. Eur. J.*, **2017**, 23, 13883–13887
285. F. Su, S. C. Mathew, L. Mohlmann, M. Antonietti, X. Wang, S. Blechert, *Angew. Chem. Int. Ed.*, **2011**, 50, 657–660
286. S. Sarina, H. Zhu, E. Jaatinen, Q. Xiao, H. Liu, J. Jia, C. Chen, J. Zhao, *J. Am. Chem. Soc.*, **2013**, 135, 5793–5801
287. J. H. Ko, N. Kang, N. Park, H-W. Shin, S. Kang, S. M. Lee, H. J. Kim, T. K. Ahn, S. U. Son, *ACS Macro Lett.*, **2015**, 4, 669–672
288. D. Lenoir, *Angew. Chem. Int. Ed.*, **2006**, 45, 3206–3210
289. M. LARGERON, *Org. Biomol. Chem.*, **2017**, 15, 4722–4730
290. M. L. Contente, F. Dall'Oglio, L. Tamborini, F. Molinari, F. Paradisi, *ChemCatChem*, **2017**, 9, 3843–3848
291. G. F. P. de Souza, T. W. von Zuben, A. G. Salles, Jr, *ACS Sustainable Chem. Eng.*, **2017**, 5, 8439–8446
292. T. J. Collins, *Acc. Chem. Res.*, **2002**, 35, 782–790
293. a) A. Sudalai, A. Khenkin, R. Neumann, *Org. Biomol. Chem.*, **2015**, 13, 4374–4394; b) A. Lauterbach, G. Ober., *Iodine and iodine compounds, Kirk Othmer Encyclopedia of Chemical Technology* (5th edition), **2005**, vol. 14, John Wiley & Sons, 353–380
294. P. Galletti, G. Martelli, G. Prandini, C. Colucci, D. Giacomini, *RSC Adv.*, **2018**, 8, 9723–9730

- 
295. a) R. Ciriminna, M. Pagliaro, *Org. Process Res. Dev.*, **2010**, *14*, 245–251; b) R.A. Sheldon, I. W. C. E. Arends, *Adv. Synth. Catal.*, **2004**, *346*, 1051–1071
296. A. L. Bartelson, K. M. Lambert, J. M. Bobbitt, W. F. Bailey, *ChemCatChem*, **2016**, *8*, 3421–3430
297. P. L. Anelli, C. Biffi, F. Montanari, S. Quici, *J. Org. Chem.*, **1987**, *52*, 2559–2562
298. a) Q. Xing, H. Lv, C. Xia, F. Li, *Chem. Commun.*, **2016**, *52*, 489–492; b) S-J. Jin, P. K. Arora, L. M. Sayre, *J. Org. Chem.*, **1990**, *55*, 3011–3018
299. P. Galletti, M. Pori, D. Giacomini, *SynLett*, **2010**, *17*, 2644–2648
300. M. Lei, R-J. Hu, Y-G. Wang, *Tetrahedron*, **2006**, *62*, 8928–8932
301. a) W. F. Bailey, J. M. Bobbitt, K. B. Wiberg, *J. Org. Chem.*, **2007**, *72*, 4504–4509; b) F. d'Acunzo, P. Baiocco, M. Fabbrini, C. Galli, P. Gentili, *Eur. J. Org. Chem.*, **2002**, *24*, 4195–4201
302. J. Rumble (editor), *Bond Dissociation Energies, Handbook of Chemistry and Physics* (98th edition), **2017**, CRC press,
303. X. Jin, K. Kataoka, T. Yatabe, K. Yamaguchi, N. Mizuno, *Angew. Chem. Int. Ed.*, **2016**, *55*, 7212–7217
304. C. Liu, H. Zhang, W. Shi, A. Lei, *Chem. Rev.*, **2011**, *111*, 1780–1824
305. J. Pitzer, K. Steiner, *J. Biotechnol.*, **2016**, *235*, 32–46
306. S. De Sarkar, A. Studer, *Org. Lett.*, **2010**, *12*, 1992–1995
307. a) Y. Suto, N. Yamagiwa, Y. Torisawa, *Tetrahedron Lett.*, **2008**, *49*, 5732–5735; b) A. Porcheddu, L. De Luca, *Adv. Synth. Catal.*, **2012**, *354*, 2949–2953; c) Z. Liu, J. Zhang, S. Chen, E. Shi, Y. Xu, X. Wan, *Angew. Chem. Int. Ed.*, **2012**, *51*, 3231–3235; d) B. Tan, N. Toda, C. F. Barbas III, *Angew. Chem. Int. Ed.*, **2012**, *51* (50), 12538–12541; e) A. M. Whittaker, V. M. Dong, *Angew. Chem. Int. Ed.*, **2015**, *54*, 1312–1315; f) R. Deshidi, M. A. Rizvi, B. A. Shah, *RSC Adv.*, **2015**, *5*, 90521–90524
308. D. Gamnara, G. A. Seoane, P. Saenz-Méndez, P. Domínguez de Maria, *Redox Biocatalysis: Fundamentals and Applications*, **2013**, John Wiley & Sons
309. H. Claus, *Micron* **2004**, *35*, 93–96
310. M. Sosna, J-M. Chrétien, J. D. Kilburn, P. N. Bartlett, *Phys. Chem. Chem. Phys.*, **2010**, *12*, 10018–10026
311. S. Riva, *Trends Biotechnol.*, **2006**, *24* (5), 219–226
312. M. Mogharabi, M. A. Faramarzi, *Adv. Synth. Catal.*, **2014**, *356*, 897–927
313. C. Pezzella, L. Guarino, A. Piscitelli, *Cell. Mol. Life Sci.*, **2015**, *72*, 923–940
314. P. Galletti, M. Pori, F. Funicello, R. Soldati, A. Ballardini, D. Giacomini, *ChemSusChem*, **2014**, *7*, 2684–2689
315. P. Galletti, F. Funicello, R. Soldati, D. Giacomini, *Adv. Synth. Catal.*, **2015**, *357*, 1840–1848

316. B. Bechi, S. Herter, S. McKenna, C. Riley, S. Leimkühler, N. J. Turner, A. J. Carnell, *Green Chem.*, **2014**, *16*, 4524–4529
317. a) M. Aresta, A. Dibenedetto, A. Angelini, *Chem. Rev.*, **2014**, *114*, 1709–1742; b) T. Sakakura, J-C. Choi, H. Yasuda, *Chem. Rev.* **2007**, *107*, 2365–2387; c) E. A. Quadrelli, G. Centi, J-L. Duplan, S. Perathoner, *ChemSusChem*, **2011**, *4*, 1194–1215
318. M. Aresta, A. Dibenedetto, *Dalton Trans.*, **2007**, 2975–2992
319. a) D. J. Darensbourg, *Inorg. Chem.*, **2010**, *49*, 10765–10780; b) R. Martin, A. W. Kleij, *ChemSusChem* **2011**, *4*, 1259–1264; c) Y. Tsuji, T. Fujihara, *Chem. Commun.*, **2012**, *48*, 9956–9964; d) K. Huang, C-L. Sun, Z-J. Shi, *Chem. Soc. Rev.*, **2011**, *40*, 2435–2452; e) C. J. Whiteoak, A. Nova, F. Maseras, A. W. Kleij, *ChemSusChem*, **2012**, *5*, 2032–2038; f) S. Nakamura, *Org. Biomol. Chem.*, **2014**, *12*, 394–405
320. S. M. Glueck, S. Gumus, W. M. F. Fabian, K. Faber, *Chem. Soc. Rev.*, **2010**, *39*, 313–328
321. a) R. Brackmann, G. Fuchs, *Eur. J. Biochem.*, **1993**, *213*, 563–571; b) M. Boll, G. Fuchs, *Biol. Chem.*, **2005**, *386*, 989–997; c) J. Gobson, C. S. Harwood, *Annu. Rev. Microbiol.*, **2002**, *56*, 345–369; d) L. Ackermann, *Angew. Chem. Int. Ed.*, **2011**, *50*, 3842–3844
322. C. Wuensch, J. Gross, G. Steinkellner, A. Lyskowski, K. Gruber, S. M. Glueck, K. Faber, *RSC Adv.*, **2014**, *4*, 9673–9679
323. a) K. Kirimura, H. Gunji, R. Wakayama, T. Hattori, Y. Ishii, *Biochem. Biophys. Res. Commun.*, **2010**, *394*, 279–284; b) K. Kirimura, S. Yanaso, S. Kosaka, K. Koyama, T. Hattori, Y. Ishii, *Chem. Lett.*, **2011**, *40*, 206–208
324. A. S. Lindsey, H. Jeskey, *Chem. Rev.*, **1957**, *57*, 583–614
325. M. P. Torrens-Spence, P. Liu, H. Ding, K. Harich, G. Gillaspay, J. Li, *J. Biol. Chem.*, **2013**, *288*, 2376–2387
326. a) R. Lewin, M. L. Thompson, J. Micklefield, *Enzyme Carboxylation and Decarboxylation*, Science of Synthesis: Biocatalysis in Organic Synthesis (Eds.: K. Faber, W-D. Fessner, N. J. Turner), **2015**, Vol. 2, Thieme, 133–157; b) A. Alissandratos, C. J. Easton, *Beilstein J. Org. Chem.*, **2015**, *11*, 2370–2387; c) C. Wuensch, T. Pavkov-Keller, G. Steinkellner, J. Gross, M. Fuchs, A. Hromic, A. Lyskowski, K. Fauland, K. Gruber, S. M. Glueck, K. Faber, *Adv. Synth. Catal.*, **2015**, *357*, 1909–1918
327. K. Plasch, V. Resch, J. Hitce, J. Popłonski, K. Faber, S. M. Glueck, *Adv. Synth. Catal.*, **2017**, *359*, 959–965
328. J. E. Smyth, N. M. Butler, P. A. Keller, *Nat. Prod. Rep.*, **2015**, *32*, 1562–1583
329. a) E. Masson, *Org. Biomol. Chem.* **2013**, *11*, 2859–2871; b) F. Grein, *J. Phys. Chem. A*, **2002**, *106*, 3823–3827
330. I. Cepanec, *Synthesis of biaryls*, Elsevier, **2004**
331. M. Rachwalski, N. Vermue, F. P. T. J. Rutjes, *Chem. Soc. Rev.*, **2013**, *42*, 9268–9282
332. S. Staniland, R. W. Adams, J. J. W. McDouall, I. Maffucci, A. Contini, D. M. Grainger, N. J. Turner, J. Clayden, *Angew. Chem. Int. Ed.*, **2016**, *55*, 10755–10759
333. a) A. Bracegirdle, J. Clayden, L. W. Lai, *Beilstein J. Org. Chem.*, **2008**, *4*, 47; b) J. Clayden, L. W. Lai, M. Helliwell, *Tetrahedron*, **2004**, *60*, 4399–4412; c) J. Clayden, L. W. Lai, *Tetrahedron Lett.*, **2001**, *42*, 3163–3166; d) J. Clayden, L. W. Lai, *Angew. Chem. Int. Ed.*, **1999**, *38*, 2556–2558; e) V. Chan, J. G. Kim, C. Jimeno, P. J. Carroll, P. J. Walsh, *Org. Lett.*, **2004**, *6*, 2051–2053

- 
334. G. A. Molander, B. Biolatto, *Org. Lett.*, **2002**, 4 (11), 1867–1870
335. M. Forghieri, C. Laggner, P. Paoli, T. Langer, G. Manao, G. Camici, L. Bondioli, F. Prati, L. Costantino, *Bioorg. Med. Chem.*, **2009**, 17, 2658–2672
336. C. Wuensch, N. Schmidt, J. Gross, B. Grischek, S. M. Glueck, K. Faber, *J. Biotechnol.*, **2013**, 168, 264–270
337. The PyMOL Molecular Graphics System, Version 1.2r3pre, Schroedinger, LLC
338. T. Maibunkaew, C. Thongsornkleeb, J. Tummatorn, A. Bunrit, S. Ruchirawat, *Synlett*, **2014**, 25 (12), 1769–1775
339. M. Schlosser (editor), *Organometallics in Synthesis* (3rd manual), **2004**, Wiley
340. a) D-H. Lee, Y. Qian, J-H. Park, J-S. Lee, S-E. Shim, M-J. Jin, *Adv. Synth. Cat.*, **2013**, 355 (9), 1729–1735; b) G. M. Scheuermann, P. Steurer, R. Muelhaupt, L. Rumi, W. Bannwarth, *J. Am. Chem. Soc.*, **2009**, 131 (23), 8262–8270; c) M. Pallavicini, R. Budriesi, L. Fumagalli, P. Ioan, A. Chiarini, C. Bolchi, M. P. Ugenti, S. Colleoni, M. Gobbi, E. Valoti, *J. Med. Chem.*, **2006**, 49 (24), 7140–7149; d) I. Y. El-Deeb, T. Funakoshi, Y. Shimomoto, R. Matsubara, M. Hayashi, *J. Org. Chem.*, **2017**, 82 (5), 2630–2640